Oil & Natural Gas Technology

DOE Award No.: DE-FC26-04NT15425

Final Report

Application of Time-Lapse Seismic Monitoring for the Control and Optimization of CO_2 Enhanced Oil Recovery Operations

Submitted by:
Schlumberger DCS
1310 Commerce Drive, Park Ridge 1
Pittsburgh, PA 15275

Prepared for:
United States Department of Energy
National Energy Technology Laboratory

March 9, 2009

Office of Fossil Energy

Application of Time-Lapse Seismic Monitoring for the Control and Optimization of CO_2 Enhanced Oil Recovery Operations

FINAL REPORT

Reporting Period: March 2004

To

March, 2009

Principal Author - Brian Toelle

Date Report Issued: March 2009

DOE Award No. DE-FC26-04NT 15425

Schlumberger DCS

1310 Commerce Drive, Park Ridge 1

Pittsburgh, PA 15275

DISCLAIMER

1 ABSTRACT

This project, “Application of Time-Lapse Seismic Monitoring for the Control and Optimization of CO_2 Enhanced Oil Recovery Operations”, investigated the potential for monitoring CO_2 floods in carbonate reservoirs through the use of standard p-wave seismic data. This primarily involved the use of 4D seismic (time lapse seismic) in an attempt to observe and map the movement of the injected CO_2 through a carbonate reservoir. The differences between certain seismic attributes, such as amplitude, were used for this purpose. This technique has recently been shown to be effective in CO_2 monitoring in Enhanced Oil Recovery (EOR) projects, such as Weyborne.

This study was conducted in the Charlton 30/31 field in the northern Michigan Basin, which is a Silurian pinnacle reef that completed its primary production in 1997 and was scheduled for enhanced oil recovery using injected CO_2. Prior to injection an initial “Base” 3D survey was obtained over the field and was then processed and interpreted. CO_2 injection within the main portion of the reef was conducted intermittently during 13 months starting in August 2005. During this time, 29,000 tons of CO_2 was injected into the Guelph formation, historically known as the Niagaran Brown formation. By September 2006, the reservoir pressure within the reef had risen to approximately 2000 lbs and oil and water production from the one producing well within the field had increased significantly.

The determination of the reservoir’s porosity distribution, a critical aspect of reservoir characterization and simulation, proved to be a significant portion of this project. In order to relate the differences observed between the seismic attributes seen on the multiple 3D seismic surveys and the actual location of the CO_2, a predictive reservoir simulation model was developed based on seismic attributes obtained from the base 3D seismic survey and available well data. This simulation predicted that the CO_2 injected into the reef would remain in the northern portion of the field. Two new wells, the State Charlton 4-30 and the Larsen 3-31, were drilled into the field in 2006 and 2008 respectively and supported this assessment.

A second (or “Monitor”) 3D seismic survey was acquired during September 2007 over most of the field and duplicated the first (Base) survey, as much as possible. However, as the simulation and new well data available at that time indicated that the CO_2 was concentrated in the northern portion of the field, the second seismic survey was not acquired over the extreme southern end of the area covered by the original (or Base) 3D survey. Basic processing was performed on the second 3D seismic survey and, finally, 4D processing methods were applied to both the Base and the Monitor surveys. In addition to this 3D data, a shear wave seismic data set was obtained at the same time.

Interpretation of the 4D seismic data indicated that a significant amplitude change, not attributable to differences in acquisition or processing, existed at the locations within the reef predicted by the reservoir simulation. The reservoir simulation was based on the porosity distribution obtained from seismic attributes from the Base 3D survey. Using this validated reservoir simulation the location of oil within the reef at the time the Monitor survey was obtained and recommendations made for the drilling of additional EOR wells. The economic impact of this project has been estimated in terms of both enhanced oil recovery and CO_2 sequestration potential. In the northern Michigan Basin alone, the Niagaran reef play is comprised of over 700 Niagaran reefs with reservoirs already depleted by primary production. Potentially there is over 1 billion bbls of oil (original oil in place minus primary recovery) remains in the reefs in Michigan, much of which could be more efficiently mobilized utilizing techniques similar to those employed in this study.

Table of Contents

Table of Contents

List of Tables

List of Graphs

List of Figures

2 LIST OF GRAPHICS

List of Figures

3 INTRODUCTION

3.1 General Background

For many years the energy demands of the United States were met through the development of existing oil fields within the country's borders and the periodic discovery of new ones. As the country's population and standard of living grew so did the energy needs, forcing oil imports from other countries. In today's rapidly industrializing world competition for oil is greater than ever before. At this same time serious concerns over the potential for global warming has resulted in the proposed solution of the underground sequestration of the greenhouse gas CO_2.

Enhanced Oil Recovery (EOR) from existing oil fields within the United States using CO_2 offers, at least in part, a potential solution to these two issues. It has been shown in a number of studies that during the primary production phase, oil fields only recover a portion of the oil in place. Injection of CO_2 into an oil reservoir has in the past been established as one possible method for recovering additional oil from these older fields. Additionally, this could also result in the sequestration of a green house gas, if properly administered.

The main issue associated with the optimization of these types of EOR operations has been predicting and controlling where the sweep goes within the reservoir. This has historically been attempted using well data and reservoir simulation and has been shown to be of use in large fields with homogeneous reservoirs which are easily modeled. However, the vast majority of the fields in the United States have reservoirs with some form of heterogeneity associated with them. Often in these cases CO_2 breakthrough occurs unexpectedly and prematurely, indicating inaccuracies in the reservoir characterization and simulations.

This project, the "Application of Time-Lapse Seismic Monitoring for the Control and Optimization of CO_2 Enhanced Oil Recovery Operations" project, investigated the potential for monitoring CO_2 floods in carbonate reservoirs through the use of standard p-wave seismic data. This involved the use of 4D seismic (time lapse seismic) in an attempt to observe the movement of the injected CO_2 through the reservoir. Seismic Amplitude, was used to detect and map the movement of CO_2 within the reservoir. This technique has been shown to be effective in CO_2 monitoring in EOR projects, such as Weyborne.

The Charlton 30/31 field is a Silurian pinnacle reef that completed its primary production in 1997. This field is still undergoing enhanced oil recovery using CO_2. The CO_2 flood was initiated at the end of 2005 when the injection of small amounts of CO_2 began in the A1 Carbonate. This injection was conducted for 2 months before being temporarily halted in order for pressure measurements to be conducted.

The determination of the reservoir's porosity distribution proved to be a significant portion of the study. In order to relate the differences observed between the seismic attributes seen on the time-lapse surveys and the actual location of the CO_2, a predictive reservoir simulation model had to be developed. From this model, an accurate determination of porosity within the carbonate reservoir needed to be obtained. For this determination of porosity certain seismic attributes have been investigated.

Reservoirs like the Charlton 30/31 field range from 50 to 400 acres in size. The relatively small area to image makes 3-D seismic data acquisition reasonably cost effective. Permeability and porosity vary considerably throughout the reef, thus it is essential to perform significant reservoir characterization and modeling prior to implementing a CO_2 flood to maximize recovery efficiency.

This same technique could be applied across a large spectrum of the industry. In the northern Michigan Basin alone, the Northern Silurian Reef Trend, see Figure 1, is comprised of over 700 Niagaran reefs with reservoirs already depleted by primary production. These reservoirs range in thickness from 200 to 400 ft and are at depths of 2000 to 5000 ft. Over 160 of these Niagaran oil fields have produced over 1 million bbls each and the total production is currently in excess of 300 million bbls and 1.4 Tcf. There could potentially be over 1 billion bbls of oil remaining in reefs in Michigan, much of which could be mobilized utilizing techniques similar to those employed in this study. Many existing fields in these trends are older and these have significant potential for enhanced oil recovery.

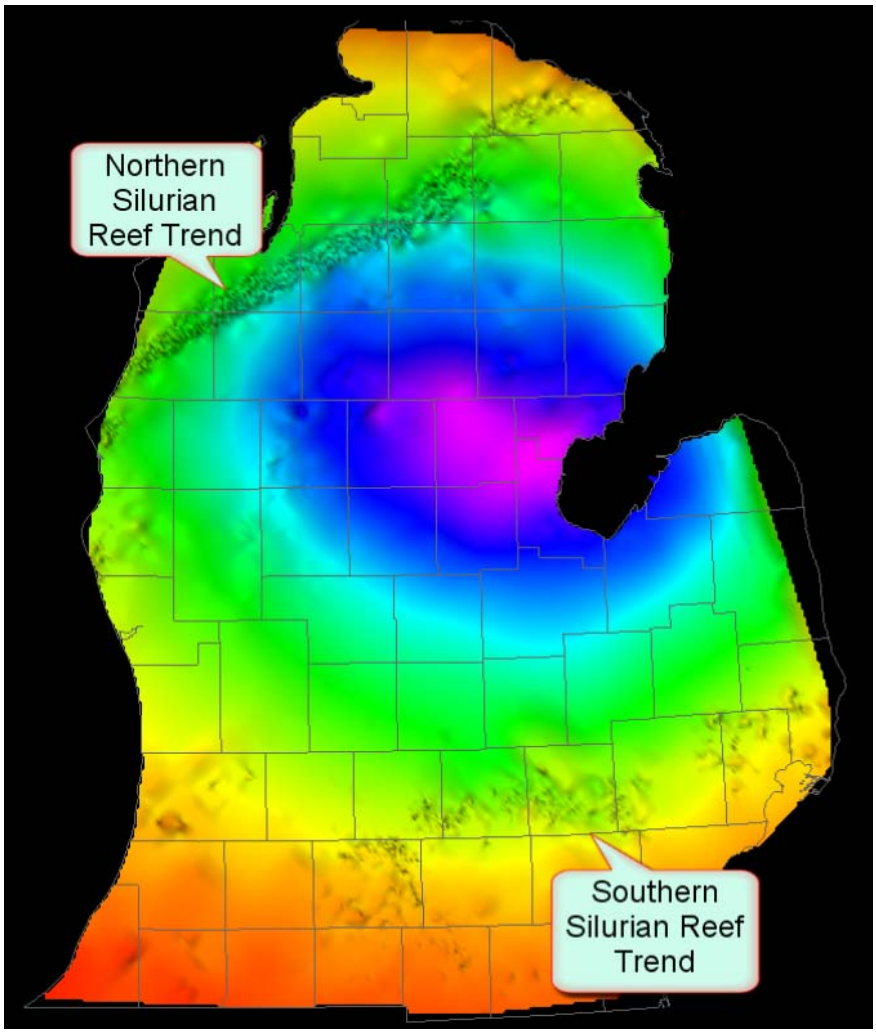

Figure 1: Structural grid for the Top of the Guelph Formation in the Michigan Basin and showing the location of the Northern and Southern Silurian Reef Trends.

These reefs occur in the Guelph Formation, which is a stratigraphic unit that has historically been referred to as the Brown Niagaran, see Figure 2. The first large commercial scale Niagaran reef field was the Boyd Field in St. Clair County. Discovered in 1952, the Boyd has produced over 2 MM bbls of oil and over 21 BCF of natural gas.

The Silurian stratigraphic units have been investigated for many decades. From the mid 1940's through the 1960's, a number of publications addressed the regional stratigraphy and paleogeography of the Silurian in the Michigan and Illinois Basins. An early lithofacies analysis of the area's Silurian was conducted by Melhorn (1958). The paleontology, petrography and geometry of northeast Illinois Silurian reefs were described by Ingels (1963). Joudry (1969) published research on potential dolomitization mechanisms in the Southern Michigan Basin Reef Trend.

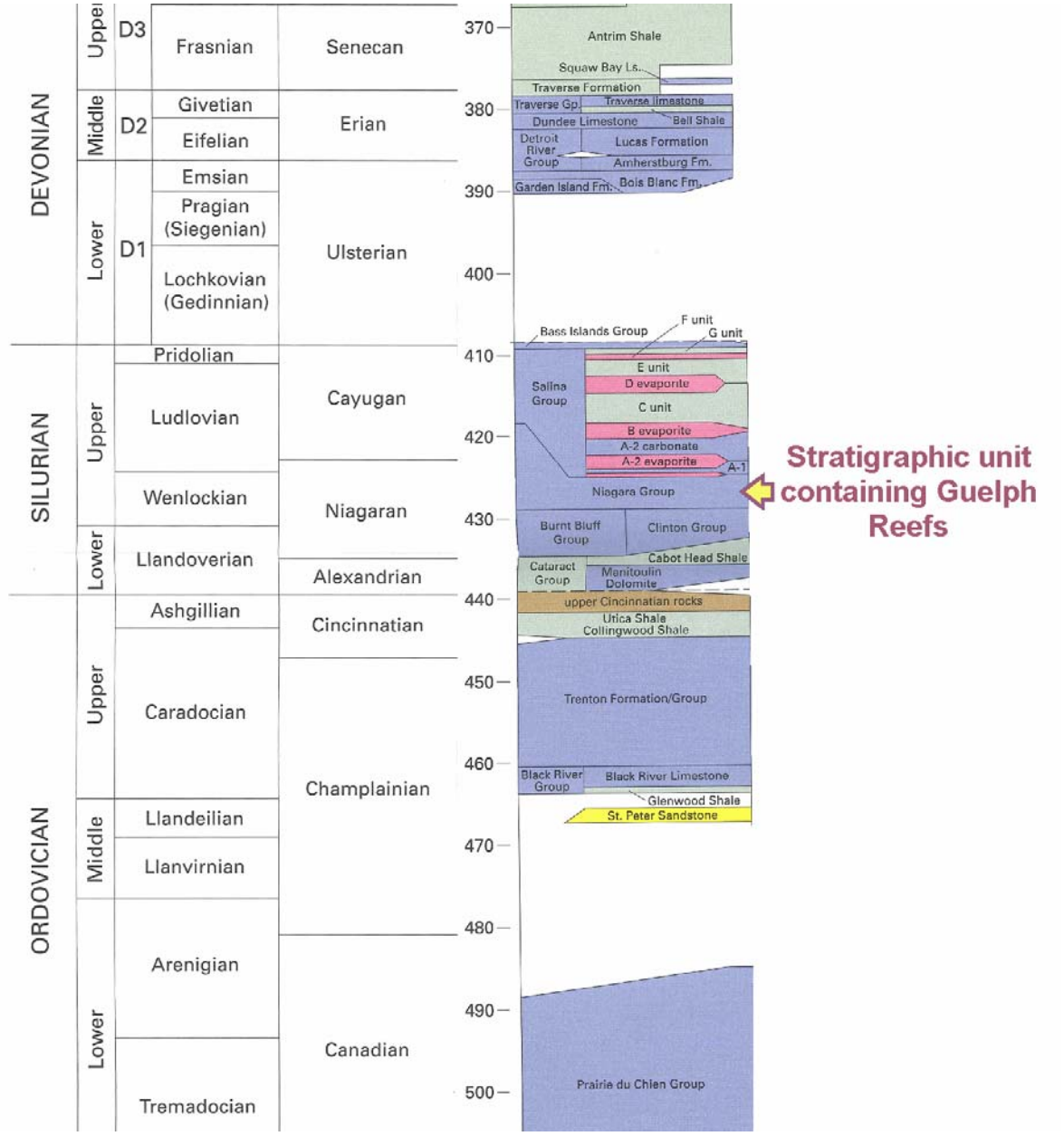

Figure 2: Pre-Mississippian Stratigraphy of the Study Area. Taken from USGS Scientific Investigations Map 2978, Swezey, 2008

In 1969, the first field in the Northern Silurian Reef Trend was discovered, leading to additional investigations of these reefs. These included works by Mesolello (1974), Shaver (1974) and (1977), Huh (1976), and Nurmi (1977). One of the more prolific workers on these structures during this time was Gill (1973, 1975, 1977 and 1979). A set of Indiana University publications (Indiana University Paleontology Seminar) in the 1970s and 1980s described the structure and stratigraphy of Silurian Reef complexes in Indiana and Ohio. In 1987 Cercone and Lohmann discussed diagenesis in these reefs.

More recently, Wylie and Wood (2005) provided an excellent description of these reefs through core data, 3D visualization techniques and well log tomography. This investigation illustrates in detail the complicated nature of these reefs. High porosity zones, which they relate to "Storage", did not necessarily correspond with zones of high permeability, which they relate to "Deliverability".

Exploration activity to locate these reefs accelerated in the 1970's with increase in oil prices. Production from these trends peaked in the late 70s – early 80s. These reservoirs range from completely dolomitized to mixed lithologies having a low porosity, low permeability limestone matrix with irregularly dolomitized intervals to entirely limestone throughout the reservoir interval. These dolomitized zones provide a network of higher porosity / permeability which controls fluid flow throughout the reservoir. Gravity segregation/gravity drainage effects are apparent as a depletion mechanism in many of these fields.

Although the fields within these trends are at the end of their primary production phase, they still contain a significant amount of oil which cannot be obtained through primary techniques. Enhanced Oil Recovery (EOR) techniques have been applied to only a few of these fields in the past. These EOR techniques included water flooding, gas recycling and, for a few fields CO_2 injection.

The CO_2 source for these projects has been the stratigraphically shallower Antrim Shale formation, see Figure 3. Natural gas production has occurred from the Antrim Shale for more than 20 years. The gas from the Antrim must be processed to remove the CO_2 in order to meet pipeline quality standards and a significant amount of the removed CO_2 is vented to the atmosphere.

In the Northern Reef Trend a number of these Guelph reefs occur where the Antrim shale is productive and CO_2 flooding has been conducted in only a few fields. CO_2 flooding was performed on two other fields in the area during the 1990's. These attempts met some success. Unfortunately, limited access to capital slowed development of these fields, which lead to these projects being abandoned.

The Charlton 30/31 Field, located in Otsego County, Michigan is one of the reefs in the Northern Michigan Basin's Silurian Reef Trend. Figure 3 shows this field's location in the northern portion of Michigan's Southern Peninsula. This field is approximately 300 acres in size and has a structural closure of just over 300 feet. Discovered by Shell in 1974 this field has produced 2.6 million barrels of oil. It is estimated that this reef originally contained 7 million barrels of oil in place. Six production wells were drilled during the 1970s and two wells, drilled in conjunction with this project, were drilled in 2006 and 2008.

Core Energy LLC., an oil and gas exploration and development company based in Traverse City, Michigan, obtained control of the oil assets and the "mothballed" CO_2

delivery system. Since controlling these assets, Core Energy has expanded operations to the point where there are now five fields in various stages of CO_2 flooding. These fields have been studied to various degrees with a number of them having 3D seismic obtained over them. One of these fields, the Charlton 30/31 field, has had a 4D seismic survey acquired over it along with a full reservoir characterization and simulation developed using this study's Base 3D Seismic survey.

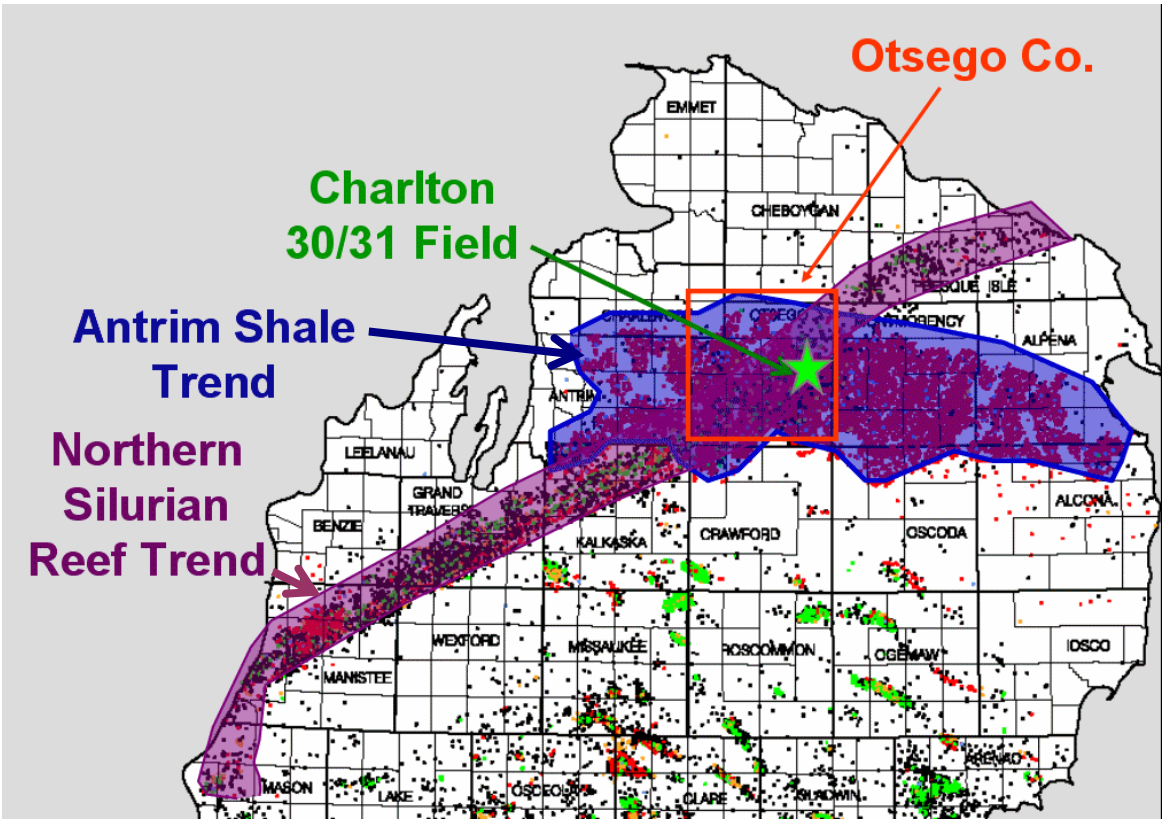

Figure 3: Location of the Charlton 30/31 Field within the Northern Silurian Reef Trend of the Michigan Basin.

As a result of these CO_2 floods a significant amount of information concerning CO_2 flooding of these types of reefs has been obtained which can be utilized in the planning of future CO_2-based EOR project within these trends. This information also allows for an estimate of the EOR potential to be made for both the Northern Silurian Reef Trend and the Southern Silurian Reef Trend.

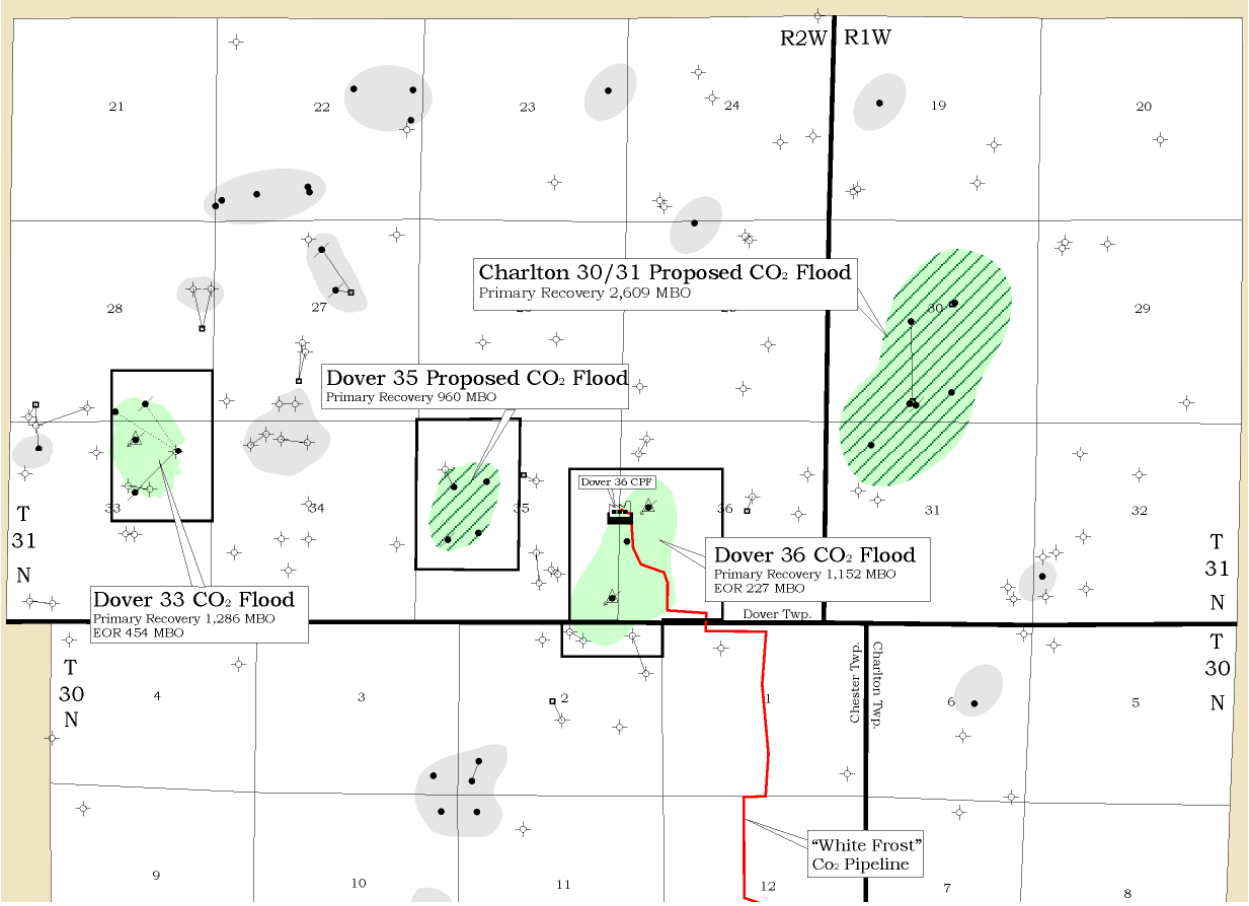

Figure 4: Map showing the location of the Charlton 30/31 field and the neighboring fields.

3.2 Project Scope

Enhanced recovery of oil by injecting CO_2 into the oil reservoir has been used in a limited number of U.S. oil reservoirs, primarily by large major producers. Independent oil producers have been hesitant to implement enhanced oil recovery using CO_2 because of the high initial investment and the technical/economic risks associated with such projects. Most of these risks are directly or indirectly associated with (1) insufficient understanding of the oil-bearing rock formation before flooding, and (2) limited understanding of what happens to the CO_2 once it is injected into the ground.

The first objective of this project was to demonstrate the use of cost-effective key and advanced technologies to better understand oil reservoirs prior to CO_2 flooding. The second objective was to demonstrate the use of advanced seismic technologies to "observe" the CO_2 flood front during injection such that "real-time" decisions can be made. The 4-year project will demonstrate the technical and cost effectiveness of the application of these technologies. Results of this project will be directly applicable to other existing oil reservoirs in the U.S., with increases in U.S. oil production envisioned during the subsequent 5 to 10 years and beyond.

A Niagaran reef oil formation in Michigan will be the target reservoir characterized for CO_2 flood potential. The characterization and modeling effort will define the geologic and

reservoir properties of the oil formation in order to optimize the flood design. The potential of both vertical and horizontal wells will be investigated. As part of the characterization phase, analysis of field data from existing and new wells is planned. Following completion of the characterization phase, field implementation of the CO_2 injection will occur. Periodic seismic surveys will be performed to "observe in real time" the movement of the CO_2 underground. These data will be used to optimize flood behavior and oil recovery

The scope of work includes a reservoir characterization effort in Phase I that will illustrate numerous advanced technologies for U.S. oil producers. The Niagaran oil reservoir in the Charleton 30/31 Field, Otsego County, Michigan will be the target for this project. In Phase I, our program calls for evaluating all existing data; shooting and analyzing an advanced 3-D seismic survey; and in one or more existing wells collecting advanced logs, analyzing production data, and developing a finite-difference reservoir simulation model. A compositional reservoir simulator will be developed with all of the existing data and used to design and estimate the CO_2 flood response. CO_2 injection will also begin in Phase 1 into the top of the reef to re-pressurize the reservoir prior to drilling horizontal production wells in Phase 2. The operator currently plans to shut-in the existing production wells during CO_2 injection until miscibility is achieved. Of course our 3-D seismic analysis and our simulation study might change the flood design.

The primary purpose of Phase II involves shooting an advanced 3-D seismic survey after 9 months and 2 years of CO_2 injection to determine the CO_2 flood front and the areal sweep efficiency. Changes may be made to modify the injection scheme based on the 3-D and reservoir simulation results. Two horizontal production wells will then be drilled into the bottom of the reef at locations determined from the 3-D survey and simulation studies. The compositional simulation model will be compared and calibrated based on this data and the actual well production data during that period.

One of our project objectives is to demonstrate advanced technologies that will better characterize oil reservoirs for CO_2 flooding. Another objective is to demonstrate advanced technologies to monitor the CO_2 flood front during injection such that "real-time" decisions can be made.

3.3 Geologic Overview and Field History

Geologic structures of the type investigated by this study use discrete pinnacle-like reefs. Some of these grow to be over 1 mile in diameter and have thicknesses of several hundred feet. These reefs can form barrier-like features that extend hundred of miles. The following figures, 5 through 9, display basic information concerning the regional geology of the basin and these reefs. Michigan basin is a bowl shaped, intercratonic basin which formed during the early Paleozoic. The center of the basin is located at the approximate midpoint of the Southern Michigan peninsula. Figure 6 is an idealized cross-section through the basin which illustrates the bowl like nature of the basin.

Figure 7 shows the orientation of these reefs to the basin and the shelf margin. During this Silurian the edge of the shelf margin is discernible by the location of the reef trends shown in figure 1. Figure 8 shows the possible internal reef structure taken from a recent DOE publication from project DE-AC26-00BC15122.

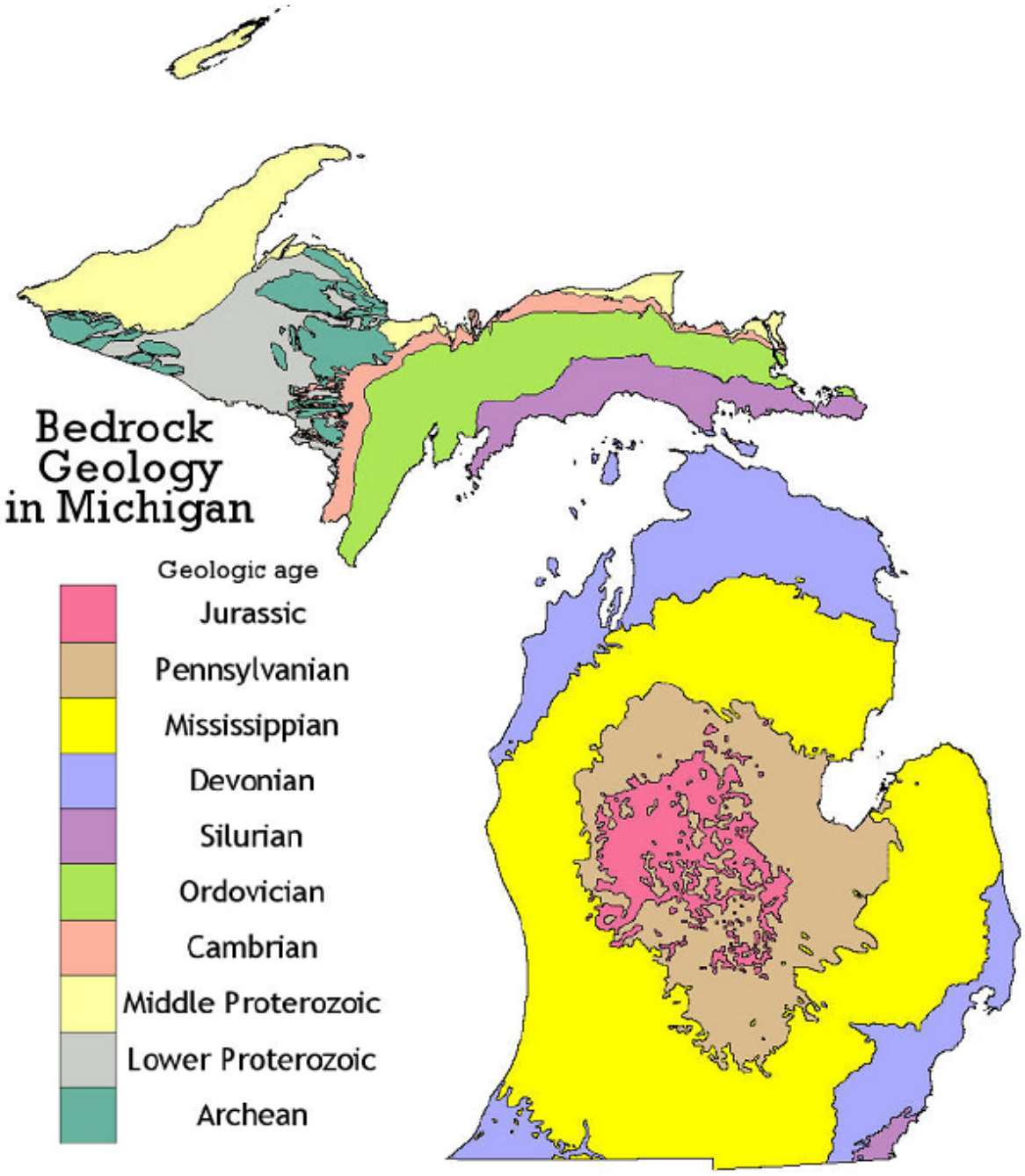

Figure **Error! Bookmark not defined.**: Bedrock geology map of Michigan taken from the Michigan Department of Environmental Quality website

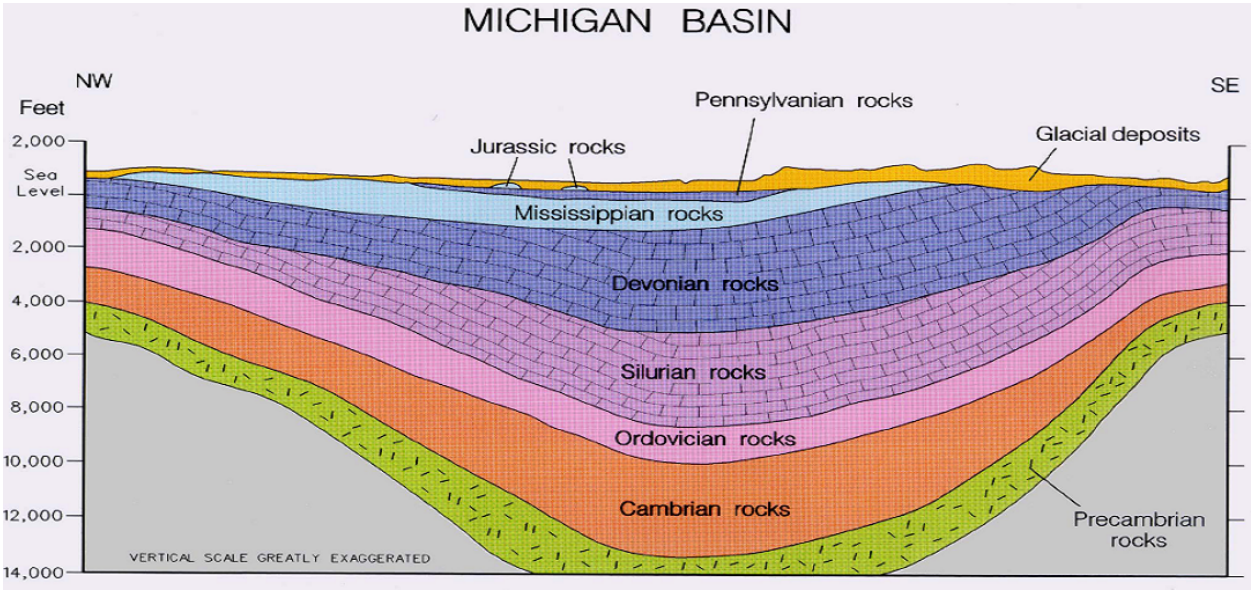

Figure 5: Idealized cross-section through the Michigan Basin taken from Michigan Department of Environmental Quality website.

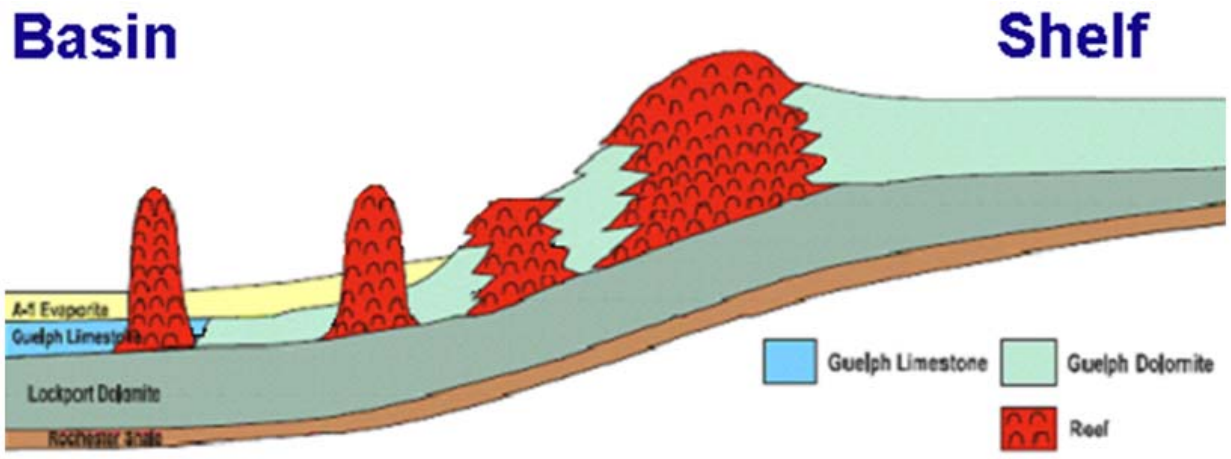

Figure 6: Idealized cross-section showing clinical and shelf margin reef development of Guelph pinnacle reefs.

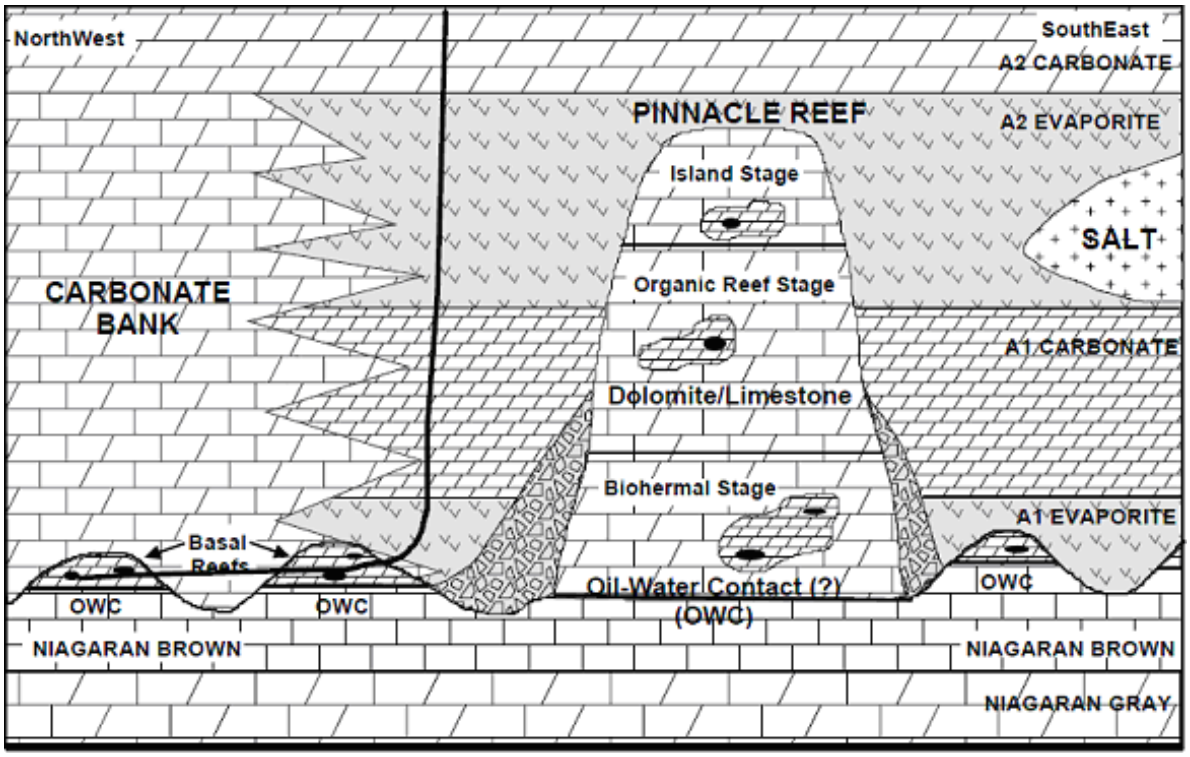

Figure 7: Possible internal reef structure taken from 2006 Department of Energy publication, project DE-AC26-00BC15122

The reefs of the Michigan Basin have been producing oil and gas since 1925 when production was established in the southern Michigan Basin Silurian Reef Trend. Production in the northern reef trend began in 1969 with peak production occurring in the late 1970s and early 1980s. The Northern Reef Trend is comprised of over 700 producing reefs, of which a significant number have produced over 1 million barrels of oil.

Historical production of oil from these two trends have occurred predominantly in the Northern Reef Trend. However, the Southern Reef Trend also contributes significantly to Michigan oil production. The Southern Reef Trend encompasses approximately 6,000 sq mi (Dolton) much less than 56,000 sq mi in the Northern Reef Trend. The Southern Reef Trend encompasses an area of about 11% the size of the Northern Reef Trend, and has a cumulative oil production of 10% of the cumulative production in the Northern Trend.

Although the southern reef hydrocarbons were first discovered in 1889, neither the DEQ nor the MTU reports oil production for these fields until 1959. Peak production in the Southern Reef Trend occurred between the 1970s and 1990s, lagging the Northern Trend productive years by 5-10 years.

Primary production from the Charlton 30/31 Field began in September 1974 and continued until November 1997 when the last producer was shut in. Cumulative oil production was 2.6 MMBbl, and cumulative gas production was 3.9 BSCF. Water production from the field was low, with a reported cumulative of 340,000 Bbl, although the accuracy of this value is questionable. The fields in this part of the play typically produce through pressure depletion / gravity segregation drive mechanisms and have no water influx or other natural pressure support mechanisms. During depletion several bottomhole

static pressure surveys were collected which clearly showed all the wells on a common pressure decline curve from an initial datum pressure of 2,959 psi to an abandonment pressure near 500 psia. A total of six wells were used to deplete the field. During their productive life these wells were aggressively managed with numerous interventions for reperforation, restimulation, gas lift and pumping. The field was not intentionally waterflooded.

In 2004, remediation efforts began in preparation for the CO_2 flood. Of the six original wells, two had been permanently abandoned, the “C”1-30 and the “C”3-30. The remaining wells were all reentered. The “C”2-30 was restored and serves as the initial injection well. The Charlton 1-30 and Charlton 2-30 were restored to producing status. However, the casing of the Charlton 1-31 well, at the southern end of the field, was so severely corroded that it was abandoned. This loss of a well at the southern end of the structure influenced the location selected for the Charlton 4-30 well which was drilled in 2007. The Charlton 4-30 was drilled as a CO_2 sequestration test well in the uphole section and it is expected to become available for operation in the reef at some later date.

Figure 9 is a cross sectional view through the Charlton 30/31 Field from south to north composed of gamma ray logs for some of these wells within the field.

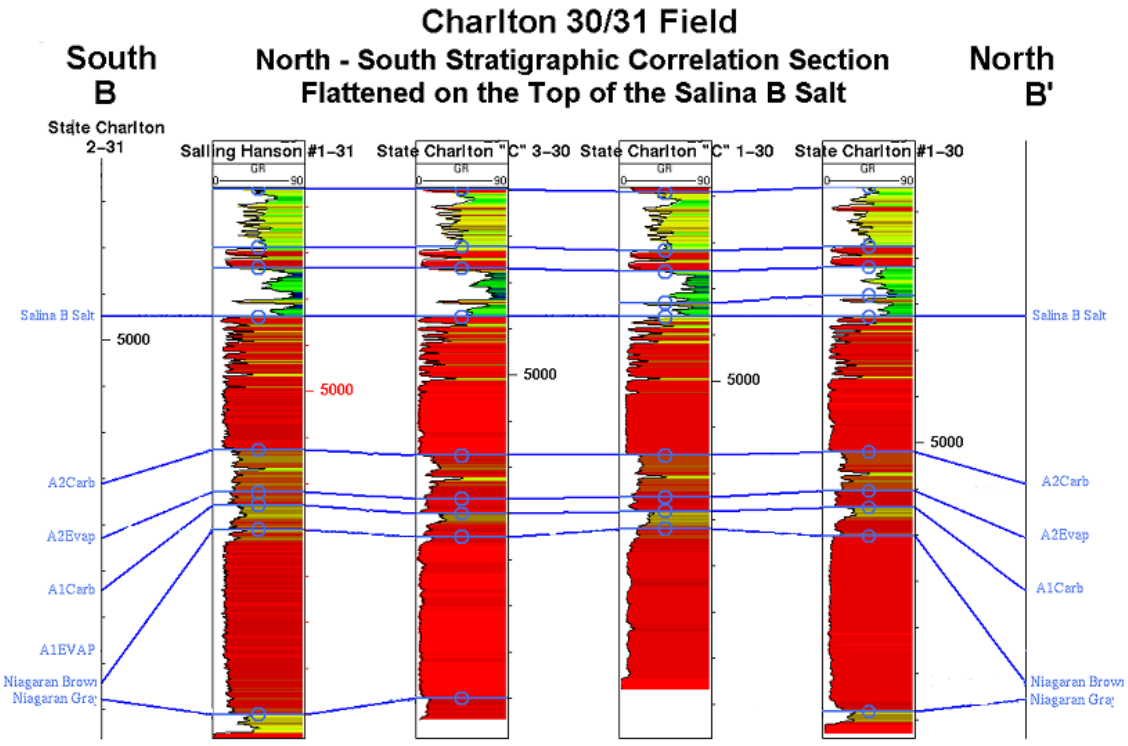

Figure 8: A cross sectional view through the Charlton 30/31 Field from south to north.

4 EXECUTIVE SUMMARY

The primary goal of the “Application of Time-Lapse Seismic Monitoring for the Control and Optimization of CO_2 Enhanced Oil Recovery Operations” project has been to investigate the use of advanced reservoir characterization and simulation techniques, including the use of 4D seismic (time lapse seismic), with regard to their use for the optimization of enhanced oil recovery projects. This project has involved a number of state-of-the-art geophysical technologies used to, first, characterize the targeted reservoir and then, second, use 4D seismic to monitor the CO_2 flood. The reservoir studied during this project has been the Silurian pinnacle reef located in the Northern Michigan Basin known as the Charlton 30/31 Field. This field, located in Otsego County, Michigan, produced 2.6 million barrels of oil during its primary production phase which ended in 1997 and was scheduled for a CO_2-based EOR project that was to begin in 2004.

As the project progressed it naturally divided into two phases due to the nature of the workflow employed. The first phase involved the imaging, characterization and simulation of this Silurian reef reservoir using the first or "Base" 3-D survey. During this phase the Base 3-D survey was planned using forward seismic modeling and then acquired, processed and interpreted using state-of-the-art geophysical software tools and methods. The results of this interpretation were used to build a reservoir characterization which then fed a production history matched, reservoir simulation that was used as a forward prediction tool. During the second phase of the project an additional 3-D survey or "Monitor" 3-D survey was acquired after the injection of what was believed to be a significant amount of CO_2. The results of the interpretation of this Monitor survey were then used to validate the predictions developed during the first phase of the project.

The most important result obtained during phase 1 of the project has been the finding that high porosity zones within these types of reservoirs may be mappable through the interpretation of certain seismic frequencies. The accurate identification and mapping of this key reservoir property proved crucial to the modeling, which was needed to predict the movement of critical phase CO_2 within the reservoir. Using this technique predictions were made prior to the drilling of two new wells concerning the amount of porosity to be encountered by these wells. These predictions were proved accurate by the drilling results. Additionally, the history matching procedure performed during the reservoir simulation supported the overall porosity distribution within the reef.

The most important phase 2 finding has been the determination that 4D (time lapse) seismic can be used to image the flow of critical phase CO_2 within these reservoirs. Seismic amplitude anomalies were observed within the areas predicted by the reservoir simulation and have a shape and location consistent with the flow of CO_2 within these types of porosity/permeability systems. The location of these amplitude anomalies supports the results of the reservoir simulation which in turn support the major findings in phase 1 of the project.

This study’s successful determination that critical phase CO_2 flow can be imaged within moderate-depthed carbonate reservoirs has broad implications with respect to not only the optimization of enhanced oil recovery projects within these types of reservoirs but also its use with regard to future CO_2 sequestration projects.

5 EXPERIMENTAL

5.1 Existing Data Analysis and 4D Survey Design

In preparation for the acquisition of the Base 3D seismic survey geologic information obtained during the initial development of the field during the 1970s was obtained and loaded into a geophysical workstation. This information was used to develop a preliminary understanding of the field's geology. Figure 10 shows the original structure map based on the results of drilling that took place during the field's initial development.

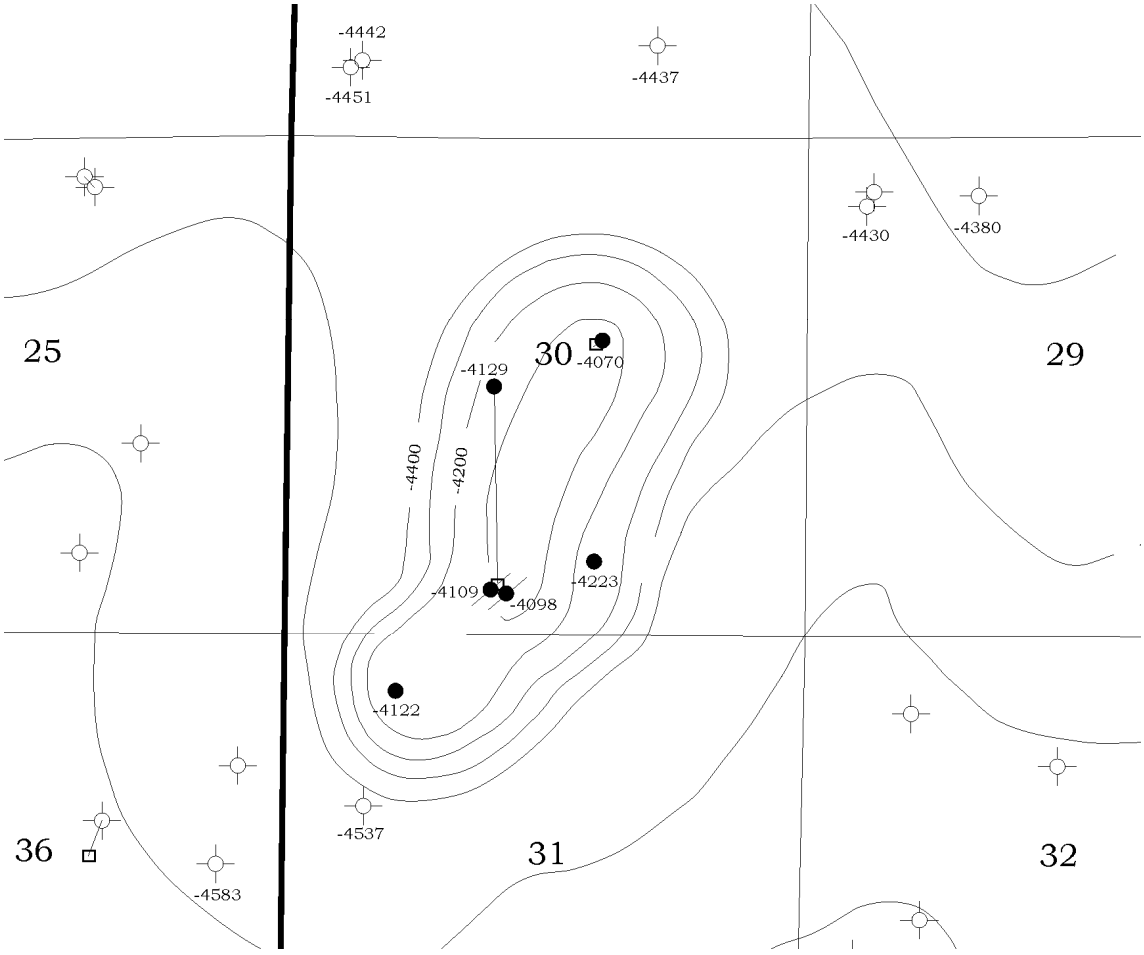

Figure 9: Original structure map of the Top of the Guelph formation based on the results of drilling that took place during the field's initial development.

This map was digitized and loaded into a GeoFrame geophysical project on a UNIX-based workstation. As a result the structure of the Guelph reef was duplicated in the GeoFrame project, see figure 11. Well logs were transmitted to the Schlumberger office in Oklahoma City where they were analyzed and interpreted by a petrophysicist. The results of this analysis were also loaded into the GeoFrame project. These logs were interpreted and used to create a number of correlation sections and cross sections through the reef. One of these, constructed with the porosity logs, is shown in figure 12. These logs were also analyzed to determine the petrophysical / geophysical properties of the various rock units from the shallow, near surface to the Niagaran Gray, the stratigraphic unit directly beneath

the productive interval in the Guelph. Table 1 shows the results of this analysis, which includes the shear-wave velocity which was calculated in AVOLOG.

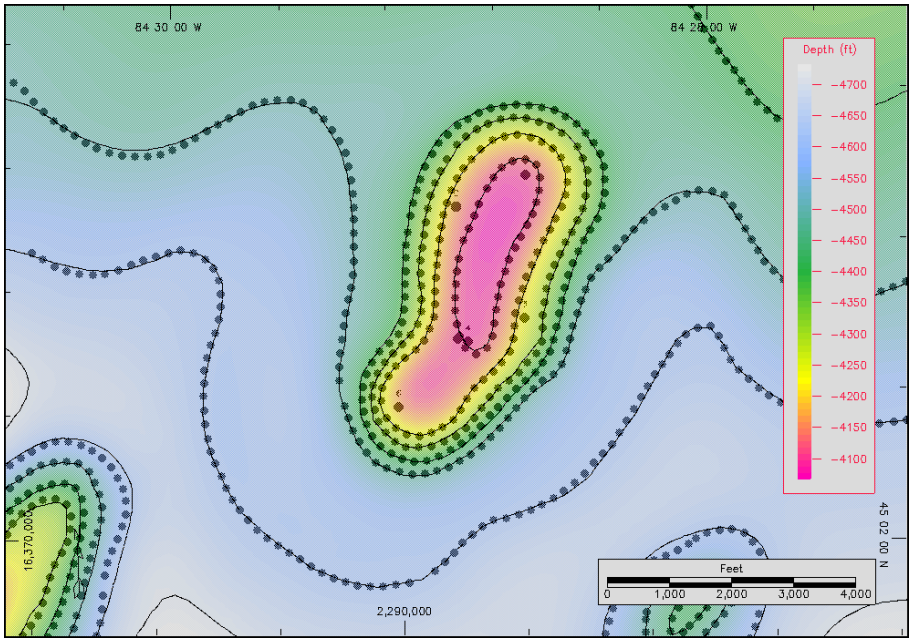

Figure 10: Original structure of the Guelph reef duplicated in the GeoFrame project based on existing data at the start of the project.

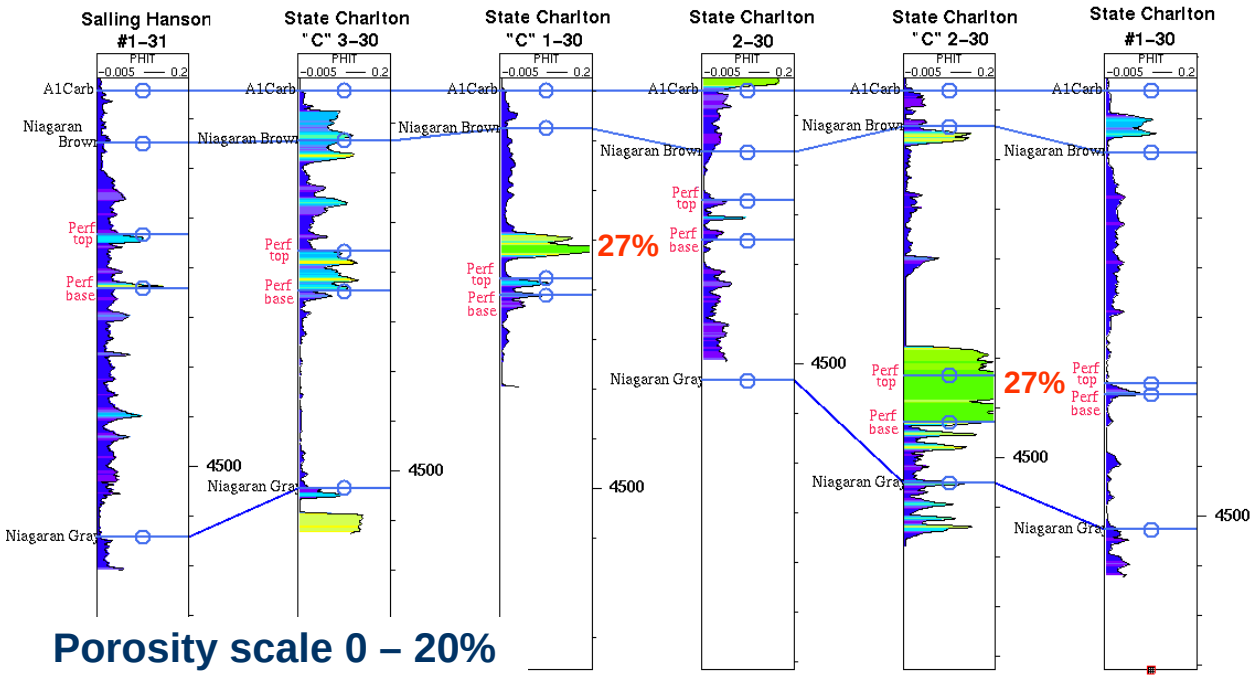

Figure 11: Porosity log correlation section through the Charlton 30/31 reef.

Off Reef / On Reef Rock Property Combination (On Reef Salling Hanson for deep units - Off Reef Black #1-11 Gr and Dtc and Weigandt Rhob for shallow units.)							
	Off / On Reef Avg. GR.	Off / On Reef Avg. P-Vel.	Off / On Reef Avg. S-Vel.		Off / On Reef Avg. rhob		
Antrim Shale	121.6698827	12971.54761	Estimated based on 50.82% of Vp	6592	Estimated based on generalized lithology	2.5	
Traverse Fm	54.22604839	16055.54182		8159		2.7	
Traverse Ls	44.50418227	18697.56389		9502		2.65	
Bell Sh.	110.5512097	10085.87022		5126		2.5	
Dundee	25.20380309	17074.7634		8677		2.7	
Detroit River	14.01371025	17294.4864		8789		2.3	
Base DR Evap	22.83129652	19509.59483		9915		2.8	
Amherstburg Fm	25.07425824	17941.4607		9118		2.8	
Bois Blanc	23.9013271	17063.70587		8672		2.76	
Bass Is.	25.8161321	19876.64786		10112		2.81	
Salina G	47.54819475	17851.37263		8586		2.67	
Salina F	27.6428653	18938.85858		10946		2.02	
Salina F Salt	27.93511549	14547.30427		7849		2.21	
Salina E	24.16752535	14124.51691		7743		2.22	
Salina D	34.52321141	14605.79662		7588		2.44	
Salina C	68.3775549	12257.22044		5329		2.47	
Salina B		1190.00000		6047		2.45	
Salina B Salt	16.69636357	14896.94055		8676		2.14	
A2Carb	24.62978261	20047.98441		8817		2.75	On-Reef Section
A2Evap	20.4262963	20118.85024		9663		2.87	
A1Carb	25.29349057	20090.8257		8735		2.70	
A1Evap	9.7566 / NA	14921.16 / NA		9110.04 /NA		2.06 / NA	
Niagaran Brown	14.385	20020.36071		11525		2.69	On-Reef Section
Niagaran Gray	26.45027523	19478.54679		9448		2.73	

Table 1: An On-Reef / Off-Reef comparison of rock properties.

It should be noted that the A1Evaporite is shown to be in the “Off-Reef” portion of Table 1 because it pinches out on the side of the reef and does not overly it. This is a significant observation as its absence from the crest of the reef places the A1Carbonate with its P-wave velocity of 20,090 feet per second directly on top of the Guelph (Niagaran Brown) with its 20,020 feet per second P-wave velocity. Additionally, the variation in rock density for these two units is very small. This indicates that virtually no acoustic impedance contrast should be expected at the top of the reef form compressional seismic energy.

However, a strong acoustic impedance difference should be seen for S-wave (Shear-wave) energy at this same boundary. The implications are that the top of the Guelph reef

should not be visible to the compression seismic energy but should be very visible in shear energy.

Using the values shown in Table 1 a 12 layer rock property model was constructed in Gemini, a forward seismic modeling program. An exploded view of this model is shown in figure 13.

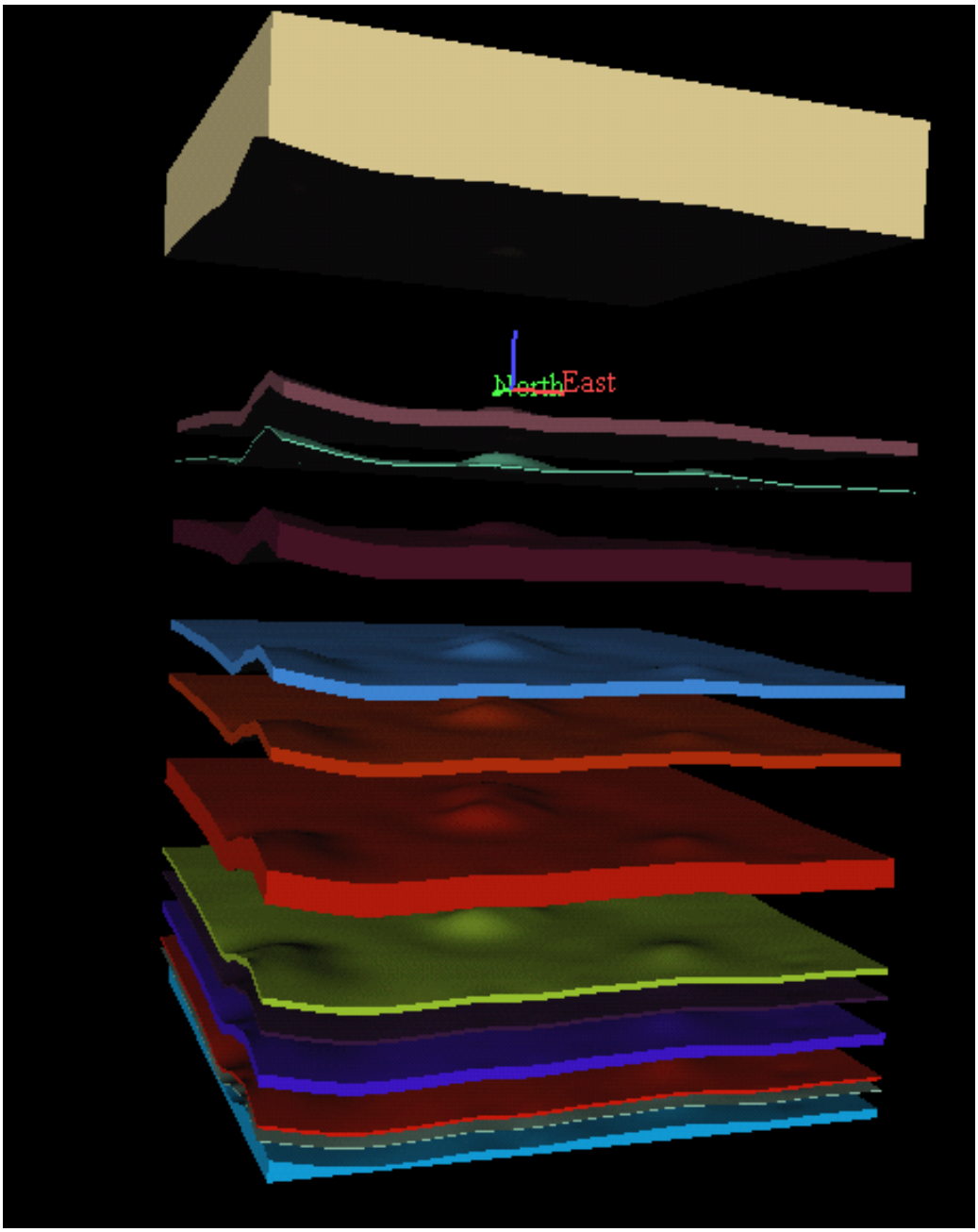

Figure 12: Exploded view of the 12 layer forward model in Gemini constructed using the rock properties shown in Table 1.

Once constructed a number of 3D seismic acquisition geometries were tested using this model. During this process various 3D shot / receiver pairs were ray traced in order to predict various seismic responses from the reef. Figures 14 through 16 show some of the model runs that were tested and the results .

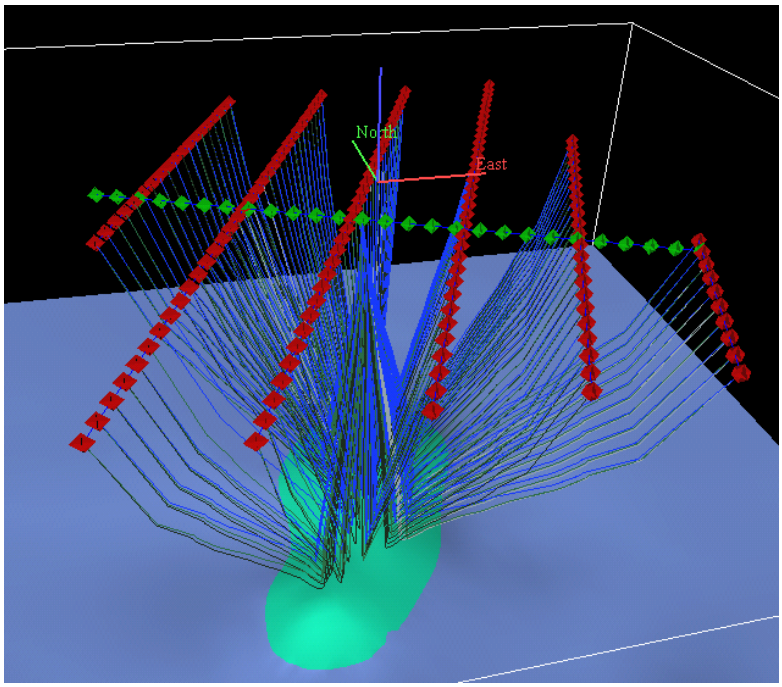

Figure 13: Display from one forward 3D seismic ray-trace model for multiple sources for a single receiver.

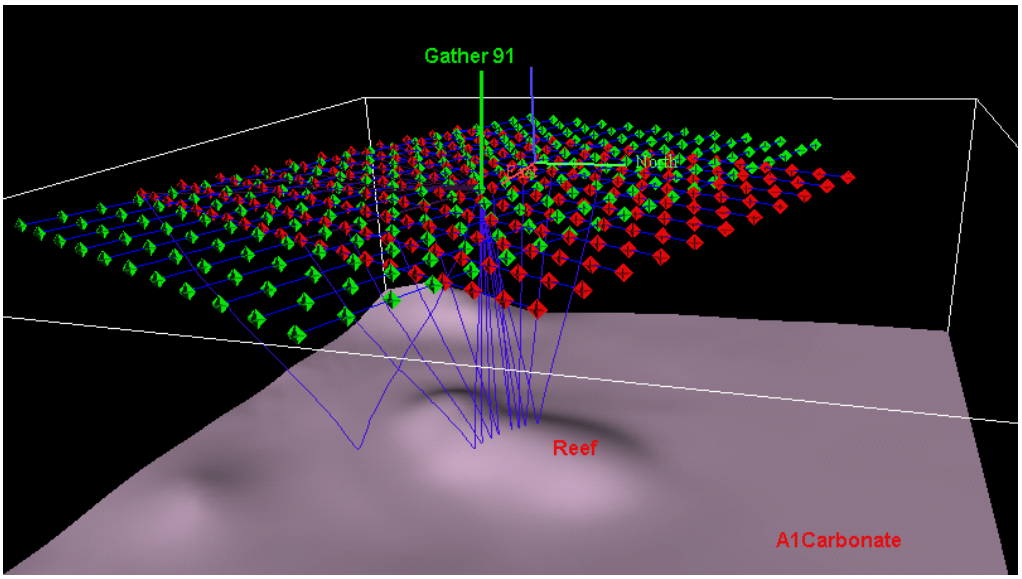

Figure 14: Forward 3D seismic ray-trace model for Gather 91.

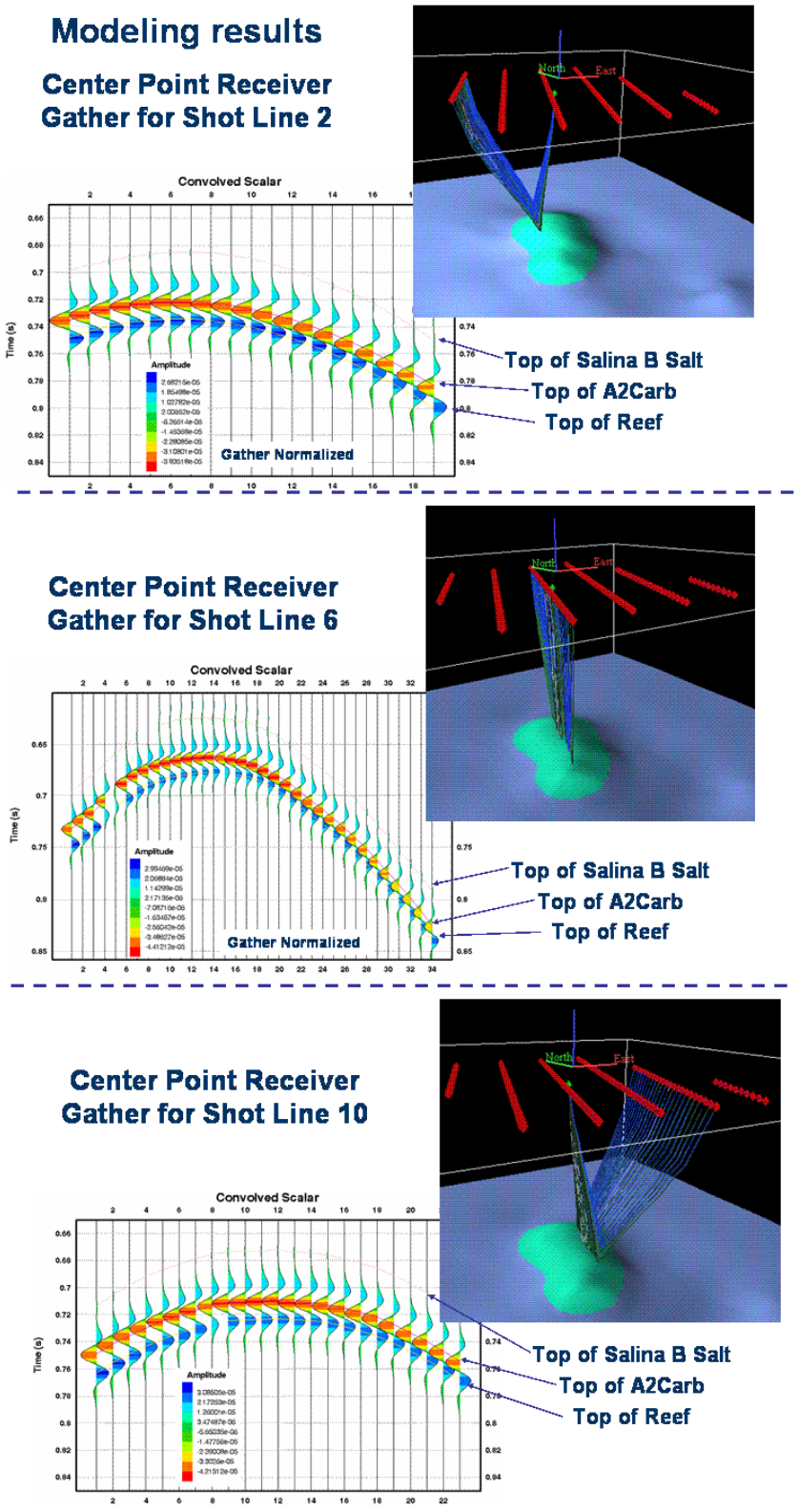

Figure 15: 3D ray trace modeling results showing predicted seismic response at top of reef.

As a result of the modeling the seismic acquisition parameters, which had been originally developed prior to the onset of the DOE project, were altered to ensure the optimum imaging of the reservoir. The final acquisition geometry is shown in Figure 17.

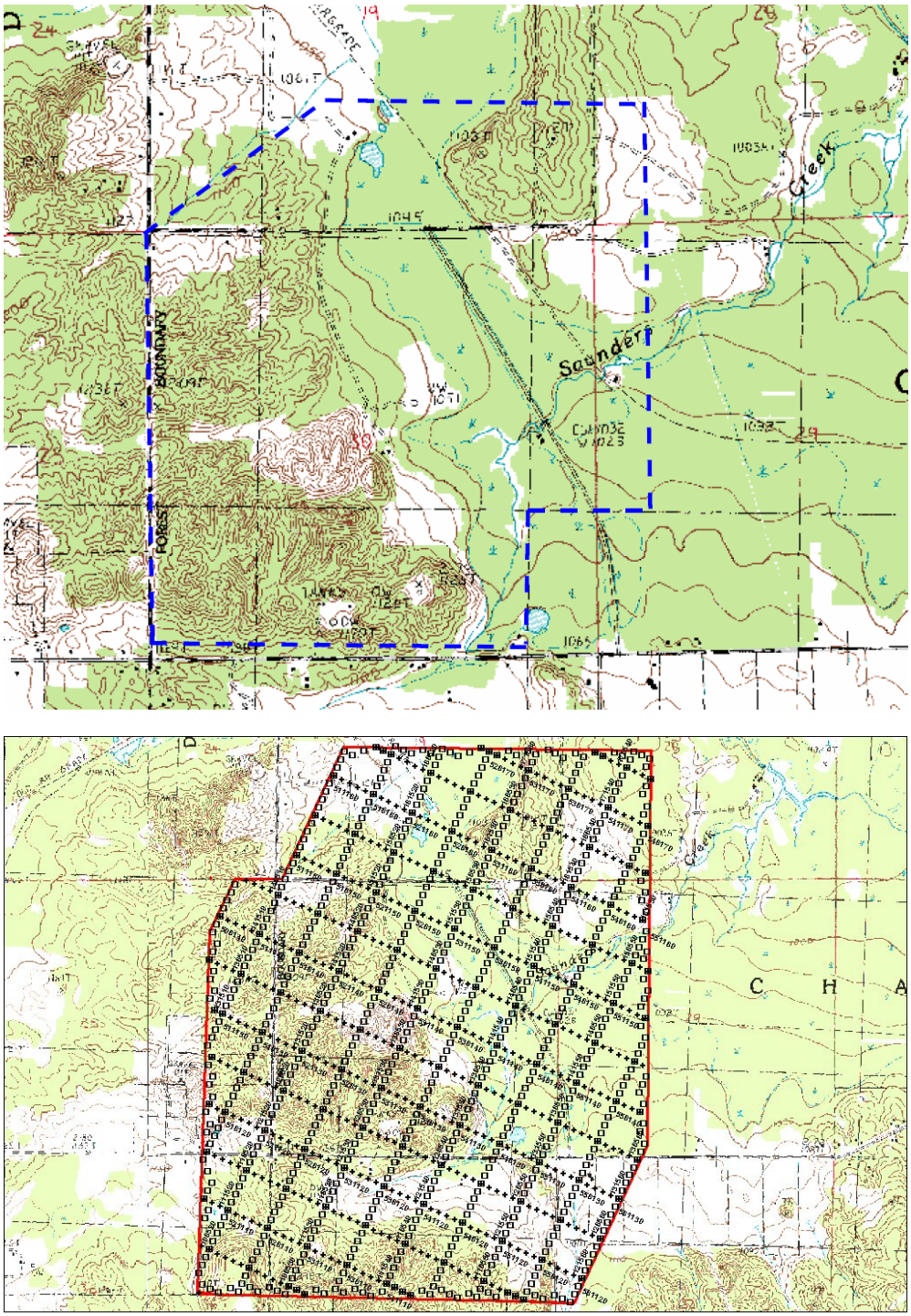

Figure 16: Topography and Final acquisition geometry of the Base 3D survey for the Charlton 30/31 field area.

5.2 Base 3D Survey Acquisition and Processing

The “Base” 3D survey was obtained in March of 2004 and covered 2.5 square miles. This survey was acquired by Great Lakes Geophysical. The resulting bin spacing was 82.5 by 82.5 foot. Five pounds of dynamite supplied the energy source and the resulting processed volume had a sample rate of 1 millisecond. During the acquisition a number of acquisition exclusion zones were encountered. These are not uncommon when acquiring seismic data and are generally compensated for by adding shot/receiver pairs in other locations and through the processing of the data. These exclusion zones are shown in Figure 18.

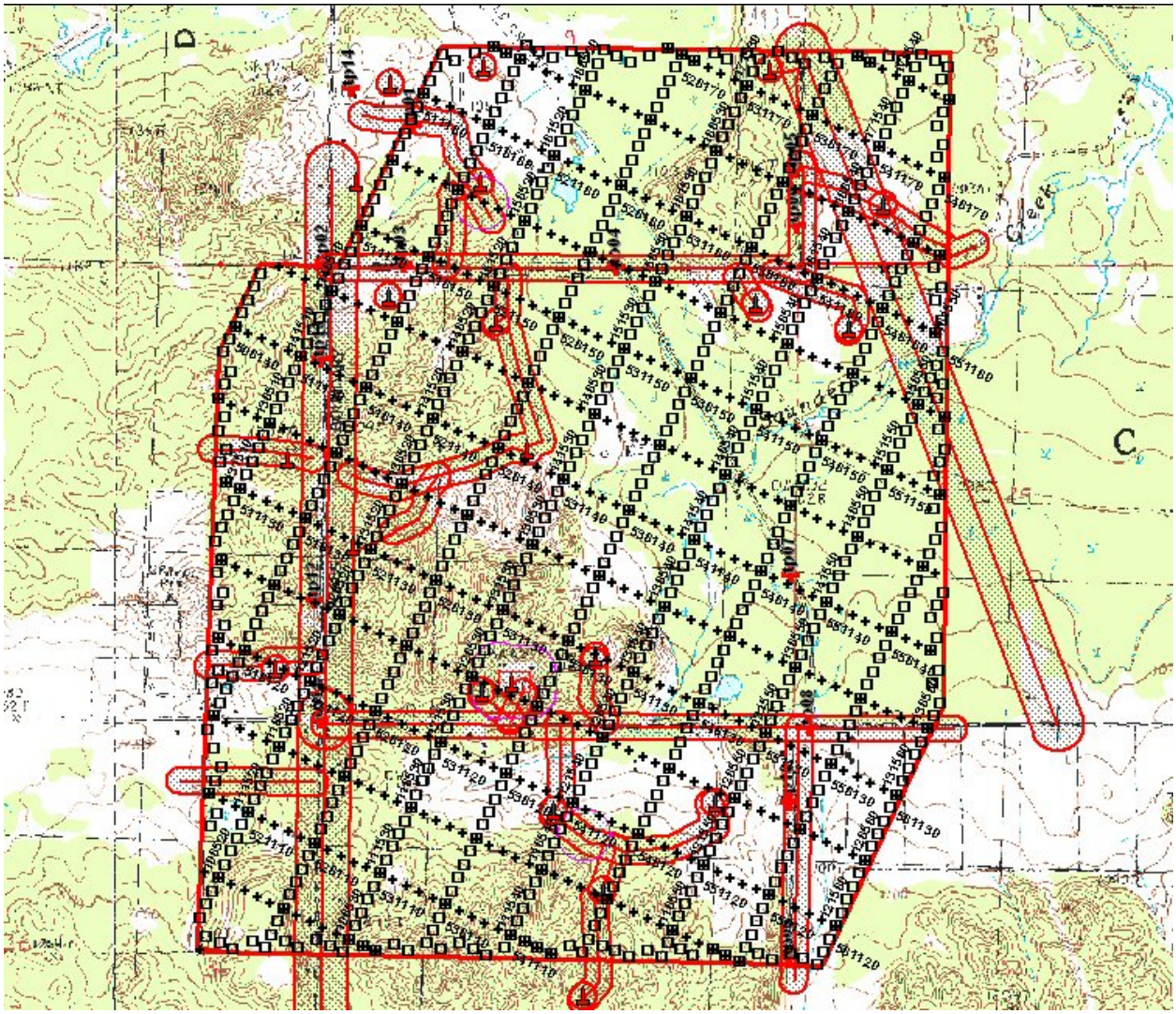

Figure 17: Acquisition exclusion zones for the Base 3D seismic survey.

Once the acquisition of the Base 3D seismic survey was completed, the raw seismic data was processed by two different processing companies. This was done to insure that any data artifacts that may have resulted from a particular company’s processing sequence would be noted and resolved prior to the interpretation of the volume. Such processing

induced artifacts may have resulted in false positives being interpreted when examining the 4D survey and incorrectly relating these to movement of the CO_2 within the reef.

The general processing sequence preformed on the Base 3D survey is as follows;

1. **Reformat SEGD to Internal Format**
2. **Spherical Divergence Correction**
3. **Trace Edits**
4. **Refraction Analysis**
5. **3D Geometry QC and Correction of Positioning of Source/Receiver**
6. **Elevation/Refraction Static Application**
7. **3D Surface Consistent Deconvolution**
8. **Zero Phase Spectral Whitening**
9. **3D CDP Sort**
10. **Velocity Analysis**
11. **3D Surface Consistent Auto Statics**
12. **Velocity Analysis**
13. **3D Surface Consistent Auto Statics**
14. **Noise Reduction as necessary**
15. **CDP Statics**
16. **3D CDP Stack**
17. **Post Stack Filter/Scaling/Decon or Whitening Application**
18. **Post Stack 3D Signal Enhancement -FXY Prediction Filter**
19. **Final Structural output**
20. **Post Stack 3D Finite Difference Migration**
21. **Post Migration 3D Signal Enhancement - FXY Prediction Filter (if necessary)**
22. **Migration output to SEGY**
23. **Targeted PSTM to Residual Velocity Field**
24. **Kirchoff Pre-Stack Time Migration (PSTM)**
25. **Residual Velocites**
26. **Pre-Stack Time Migration Stack output to SEGY**

In addition to the basic processing sequence described above one processing company, WesternGeco, was requested to perform advanced, azimuthal velocity analysis and processing on the Base 3D survey. As a result of this advanced processing techniques, four azimuth-limited volumes were developed. These were developed on 45 degree angular swaths corresponding to the following azimuths

- 2.5 to 47.5 degrees (with the reciprocal 182.5 to 227.5 degrees),
- 47.5 to 92.5 degrees (reciprocal 227.5 to 272.5 degrees),
- 92.5 to 137.5 degrees (reciprocal 272.5 to 317.5 degrees) and
- 137.5 to 182.5 degrees (reciprocal 317.5 to 360.0, 0.0 to 2.5 degrees).

All volumes were developed on a pre-stack migration.

5.3 Base Survey Interpretation and Porosity Mapping

5.3.1 Wavelet and Frequency Analysis and Well-to-Seismic Ties

A number of geophysical analyses were performed on the resulting Base 3D seismic data set. Wavelet analysis was conducted in a number of locations within the volume in the vicinity of those wells that had acquired sonic logs. A deterministic method was used for this wavelet extraction which includes the reflection coefficients (RC) calculated from the well log data. This method of crosscorrelation between the seismic data and the RC series results in a highly accurate determination of the wavelet at the well location. The extracted wavelets were combined with the log data to produce good quality well to seismic ties. For this analysis both a long and short seismic time window was used for the extraction of the wavelet. Figure 19 shows a screen capture of Plate 1 that documents the results of the short windowed wavelet extraction.

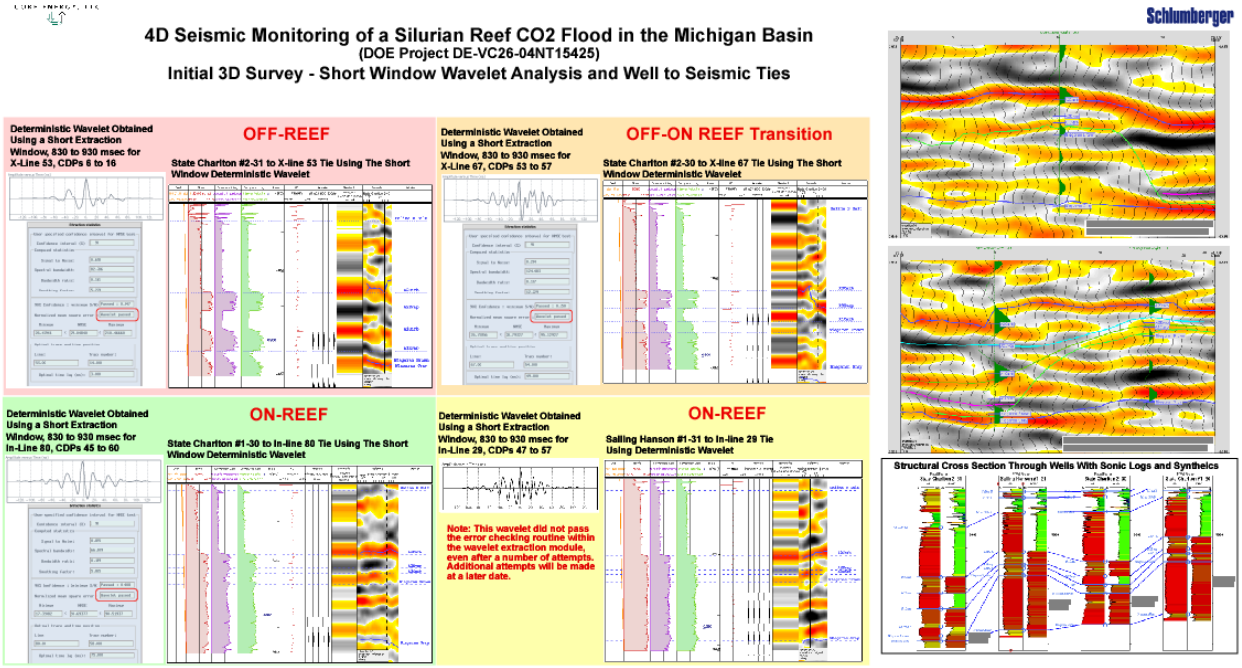

Figure 18: Screen capture of Plate 1 illustrating the results of the short windowed wavelet extraction.

In this display a number of wavelets were extracted from the Base seismic volume, used in the development of synthetic seismograms which, in turn, were used for the well-to-seismic ties. Figure 20 shows the short windowed wavelet extracted from cross line 67 over a window from 830 to 930 msec in the vicinity of the State Charlton 2-30 well. This wavelet is clearly minimum phase, as expected for the type of survey acquired. The synthetic seismogram that was generated with this wavelet is also shown in this same figure.

Figure 21 shows the well to seismic tie developed with this synthetic. In this display the seismic is displayed in the red-yellow-white-gray-black color map where red is a strong positive (or peak) value and the black is a strong negative (or trough) value. The synthetic is shown in green as a traditional wiggle trace. This tie was judged to be “fair” in quality.

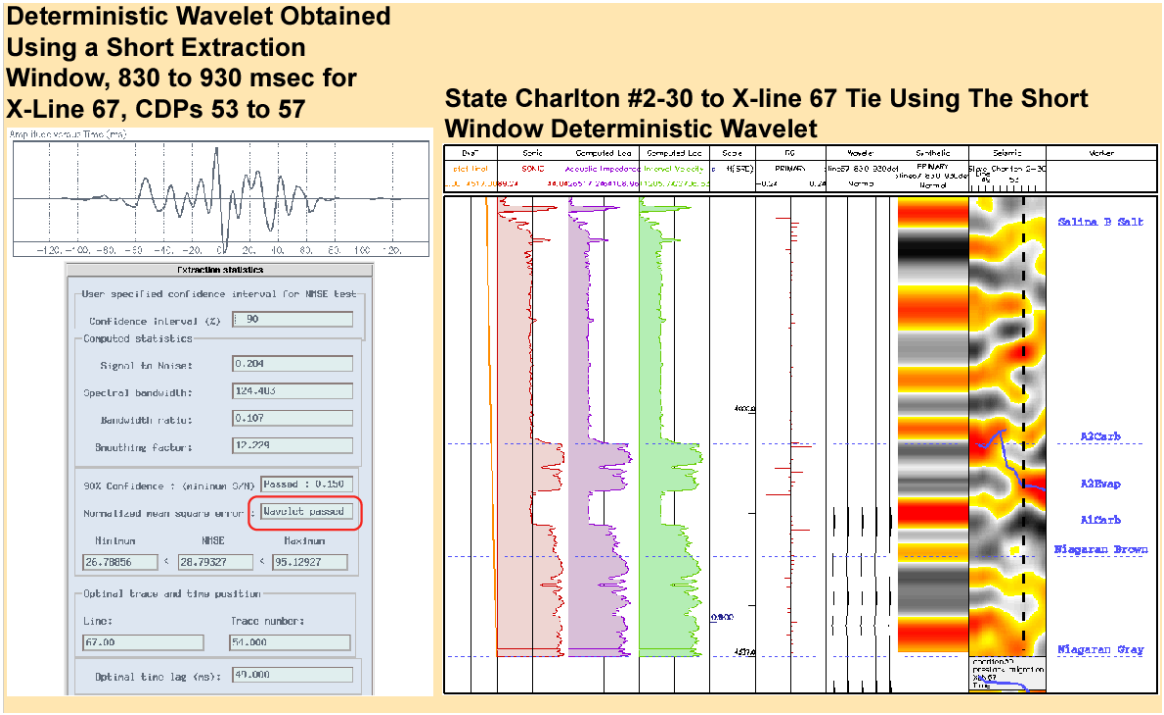

Figure 19: The short windowed wavelet extracted from the vicinity of the State Charlton 2-30 well.

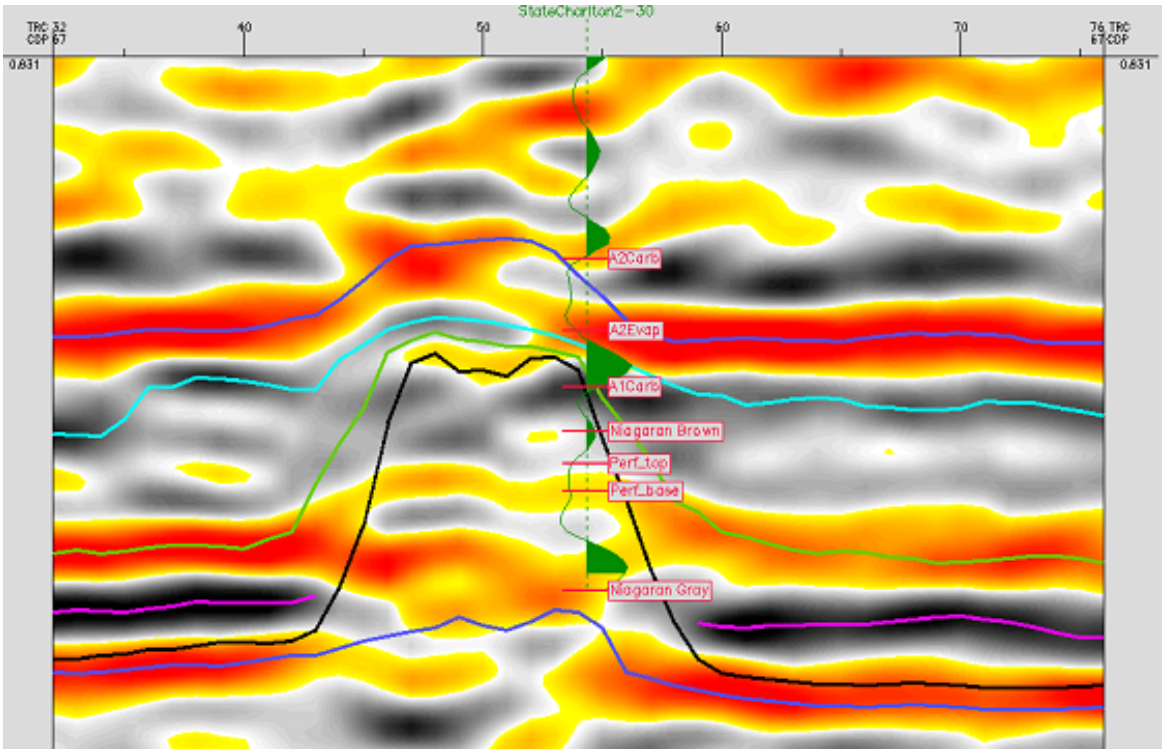

Figure 20: Well to seismic tie developed with the short windowed extracted wavelet for the State Charlton #2-30 well

Figures 22 and 23 show the same information as in figures 20 and 21, but for the State Charlton 1-30 well and its well-to-seismic tie on in-line 80. This tie was judged to be of “excellent” quality.

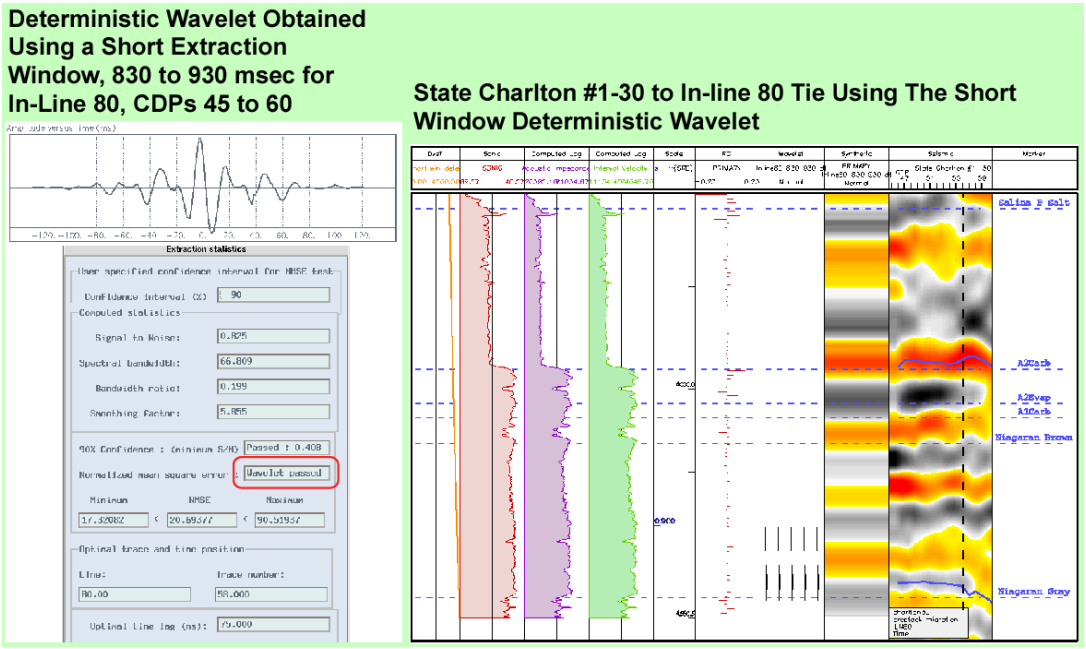

Figure 21**:** The short windowed wavelet extracted from the vicinity of the State Charlton 2-30 well and the synthetic seismogram developed using this wavelet.

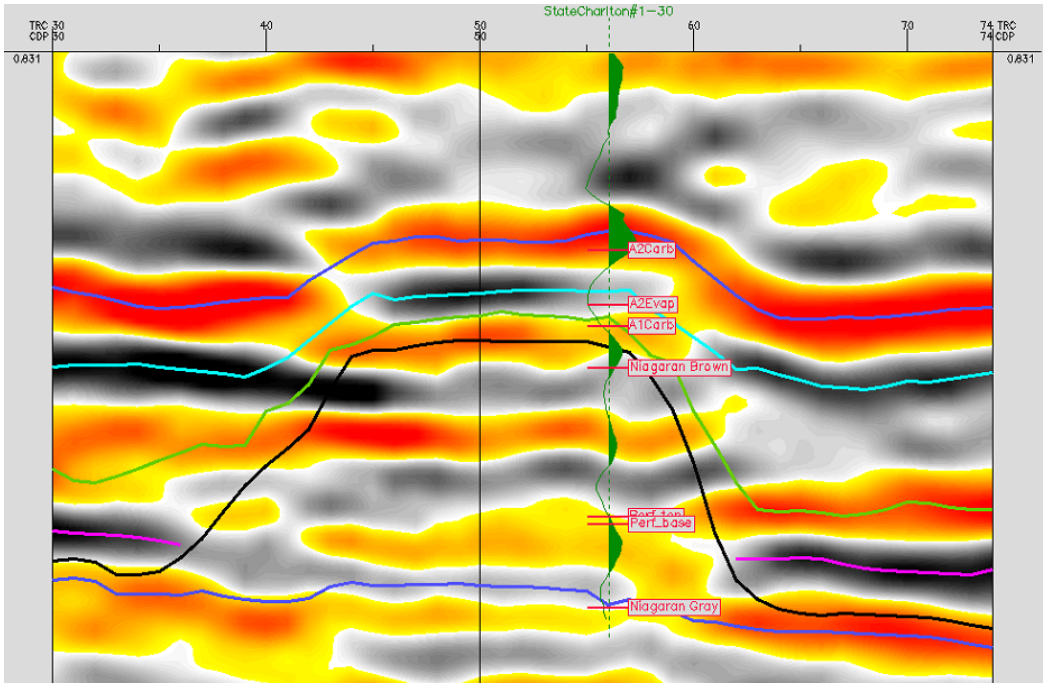

Figure 22: Well to seismic tie developed with the short windowed extracted wavelet for the State Charlton #1-30 well

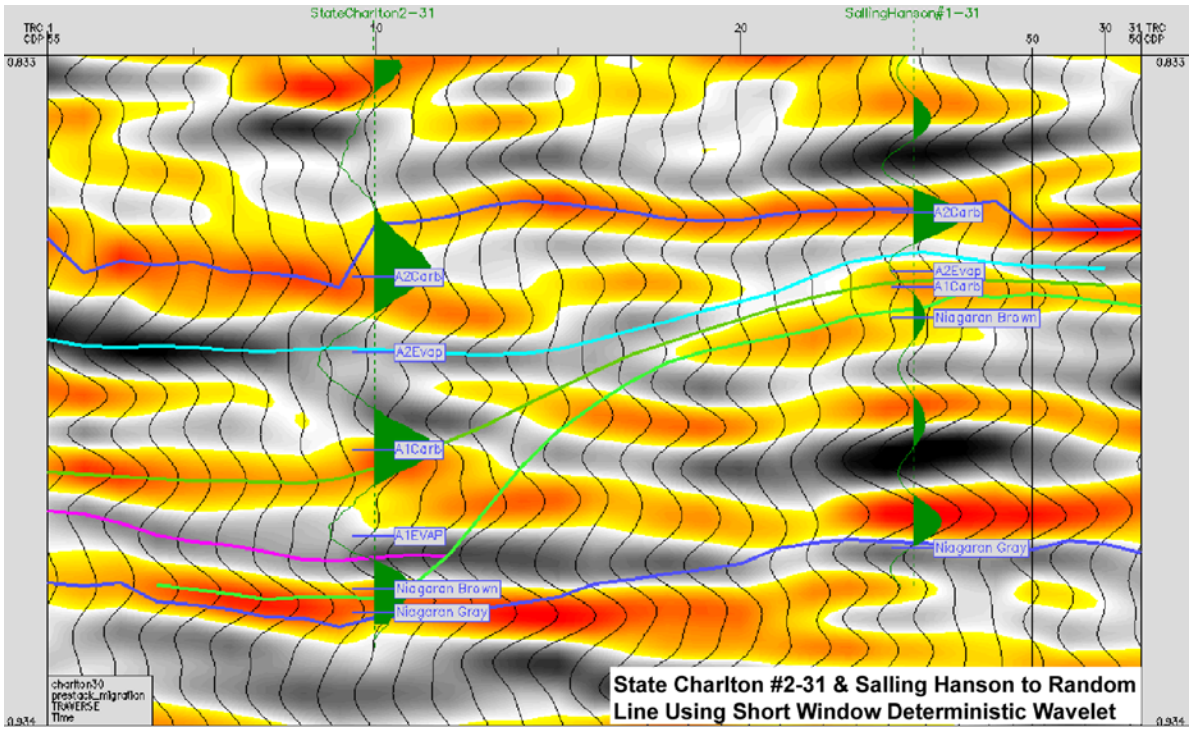

Figure 23: Well-to-seismic tie along a random line developed with the short windowed extracted wavelet for the State Charlton #2-31 well and the Salling Hanson #1-31 well.

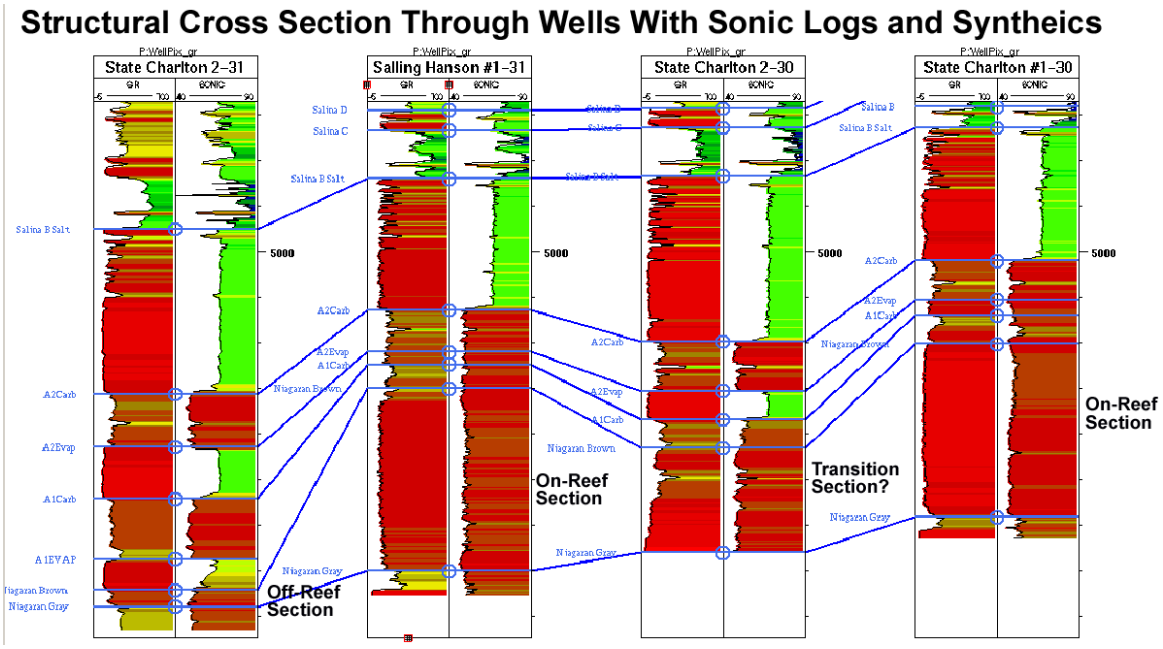

Figure 24: Correlation section showing all wells with sonic logs. These wells were use it the construction

Two well-to-seismic ties were generated, one for the State Charlton #2-31 well (an off-reef well) and another for the Salling Hansen #1-31 well (an on-reef well). Both of these wells are located in the southern part of the seismic survey. Figure 24 shows a random line that runs through both wells, and the resulting well-to-seismic ties. Both of these ties are judged to be “good” to “very good” in quality. This display helps to illustrate the change in seismic character that was used to identify and map the reef.

In nearly all of the synthetics the top of the A2-Carbonate is the strongest peak event immediately above the top of the reef. This observation was to prove instrumental later in the study when the 4D analysis was conducted. In the Salling Hansen #1-31 well three peak seismic events occur between the A2-Carbonate peak event and the reef’s base, the Niagaran Gray, which is a positive to negative zero-crossing at this location. In the State Charlton #2-31 well, the only off-reef well with a sonic log and hence the only off-reef well for which a synthetic could be developed, only two peak events occur between the A2-Carbonate and the Niagaran Gray, also a positive to negative zero-crossing.

This change in seismic character, from three peaks on-reef to two peaks off-reef, proved to be consistent across the study area. The well-to-seismic tie for the State Charlton #1-30 in the northern portion of the field also exhibits this same on-reef seismic character. This change was used to distinguish the on and off-reef portions of the Niagaran Brown (Guelph) reef was identified and mapped within the Base 3D survey.

This same well-to-seismic tie analysis was performed using wavelets extracted over a much longer time window, 700 msec. Figure 26 shows a screen capture of Plate 2 which documents the results of the long windowed wavelet extraction. The well-to-seismic ties that were generated from this analysis did not tie as well to the seismic data as those generated using the wavelets extracted over the shorter time window.

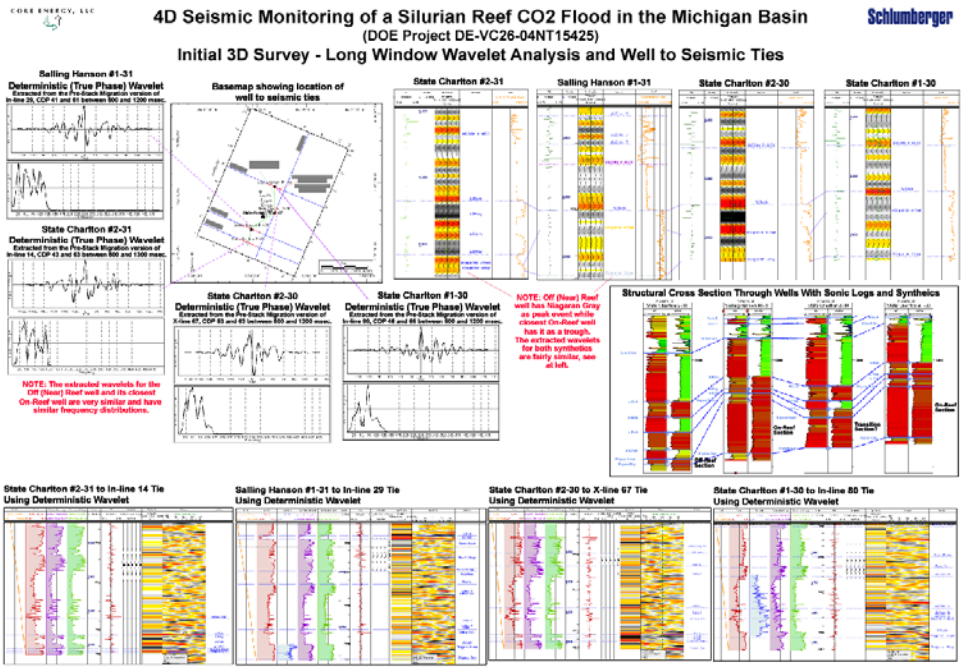

Figure 25: Screen capture of Plate 2 illustrating the results of the long windowed wavelet extraction.

In addition to the wavelet analysis a frequency analysis was also conducted. Figure 27 shows the frequency content of the seismic in the vicinity of each well-to-seismic tie as extracted during the long window wavelet analysis. The range of frequencies in the data shown in figure 27 is fairly consistent at approximately 10 to 120 hz.

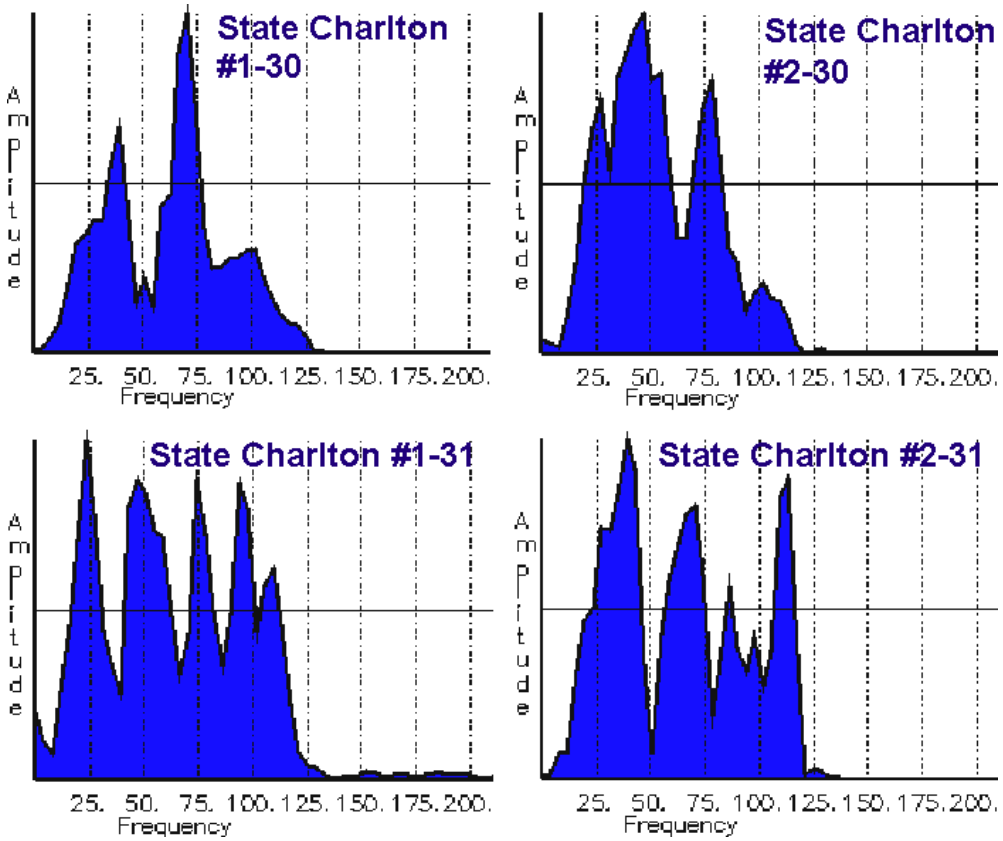

Figure 26: Frequency content graphs for each well-to-seismic tie created using wavelets extracted using long time windows.

5.3.2 Blended Seismic Attribute Analysis and Time, Velocity and Depth Mapping

Using the well-to-seismic ties the top and base of the reef and various horizons immediately above the reef were identified and interpreted. In addition to the well-to-seismic ties blended seismic attributes were developed in order to aid with this interpretation. Specifically, seismic variance and amplitude were found to be of value with this task.

Seismic variance is a measurement of how rapidly the seismic data is changing. The higher the variance attribute that higher the rate of change. This attribute is often employed in order to identify locations in 3D seismic volumes where rapid structural changes are occurring, such as at a fault, or where changes in stratigraphy are occurring, such as a channel edge.

Seismic variance was extracted from the Base 3D survey using a 100 msec. time window and a 3 by 3 trace setting. Next the high portion of the variance values were blended with the high peak amplitude values for the volume and then displayed and interpreted using GeoViz, a 3D visualization and interpretation program. The edges on the reef were clearly visible with this method. Figure 28 shows a time slab from 855 to 860 milliseconds. The edge of the reef is clearly visible in the high variance shown in blue. High peak amplitudes are shown red-orange. Using these blended attribute displays greatly aided the identification and interpretation of the reef and led to a more detailed interpretation in a shorter amount of time.

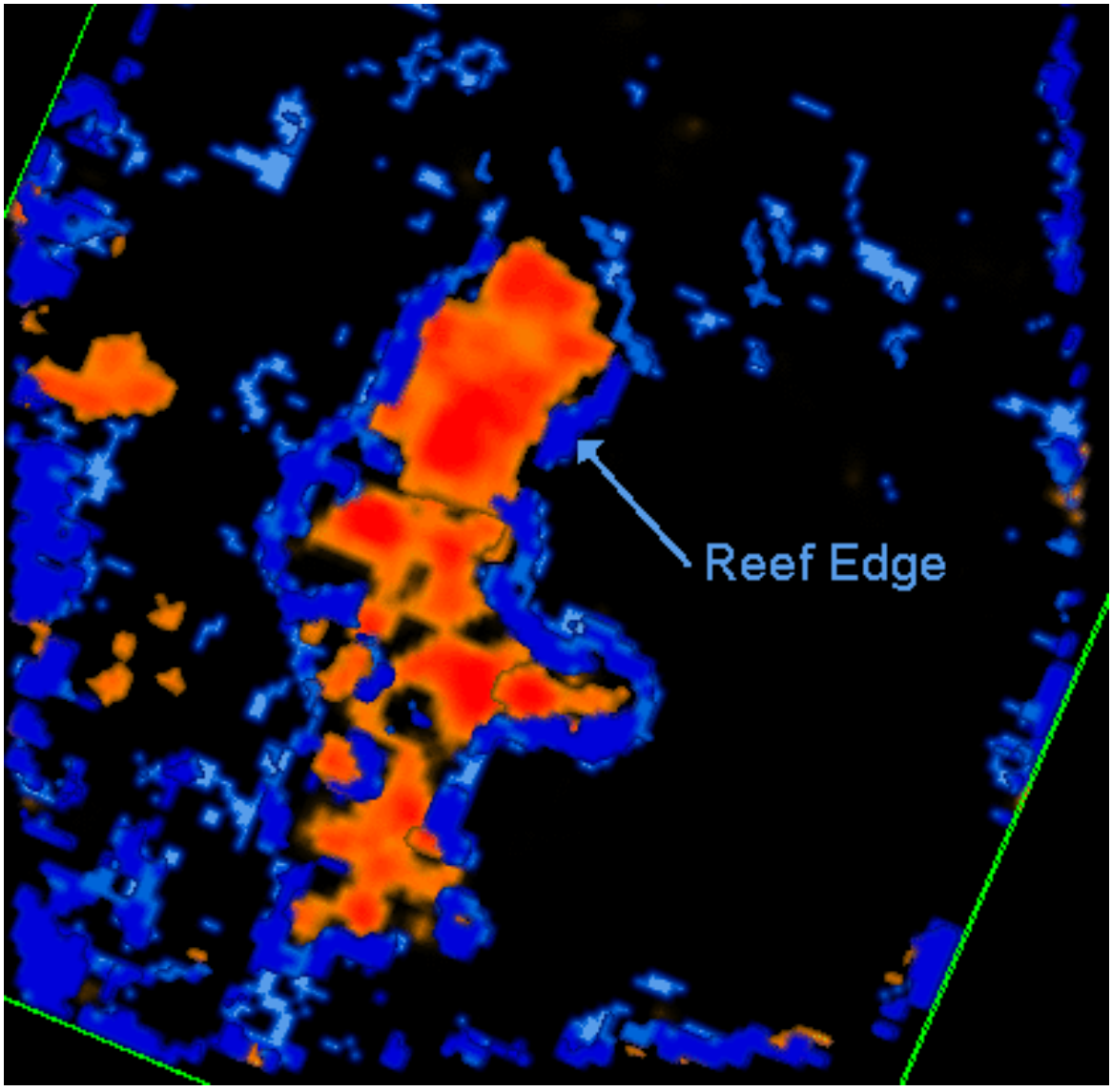

Figure 27: Blended seismic attribute time slab 855 to 860 msec. – high variance (in blue) and high amplitude (red-orange).

Additional blended attribute displays are shown in Appendix D.

A seismic time map was produced from the interpretation based on the blended attribute analysis and the well-to-seismic ties. This map is included at the back of the report as Plate 3. A screen capture of this plate is shown in Figure 29.

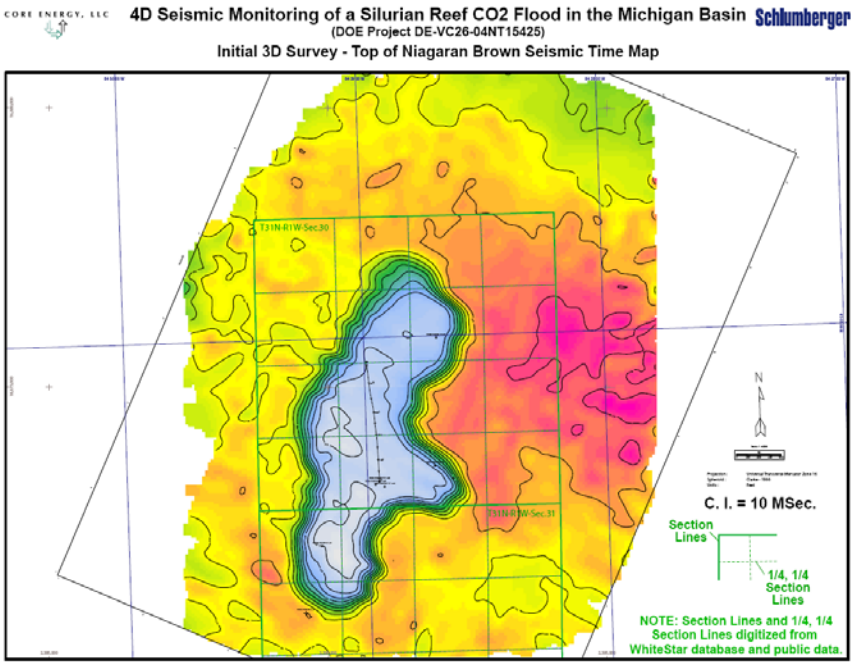

Figure 28: Screen capture of Plate 3 - Seismic time map based on interpretation guided by the well-to-seismic ties.

In addition to helping relate specific seismic events to the various formations in the study area the well-to-seismic ties also helped to establish the seismic velocity field for these same horizons. Figure 30 is a screen capture of the Apparent Velocity Map for the Top of Niagaran Brown formation (which includes the Guelph reef). This is provided at the back of the report as Plate 4.

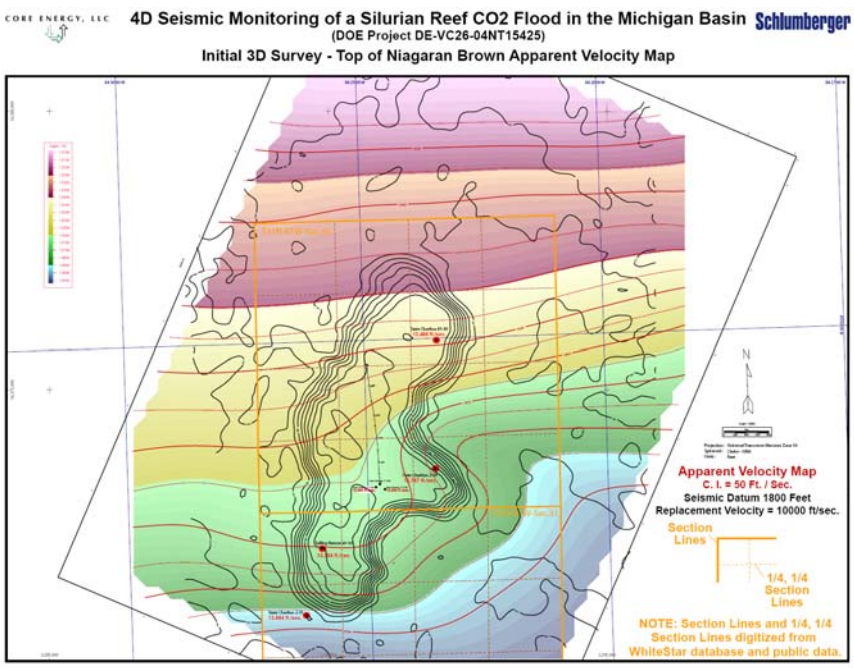

Figure 29: Screen capture of plate 4 - Apparent Velocity Map for the Top of the Niagaran Brown formation.

Once the time and velocity maps were developed they were combined to produce preliminary depth maps for the top and base of the reservoir and the overlaying A1 Carbonate. This map is included at the back of this report as Plate 5, a screen capture of this is shown in Figure 31.

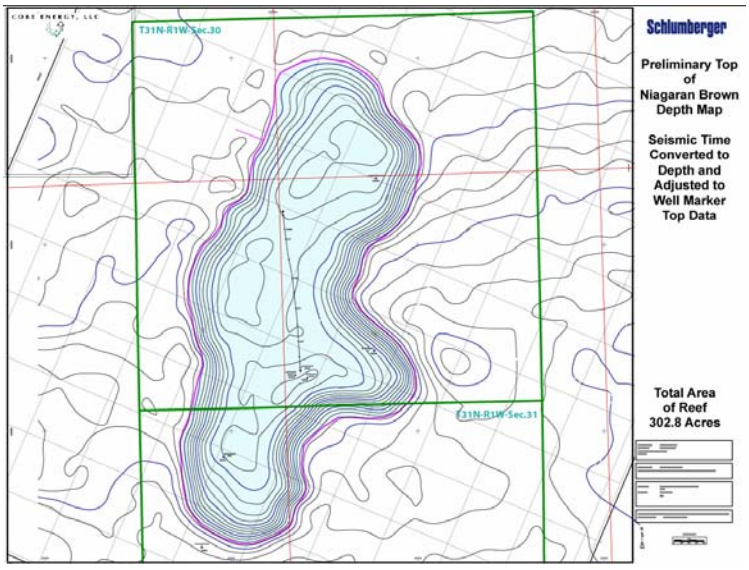

Figure 30: Screen capture of Plate 5, a preliminary depth map of the Top of Niagaran Brown (Guelph) Formation.

All available time, velocity and well to seismic tie information was reviewed again in order to quality control the preliminary depth maps. Finalized versions of all structure maps were then generated. Figure 32 shows the finalized depth map generated for the top of the Guelph (formerly known as the Niagaran Brown) Formation using the Base 3-D survey and all wells available when the Base 3-D was acquired.

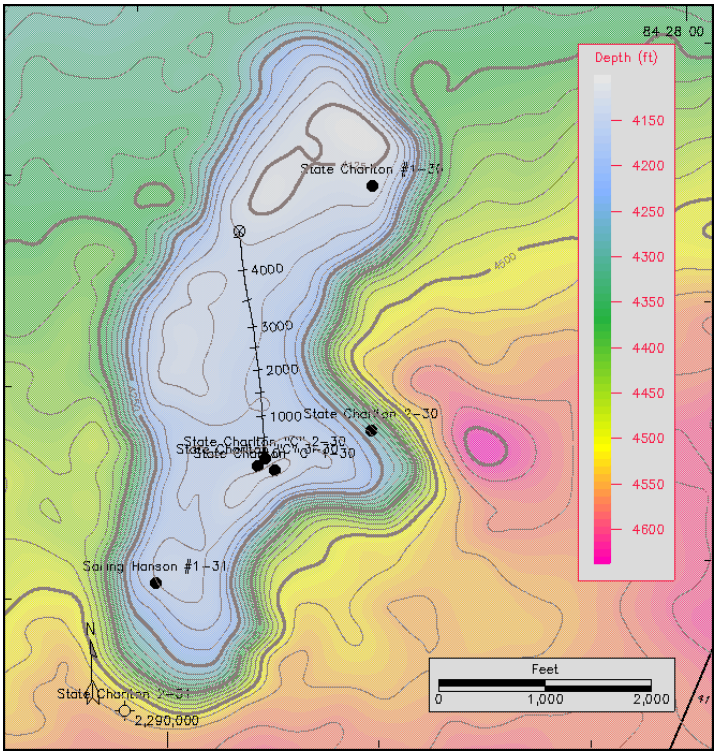

Figure 31: Finalized depth map of the Top of Niagaran Brown Formation, Charlton 30/31 Field

5.3.3 Porosity Detection and Distribution Mapping

Once the basic structure of the reef was identified and mapped the investigation into the internal stratigraphy of the reef could begin. Seismic attribute analyses were again performed on the Base 3-D volume to help identify internal stratigraphy. A number of different attributes were extracted from the volumes and examined. These attributes were compared to the porosity measurements obtained with the well log data.

Initially, time slices through the seismic volume at 2 ms intervals were converted to depth using velocities established during the well-to-seismic ties. Log porosity values were averaged within the interval bounded by these 2 ms depthed time slices. Figure 33 shows a correlation section through various wells in the field and displays the porosity log as recorded in track 1 and then blocked on the 2 msec intervals in track 2.

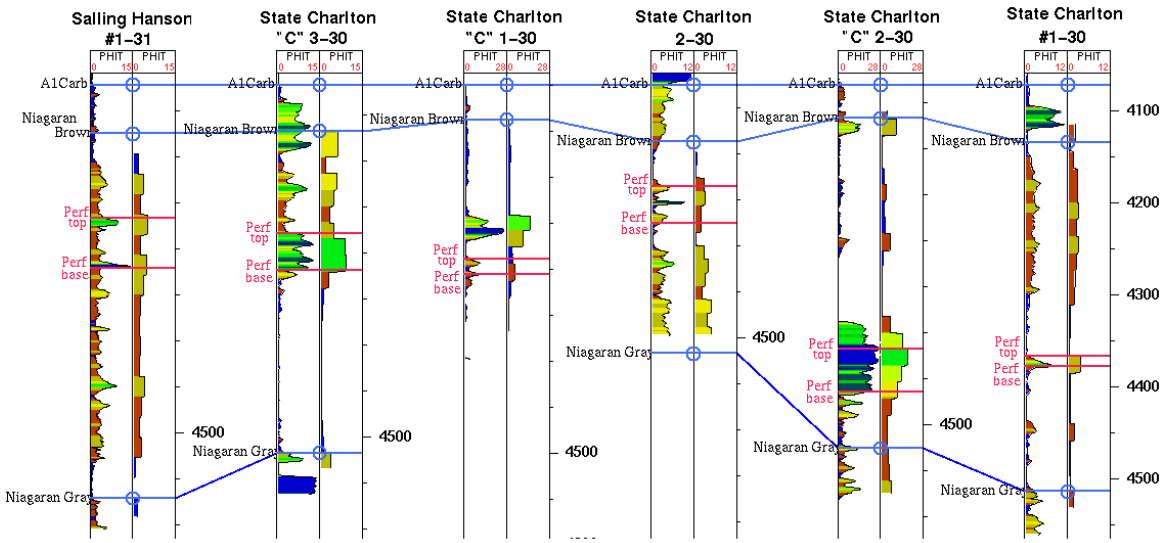

Figure 32: Original porosity logs and the averaged porosity values blocked 2 msec time intervals that were adjusted to depth.

These averaged porosity log values were then compared with each of the seismic attributes that had been extracted from the seismic volume along the well bore locations. This analysis suggested a correlation between instantaneous frequency and porosity values greater than 5%. This relationship is not well-defined but thought to be usable when characterizing the reef. Graph #1 illustrates this relationship for all data pairs within the reef. A "shotgun pattern" exists for all porosity values less than 5%, indicating that all frequencies, high and low, are being returned by the lower porosity portion of the reservoir. However, a potential correlation can be seen for values above 5%. The porosity / frequency pairs suggesting this relationship have been designated in red on Graph #1.

The discovery of this relationship, if confirmed, could have a significant impact on the characterization of this reef and, potentially many others in this trend. To further this investigation a number of instantaneous frequency volumes were generated from the Base 3D survey using various parameter settings and then compared to the well data. Figures 34, 35 and 36 show lines through one of these instantaneous frequency volume at the same locations as those shown for the well-to-seismic ties in the previous section. In these displays lower frequency is indicated by the lightest blue.

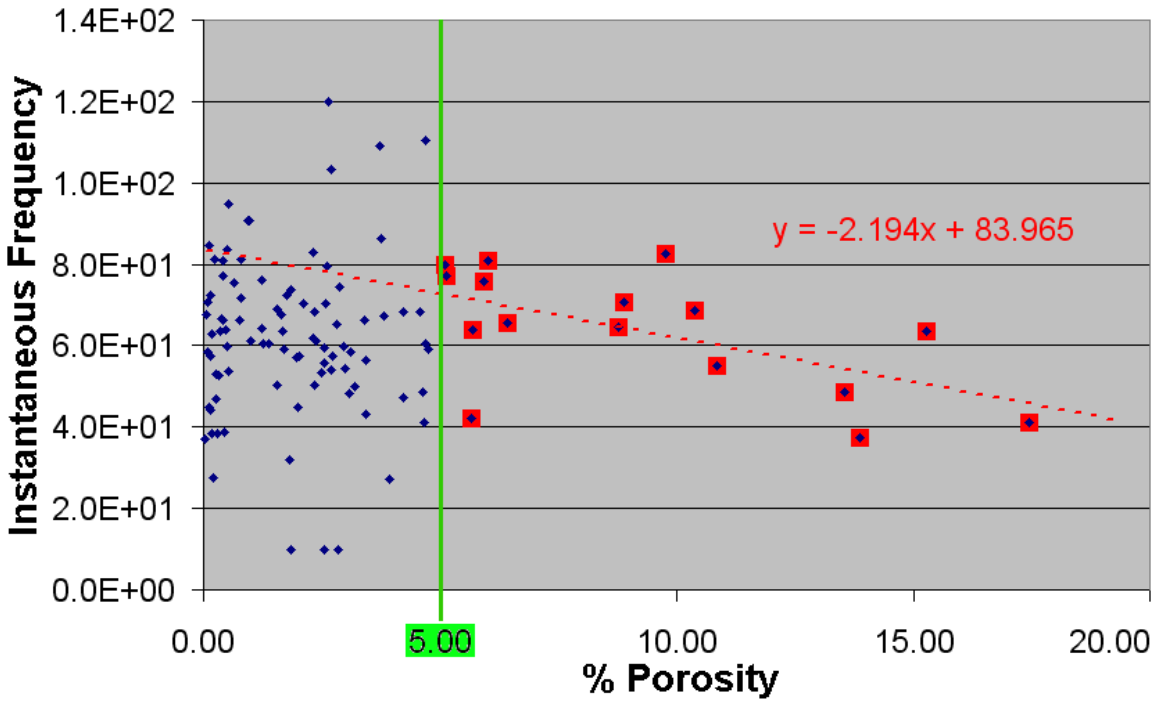

Graph 1: Blocked log porosity values within reef for all wells versus instantaneous frequency values for 2 msec time slices.

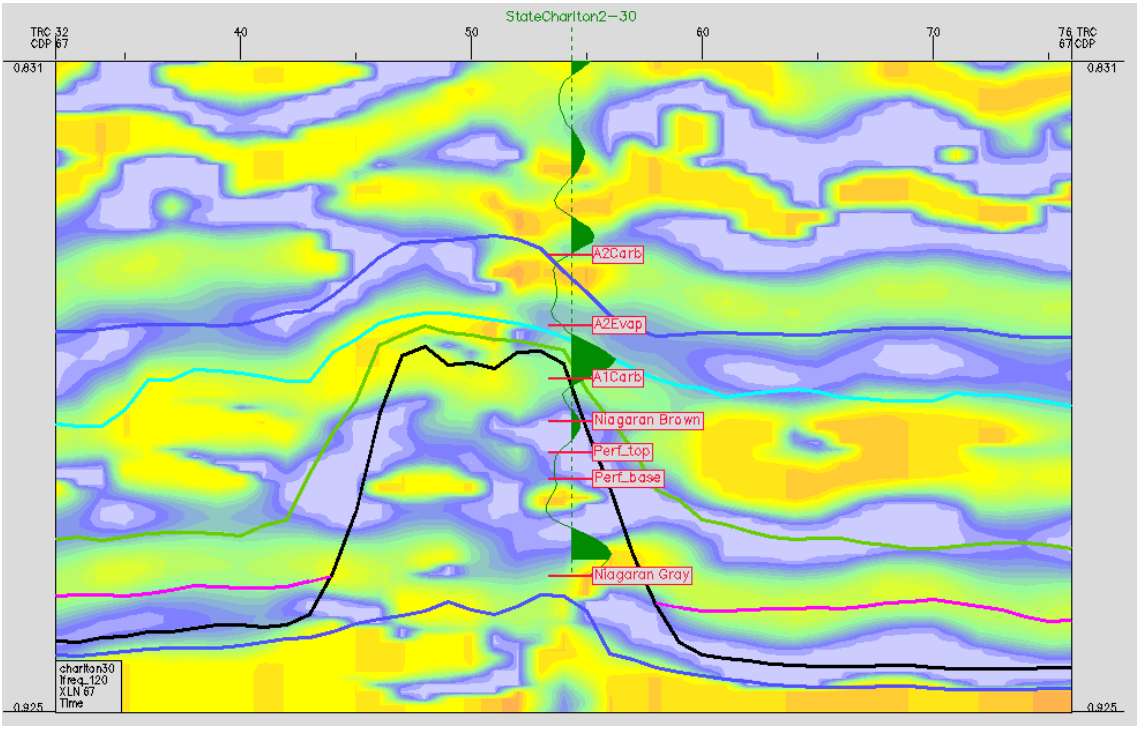

Figure 33: Instantaneous frequency display for the same line shown in Figure 21.

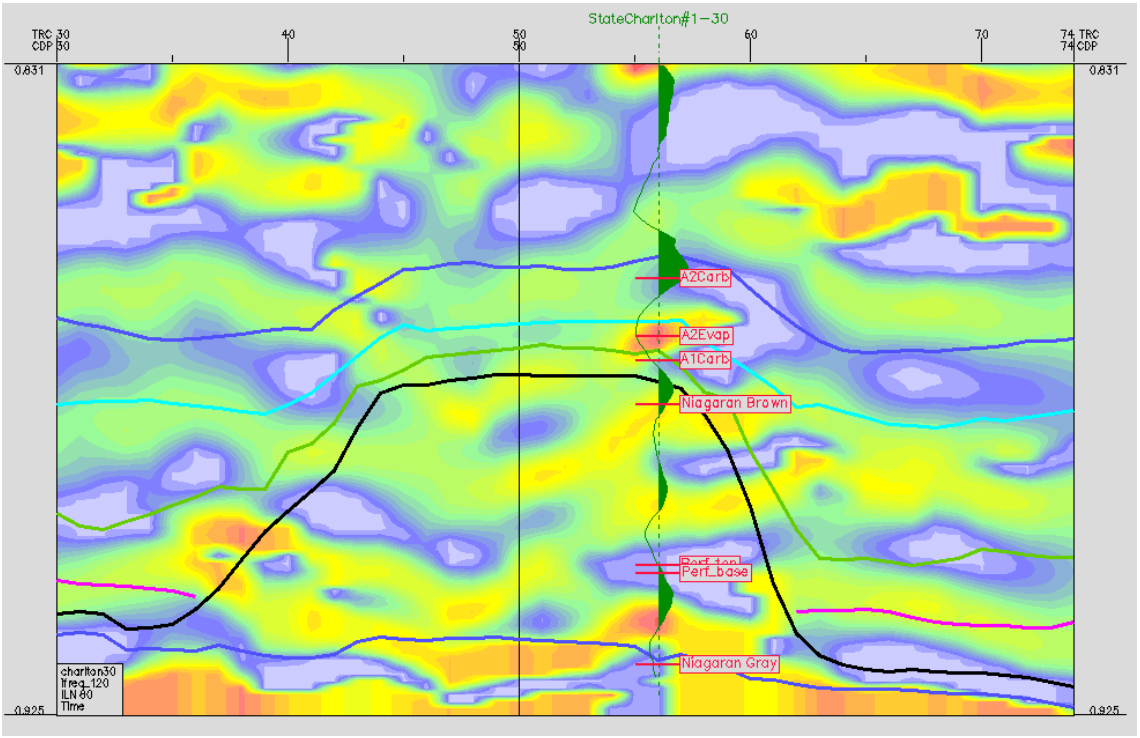

Figure 34: Instantaneous frequency display for the same line shown in Figure 23.

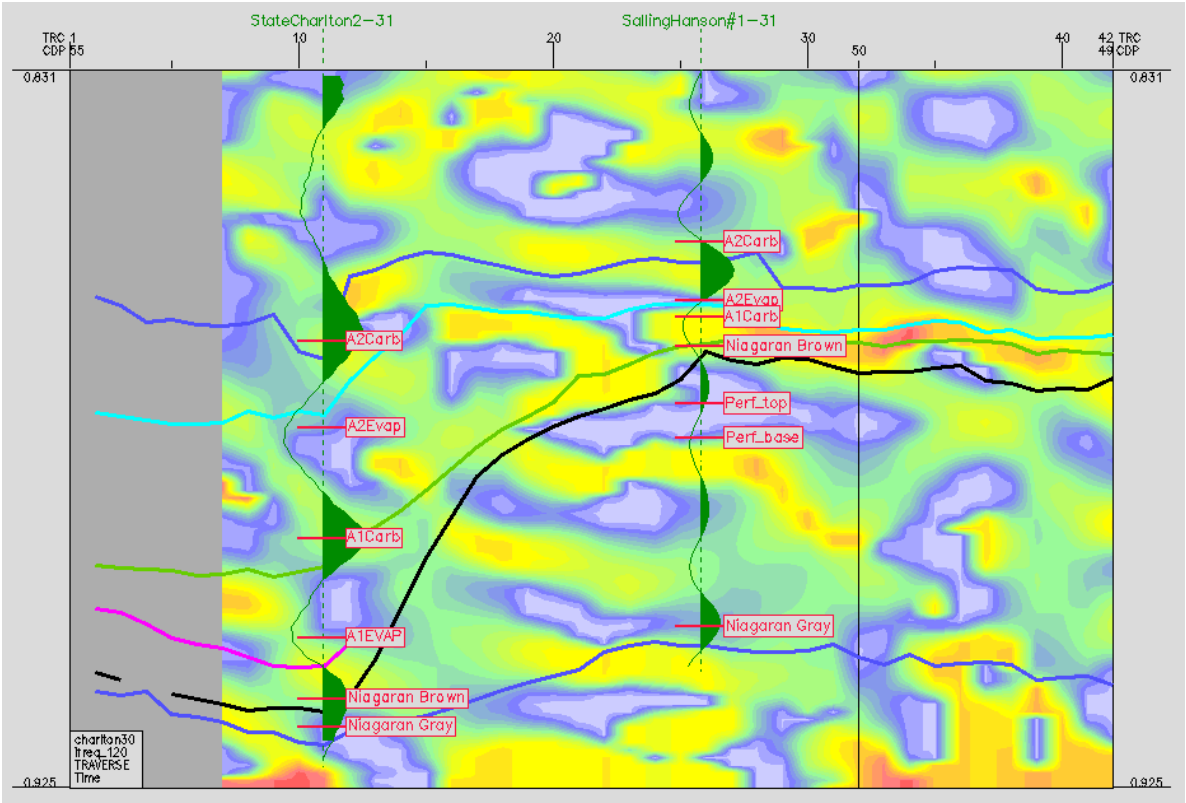

Figure 35: Instantaneous frequency display for the same line shown in Figure 24.

Examination of these instantaneous frequency displays immediately revealed that the intervals perforated during the well's primary production phase all aligned with zones of low frequency. Since it is a normal industry practice to perforate in zones of high porosity this was taken as support for the relationship shown in Graph 1, namely that lower frequencies were associated with higher porosity zones in the reef.

A literature search indicated that there was support in past publications for this relationship. This research was initiated by Biot in the 1950s and dealt with the attenuation of higher frequencies due to fluid movement within porous zones. His papers, "Theory of Elasticity and Consolidation for a Porous Anisotropic Solid" (1955) and "Theory of Deformation of a Porous Viscoelastic Anisotropic Solid" (1956), both in the Journal of Applied Physics describe this phenomenon. An early effort to apply this work to the geosciences was performed by H. C. Misra in 1965 with the publication of a thesis entitled "Permeability of porous media to transient flow". In this work Misra theorized that "the permeability of the porous medium, as it occurs in the equations of motion, is frequency-dependent."

An initial attempt to use this relationship to generate a porosity volume for the reef for use in the reservoir characterization was attempted. Instantaneous frequency values from the time slices between the 2 millisecond bounding surfaces were used to influence the gridding of the log porosity values. Figure 37 shows the instantaneous frequency map on the right for one of the 2 msec time slices, 889 msec, and the resulting porosity distribution map created using the frequencies as a guide on the left. Additional comparison displays for other time slices are included in Appendix G.

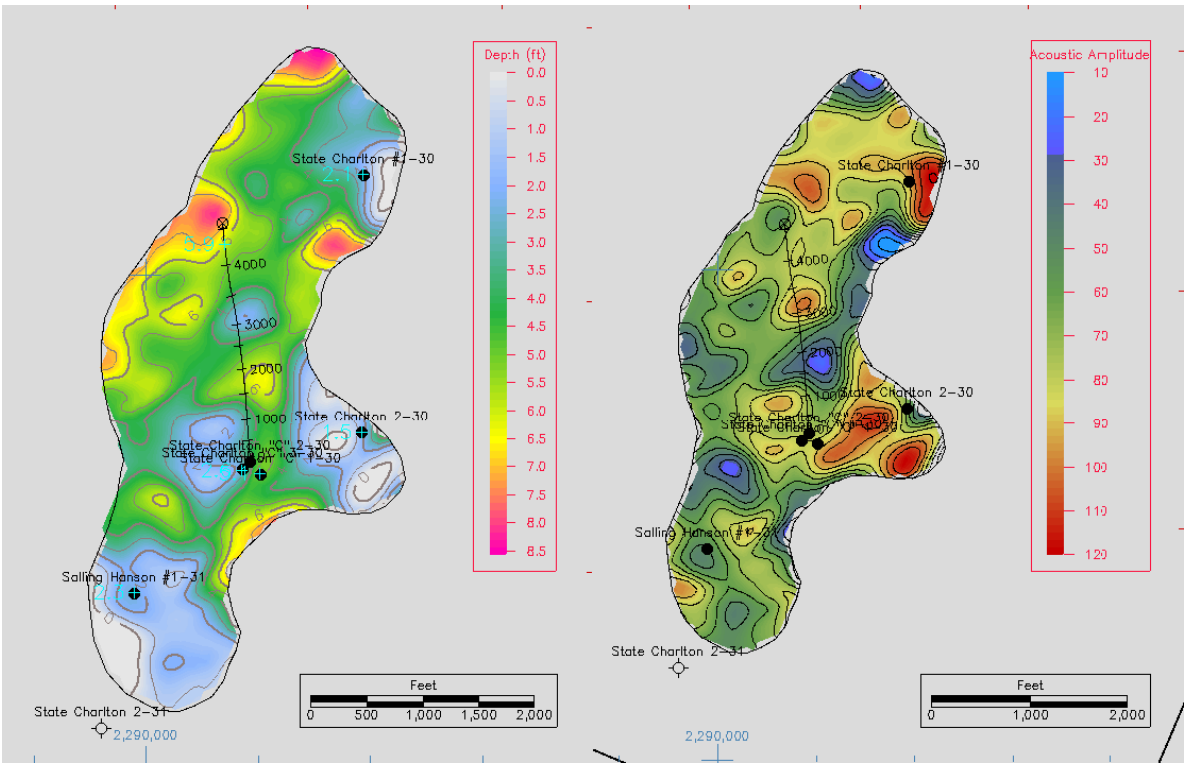

Figure 36: Porosity distribution map for time slice 889 (left) and the map of instantaneous frequencies (right) on with it was based.

Log porosity values for each time slice, shown in light blue on the porosity distribution map (left) of Figure 37 were also used to constrain the resulting surfaces. It should be noted that due to software constraints the titles for the color bar scales on both images are incorrect. For the porosity distribution map on the left scale should read “Percent” and not “Depth”. For the instantaneous frequency map on the right the title should read “Hertz” and not “Acoustic Amplitude”. These 2 msec porosity distribution grids were used to construct a geologic model that was then used in an initial reservoir simulation of the field. The results from this initial simulation, which was based on the initial attempts to use gridded surfaces generated with the frequency – porosity relationship, indicated that the overall pore volume was too high but the porosity distribution was quite reasonable.

It was concluded that low frequency values, which were also being returned from the low porosity portion of the reservoir (see Graph 1), were pulling up the overall porosity in the simulation. This accounted for the pore volume being too high. However, the porosity distribution indicated favorably corresponded with the well production history thus supporting the relationship.

A second attempt was made to use this method to characterize the reservoir’s porosity distribution using this method, but with a slightly different approach and with an attempt to further validate the method. The instantaneous frequency volume was regenerated using a new version of the software and with slightly more constrained parameters. Figure 38 shows in-line 80 through the State Charlton #1-30 well from the second instantaneous frequency volume. While this attribute section is slightly visually different from the initial volume, see figure 35, the frequency distribution is the same and the low frequency zones occur in the same locations.

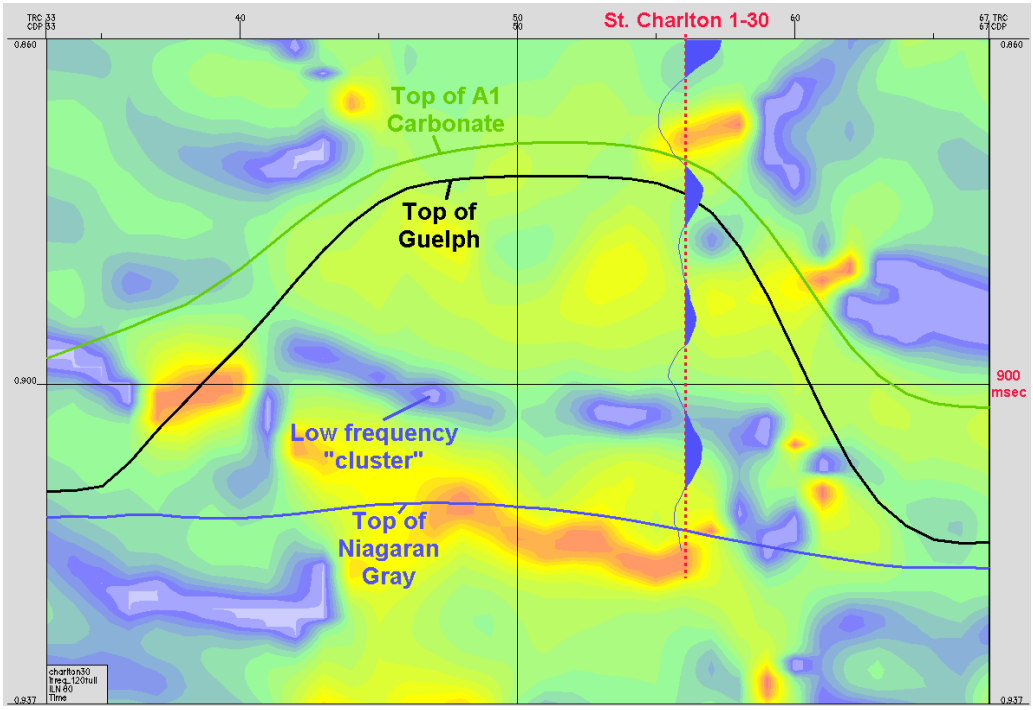

Figure 37: Instantaneous frequency display for In-line 80 through the State Charlton 1-30 well.

Using GeoFrame's IESX seismic interpretation application the instantaneous frequency volume was displayed and interpreted. The color map of the application's display was selected to help rapidly identify clusters of lower frequency within the seismic volume. The tops and bases of these low frequency "clusters" were interpreted. This interpretation, along with the instantaneous frequency volume, was then transferred into a geologic model construction program. Within this program the porosity to frequency relationship shown in Graph 1 was applied to the volume within the low frequency clusters. Within these zones the porosity distribution was set to greater than 5% using a deterministic method that was guided by the actual instantaneous frequency values. Outside of these "clusters" a stochastic distribution of 1 to 5% porosity was used.

This second porosity volume was believed to be more finely tuned than the original one and this new volume was used in the creation of a new geologic model and reservoir simulation. This new porosity distribution proved to be a very good starting point for the history matching process. Areas around four of the six production wells required little or no adjustment to create a reasonable history match. The remaining two wells, which clearly showed production interference effects between them, required additional history matching efforts, including regional reduction of the porosity array.

5.4 Reservoir Simulation, History Matching and Prediction

The simulation was designed to take maximum advantage of the high resolution 3-D seismic survey. The simulation grid was laid out parallel to the seismic lines and cell size was set as 82.5 foot squares, the same as the bin spacing of the seismic data. Also, grid cell thickness was set at 9 feet, equivalent to the seismic sample rate of 1 millisecond resolution.

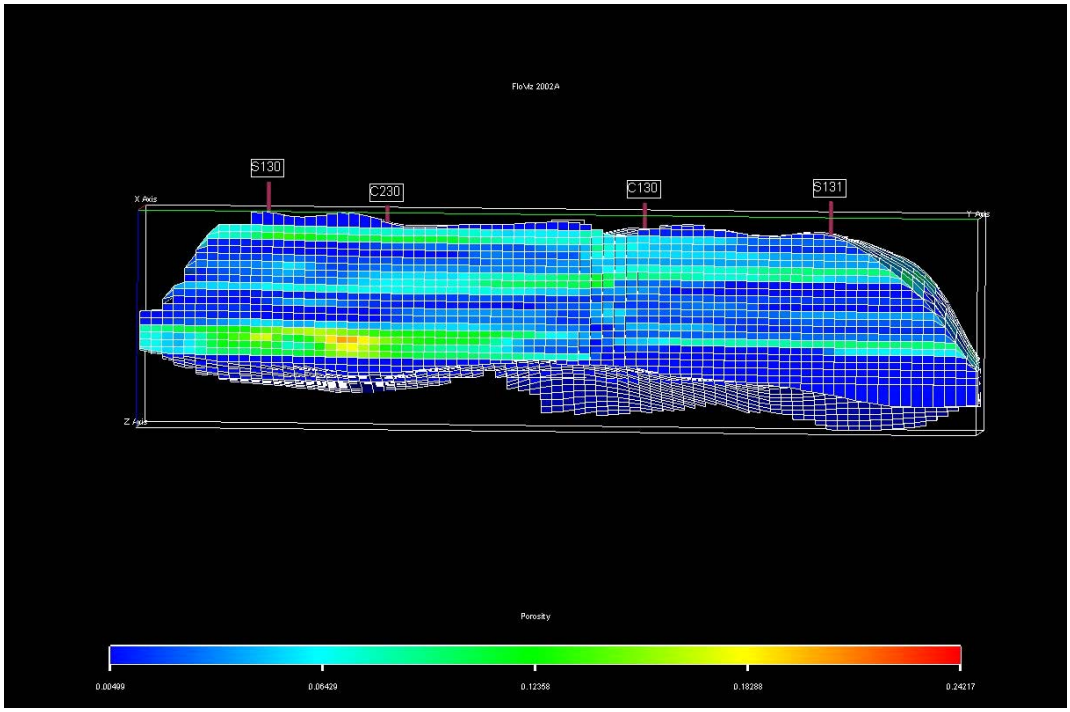

Figure 38: Cross section of simulation showing grid structure and seismic porosity distribution.

This effectively created one simulation grid cell for each seismic sample point, with the effect of eliminating the need for upscaling of the seismically derived data. The resulting simulation grid contained 48 x 87 x 29 cells. Within the reef isopach, there is no easily identifiable layered stratigraphy that might be considered as coherent flow units. Partial dolomitzation of the reef limestone creates much of the storage capacity and most of the permeability in the reef. This allowed for uniform horizontal layering in the simulator. The resulting grid structure with the seismically derived porosity distribution is shown in Figure 39.

History matching was accomplished using the seismically derived static model with relatively few modifications. The overall pore volume from the static model was reduced by about 20% to achieve the observed field pressure decline, but the field porosity distribution was retained with only one exception. The exception area was between the "C"2-30 and Charlton 1-30 wells which have showed clear interference effects between them during depletion, pre-CO_2 flood testing and during early CO_2 flood operations. Additional pore volume reduction between these wells was required to match the effects seen between these two wells. The history match of the field's depletion history is shown in Figure 40.

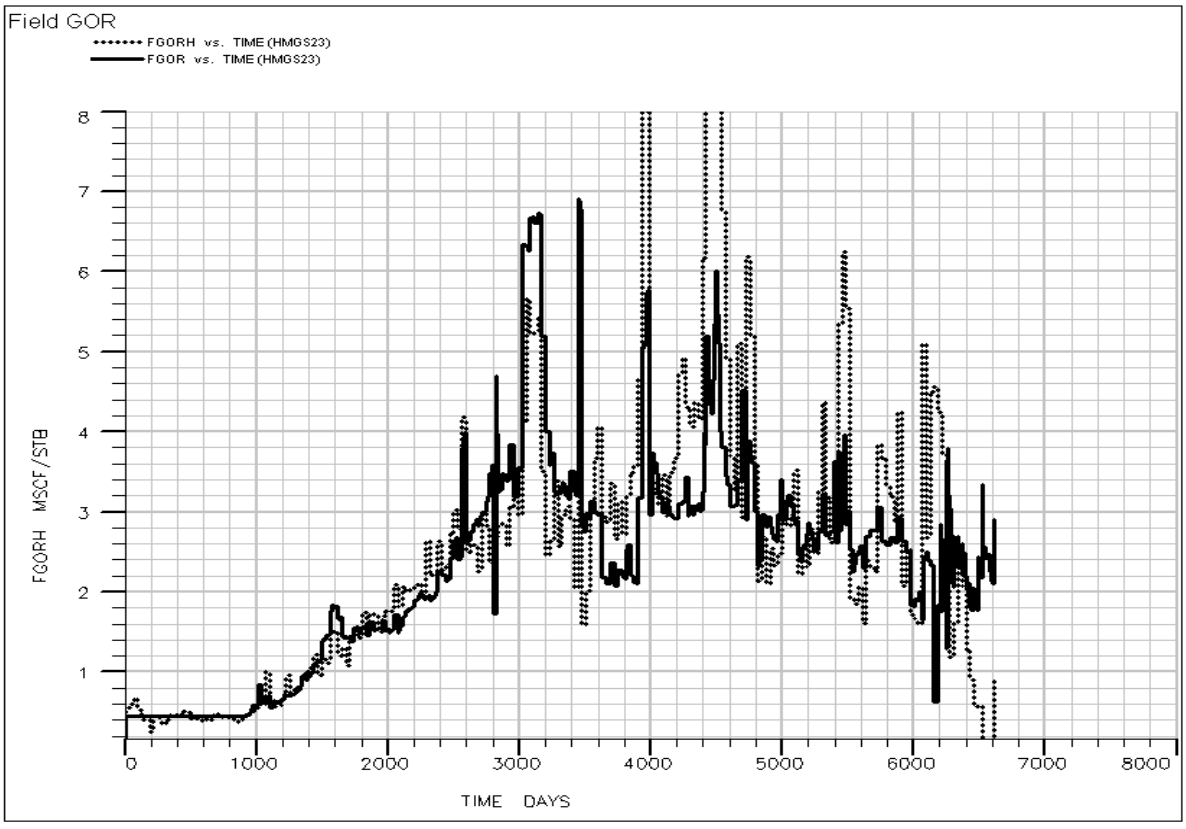

Figure 39: History match showing 18 years of field GOR history, dashed line, and simulated GOR, solid line.

The results of the history matched reservoir simulation support the relationship suggested in Graph #1. As noted previously a relationship exists between lower instantaneous frequency and higher porosity when porosity values are greater than 5%. Unfortunately, lower instantaneous frequencies can also be found in rocks with less than 5% porosity. When the relationship shown in Graph #1 is applied to the entire reef, rocks with porosities lower than 5% are artificially boosted to higher porosity values, and this somewhat optimistic estimation of pore volume was confirmed by the need to reduce pore volume in the simulation.

The period of the dump flood also had to be "history matched". This was the time between the end of primary production in 1997 and the start of the 2004 well remediation program. The bottomhole pressures recorded in 2004 and 2005 confirmed that pore pressure in the reef was in the range of 1,600 to 1,800 psi. This roughly coincides to the height of a column of salt water between the reef perforations and the source Dundee Formation. Therefore, the dump flood was replicated in the simulator by introducing constant pressure water injectors at the wells with known casing leaks. This injected 2.3 million barrels of water into the simulated reservoir and repressured it to 1,650 psi.

After repressuring, the history matched model was used to create a variety of CO_2 flood development scenarios. The simulator was constructed using black oil PVT data and CO_2 injection was handled by using the 4-component solvent model methodology with CO_2 as the solvent. The Todd-Longstaff miscible fluid mixing parameter technique was applied. The most advantageous CO_2 flood development plan was not immediately apparent. Several factors were important considerations, including:

1) The highly irregular yet continuous high porosity and permeability distribution due to dolomitization.

2) The thick oil column, over 300 feet, and the apparent gravity drainage effects seen during depletion.

3) The elongate shape of the reef structure.

4) The limited number of wellbores to create an effective injection/ production pattern.

The most effective simulation scenario involved injection into the two most northerly wells, sweeping oil to the southern wells. Core Energy ultimately adopted a variation of this scenario by initially injecting into the second most northerly well, the "C"2-30, and temporarily producing from the most northerly well, the Charlton 1-30. The intent was that after approximately one year, when the Charlton 1-30 began cycling unacceptable amounts of CO_2, it would also be converted to injection to push remaining oil toward the southern producers.

5.5 CO_2 Injection

Injection of CO_2 at the Charlton 30/31 field began in August 2005 through the deviated Charlton "C"2-30 well and was maintained at varying rates until September 2006. Injection during this time period was not continuous and was suspended for extended periods of time due to reservoir testing programs or balancing of system CO_2 requirements among the several CO_2 flood fields operating within the Core Energy project area. By April 2007

29,000 tons of CO_2 had been injected into the northern end of the field with a monthly average rate as high as 3.9 MMSCFD.

An adjacent well, also in the northern portion of the field, the Charlton 1-30 well, was opened for production during this same time period. This well produced an average of 313 BWPD for 5 months without producing oil. The production of this large amount of water was unexpected and initially the source was undetermined. However, further investigation determined that water had entered the reef as the result of an inadvertent dump-flood. This had occurred when caustic waters within a shallower disposal zone corroded through the casings of the temporarily abandoned wells and flowed down into the reef.

First oil was produced in June 2006 and continued through to April 2007 at an average of 10 BOPD and 337 BWPD. CO_2 break through occurred in the production stream in July 2006. Since then CO_2 production has totaled approximately 10% of what had been injected during the first injection phase.

Injection resumed in November of 2007. Up to this time approximately 3,000 bbls of CO_2-enhanced incremental oil have been recovered. However, recent work-over activity revealed a significant amount of oil within the annulus of the producing well. It is apparent that field response in Charlton 30/31 is still in its very early stages. Only a small fraction of the projected CO_2 quantity has been injected to date. Compared to the other four fields in the area with ongoing CO_2 floods, Charlton 30/31 is the only field that has experienced the inadvertent dump flood conditions which have complicated operations. The produced gas mixture is currently recycled into the Core Energy CO_2 system.

5.6 Dump Flood

During the well remediation phase, it became apparent that pore pressure in the reef was much higher than the estimated 1997 abandonment pressure of 500 psia. In December 2004 a bottomhole pressure gauge recorded over 1,700 psi. Several other BHP measurements confirmed the anomalous high formation pressure and an explanation was sought.

The well remediation program revealed a serious condition common to all the wells, corroded casing. In the case of the Charlton 1-31 and Charlton 2-30 wells, casing leaks were severe and water was entering the wellbores from shallower formations, particularly the Dundee Formation. Locally, the Dundee is used as a produced water disposal zone for other projects. It is unknown when the inadvertent injection, or “dump flooding” of water began in the reef, how many injection points there were, and what the cumulative volume injected was.

Discovery of the dump flood has helped explain the reported increase of produced water from the Charlton 2-30 well in 1985 and the sudden arrival of 100% water cut in the “C”2-30 well in 1997, which ended primary production from the field. 2004 remediation work on the “C”2-30 and Charlton 1-30 wells did not find any casing leaks across the Dundee Formation, but the condition of the casing in the abandoned “C”1-30 and “C”3-30 wells is unknown.

The dump flood, and the limited understanding of it, has been an important complicating factor in forward planning and execution of the CO_2 flood. Simulation efforts have

replicated the repressuring of the reef with dumpflood water. An estimated 2.3 million barrels of dump flood water have been added to the reef system between 1985 and 2005, at which time known casing leaks were repaired.

5.7 Planning and Drilling of First New Well

During the summer of 2006 plans were made for the drilling of the first new well in the Charlton 30/31 field since the ending of its primary production development phase. This well, the Charlton 4 - 30, was being drilled into conjunction with a CO_2 sequestration study project that was to take place in a shallower reservoir. This well was to be deepened to test the reef's western edge. Figure 41 shows the location of this well.

The drilling of this new well provided an opportunity to test the porosity distribution model developed using the instantaneous frequency method described previously in this report. Through this method it was predicted that this well would have little to no porosity greater than 5%. Additionally, the reservoir simulation, which was based on the porosity model that was developed with the initial "Base" 3-D survey, predicted that no CO_2 would be encountered in the reef at this location and time.

The Charlton 4-30 well was drilled at the end of 2006. Well logging and sidewall cores were taken throughout the reef section. Results of this drilling program are discussed in the "Results and Discussion" of this report.

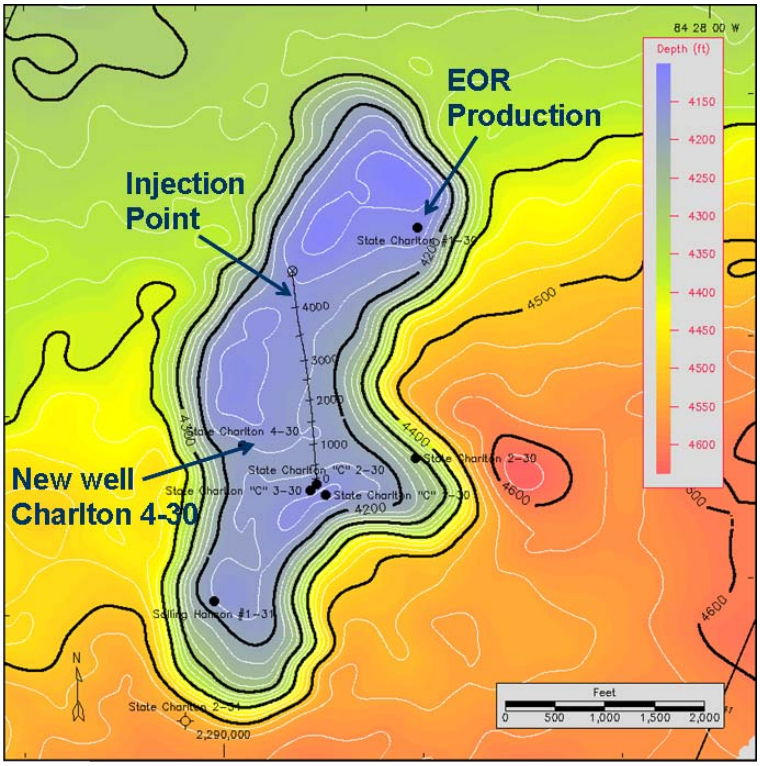

Figure 40: Showing the location of the Charlton 4 - 30 well

5.8 Monitor 3D Survey and Shear Wave Acquisition

The Monitor survey was acquired using the same acquisition company and parameters that were used in the acquisition of the Base 3-D survey. Unfortunately, due to the timing of the project it was not possible to acquire the Monitor survey at the same time of year as the Base 3-D survey. The Monitor 3-D seismic survey was acquired in September 2007 at the end of the summer and beginning of the fall, whereas, the Base survey was acquired in March at the end of the winter and beginning of the spring.

This difference in the time of year when the acquisitions occurred is believed to have had some effect on the two data sets. This is most likely due to the water saturation of the surface formations. The study area is extensively covered with significant amount of glacial drift. At the end of the winter/beginning of spring these materials become saturated with snowmelt water. At the end of the summer/beginning of fall this water would not be present to the same degree. The presence or absence of water in these materials would have some effect on the seismic signal. This variation of signal was adjusted for at the time the two surveys are processed. Although processing of the data enhanced the lost signal due to the effects of glacial drift saturation, it still must be taken into account.

An attempt was made to acquire a small, 3-D multicomponent data set at the same time the Monitor P-wave survey was being acquired. A 48 channel Geometrics Strataview system with 24 3-component 40/100Hz Geophones was obtained through the Geoscience Department of Michigan State University and deployed within the center of the Charlton 30/31 field. It was hoped that an electrical signal cable could be run between the doghouse of the P-wave survey and the Geometrics Strataview system in order to synchronize the two systems. This would have allowed the seismic energy from the dynamite shots prepared by the P-wave survey crew to be used as energy sources for the multicomponent acquisition.

Both the P-wave survey doghouse and the multicomponent system were stationed at the same time at the surface location of the CO_2 injector well. A number of attempts were made to synchronize these two acquisition systems in order to ensure that their recording clocks started with the trigger of the dynamite shot. Unfortunately, all attempts to do this in an automatic manner failed due to equipment incompatibility. In order to resolve this issue the multicomponent acquisition crew triggered the recording of each shot manually once the triggering tone was heard by radio.

This method proved to be highly inefficient and inaccurate. As a result of these inaccuracies as well as the project timeline the multicomponent data that was recorded was not analyze during this study.

5.9 Processing of 4D Seismic Survey and Interpretation

5.9.1 Separate Base and Monitor 3D Survey Processing

During the initial stages of the project only the Base 3-D survey was available for use. This survey, acquired in March of 2004, imaged the Charlton 30/31 reef prior to the injection of CO_2. Basic processing was performed on this data set by two different processing companies, Sterling Seismic and WesternGeco. Advanced azimuthal processing was also performed by WesternGeco. The initial interpretation of these basic seismic volumes is covered under previously reported sections.

Once the Monitor 3D survey was acquired in September, 2007 the same processing sequence was performed on it by both companies. Both of these data sets were examined to determine the quality of the data with respect to that of the Base 3D surveys. It was determined that the structure and seismic signature of the reef was the same within each processing set.

5.9.2 4D Survey Processing

The basic field data for both the Base and Monitor surveys were then returned to WesternGeco and a complete 4D processing sequence was performed. Because the correct 4D seismic data processing sequence is critical to the success of a project of this type additional details are described here concerning the sequence applied to this 4D data set. The complete report from WesternGeco concerning this 4D processing sequence is shown in Appendix C.

5.9.3 4D Survey Reef Signature Comparison

Upon completion of the 4D processing both data sets, the 4D Base Survey and the 4D Monitor Survey, were loaded into a LINX-based GeoFrame 4.4 project. Additionally, all available well data previously used in this project was loaded into this new workstation project. Wavelet analysis and well to seismic ties were performed on both of these surveys and then compared with those generated for the original (non-4D processed) volumes.

This comparison found that an upward shift of 80 msec on the 4-D surveys had occurred to the seismic events associated with the reef as originally processed by WesternGeco for the Base 3-D survey in 2004. This was determined to be due to a variation in the velocity field used during the different processing sequences.

The seismic signature of the reef on the Base 3D survey matched the Monitor 3D in character. The on-reef section is composed of four peak events from the top of the A2-Carbonate to the top of the Niagaran Gray. The seismic signature can be seen in both processing sequences and is confirmed by the well to seismic ties. This transitions to the off-reef section, which is composed of only three peak events from the top of the A2-Carbonate to the top of the Niagaran Gray on both sequences. This transition is the result of the 90% decrease in isopach of the Guelph formation as the pinnacle reef facies (approximately 380 feet thick) rapidly transitions to the non-reef facies.

This same seismic signature can be seen on the original 3D processing as well as the 4D processing. Additional investigation confirmed that the original horizon interpretation performed on the 3D data set matched the 4D seismic processing quite well. Some adjustments to the interpretation had to be performed but these adjustments were minor.

5.9.4 A2-Carbonate Interpretation on the 4D Base and Monitor survey.

Since both the Base and Monitor 3-D surveys were developed with the exact same processing sequence during the 4-D processing, significant variations in amplitude between the two volumes due to processing effects were not expected. One possible source of amplitude variation between the two surveys was believed to be due to the differences in the time of year when the surveys were acquired, as discussed previously. Another possible source of amplitude variation is minor change in acquisition geometry.

The monitor survey was not extended as far to the south because reservoir simulations of the CO_2 injection, based on the original Base 3D survey, indicated that the CO_2 would be concentrated within the northern end of the reef. Additionally, some minor changes in the source and receiver geometry were necessary for the Monitor survey due to licensing and landowner restrictions. These, however, were kept to a minimum and their effect believed to be negligible.

In order to determine the variations in signal strength that might be due to these minor changes in acquisition geometry, a strong reflection event from a non-reservoir stratigraphic unit was selected for interpretation that was within the immediate vicinity of the reef. The A2-Carbonate was selected for this comparison. This stratigraphic unit is the strongest reflector immediately above the reef and is easily recognizable across the area. This event was easily and rapidly interpreted on both the Base and Monitor 4-D surveys.

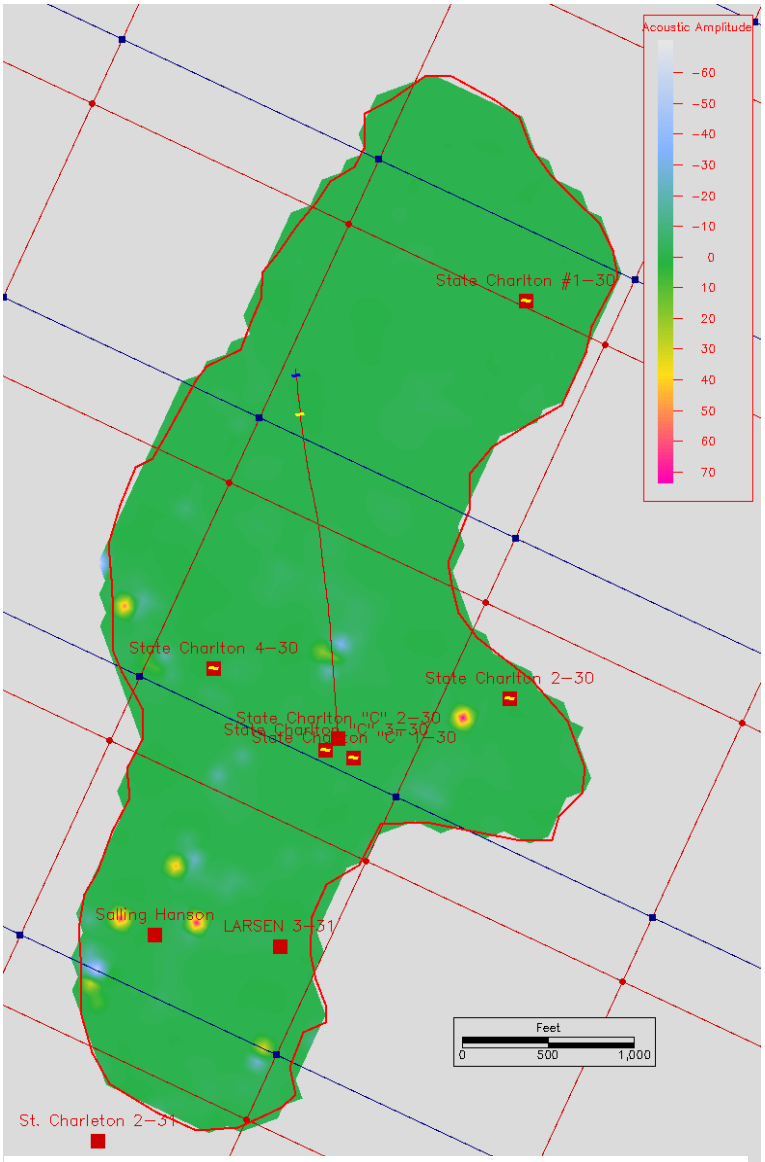

Figure 42: Percent amplitude difference for A2-Carbonate between Monitor and Base surveys.

The amplitude of the A2-Carbonate peak event was mapped for both surveys. The amplitude ranges for the area directly above the reef were compared on both surveys. It was found that the amplitude variation was extremely similar. For the Base survey the A2-Carbonate amplitudes ranged from -155 to 4529. For the Monitor survey the A2-Carbonate amplitude ranged from -34 to 4691. In order to bring these two surveys into a closer alignment for comparison purposes the A2-Carbonate amplitude was gridded for the monitor survey and scaled by .99 and biased by -120. This produced an amplitude range of -153 to 4524. This adjustment brought the amplitude range for the A2-Carbonate into alignment for both surveys.

An amplitude difference map was then created by subtracting the A2-Carbonate amplitudes from the adjusted Monitor survey from the Base survey.

While this amplitude difference map for the A2-Carbonate was informative concerning the amplitude variation for this single stratigraphic unit it, was not believed to be significant for the adjustment of the two surveys signal strength brought about due to differences in the acquisition geometry. Amplitude variations within the reef due to acquisition geometry or pore fluid replacement would not necessarily be confined to peak (+) events and could be associated with trough (-) events or some other (mixed) event.

It was decided that the best method for accounting for the signal strength variation due to acquisition geometry was the use of an amplitude percent difference approach. The amplitude difference grid for the A2-Carbonate events was then divided by the amplitude of the A2-Carbonate on the monitor survey. This produced an amplitude percent difference grid between the adjusted A2-Carbonate amplitudes of the Monitor survey and the Base survey. This is shown in figure 42.

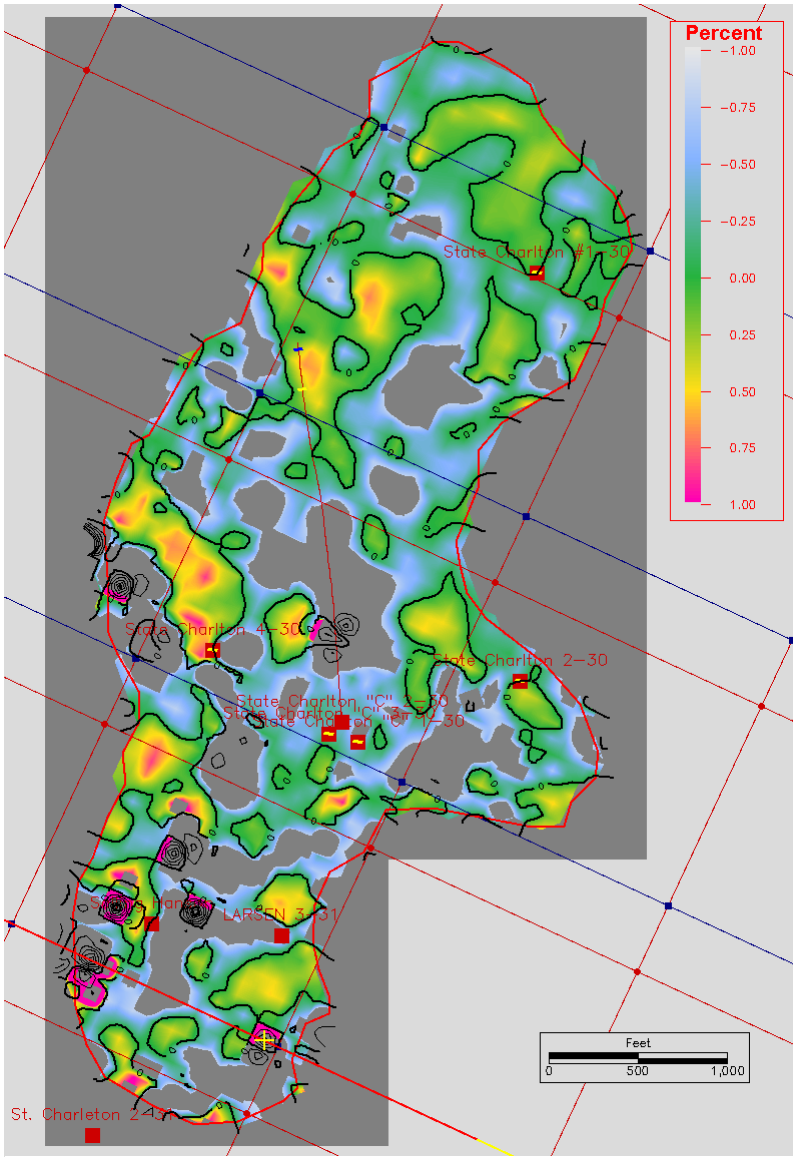

Figure 43: A2-Carbonate percent amplitude difference map. Dark gray areas exceed 100% difference. Colored areas have difference of less than 100%.

The resulting percent difference grid contained several localities within the reef where the amplitude difference between the monitor and the peak surveys approached 7000%. These were all in the southern half of the survey and are believed to be related to the decreased fold in that portion of the monitor survey. Some of the high percentage change events were determined to be static “busts” but others were found to be legitimate. These can easily be seen as bright red or blue points in the southern part of the survey shown on

figure 42. However, these are clearly isolated occurrences, restricted in all cases to single traces.

The vast majority of the northern portion of the reef showed an amplitude variation between the Base and the Monitor surveys of 100% or less. Figure 43 shows the A2-Carbonate amplitude difference in percent between the Monitor and Base surveys with the display scale set to 100% to -100%. Those portions of the grid that are outside these ranges are displayed in dark gray. As can be seen in the northern portion of the reef there are small and isolated areas that have amplitude differences greater than 100%, however, the majority of the grid is near the scale midpoint of 0%.

Since the 4-D processing for both the Base and the Monitor surveys were identical, the difference in amplitude strength for the A2-Carbonate (a non-reservoir stratigraphic unit with high acoustic impedance contrast with the overlying sedimentary unit) shown in figure 43 is believed to be due to minor differences in the acquisition of the two surveys. This would be the result of the few, minor changes in the source and receiver geometry brought about due to licensing and landowner restrictions mentioned earlier. Additionally, variations in the amount of geophone coupling with the ground and signal-to-noise ratio may have contributed to the variation in signal strength, as well as the amount of water saturation in the near surface materials at the time of year when each survey was acquired.

The determination of the variation in signal strength due to acquisition provided the basis for the interpretation of amplitude differences noted between the Base and adjusted Monitor surveys. Throughout most of the northern portion of the reef amplitude differences of 100% or less could be attributable to acquisition related effects. Differences of greater than 100% would need to be examined in more detail as they could be attributable to changes within the reservoir or acquisition if they occur within those few areas denoted in dark gray on figure43.

5.9.5 Flattening of the seismic volumes on the A2 Carb

In an attempt to compensate for slight variations in event time that may have occurred to the top of the reef it was decided that the 4-D interpretation would be conducted on seismic volumes that had been flattened on the A2 Carbonate. Since the A2-Carbonate is such a strong event and easily interpreted it could be used as a datum from which events in the reef could be referenced. This would minimize any time differences that could be significant when attempting to relate events within the two seismic surveys.

The A2-Carbonate horizon was interpreted within GeoFrame's IESX seismic interpretation module on both the Base and the Monitor volumes. Time maps of both interpreted horizons (A2-Carbonate Base and A2-Carbonate Monitor) were generated and subtracted from one another. Differences between these two surfaces would, theoretically, be nonexistent only if both surveys had been acquired and processed in exactly the same manner. This, of course, was not achievable for a number of reasons, which were discussed earlier.

Significant time changes between the A2-Carbonate Time maps for the Base and Monitor surveys were investigated and quality controlled. Adjustments were made to the interpretation where indicated. Some differences remained as a result of static busts and other minor data disruptions. However, after the quality control process valid A2-

Carbonate time surfaces for both the Base and Monitor surveys were produced with minimal time differences.

Flattened seismic volumes of the Base and Monitor 4-D seismic surveys were then generated using the A2-Carbonate as the flattened reference datum and moving this event to a time of 0 ms. Comparisons were then made between these two volumes as well as the results of the reservoir simulation. The results of these comparisons are discussed in section 6.1.3.

5.10 Planning and Drilling of Second New Well

At the beginning of 2008 another new well, the Larson 3 - 30, was planned for the southern end of the field. Again, the reservoir simulation based on the porosity model developed with the Base 3-D seismic survey predicted that no CO_2 would be encountered at this location. Another prediction concerning the amount of porosity greater than 5% that would be encountered at this location by this new well was made using the instantaneous frequency method described earlier in this report. Using this method it was predicted that a moderate zone of porosity would be encountered approximately midway through the reef.

The Larson #3-30 well was drilled and logs in May of 2008. The results of these drilling operations will be discussed in the "Results and Discussions" section.

5.11 Additional Geophysical Investigations

In additional to the analyses described in the previous sections a depthed 3D seismic volume was generated for the Base 3D survey. This volume was briefly examined and used to confirm the depth maps developed with the time-velocity-depthing method. Additionally, a wave number analysis was attempted to see if the relationship identified with the time/frequency volume could be duplicated with this data set. This relationship was readily discernible within a reasonable amount of time and this investigation was halted.

5.12 CO2 Density Determination

Calculations where made to determine the density of the CO_2 within the reservoir. Graph 2 shows the results of this determination.

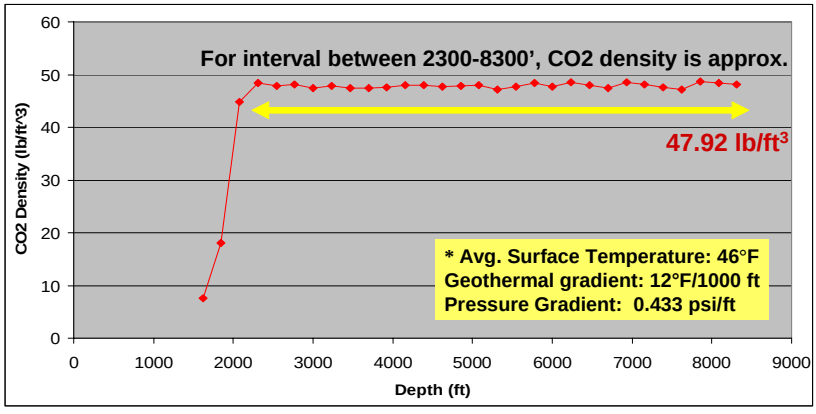

*** From Geothermal Gradient Map of North America, AAPG and U.S. Geological Survey, 1976**

Graph 2: CO_2 Density Determination for Reservoir

6 RESULTS AND DISCUSSION

6.1 Porosity Detection using Seismic Attributes

A number of seismic attributes were investigated in an attempt to characterize the porosity distribution within the reef. The mapping of instantaneous frequency proved to be useful for this task. Twice during the project predictions were made prior to the drilling of wells concerning the location and amount of porosity to be encountered at those locations. In both instances these predictions were proven by the drilling results.

6.1.1 State Charlton #4-30 Well

Prior to the drilling of the State Charlton #4-30 well the portion of the reef that was to be drilled into was examined using the instantaneous frequency seismic volume. This well was planned for the far western side of the reef, see Figure 41. It was found that no low frequency zones existed in the reef at this location. As a result it was interpreted that no porosity zones greater than 5% porosity would be encountered at this location. However, immediately to the northeast, approximately 250 feet, a low frequency zone was observed. It was recommended that the well location be moved in order for this zone to be tested. Unfortunately, since the State Charlton #4-30 well was also being drilled in association with another DOE project in order to test a shallower zone, it was not possible to change the well's surface location.

Recommendations were then made to use directional drilling techniques to deviate the borehole to the potential high porosity zone once the well was below the shallower zone that was the focus of the other DOE project. This was decided to be too costly and was not attempted. As a result the well was drilled through the reef at the location directly below the surface location and in a portion of the reef predicted to have little to no porosity greater than 5%. Well logs and sidewall cores obtained through the reef section by the State Charlton #4-30 revealed that a small (less than 6 feet thick) section near the middle of the reef exceeded 5% porosity. Although the reef's porosity at this location did exceed 5%, the zone's thickness was determined to be below the resolution of the seismic volume.

However, a large zone of porosity greater than 5% at the base of the reef was logged. The original prediction that no significant porosity zones would be encountered in the reef was re-examined. It was determined that a moderate low frequency zone was observed within this portion of the reef but had originally been interpreted as being below the base of the reef section and in the Niagaran Gray formation. The new well log data allowed a reinterpretation for the top of the Niagaran Gray formation which moved the seismic horizon downward until the zone of low frequency could be seen to be included within the reef.

As predicted by the reservoir simulation no CO_2 was encountered at this portion of the reef at this time.

6.1.2 Larsen 3-31 well

The Larsen 3-31 well was drilled in May of 2008 in the southern portion of the reef. This well encountered the zone of porosity predicted through the use of instantaneous

frequency analysis. Additionally, as predicted by the reservoir simulation no CO_2 was encountered at this portion of the reef at this time.

6.2 Monitoring of CO_2 Flood using 4D Seismic

Using the signal variation between the two surveys discussed in section 5.9.4 as a consideration, the A2-Carbonate flattened volumes for the Base and the scale adjusted Monitor seismic surveys were reviewed in an attempt to locate any amplitude anomalies that would indicate the replacement of oil/water with CO_2. As indicated in section 5.9.4 for most of the northern portion of the reef the percent amplitude difference between the Base and Monitor survey for the A2-Carbonate reflector is less than 100%. Therefore, amplitude differences significantly greater than 100% would indicate a change that is related to some variable other than acquisition differences.

During this review a number of a few strong amplitude differences were noted. Figure 44 shows the crossline 5045 for both the Base (shown above in figure) and Monitor surveys (shown below in the figure). As can be seen on the percent amplitude difference map crossline 5045, shown as a blue line trending north northeast, is primarily located in the northern portion of the reef in areas with less than 100% amplitude difference. However, a significant amplitude difference was noted at the top of the Guelph reef between traces 68 to 75. The highest amplitude difference that should be seen in this area is 50% (colored yellow).

Figure 45 shows the same two lines with the amplitude for a single sample on the same trace on both surveys being annotated. This sample, shown at the center of the green rectangle, has an amplitude value of -186. Using the maximum value for the area of 50% the highest amplitude expected on the Monitor survey that would be related to differences in acquisition would be -279 or -93. The value for the same sample on the Monitor survey is 1420. Not only is this a difference of over 700% but there is also a sign change. Therefore, this difference is too great to be associated with acquisition related differences.

It is also noted that this major increase in amplitude appears to be following the top of the reef as shown by the dark blue interpretation line.

Figure 46 shows this same amplitude anomaly but along in line 1072. Again, on the maps shown on the right percentage values that exceed 100% are shown in dark gray. A portion of this line does run across one of these areas. However, the anomaly is located on the western side of the reef in an area indicated to have almost 0% difference between the two surveys.

The sample selected for comparison shows an amplitude of 1234 on the Base survey and 2101 on the Monitor survey, shown in figure 47. If the maximum value in the area associated with amplitude variations associated with acquisition and processing is 50% then the highest amplitude should be 1851 or less. The value of 2101 on the Monitor survey is more than 70% higher than the amplitude on the Base survey. This difference is not as great as the sampling described above along crossline 5045, however, the anomaly has the same orientation in that it occurs just below and following the upper surface of the reef. This orientation also supports the concept that this anomaly is associated with the injected CO_2 plume.

In addition to reviewing the flattened Base and flattened Monitor surveys using in-line and crossline comparisons a number of times slices through the flattened Monitor survey were generated and examined. In the survey that has been flattened on the A2-Carbonate the upper surface of the Guelph formation in the northern portion of the reef occurs at approximately 10 ms in many places. Times slices through this Monitor seismic volume flattened on the A2-Carbonate starting at 10 ms down to 20 ms below the A2-Carbonate can be seen in appendix 10.2 at the back of this report. The 11 time slices shown (10 ms to 20 ms inclusive) image approximately the upper quarter of the reef, as the reef base in this area occurs between 50 and 53 ms below the top of the A2 carbonate, the reef being approximately 40 ms in thickness.

An examination of this sequence reveals a small high amplitude anomaly just east of the injection point, which occurs between the small yellow and blue markers along the Charlton “C”2-30 borehole. This anomaly grows in size and strength with subsequently deeper time slices. A complete set of these amplitude time slices are included in Appendix E for the Base survey and Appendix F for the Monitor survey.

Figure 48 shows the time slice from this A2-Carbonate flattened Monitor survey at 15 ms below the top of the A2 carbonate. The high amplitude anomaly at this depth is shown in the shape of a “jet” moving to the east from the injection point towards the enhanced oil recovery production well, the State Charlton #1 - 30. The shape and location of this “jet”, along with the amplitude evidence presented above, strongly suggests that this is the CO_2 plume moving between the injector and EOR well near the top of the reef. Other high amplitude anomalies can be seen occurring in this time slice just east of the jet and also just north of the EOR well.

Figure 49 shows the time slice 17 ms below the top of the A2-Carbonate. At this point the anomaly appears to bifurcate into two arms that move around an area immediately to the west of the EOR well. The southern arm is slightly less than amplitude while the northern arm appears to be taking a more contorted path before the CO_2 reaches the EOR well. This image also suggests a "pooling" of the CO_2 in the northernmost portion of the reef.

Figure 50 Shows time slice 20 ms below the top of the A2-Carbonate. At this depth the anomaly appears to be losing strength but is still moving around the area immediately to the west of the EOR well.

These amplitude time slices provide strong evidence for the location of the injected CO_2 within the reservoir. The location and shape of these anomalies are consistent with what would be expected for this injector/EOR configuration. The CO_2, injected in the State Charlton “C”2 - 30 borehole approximately 3/4 of the way into the reef, immediately flows upward until encountering the barrier that is the top of the reef. From this point it moves northeast as indicated by the "jet" seen on time slice 15 ms. Approximately half way between the two wells (in map orientation view) the CO_2 encounters a zone of low porosity/permeability and is forced around it. These two flow paths apparently come together just to the northeast of the EOR well.

This evidence provides strong support for monitoring CO_2 that has been injected into reservoir with 4D surface seismic, even at a depth of over 5000 feet and in high velocity carbonate rocks.

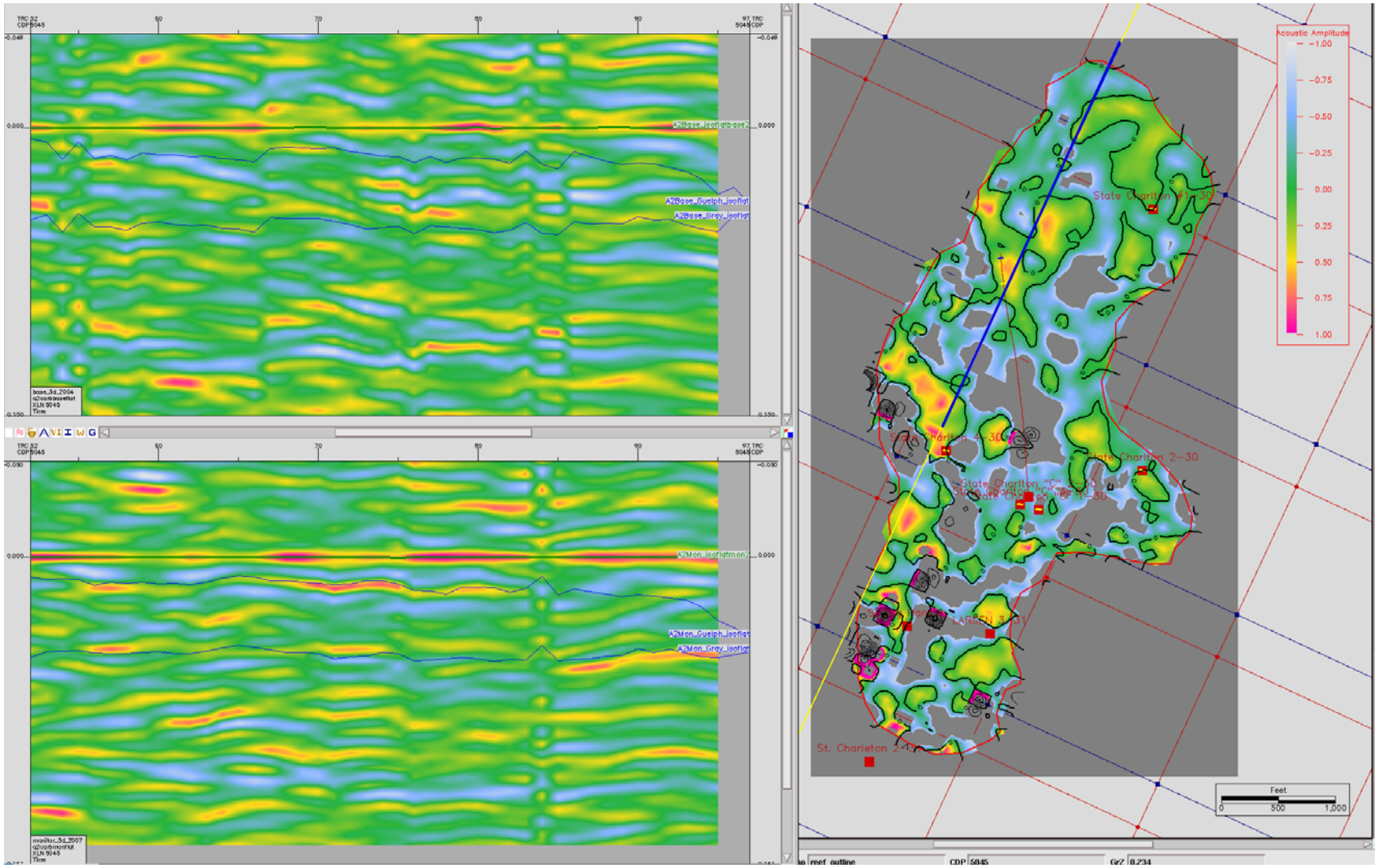

Figure 43: Crossline 5045 (Base survey above, Monitor survey below) flattened on the top of the A2 carbonate. Location of the crossline is shown as a blue line on the percent amplitude difference map at right. Dark gray color indicates percentages beyond 100%.

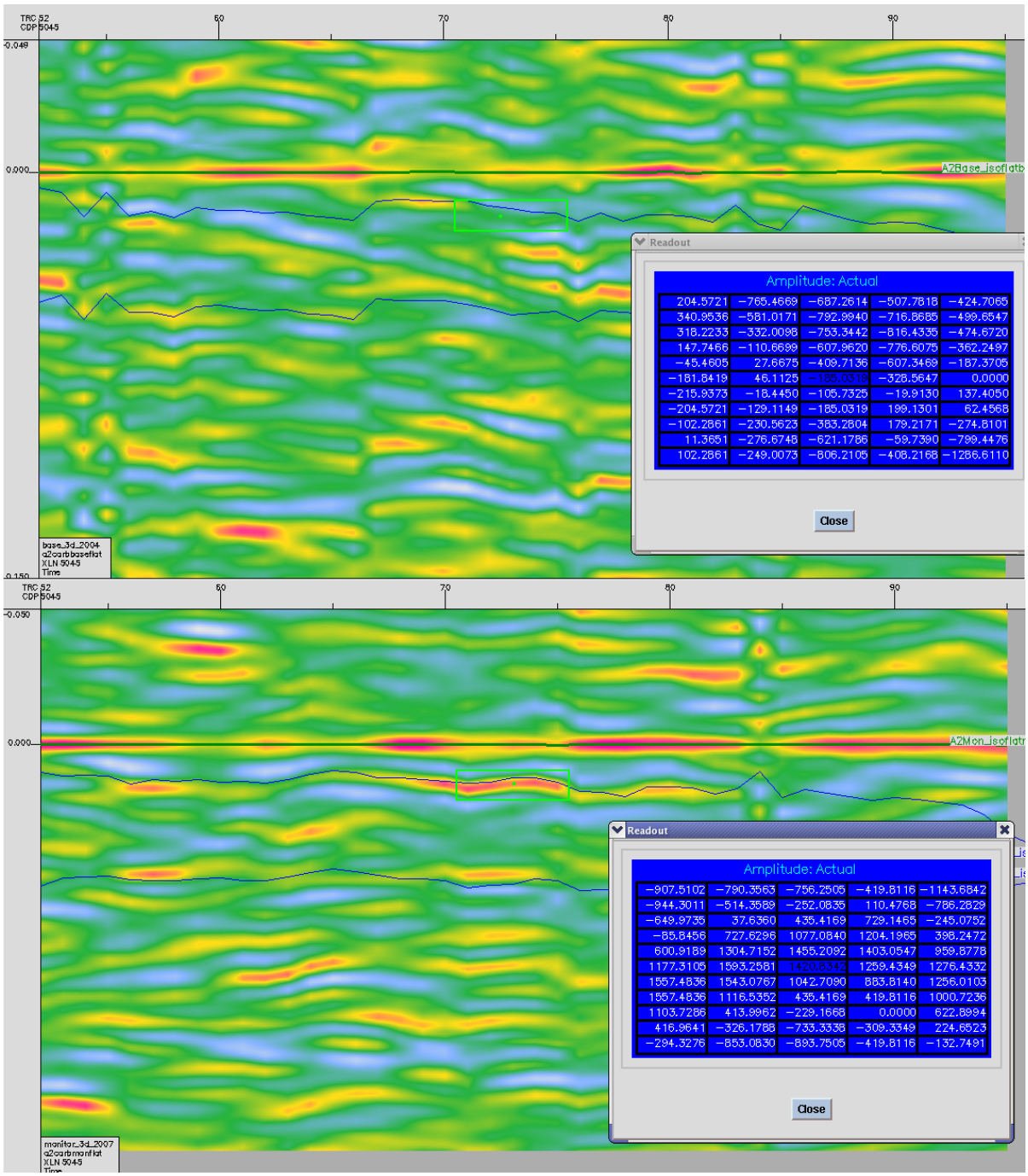

Figure 44: Crossline 5045 (Base survey above, Monitor survey below) flattened on the top of the A2-Carbonate with single sample amplitude annotated.

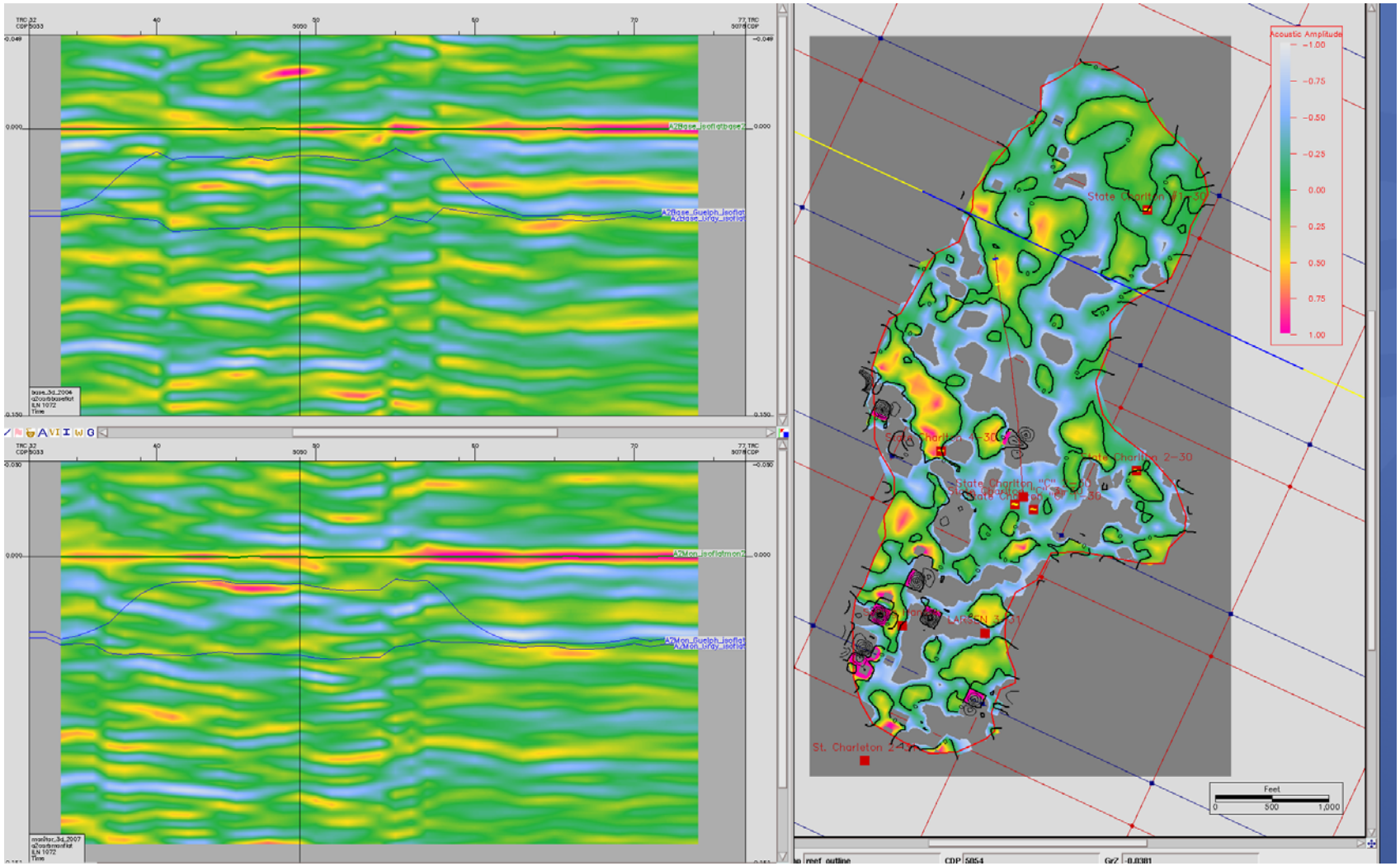

Figure 45: In-line 1072 (Base survey above, Monitor survey below) flattened on the top of the A2 carbonate. Location of the crossline is shown as a blue line on the percent amplitude difference map at right. Dark gray color indicates percentages beyond 100%.

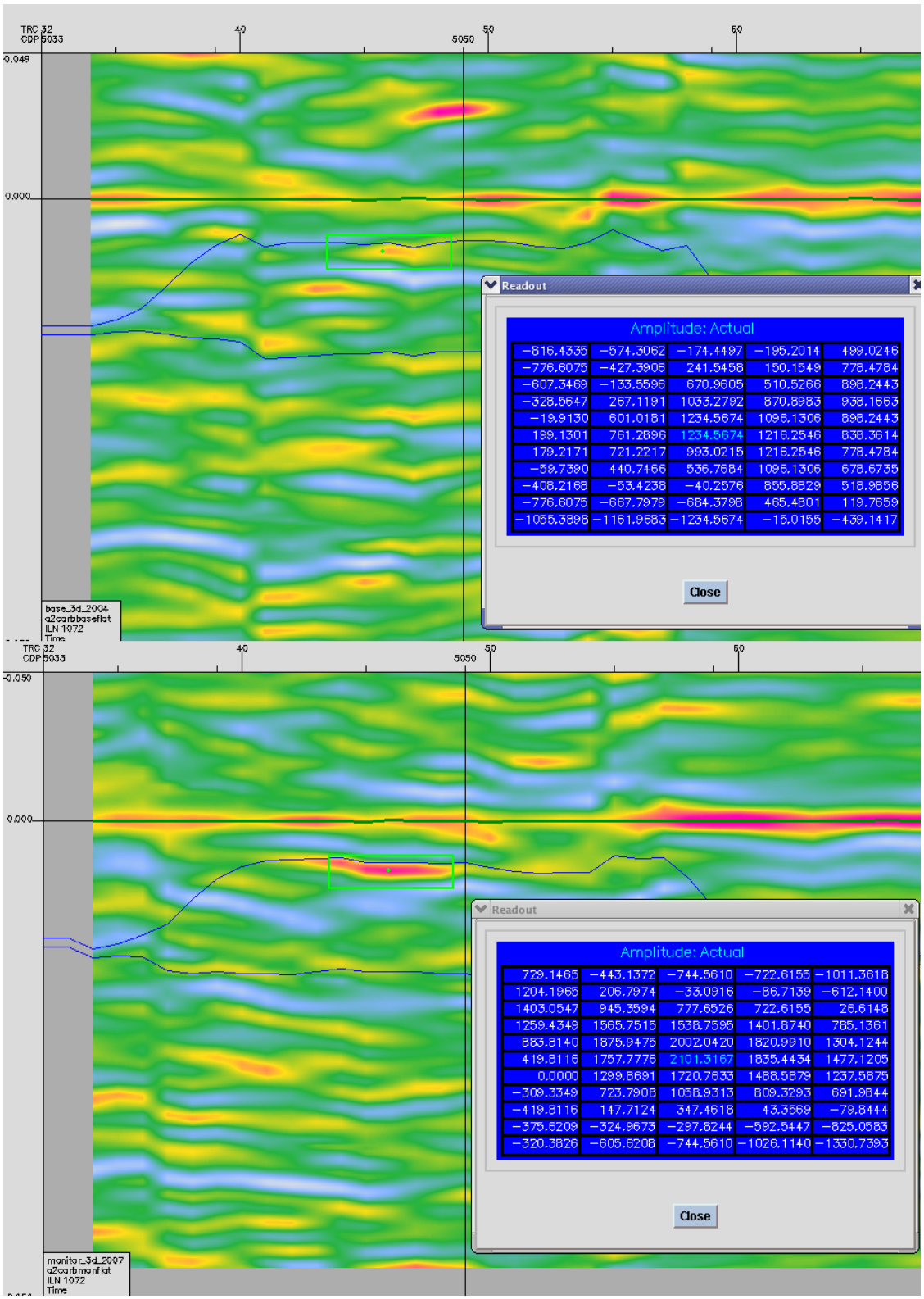

Figure 46: In line 1072 (Base survey above, Monitor survey below) flattened on the top of the A2-Carbonate with single sample amplitude annotated.

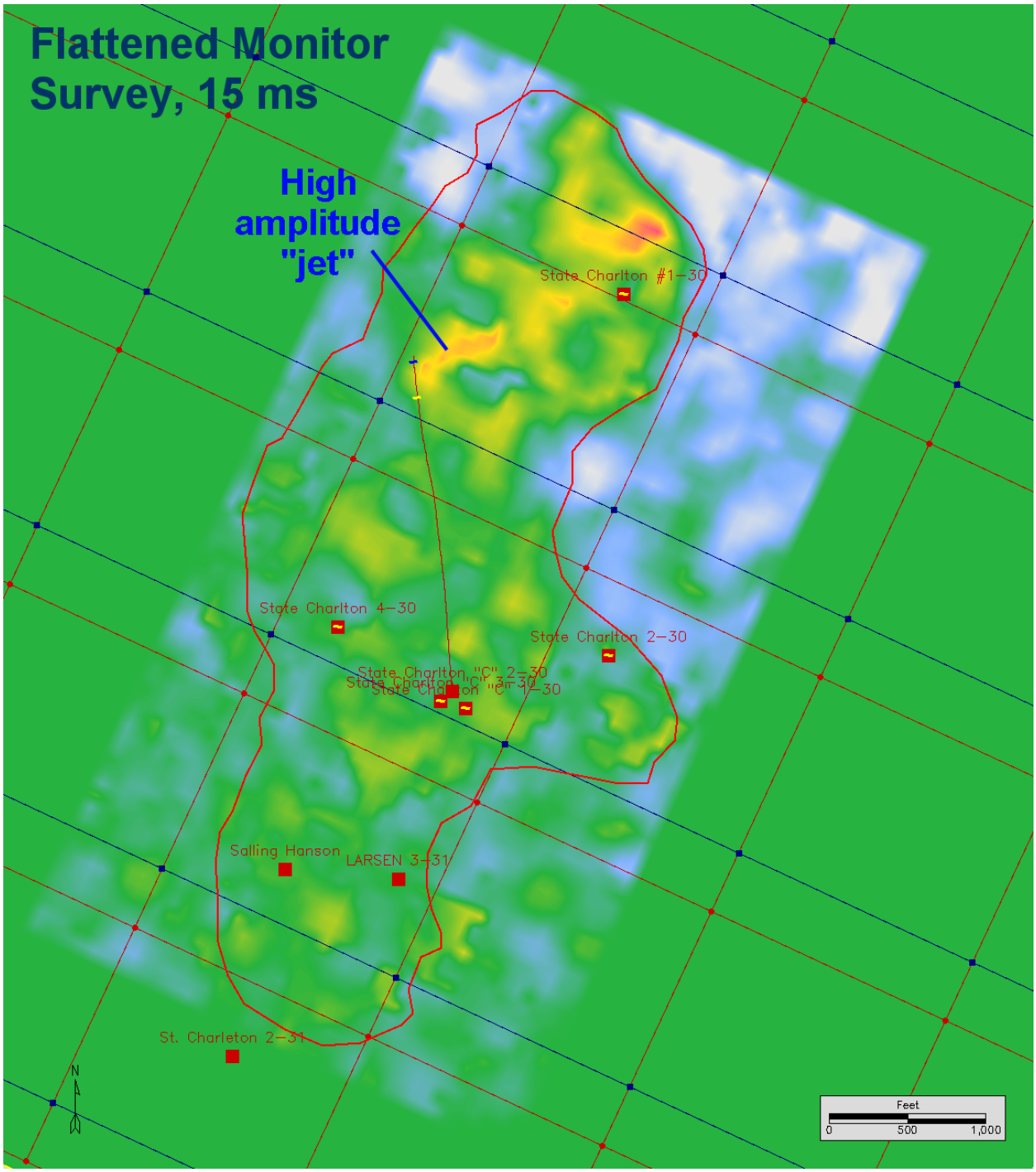

Figure 47: Time slice 15 ms from the A2-Carbonate flattened Monitor survey showing a high amplitude anomaly" just east of the injection point "jetting" toward the enhanced oil recovery production well.

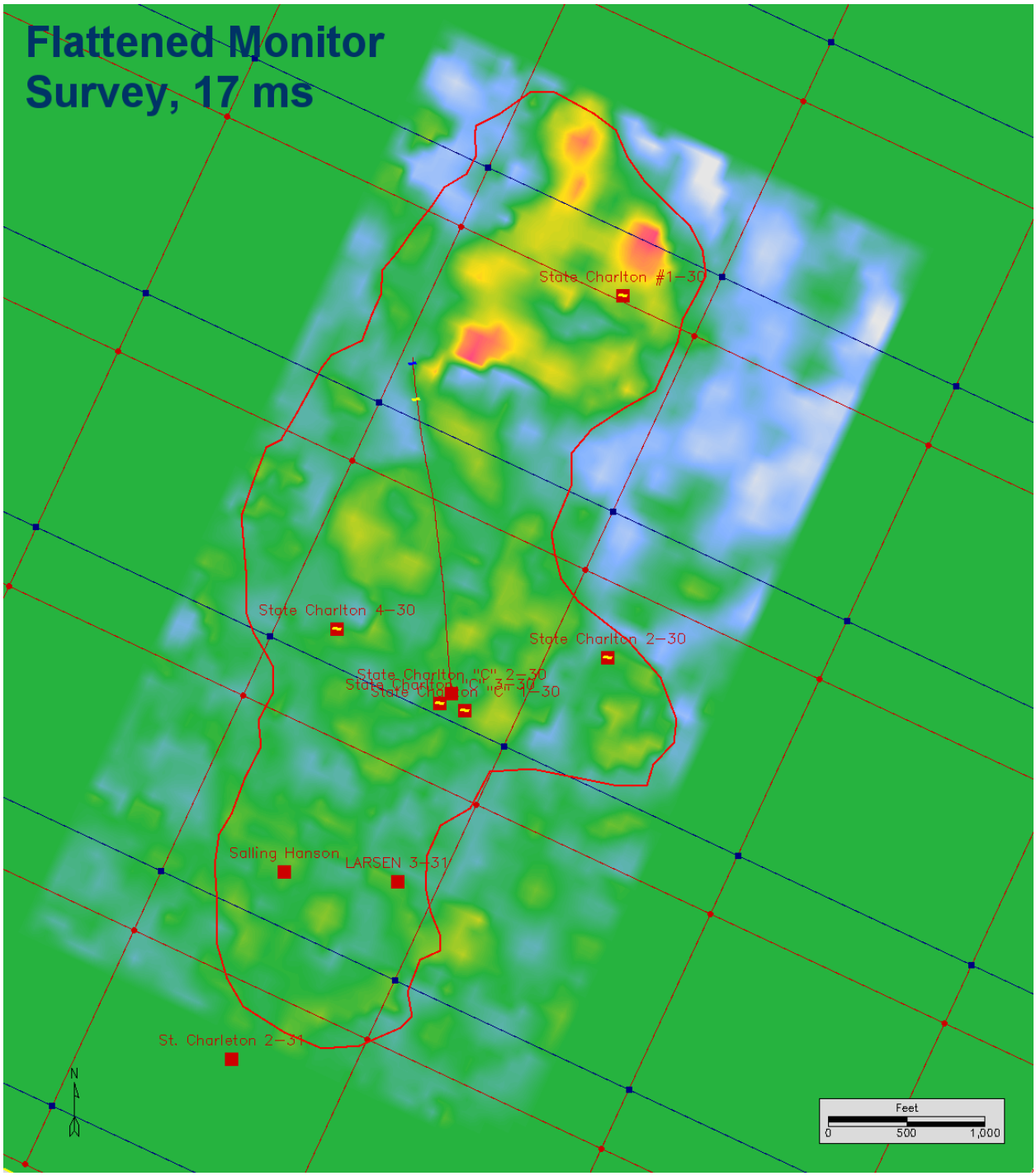

Figure 48: Time slice 17 ms from the A2-Carbonate flattened Monitor survey showing that the high amplitude anomaly appears to be bifurcating around an area immediately west of the EOR well.

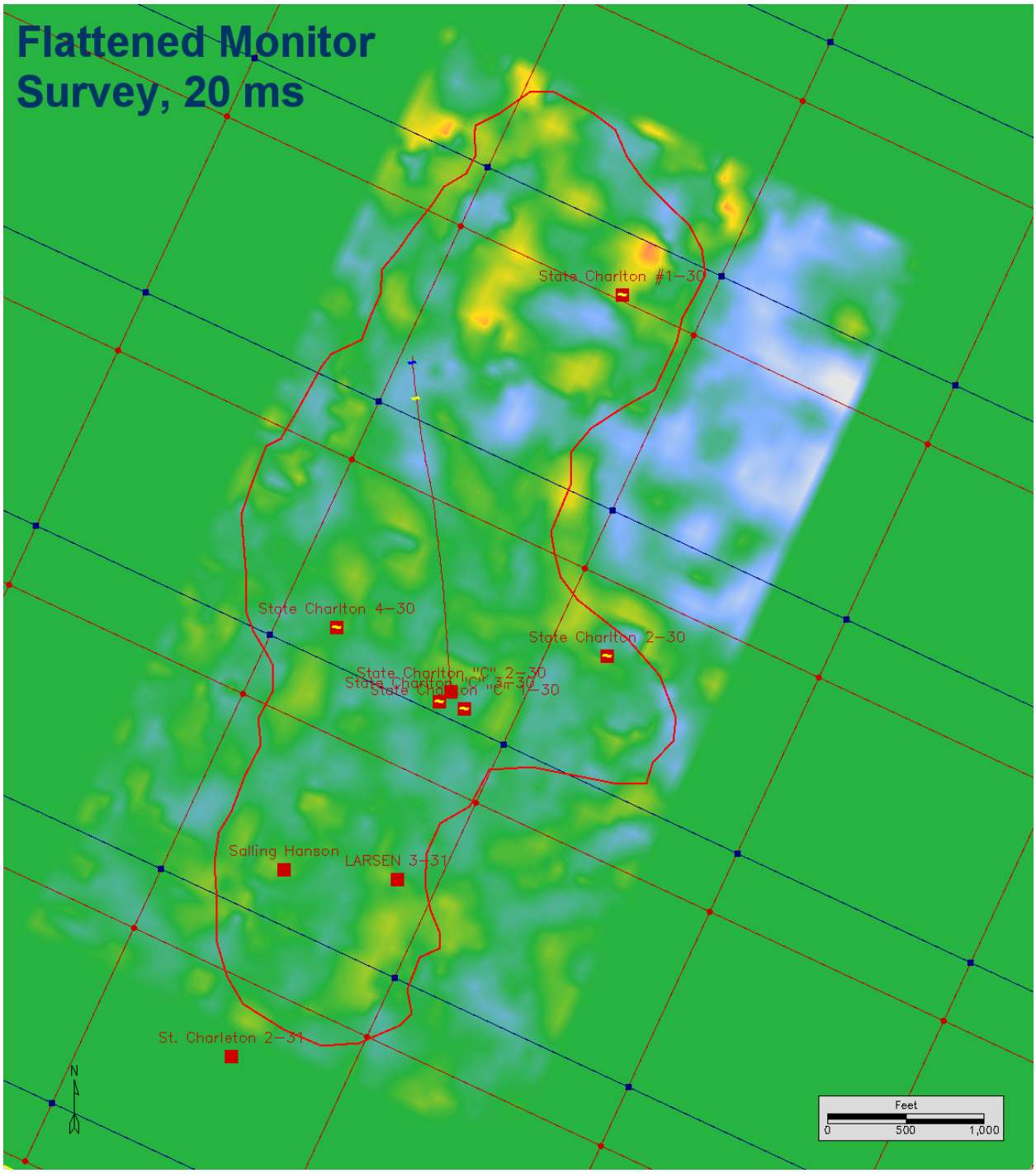

Figure 49: Time slice 20 ms from the A2-Carbonate flattened Monitor survey showing that the high amplitude anomaly appears to be weakening in strength but still suggesting a horseshoe shaped orientation around the area immediately west of the State Charlton #1 - 30 well.

6.2.1 Reservoir prediction and 4D seismic confirmation

The results of the reservoir simulation, which were ultimately based on the static model generated with the porosity distribution obtained through the instantaneous frequency analysis, was compared to the A2-Carbonate flattened Monitor seismic volume. The purpose of this comparison was to determine if the high amplitude anomalies, that are believed to indicate the presence of injected CO_2, correspondent with the CO_2 locations from the model and the reservoir simulation. Note that in the reservoir simulation displays only CO_2 concentrations of 60% or higher are shown.

Figures 51 through 55 show this comparison for key time slices and their corresponding reservoir simulation layers. Figure 51 shows time slice 12 ms and the corresponding reservoir simulation layer, #6. In this figure a high amplitude anomaly just west of the State Charlton #1 - 30 well can be seen on the amplitude time slice. The corresponding reservoir layer, layer #6, predicts a concentration of CO_2 at concentrations greater than 60% at a similar location.

Figure 52 shows time slice 13 ms in the reservoir simulation layer #7.

Figure 53 shows time slice 14 ms and reservoir simulation layer #8. High amplitudes can be seen just east of the injection point along with a corresponding predicted high concentration of CO_2 on the simulation layer at the same location. The simulation also predicts a concentration of CO_2 greater than 60% to the north of this location with a small gap between the two concentrations. The time slice also shows a low amplitude area separating to higher amplitude areas in a similar location.

Figure 54 shows time slice 15 ms and its corresponding reservoir simulation layer #9. High amplitudes are still shown east of the injection point, however, the CO_2 "jet" is not obvious within the simulation layer. The reason for this is unknown, however, it is possible that the “jet” is the result of CO_2 movement along a linear trending, open natural fracture system. The long, linear orientation of this “jet” supports this theory. Another possible explanation for the location of this strong amplitude anomaly not corresponding with the reservoir simulation results is a local change in the in the frequency to porosity relationship described earlier in this report.

Figure 55 shows time slice 16 ms and its corresponding reservoir simulation layer #10. Strengthen the amplitudes have increased east of the injection point.

The locations of the amplitude anomalies noted on the flattened, scale adjusted Monitor survey and the reservoir simulation modeled CO_2 porosity distributions cannot be considered coincident. However, given the large number of variables involved in the seismic acquisition, processing, attribute interpretation, porosity modeling and reservoir simulation, the relationship suggested must be considered more than tenuous.

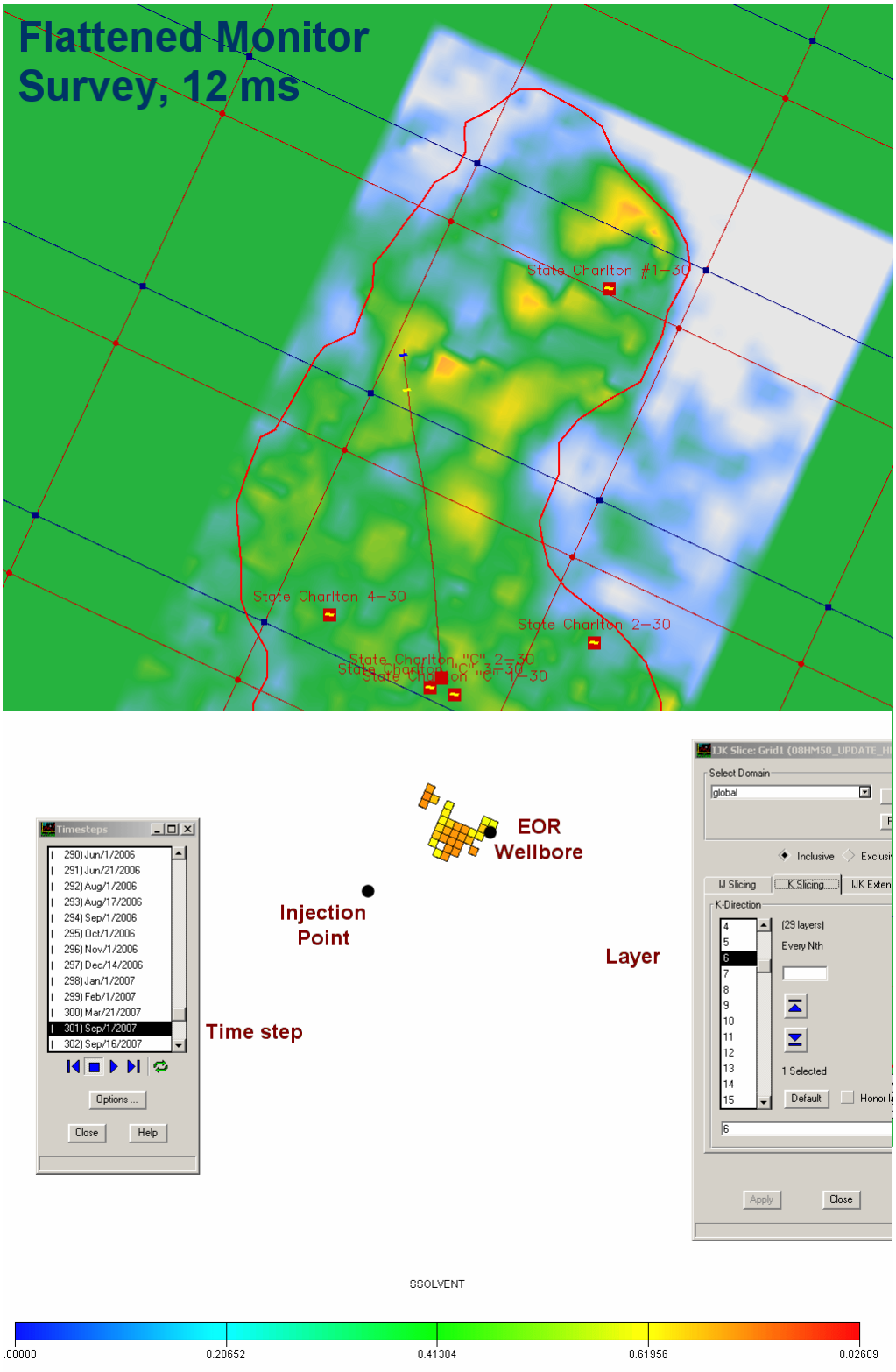

Figure 50: A2-Carbonate flattened Monitor survey time slice 12 ms with the layer 6 from the final reservoir simulation at times step September 2007.

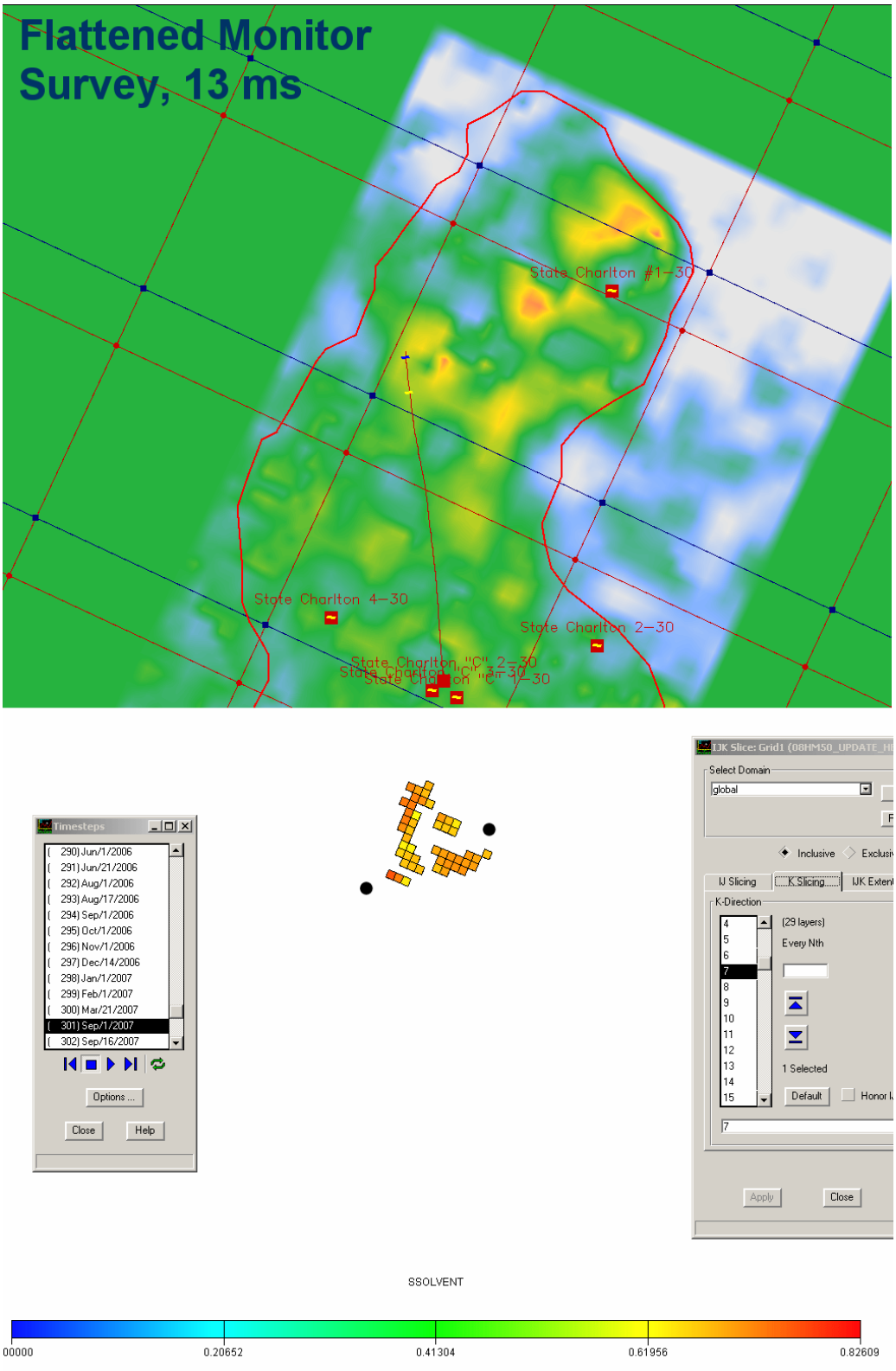

Figure 51: A2-Carbonate flattened Monitor survey time slice 13 ms with the layer 7 from the final reservoir simulation at times step September 2007.

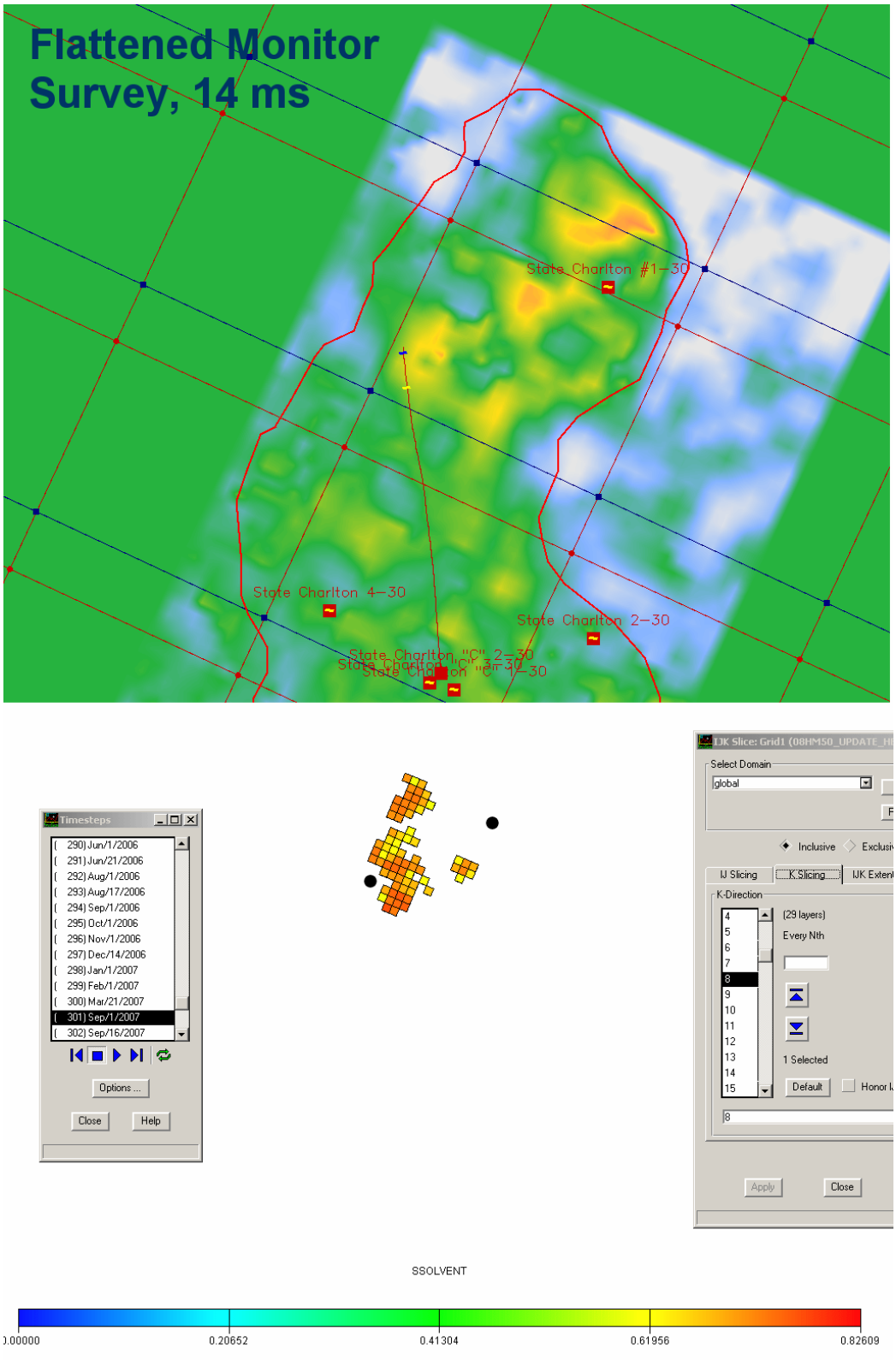

Figure 52: A2-Carbonate flattened Monitor survey time slice 14 ms with the layer 8 from the final reservoir simulation at times step September 2007.

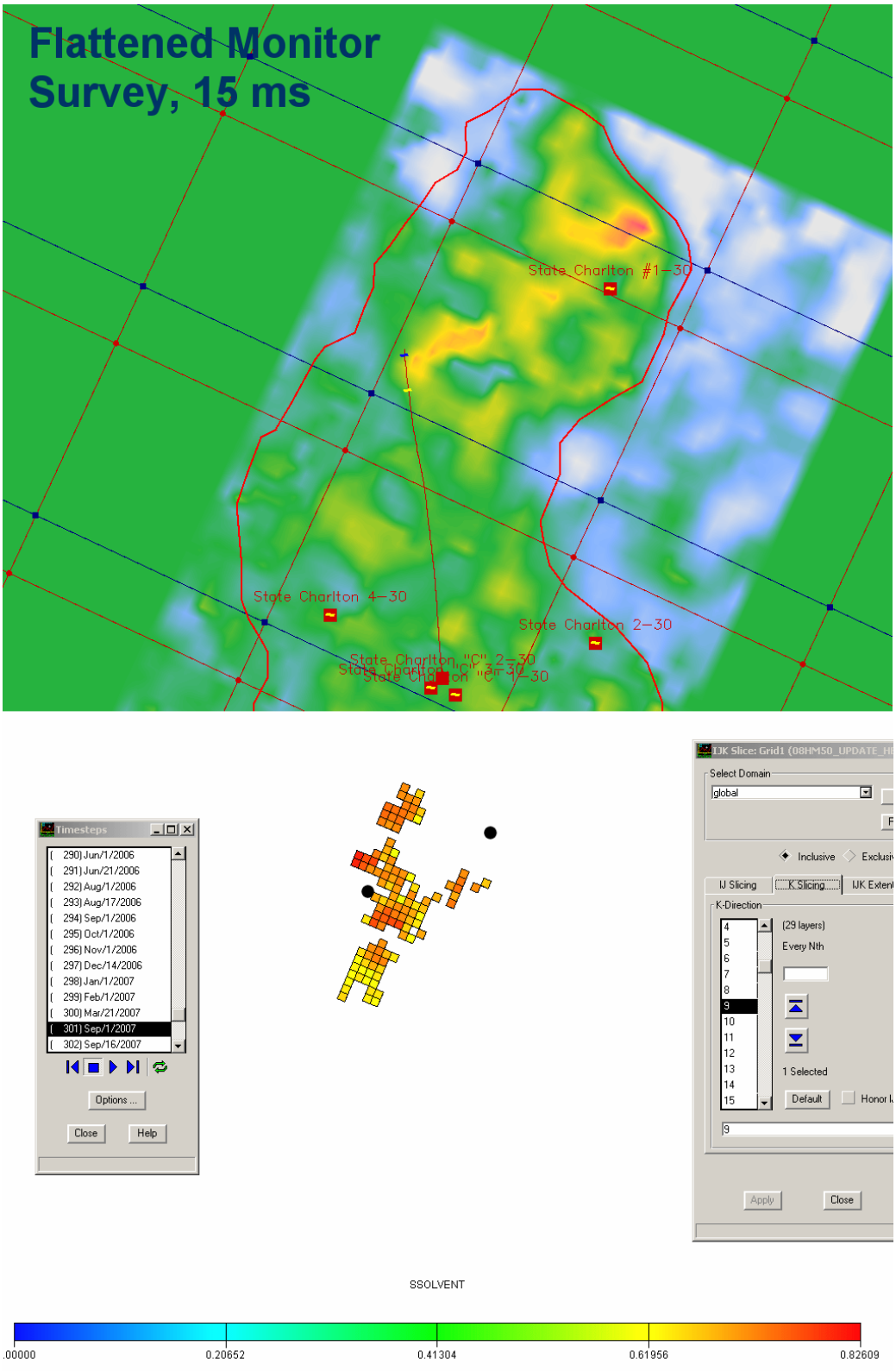

Figure 53: A2-Carbonate flattened Monitor survey time slice 15 ms with the layer 9 from the final reservoir simulation at times step September 2007.

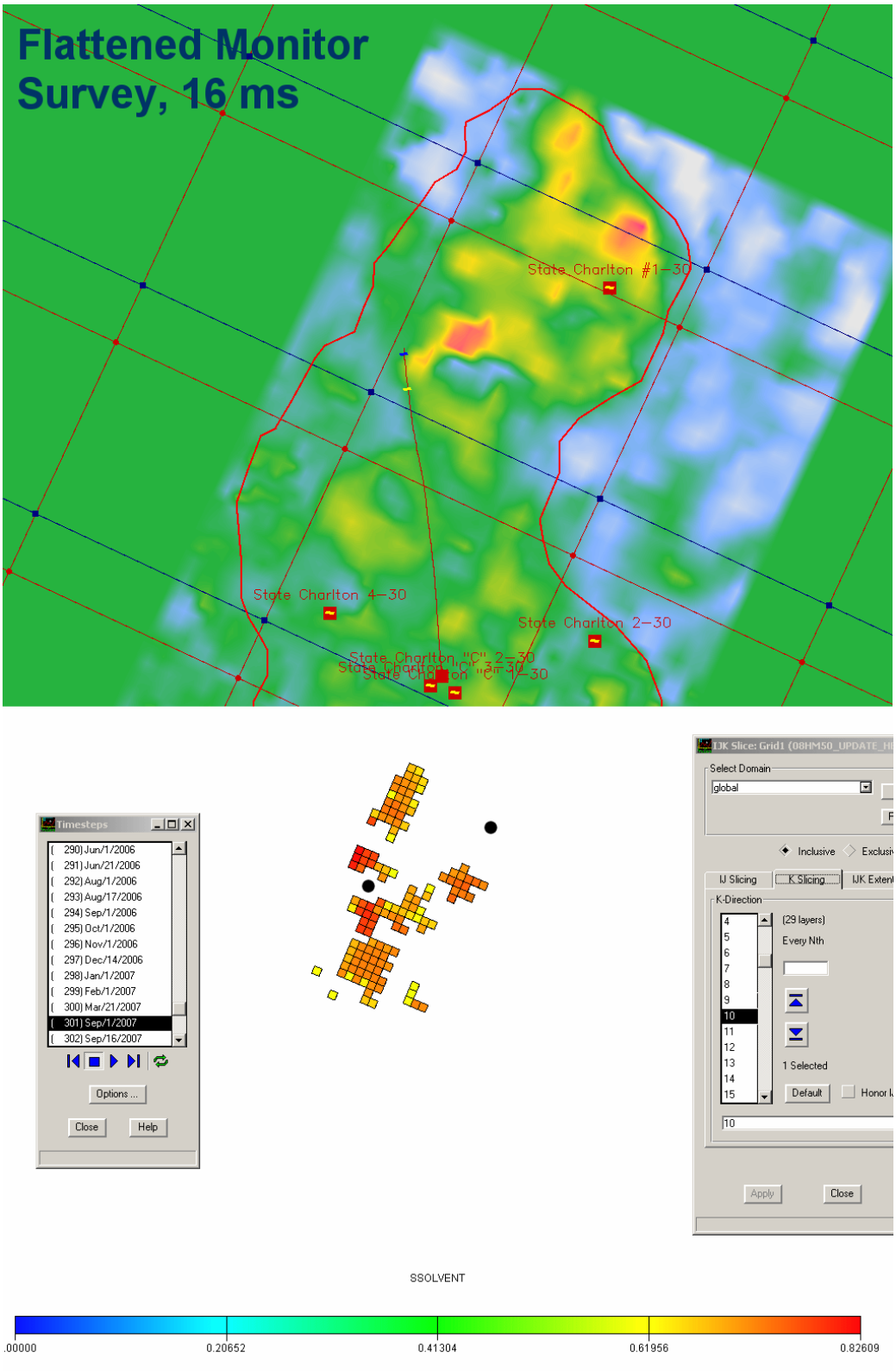

Figure 54: A2-Carbonate flattened Monitor survey time slice 16 ms with the layer 10 from the final reservoir simulation at times step September 2007.

6.3 Economic Impact

6.3.1 Northern Reef Trend's CO_2 EOR Potential

Given the understanding of the porosity distribution obtained during the investigation of Michigan's Northern Silurian Reef Trend and production performance from the most mature of the CO_2 floods, an estimate of the EOR potential for the entire reef trend can be made. Indicated EOR recovery from the mature floods in the trend is approximately 10% of the original oil in place (OOIP). The primary production phase of these carbonate reservoirs recovers approximately 25% of the OOIP, although, this can vary significantly depending upon well spacing effectiveness, reservoir compartmentalization, production strategy and drive mechanism, such as the degree of gravity segregation that may occur in the reservoir.

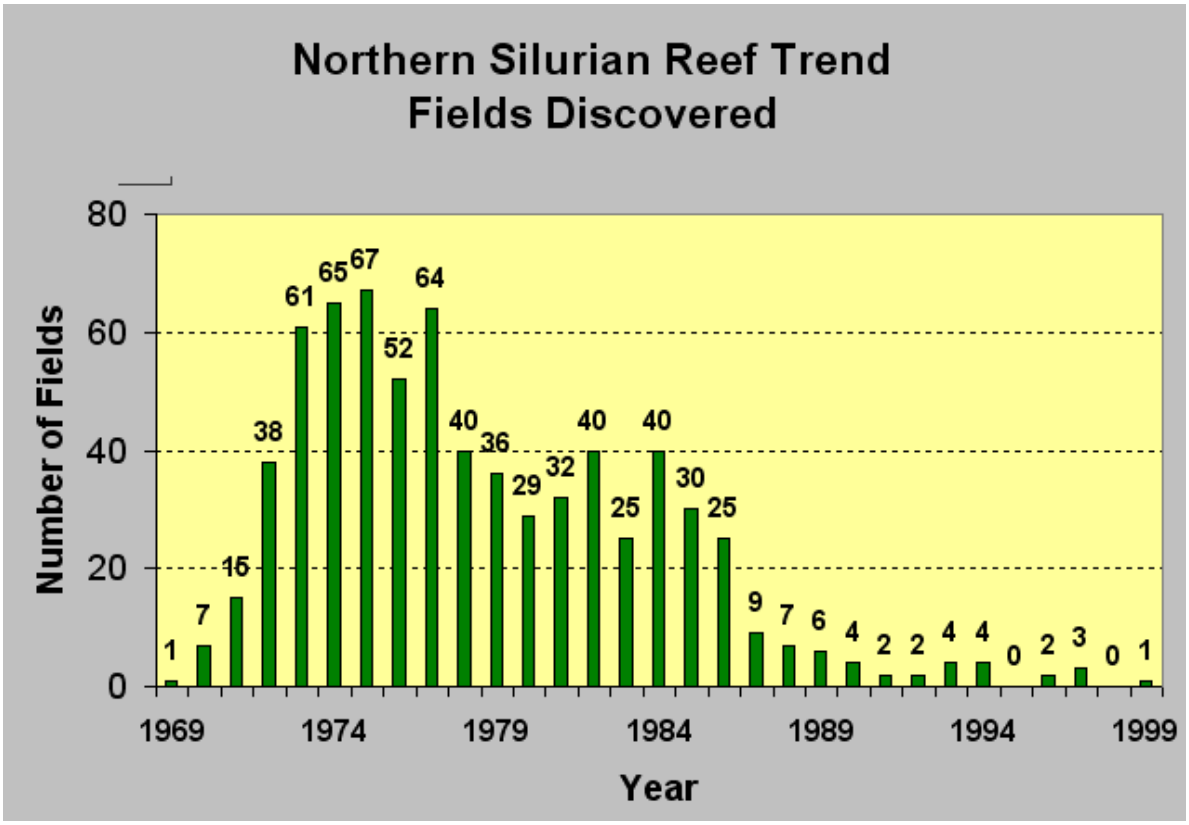

Graph 3: Reef discoveries by year for the Northern Reef Trend.

Data obtained from Michigan's DEQ, converted into digital form by Dr. Wood and his team at Michigan Technological University and evaluated during this project indicates that a total of 721 fields in the Northern Reef Trend have produced a total of 386.3 million barrels from 1969 until Nov 2007. This value includes production from secondary water flooding. Brock (1995) investigated hearing files at the MDEQ to identify fields permitted for secondary recovery efforts. Using this list and updating with additional MDEQ data sources, production from these fields, obtained after the start of water injection, is 37.3 MM bbls to November, 2007. When this is removed from the trend's primary production

349 MMBO may be attributed to primary production from the Northern Reef Trend. Graph 3 illustrates the discovery rate for the fields within this trend and indicates that the vast majority of the fields have been located and produced, although it should be noted that new reef discoveries are still being made, particularly in the western portion of the state. Graph 4 shows the oil production from the trend and indicates that the majority of the oil that should be expected to be produced during the primary production portion of these fields has occurred.

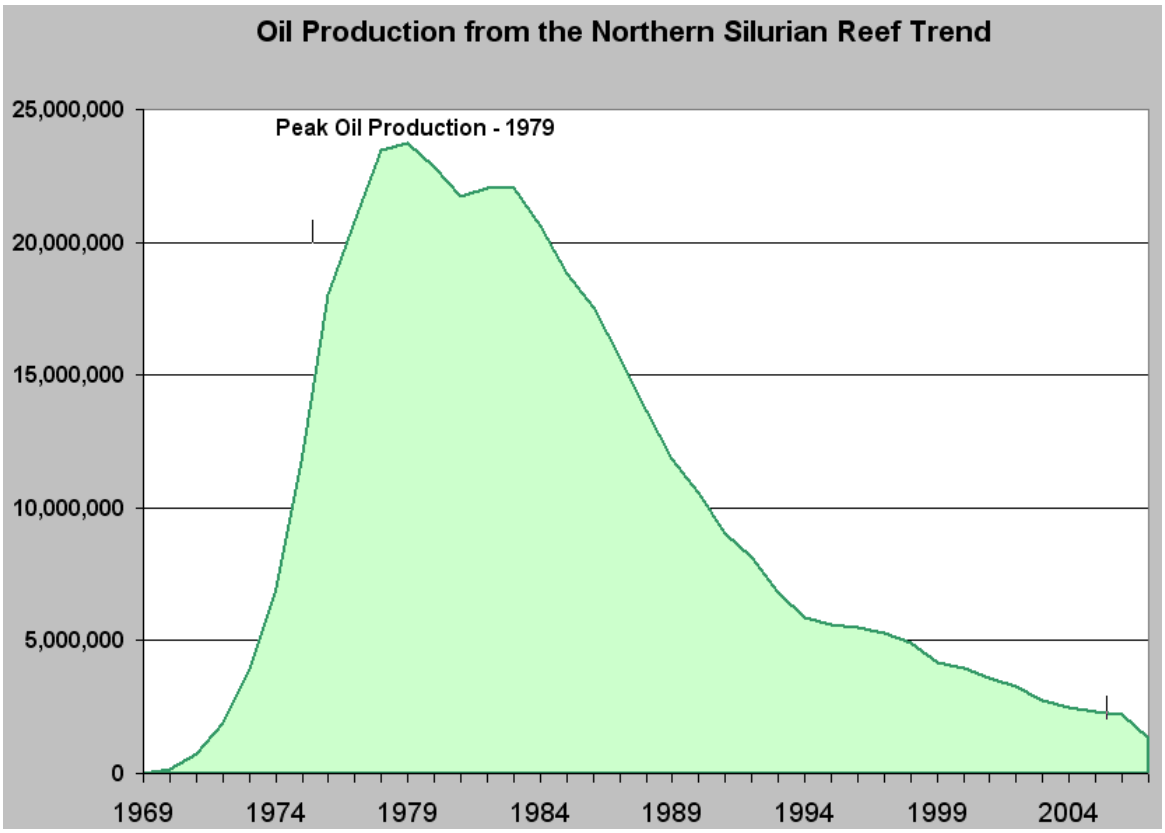

Graph 4: Oil Production by year since the discovery of the Northern Silurian Reef Trend.

If the 349 MMBO produced represents 25% of the OOIP, the Northern Reef Trend originally contained 1.4 billion barrels of oil and approximately 140 MMBO could be expected from CO_2 EOR processes. However, it is unrealistic to expect that it would be financially feasible to perform EOR operations on all 721 fields in the trend. Some economic cutoff, depending on the field's reserves and proximity to the CO_2 pipeline, would prevent operations within many of the smaller fields, at least until the CO_2 infrastructure had expanded significantly.

Using the available data set, 167 fields have been identified within the Northern Reef Trend as currently having cumulative production of 1 MMBO or more. Given today's oil price many operators would find the potential EOR yield from one of these fields to be quite attractive. This figure of 167 fields is in-line with Charpentier (1989) USGS Open-file Report 89-216 who reported that 224 fields within the trend had produced 1 MMBO equivalent. When the 62 gas fields that he had including in this figure are removed 162 oil fields had achieved this production figure at that time.

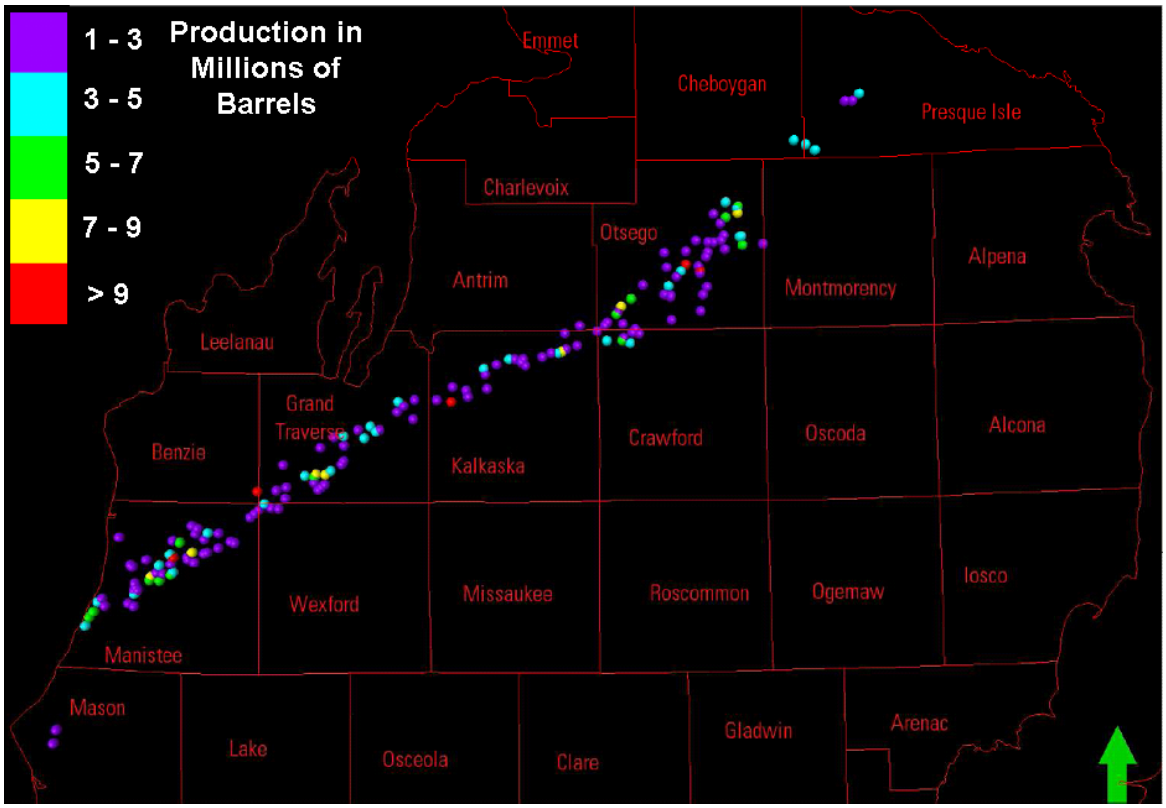

Figure 55: 167 fields that have produced 1 MMBO or more in the Northern Reef Trend.

These 167 fields have reportedly produced 271.2 million barrels from 1969 to November of 2007. Of these 167 fields 10 of them are reported to have been water flooded and have water injection wells. These fields have reported total production of 22.6 MMBO. When this production is removed the primary production from these fields is an estimated 248.6 million barrels. These figures reveal that 23% of the fields have produced 72% of all the Northern Reef Trend's primary oil production. Again, assuming that this figure represents 25% of the OOIP for these 167 fields, 99.5 MM bbls of EOR could be expected from these fields with CO_2. Figure #56 shows the location of these 167 fields and color codes them according to the amount of cumulative primary production. As can be seen in this figure these larger fields are not concentrated at any one location within the trend but are instead distributed throughout the trend indicating a general uniformity in production characteristics. This distribution would make the spread of the infrastructure needed to transport the CO_2 much more financially viable as it would be able to spread from larger field to larger field over short distances.

6.3.2 Northern Reef Trend's CO_2 Source Considerations

Associated CO_2 is currently removed from Devonian Antrim Shale formation natural gas at centralized gas processing plants in Otsego and adjacent counties. The majority of this processed CO_2 is currently vented to the atmosphere. However, as noted earlier Core Energy LLC. has been taking CO_2 from the emissions stream for use in their EOR operations and is capable of handling up to 11 MMcf/day in their compression and pipeline facilities. The largest gas processing plant has had an average annual production

of CO_2 for the last ten years of over 1 bcf/month. Total CO_2 production from all Antrim gas processing plants averages approximately 21bcf/year.

Cumulative production to date of combustible gas from the Antrim formation is approximately 2.5 TCF. Continued production from this play is estimated at an additional 23-28 years, resulting in total gas recovery of 5 TCF. CO_2 content, estimated at 15-30% in Antrim gas, would result in an ultimate resource of 375-750 BCF from Northern Michigan gas processing plants over the projected life of the play. This compares closely to the estimated total cumulative production from the Antrim of 525-630 BCF of CO_2.

Net CO_2 utilization factors range from 10-50 mcf/ bbl in CO_2-based EOR operations (Steve Meltzer, pers. comm.). Given the estimates of gross CO_2 supply, projected ultimate CO_2-based EOR from Niagaran reef reservoirs (using all Antrim gas processing plants CO_2 sources) is 25-75 MMBO. Initial estimates of net utilization factors of 6 mcf/bbl for CO_2-based EOR in two mature flood fields, Dover 33 and 36, suggest that estimates of incremental CO_2-based EOR using Antrim CO_2 may be more optimistic, and as high as 125 MMBO, if applied to the entire northern Niagaran reef trend. However, these estimates do not consider CO_2 recycling and re-injection, a method currently practiced in a number of these EOR projects.

6.3.3 Southern Reef Trend CO_2 EOR Potential

Using the methodology described in the previous section an estimate for the CO_2 EOR potential of Michigan's Southern Silurian Reef Trend can also be made. Since the porosity distribution within the Charlton 30/31 field was found to have a similar morphology as that reported by Wylie and Wood (2005) the same method for calculating the trend's EOR potential can be applied.

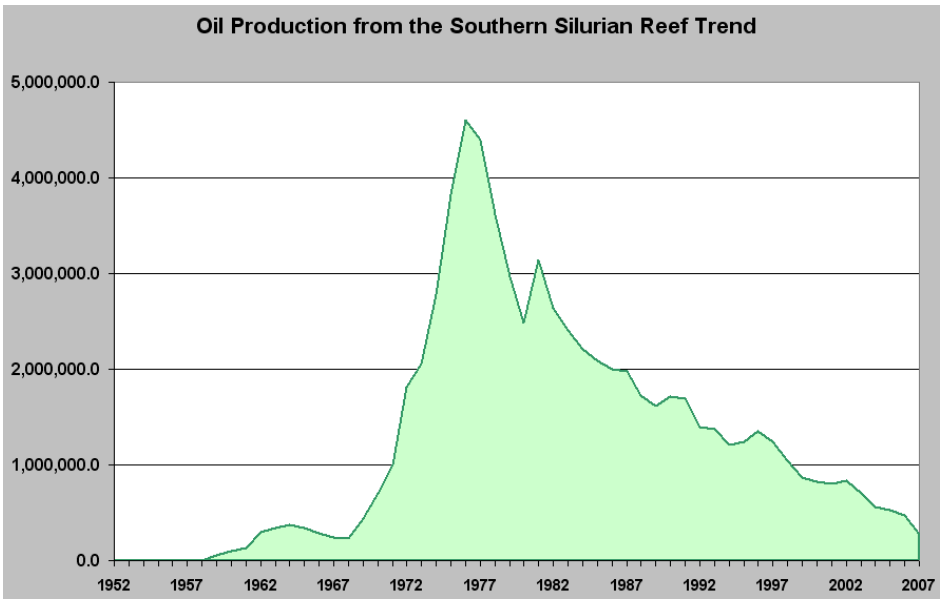

Graph 5: Oil Production by year since the discovery of the Southern Silurian Reef Trend.

Since its discovery in 1958 the Southern Silurian Reef Trend of the Michigan Basin has reportedly produced 71 million barrels of oil, see Graph 5. This production has been obtained from 333 fields. Using the same assumptions presented in the previous section, which includes removing 13.4 MMBO due to water injection, the total EOR potential for the Southern Trend is approximately 23 million barrels of oil.

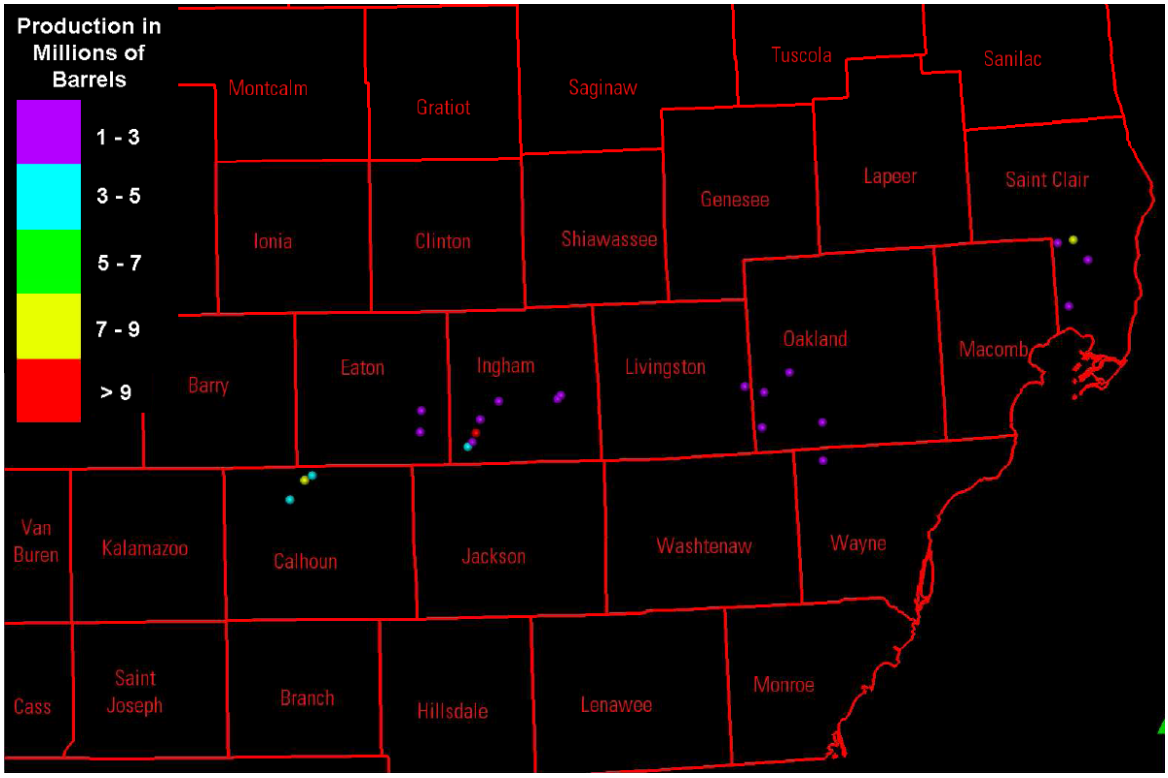

Figure 56: 23 fields that have produced 1 MMBO or more in the Southern Reef Trend.

Again many of these fields would not be immediately considered economic for conducting EOR operations with CO_2 because 310 of the fields (93% of the fields in the trend) have produced less than 1 million barrels of oil during their primary production phase. The remaining 7% (23 fields) have produced 37.2 million barrels or 52% of the trend's production. Figure 57 shows the location of these 23 fields. The EOR potential for these fields is calculated to be 10.1 million barrels.

An important concern with CO_2-based EOR projects in the Southern Reef Trend is the absence of the Antrim play in the southern part of Michigan to act as the source. However, other anthropogenic sources might be available. Four power generation facilities exist within the area of the Southern Reef Trend that produced significant amounts of CO_2. These four CO_2 sources have averaged a total of slightly more than 11 million tons of CO_2 a year for the past 10 years according to data obtained from the EPA's Clean Air Markets database. These are Detroit Edison's Saint Clair, MI facility (7.6 million tons per year average) located at the east end of the trend, the Lansing Board of Water and Light's Eckert Station facility (2 million tons per year average), the Lansing Board of Water and Light's Erickson facility (1 million tons per year average) and the Michigan South Central Power Agency's Endicott Generating facility (.5 million ton per year average) located just south of the trend.

These facilities are significant point sources of CO_2 that may eventually need to capture and sequester these CO_2 emissions. The amount of CO_2 produced by these power generation plants could easily fill a large number of reefs.

6.3.4 Economic Analysis Summary

The fields within Michigan's Silurian Reef Trends have produced almost a half billion (457 MM) barrels of oil and represent a significant oil resource within Michigan that could be exploited through CO_2 EOR operations. This is particularly true for the Northern Reef Trend. The total EOR potential for these two trends using CO_2 is estimated to be 168 MMBO. However, a more realistic figure, considering economic limitations, is believed to be 110 million barrels, 90% of this would be from the Northern Reef Trend.

7 CONCLUSIONS

7.1 Demonstration of cost-effective reservoir characterization technologies in preparation of CO_2 flooding.

This project has demonstrated that state-of-the-art, cost-effective, geophysically-based reservoir characterization technologies can be used to effectively image moderately deep, carbonate reservoirs. These technologies, when combined in a fully integrated geoscience/reservoir engineering approach, have been shown to produce a good understanding of key reservoir properties within these types of fields. This integration has included the following technologies;

- Rock property determination
- Forward seismic acquisition modeling
- 3-D seismic acquisition
- Seismic wavelet determination and analysis
- Well to seismic time generation
- Seismic frequency analysis
- Seismic attribute generation and interpretation
- Reservoir engineering data analysis
- Reservoir characterization methodologies
- Reservoir simulation
- Production history matching

These technologies have been combined to the extent that reservoir controlling properties, such as the porosity/permeability systems, have been accurately mapped out and used in the planning of CO_2 based enhanced oil recovery projects. The porosity predictions made prior to the drilling of the two new wells in the Charlton 30/31 Field strongly indicate that the low-frequency relationship with porosity zones greater than 5% does exist.

This relationship is also supported by the association of high amplitude anomalies on the A2-carbonate flattened, amplitude range shifted Monitor survey with the reservoir simulation predictions for the higher concentrations of CO_2 within the reef. Additionally, the porosity volume developed using the instantaneous frequency attribute from the Base 3-D survey also supported by the reservoir simulation history match.

This relationship is considered a major finding of the study having significant implications for the subsurface characterization of potential reservoirs. The accurate mapping of controlling reservoir properties when combined with detailed, reservoir simulations that have been validated through production history matching, will provide optimized and detailed plans for conducting enhanced oil recovery projects in the future. These optimized EOR projects will be the key to recovering not only the potential 168 million barrels of oil contained in the Silurian reef trends of the Northern and Southern Michigan basin but also the hundreds of millions of barrels of oil still contained in other reservoirs of the same type throughout the United States.

Additionally, these technologies may be applicable to the characterization of reservoirs under consideration for CO_2 sequestration projects. The identification of high porosity

zones within carbonates that may be under consideration for these types of projects would be extremely valuable when considering wellbore placement and CO_2 injectability.

7.2 Demonstration of advanced seismic technologies for monitoring CO_2 injection

This project has demonstrated that the monitoring of critical-phase CO_2 injected into moderate depth, carbonate reservoirs can be accomplished using state-of-the-art, cost-effective, 4D seismic technologies. While this project attempted precise 3-D survey repeatability it was not entirely achieved. However, the slight variations within the 4D seismic survey did not prevent the identification of the CO_2 within the subsurface.

Strong seismic amplitude anomalies are observable on the Monitor survey, which correspond approximately to zones of higher CO_2 concentrations predicted by the reservoir simulation. The amplitude differences observed between the A2-Carbonate flattened Base 3-D survey and the A2-Carbonate flattened, amplitude shifted Monitor survey have been shown to be stronger than those associated with the acquisition and processing of the data set. These amplitude anomalies are not only located within the upper portion of the reservoir but appear to follow its upper surface, as predicted by the reservoir simulation. This illustrates that the 4D seismic survey not only provides imaging of the CO_2 flood areally but also vertically within the reservoir. Additionally, the predictions that no CO_2 would be encountered at the new well locations at the time of their drilling support the understanding of the CO_2 distribution within the reservoir, which is supported by the 4D seismic survey.

The location of the amplitude anomalies confirm that the porosity/permeability system, developed from an understanding of the frequencies within the seismic data, is accurate. This confirmation allows the results from the reservoir simulation to be used in the planning of additional enhanced oil recovery wells, and thus optimizing the ultimate recovery from these reservoirs. This monitoring capability provides confirmation that the reservoir controlling parameters are either understood and that the EOR project should continue as planned or indicates that adjustments will need to be made. Recommendations for the drilling of additional wells into zones of higher porosity containing additional oil reserves were made as a result of this study.

The finding that critical phase CO_2 injected into moderate depth carbonate reservoirs can be monitored through the use of 4D seismic should be considered a key result of this project that has significant implications. The use of 4D seismic to monitor CO_2 based EOR projects will not only allow the adjustment of injector locations and injection parameters but will also help to identify zones that have been bypassed by the CO_2 sweep. These bypassed zones can then be targeted with additional boreholes. As a result a significant amount of the 168 million barrels of oil in the Northern and Southern Michigan basin reef trends could be recoverable.

The application of this technology to image critical phase CO_2 injected into carbonate reservoirs has implications outside of the enhanced oil recovery industry. In the near future subsurface CO_2 sequestration projects will be conducted throughout the world. It is believed that this 4D surface seismic technology provides considerable advantages for these projects. Surface, P-wave 3-D seismic surveys can be acquired over large areas prior to the drilling of wells. Interpretation of these surveys will be of great benefit for reservoir characterization and cap rock integrity studies and the planning of the well or wells to be used for injection. Once injection has commenced and progressed to a certain

point additional 3-D surveys can be acquired in order to ensure the injected CO_2 is remaining within the targeted reservoir and the cap rock integrity is being maintained.

The successful application of the technologies and methodologies discussed in this report demonstrate how enhanced oil recovery projects can be optimized. As a result of the reservoir characterization developed from the seismic attributes extracted from the Base 3D survey the understanding of the porosity/permeability system within this reef was greatly increased. The confirmation, or at least the support, that this understand is essentially correct was provided by the results from two new wells and the amplitude anomalies seen on the Monitor survey.

This supported the results of the reservoir simulation and allowed recommendations concerning the additional drilling and the distribution of oil within the reservoir. See Appendix H for results from the reservoir simulation concerning the oil distribution within the reef at time step September, 2007.

8 REFERENCES

Cercone, Karen Rose, and Lohmann, Kyger C., 1987, Late Burial Diagenesis of Niagaran (Middle Silurian) Pinnacle Reefs in Michigan Basin: Bulletin of the American Association of Petroleum Geologists, Vol. 71, NO. 2, PP 156-166

Ferdinand, Kevin, The Integration of Seismic Attributes and Rock Properties for Mapping Porosity Thickness in the Heterogeneous Grayburg Carbonate Reservoir, Corrigan Cowden Unit West Texas, AAPG Annual Meeting, March 10-13, 2002 Houston, Texas

Gill, D., 1973, Stratigraphy facies, evolution and diagenesis of productive Niagaran Guelph reefs and Cayugan sabkha deposits, the Belle River Mills gas field, Michigan Basin: Unpublished Ph.D. Thesis, University of Michigan, 275 p.

Gill, D., 1977, Salina A-1 Sabkha Cycles and the late Silurian Paleogeography of the Michigan Basin: Journal of Sedimentary Petrology, Vol. 47, NO. 3, PP 979-1017

Gill, D., 1979, Differential Entrapment of Oil and Gas in Niagaran Pinnacle-Reef Belt of Northern Michigan, Bulletin of the American Association of Petroleum Geologists, Vol. 63, NO. 4, PP 608-620

Gill, D., 1994, Niagaran Reefs of Northern Michigan, Part I: Exploration Portrait: Journal of Petroleum Geology, Vol. 17(1), PP99-110

Indiana University Paleontology Seminar, 1980, Stratigraphy, Structure, and Zonation of Large Silurian Reef at Delphi, Indiana: Bulletin of the American Association of Petroleum Geologists, Vol. 64, NO. 1, PP 115-131

Indiana University Paleontology Seminar, 1976, Silurian Reef Complex, Rockford, Ohio: Constitution, Growth, and Significance: Bulletin of the American Association of Petroleum Geologists, Vol. 60, NO. 3, PP 428-451

Ingels, Jerome J. C., 1963, Geometry, Paleontology, and Petrography of Thornton Reef Complet, Silurian of Northeastern Illinois: Bulletin of the American Association of Petroleum Geologists, Vol. 47, NO. 3, PP 405-440

Jodry, Richard L., 1969, Growth and Dolomitization of Silurian Reefs, St. Clair County, Michigan: Bulletin of the American Association of Petroleum Geologists, Vol. 53, NO. 4, PP 957-981

Melhorn, Wilton N., 1958, Stratigraphic Analysis of Silurian Rocks in Michigan Basin: Bulletin of the American Association of Petroleum Geologists, Vol. 42, NO. 4, PP 816-838

Mesolella, K. J., Robinson, J. D., McCormick, L. M. and Ormiston, A. R., Cyclic Deposition of Silurian Carbonates and Evaporites in Michigan Basin: Bulletin of the American Association of Petroleum Geologists, Vol. 58, NO. 1, PP 34-62

Shaver, Robert H., 1974, Silurian Reefs of Northern Indiana: Reef and Interreef Macrofaunas: Bulletin of the American Association of Petroleum Geologists, Vol. 58, NO. 6, PP 934-956

Shaver, Robert H., 1977, Silurian Reef Geometry – New Dimensions to Explore: Journal of Sedimentary Petrology, Vol. 47, NO. 4, PP 1409-1424

Simo, J. A. and Lehmann, Patrick J., 2000, Diagenetic History of Pipe Creek JR. Reef, Silurian, North-Central Indiana, U.S.A.: Journal of Sedimentary Research, Vol. 70, NO. 4, PP 937-951

Wylie, Albert S. and Wood, James R., 2005, Well-log tomography and 3-D Imaging of Core and Log-Curve Amplitudes in a Niagraran Reef, Belle River Mills Field, St. Clair County, Michigan, United States.

9 LIST OF ACRONYMS

ANA – Anomalous noise attenuation

API American Petroleum Institute

AVAZ Amplitude versus azimuth

AVO Amplitude versus offset

BARS Borehole Acoustic Reflection Survey

Bbls - barrels

BCF – Billions of cubic feet

BHP – Bottom hole pressure

BOPD – Barrels of oil per day

BOWD – Barrels of water per day

CDP – common depth point

CO2 – Carbon Dioxide

COR Contracting Officer's Representative

CPS-3 (binary format) –

DCS Data and Consulting Services

DOE – Department of Energy

ECS Elemental Capture Spectroscopy

EOR – Enhanced Oil Recovery

Ft - feet

FXCNS – FX Coherent noise suppression

GOR – Gas to Oil Ratio

IESX -

LPM Log Property Mapping

MBWP- Model-based wavelet processing

MI DEQ – Michigan Department of Environmental Quality

MI – Michigan

MMBO – million barrels of oil

MMSCF – Million standard cubic feet

MMSCFD – Million standard cubic feet per day

MTU – Michigan Technological University

NETL National Energy Technology Laboratory

OOIP – Original oil in place

OTA Office of Technology Assessment

PSTM – Pre-stack time migration

p-wave – Primary [seismic] wave

QC – Quality control

SCAC – Surface-consistent amplitude compensation

TCF – Trillion cubic feet

US – United States

VSP – Vertical Seismic Profile

WV West Virginia

10 Tools Used

Petrel static model construction package

GeoFrame geophysical workstation

Gemini Forward Ray-traced modeling package

AVOlog

11 APPENDICES

11.1 Appendix A - Reservoir Simulation Results – CO_2 Concentrations greater than 60% at Time Step September, 2007

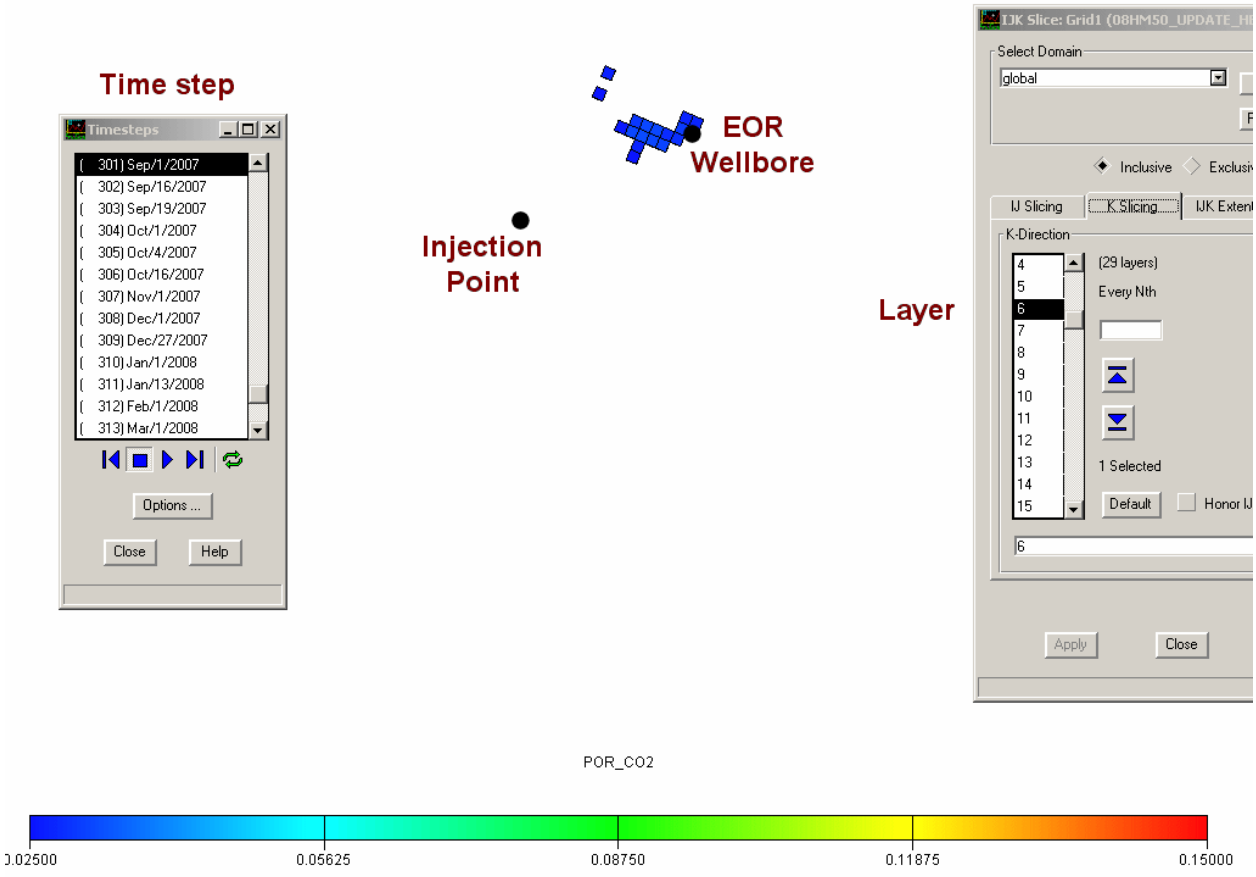

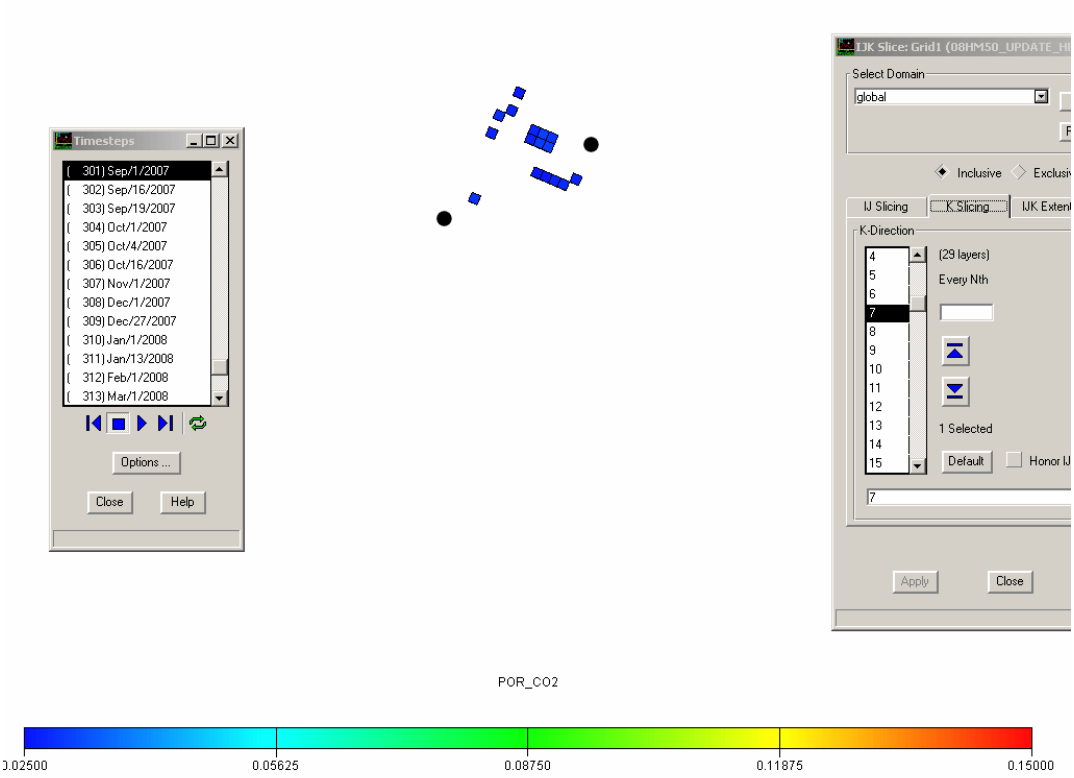
Timesteps
(301) Sep/1/2007
(302) Sep/16/2007
(303) Sep/19/2007
(304) Oct/1/2007
(305) Oct/4/2007
(306) Oct/16/2007
(307) Nov/1/2007
(308) Dec/1/2007
(309) Dec/27/2007
(310) Jan/1/2008
(311) Jan/13/2008
(312) Feb/1/2008
(313) Mar/1/2008
Options ...
Close
Help
IJK Slice: Grid1 (08HM50_UPDATE_HI
Select Domain
global
Inclusive
IJ Slicing
K Slicing
IJK Extent
K-Direction
4
5
6
7
8
9
10
11
12
13
14
15
(29 layers)
Every Nth
1 Selected
Default
Honor IJ
7
Apply
Close
POR_CO2
0.02500
0.05625
0.08750
0.11875
0.15000

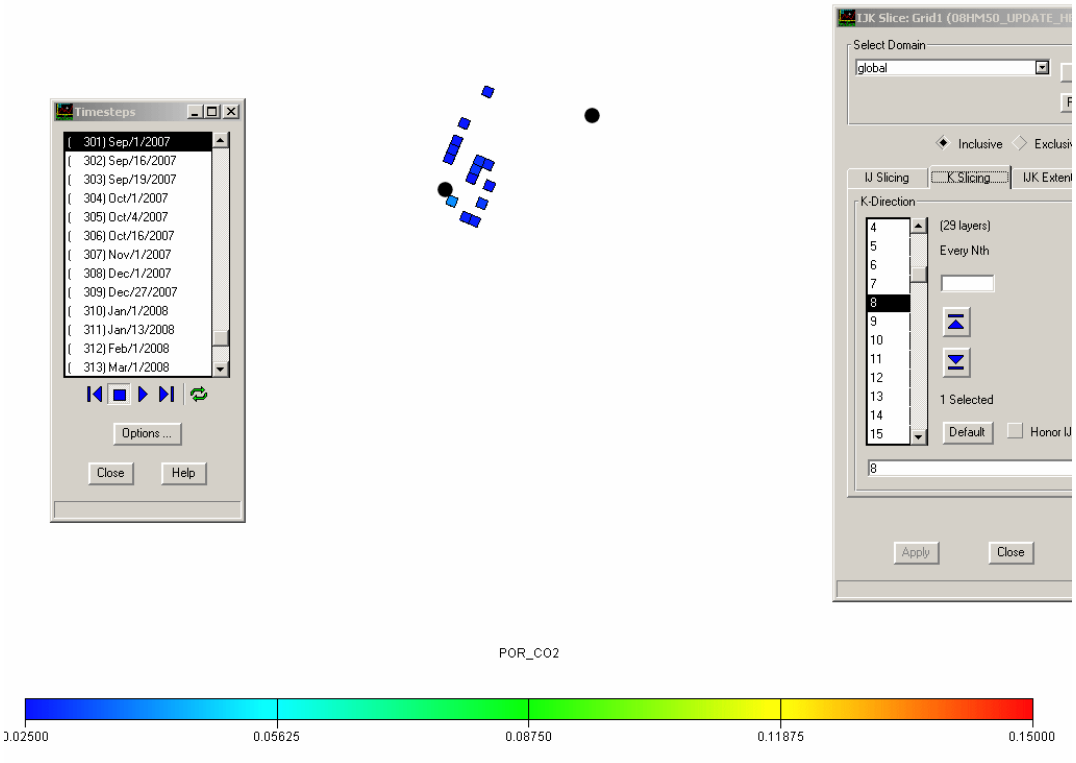
Timesteps
(301) Sep/1/2007
(302) Sep/16/2007
(303) Sep/19/2007
(304) Oct/1/2007
(305) Oct/4/2007
(306) Oct/16/2007
(307) Nov/1/2007
(308) Dec/1/2007
(309) Dec/27/2007
(310) Jan/1/2008
(311) Jan/13/2008
(312) Feb/1/2008
(313) Mar/1/2008
Options ...
Close
Help
IJK Slice: Grid1 (08HM50_UPDATE_H
Select Domain
global
Inclusive
IJ Slicing
K Slicing
IJK Extent
K-Direction
4
5
6
7
8
9
10
11
12
13
14
15
(29 layers)
Every Nth
1 Selected
Default
Honor IJ
8
Apply
Close
POR_CO2
0.02500
0.05625
0.08750
0.11875
0.15000

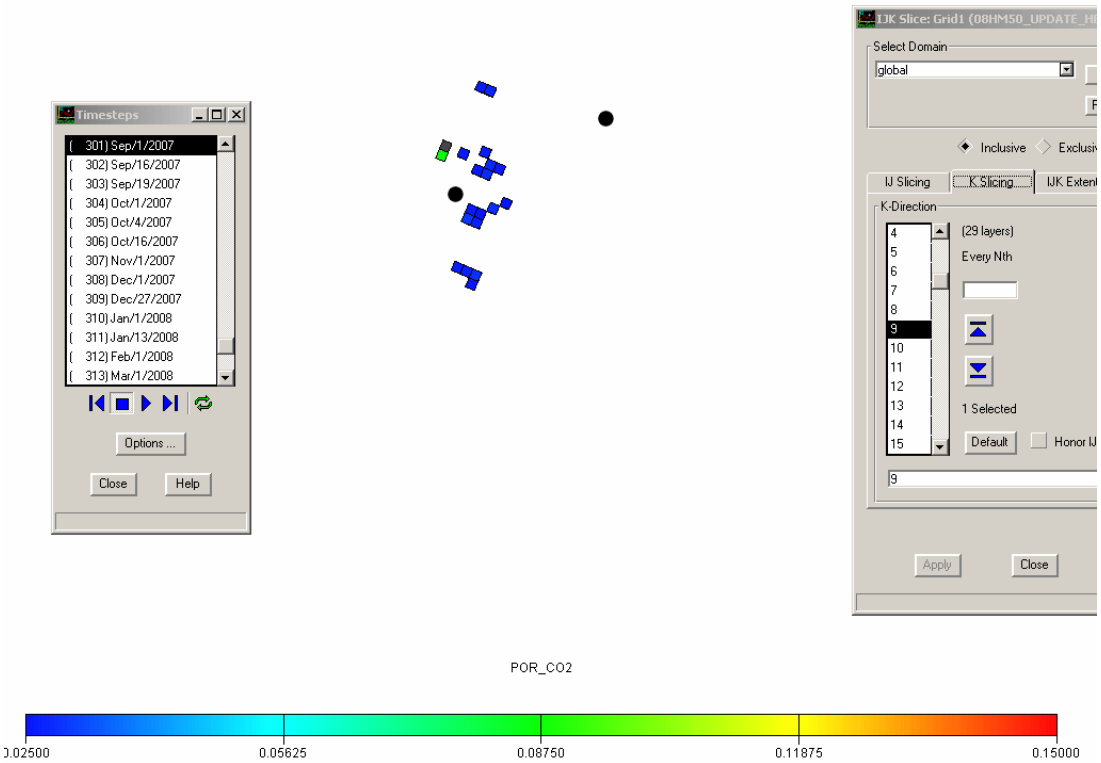
Timesteps
(301) Sep/1/2007
(302) Sep/16/2007
(303) Sep/19/2007
(304) Oct/1/2007
(305) Oct/4/2007
(306) Oct/16/2007
(307) Nov/1/2007
(308) Dec/1/2007
(309) Dec/27/2007
(310) Jan/1/2008
(311) Jan/13/2008
(312) Feb/1/2008
(313) Mar/1/2008
Options ...
Close
Help
IJK Slice: Grid1 (08HM50_UPDATE_H
Select Domain
global
Inclusive
IJ Slicing
K Slicing
IJK Extent
K-Direction
4
5
6
7
8
9
10
11
12
13
14
15
(29 layers)
Every Nth
1 Selected
Default
Honor IJ
9
Apply
Close
POR_CO2
0.02500
0.05625
0.08750
0.11875
0.15000

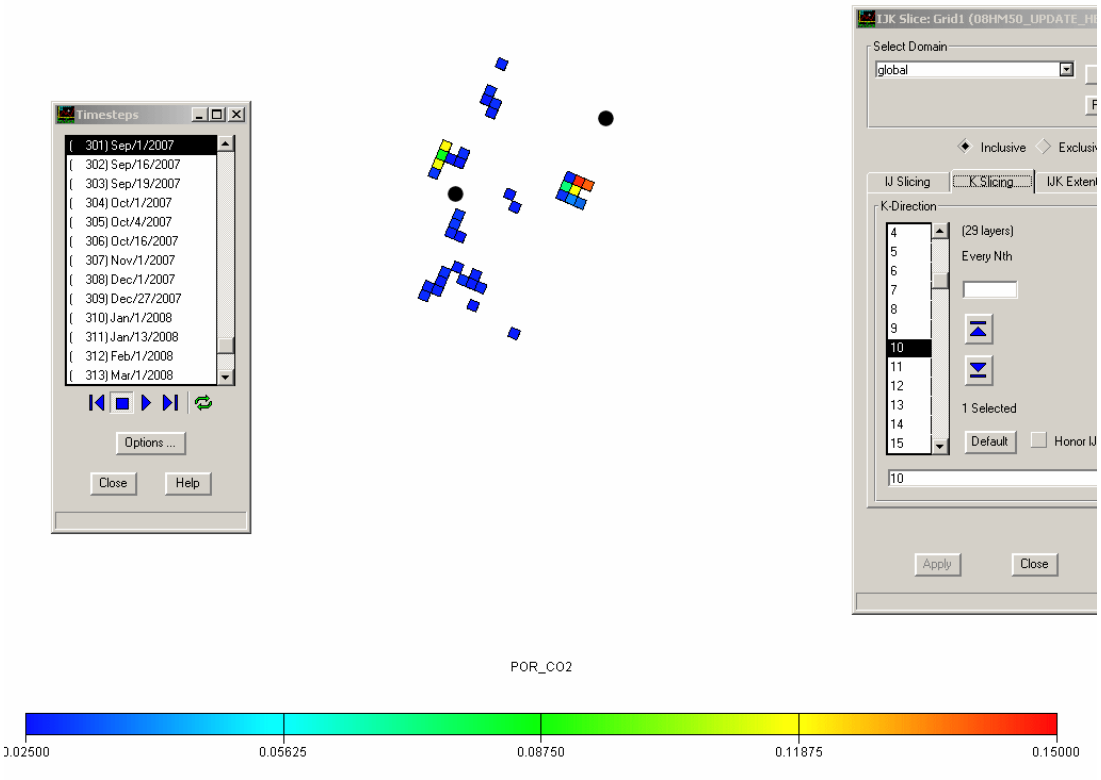
Timesteps
301] Sep/1/2007
302] Sep/16/2007
303] Sep/19/2007
304] Oct/1/2007
305] Oct/4/2007
306] Oct/16/2007
307] Nov/1/2007
308] Dec/1/2007
309] Dec/27/2007
310] Jan/1/2008
311] Jan/13/2008
312] Feb/1/2008
313] Mar/1/2008
Options ...
Close
Help
IJK Slice: Grid1 (08HM50_UPDATE_H
Select Domain
global
Inclusive
IJ Slicing
K Slicing...
K-Direction
(29 layers)
Every Nth
1 Selected
Default
10
Apply
Close
POR_CO2
0.02500
0.05625
0.08750
0.11875
0.15000

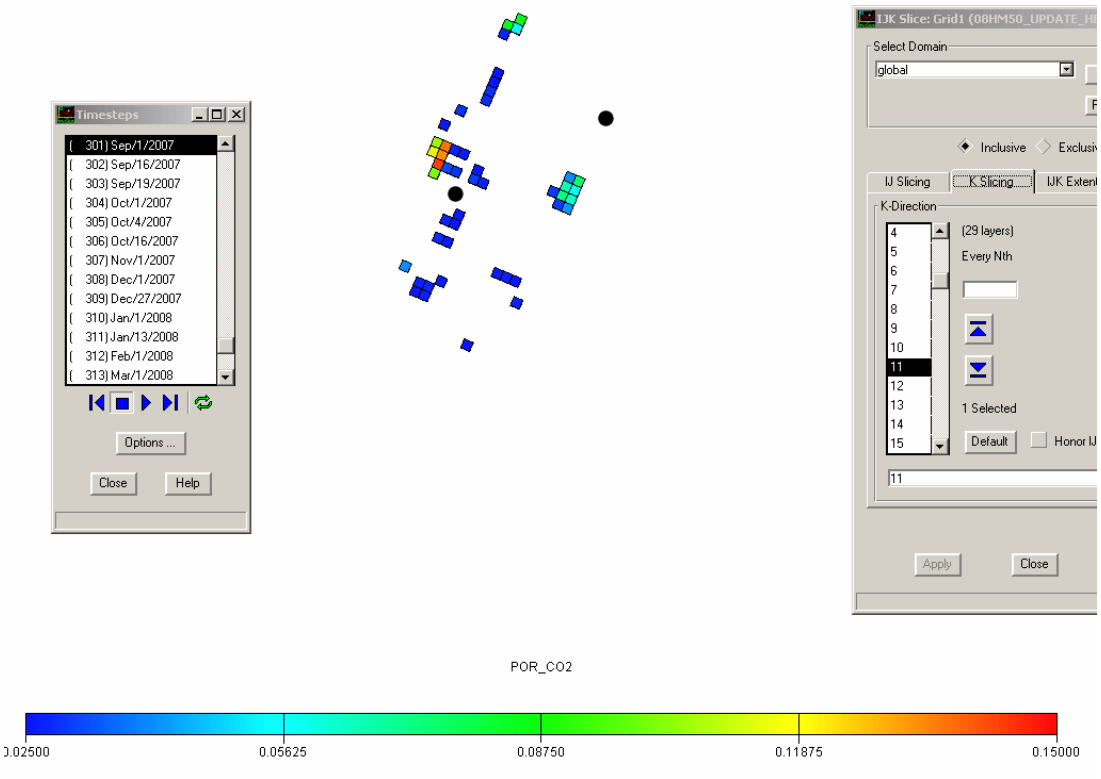
Timesteps
301] Sep/1/2007
302] Sep/16/2007
303] Sep/19/2007
304] Oct/1/2007
305] Oct/4/2007
306] Oct/16/2007
307] Nov/1/2007
308] Dec/1/2007
309] Dec/27/2007
310] Jan/1/2008
311] Jan/13/2008
312] Feb/1/2008
313] Mar/1/2008
Options ...
Close
Help
IJK Slice: Grid1 (08HM50_UPDATE_H
Select Domain
global
Inclusive
IJ Slicing
K Slicing...
K-Direction
(29 layers)
Every Nth
1 Selected
Default
11
Apply
Close
POR_CO2
0.02500
0.05625
0.08750
0.11875
0.15000

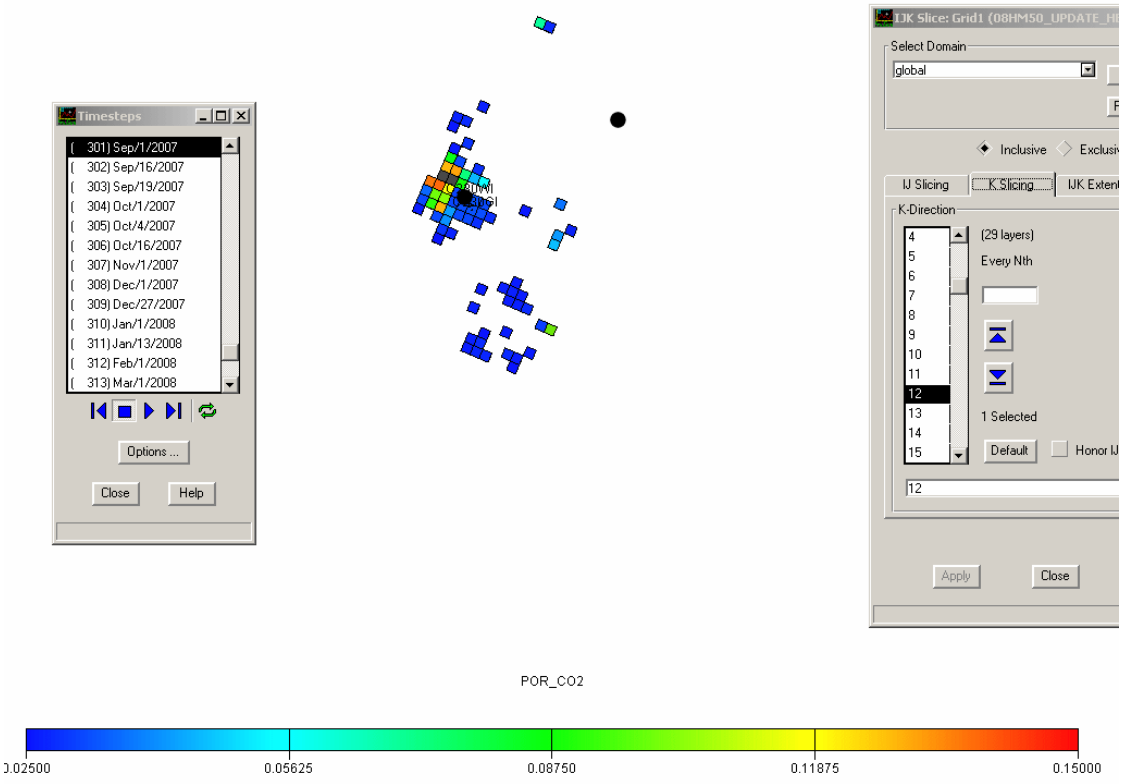
Timesteps
(301) Sep/1/2007
(302) Sep/16/2007
(303) Sep/19/2007
(304) Oct/1/2007
(305) Oct/4/2007
(306) Oct/16/2007
(307) Nov/1/2007
(308) Dec/1/2007
(309) Dec/27/2007
(310) Jan/1/2008
(311) Jan/13/2008
(312) Feb/1/2008
(313) Mar/1/2008
Options ...
Close
Help
IJK Slice: Grid1 (08HM50_UPDATE_HI
Select Domain
global
Inclusive
IJ Slicing
K Slicing
IJK Extent
K-Direction
4
5
6
7
8
9
10
11
12
13
14
15
(29 layers)
Every Nth
1 Selected
Default
Honor IJ
12
Apply
Close
POR_CO2
0.02500
0.05625
0.08750
0.11875
0.15000

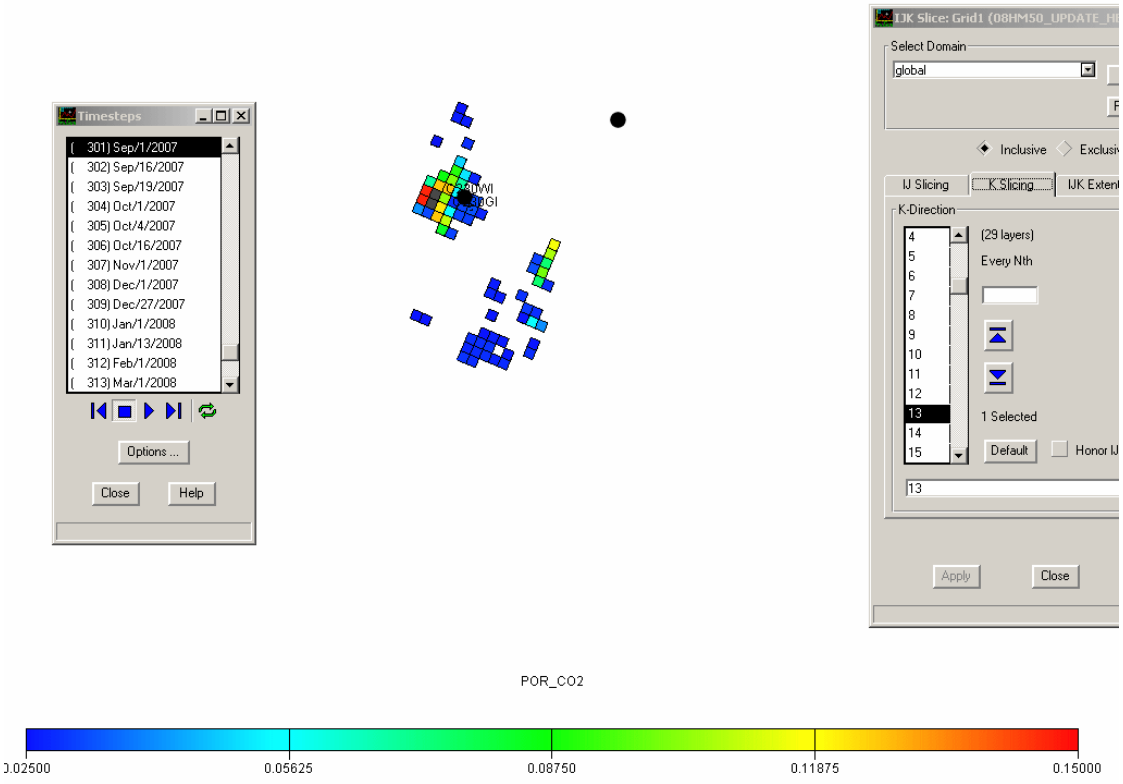
Timesteps
(301) Sep/1/2007
(302) Sep/16/2007
(303) Sep/19/2007
(304) Oct/1/2007
(305) Oct/4/2007
(306) Oct/16/2007
(307) Nov/1/2007
(308) Dec/1/2007
(309) Dec/27/2007
(310) Jan/1/2008
(311) Jan/13/2008
(312) Feb/1/2008
(313) Mar/1/2008
Options ...
Close
Help
IJK Slice: Grid1 (08HM50_UPDATE_HI
Select Domain
global
Inclusive
IJ Slicing
K Slicing
IJK Extent
K-Direction
4
5
6
7
8
9
10
11
12
13
14
15
(29 layers)
Every Nth
1 Selected
Default
Honor IJ
13
Apply
Close
POR_CO2
0.02500
0.05625
0.08750
0.11875
0.15000

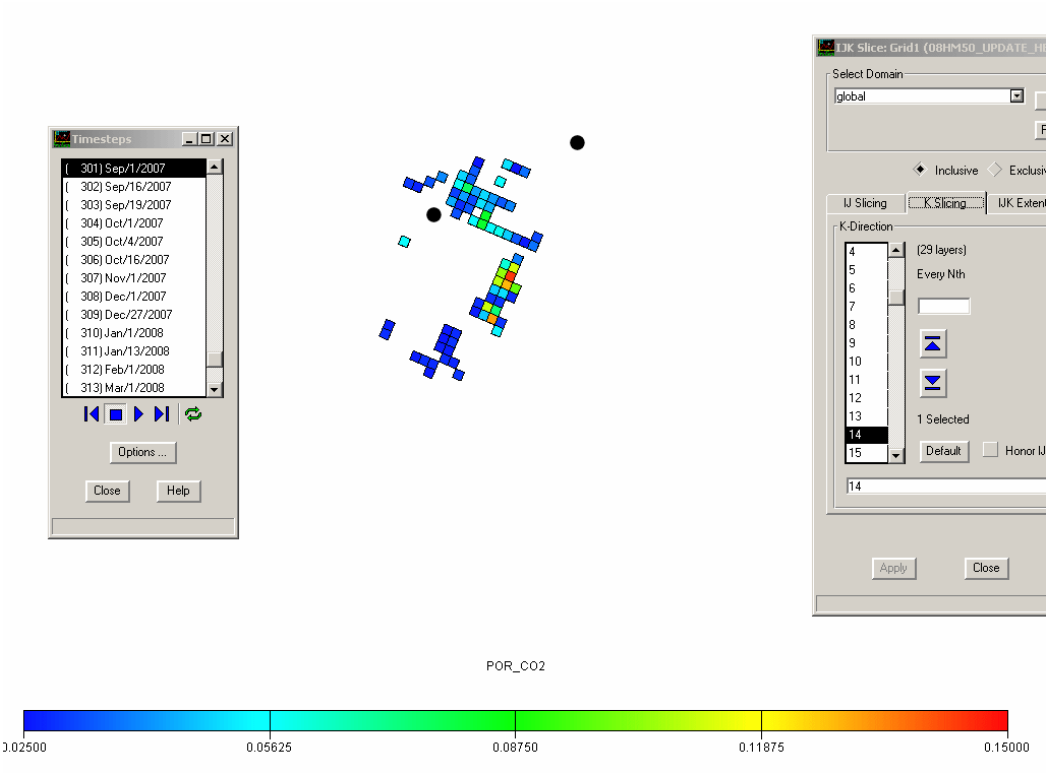
Timesteps
(301) Sep/1/2007
(302) Sep/16/2007
(303) Sep/19/2007
(304) Oct/1/2007
(305) Oct/4/2007
(306) Oct/16/2007
(307) Nov/1/2007
(308) Dec/1/2007
(309) Dec/27/2007
(310) Jan/1/2008
(311) Jan/13/2008
(312) Feb/1/2008
(313) Mar/1/2008
Options ...
Close
Help
IJK Slice: Grid1 (08HM50_UPDATE_HI
Select Domain
global
Inclusive
IJ Slicing
K Slicing
IJK Extent
K-Direction
(29 layers)
Every Nth
1 Selected
Default
Honor IJ
14
Apply
Close
POR_CO2
0.02500
0.05625
0.08750
0.11875
0.15000

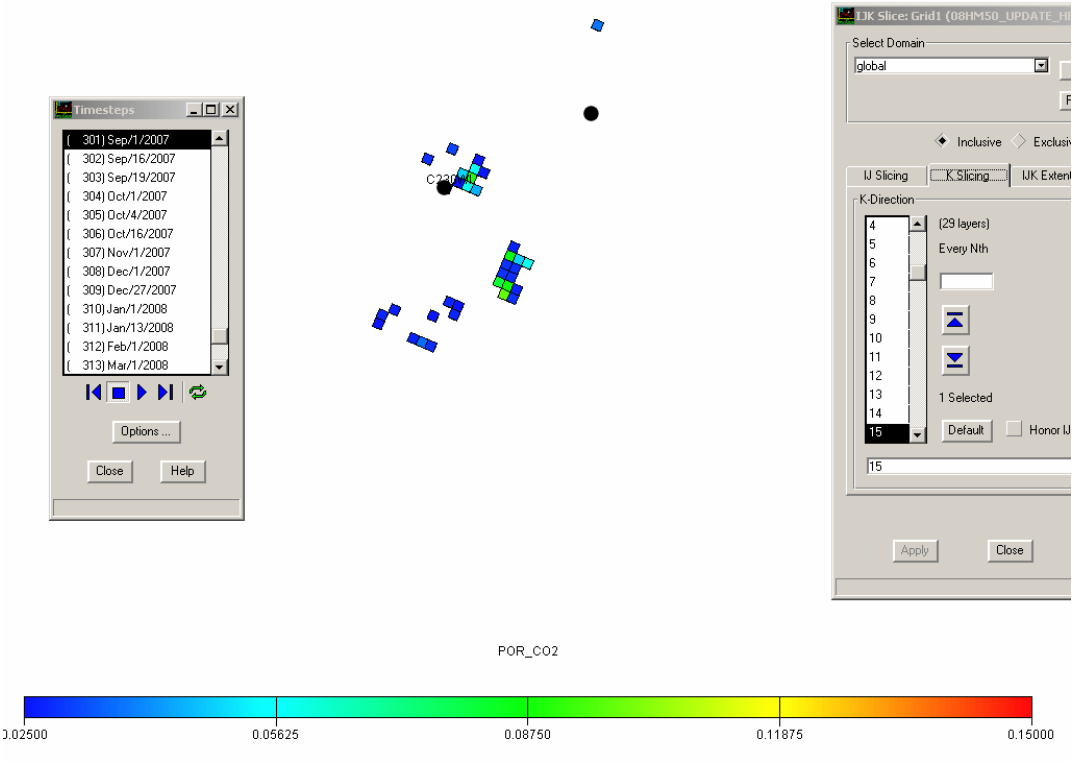
Timesteps
(301) Sep/1/2007
(302) Sep/16/2007
(303) Sep/19/2007
(304) Oct/1/2007
(305) Oct/4/2007
(306) Oct/16/2007
(307) Nov/1/2007
(308) Dec/1/2007
(309) Dec/27/2007
(310) Jan/1/2008
(311) Jan/13/2008
(312) Feb/1/2008
(313) Mar/1/2008
Options ...
Close
Help
IJK Slice: Grid1 (08HM50_UPDATE_HI
Select Domain
global
Inclusive
IJ Slicing
K Slicing
IJK Extent
K-Direction
(29 layers)
Every Nth
1 Selected
Default
Honor IJ
15
Apply
Close
POR_CO2
0.02500
0.05625
0.08750
0.11875
0.15000

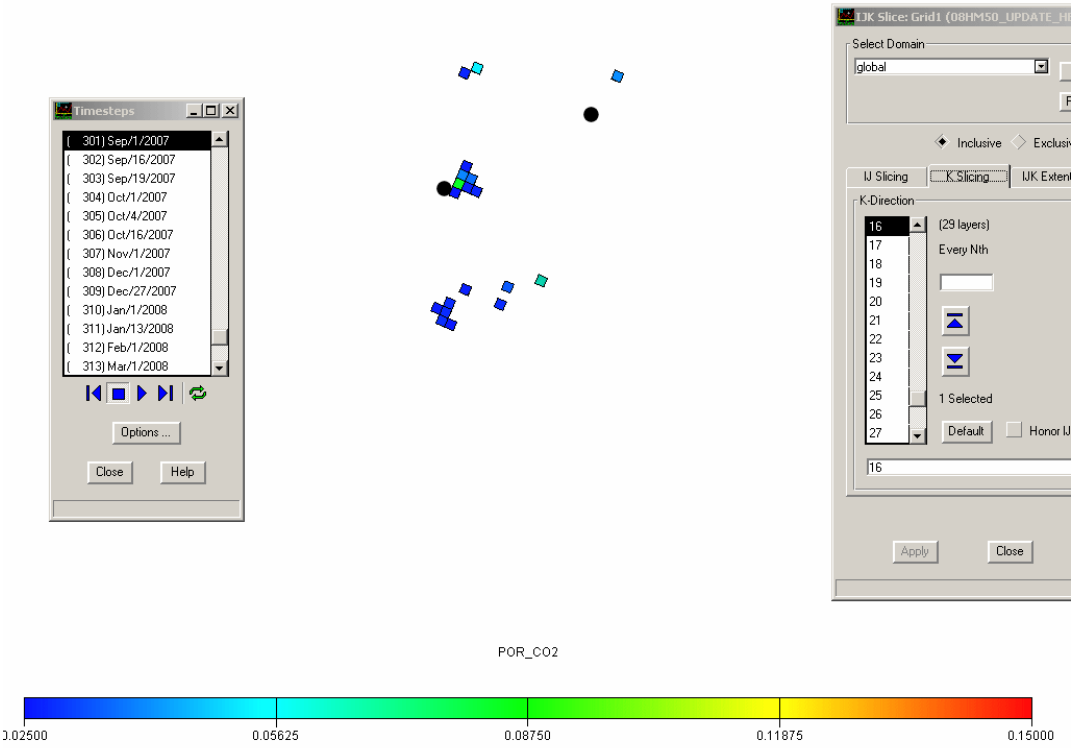
Timesteps
(301) Sep/1/2007
(302) Sep/16/2007
(303) Sep/19/2007
(304) Oct/1/2007
(305) Oct/4/2007
(306) Oct/16/2007
(307) Nov/1/2007
(308) Dec/1/2007
(309) Dec/27/2007
(310) Jan/1/2008
(311) Jan/13/2008
(312) Feb/1/2008
(313) Mar/1/2008
Options ...
Close
Help
IJK Slice: Grid1 (08HM50_UPDATE_H
Select Domain
global
Inclusive
IJ Slicing
K Slicing
IJK Extent
K-Direction
16
17
18
19
20
21
22
23
24
25
26
27
(29 layers)
Every Nth
1 Selected
Default
Honor IJ
16
Apply
Close
POR_CO2
0.02500
0.05625
0.08750
0.11875
0.15000

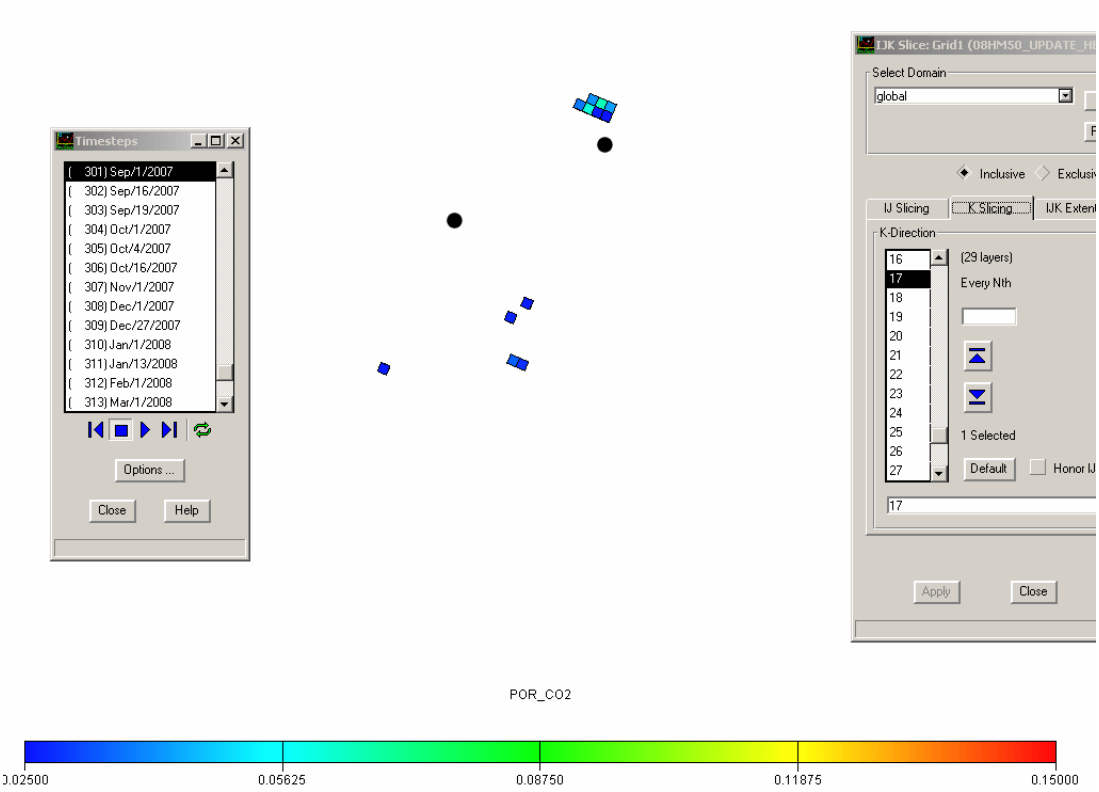
Timesteps
(301) Sep/1/2007
(302) Sep/16/2007
(303) Sep/19/2007
(304) Oct/1/2007
(305) Oct/4/2007
(306) Oct/16/2007
(307) Nov/1/2007
(308) Dec/1/2007
(309) Dec/27/2007
(310) Jan/1/2008
(311) Jan/13/2008
(312) Feb/1/2008
(313) Mar/1/2008
Options ...
Close
Help
IJK Slice: Grid1 (08HM50_UPDATE_H
Select Domain
global
Inclusive
IJ Slicing
K Slicing
IJK Extent
K-Direction
16
17
18
19
20
21
22
23
24
25
26
27
(29 layers)
Every Nth
1 Selected
Default
Honor IJ
17
Apply
Close
POR_CO2
0.02500
0.05625
0.08750
0.11875
0.15000

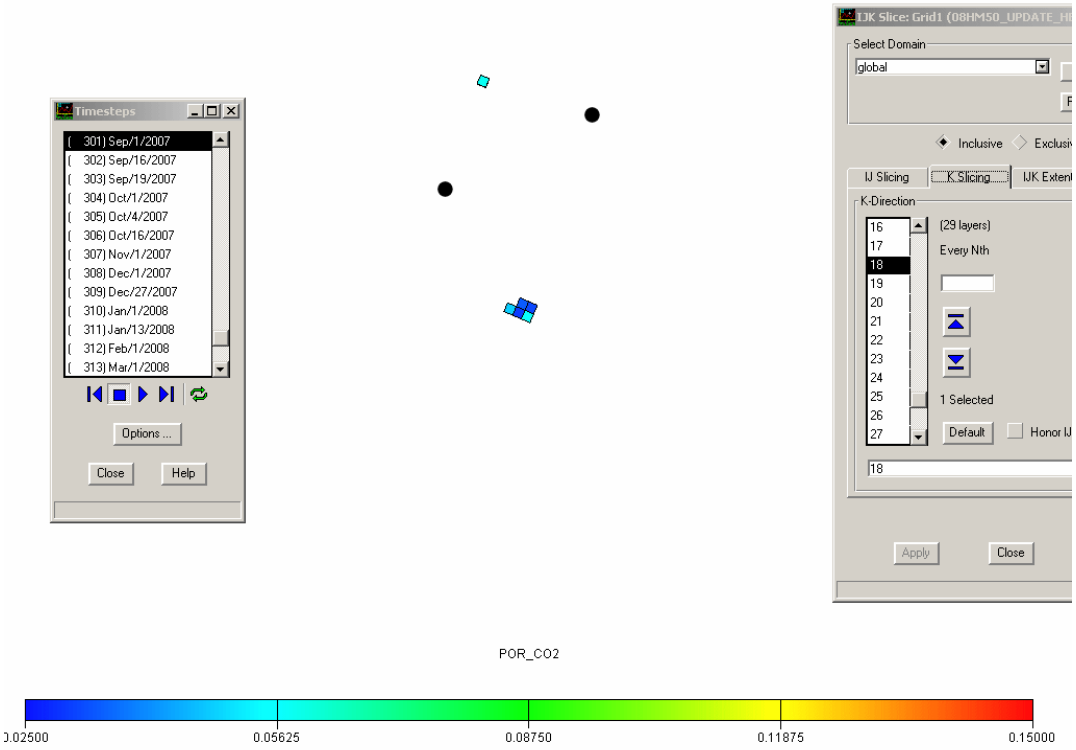
Timesteps
(301) Sep/1/2007
(302) Sep/16/2007
(303) Sep/19/2007
(304) Oct/1/2007
(305) Oct/4/2007
(306) Oct/16/2007
(307) Nov/1/2007
(308) Dec/1/2007
(309) Dec/27/2007
(310) Jan/1/2008
(311) Jan/13/2008
(312) Feb/1/2008
(313) Mar/1/2008
Options ...
Close
Help
IJK Slice: Grid1 (08HM50_UPDATE_HI
Select Domain
global
Inclusive
IJ Slicing
K Slicing
IJK Extent
K-Direction
16
17
18
19
20
21
22
23
24
25
26
27
(29 layers)
Every Nth
1 Selected
Default
Honor IJ
18
Apply
Close
POR_CO2
0.02500
0.05625
0.08750
0.11875
0.15000

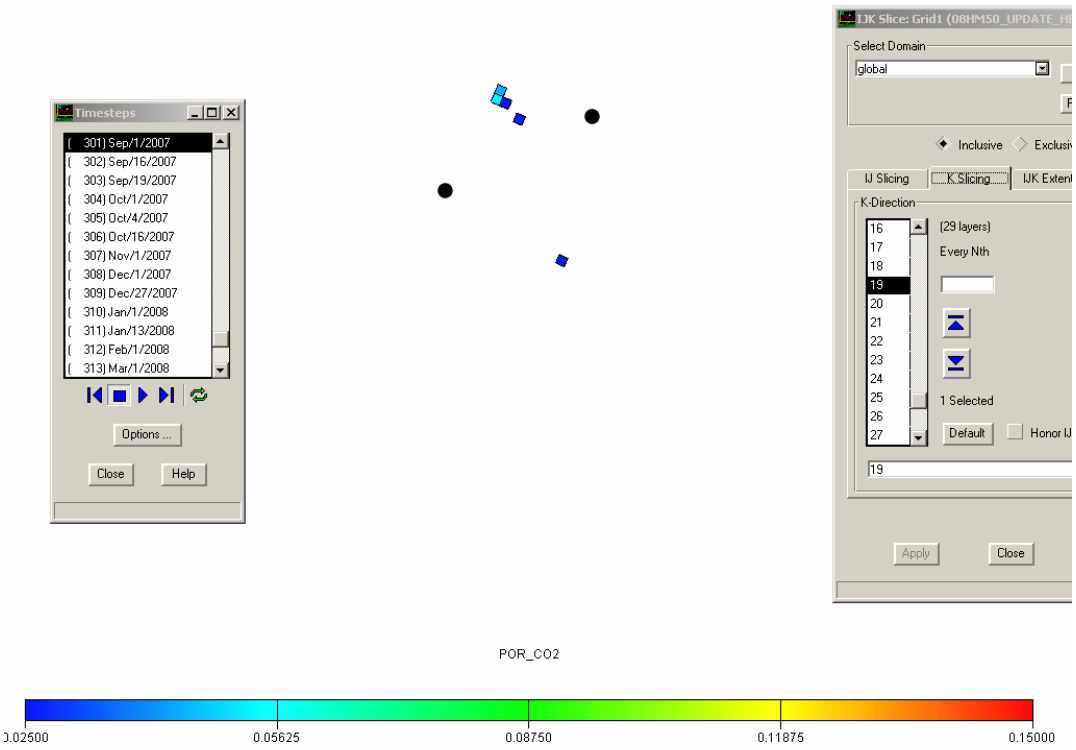
Timesteps
(301) Sep/1/2007
(302) Sep/16/2007
(303) Sep/19/2007
(304) Oct/1/2007
(305) Oct/4/2007
(306) Oct/16/2007
(307) Nov/1/2007
(308) Dec/1/2007
(309) Dec/27/2007
(310) Jan/1/2008
(311) Jan/13/2008
(312) Feb/1/2008
(313) Mar/1/2008
Options ...
Close
Help
IJK Slice: Grid1 (08HM50_UPDATE_HI
Select Domain
global
Inclusive
IJ Slicing
K Slicing
IJK Extent
K-Direction
16
17
18
19
20
21
22
23
24
25
26
27
(29 layers)
Every Nth
1 Selected
Default
Honor IJ
19
Apply
Close
POR_CO2
0.02500
0.05625
0.08750
0.11875
0.15000

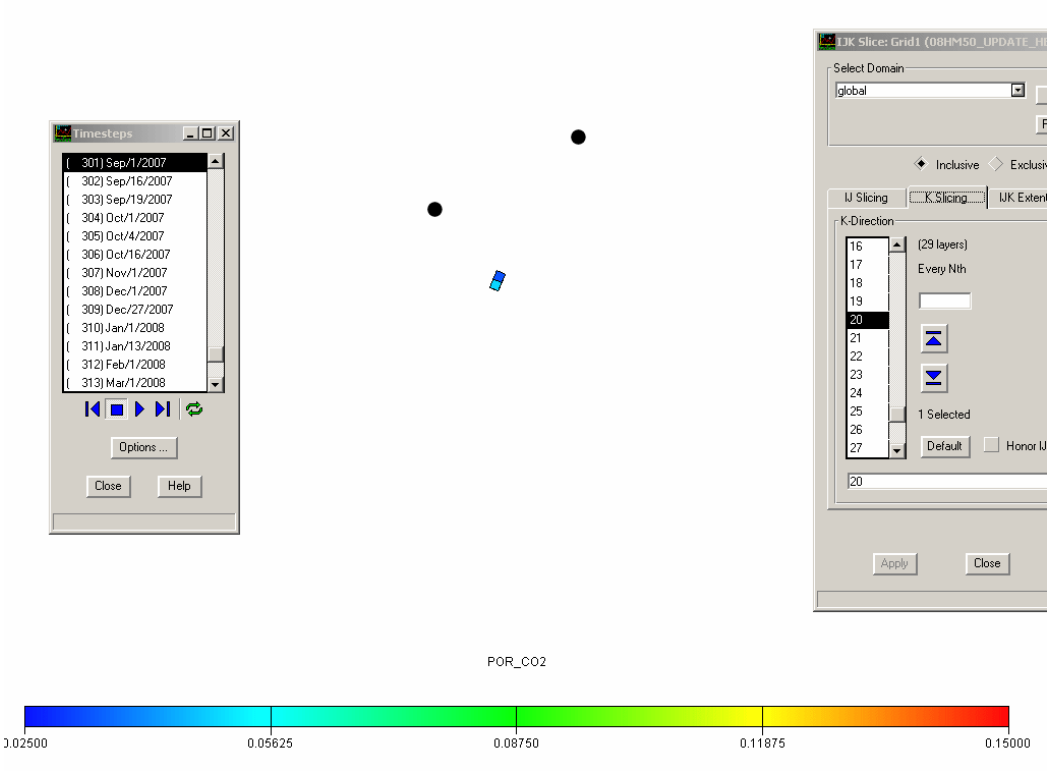
Timesteps
(301) Sep/1/2007
(302) Sep/16/2007
(303) Sep/19/2007
(304) Oct/1/2007
(305) Oct/4/2007
(306) Oct/16/2007
(307) Nov/1/2007
(308) Dec/1/2007
(309) Dec/27/2007
(310) Jan/1/2008
(311) Jan/13/2008
(312) Feb/1/2008
(313) Mar/1/2008
Options ...
Close
Help
IJK Slice: Grid1 (08HM50_UPDATE_HI
Select Domain
global
Inclusive
IJ Slicing
K Slicing
K-Direction
16
17
18
19
20
21
22
23
24
25
26
27
(29 layers)
Every Nth
1 Selected
Default
20
Apply
Close
POR_CO2
0.02500
0.05625
0.08750
0.11875
0.15000

11.2 Appendix B – Selected Amplitude Time Slices from the A2Carbonate Flattened 4D Seismic Monitor Survey

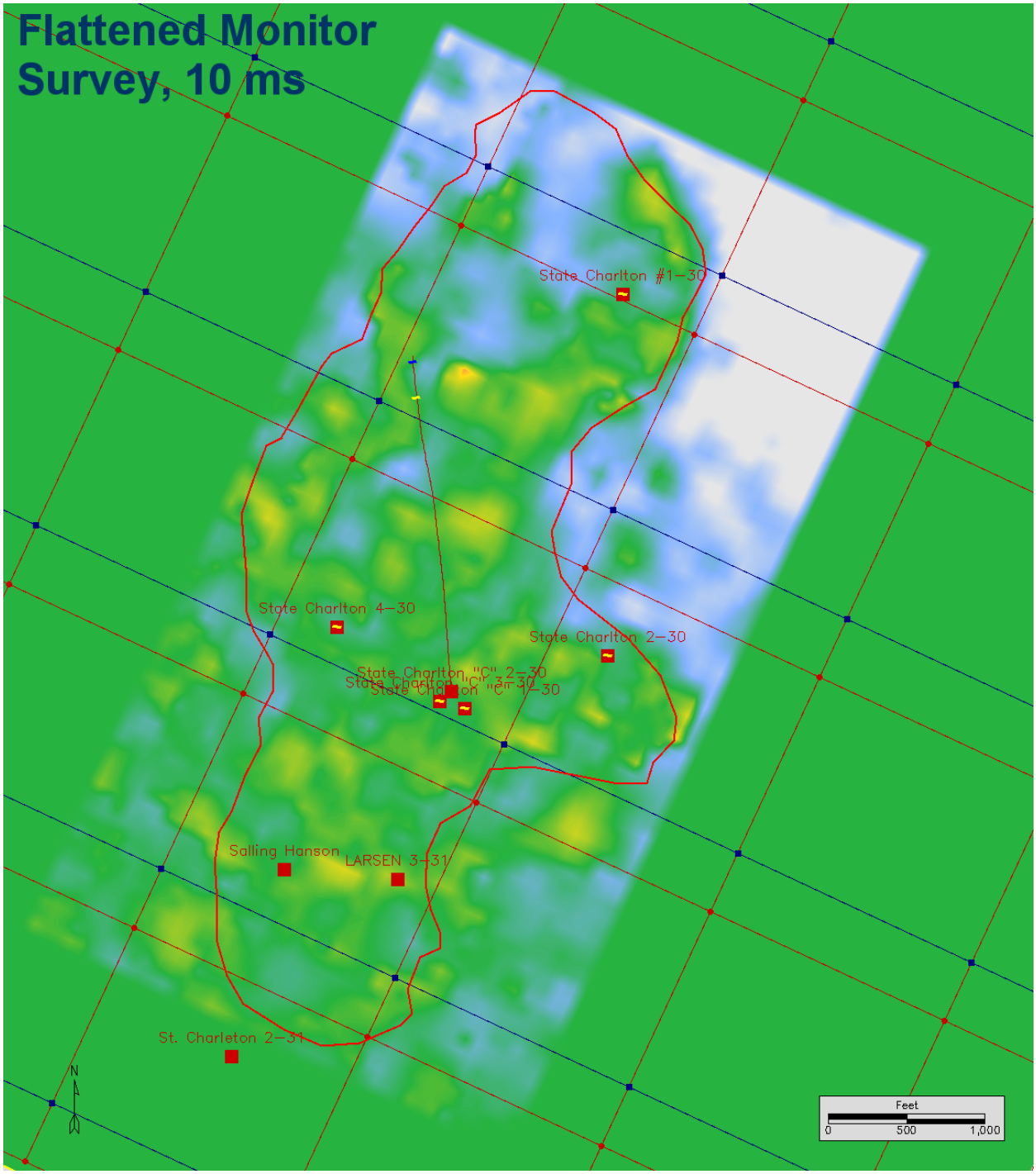

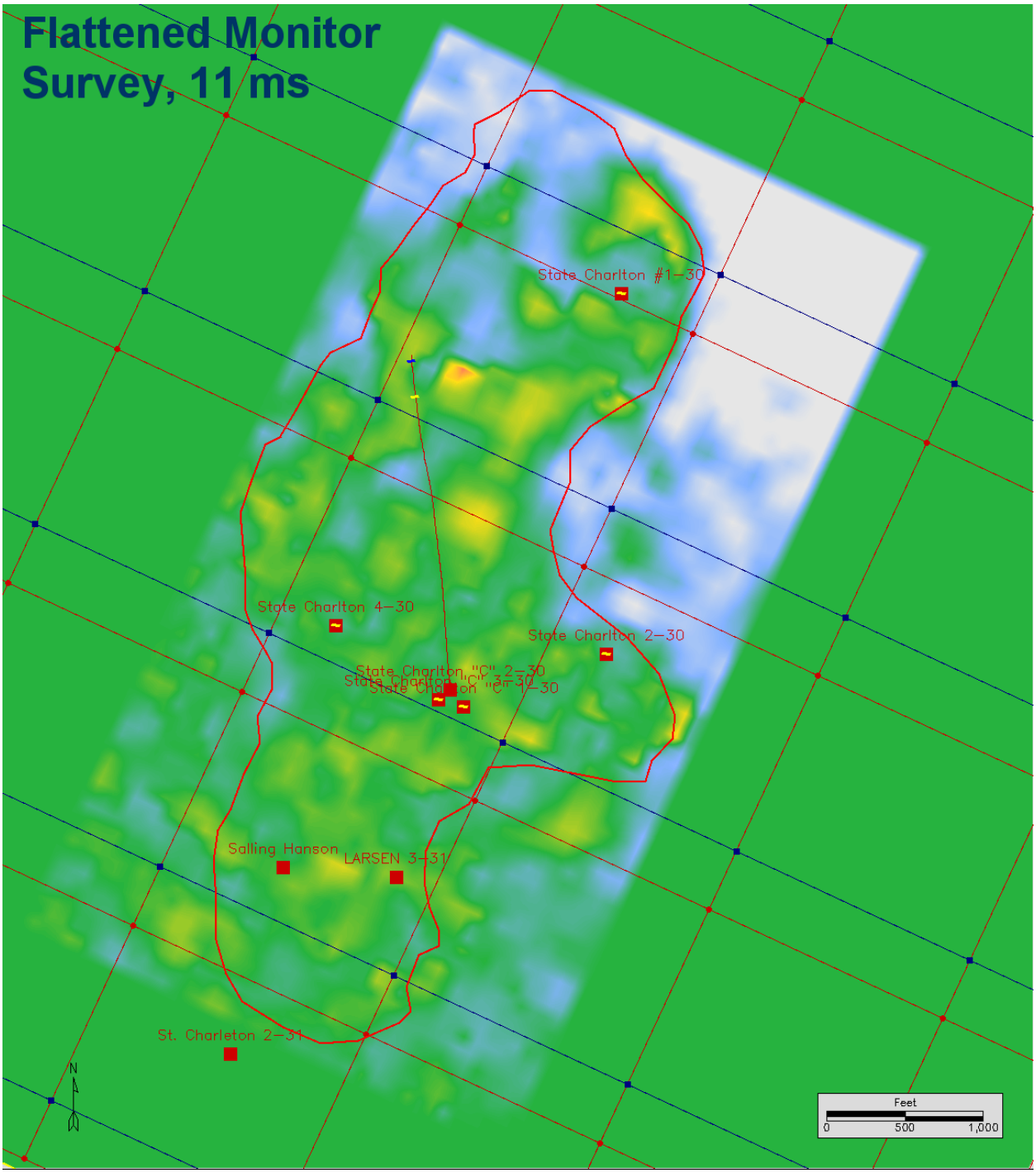
Flattened Monitor Survey, 11 ms
State Charlton #1–30
State Charlton 4–30
State Charlton 2–30
State Charlton "C" 2–30
State Charlton "C" 3–30
State Charlton "C" 1–30
Salling Hanson
LARSEN 3–31
St. Charleton 2–31
N
Feet
0
500
1,000

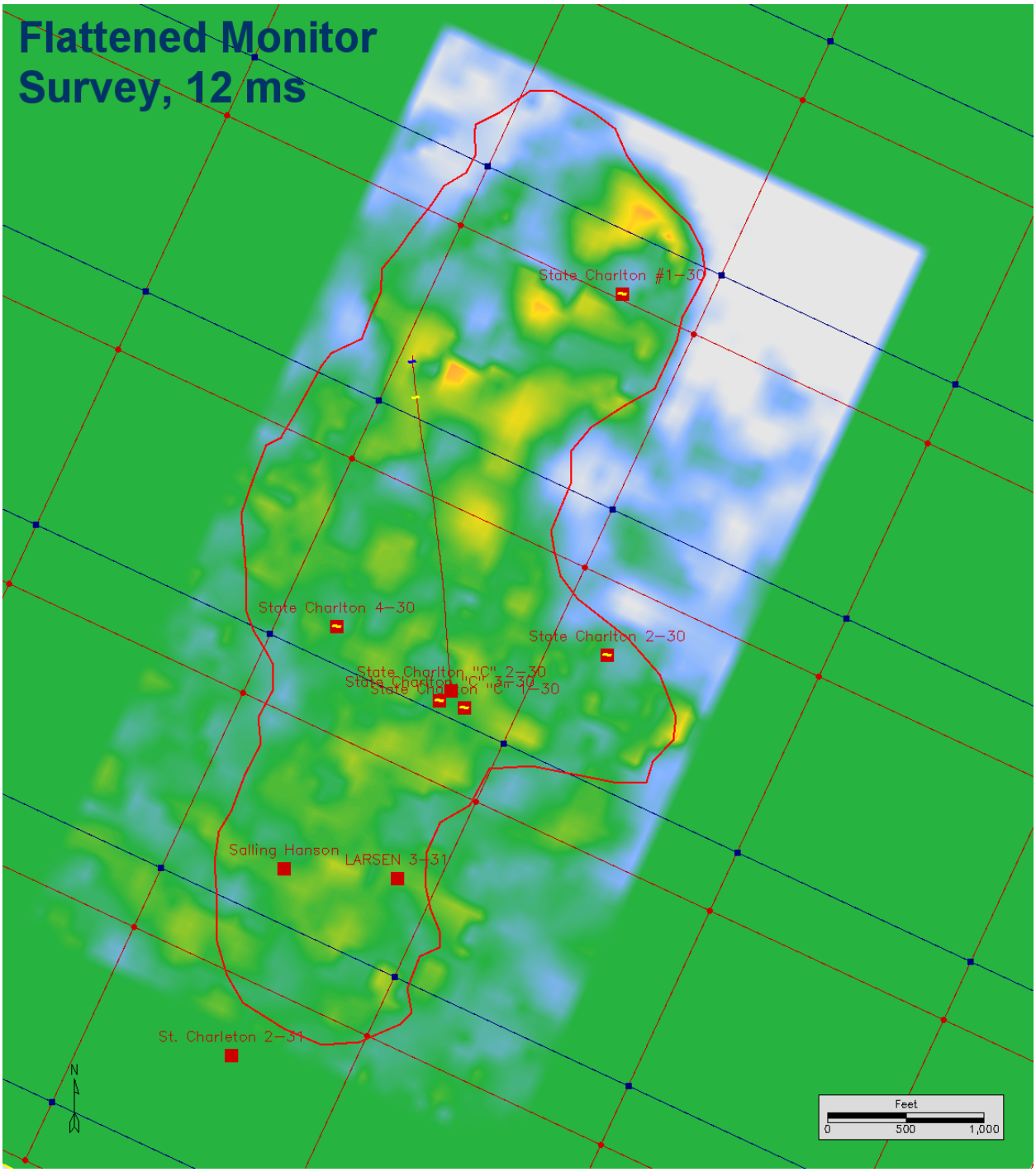
Flattened Monitor Survey, 12 ms
State Charlton #1-30
State Charlton 4-30
State Charlton 2-30
State Charlton "C" 2-30
State Charlton "C" 3-30
State Charlton "C" 1-30
Salling Hanson
LARSEN 3-31
St. Charleton 2-31
N
Feet
0
500
1,000

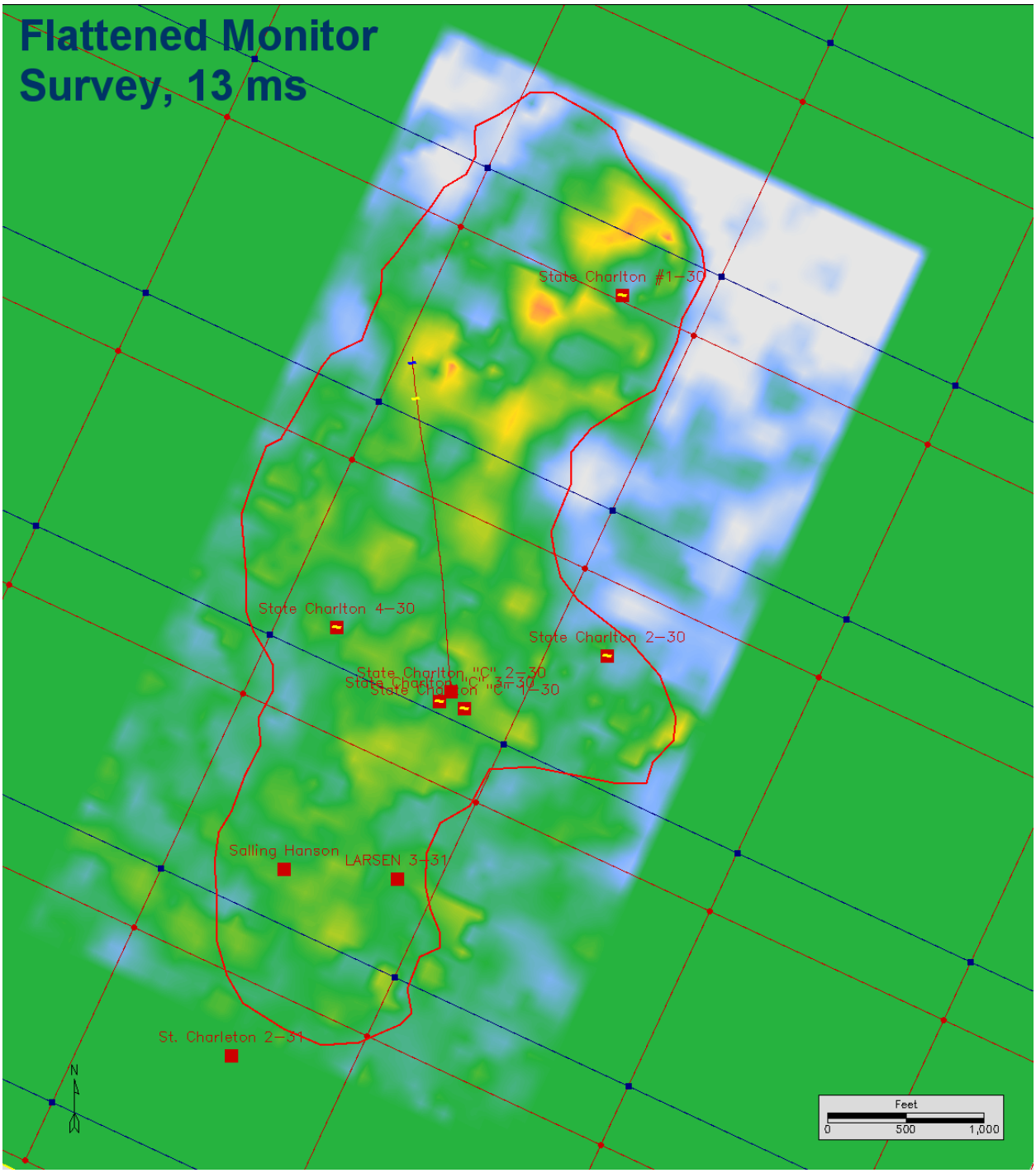
Flattened Monitor Survey, 13 ms
State Charlton #1-30
State Charlton 4-30
State Charlton 2-30
State Charlton "C" 2-30
State Charlton "C" 3-30
State Charlton "C" 1-30
Salling Hanson
LARSEN 3-31
St. Charleton 2-31
N
Feet
0
500
1,000

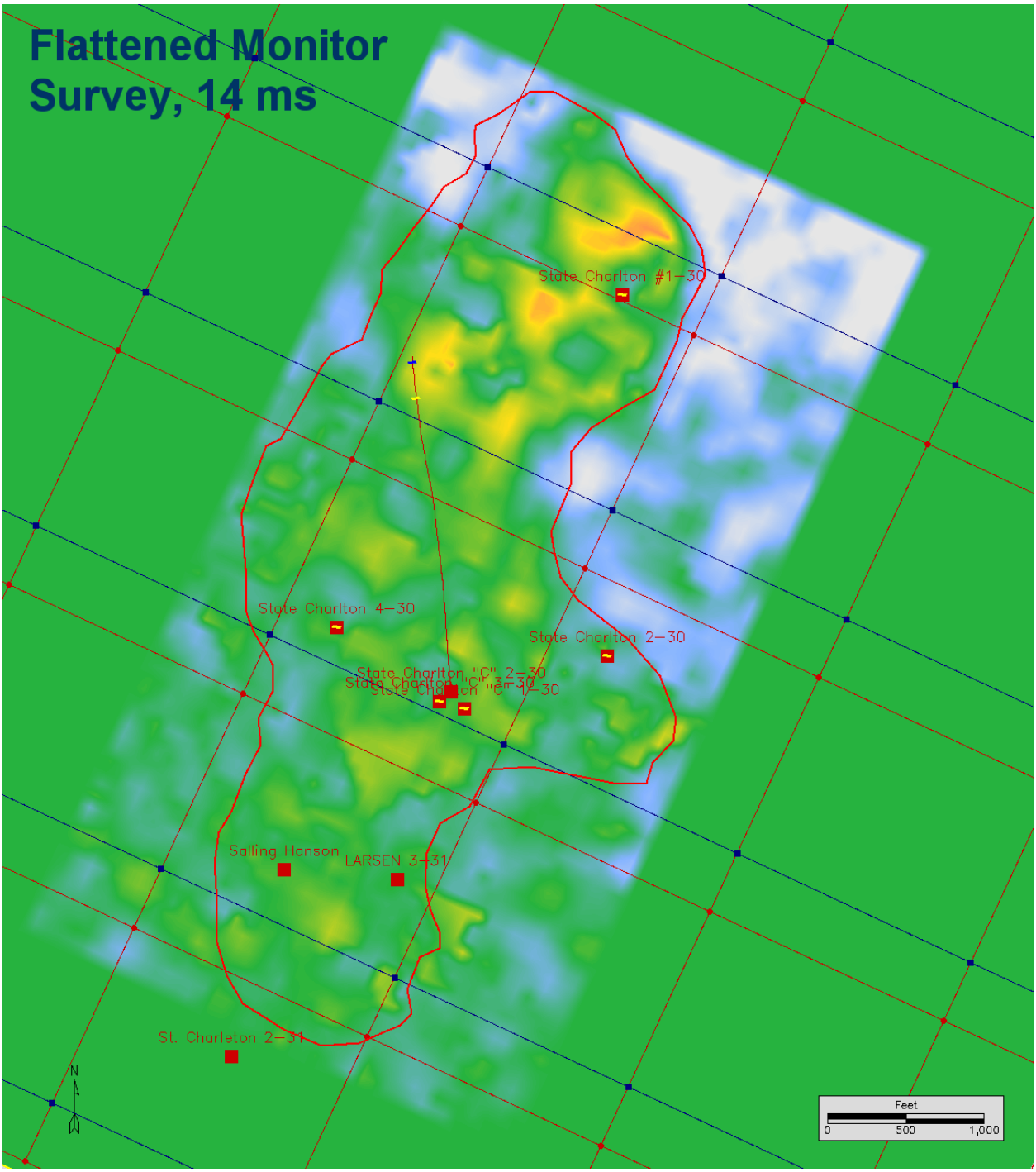
Flattened Monitor Survey, 14 ms
State Charlton #1–30
State Charlton 4–30
State Charlton 2–30
State Charlton "C" 2–30
State Charlton "C" 3–30
State Charlton "C" 1–30
Salling Hanson
LARSEN 3–31
St. Charleton 2–31
N
Feet
0
500
1,000

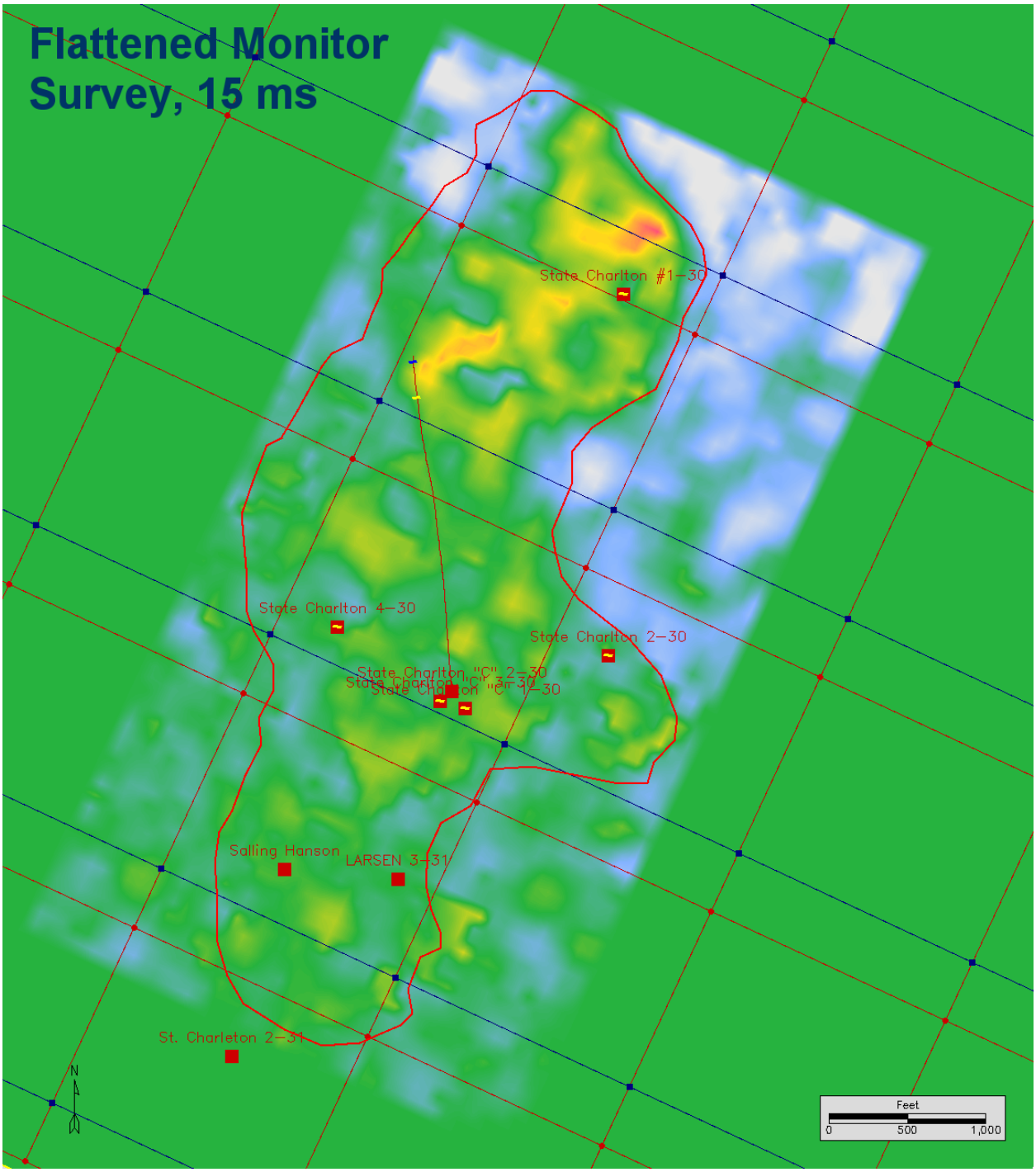
Flattened Monitor Survey, 15 ms
State Charlton #1-30
State Charlton 4-30
State Charlton 2-30
State Charlton "C" 2-30
State Charlton "C" 3-30
State Charlton "C" 4-30
Salling Hanson
LARSEN 3-31
St. Charleton 2-31
N
Feet
0
500
1,000

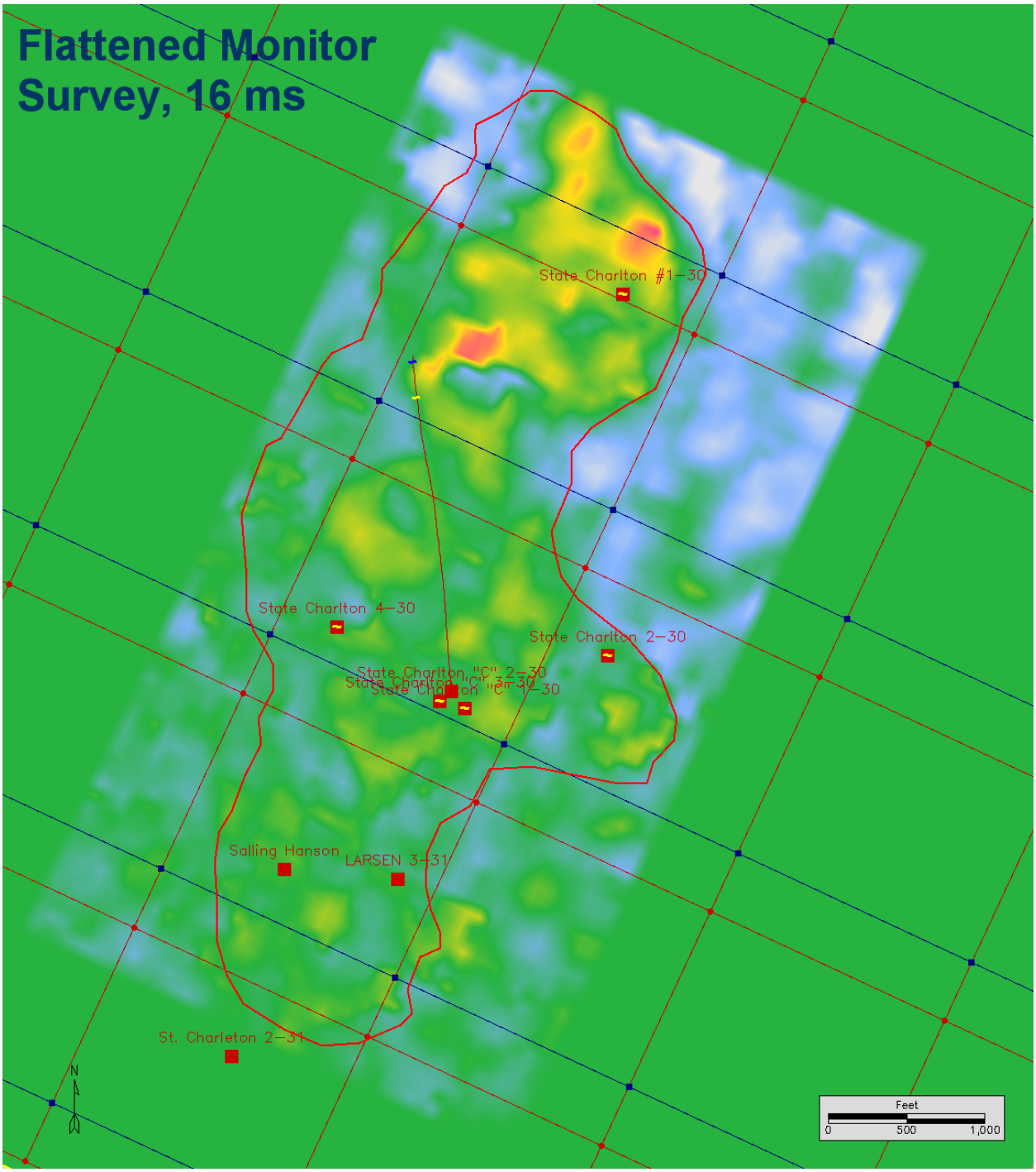
Flattened Monitor Survey, 16 ms
State Charlton #1-30
State Charlton 4-30
State Charlton 2-30
State Charlton "C" 2-30
State Charlton "C" 3-30
State Charlton "C" 1-30
Salling Hanson
LARSEN 3-31
St. Charleton 2-31
N
Feet
0
500
1,000

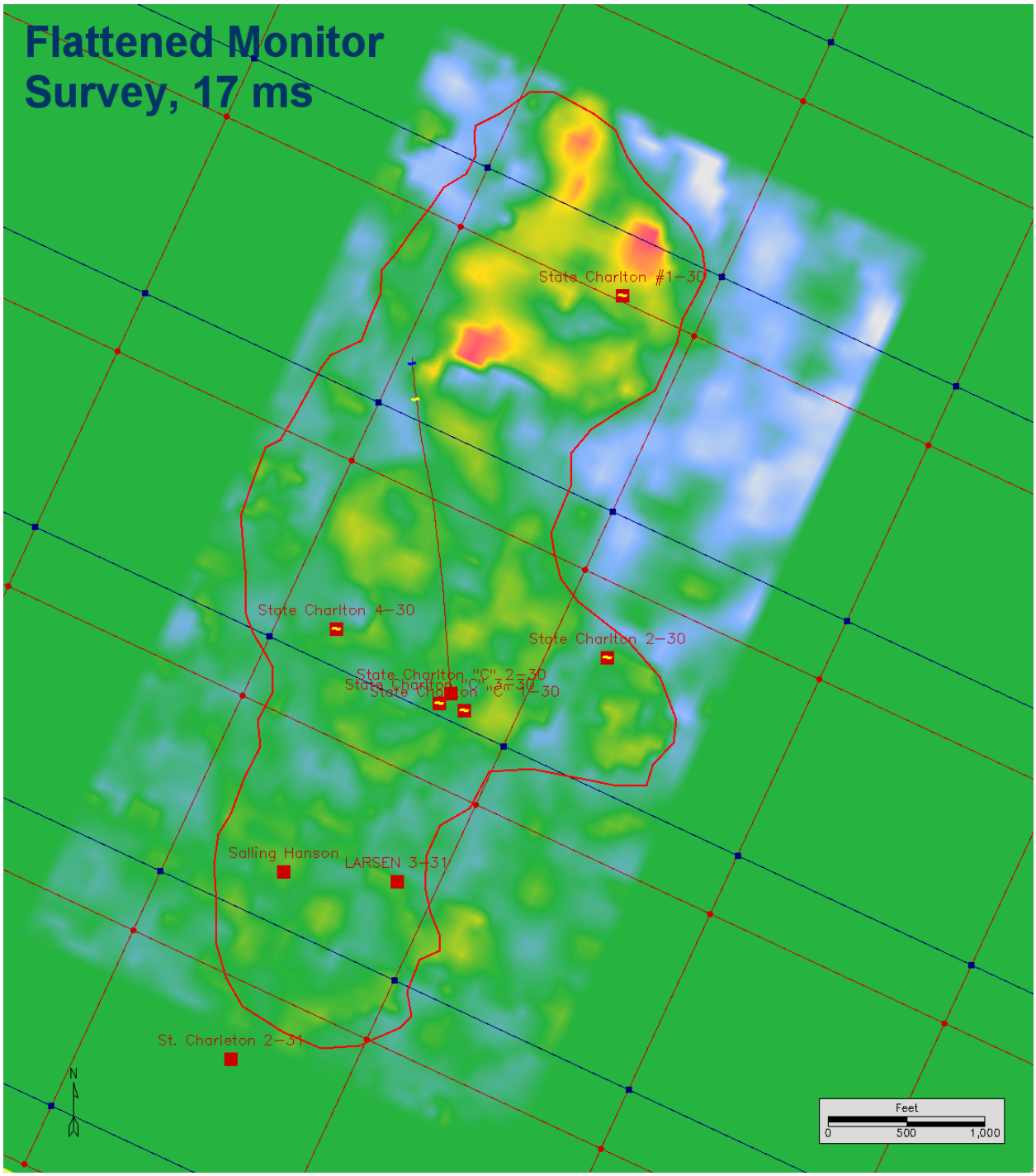
Flattened Monitor Survey, 17 ms
State Charlton #1-30
State Charlton 4-30
State Charlton 2-30
State Charlton "C" 2-30
State Charlton "C" 3-30
State Charlton "C" 1-30
Salling Hanson
LARSEN 3-31
St. Charleton 2-31
N
Feet
0
500
1,000

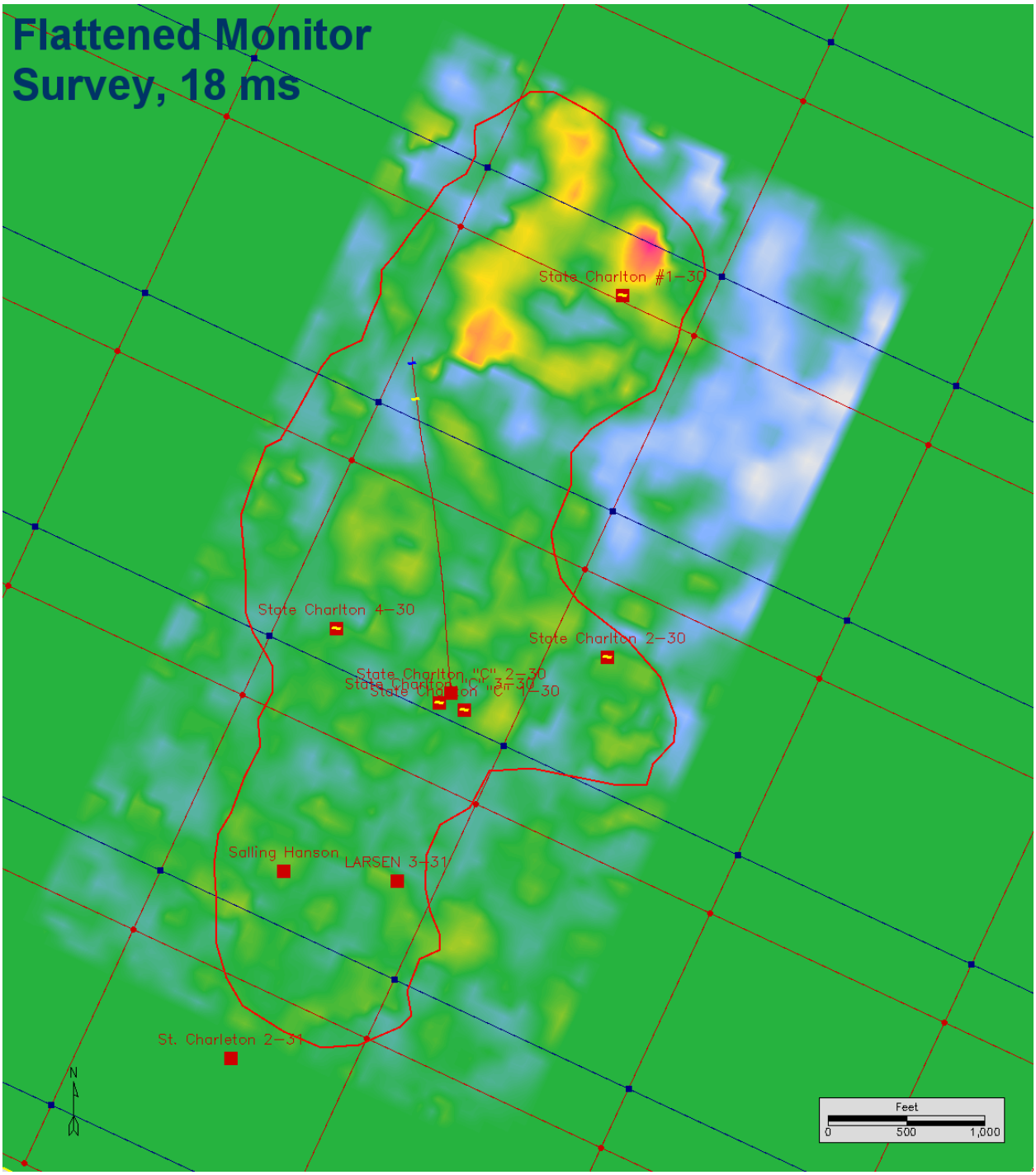
Flattened Monitor Survey, 18 ms
State Charlton #1-30
State Charlton 4-30
State Charlton 2-30
State Charlton "C" 2-30
State Charlton "C" 3-30
State Charlton "C" 1-30
Salling Hanson
LARSEN 3-31
St. Charleton 2-31
N
Feet
0
500
1,000

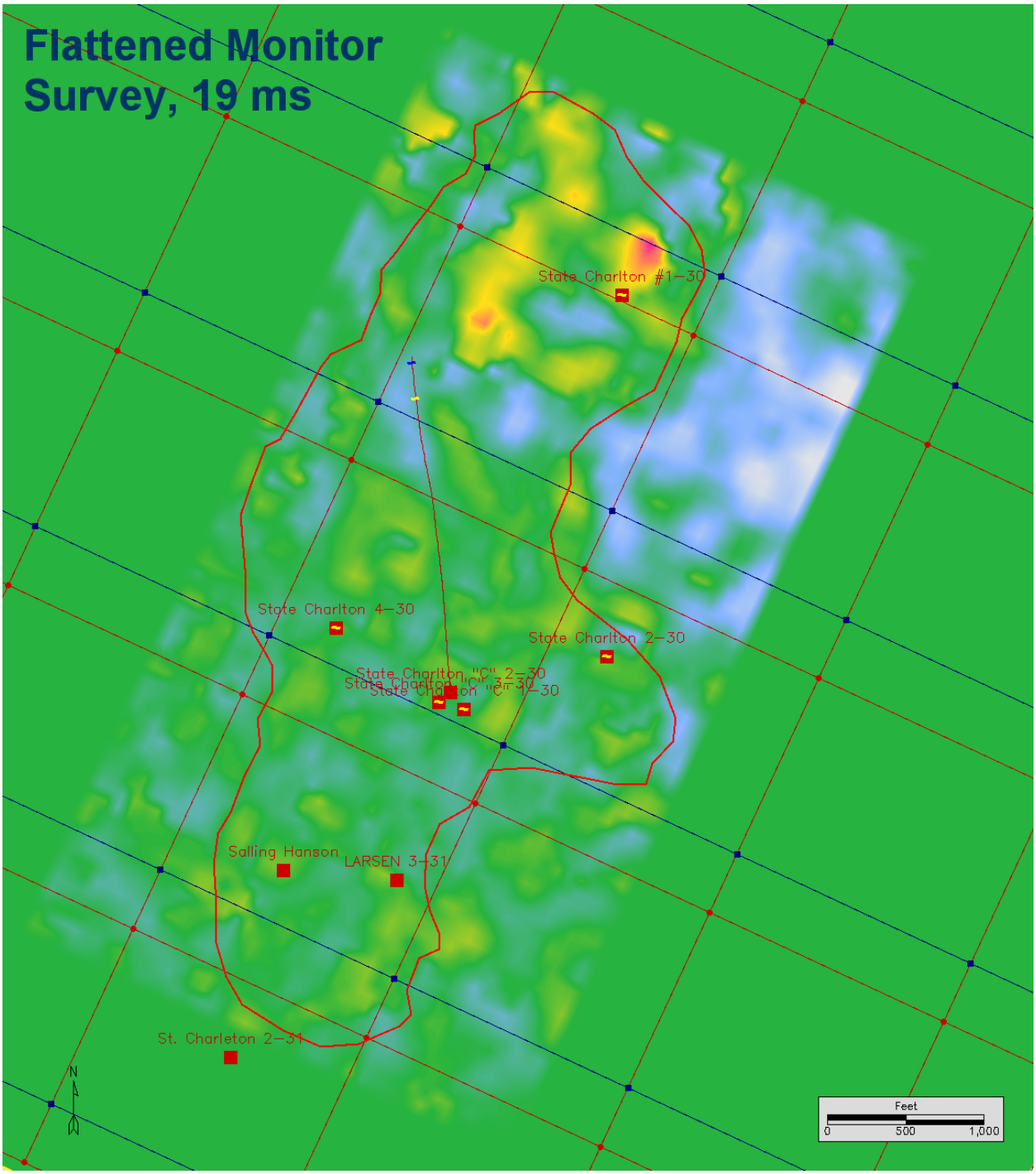
Flattened Monitor Survey, 19 ms
State Charlton #1–30
State Charlton 4–30
State Charlton 2–30
State Charlton "C" 2–30
State Charlton "C" 3–30
State Charlton "C" 1–30
Salling Hanson
LARSEN 3-31
St. Charleton 2–31
N
Feet
0
500
1,000

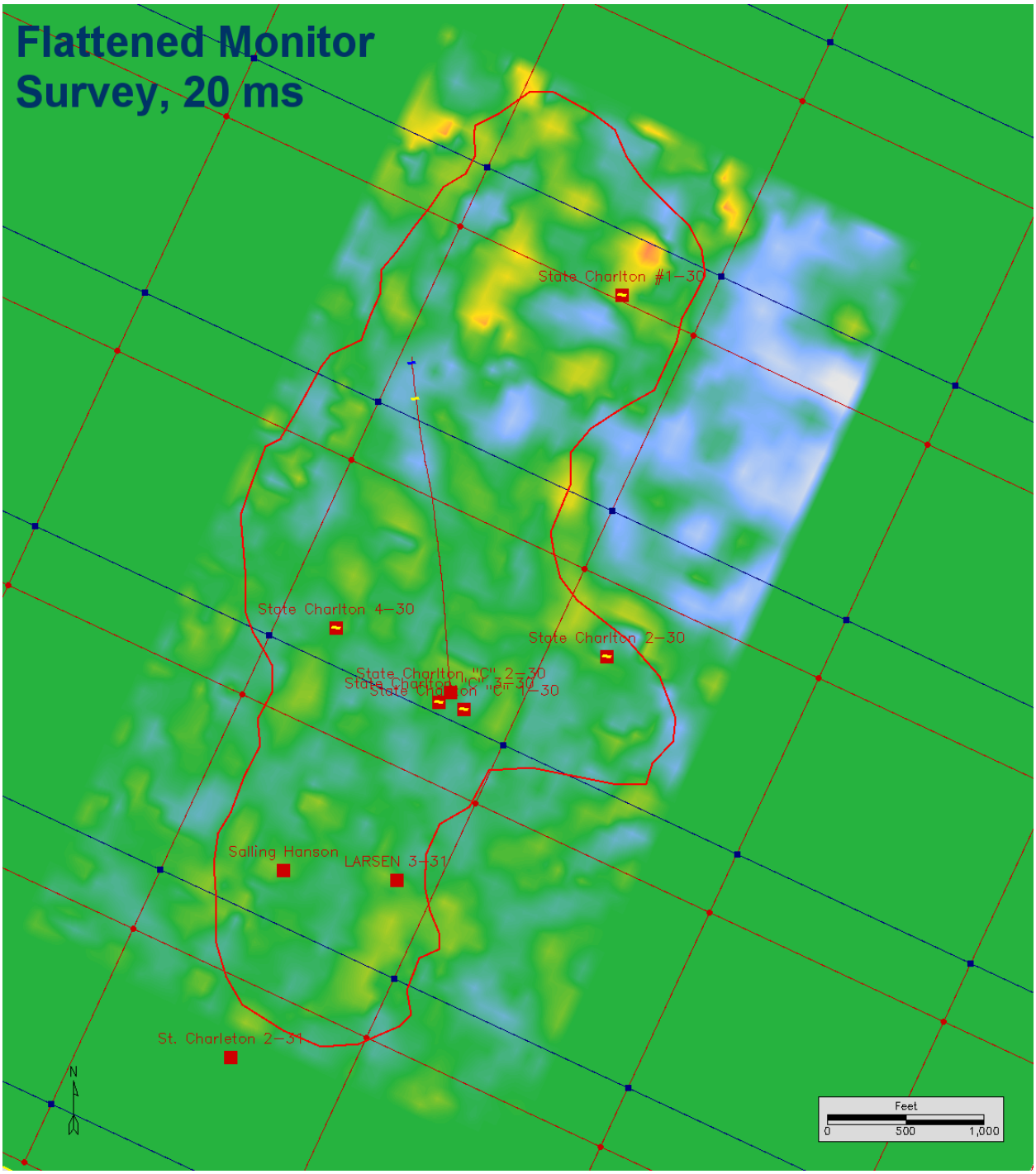
Flattened Monitor Survey, 20 ms
State Charlton #1–30
State Charlton 4–30
State Charlton 2–30
State Charlton "C" 2–30
Salling Hanson
LARSEN 3-31
St. Charleton 2–31
N
Feet
0
500
1,000

Appendix C

Data Processing Report

For

Schlumberger DCS

Area: Silurian Reef 4D

WG Lawson Code: BV58
Date: September 16, 2008

WesternGeco
1625 Broadway, Suite 1300, Denver, Colorado 80202 USA

Report Author
Adrian Montgomery

Table of Contents

1.0 Introduction

This is a 4D project as such great care and effort was put into preserving relative amplitudes while accounting for noise levels in the data. Two vintages of data were collected for this processing effort, a baseline survey in 2004 and a monitor survey acquired in 2007. The two data vintages had very well repeated source and receiver locations. Non-co-located source and receiver locations were processed up to migration and then discarded. Overall the data is characterized by low signal to noise ratio with high amplitude ground roll and pervasive random noise which only resolved into coherent energy during migration.

2.0 Seismic Data Processing

2.1 Survey/Seismic Data Merge

The survey geometry information was used to update the seismic trace header literals with the source and detector X, Y, Z information. The two sets of data were matched using unique field source point and field detector point numbers. At this point start times were assigned to the trace headers using a velocity of 8200 ft/sec.

2.2 Resample

It was determined that a 1ms sample rate would preserve a frequency range in which the data existed. Both surveys were output at a similar trace length and sample rate. An antialias filter was applied prior to the data being resampled.

Vintage	Input Sample Rate	Output Sample Rate	Input trace length	Output trace length
2004	2	1	4000 ms	3000 ms
2007	1	1	3000 ms	3000 ms

2.3 Refraction Tomography

A near surface model was derived by tomographic inversion of first-arrival times and statics were computed from it. In this case the data from the 2007 dataset was picked and the resulting static values were interpolated to stations of both the 2004 and 2007 datasets.

First-breaks were digitized over all or a range of offsets on all shots. These picked times were then input to the program together with an initial estimate of the weathering velocity field (from upholes, LVL surveys or geological information of the area). The process works by decomposing the first-arrival picks into mean 3-D traveltime / offset functions. These 3-D functions are then locally inverted into a 3-D velocity/depth model. The decomposition is done through a linear inversion that does not require explicit ray tracing and is therefore independent of the initial model. In the local inversion the residuals between the input picks and the predicted picks are back-projected onto the model grid.
The entire process is iterated several times to produce a model that is consistent with the observed first-break times within preset limits.

Parameter Values:

Picked Offset Range Minimum: 200 ft
Picked Offset Range Maximum: 5,280 ft
Source of Weathering Model Information: Direct Arrivals
Velocity Smoothing Length: 3000 ft
Thickness (or Elevation) Smoothing Length: 3,000 ft
Final Datum Elevation: 1,000 ft
Replacement Velocity: 10,000 ft/sec

2.4 Time Function Gain

This process scales trace samples by first raising the time (in seconds) to a user-supplied exponential value, then multiplying the result by the amplitude of the sample at that time. That is:

$A_o(t) = A_i(t)\ t^x$

where:

$A_o(t)$ is the amplitude of output trace sample at time t

$A_i(t)$ is the amplitude of input trace sample at time t

t is the time in seconds

x is the value of gain exponent

Parameter values:

Exponent Value : 2

2.5 F-X Coherent Noise Suppression (FXCNS)

Many acquisition and processing techniques are successful in suppressing coherent noise in '2D' data, however such methods are often ineffective for the 3D case. In the 2D case, the seismic wavefield is spatially sampled in a regular manner along a single direction, and filtering methods such as those in the frequency-wavenumber (f-k) or Radon transform (Tau-p) domains are effective at reducing coherent noise. However for 3D data, signal and noise arrive at receivers from a wide range of azimuths. Therefore, in any given propagation direction, the wavefield is not uniformly sampled and the use of f-k or Tau-p filters is problematic.

FXCNS is an approach to coherent noise suppression for 3D acquired data that can handle irregular sampling and noise variability. This is accomplished by azimuthally binning each gather prior to filtering . Each azimuth is then filtered independently using f-x domain fan filters and a least-squares optimization scheme. Noise is then estimated for a specific range of apparent velocities

The process is run on receiver gathers, azimuthally binning each gather prior to filtering. Using f-x domain fan filters and a least-squares optimization scheme, noise is then estimated for each gather over a specific range of apparent velocities, and then subtracted from the input data.

Parameter values:

High pass velocity: Tapered off from 3000 - 3500 ms^{-1}
Low pass velocity: Tapered on from 100 - 400 ms^{-1}

Number of azimuth bins: 50

2.6 Swell Noise Attenuation (SWATT)

Swell noise is caused by data acquisition in rough sea conditions, particularly when the cables are being towed at a relatively shallow depth. SWATT aims to attenuate this noise by transforming the processing gather into the frequency domain and applying a spatial median filter. Frequency bands that deviate from the median amplitude by a specified threshold are either zeroed, or replaced by good frequency bands interpolated from neighboring traces.

Parameter values:

Processing Domain : Shot

Width of Spatial Median Filter : 21 Traces
Frequency Range Processed : 0 to Nyquist Hz
Width of Frequency Bands to Process : 5 Hz

Threshold Values:

Time (ms)	Threshold (%)
0	10

2.7 Surface Consistent Deconvolution

Deconvolution can be formulated in the form of a surface-consistent spectral decomposition (Taner,1981). The aim is to decompose the seismic trace into the convolutional effects of source, detector, offset and the earth's reflectivity, and then inverse filter to recover the reflectivity component. The convolutional model used in the conventional Wiener-Levinson deconvolution scheme is give in equation 1

$$x(t) = w(t) \bullet y(t) + n(t) \qquad (1)$$

where x(t) is the recorded seismogram, w(t) is the waveform, y(t) is the earth's reflectivity that is to be estimated, n(t) is additive noise. The surface-consistent convolution model describes the wavelet for the trace with the source at location j and the detector at location I as the combination of several effects as shown in equation 2

$$W_{ij}(t) = s_j(t) \bullet r_i(t) \bullet g(t)_{\frac{(i+j)}{2}} \bullet m(t)_{\frac{(i-j)}{2}} \qquad (2)$$

Where;

$s_j(t)$ = Component of the wavelet associated with the variations in the vicinity of the source location *j*

$r_i(t)$ = Component associated with the variations in the vicinity of the detector location *i*

$g(t)_{\frac{(i+j)}{2}}$ = Component associated with the midpoint dependence of the wavelet

$m(t)_{\frac{(i-j)}{2}}$ = Component associated with the offset dependence of the wavelet

Equation 2 is Fourier transformed to yield equation 3

$$W(\omega)=S(\omega)R(\omega)G(\omega)M(\omega) \quad (3)$$

Where ω is angular frequency.

Equation 3 can be separated into amplitude components and phase spectral components, equations 4 and 5.

$$A_w = A_s\, A_r\, A_g\, A_m \quad (4)$$

$$\phi_w = \phi_s+\phi_r+\phi_g+\phi_m \quad (5)$$

Where;

A_w = Amplitude spectrum of the wavelet (or power spectrum of the input trace)

A_s = Amplitude spectrum of the near-surface filter in the vicinity of the source

A_r = Amplitude spectrum of the near-surface filter in the vicinity of the detector

A_g = Amplitude spectrum of the subsurface filter in the vicinity of the midpoint

A_m = Amplitude spectrum of the filter associated with the offset distance

ϕ_w, ϕ_s, ,ϕ_r, ϕ_g, ϕ_m = Associated phase spectra

Making the minimum phase assumption, only the amplitude spectra need to be determined. Equation 4 can now be linearized by taking the logarithm of both sides as shown in equation 6

$$\ln A_w = \ln A_s + \ln A_r + \ln A_g + \ln A_m \quad (6)$$

Given the amplitude spectrum of the wavelet (or power spectrum of the trace) for each input trace, (A_w) the Gauss-Seidel method is used to derive the logarithmic amplitude spectra for all source locations, detector locations, midpoint locations, and offset distances. When these logarithmic amplitude spectra are summed according to equation 6, the resulting logarithmic spectrum A_w is the best match for the input logarithmic spectrum A_w.

The desired spectral components are those that minimize the rms error (E) defined as the sum of the squares of the observational errors, or the differences between the input spectra and the spectra obtained by summing the derived components given by equation 7.

$$E = \sum_{i,j} \left(A_{w_{ij}} - A'_{w_{ij}} \right)^2 \quad (7)$$

The resulting source, detector, midpoint, and offset logarithmic amplitude spectra are combined according to equation 6 and used to design a minimum-phase operator to deconvolve each trace in a surface consistent manner.

2.7.1 Deconvolution Operator Design

Parameter values:

Total Operator Length	: 160 ms
Active Operator Length	: 161 ms
Prediction Distance	: 1 ms
Percent White Noise	: 0.01

2.7.2 Window Specification

The window start and stop times for each trace were obtained by adding a moveout velocity to a zero-offset time.

Parameter values:

Moveout Velocity : Linear

	Zero-Offset Time (ms)	Moveout Velocity (Feet)
Window Start Time	200	10,000
Window Stop Time	2000	20,000

2.7.3 Surface Consistent Decomposition

Parameter values:

Decomposition order: Source/Detector
Application order : Source/Detector

2.8 Time Variant Spectral Whitening

This process flattens the amplitude spectra of seismic traces over a user-defined frequency band. Amplitudes at frequencies outside this band are suppressed. The action on each trace is similar to a single-channel, zero-phase deconvolution.

An input trace is passed, in parallel, through a number of different zero-phase filters spanning the desired output frequency passband. The filter specifications are generated automatically based on the defined output frequency passband and on the number of filters required to cover this band.

Each of the filtered versions of the input trace are then AGC scaled. More precisely, the scale factors are computed on the amplitude envelope of the trace. To stabilize the process, white noise is added to the envelope before computing the scalar. This addition of white noise prevents exaggeration of weak signal frequencies.

Finally, the filtered and gained versions of the input trace are summed and the whole scaled so that the amplitude envelope of the output is equivalent to the envelope of the input trace. In this way, relative amplitude is broadly preserved.

Parameter values:

Filter Specification : Automatic
Number of Filters Generated : 10

Passband CORNER FREQUENCIES (Hz)	Passband AMPLITUDES
6 : 12 : 120 : 180	0.01 : 1.0 : 1.0 : 0.01

Gain Window Length : 400 ms
Percent White Noise : 0.01

2.9 Residual Statics (Miser 1)

Surface consistent reflection residual statics were calculated from pre-processed CDP gathers. The process is split into two phases – the first (termed XPERT) picks the time shifts for each prestack trace and the second (termed MISER) computes surface consistent statics from these picks.

In the XPERT program, one or more time and space variant gates that contain reflection events are defined. A model trace is generated by performing a rolling average of the stacked traces within the time gate and then, for each CMP gather, unstacked traces are cross-correlated with the model trace. The peaks of these cross-correlations are picked and the differential times between the peak time and the zero lag computed. These represent the sum of the residual shot and receiver statics plus any structural and residual moveout terms.

In the MISER (Modular Iterative Statics Evaluation Routine) program, an iterative Gauss-Seidel decomposition technique is used to derive the individual components of the time shift, that is, Source, Receiver, Midpoint and Residual NMO terms. The static values for each trace are written into that trace's header so that they are available for subsequent processing.

Parameter Values:

Model Window(s) : 200 ms to 1000 ms
Maximum Correlation Shift : 32 ms
Inline and Crossline Model Extent : 7

2.10 Preliminary Velocity Analysis

Velocity analysis was performed using **WesternGeco's** Interactive Velocity Analysis (INVA) package. At regular intervals across the survey CMP gather data were selected. From this data Multi-Velocity Function (MVF) stacks and velocity semblance values were computed. For each velocity location, MVF data, semblances and gathers are displayed interactively allowing stacking velocities to be interpreted.

Percentage stacks and NMO-corrected gathers are then produced to check the validity of the picks and any necessary changes made before the velocity field is output.

Parameter Values:	
Analysis Spacing	: 825 ft
Number of CMP's per Analysis (MVF Stack)	: 11
Number of CMP's per Analysis (Semblance Display)	: 5

2.11 Residual Statics (Miser 2)

Surface consistent reflection residual statics were calculated from pre-processed CDP gathers. The process is split into two phases – the first (termed XPERT) picks the time shifts for each prestack trace and the second (termed MISER) computes surface consistent statics from these picks.

In the XPERT program, one or more time and space variant gates that contain reflection events are defined. A model trace is generated by performing a rolling average of the stacked traces within the time gate and then, for each CMP gather, unstacked traces are cross-correlated with the model trace. The peaks of these cross-correlations are picked and the differential times between the peak time and the zero lag computed. These represent the sum of the residual shot and receiver statics plus any structural and residual moveout terms.

In the MISER (Modular Iterative Statics Evaluation Routine) program, an iterative Gauss-Seidel decomposition technique is used to derive the individual components of the time shift, that is, Source, Receiver, Midpoint and Residual NMO terms. The static values for each trace are written into that trace's header so that they are available for subsequent processing.

Parameter Values:	
Model Window(s)	: 200 ms to 1000 ms
Maximum Correlation Shift	: 32 ms
Inline and Crossline Model Extent	: 7

2.12 Preliminary Velocity Analysis

Velocity analysis was performed using **WesternGeco's** Interactive Velocity Analysis (INVA) package. At regular intervals across the survey CMP gather data were selected. From this data Multi-Velocity Function (MVF) stacks and velocity semblance values were computed. For each velocity location, MVF data, semblances and gathers are displayed interactively allowing stacking velocities to be interpreted.

Percentage stacks and NMO-corrected gathers are then produced to check the validity of the picks and any necessary changes made before the velocity field is output.

Parameter Values:	
Analysis Spacing	: 825 ft
Number of CMP's per Analysis (MVF Stack)	: 11
Number of CMP's per Analysis (Semblance Display)	: 5

2.13 Surface-Consistent Amplitude Compensation (SCAC)

SCAC compensates for shot, detector and offset amplitude variations that are caused by acquisition effects and are not a consequence of the subsurface geology.

The amplitude of a given time window is determined for every trace using either a root-mean-square (rms) or a mean-absolute amplitude criterion. The amplitudes measured can then be expressed as the product of surface-consistent source, receiver and offset terms, and a subsurface-consistent geology (CMP) term. Taking the logarithm allows the amplitude to be expressed as a sum of the above terms which, in turn, allows the surface consistent terms to be computed using a Gauss-Seidel iterative decomposition.

Scaling factors are then computed and applied to each trace. In this computation the CMP term is ignored, the scaling factor being the ratio of the geometric mean of all the SCAC source, detector and offset terms to the individual trace's source, detector and offset term.

Parameter Values:

Amplitude Criterion : RMS
Time Window : 500 ms to 3000 ms

2.14 Residual Amplitude Analysis/Compensation (RAAC)

Where true-amplitude information needs to be retained in the data, the application of data dependent scaling is undesirable; yet the failure to apply scaling can result in data which is difficult to display due to the range of amplitudes (dynamic range) present. The RAAC process uses statistical means to retain anomalous amplitude information, such as bright spots, while allowing the data to be scaled.

The analysis step of RAAC computes, for each trace, the amplitudes of multiple windows using an rms-amplitude criterion. The Residual Amplitude Compensation (RAC) value of each window is then the reciprocal of this computed amplitude. The center of each time window defines the position of its associated RAC value. Knowing the X-Y location and time of each RAC value allows both spatial and temporal smoothing to be applied to the RAC values.

The application step of RAAC takes the smoothed RAC values, interpolates to every sample, and applies the resulting scalars to the input traces.

Parameter values:

Number of Offset Windows : 80
Analysis Window Start : The first analysis window began at the trace start time (the RAC value corresponding to this start time was applied to all data from the start time to the first sample))
Window Length : 1000
Window Advance : 500
Amplitude Analysis Type : rms
Note: If the amount of live data within a window is not equal to at least one-half the window advance, then the RAC value for the previous window is used.
Temporal Smoothing at Top of Data : 3
Temporal Smoothing at Bottom of Data : 3
Spatial Smoothing Width : 5

2.15 Swell Noise Attenuation (SWATT)

Swell noise is caused by data acquisition in rough sea conditions, particularly when the cables are being towed at a relatively shallow depth. SWATT aims to attenuate this noise by transforming the processing gather into the frequency domain and applying a spatial median filter. Frequency bands that deviate from the median amplitude by a specified threshold are either zeroed, or replaced by good frequency bands interpolated from neighboring traces.

Parameter values:

Processing Domain : Shot

Width of Spatial Median Filter : 11 Traces
Frequency Range Processed : 0 to Nyquist Hz
Width of Frequency Bands to Process : 4 Hz

Threshold Values:

Time (ms)	Threshold (%)
0	15
3000	10

2.16 Surface-Consistent Amplitude Compensation (SCAC)

SCAC compensates for shot, detector and offset amplitude variations that are caused by acquisition effects and are not a consequence of the subsurface geology.

The amplitude of a given time window is determined for every trace using either a root-mean-square (rms) or a mean-absolute amplitude criterion. The amplitudes measured can then be expressed as the product of surface-consistent source, receiver and offset terms, and a subsurface-consistent geology (CMP) term. Taking the logarithm allows the amplitude to be expressed as a sum of the above terms which, in turn, allows the surface consistent terms to be computed using a Gauss-Seidel iterative decomposition.

Scaling factors are then computed and applied to each trace. In this computation the CMP term is ignored, the scaling factor being the ratio of the geometric mean of all the SCAC source, detector and offset terms to the individual trace's source, detector and offset term.

Parameter Values:

Amplitude Criterion : RMS
Time Window : 500 ms to 3000 ms

2.17 4D Data Matching

Source and receiver locations that were common to both the baseline and monitor surveys were kept at this point all other stations were excluded from further processing. This method of matching was used to maximize the input fold to the migration.

2.18 Pre Migration Filter

A zero-phase TVF (Time Variant Filter) was applied to the data. The filter passbands were described by low- and high-cut frequencies and associated dB/octave cutoff slopes. The specified cutoff frequencies are located at the half-power (-3 dB in amplitude) response points and the slopes at these frequencies are equal to the respective dB/octave values. The slope is an approximate cosine squared function in the amplitude domain. The filters were normalized so that the output amplitudes were the same as the input amplitudes for frequency components within the passband.

Parameter values:

Filter Centre Time (ms)	Low-cut Frequency (Hz)	Low-cut Slope (dB/octave)	High-cut Frequency (Hz)	High-cut Slope (dB/octave)
0	6	18	160	180
2000	6	18	120	160
3000	6	18	80	100

Note: The times are those at the centre of the filter where the full effect of the filter is attained
The first filter was applied from the beginning of the trace to the first filter centre time
Intermediate filters were linearly tapered and blended with the preceding and succeeding filter between the filter centre times
The last filter was applied from the last filter centre time to the end of the data

2.19 Kirchhoff Pre-Stack Time Migration

All data were input, and the entire volume was output from Kirchhoff summation prestack time migration. In this method, the migrated image is constructed by summing weighted amplitudes along diffraction curves. These diffraction curves are determined by two-way travel times from the surface to subsurface scatterers that are computed from the supplied velocity field. Ray-bending corrections were included in the travel time computation.

A V^2T amplitude correction is effectively applied during the migration process, so the corresponding geometrical spreading correction was removed prior to migration.

2.19.1 Velocity Analysis

The migration is run on common offset volumes, and as migrated velocities are required, it is run in an iterative fashion, giving improved velocity control with each pass. The iterative sequence is illustrated below.

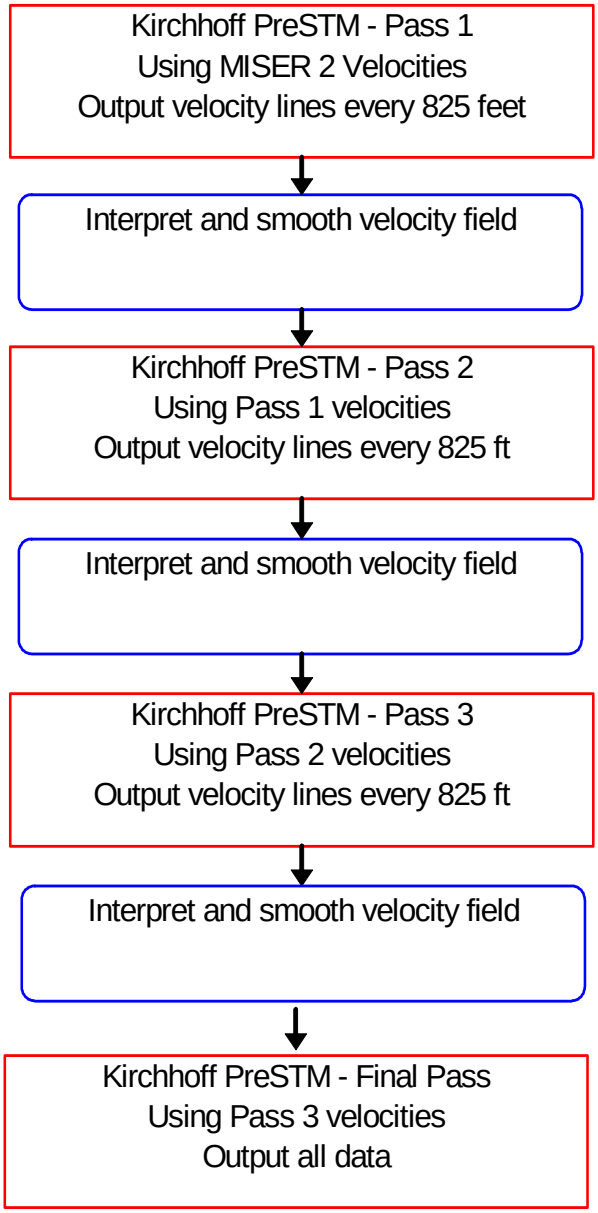

Parameter values:

Traveltime computation : Isotropic Ray Bending
Max aperture : 5280 ft
Amplitude compensation mode : 3D
Dip limit : 73 Degrees
Input Bin Size : 82.5 ft x 82.5 ft
Output Bin Size : 82.5 ft x 82.5 ft
Output End Time: : 3000 ms

Time variant frequency limits:

Time (ms)	Frequency (Hz)
0	195
2000	150
3000	100

26 offsets were output from the migration in the following manner.

Min offset input to KrPSTM	Max offset input to KrPSTM	Offset output from KrPSTM
0	1200	1020
1200	1560	1380
1560	1920	1740
1920	2280	2100
2280	2640	2460
2640	3000	2820
3000	3360	3180
3360	3720	3540
3720	4080	3900
4080	4440	4260
4440	4800	4620
4800	5160	4980
5160	5520	5340
5520	5880	5700
5880	6240	6060
6240	6600	6420
6600	6960	6780
6960	7320	7140
7320	7680	7500
7680	8040	7860
8040	8400	8220
8400	8760	8580
8760	9120	8940
9120	9480	9300
9480	9840	9660
9840	10200	10020

2.20 Final Velocity Analysis

Velocity analysis was performed using **WesternGeco's** INVA package. At regular intervals across the survey CMP gather data were selected. From this data Multi-Velocity Function (MVF) stacks and velocity semblance values were computed. For each velocity location, MVF data, semblances and gathers are displayed interactively allowing stacking velocities to be interpreted.

Percentage stacks and NMO-corrected gathers are then produced to check the validity of the picks and any necessary changes made before the velocity field is output.

Parameter Values:

Analysis Spacing	: 825 ft
Number of CMP's per Analysis (MVF Stack)	: 11
Number of CMP's per Analysis (Semblance Display)	: 5

2.21 NMO Compensation

Hyperbolic moveout was applied to the data. This corrected the reflection events to their zero offset position by:

$$t_o = \sqrt{t^2 - \frac{X^2}{V^2}}$$

where:

t is the traveltime at offset X

t_o is the zero offset traveltime

X is the absolute value of the source-to-detector offset distance

V is the moveout velocity

As the input trace samples were moveout corrected, they were stretched across a longer output time, so distorting the original data. The effect of this distortion was limited by muting the data according to a limiting stretch value that is (where this value is represented by the variable N) the output data were muted when the output time interval exceeded N% of the corresponding input time interval.

Muting was not performed on traces with a source-to-detector offset distance less than that specified below, so allowing the near-surface, near-offset data to remain unmuted.

Parameter values:

Mute:	
Limiting Stretch Value	: 2 times input time interval

2.22 Outer Trace Mute

An outer (long offset) trace mute was applied to the data in order to suppress direct arrivals, refractions and wide angle reflections.

The data were tapered from zero to full amplitude over a taper zone.

Parameter values:

Taper Zone Length: 64 ms (starting from the mute times detailed below)

Source-to-Detector Offset (Feet)	Mute Time (ms)
1,021	0
1,030	200
1,900	400
3,070	704
4,885	990
12,436	1,811

Note: Mute times were linearly interpolated between the specified offsets and extrapolated for offsets larger than the last offset specified.

2.23 Stack

The traces within each gather are stacked to form a single output trace. The resultant trace is normalized sample by sample using the following function;

NOISE FACTOR = 1

$$s(t) = \frac{1}{\sqrt{(w(t) \bullet (w(t)+nfac))}}$$

where:

w(t) is the summed weight function for a given output trace

nfac is the noise factor for trace balance

2.24 Datum Correction

The data was time shifted from recording surface to the final datum. The datum was 1000 ft. and the replacement velocity was 10,000 ft/sec.

2.25 Conclusions

4D QC's showed consistent results trough out the processing sequence demonstrating that the processing preserved the 4D footprint. On the final migrations clear differences could be seen between the baseline and monitor surveys.

3.0 Repeatability

Throughout the processing of these data the Baseline and Monitor surveys were compared to ensure that the processing was bringing them closer together. I.e making them more repeatable.

3.1 Repeatability Measurements

The primary measure (metric) used to monitor repeatability, on this survey was to take a normalised difference averaged over the whole volume. We used the RMS of the difference over the sum of the RMS for the co-incident data. The table below shows the results for the data volume cube created from the shared source and receiver locations. Analysis was performed in a time window from 100 - 700ms.

A – Baseline survey
B – Monitor survey

$$\text{Repeatability} = 200 \times \frac{2 \times \text{RMS}(A - B)}{\text{RMS } A + \text{RMS } B}$$

The table shows that the processing in improving the repeatability. The largest improvements came from the amplitude processing and imaging.

Process	NRMS
Raw	114
Noise Attenuation	117
SCD	118
SCAC	107
Final Migration	100

4.0 Personnel

QC Supervisors
John Young
Dave Dangle

Area Geophysicists
Tony Clark
Greg Wimpey

Processor
Adrian Montgomery

5.0 Appendices

5.1 Acquisition Information

5.1.1 Baseline Survey (2004)

Parameter	Value
Contractor's Name	GREAT LAKES GEOPHYSICAL INC.
Client's Name	CORE ENERGY LLC
Observer's Name	RANDY SMITH
Country	USA
State or Province	MI.
County	OTSEGO
Survey Name	CHARLTON 30 3D
Manufacture of Recording System	SERCEL
Model of Recording System	388
Number of Channels	585
Sampling Interval (in Seconds)	0.002
Record Length (in Seconds)	3.072
Recording System's Low-cut Frequency (in Hz)	3
Recording System's Low-cut Slope (in dB/Octave)	72
Recording System's High cut Frequency (in Hz)	250
Recording System's High cut Slope (in dB/Octave)	72
Recording System's Notch Frequency (in Hz)	0
Type of Source	Dynamite
Comment about the Source	5-6' X 1/2LB. OR X 1/3LB. WET AREAS
Receiver Manufacture	GEO SPACE
Receiver Model	20 D
Type of Receiver Base	Spike
Receiver's Natural Frequency (in Hz)	10
Number of Receivers in a Group	6
Type of Receiver Pattern	Linear/80'
Comment About the Receivers	CENTERED ON STA.
Source Interval	165
Receiver's Natural Frequency (in Hz)	165
Units of Measure	Feet
Number of Receiver Lines	15
Distance Between Receiver Lines	825

5.1.2 Monitor Survey (2007)

Parameter	Value
Contractor's Name	Great Lakes Geo.
Client's Name	CORE ENERGY LLC

Observer's Name	DAVE A BICE
Country	U.S.A.
State or Province	MI
County	OTSEGO CO.
Survey Name	CHARLTON 30/31 3-D
Manufacture of Recording System	SERCEL
Model of Recording System	408
Number of Channels	572
Sampling Interval (in Seconds)	0.001
Record Length (in Seconds)	4
Recording System's Low-cut Frequency (in Hz)	3
Recording System's Low-cut Slope (in dB/Octave)	0
Recording System's High cut Frequency (in Hz)	400
Recording System's High cut Slope (in dB/Octave)	72
Recording System's Notch Frequency (in Hz)	0
Type of Source	Dynamite
Comment about the Source	5X10'X1/2LB-5X5'X1/3LB
Receiver Manufacture	GEO-SPACE
Receiver Model	GS-30-CT
Type of Receiver Base	Spike
Receiver's Natural Frequency (in Hz)	10
Number of Receivers in a Group	6
Type of Receiver Pattern	Linear
Comment About the Receivers	6 PHONES@ 80.0' CENTERED ON THE FLAG
Source Interval	165
Receiver's Natural Frequency (in Hz)	165
Units of Measure	Feet
Number of Receiver Lines	16
Distance Between Receiver Lines	660

5.2 Grid Information

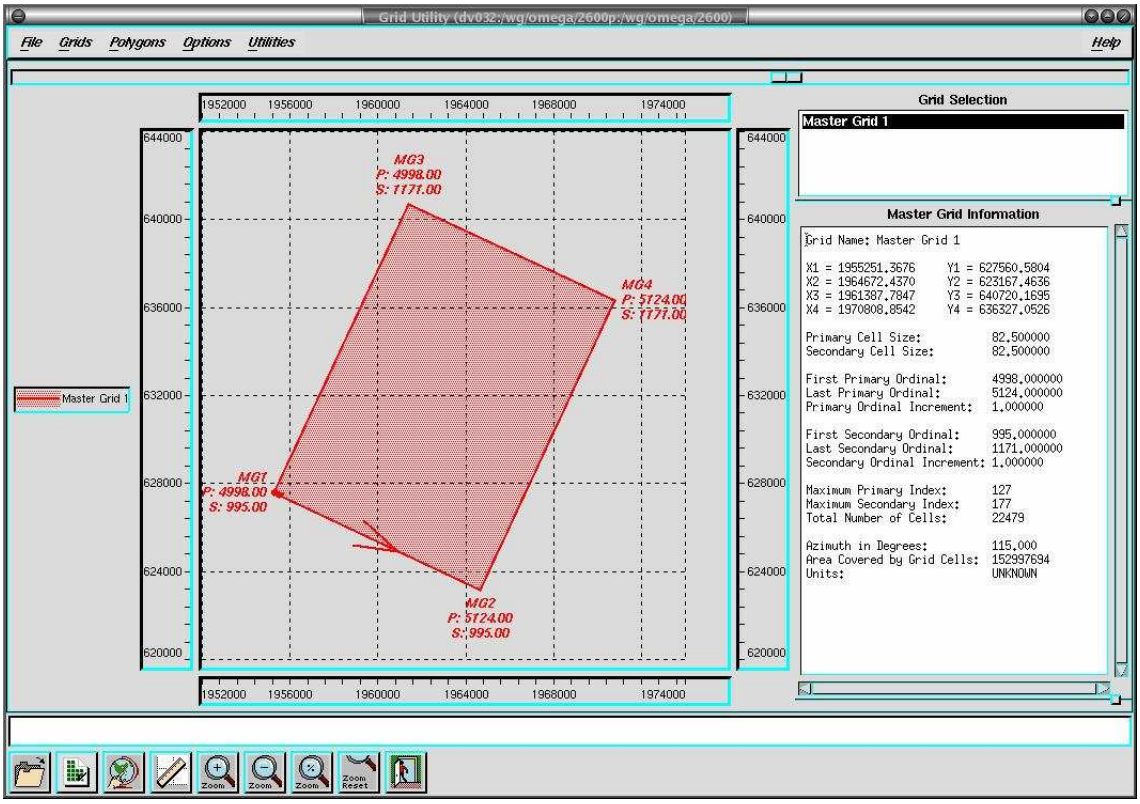

5.3 Data Examples

5.3.1 2004 XL stack after FXCNS and AAA

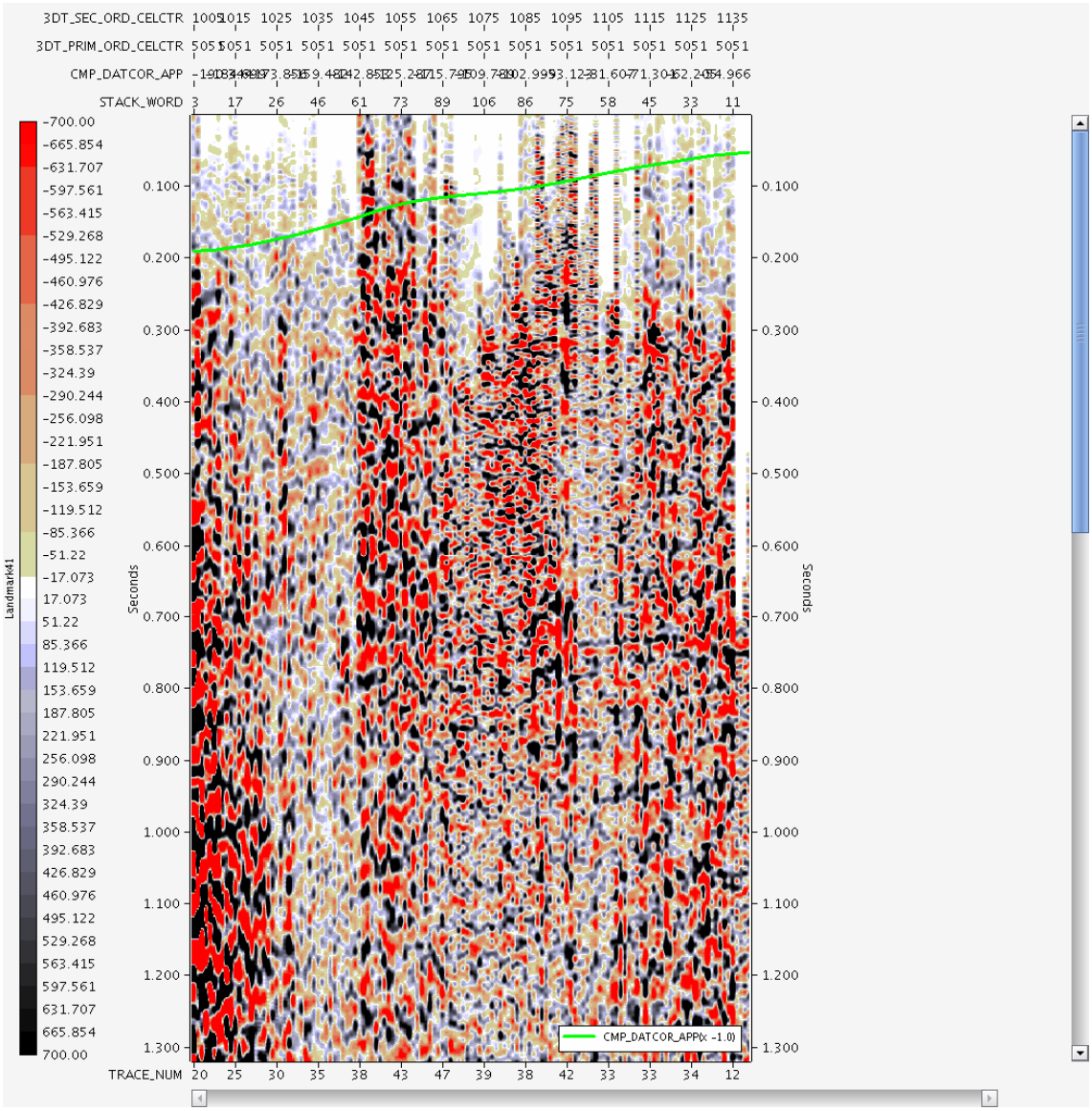

5.3.2 2007 XL stack after FXCNS and AAA

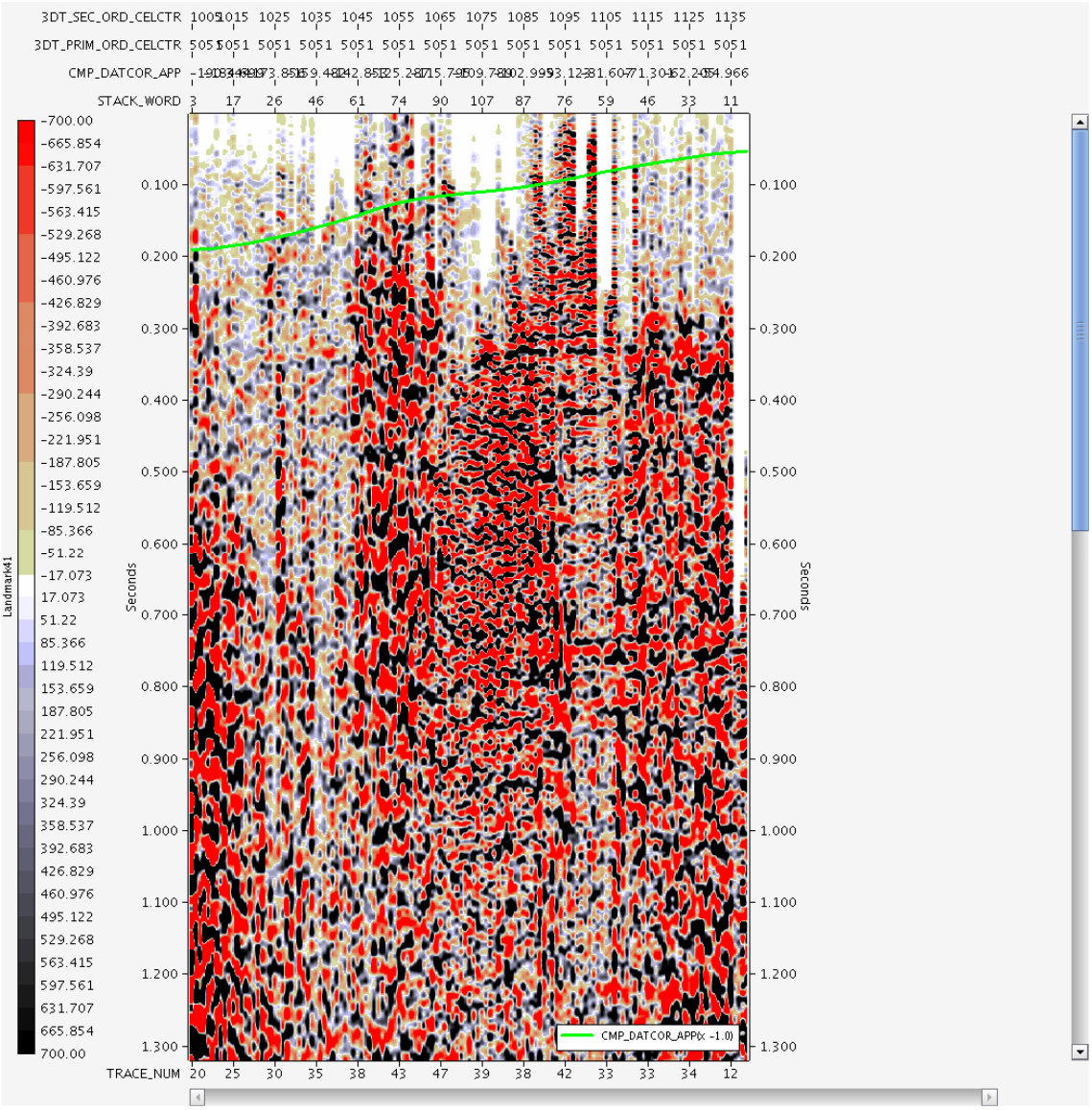

5.3.3 2004 XL stack after Surface Consistent Deconvolution

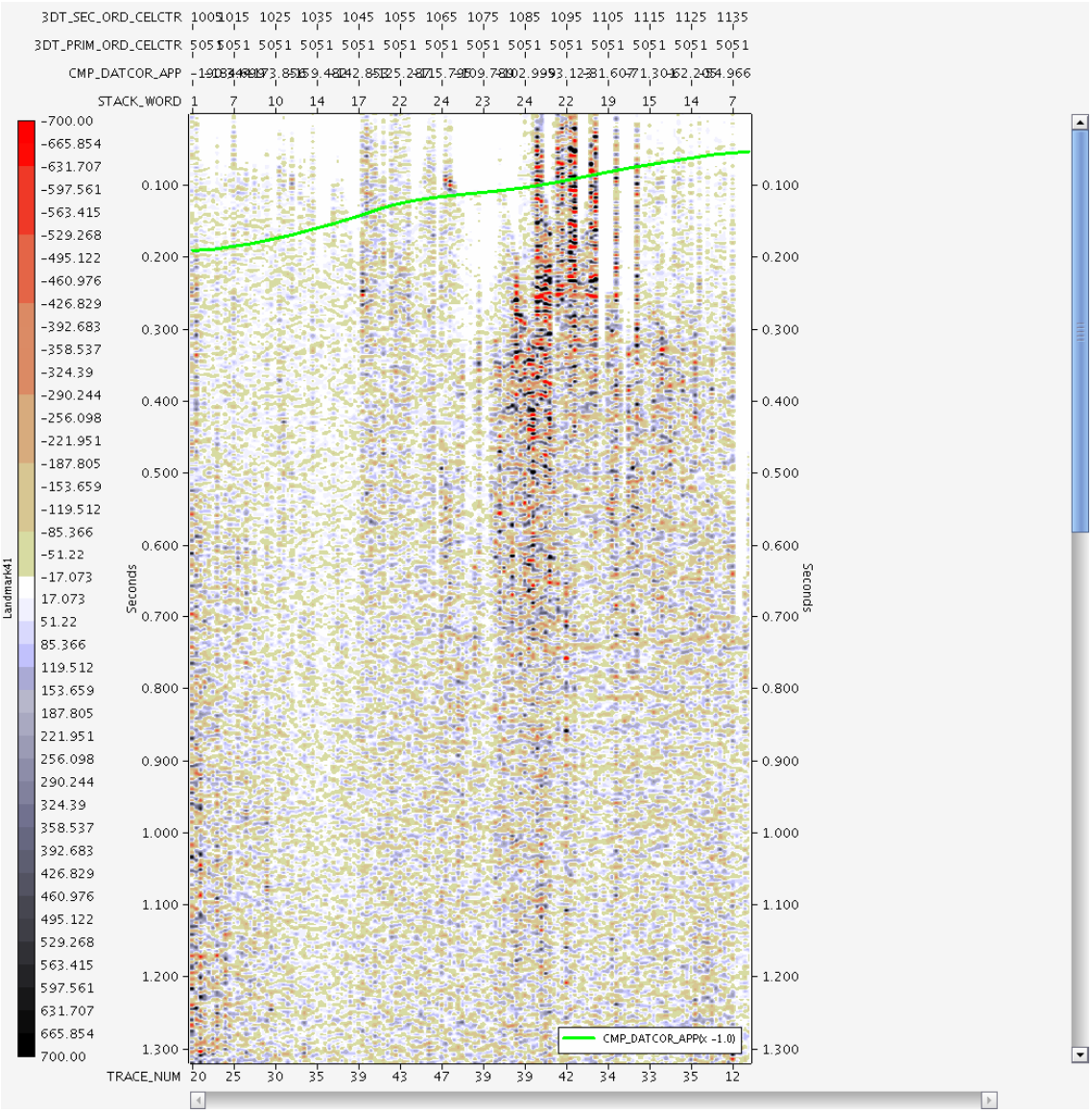

5.3.4 2007 XL stack after Surface Consistent Deconvolution

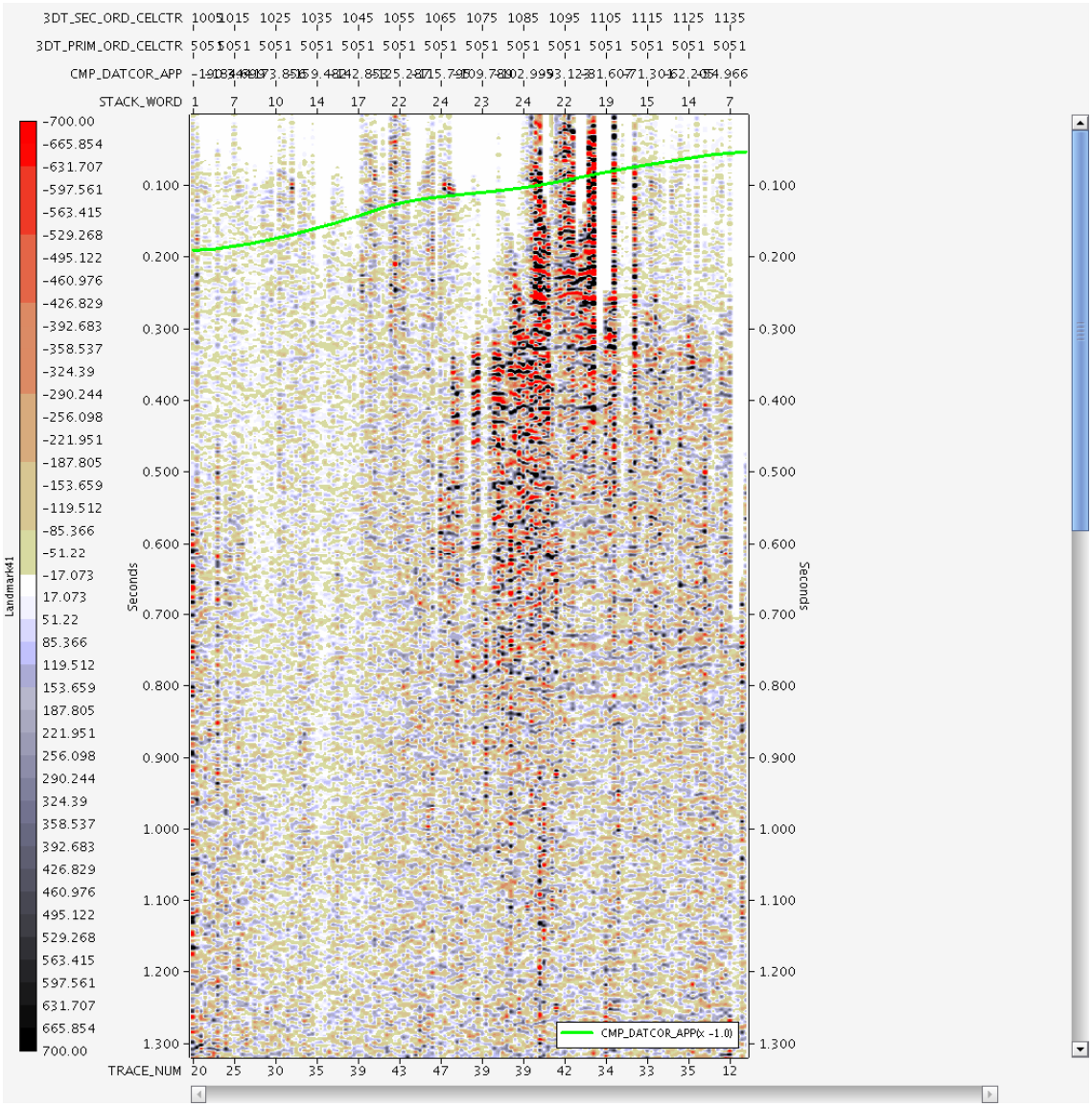

5.3.5 2004 XL stack after Surface Consistent Amplitude Compensation

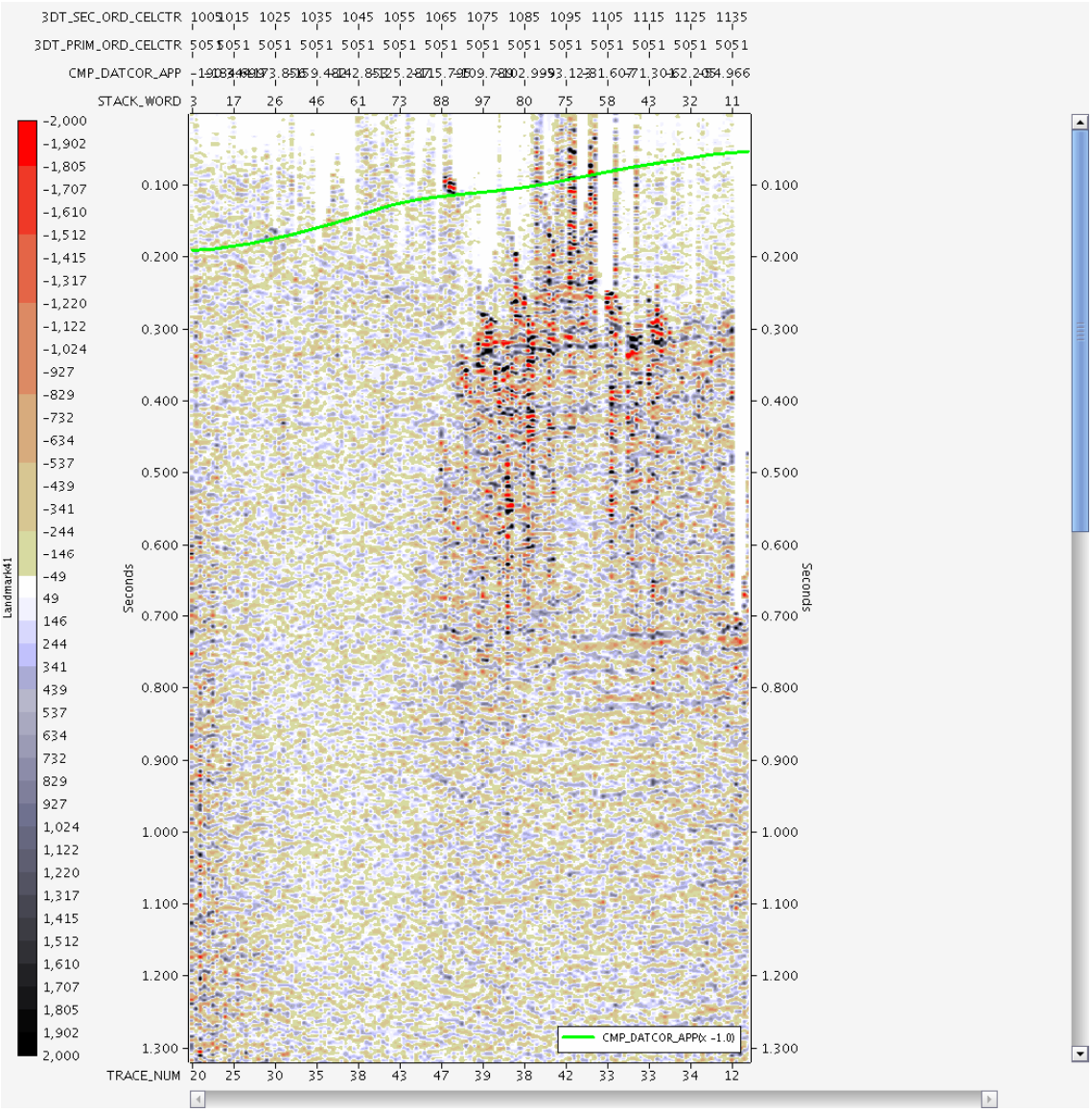

5.3.6 2007 XL stack after Surface Consistent Amplitude Compensation

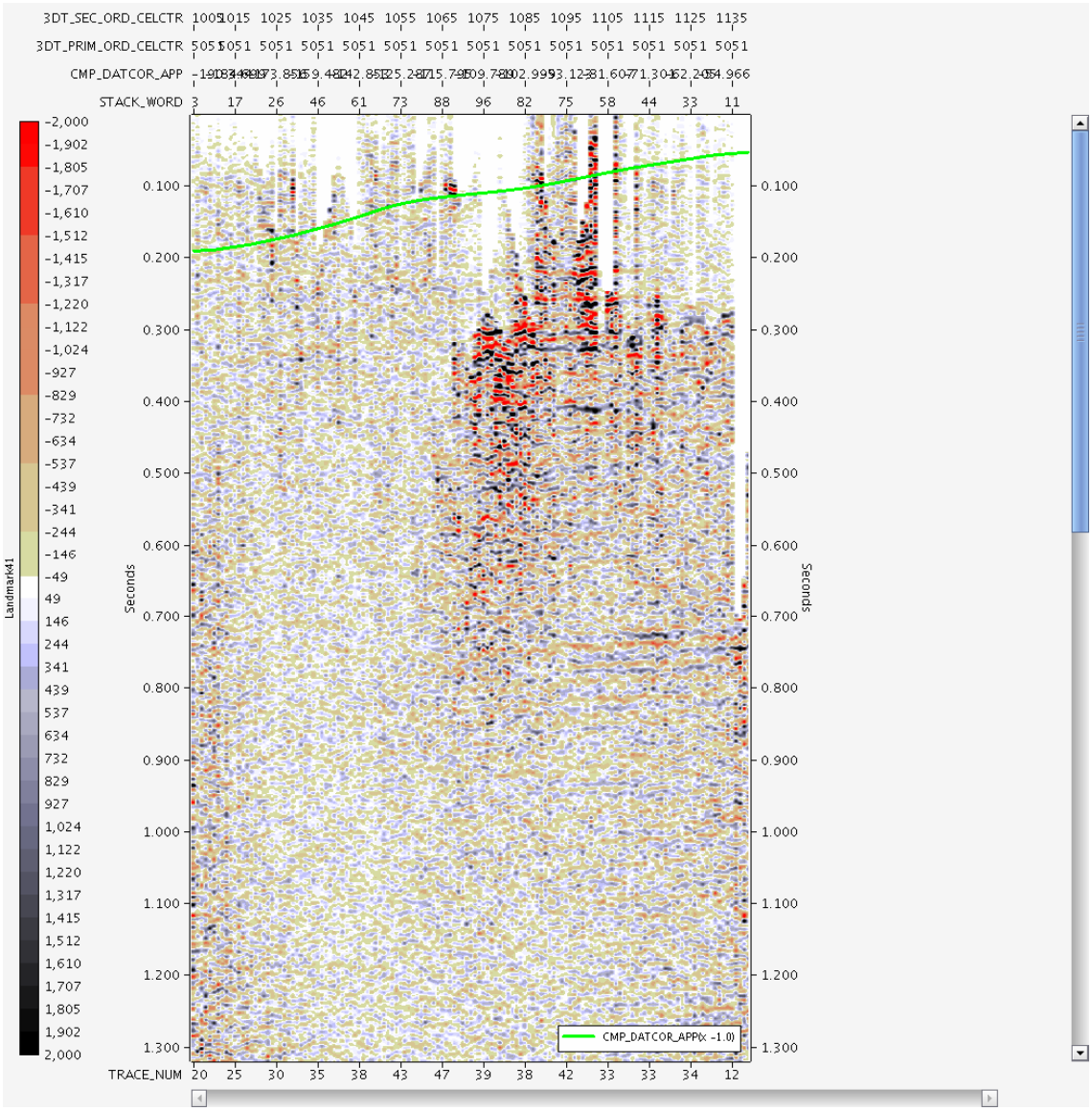

5.3.7 2004 XL from migrated volume

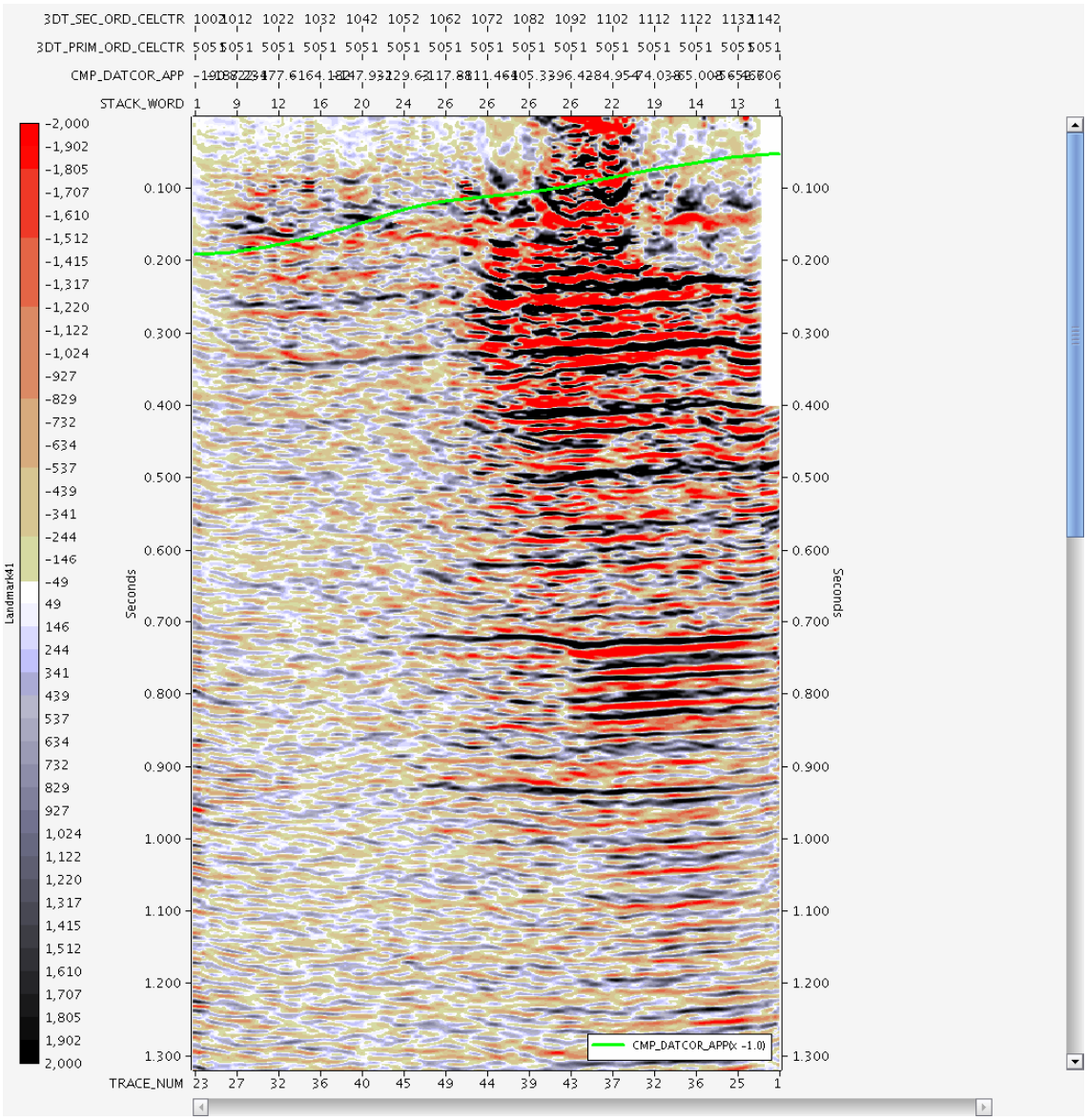

5.3.8 2007 XL from migrated volume

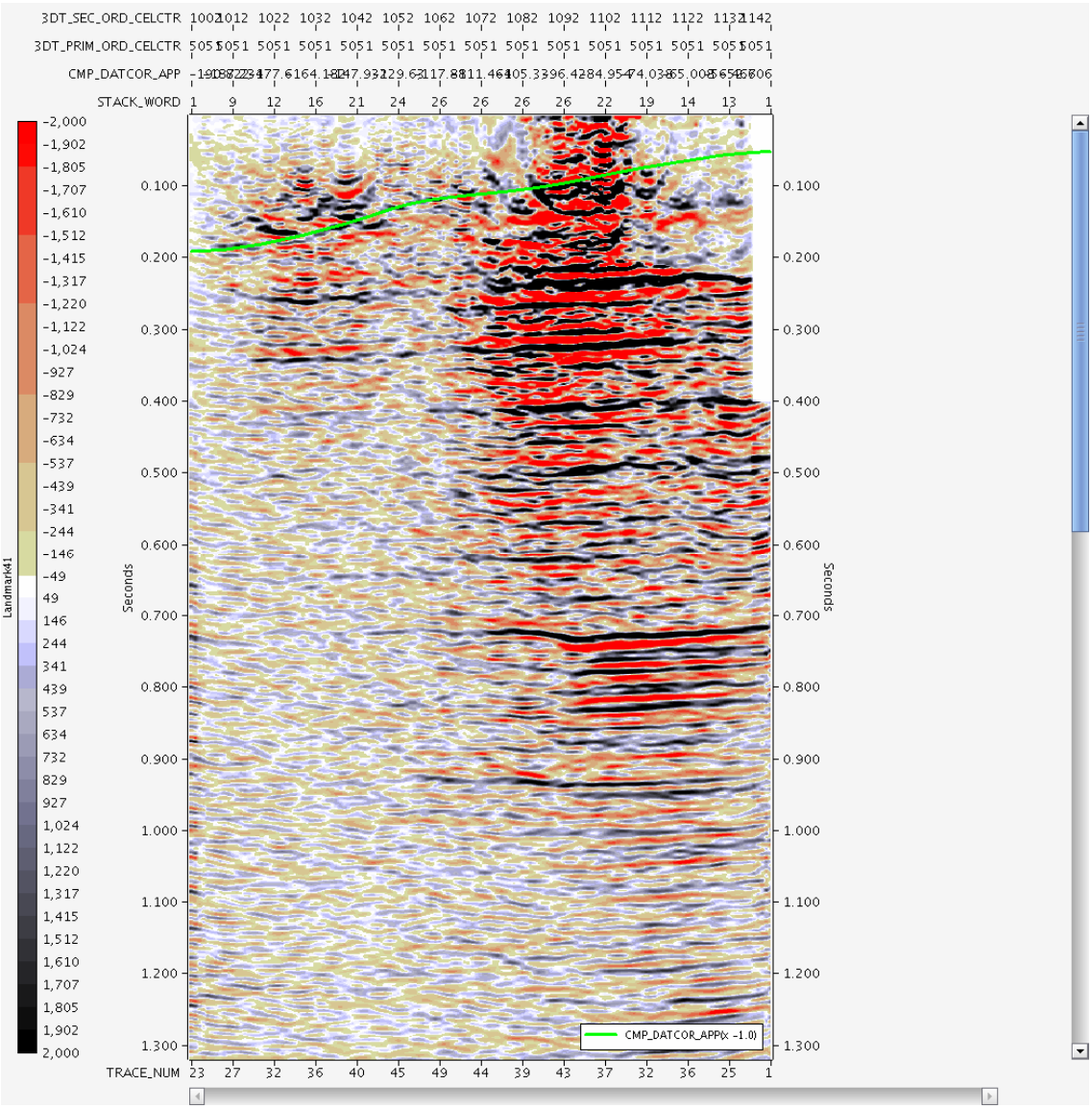

5.3.9 Difference section of migrated volumes

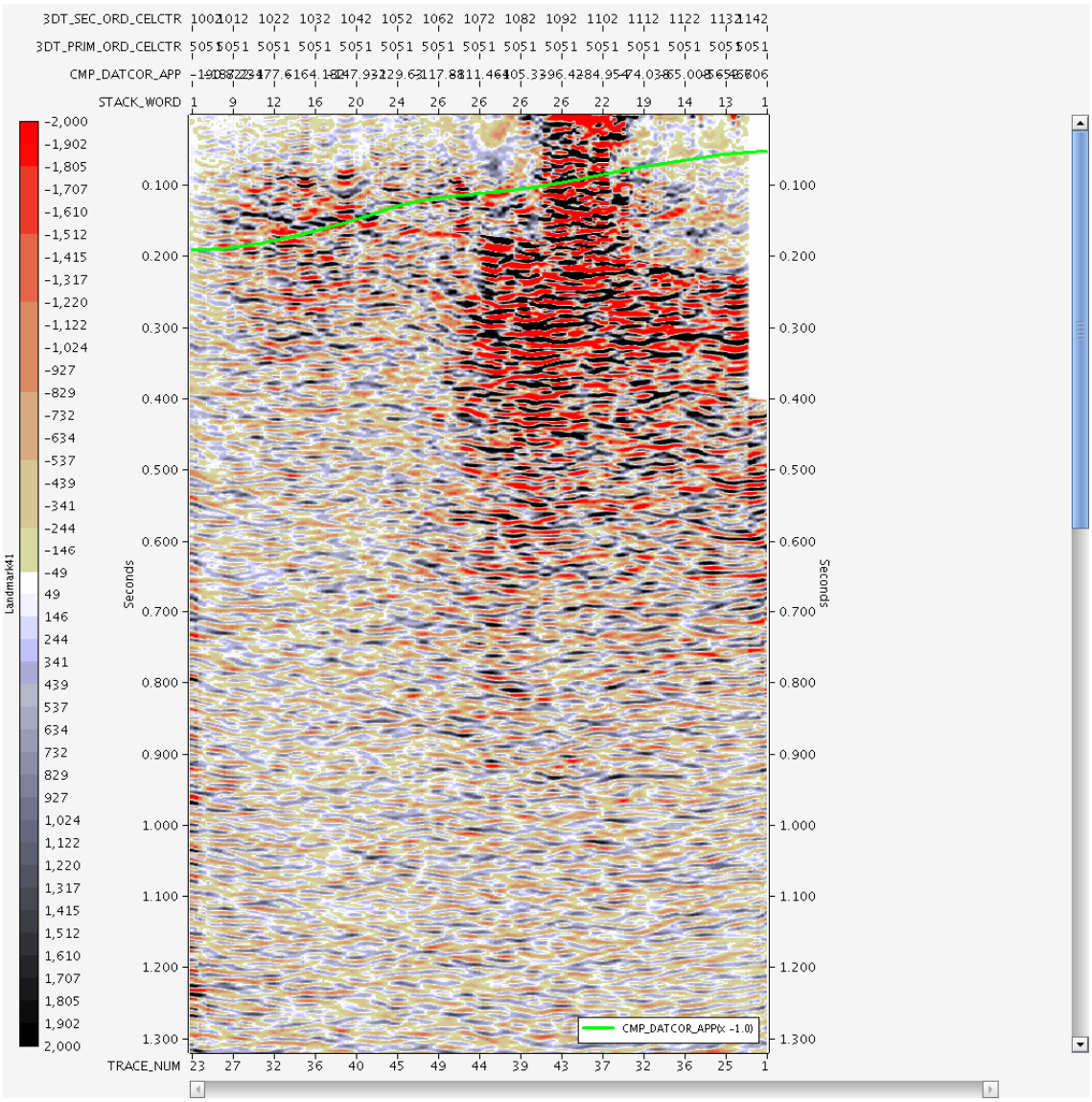

5.3.10 NRMS QC Plot of Migrated Data

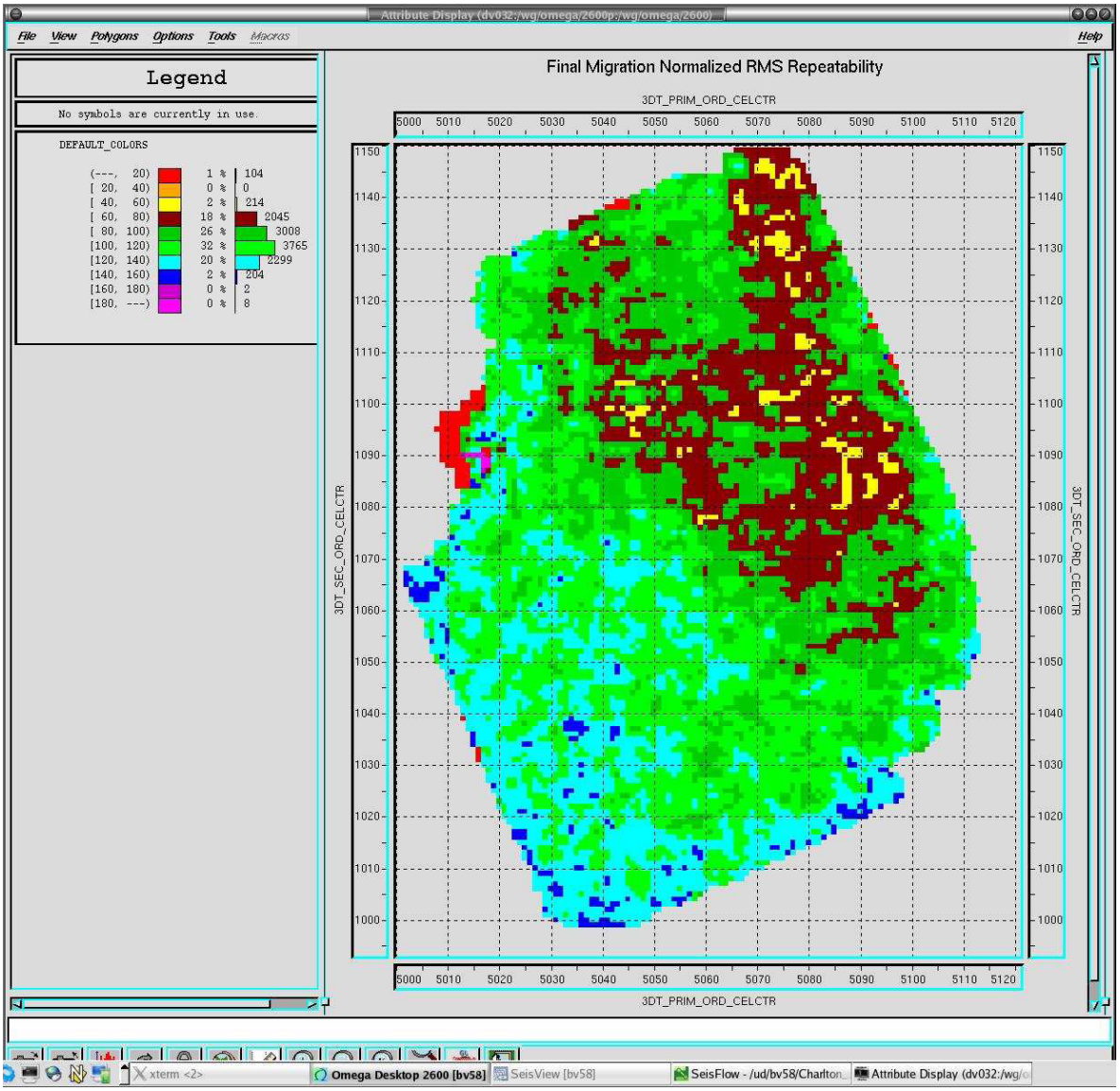

10.3 - APPENDIX D - Blended Seismic Attribute Analysis – High Amplitude blended with High Variance

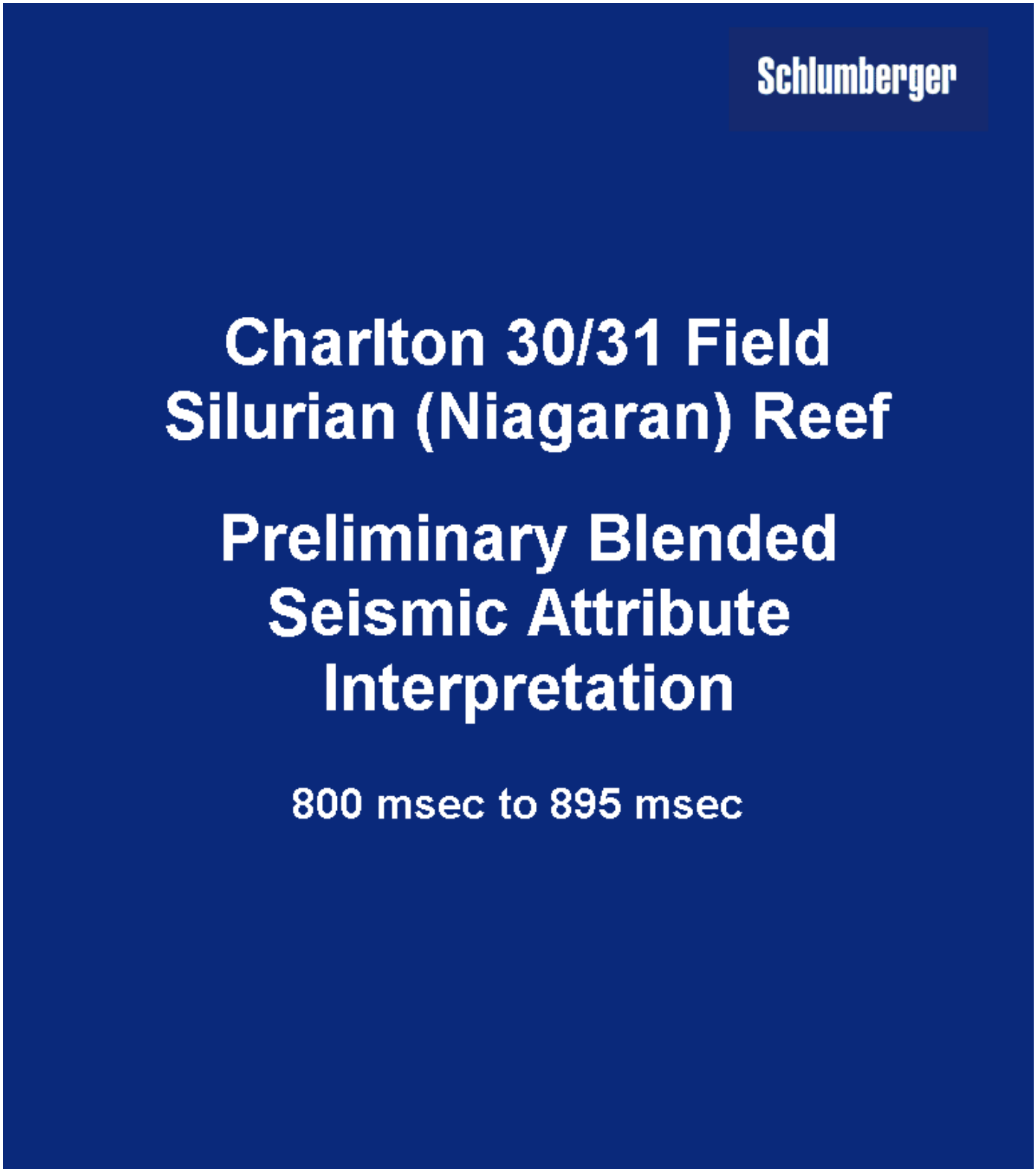

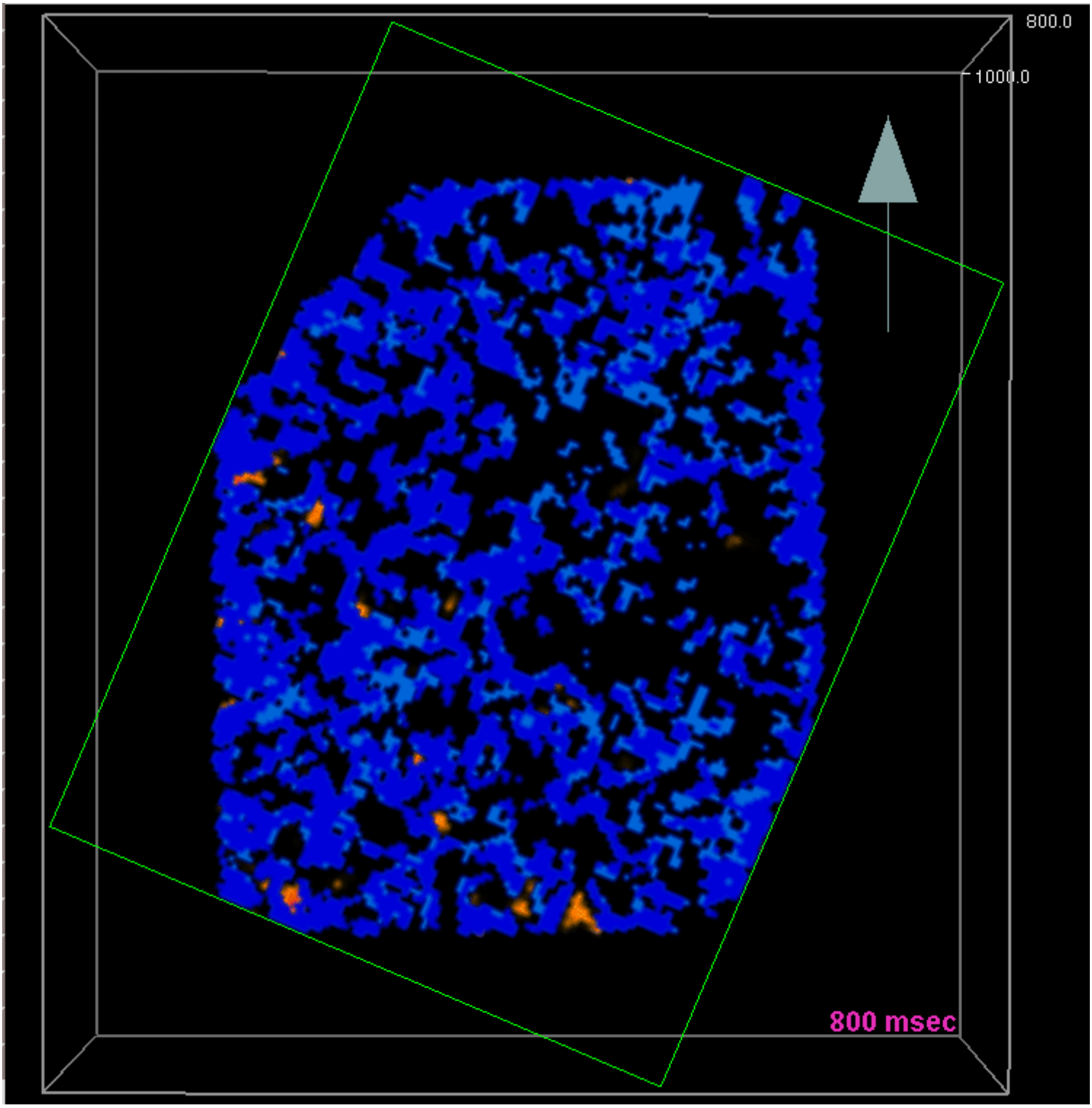
800.0
1000.0
800 msec

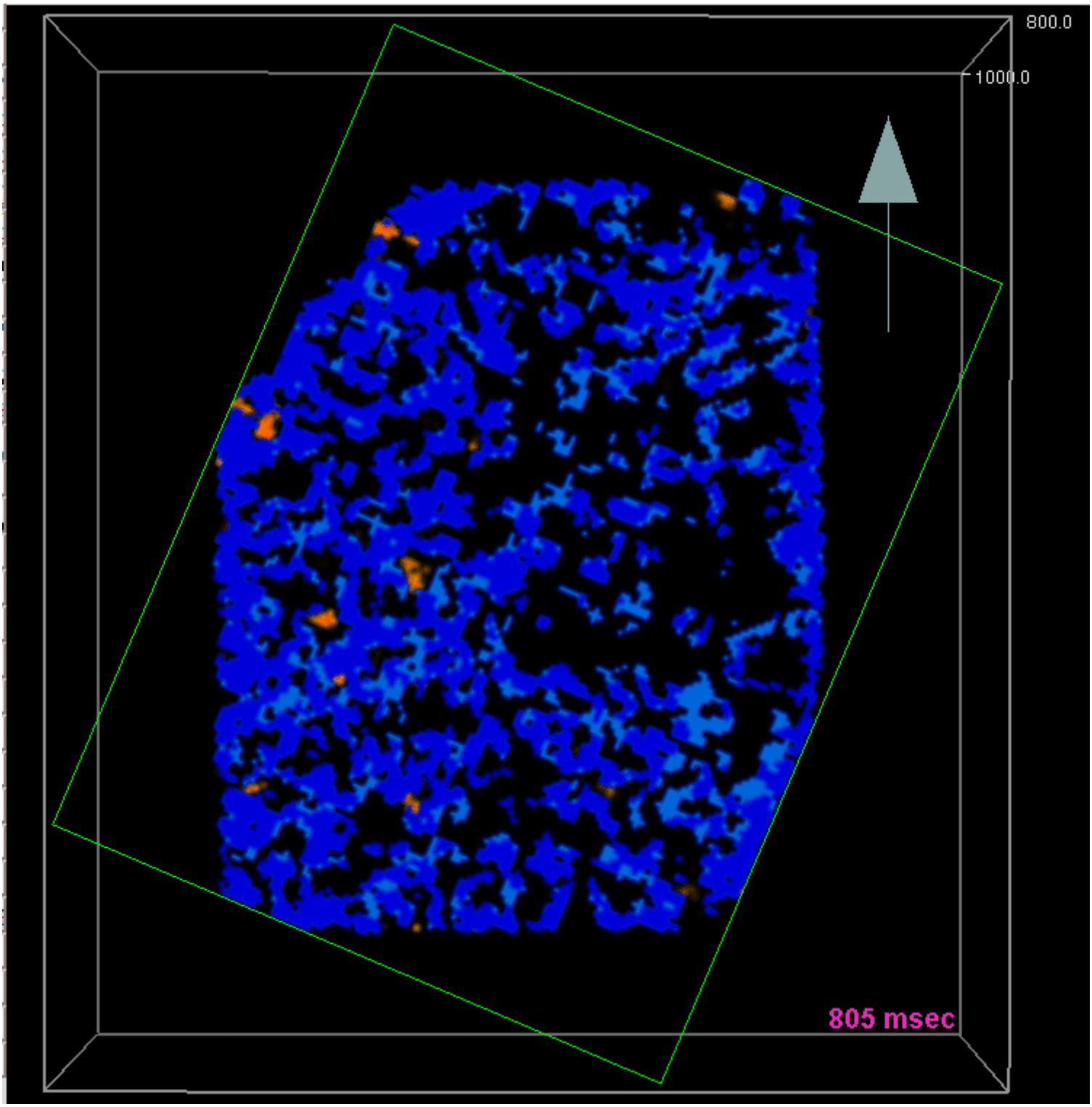
800.0
1000.0
805 msec

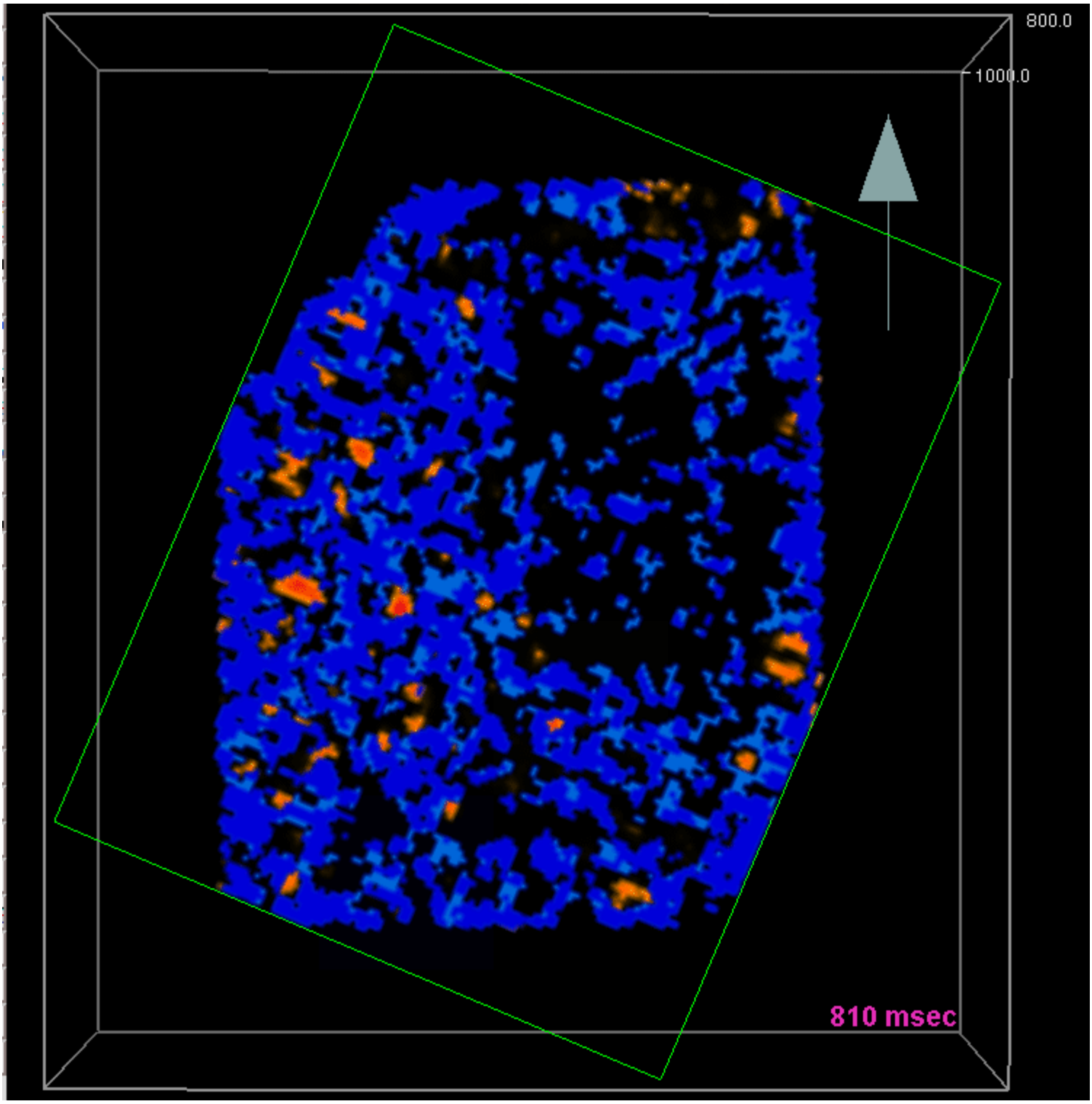
800.0
1000.0
810 msec

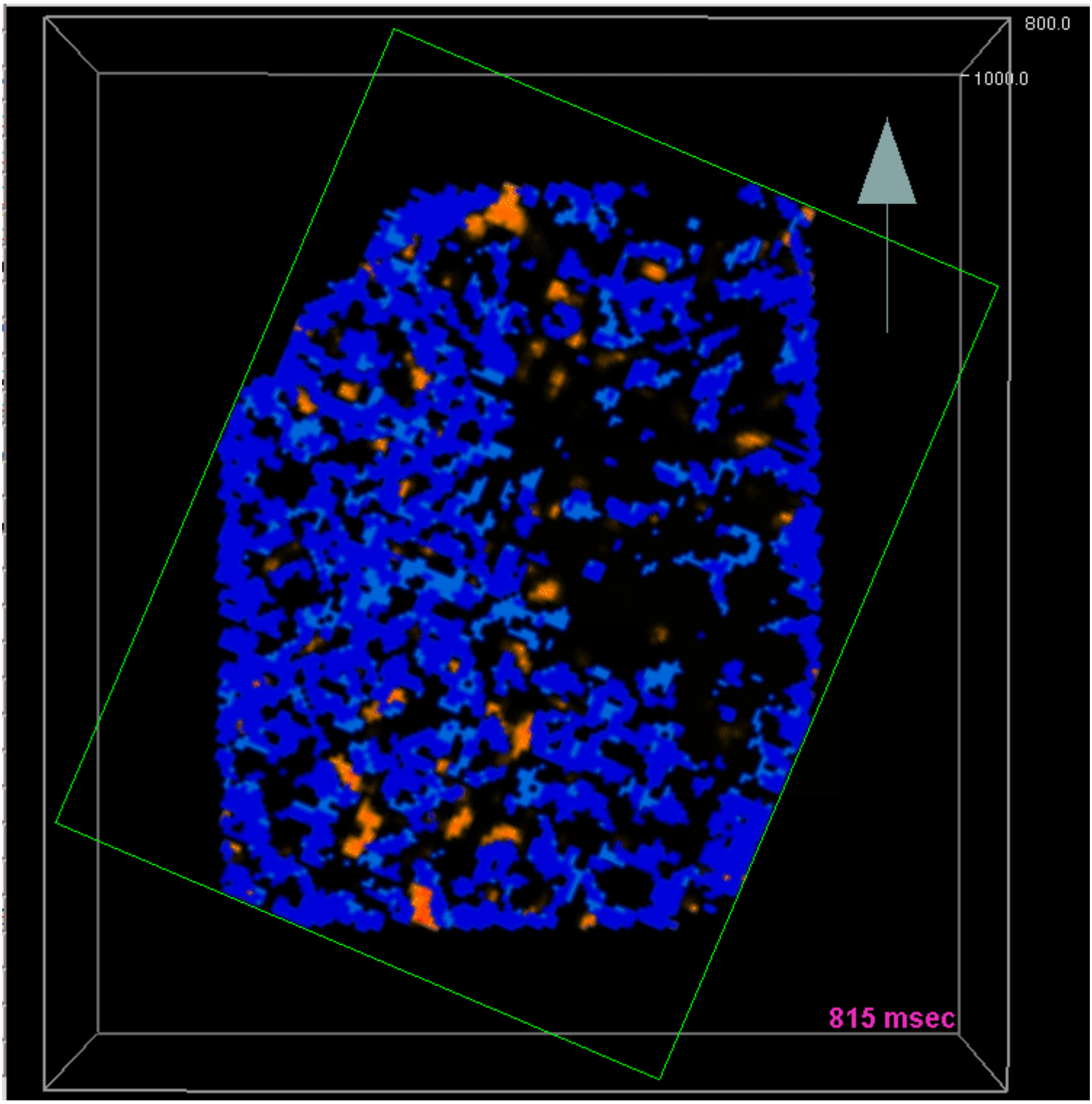
800.0
1000.0
815 msec

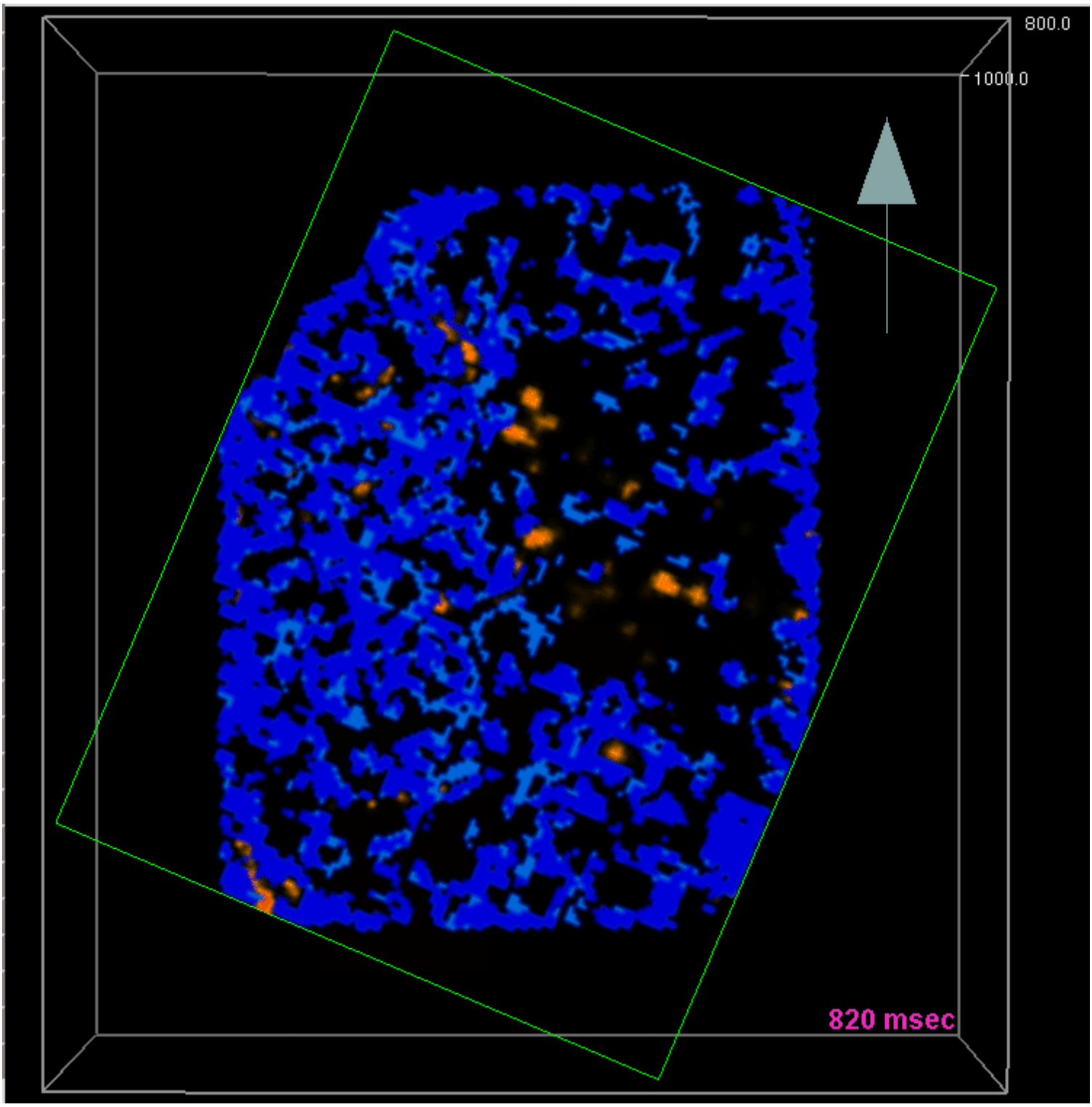
800.0
1000.0
820 msec

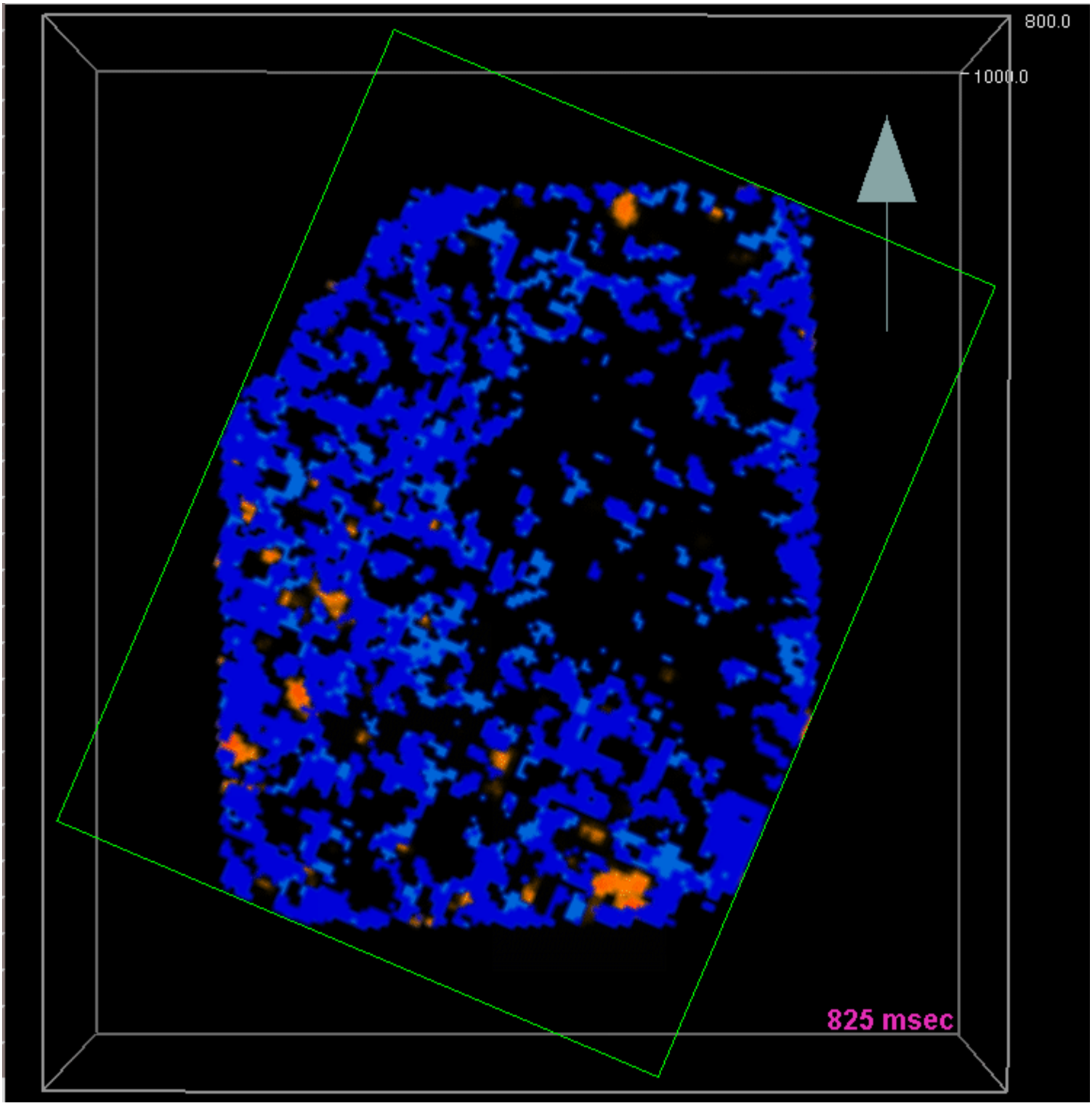
800.0
1000.0
825 msec

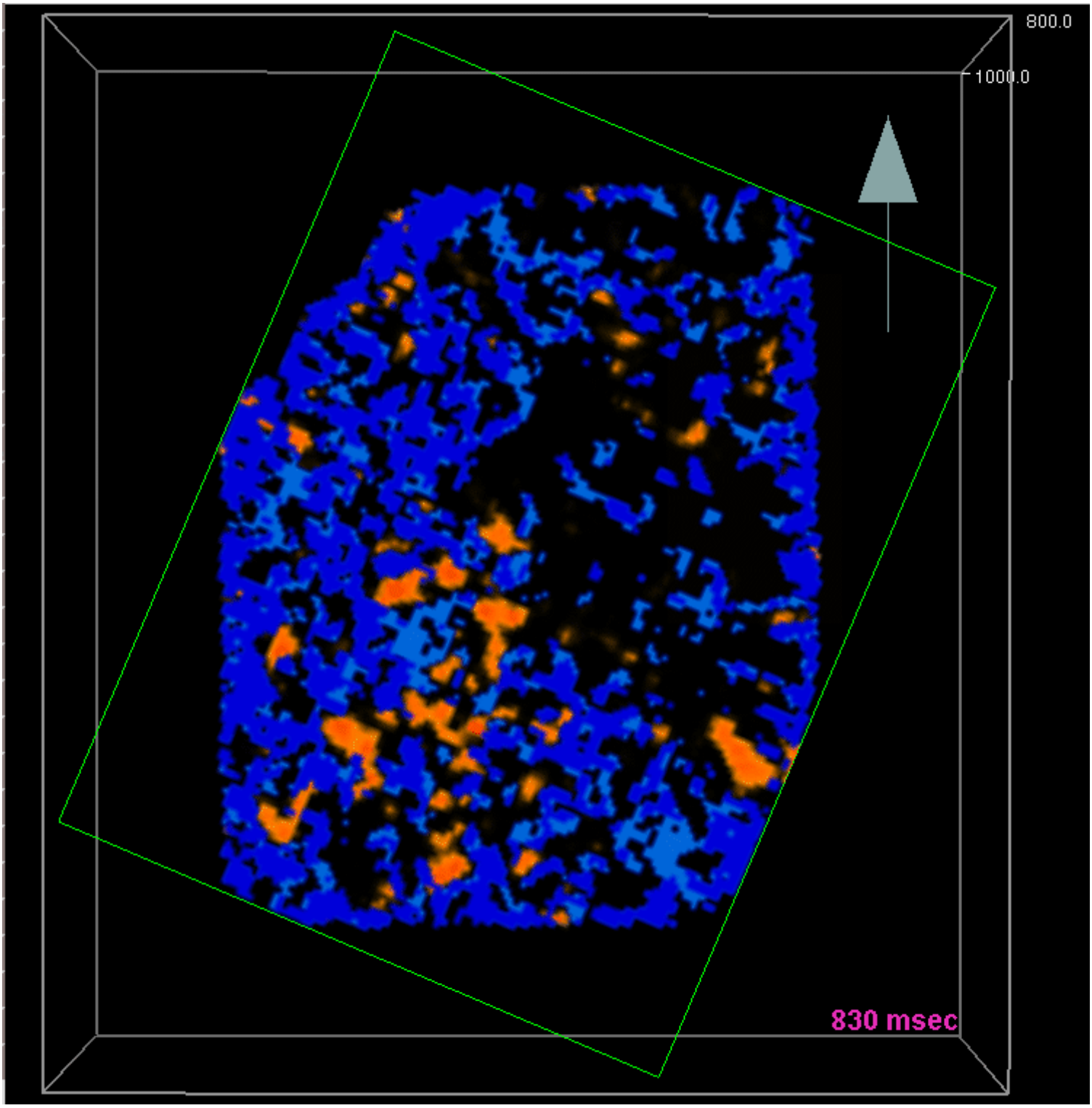
800.0
1000.0
830 msec

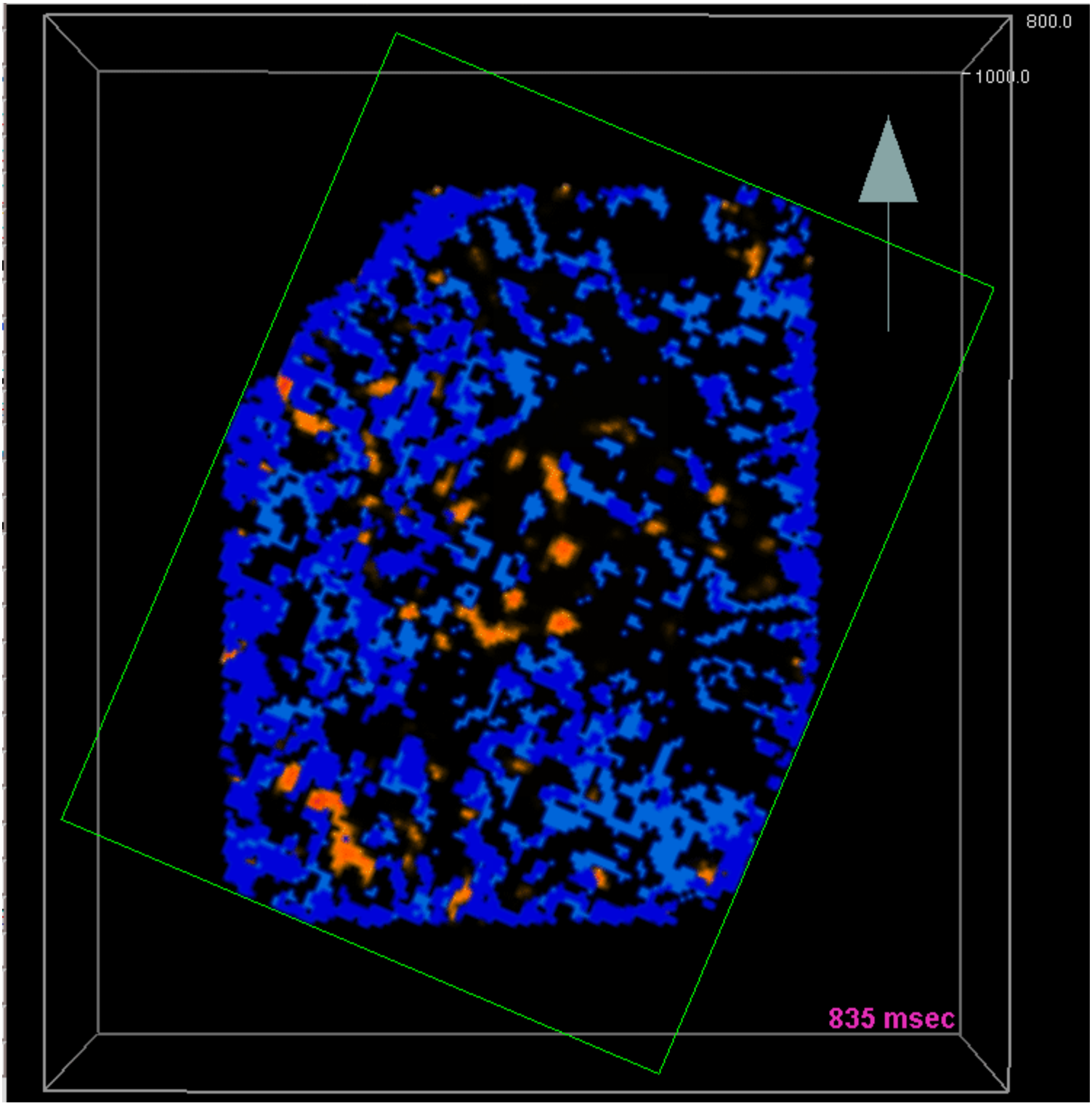
800.0
1000.0
835 msec

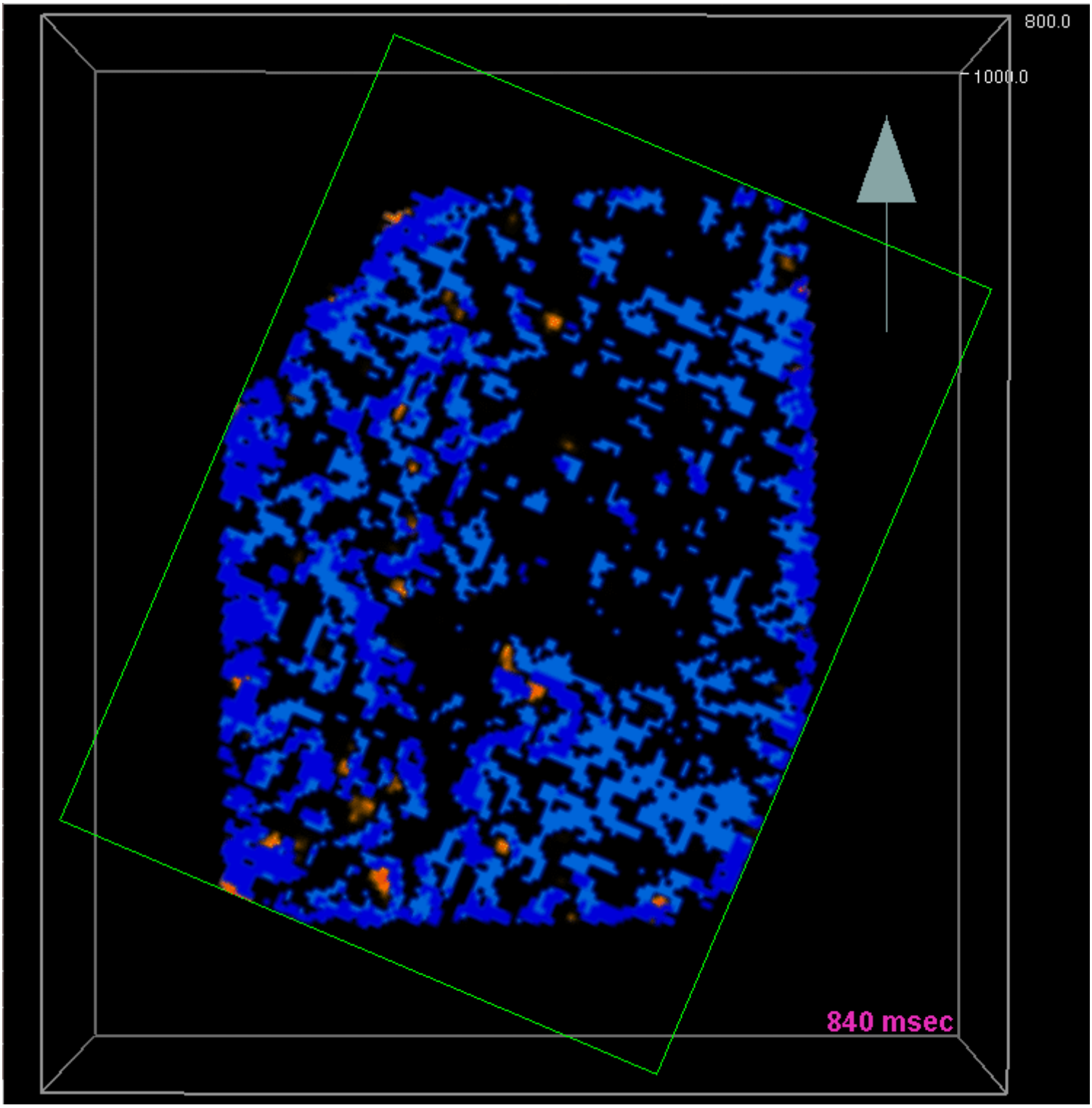
800.0
1000.0
840 msec

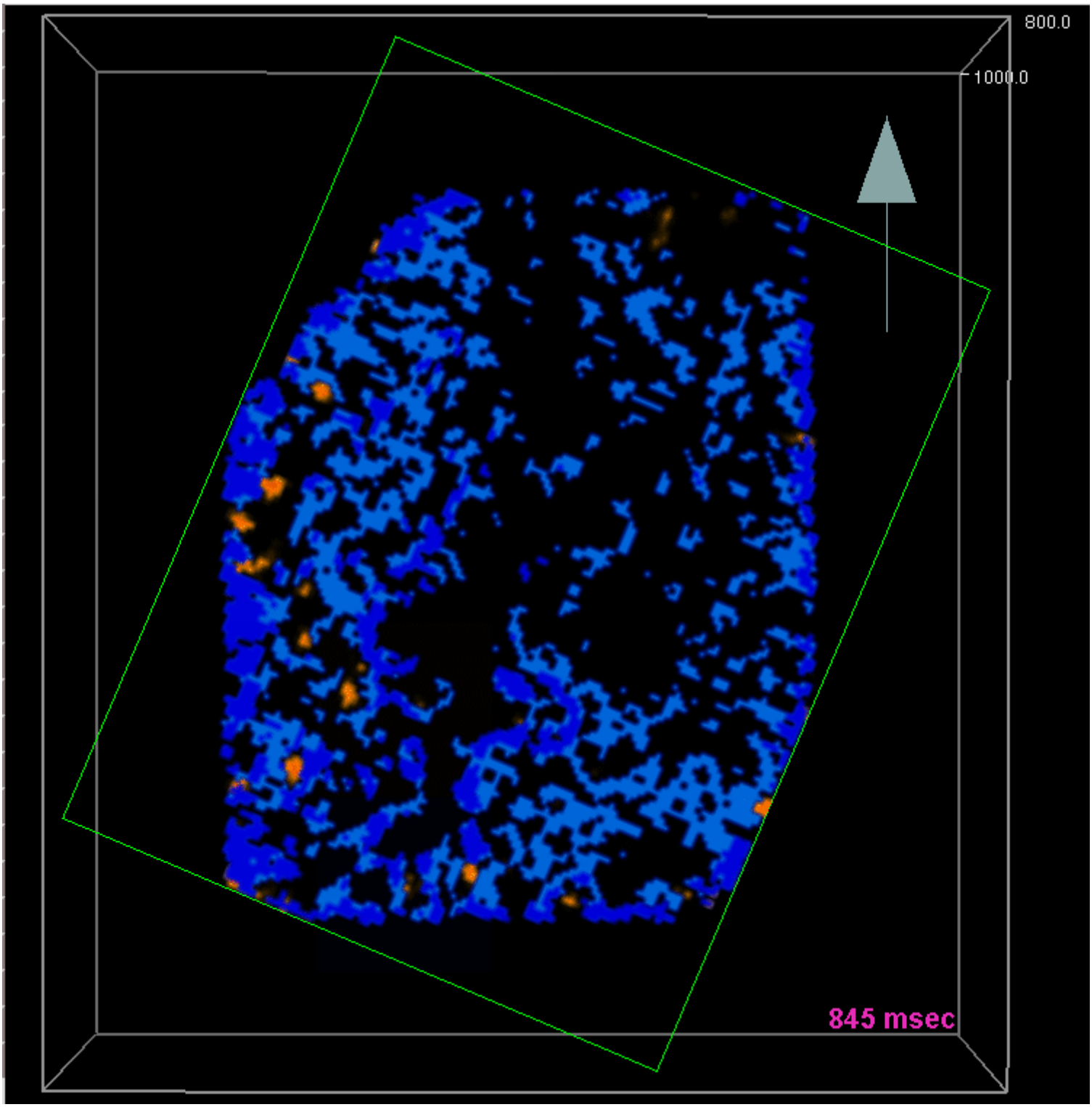
800.0
1000.0
845 msec

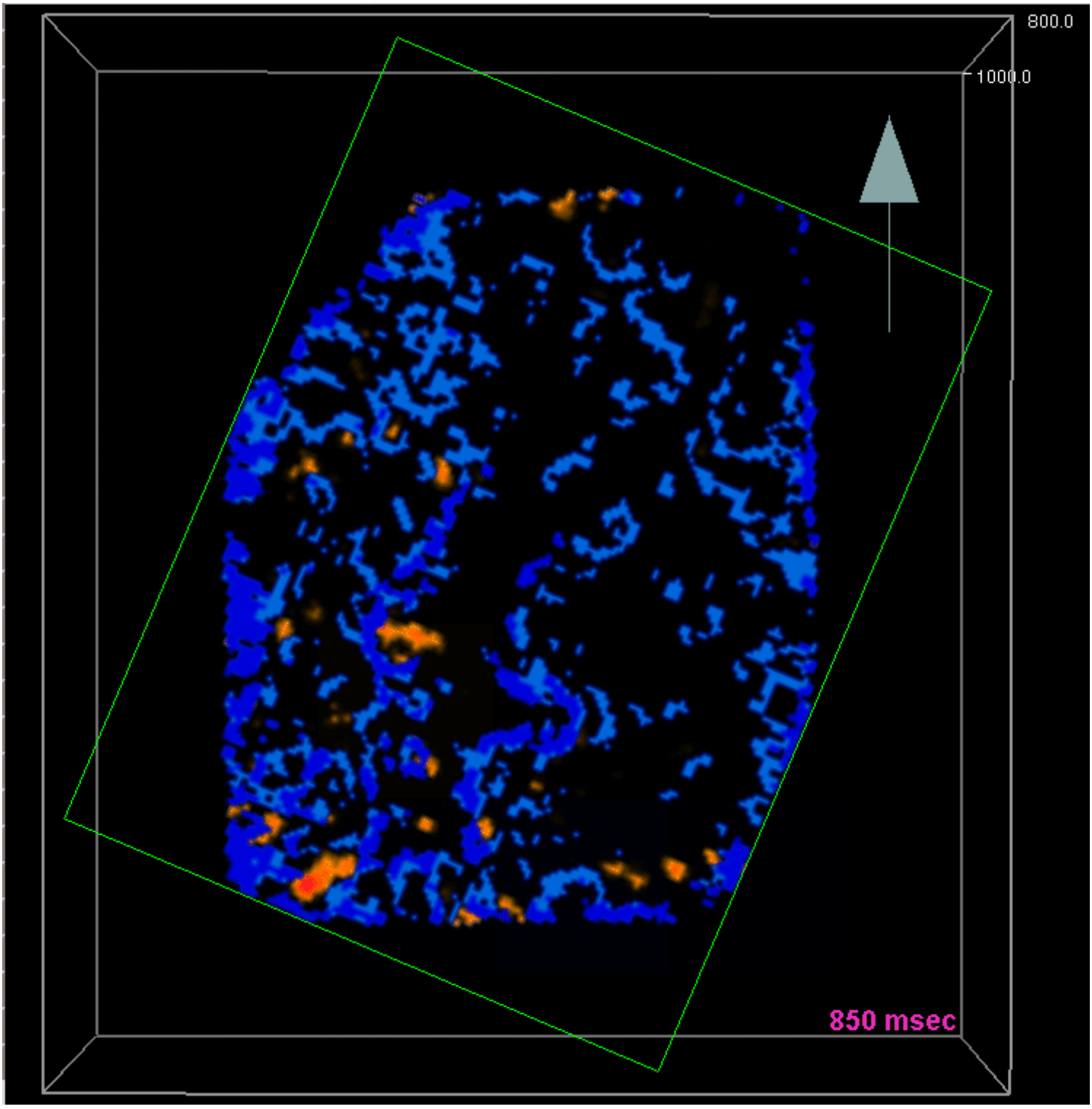
800.0
1000.0
850 msec

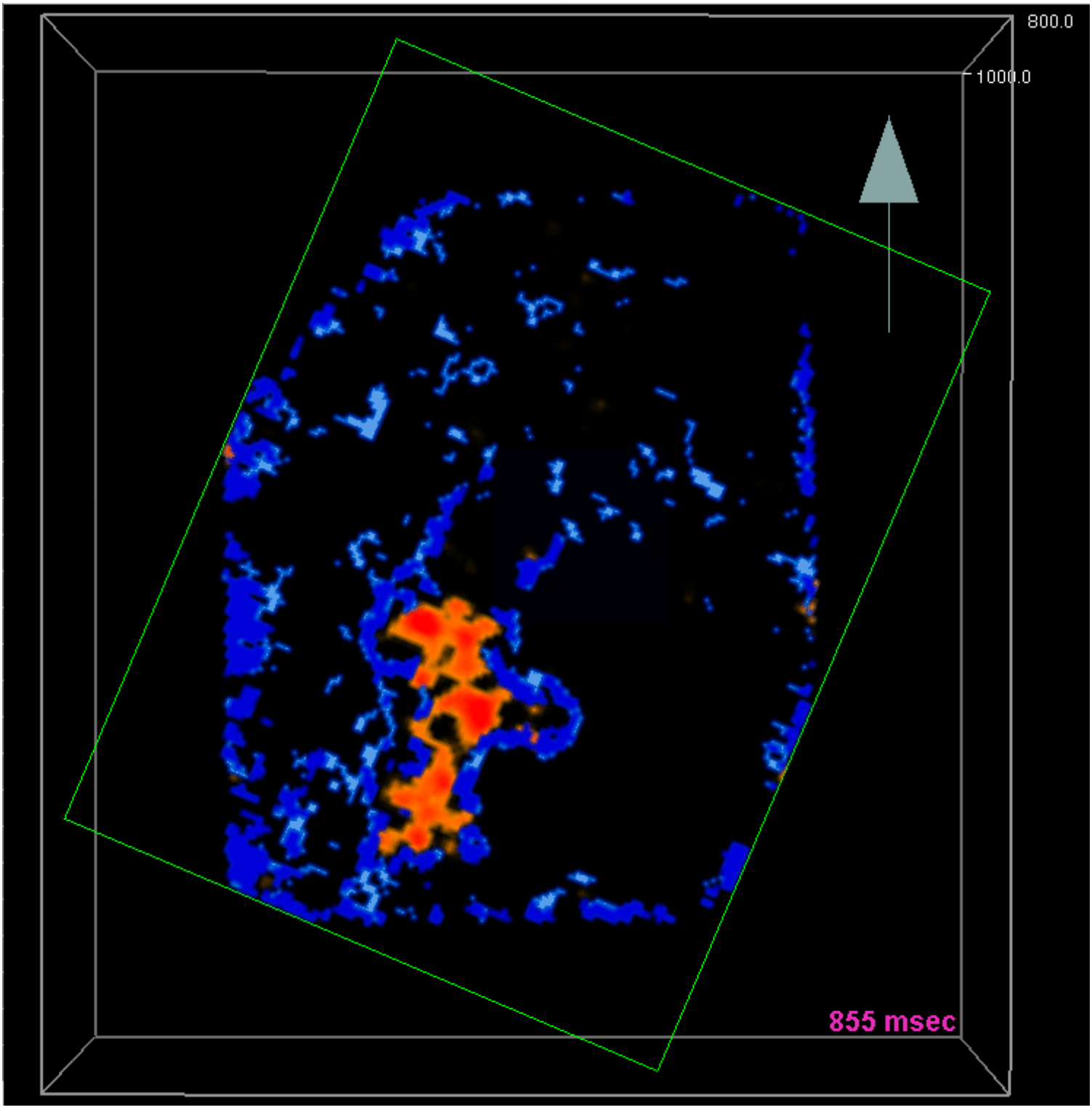
800.0
1000.0
855 msec

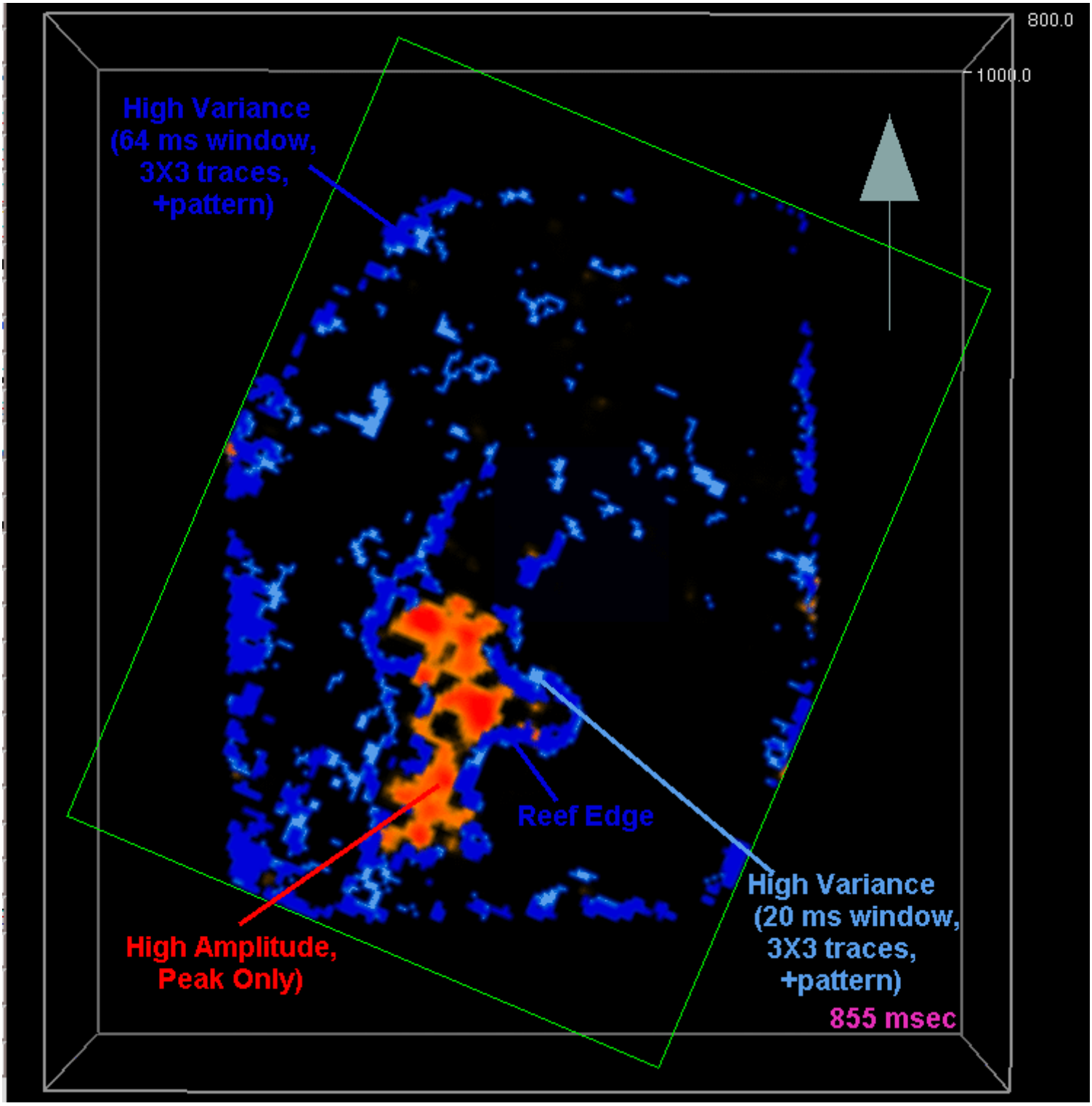
800.0
1000.0
High Variance
(64 ms window,
3X3 traces,
+pattern)
Reef Edge
High Variance
(20 ms window,
3X3 traces,
+pattern)
855 msec
High Amplitude,
Peak Only)

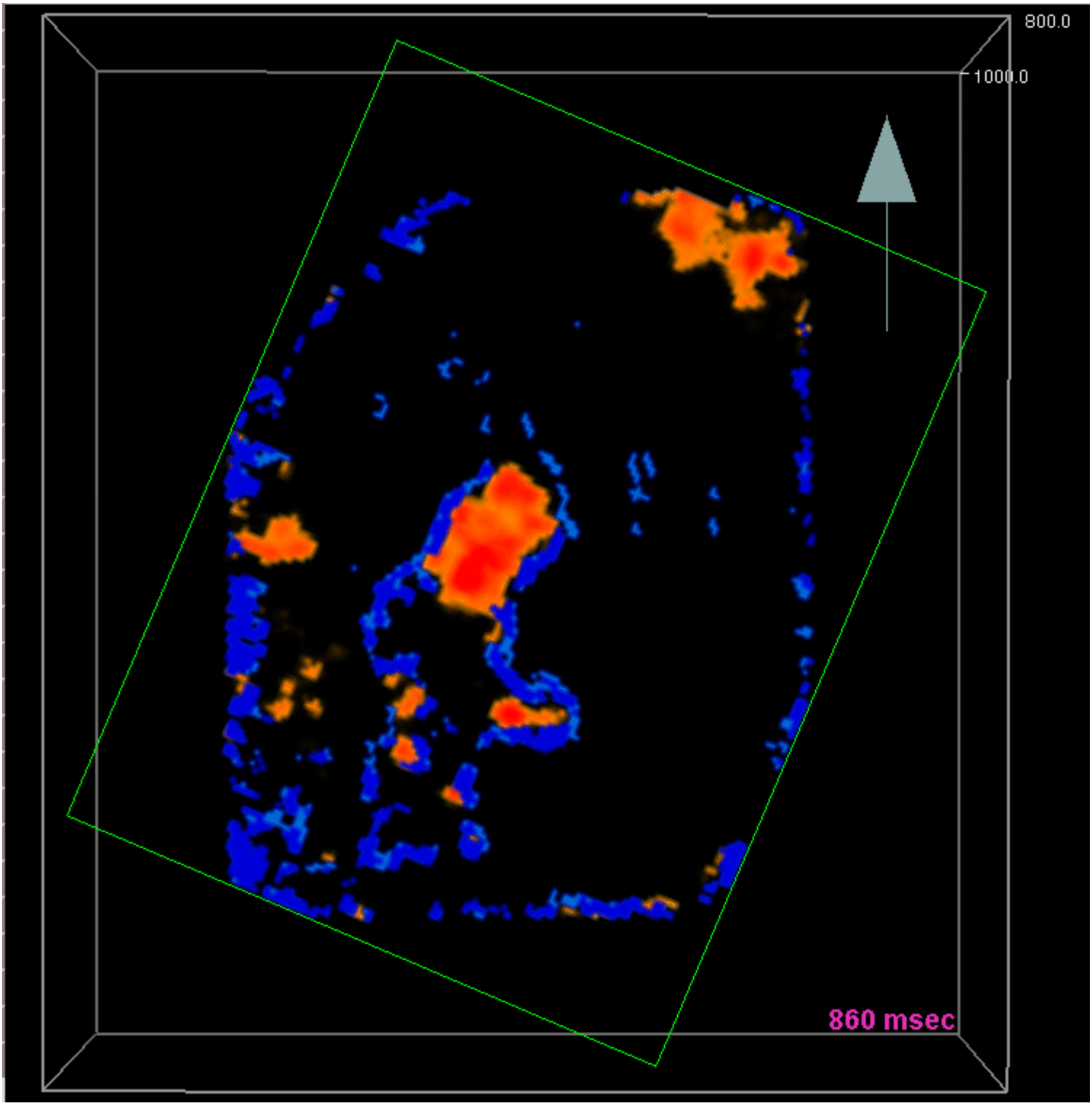
800.0
1000.0
860 msec

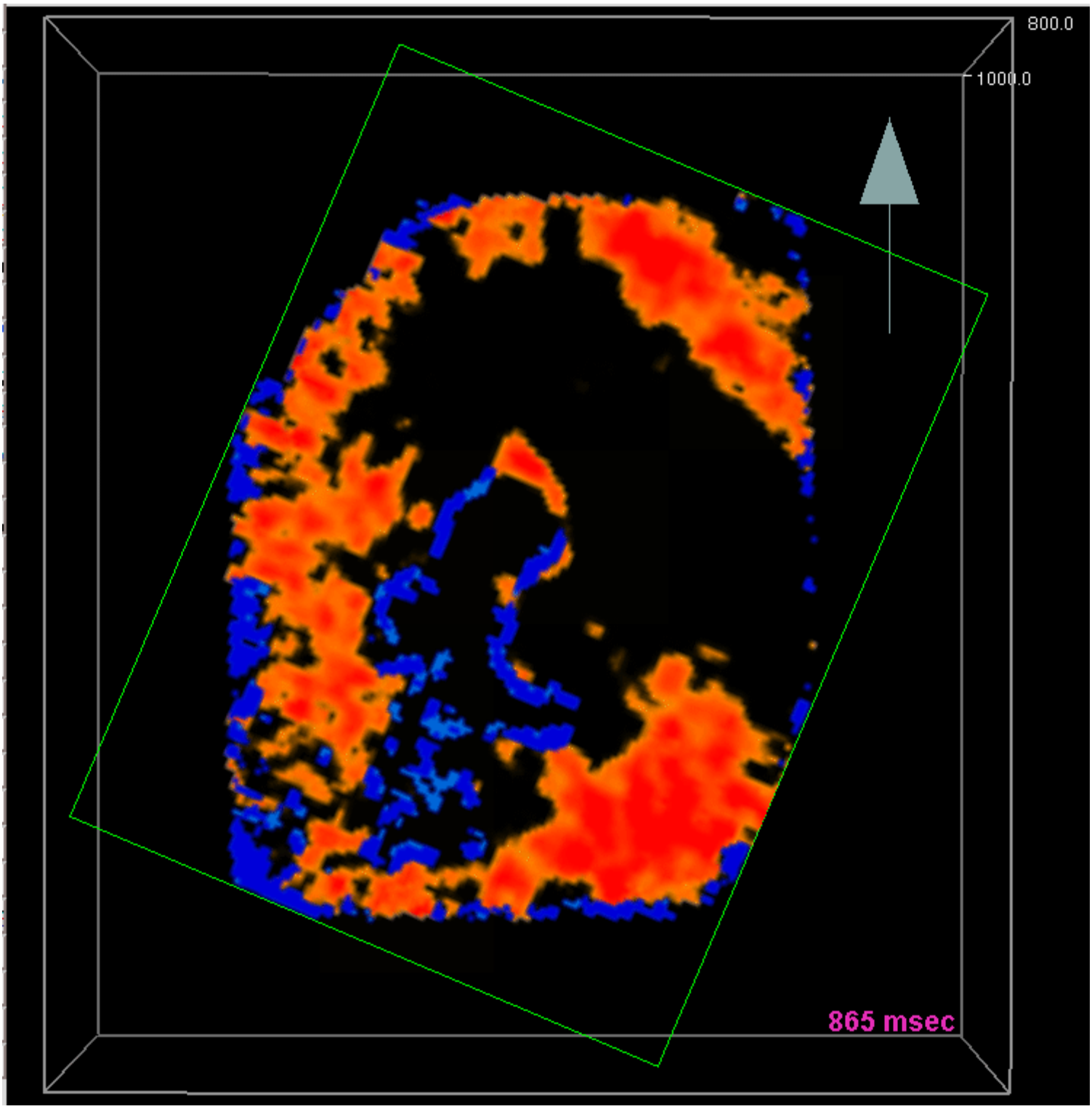
800.0
1000.0
865 msec

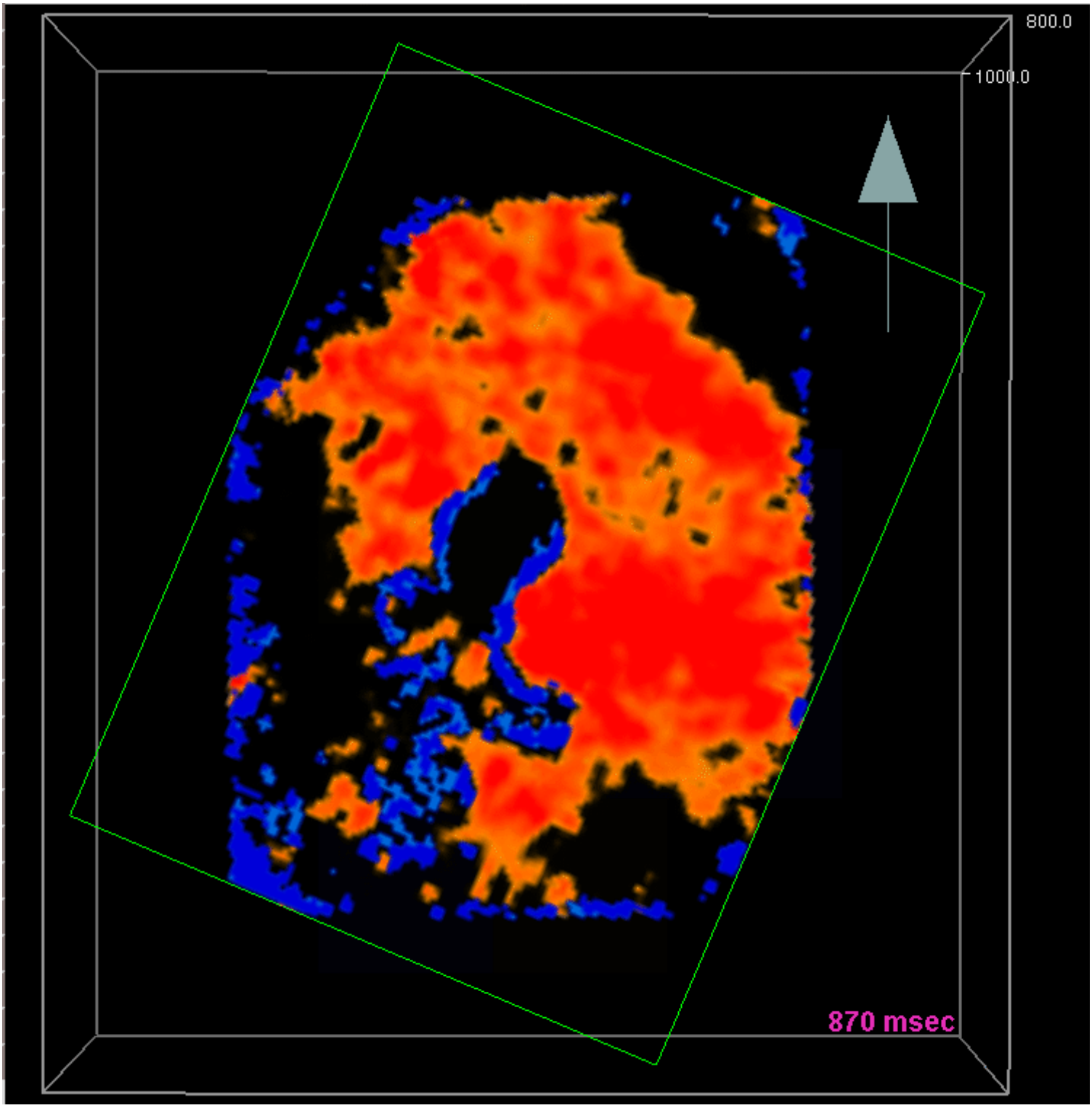
800.0
1000.0
870 msec

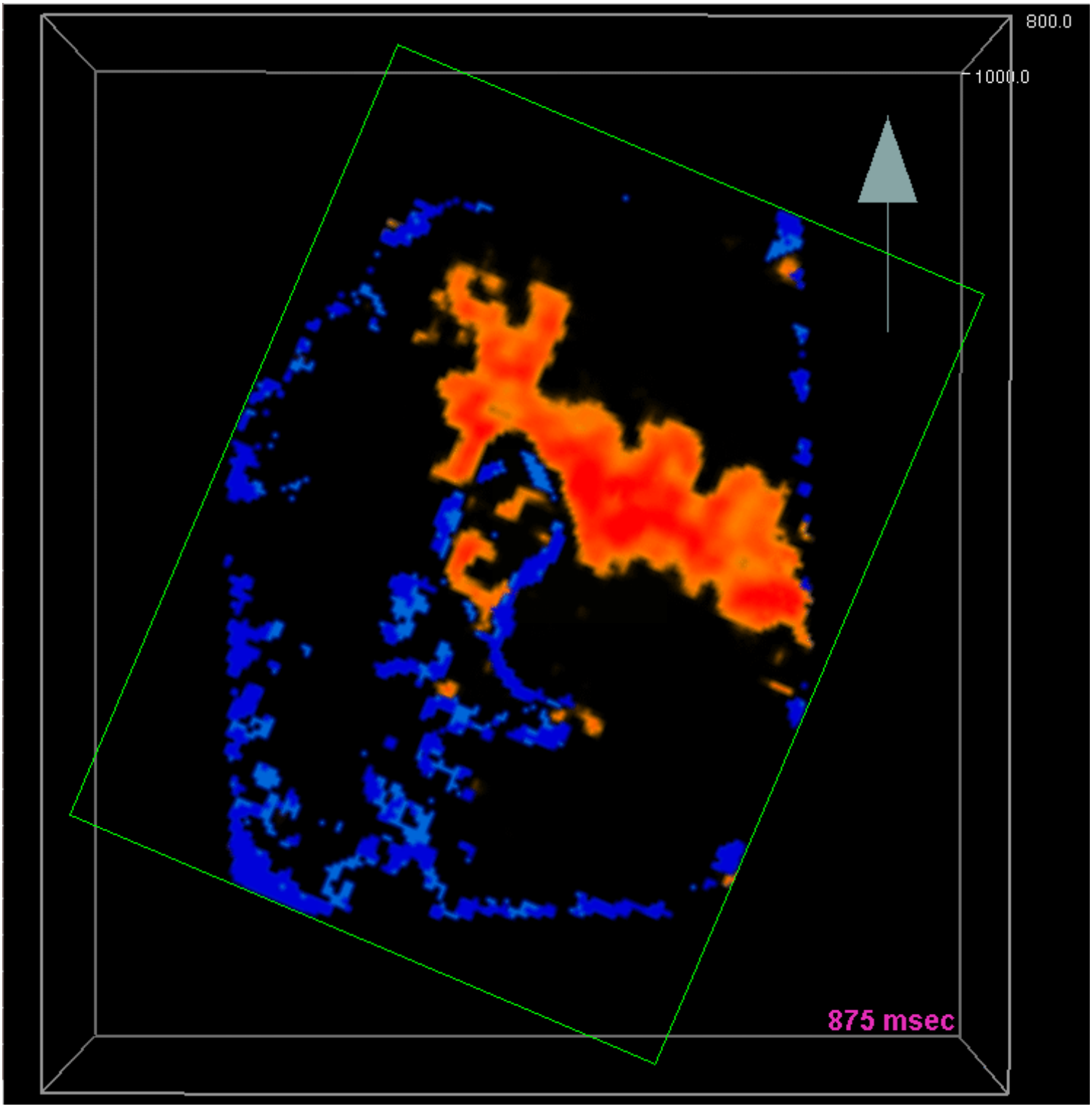
800.0
1000.0
875 msec

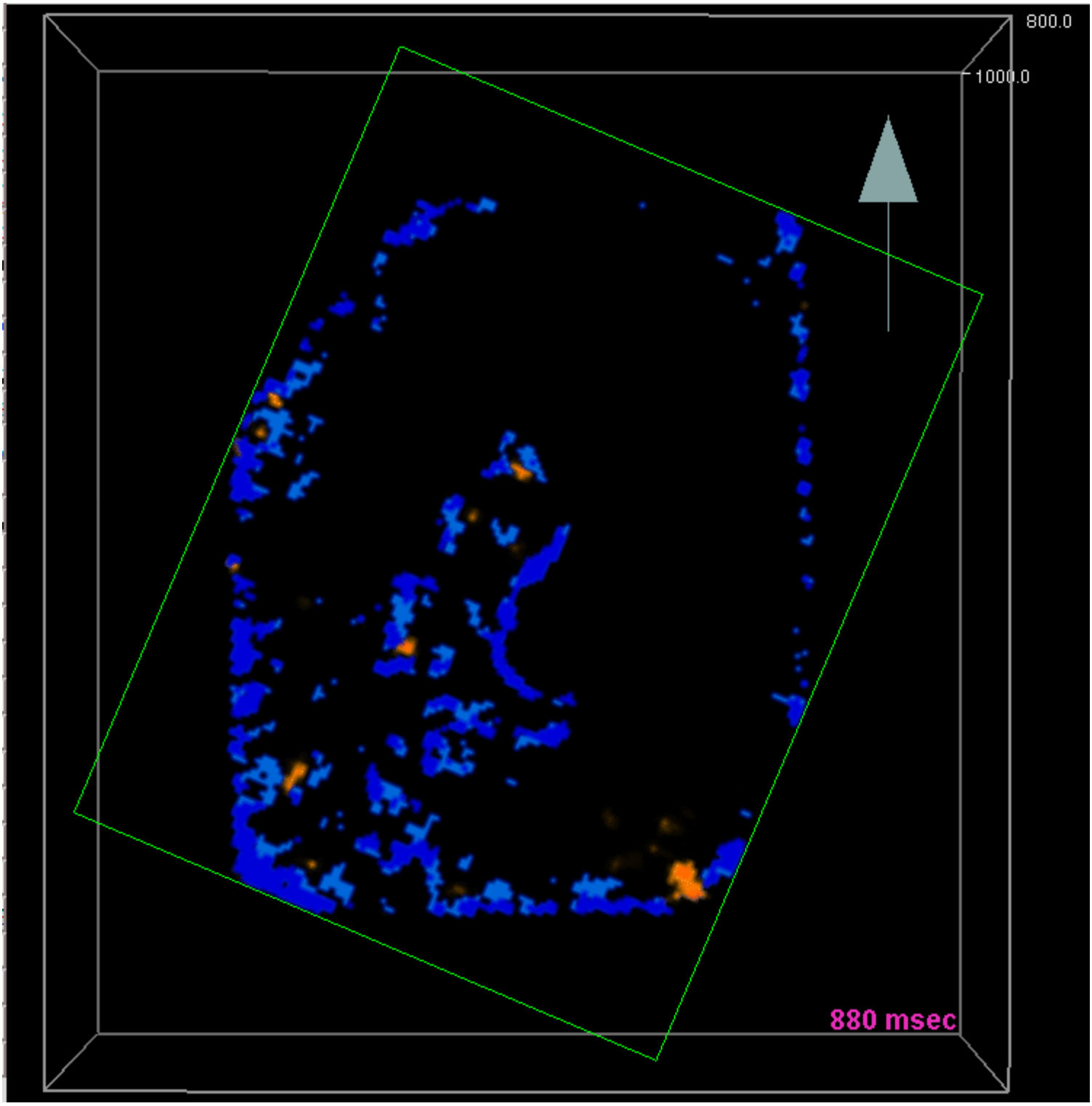
800.0
1000.0
880 msec

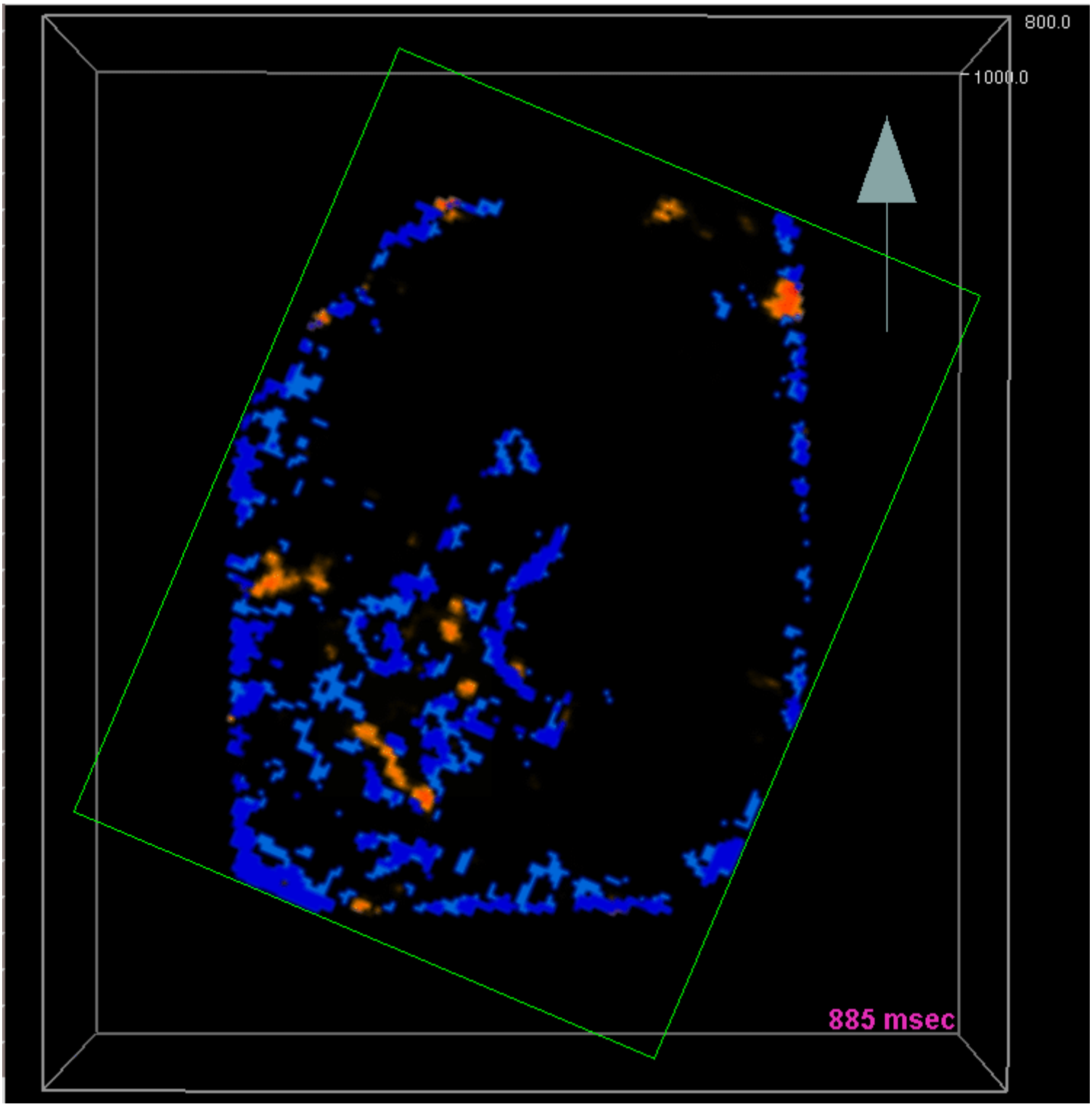
800.0
1000.0
885 msec

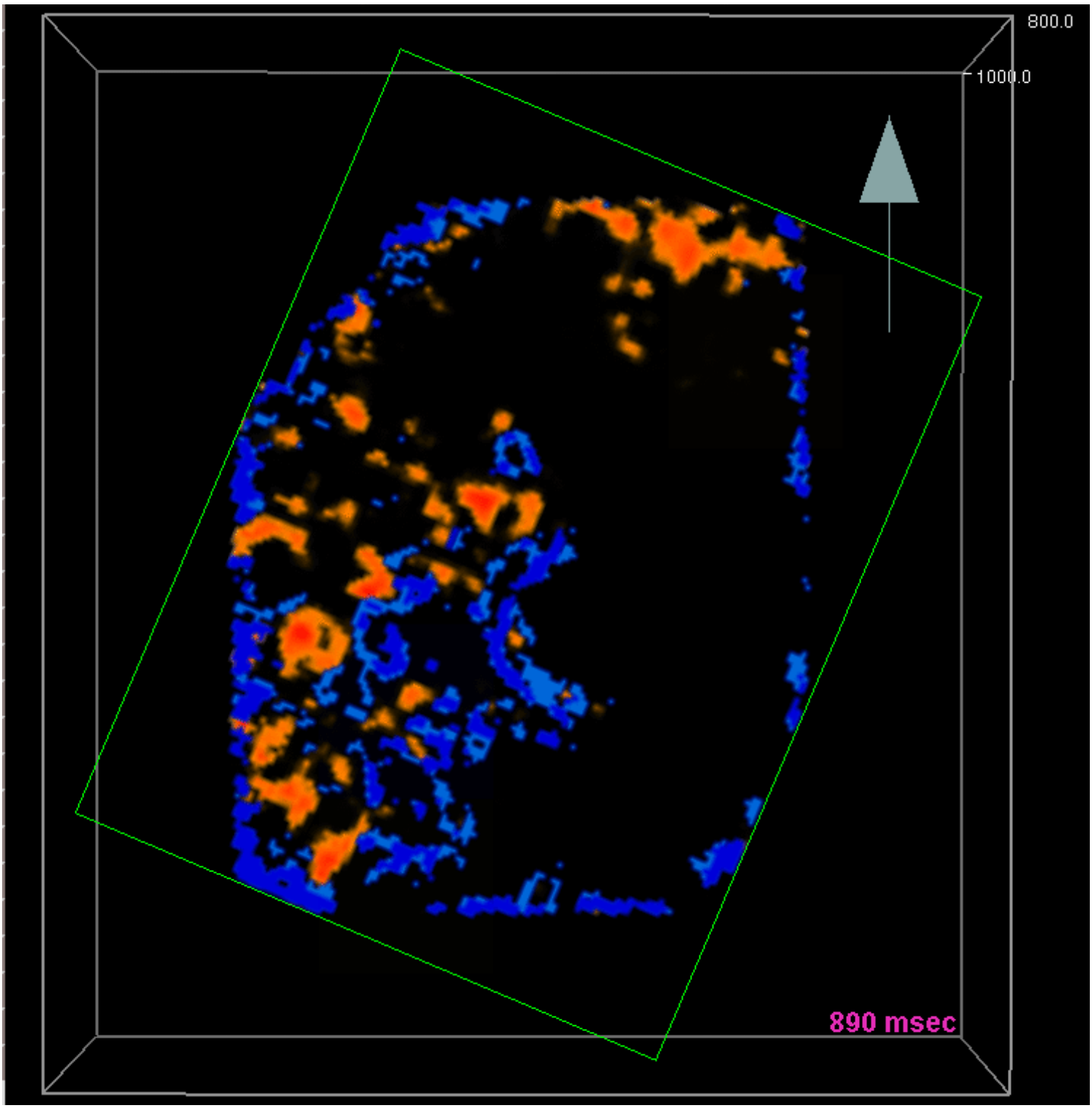
800.0
1000.0
890 msec

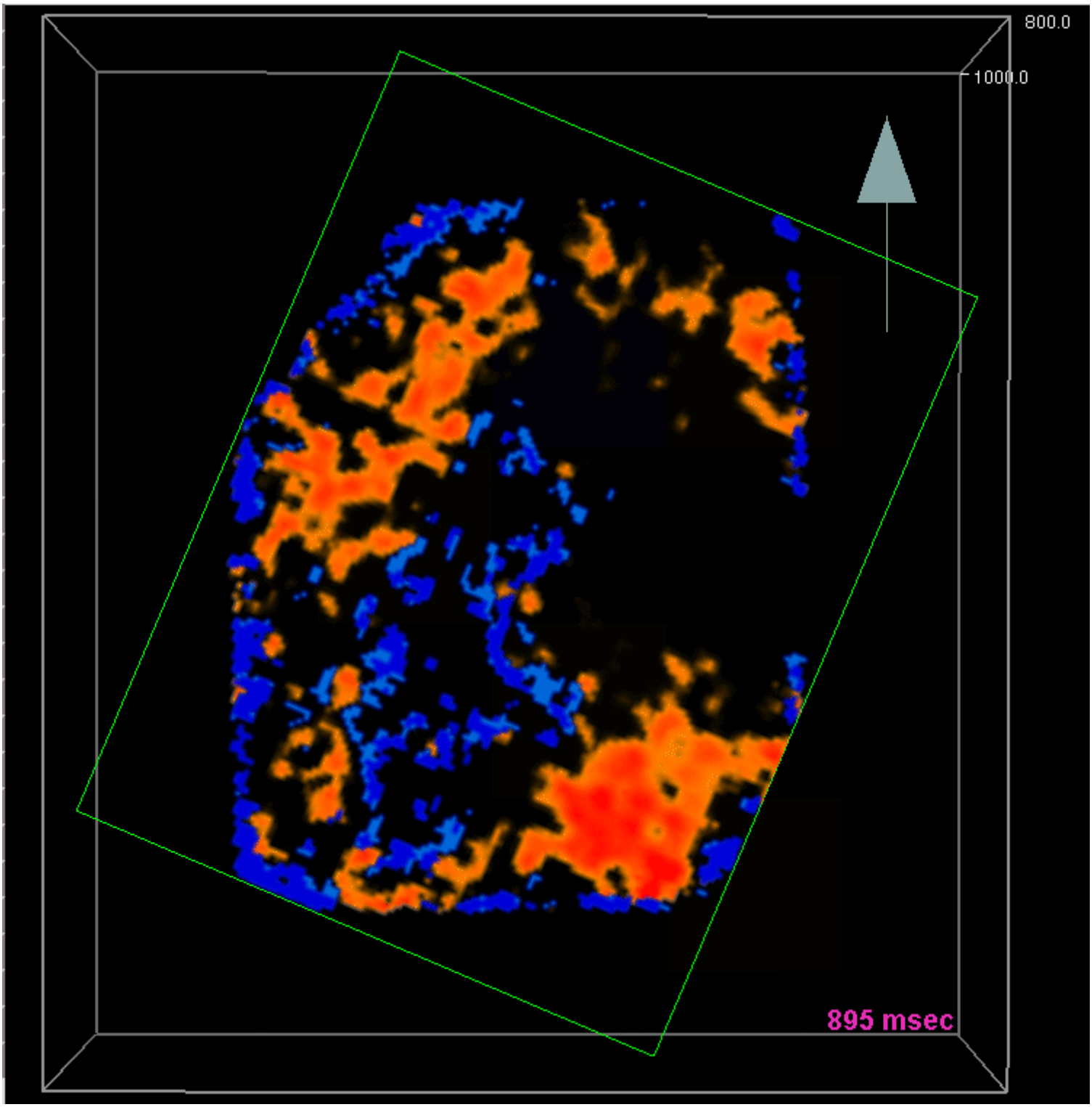
800.0
1000.0
895 msec

Composite blended seismic attribute interpretation – 855 msec – 860 msec

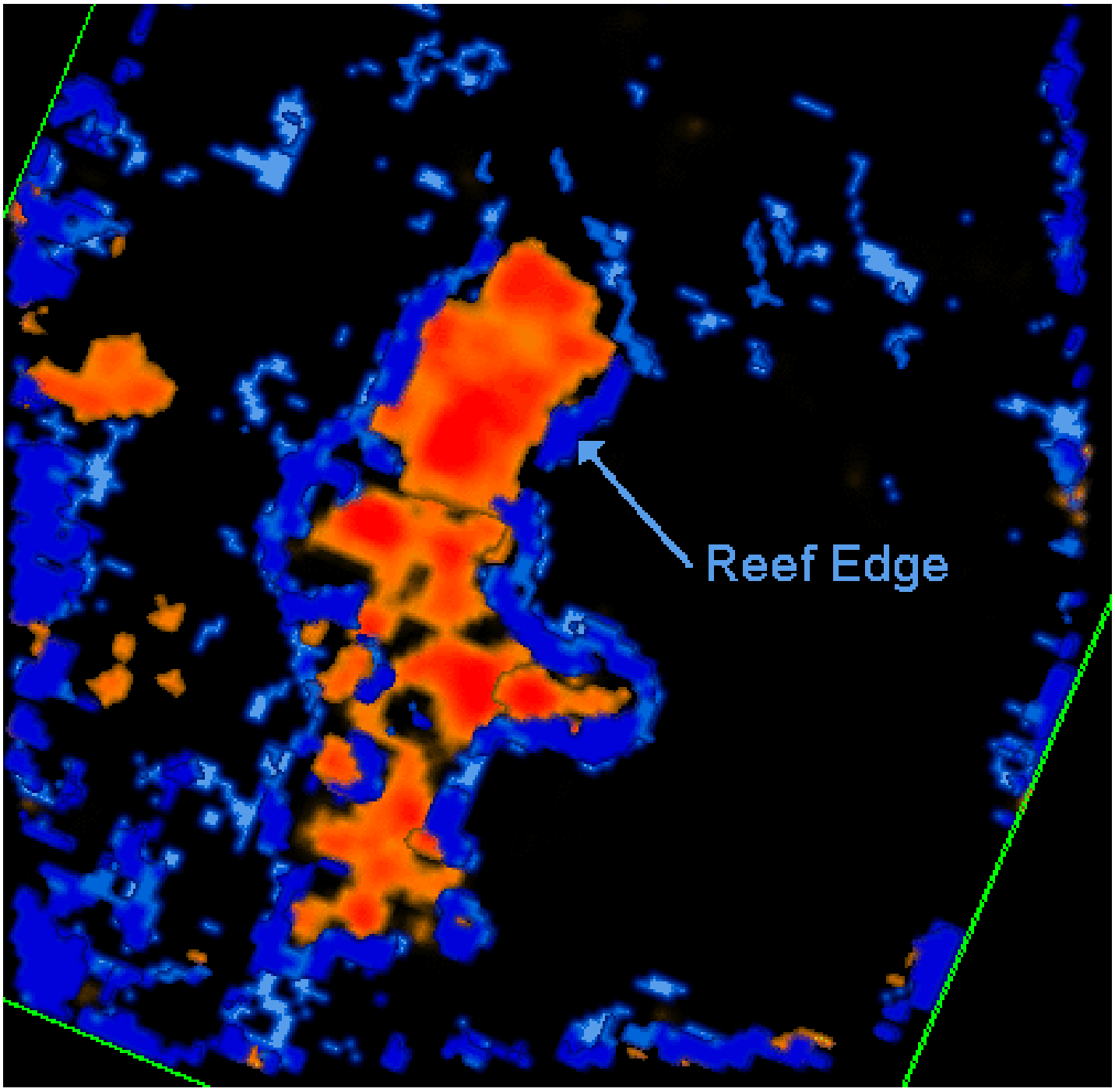

10.4 APPENDIX E - 4-D Base Seismic Survey (Flattened on A2Carbonate) – Time slices (0-70 ms)

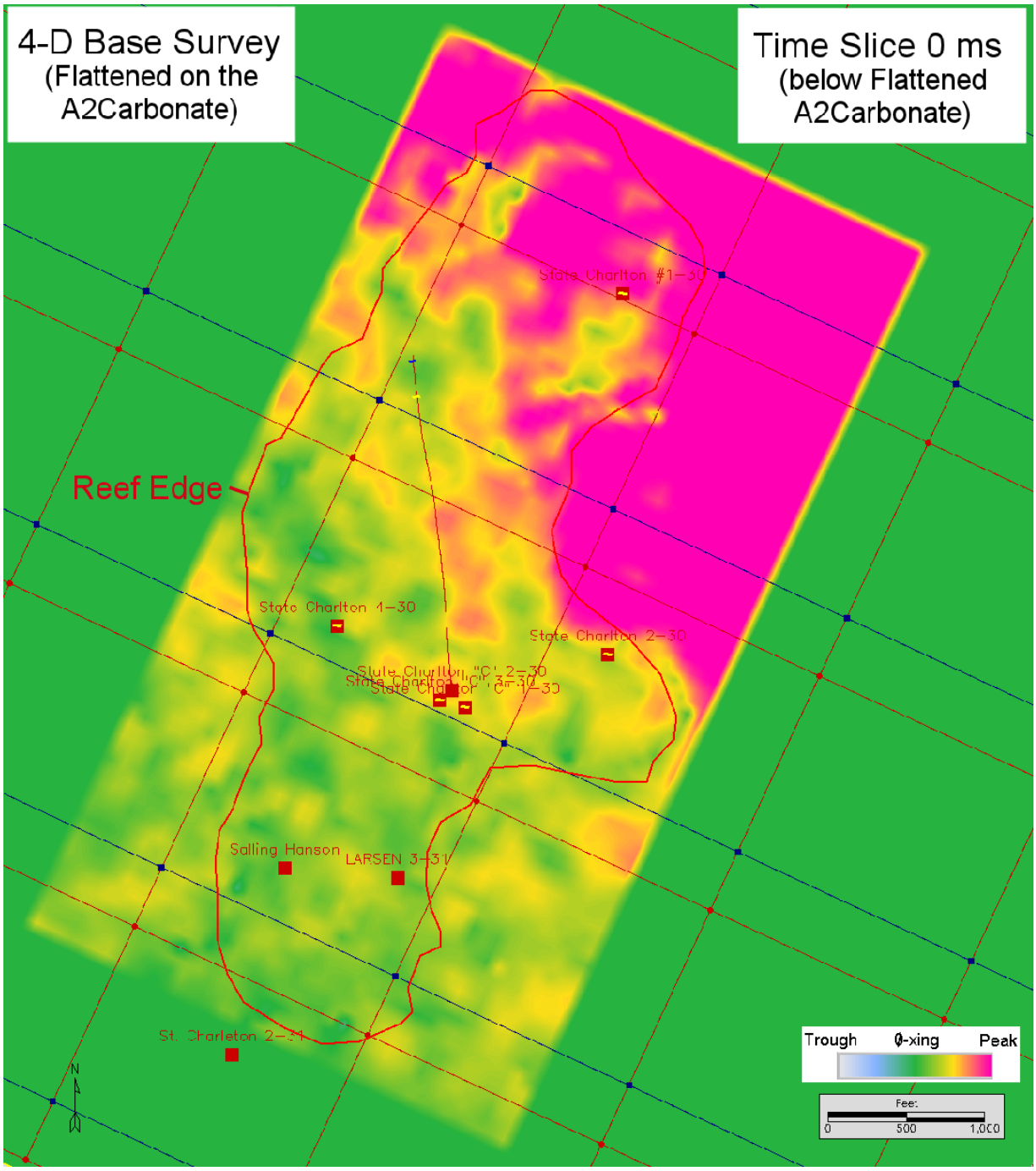

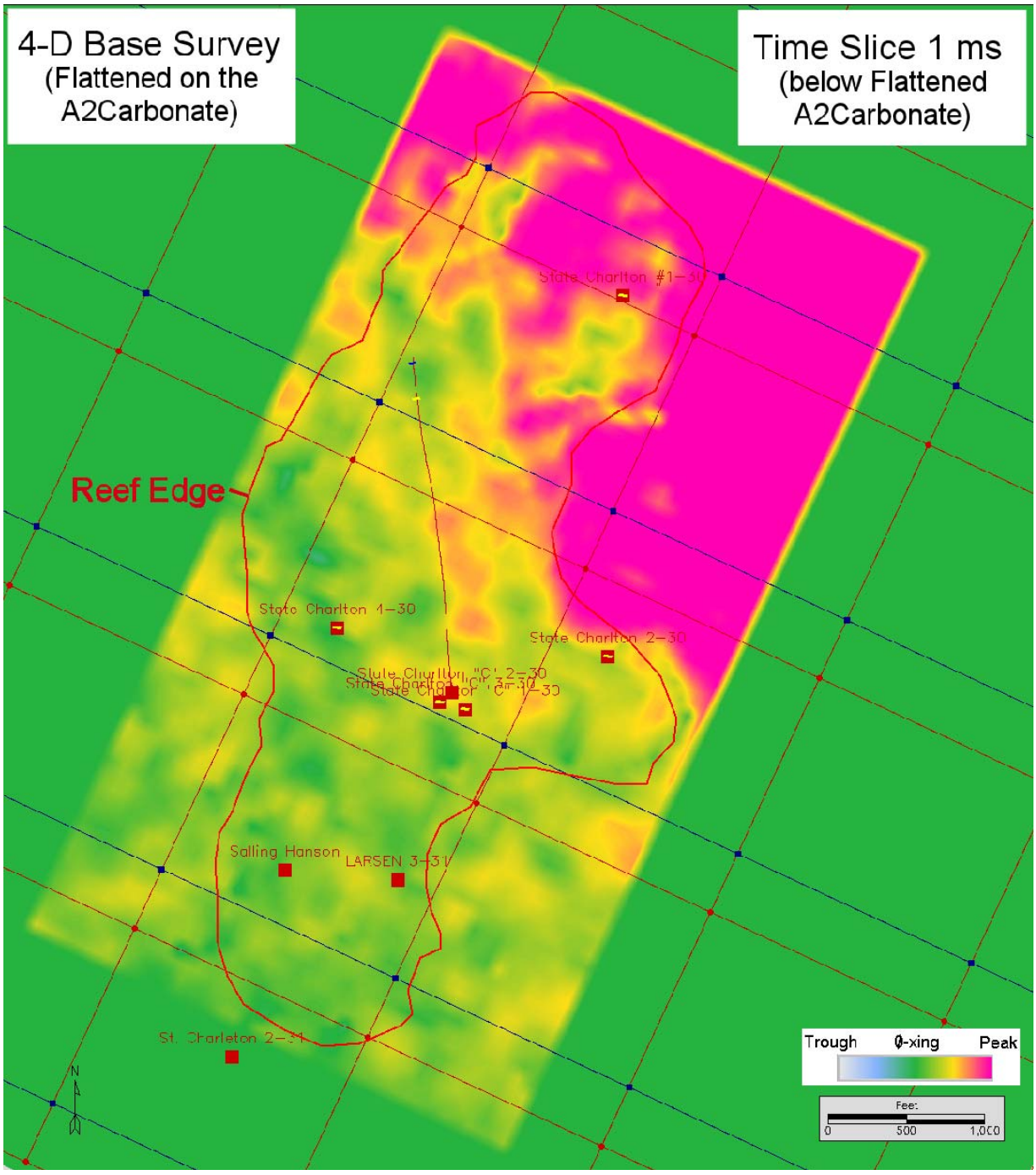
4-D Base Survey
(Flattened on the
A2Carbonate)
Time Slice 1 ms
(below Flattened
A2Carbonate)
Reef Edge
State Charlton #1-30
State Charlton 1-30
State Charlton 2-30
Salling Hanson
LARSEN 3-31
St. Charleton 2-31
Trough
0-xing
Peak
Fee:
0
500
1,000
N

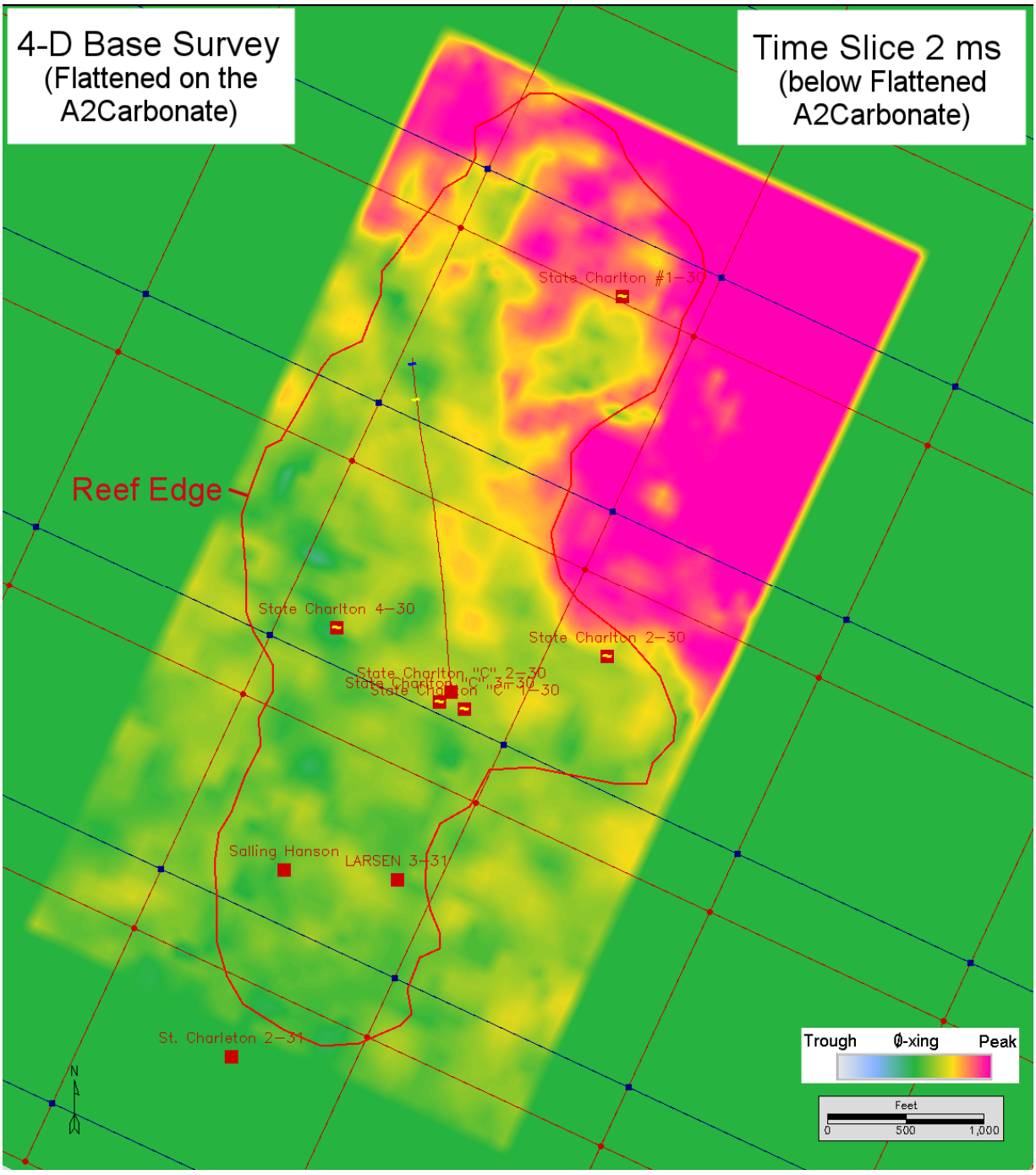
4-D Base Survey
(Flattened on the
A2Carbonate)
Time Slice 2 ms
(below Flattened
A2Carbonate)
State Charlton #1-30
Reef Edge
State Charlton 4-30
State Charlton 2-30
State Charlton "C" 2-30
State Charlton "C" 3-30
State Charlton "C" 1-30
Salling Hanson
LARSEN 3-31
St. Charleton 2-31
N
Trough
Ø-xing
Peak
Feet
0
500
1,000

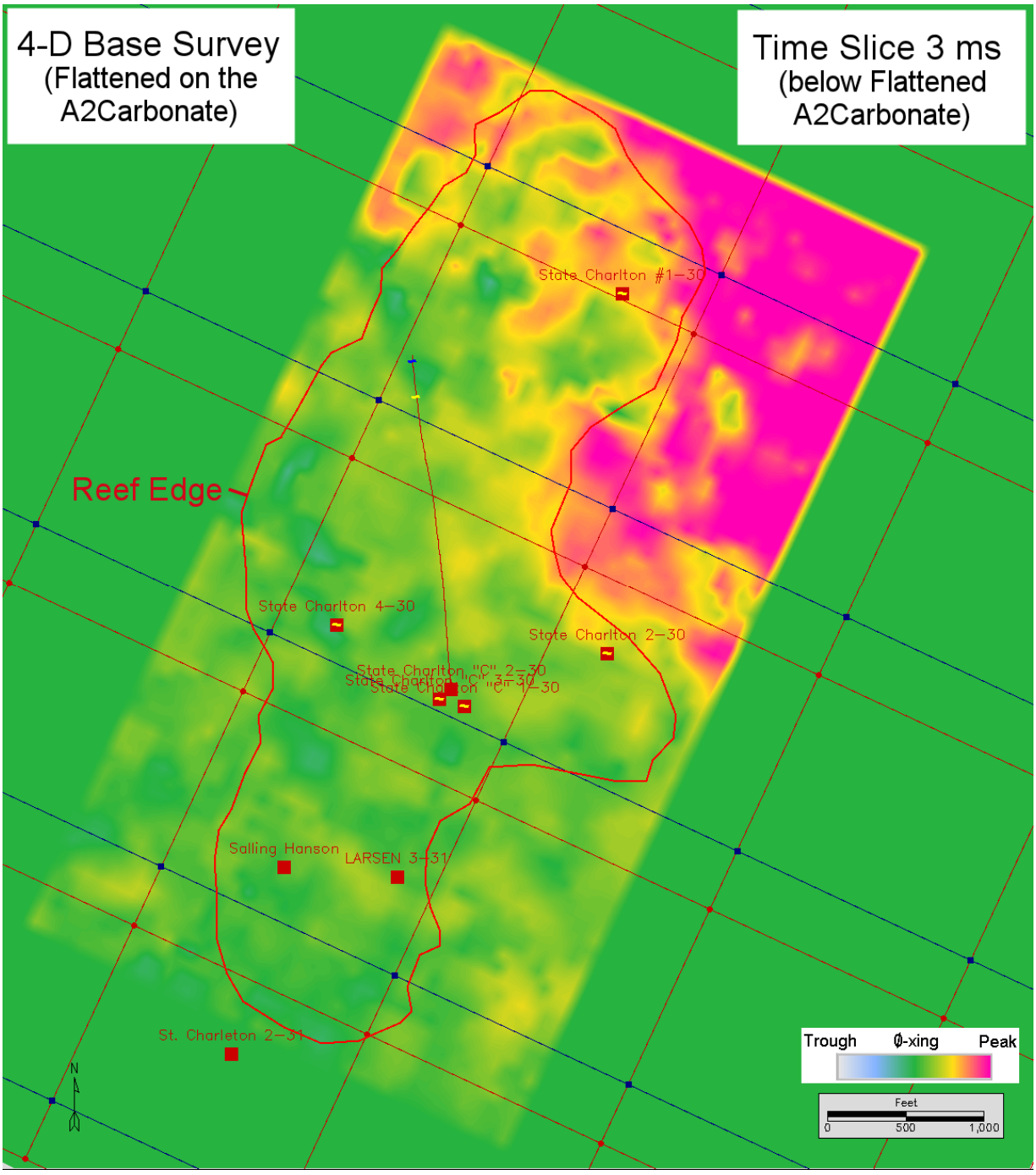
4-D Base Survey
(Flattened on the
A2Carbonate)
Time Slice 3 ms
(below Flattened
A2Carbonate)
State Charlton #1–30
Reef Edge
State Charlton 4–30
State Charlton 2–30
State Charlton "C" 2–30
State Charlton "C" 3–30
State Charlton "C" 1–30
Salling Hanson
LARSEN 3–31
St. Charleton 2–31
N
Trough
Ø-xing
Peak
Feet
0
500
1,000

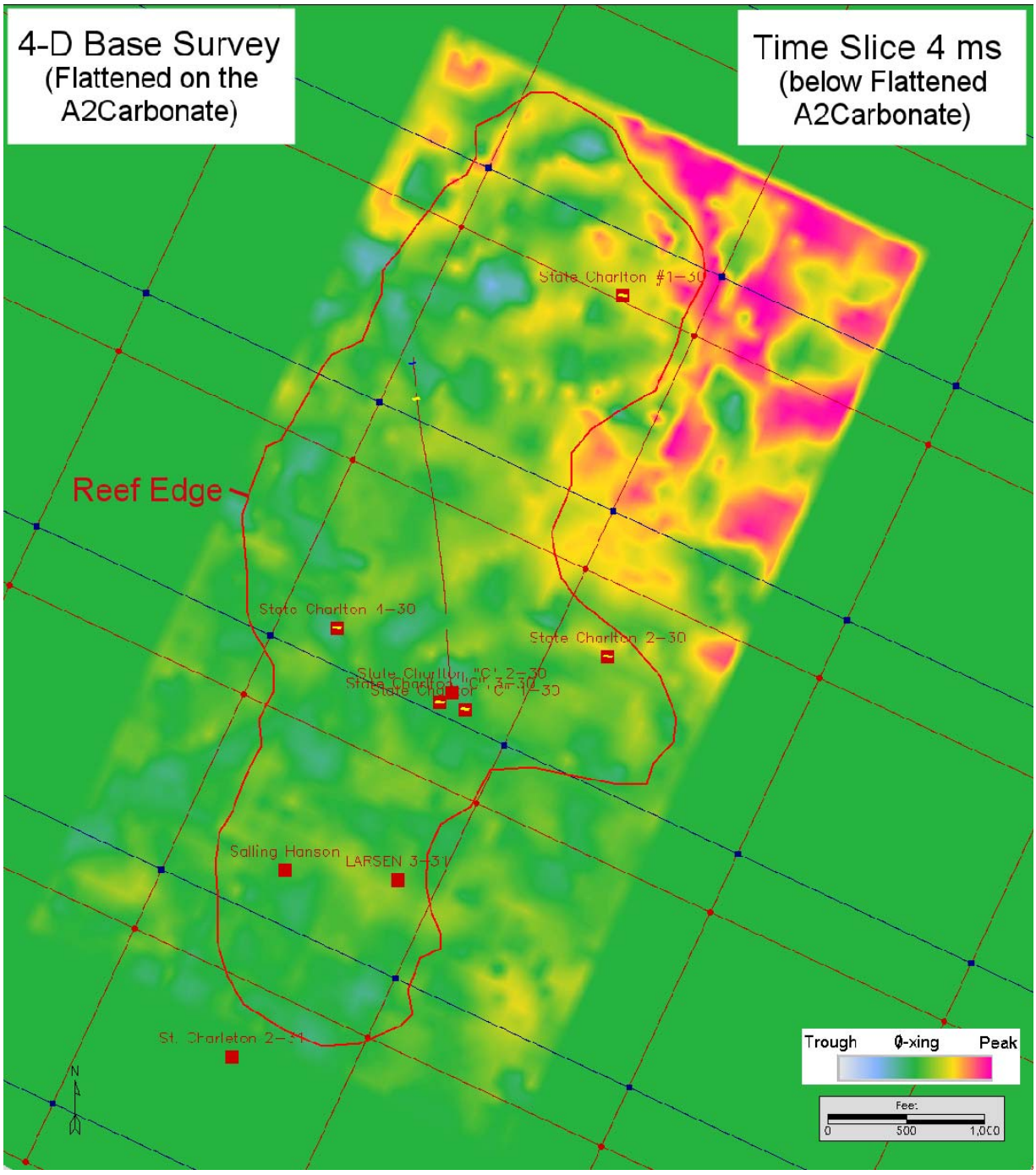
4-D Base Survey
(Flattened on the
A2Carbonate)
Time Slice 4 ms
(below Flattened
A2Carbonate)
State Charlton #1-30
Reef Edge
State Charlton 1-30
State Charlton 2-30
Salling Hanson
LARSEN 3-31
St. Charleton 2-31
Trough
0-xing
Peak
Fee:
0
500
1,000

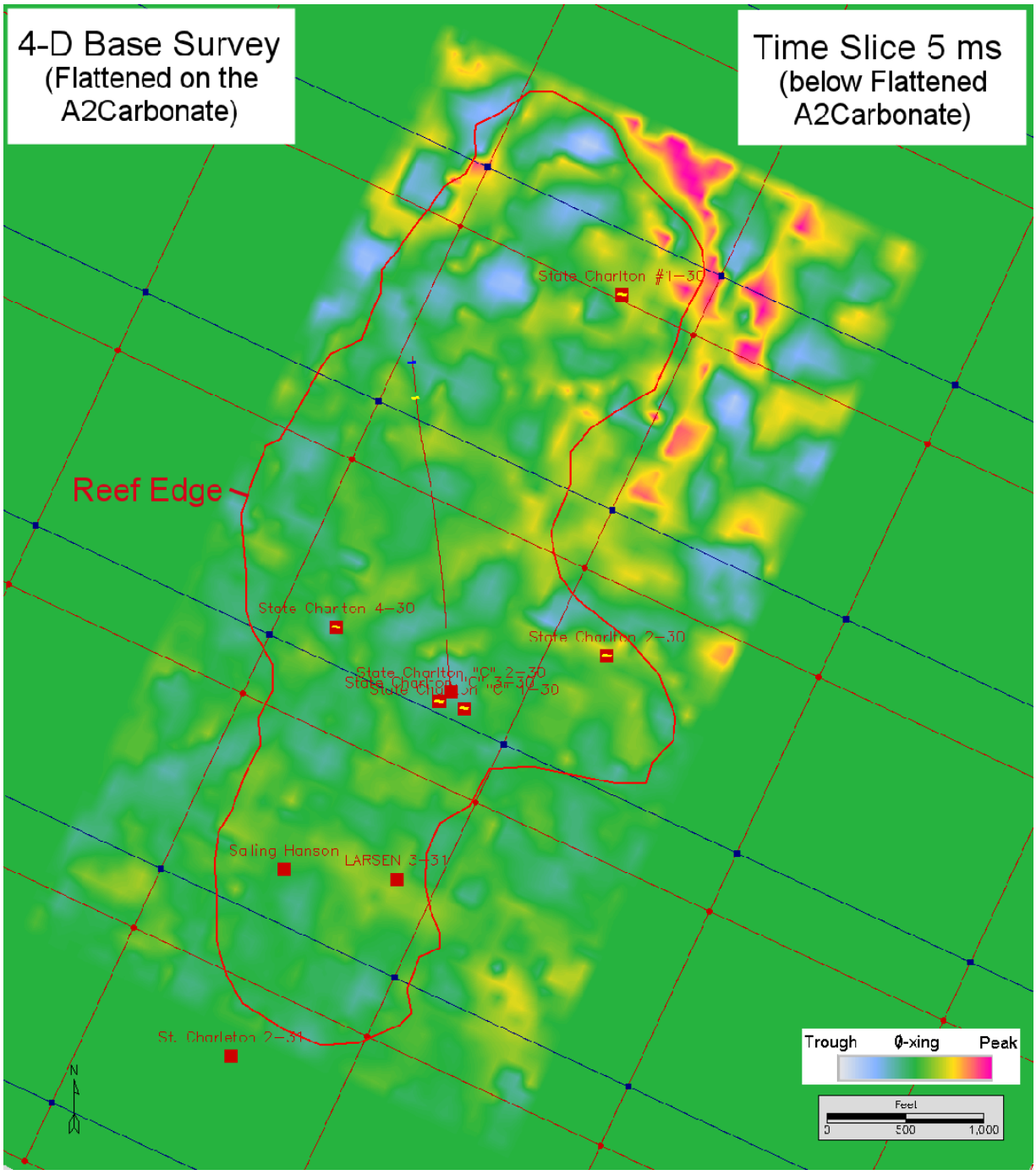
4-D Base Survey
(Flattened on the
A2Carbonate)
Time Slice 5 ms
(below Flattened
A2Carbonate)
State Charlton #1-30
Reef Edge
State Charlton 4-30
State Charlton 2-30
Saling Hanson
LARSEN 3-31
St. Charleton 2-31
N
Trough
0-xing
Peak
Feet
0
500
1,000

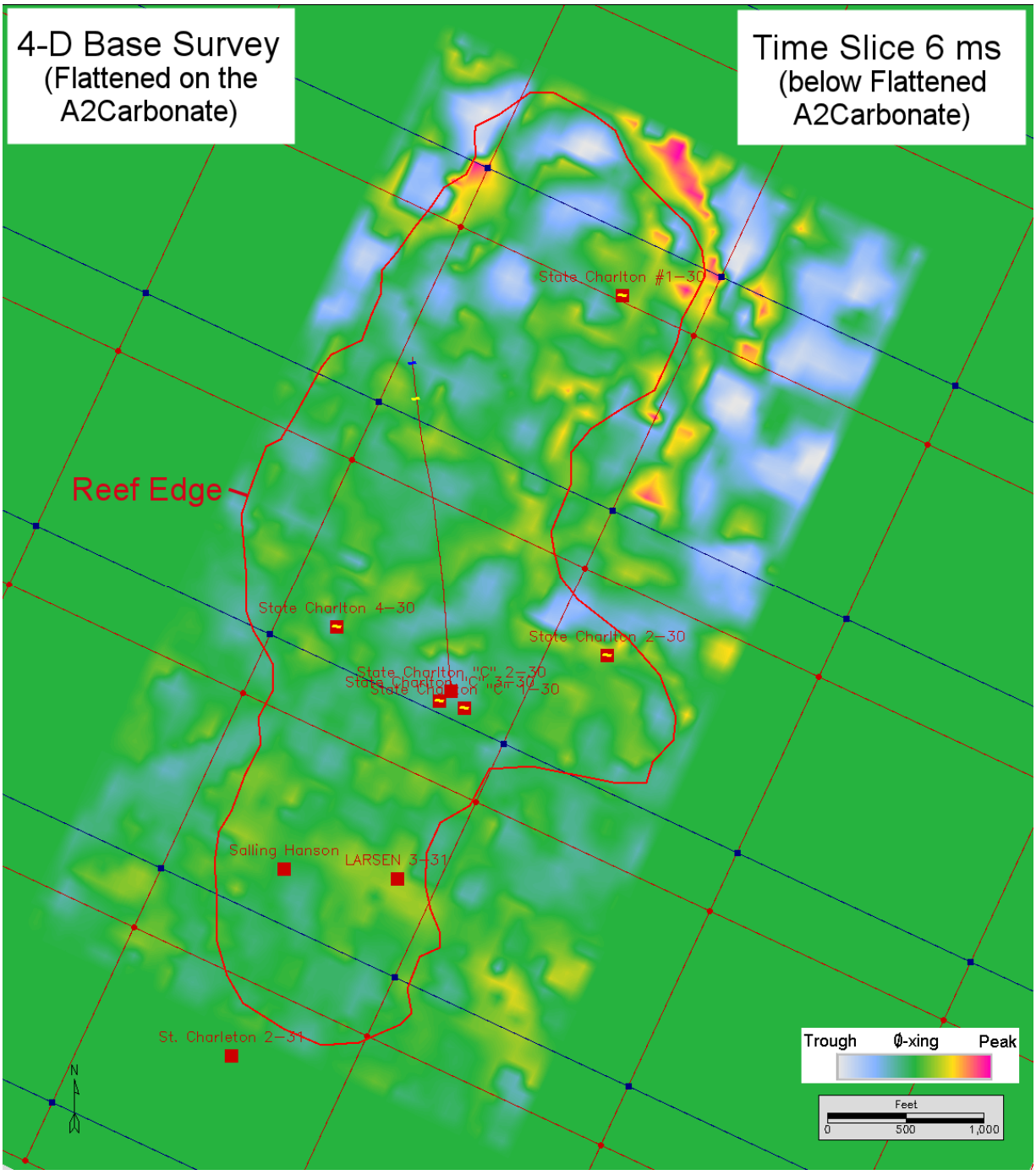
4-D Base Survey
(Flattened on the
A2Carbonate)
Time Slice 6 ms
(below Flattened
A2Carbonate)
State Charlton #1-30
Reef Edge
State Charlton 4-30
State Charlton 2-30
State Charlton "C" 2-30
State Charlton "C" 3-30
State Charlton "C" 1-30
Salling Hanson
LARSEN 3-31
St. Charleton 2-31
N
Trough
Ø-xing
Peak
Feet
0
500
1,000

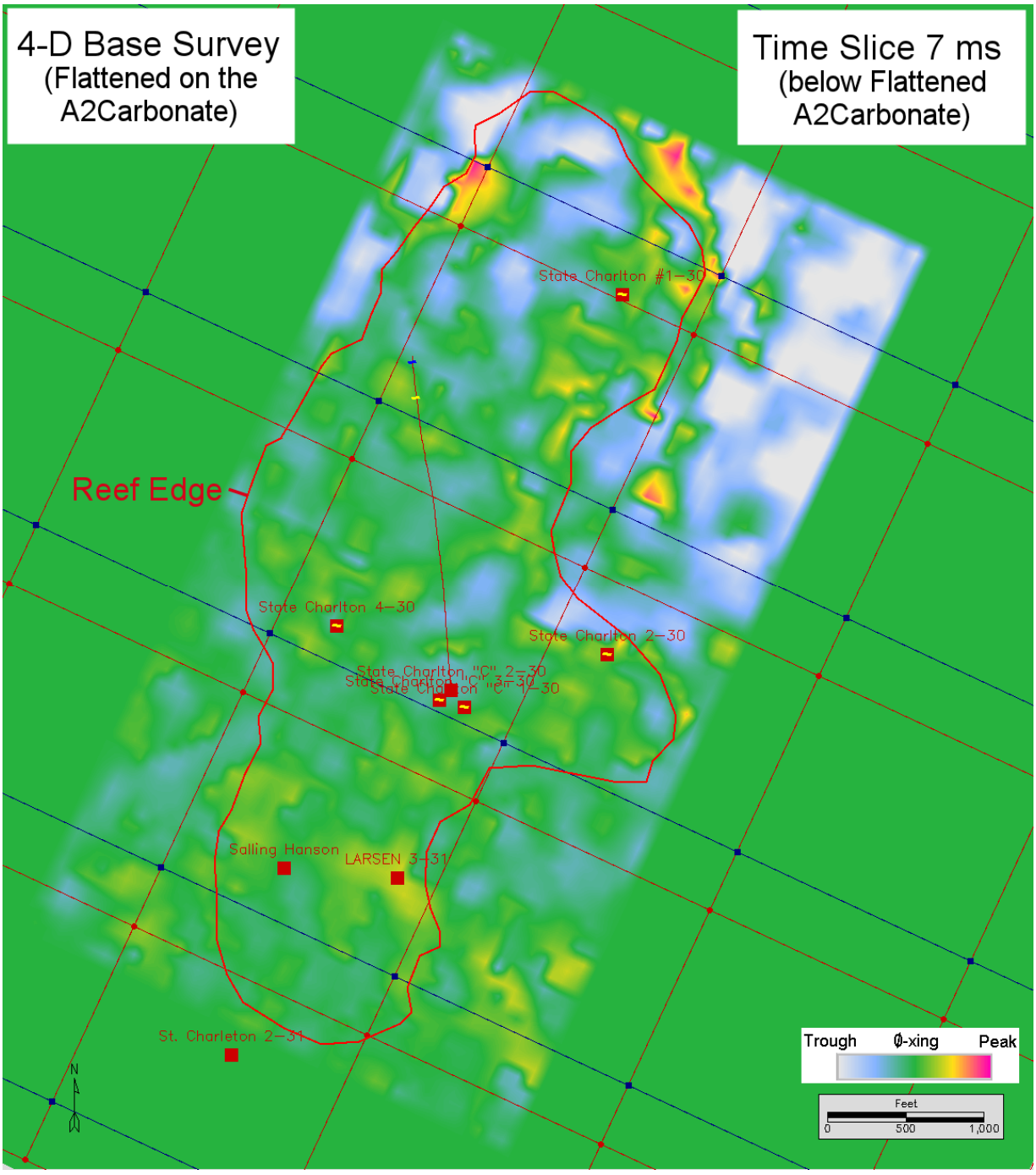
4-D Base Survey
(Flattened on the
A2Carbonate)
Time Slice 7 ms
(below Flattened
A2Carbonate)
State Charlton #1-30
Reef Edge
State Charlton 4-30
State Charlton 2-30
State Charlton "C" 2-30
State Charlton "C" 3-30
State Charlton "C" 1-30
Salling Hanson
LARSEN 3-31
St. Charleton 2-31
N
Trough
Ø-xing
Peak
Feet
0
500
1,000

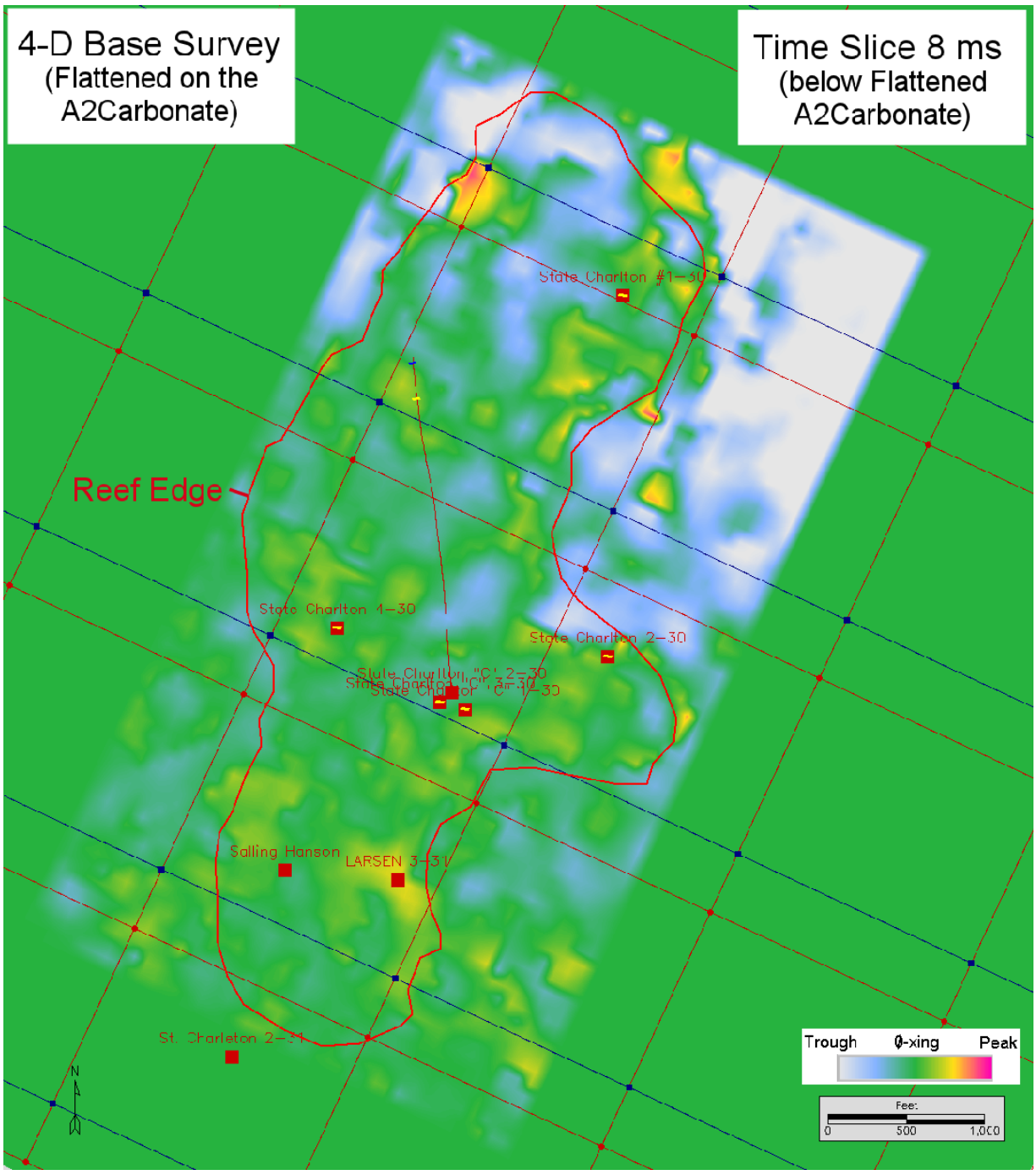
4-D Base Survey
(Flattened on the
A2Carbonate)
Time Slice 8 ms
(below Flattened
A2Carbonate)
Reef Edge
State Charlton #1-30
State Charlton 1-30
State Charlton 2-30
Salling Hanson
LARSEN 3-31
St. Charleton 2-31
N
Trough
0-xing
Peak
Fee:
0
500
1,000

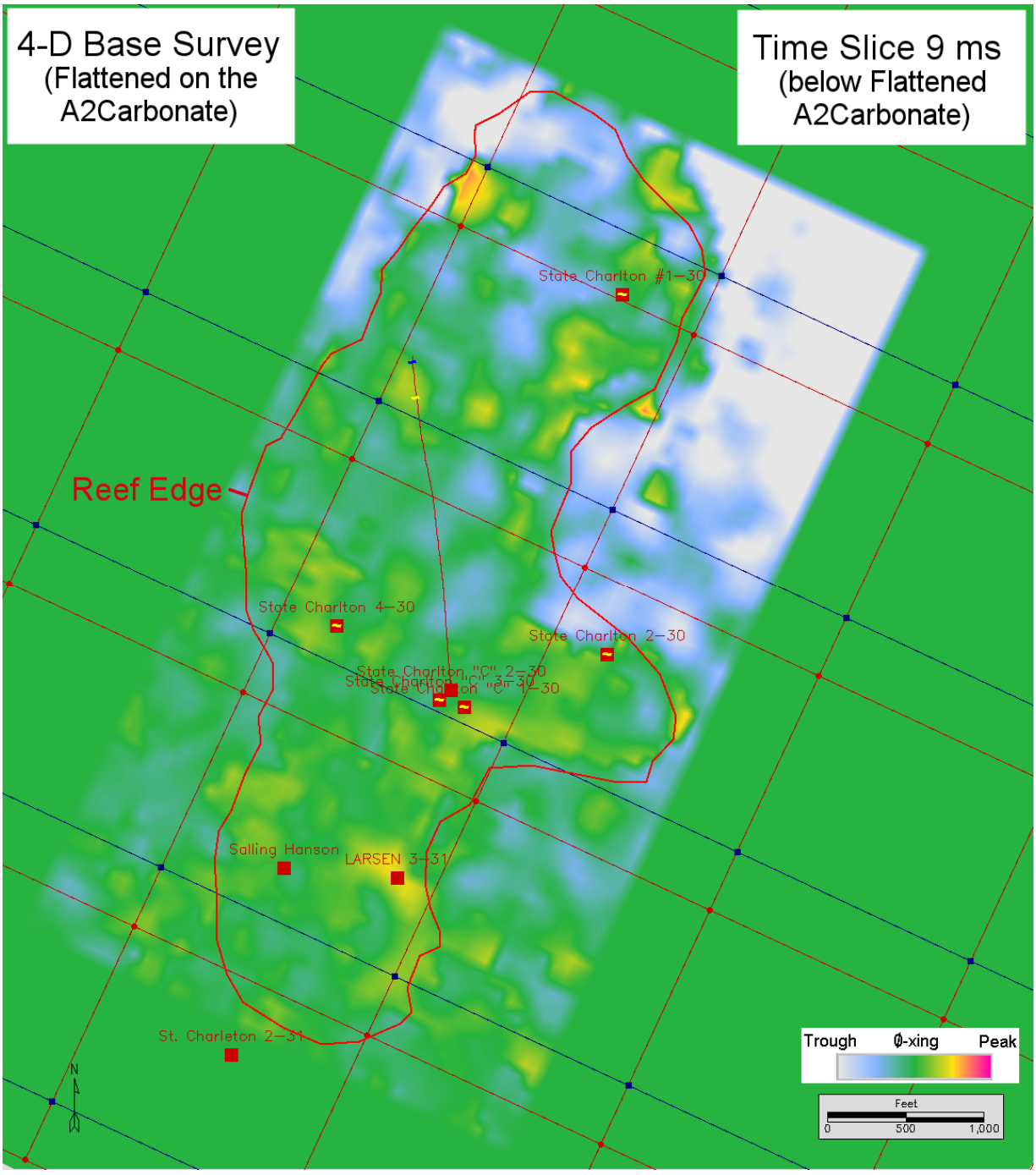
4-D Base Survey
(Flattened on the
A2Carbonate)
Time Slice 9 ms
(below Flattened
A2Carbonate)
State Charlton #1-30
Reef Edge
State Charlton 4-30
State Charlton 2-30
State Charlton "C" 2-30
State Charlton "C" 3-30
State Charlton "C" 1-30
Salling Hanson
LARSEN 3-31
St. Charleton 2-31
N
Trough
Ø-xing
Peak
Feet
0
500
1,000

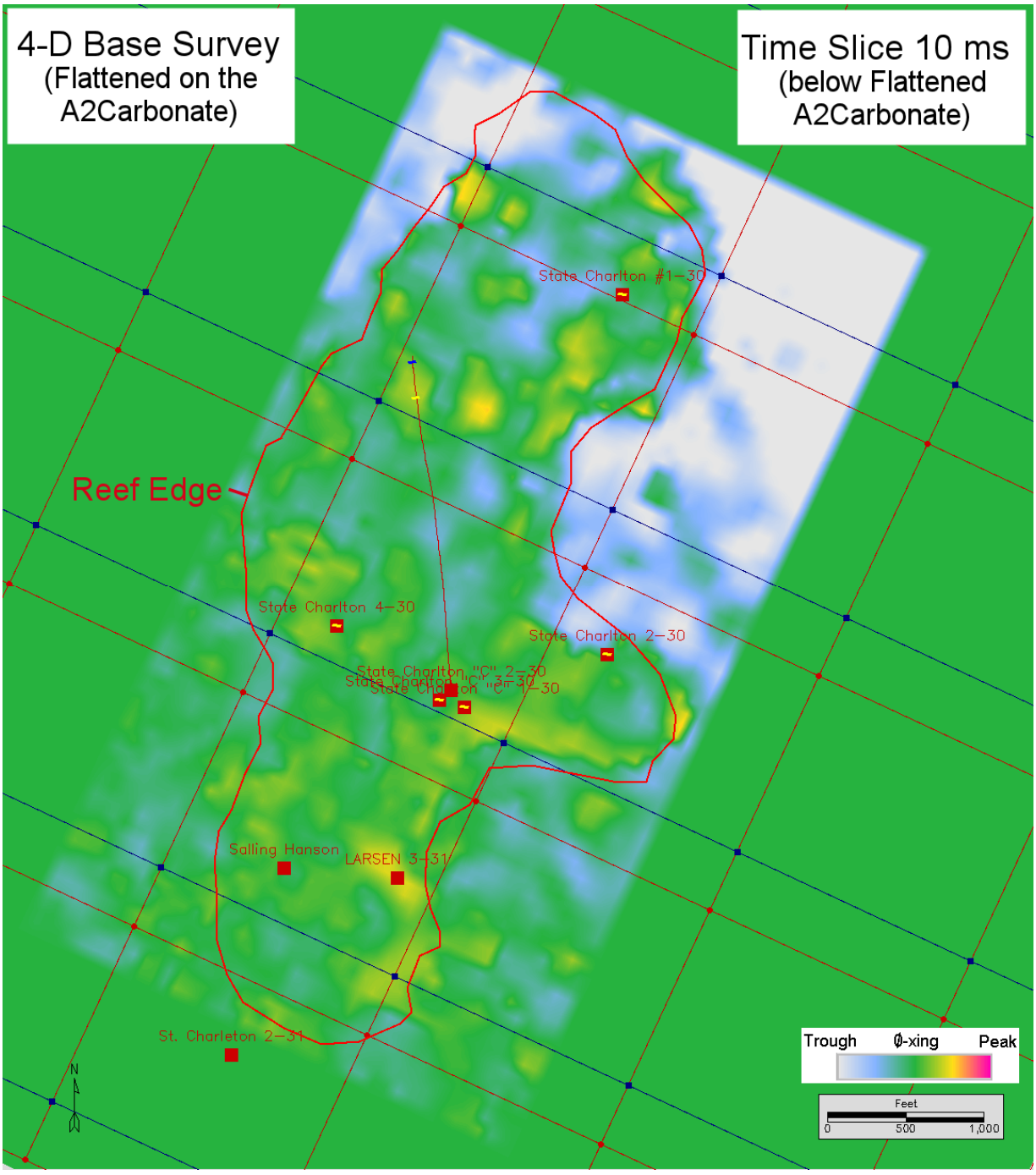
4-D Base Survey
(Flattened on the
A2Carbonate)
Time Slice 10 ms
(below Flattened
A2Carbonate)
State Charlton #1-30
Reef Edge
State Charlton 4-30
State Charlton 2-30
State Charlton "C" 2-30
State Charlton "C" 3-30
State Charlton "C" 1-30
Salling Hanson
LARSEN 3-31
St. Charleton 2-31
N
Trough
Ø-xing
Peak
Feet
0
500
1,000

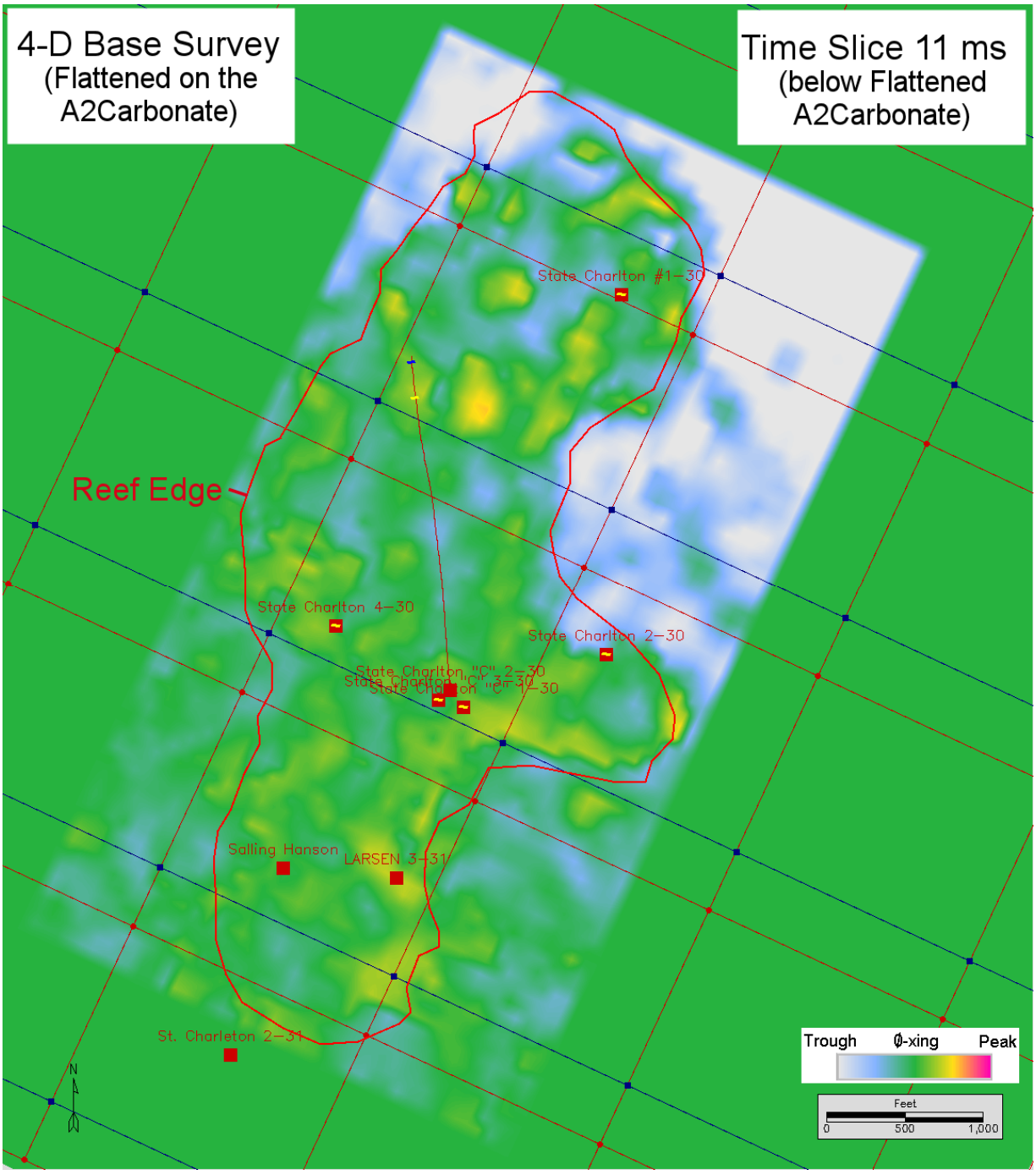
4-D Base Survey
(Flattened on the
A2Carbonate)
Time Slice 11 ms
(below Flattened
A2Carbonate)
State Charlton #1-30
Reef Edge
State Charlton 4-30
State Charlton 2-30
State Charlton "C" 2-30
State Charlton "C" 3-30
State Charlton "C" 1-30
Salling Hanson
LARSEN 3-31
St. Charleton 2-31
N
Trough
Ø-xing
Peak
Feet
0
500
1,000

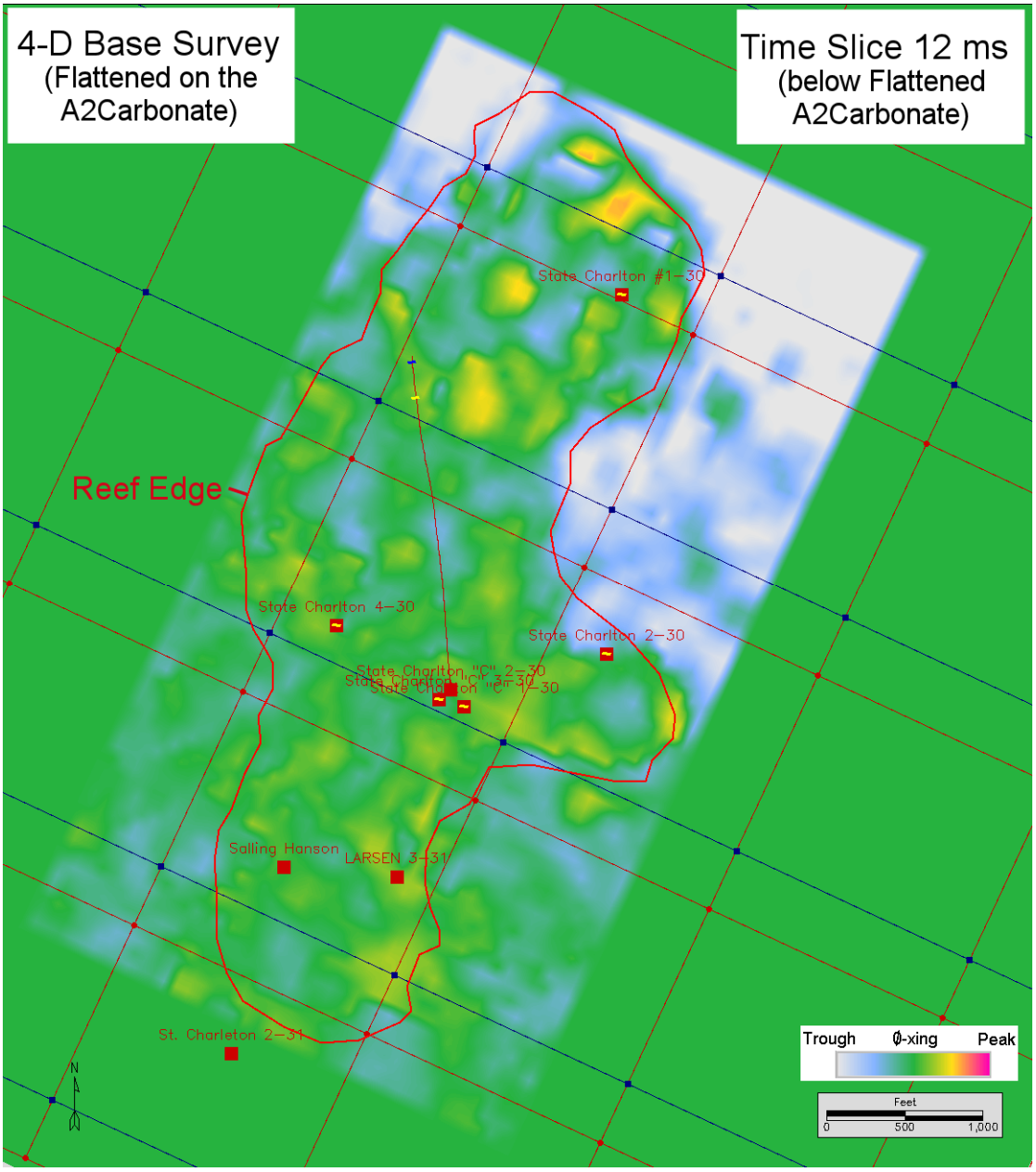
4-D Base Survey
(Flattened on the
A2Carbonate)
Time Slice 12 ms
(below Flattened
A2Carbonate)
State Charlton #1-30
Reef Edge
State Charlton 4-30
State Charlton 2-30
State Charlton "C" 2-30
State Charlton "C" 3-30
Salling Hanson
LARSEN 3-31
St. Charleton 2-31
N
Trough
Ø-xing
Peak
Feet
0
500
1,000

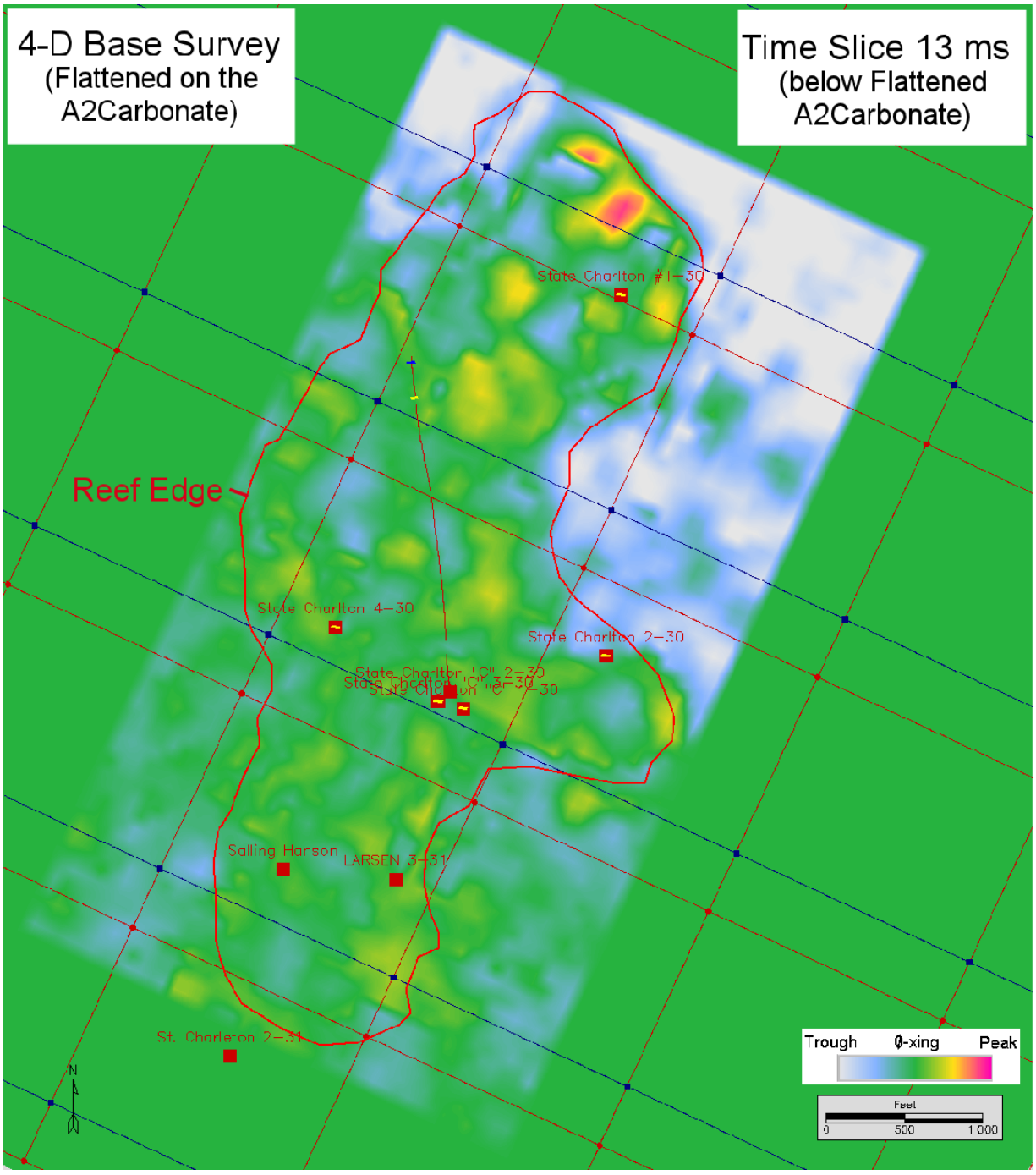
4-D Base Survey
(Flattened on the
A2Carbonate)
Time Slice 13 ms
(below Flattened
A2Carbonate)
State Charlton #1-30
Reef Edge
State Charlton 4-30
State Charlton 2-30
Salling Harson
LARSEN 3-31
St. Charleron 2-31
Trough
0-xing
Peak
Feet
0
500
1 000
N

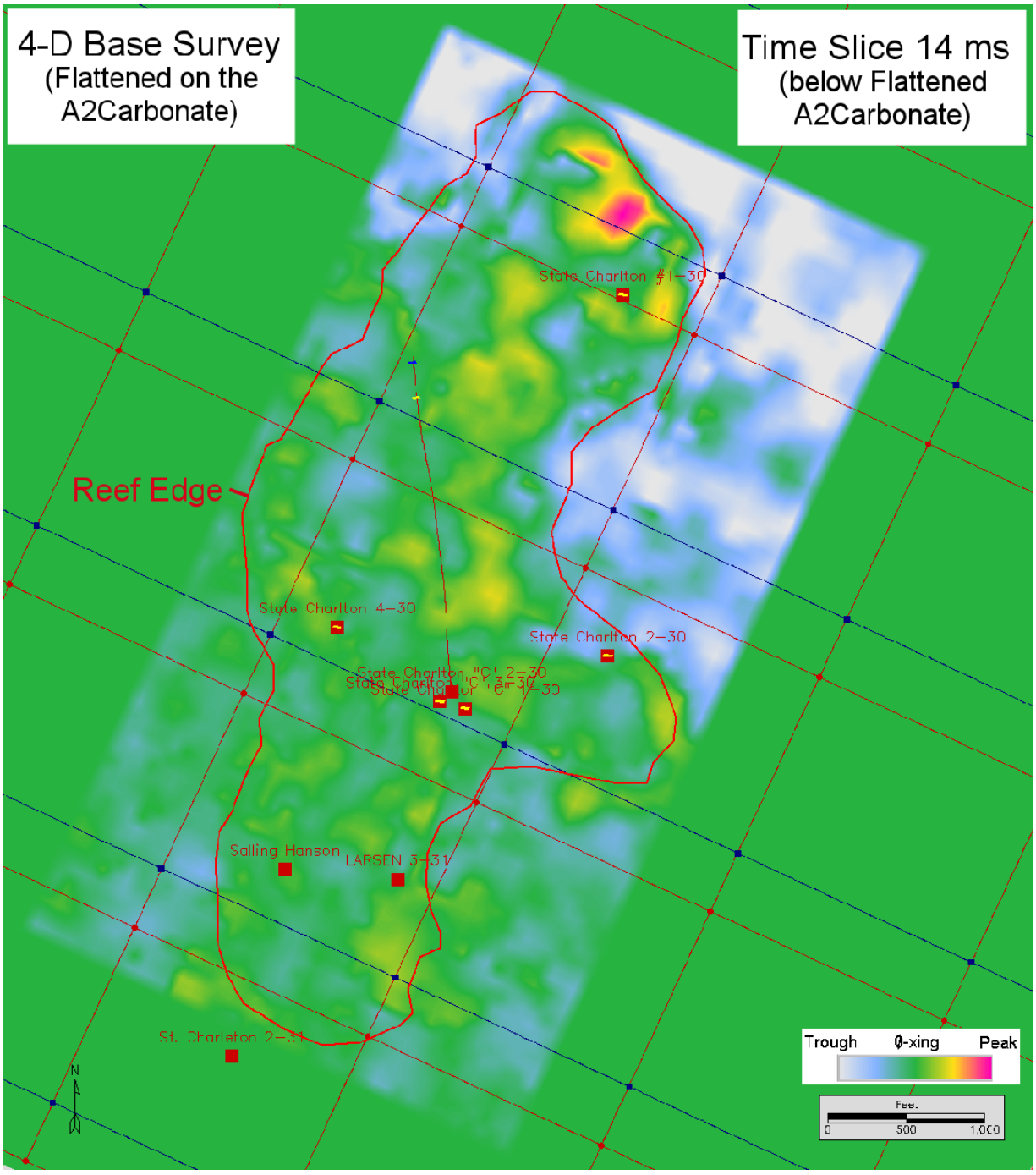
4-D Base Survey
(Flattened on the
A2Carbonate)
Time Slice 14 ms
(below Flattened
A2Carbonate)
State Charlton #1-30
Reef Edge
State Charlton 4-30
State Charlton 2-30
Salling Hanson
LARSEN 3-31
Trough
0-xing
Peak
Feet
0
500
1,000
N

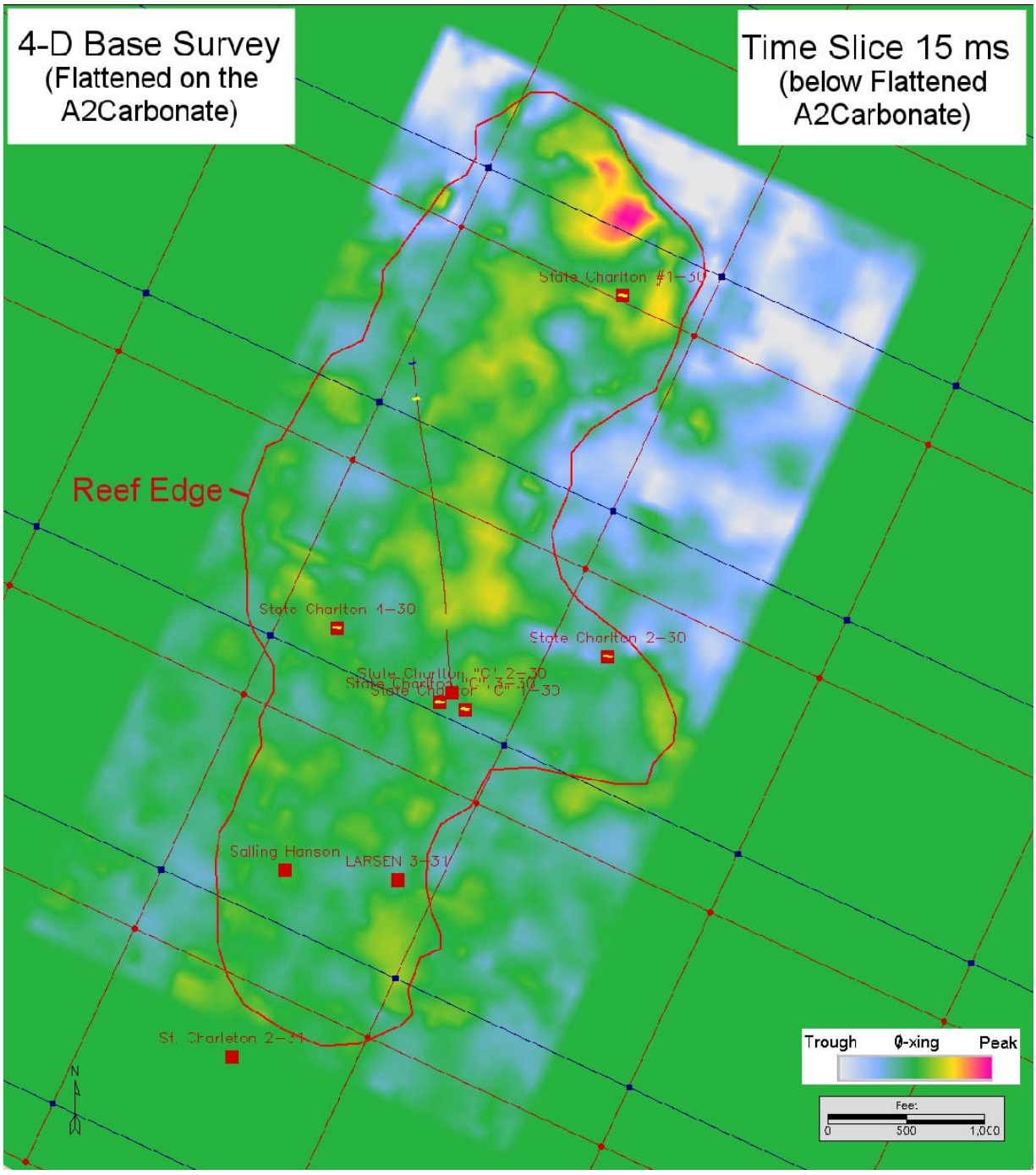
4-D Base Survey
(Flattened on the
A2Carbonate)
Time Slice 15 ms
(below Flattened
A2Carbonate)
State Charlton #1-30
Reef Edge
State Charlton 1-30
State Charlton 2-30
Salling Hanson
LARSEN 3-31
St. Charleton 2-31
Trough
0-xing
Peak
Fee:
0
500
1,000

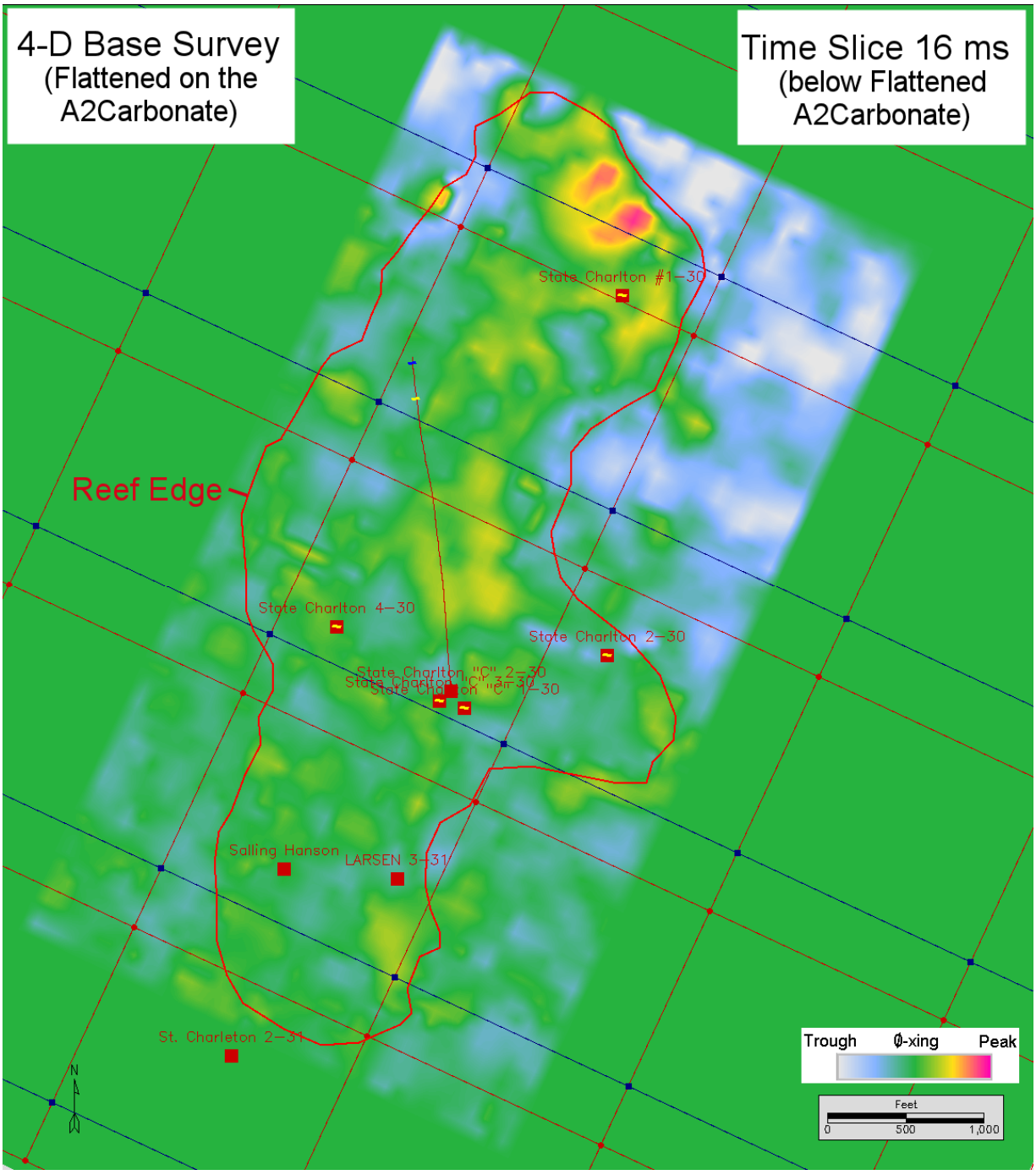
4-D Base Survey
(Flattened on the
A2Carbonate)
Time Slice 16 ms
(below Flattened
A2Carbonate)
State Charlton #1-30
Reef Edge
State Charlton 4-30
State Charlton 2-30
State Charlton "C" 2-30
State Charlton "C" 3-30
State Charlton "C" 1-30
Salling Hanson
LARSEN 3-31
St. Charleton 2-31
N
Trough
Ø-xing
Peak
Feet
0
500
1,000

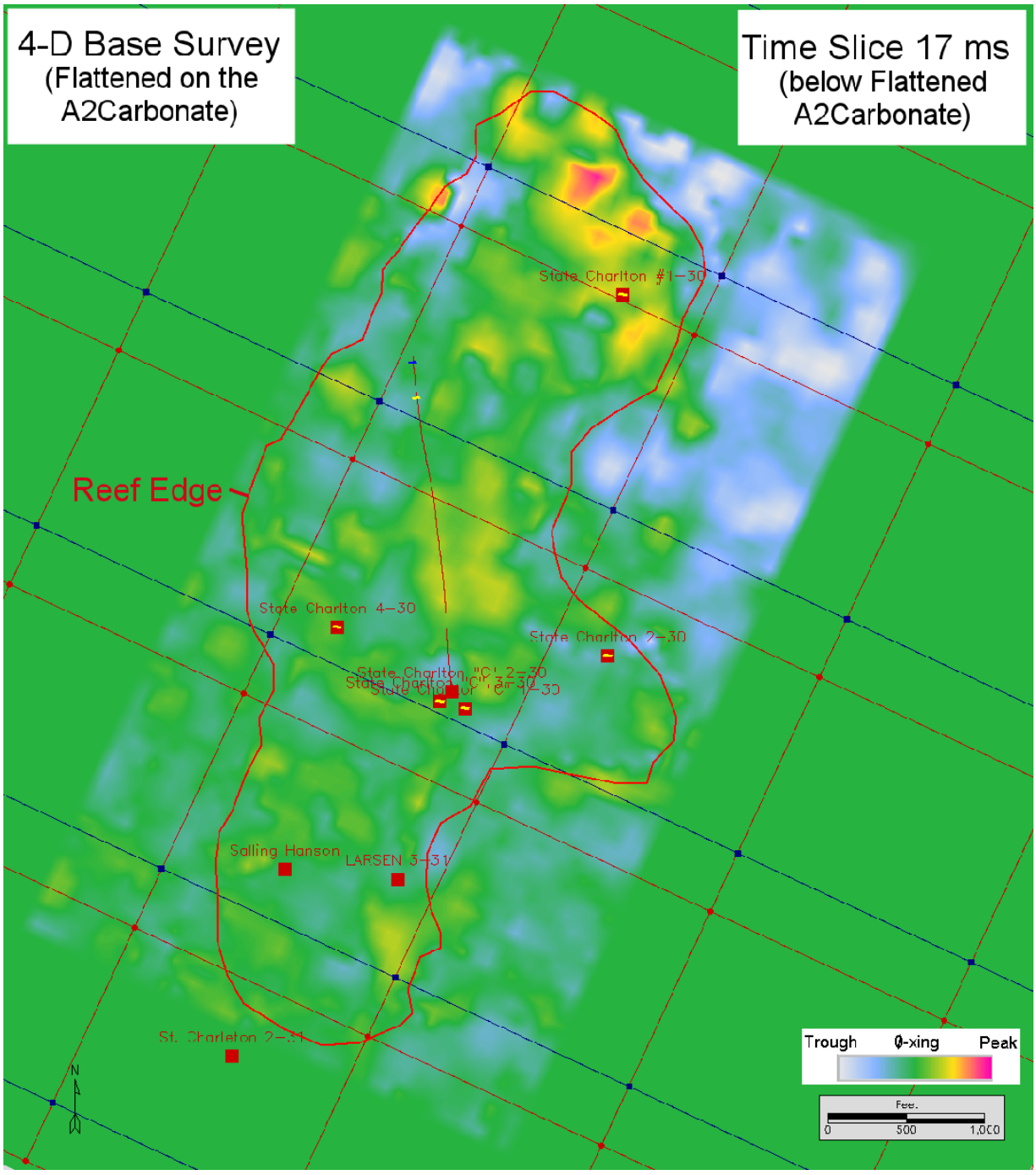
4-D Base Survey
(Flattened on the
A2Carbonate)
Time Slice 17 ms
(below Flattened
A2Carbonate)
State Charlton #1-30
Reef Edge
State Charlton 4-30
State Charlton 2-30
Salling Hanson
LARSEN 3-31
Trough
0-xing
Peak
Feet
0
500
1,000
N

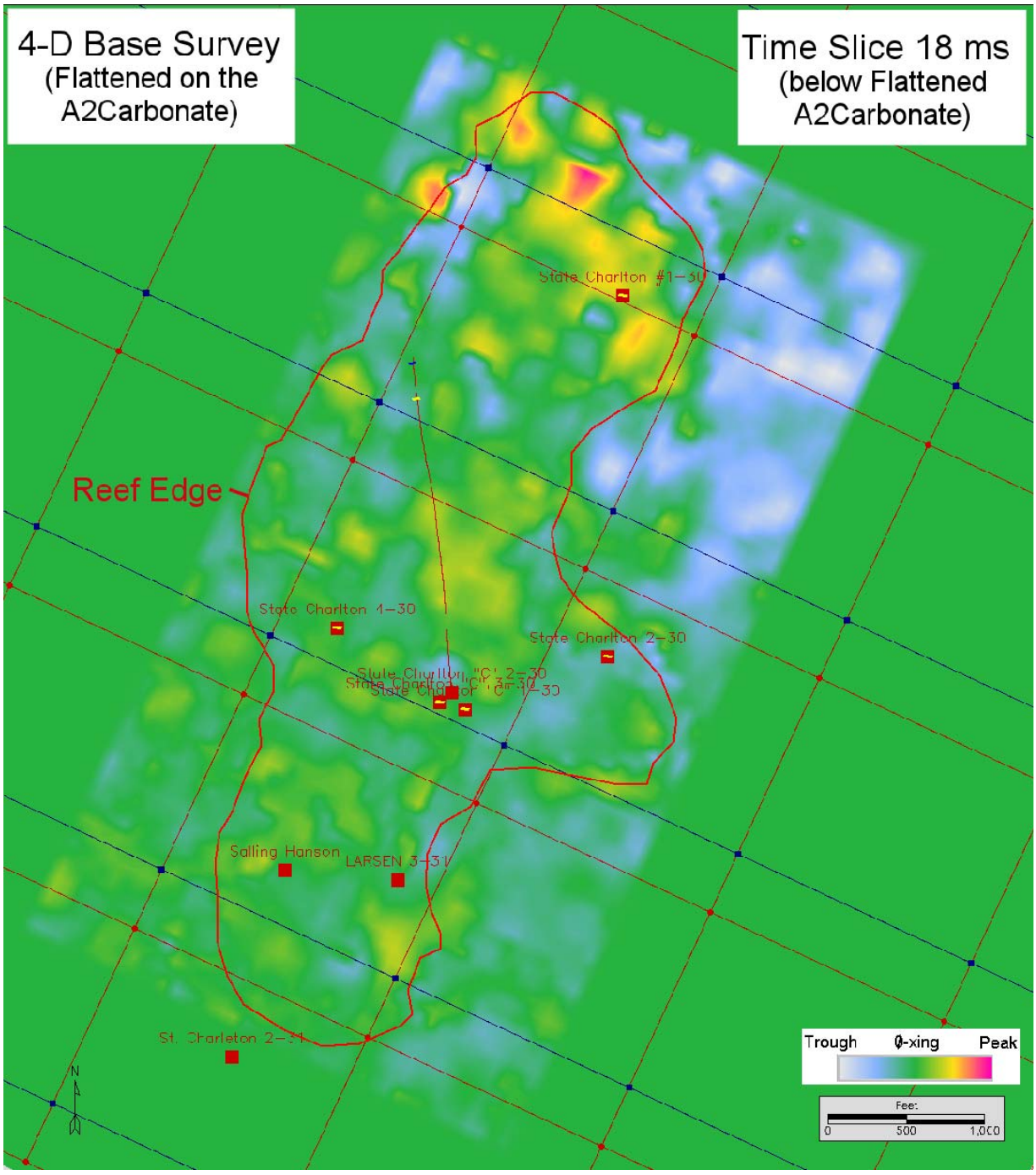
4-D Base Survey
(Flattened on the
A2Carbonate)
Time Slice 18 ms
(below Flattened
A2Carbonate)
State Charlton #1-30
Reef Edge
State Charlton 1-30
State Charlton 2-30
Salling Hanson
LARSEN 3-31
St. Charleton 2-31
Trough
0-xing
Peak
Fee:
0
500
1,000
N

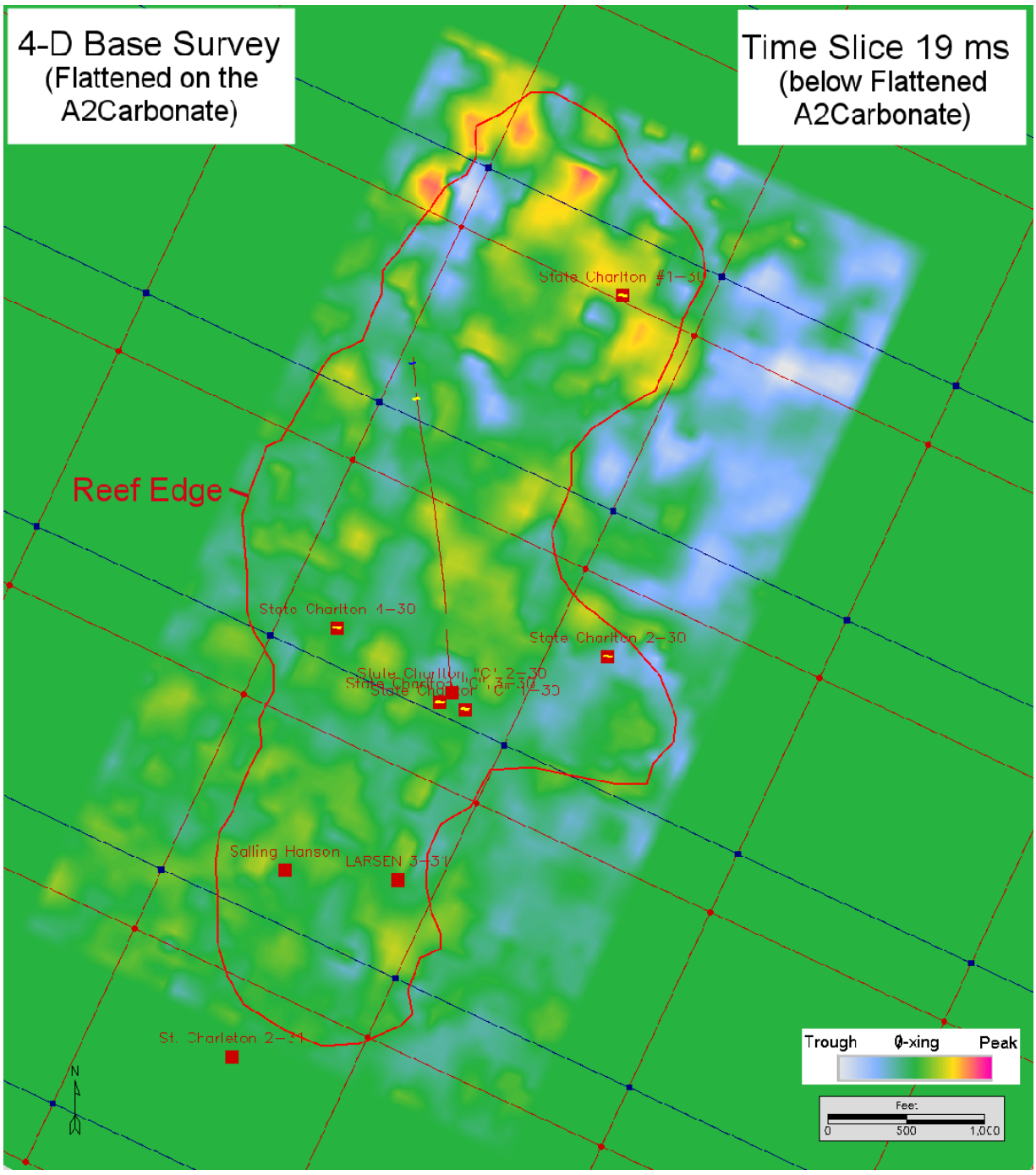
4-D Base Survey
(Flattened on the
A2Carbonate)
Time Slice 19 ms
(below Flattened
A2Carbonate)
State Charlton #1-30
Reef Edge
State Charlton 1-30
State Charlton 2-30
Salling Hanson
LARSEN 3-31
St. Charleton 2-31
Trough
0-xing
Peak
Fee:
0
500
1,000
N

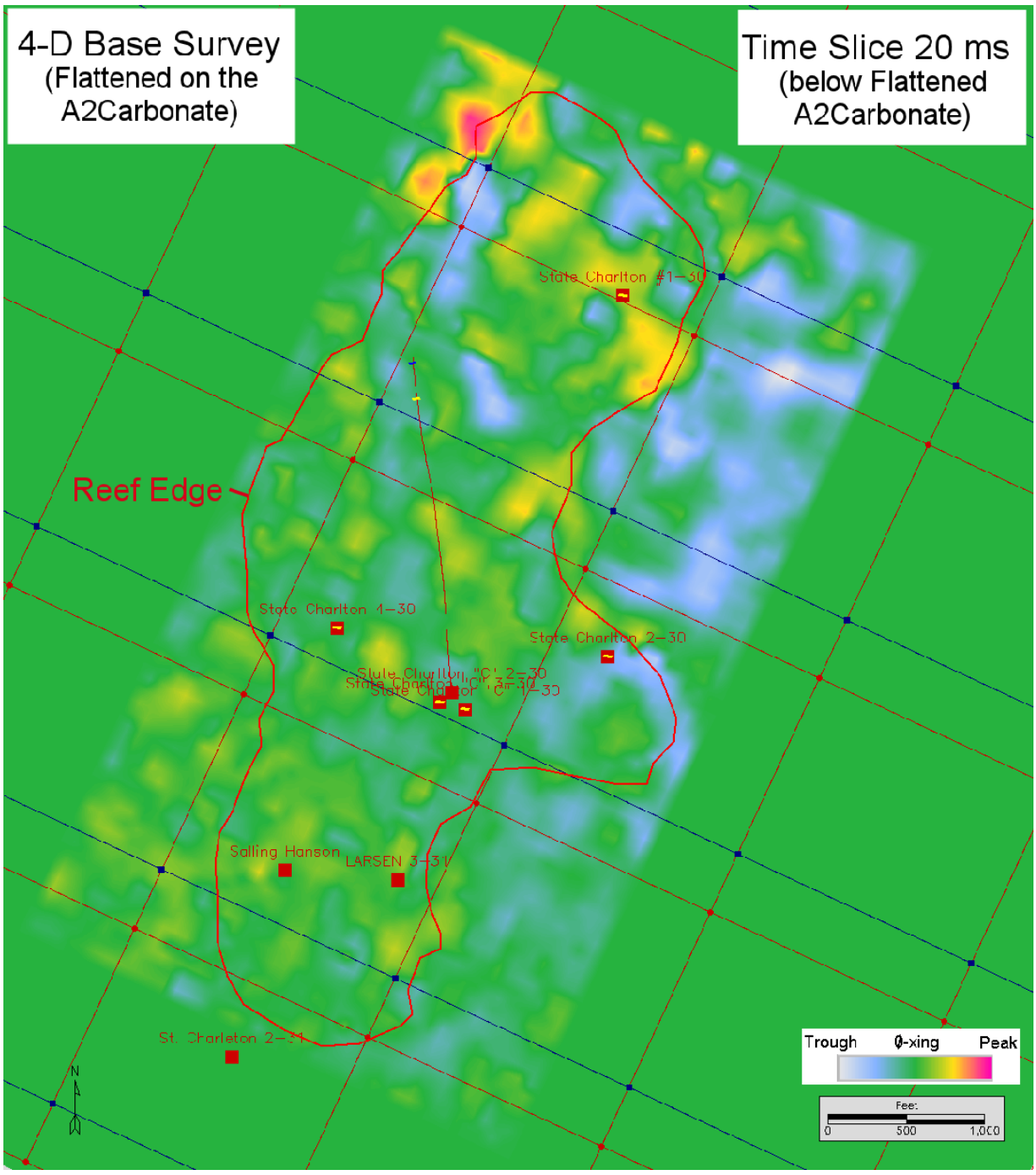
4-D Base Survey
(Flattened on the
A2Carbonate)
Time Slice 20 ms
(below Flattened
A2Carbonate)
State Charlton #1-30
Reef Edge
State Charlton 1-30
State Charlton 2-30
Salling Hanson
LARSEN 3-31
St. Charleton 2-31
Trough
0-xing
Peak
Fee:
0
500
1,000
N

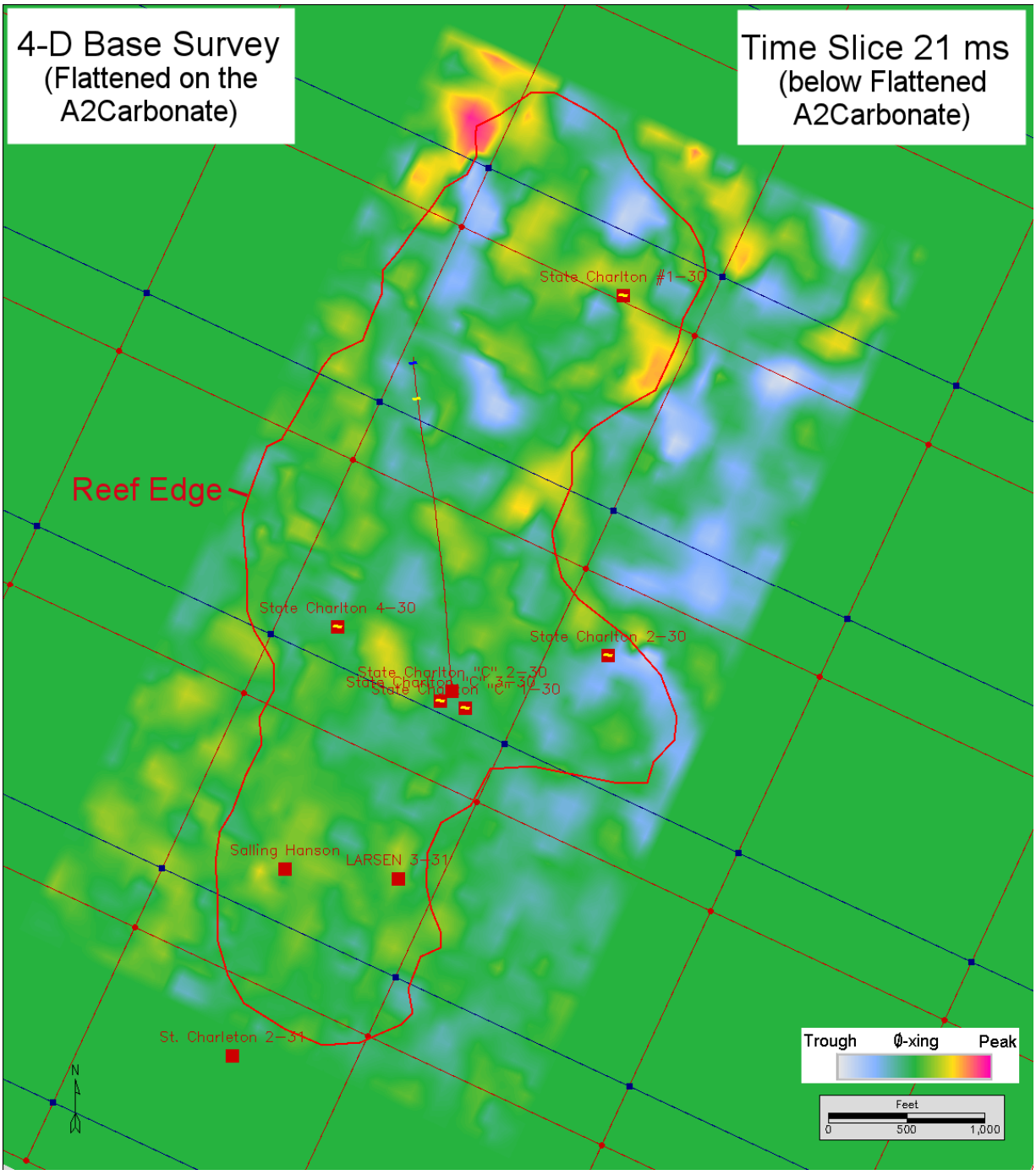
4-D Base Survey
(Flattened on the
A2Carbonate)
Time Slice 21 ms
(below Flattened
A2Carbonate)
State Charlton #1-30
Reef Edge
State Charlton 4-30
State Charlton 2-30
State Charlton "C" 2-30
Salling Hanson
LARSEN 3-31
St. Charleton 2-31
N
Trough
Ø-xing
Peak
Feet
0
500
1,000

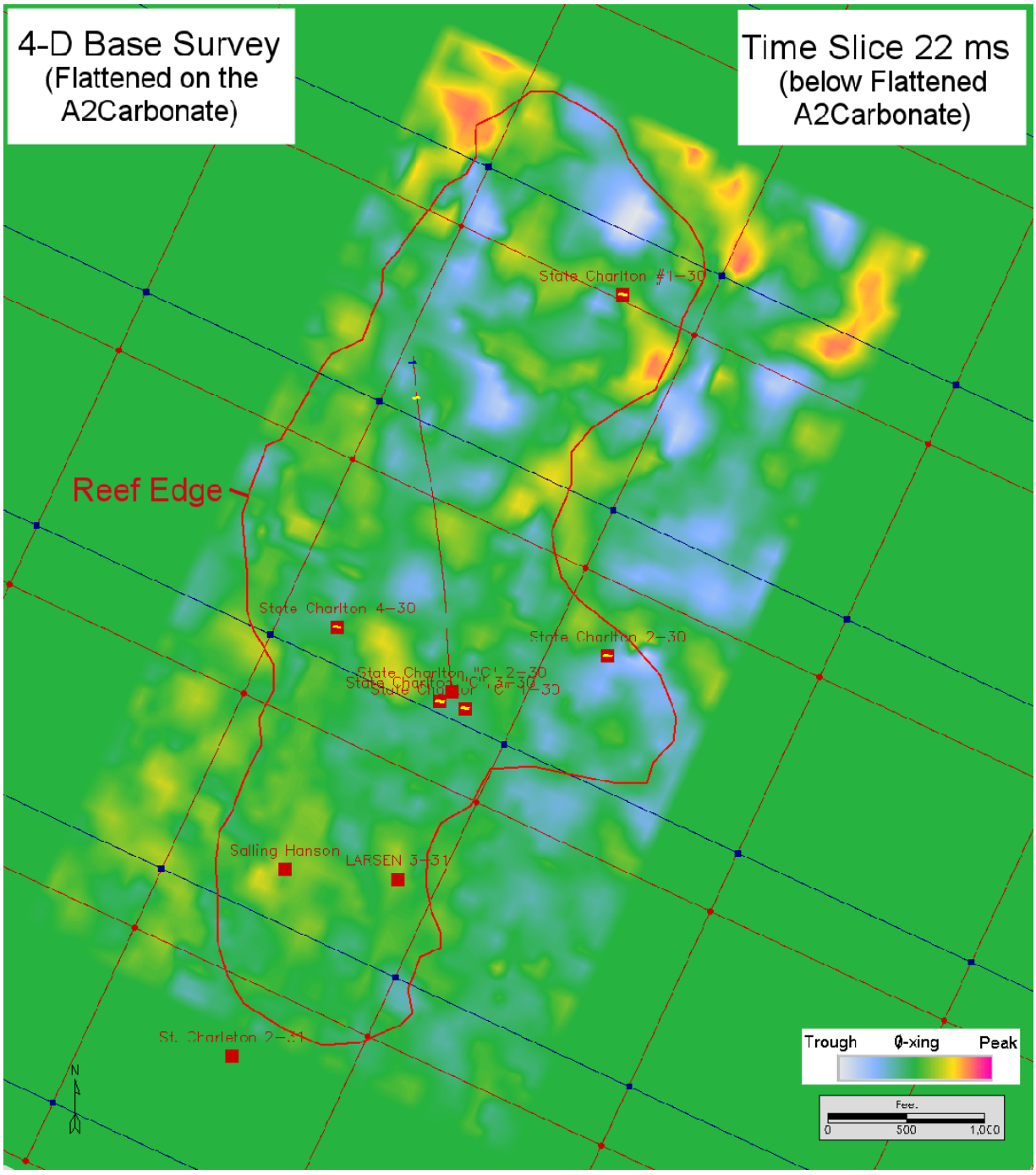
4-D Base Survey
(Flattened on the
A2Carbonate)
Time Slice 22 ms
(below Flattened
A2Carbonate)
State Charlton #1-30
Reef Edge
State Charlton 4-30
State Charlton 2-30
Salling Hanson
LARSEN 3-31
St. Charleton 2-31
Trough
0-xing
Peak
Feet
0
500
1,000
N

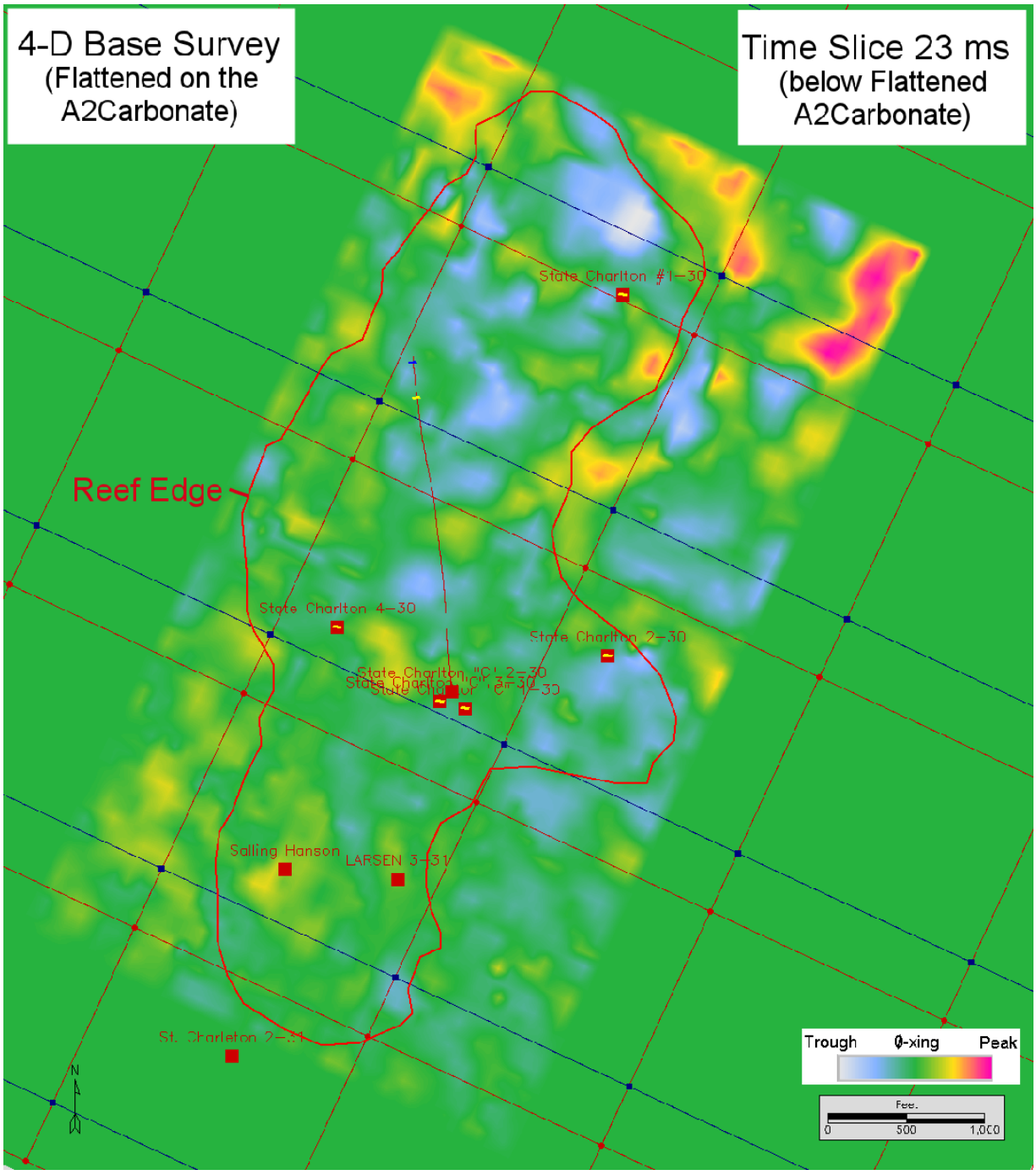
4-D Base Survey
(Flattened on the
A2Carbonate)
Time Slice 23 ms
(below Flattened
A2Carbonate)
State Charlton #1-30
Reef Edge
State Charlton 4-30
State Charlton 2-30
Salling Hanson
LARSEN 3-31
St. Charleton 2-31
N
Trough
0-xing
Peak
Feet
0
500
1,000

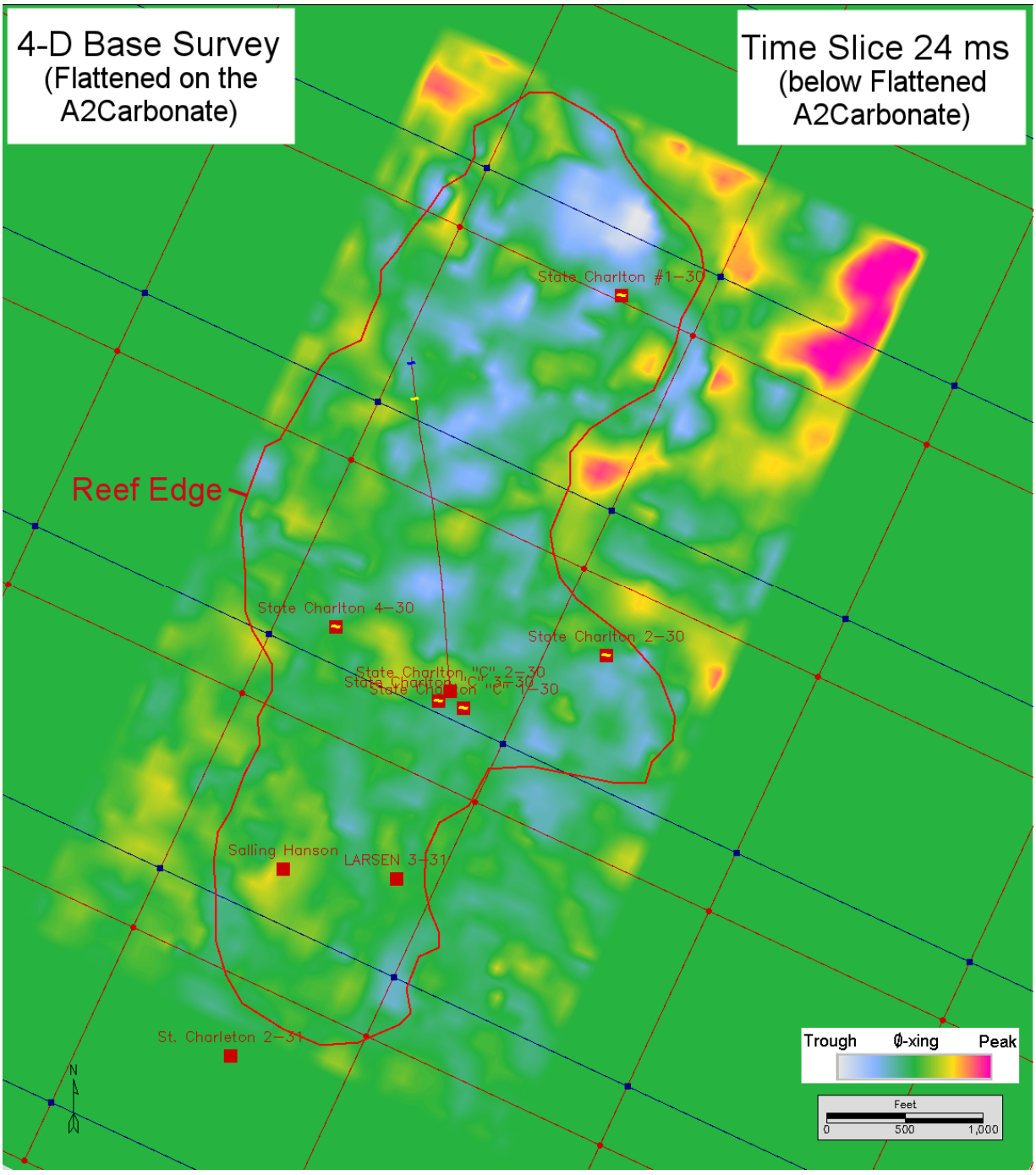
4-D Base Survey
(Flattened on the
A2Carbonate)
Time Slice 24 ms
(below Flattened
A2Carbonate)
State Charlton #1-30
Reef Edge
State Charlton 4-30
State Charlton 2-30
State Charlton "C" 2-30
Salling Hanson
LARSEN 3-31
St. Charleton 2-31
Trough
Ø-xing
Peak
Feet
0
500
1,000
N

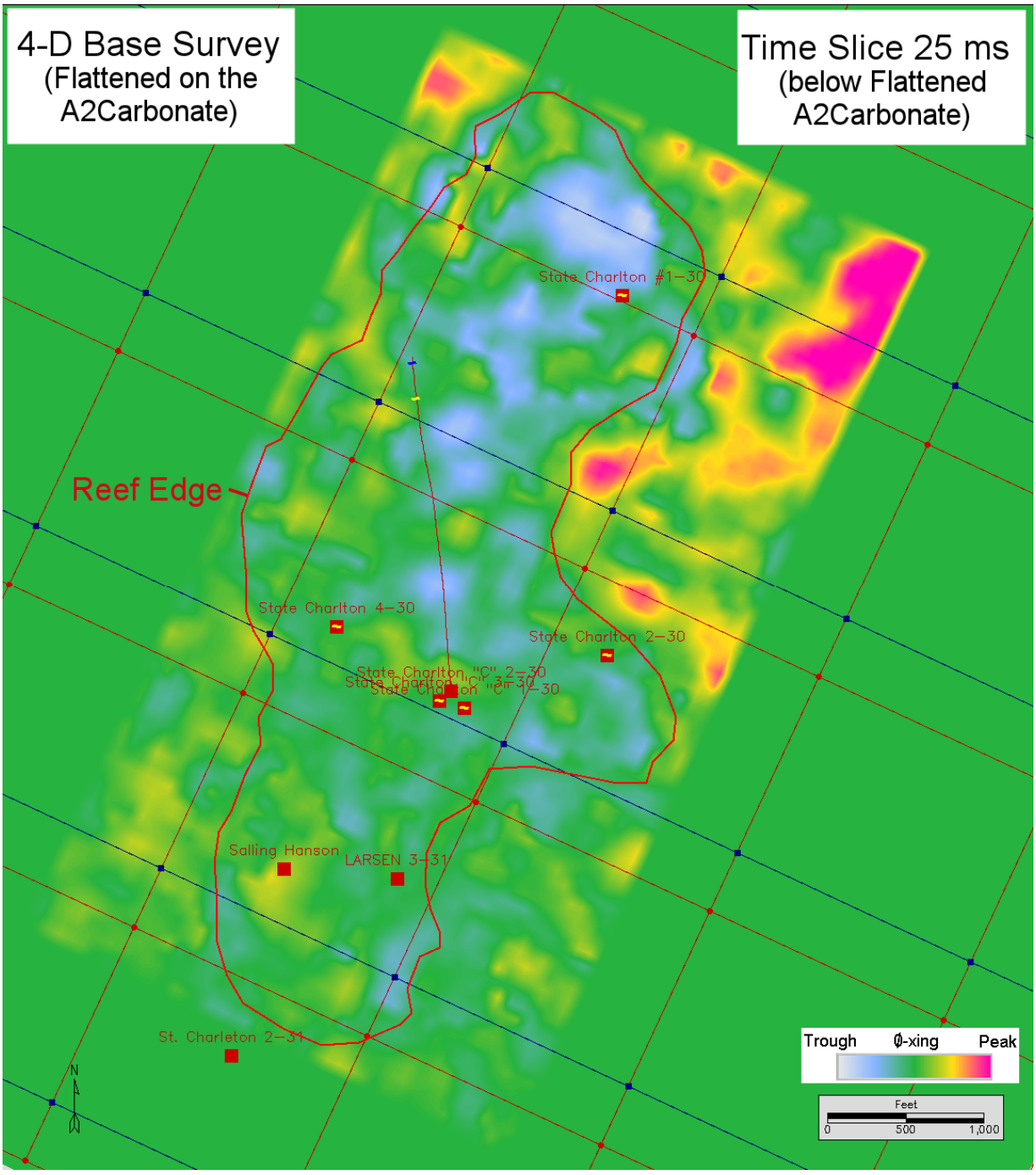
4-D Base Survey
(Flattened on the
A2Carbonate)
Time Slice 25 ms
(below Flattened
A2Carbonate)
State Charlton #1-30
Reef Edge
State Charlton 4-30
State Charlton 2-30
State Charlton "C" 2-30
State Charlton "C" 3-30
State Charlton "C" 1-30
Salling Hanson
LARSEN 3-31
St. Charleton 2-31
N
Trough
Ø-xing
Peak
Feet
0
500
1,000

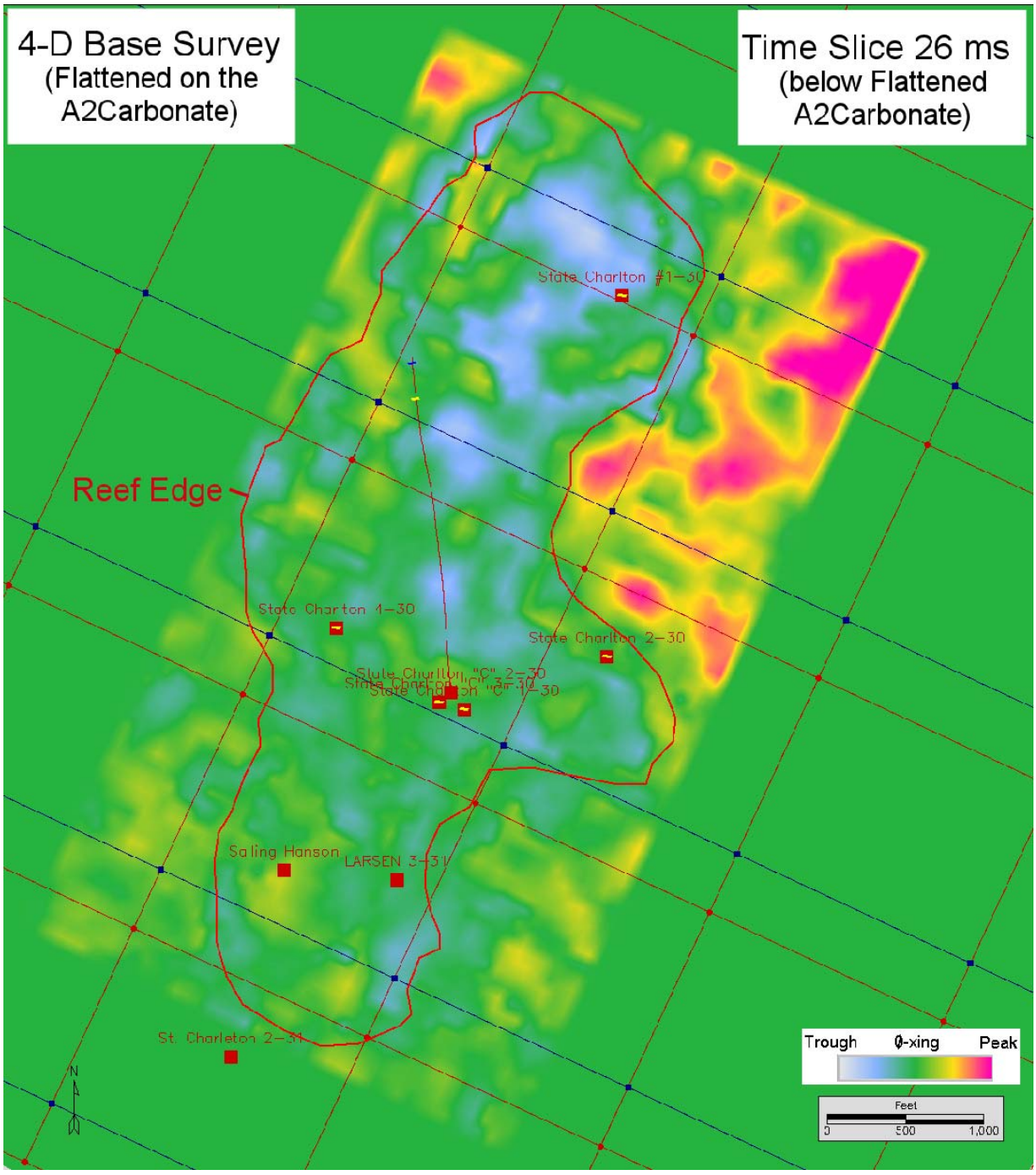
4-D Base Survey
(Flattened on the
A2Carbonate)
Time Slice 26 ms
(below Flattened
A2Carbonate)
Reef Edge
State Charlton #1-30
State Charlton 1-30
State Charlton 2-30
Saling Hanson
LARSEN 3-31
St. Charleton 2-31
Trough
0-xing
Peak
Feet
0
500
1,000
N

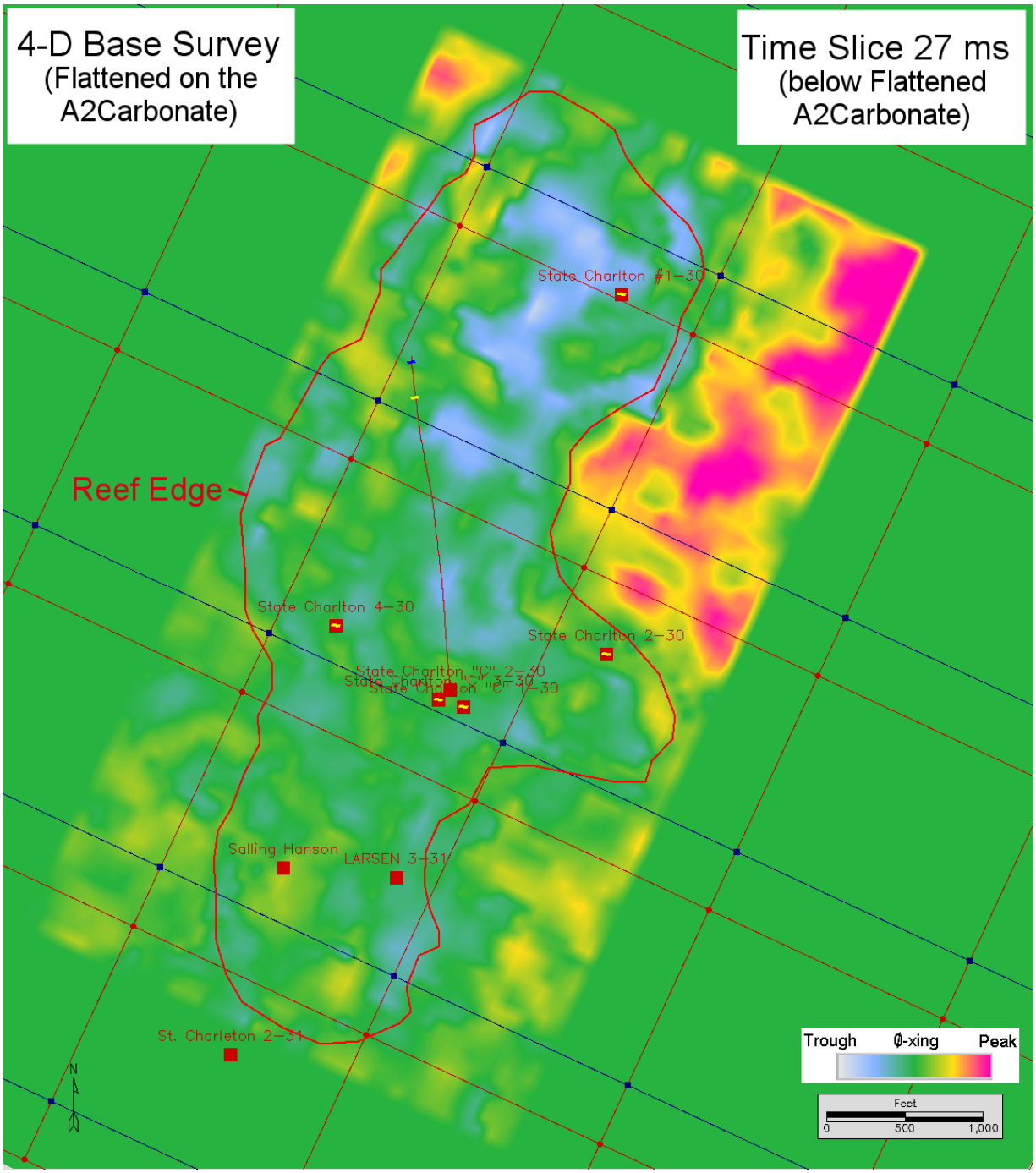
4-D Base Survey
(Flattened on the
A2Carbonate)
Time Slice 27 ms
(below Flattened
A2Carbonate)
State Charlton #1-30
Reef Edge
State Charlton 4-30
State Charlton 2-30
State Charlton "C" 2-30
State Charlton "C" 3-30
State Charlton "C" 1-30
Salling Hanson
LARSEN 3-31
St. Charleton 2-31
N
Trough
Ø-xing
Peak
Feet
0
500
1,000

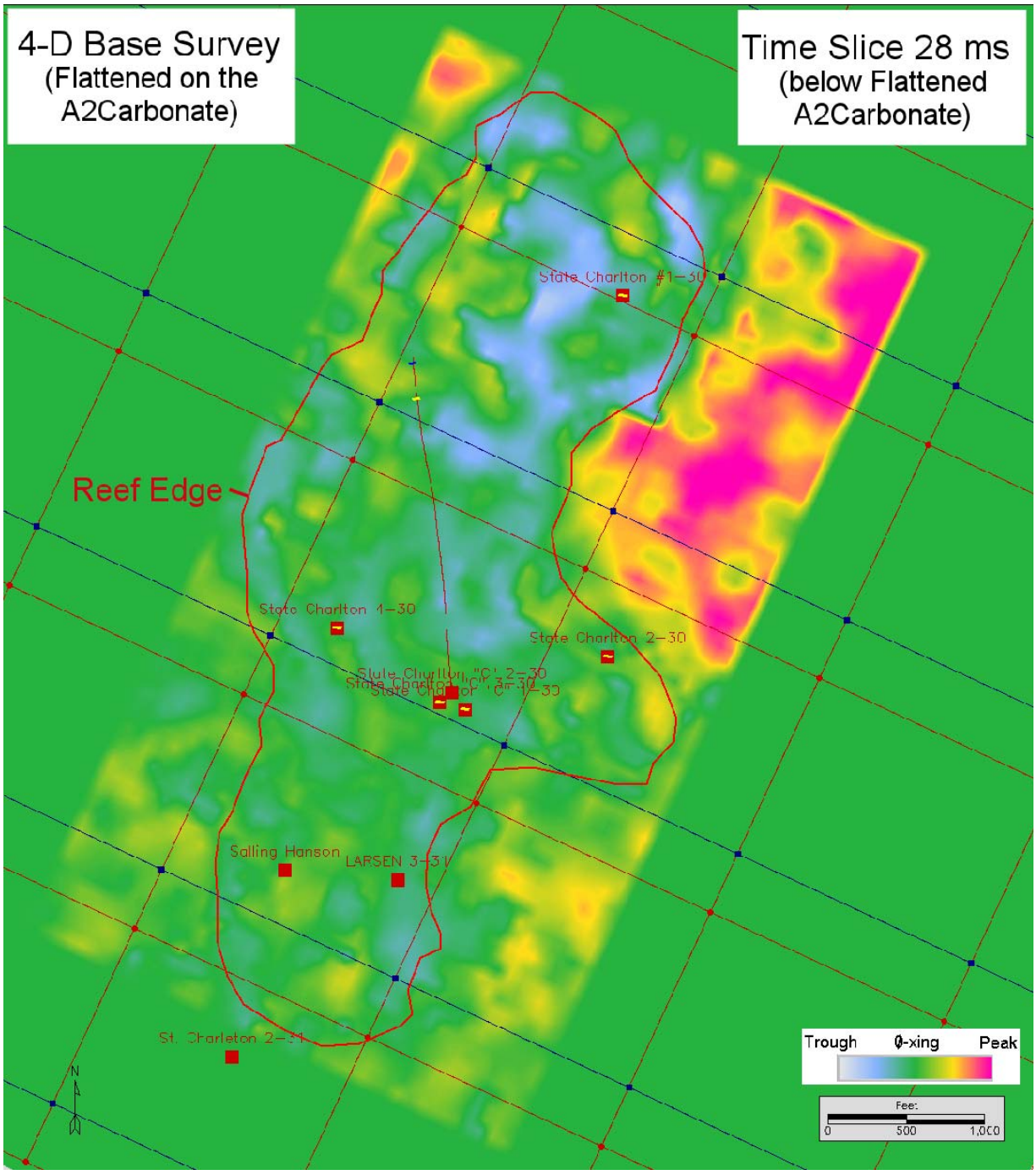
4-D Base Survey
(Flattened on the
A2Carbonate)
Time Slice 28 ms
(below Flattened
A2Carbonate)
State Charlton #1-30
Reef Edge
State Charlton 1-30
State Charlton 2-30
Salling Hanson
LARSEN 3-31
St. Charleton 2-31
Trough
0-xing
Peak
Fee:
0
500
1,000
N

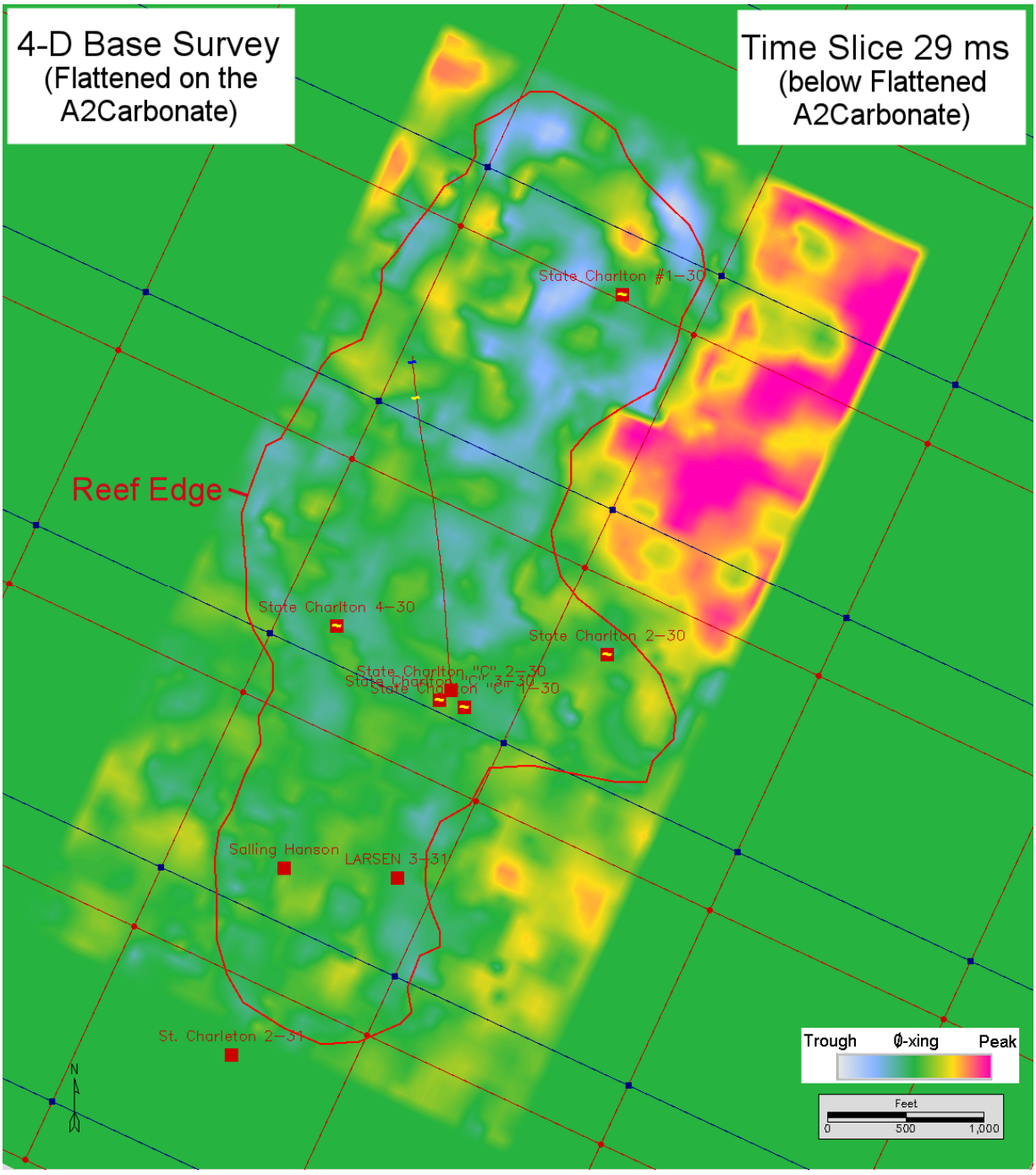
4-D Base Survey
(Flattened on the
A2Carbonate)
Time Slice 29 ms
(below Flattened
A2Carbonate)
State Charlton #1-30
Reef Edge
State Charlton 4-30
State Charlton 2-30
State Charlton "C" 2-30
State Charlton "C" 3-30
State Charlton "C" 1-30
Salling Hanson
LARSEN 3-31
St. Charleton 2-31
N
Trough
Ø-xing
Peak
Feet
0
500
1,000

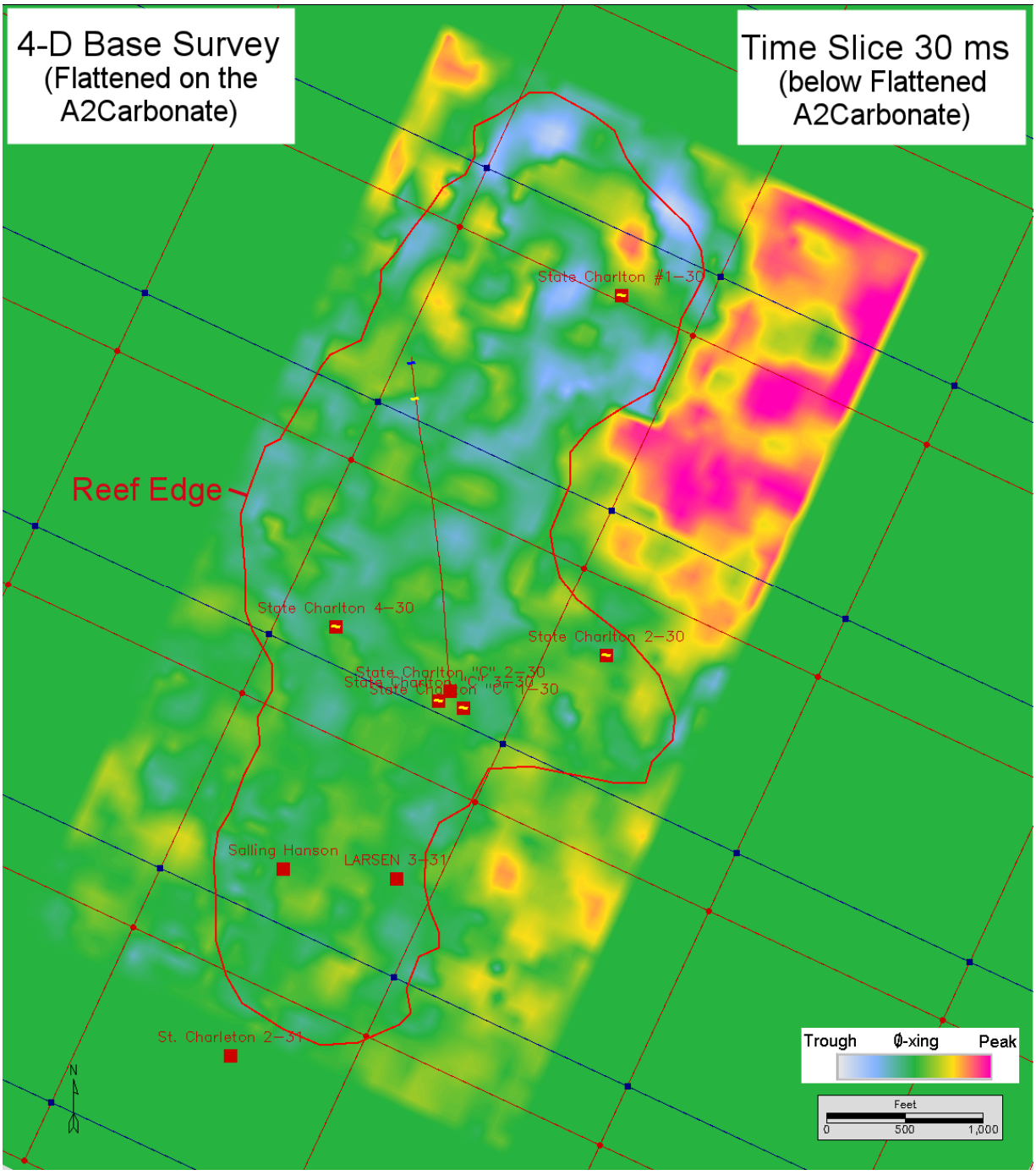
4-D Base Survey
(Flattened on the
A2Carbonate)
Time Slice 30 ms
(below Flattened
A2Carbonate)
State Charlton #1-30
Reef Edge
State Charlton 4-30
State Charlton 2-30
State Charlton "C" 2-30
Salling Hanson
LARSEN 3-31
St. Charleton 2-31
N
Trough
Ø-xing
Peak
Feet
0
500
1,000

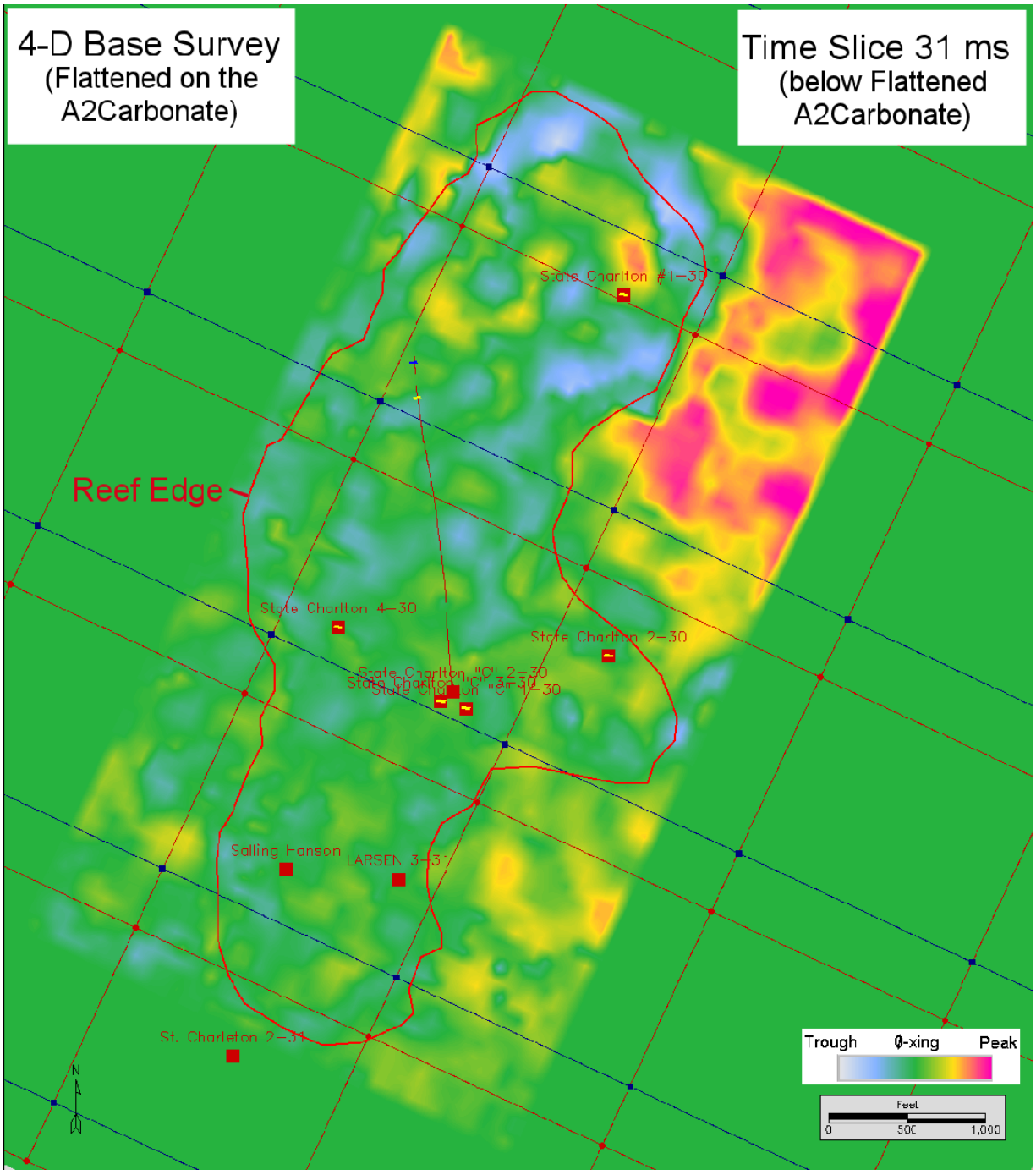
4-D Base Survey
(Flattened on the
A2Carbonate)
Time Slice 31 ms
(below Flattened
A2Carbonate)
State Charlton #1-30
Reef Edge
State Charlton 4-30
State Charlton 2-30
Salling Hanson
LARSEN 3-31
St. Charleton 2-31
Trough
0-xing
Peak
Feet
0
500
1,000
N

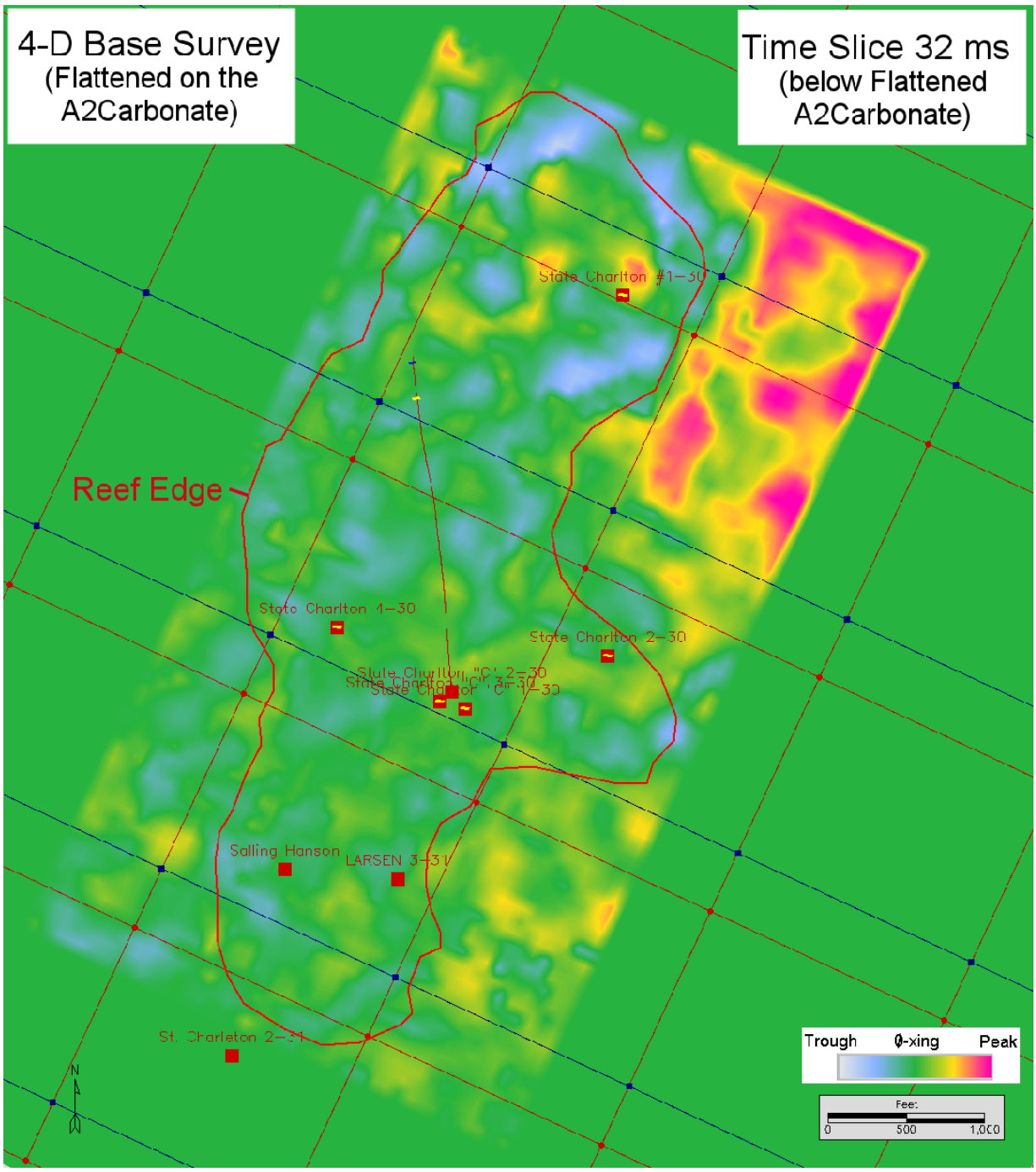
4-D Base Survey
(Flattened on the
A2Carbonate)
Time Slice 32 ms
(below Flattened
A2Carbonate)
State Charlton #1-30
Reef Edge
State Charlton 1-30
State Charlton 2-30
Salling Hanson
LARSEN 3-31
St. Charleton 2-31
N
Trough
0-xing
Peak
Feet
0
500
1,000

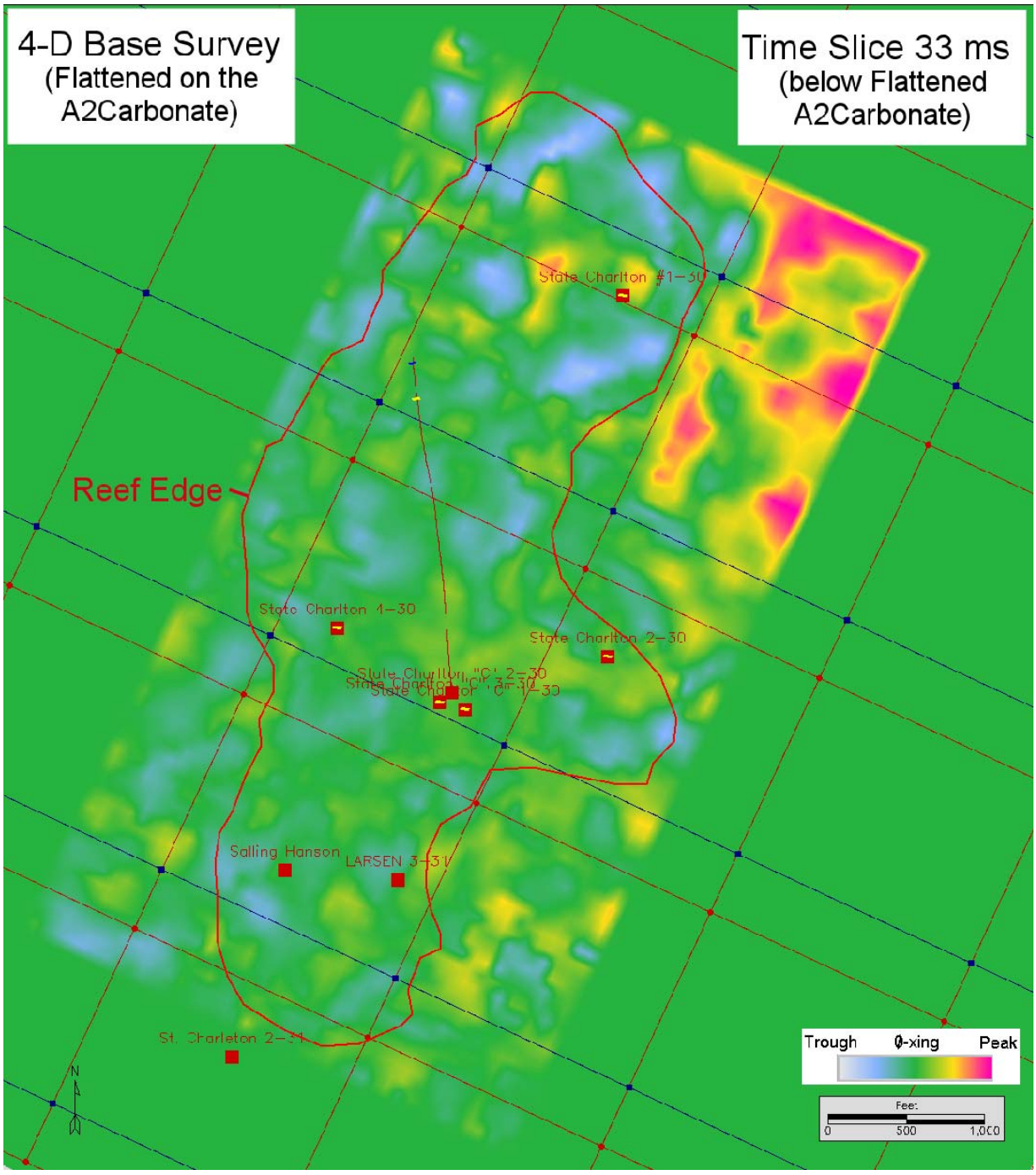
4-D Base Survey
(Flattened on the
A2Carbonate)
Time Slice 33 ms
(below Flattened
A2Carbonate)
State Charlton #1-30
Reef Edge
State Charlton 1-30
State Charlton 2-30
Salling Hanson
LARSEN 3-31
St. Charleton 2-31
Trough
0-xing
Peak
Fee:
0
500
1,000
N

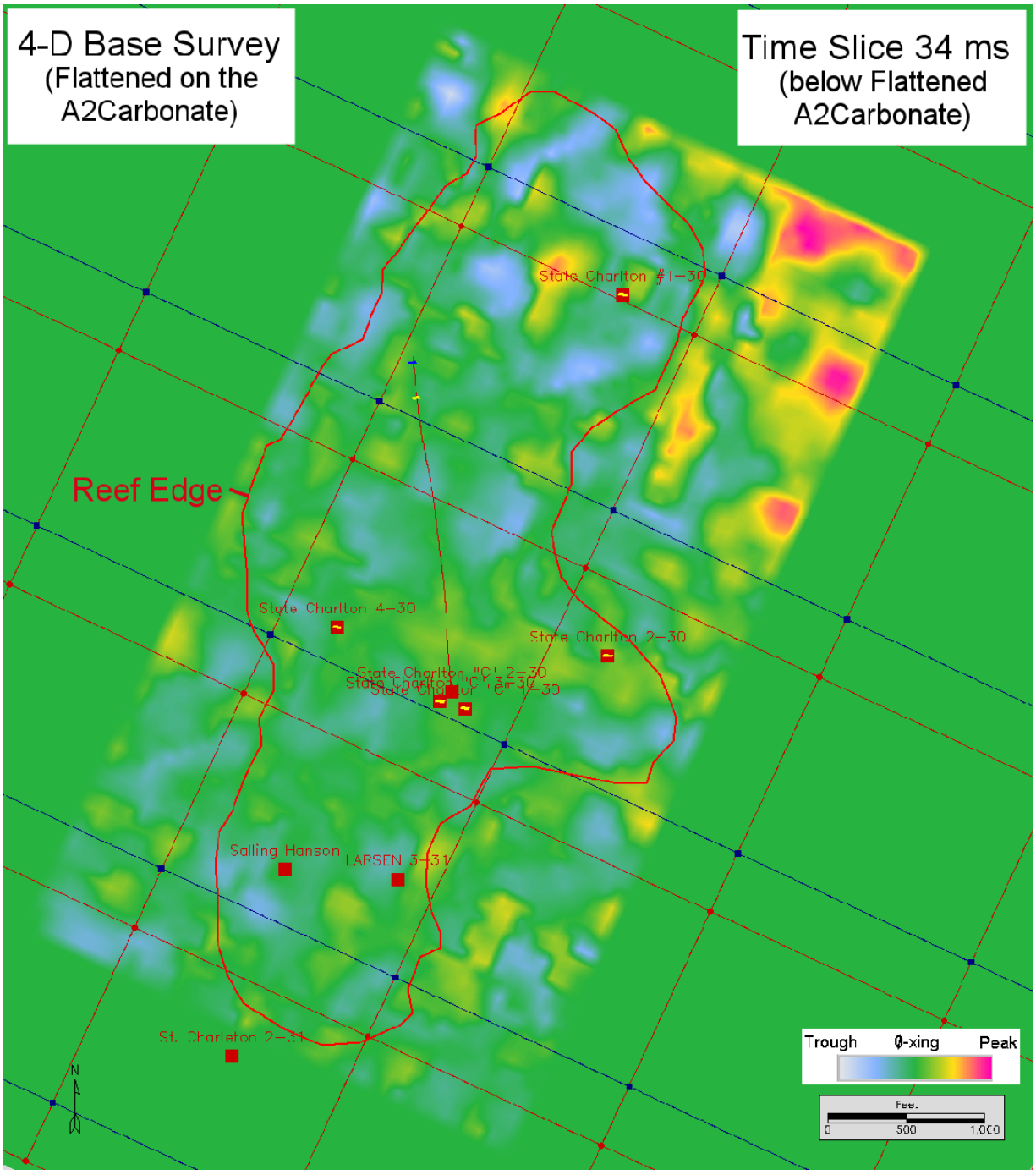
4-D Base Survey
(Flattened on the
A2Carbonate)
Time Slice 34 ms
(below Flattened
A2Carbonate)
State Charlton #1-30
Reef Edge
State Charlton 4-30
State Charlton 2-30
Salling Hanson
LARSEN 3-31
St. Charleton 2-31
N
Trough
0-xing
Peak
Feet
0
500
1,000

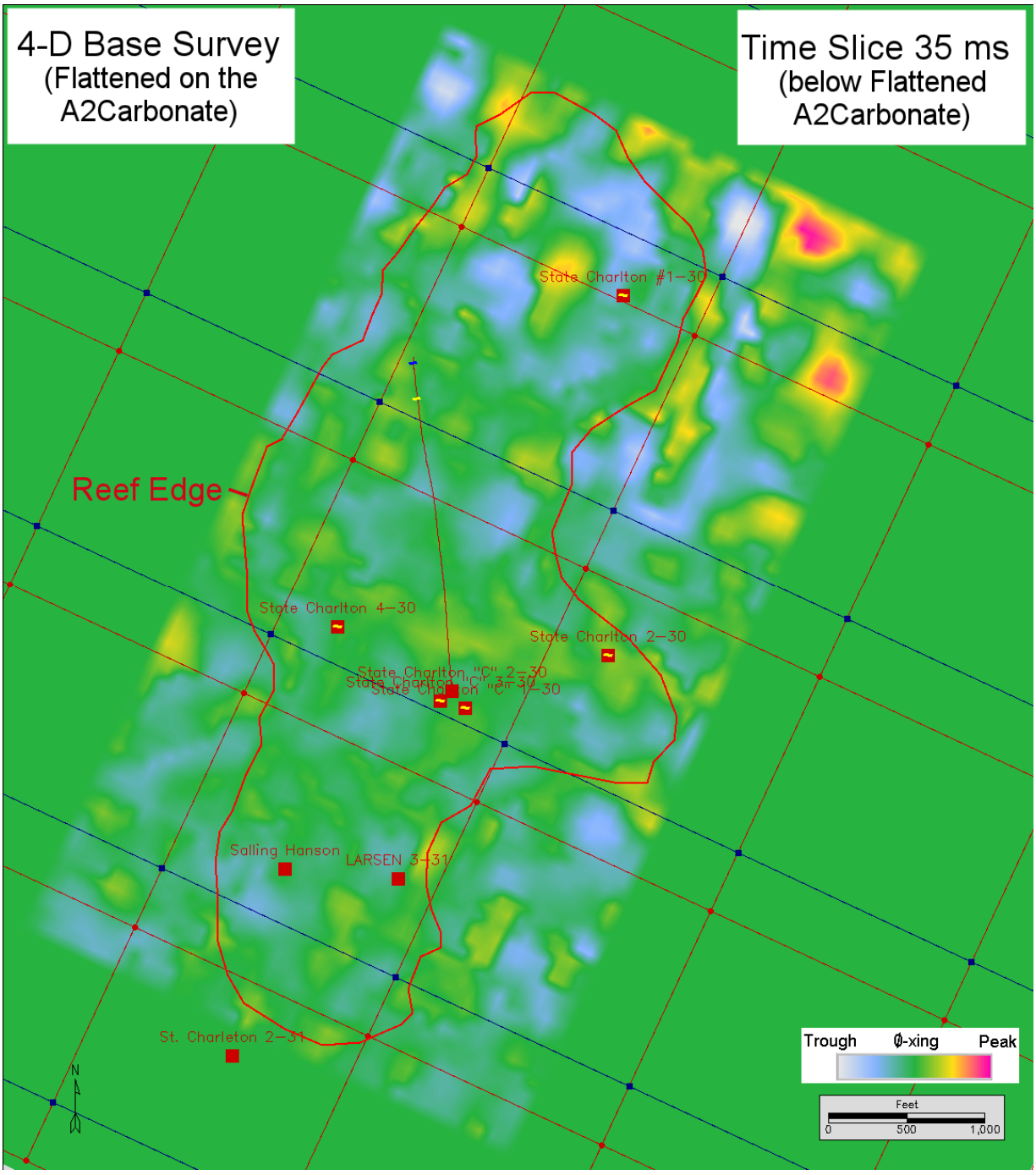
4-D Base Survey
(Flattened on the
A2Carbonate)
Time Slice 35 ms
(below Flattened
A2Carbonate)
State Charlton #1-30
Reef Edge
State Charlton 4-30
State Charlton 2-30
State Charlton "C" 2-30
Salling Hanson
LARSEN 3-31
St. Charleton 2-31
N
Trough
Ø-xing
Peak
Feet
0
500
1,000

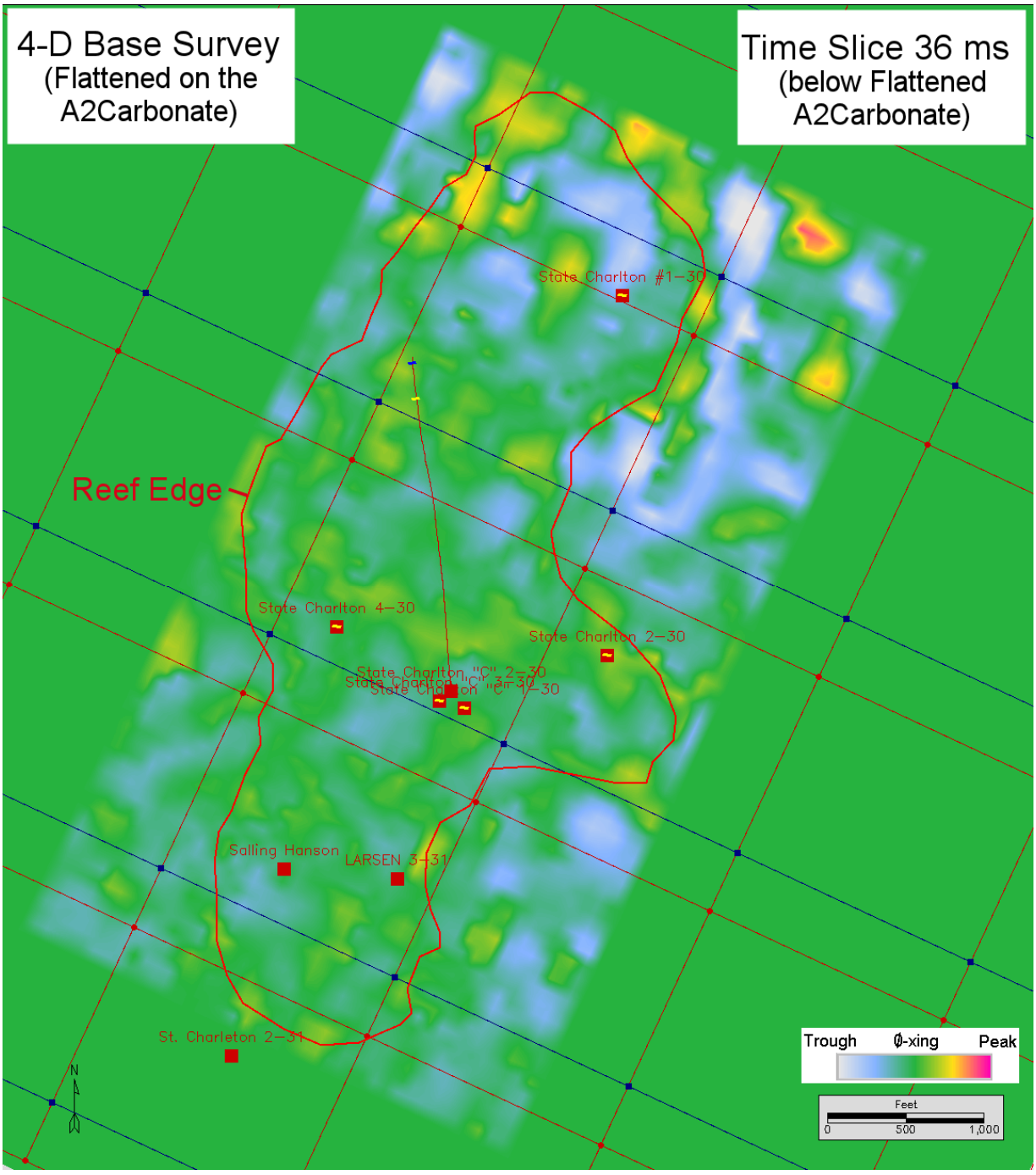
4-D Base Survey
(Flattened on the
A2Carbonate)
Time Slice 36 ms
(below Flattened
A2Carbonate)
State Charlton #1-30
Reef Edge
State Charlton 4-30
State Charlton 2-30
State Charlton "C" 2-30
State Charlton "C" 3-30
State Charlton "C" 1-30
Salling Hanson
LARSEN 3-31
St. Charleton 2-31
N
Trough
Ø-xing
Peak
Feet
0
500
1,000

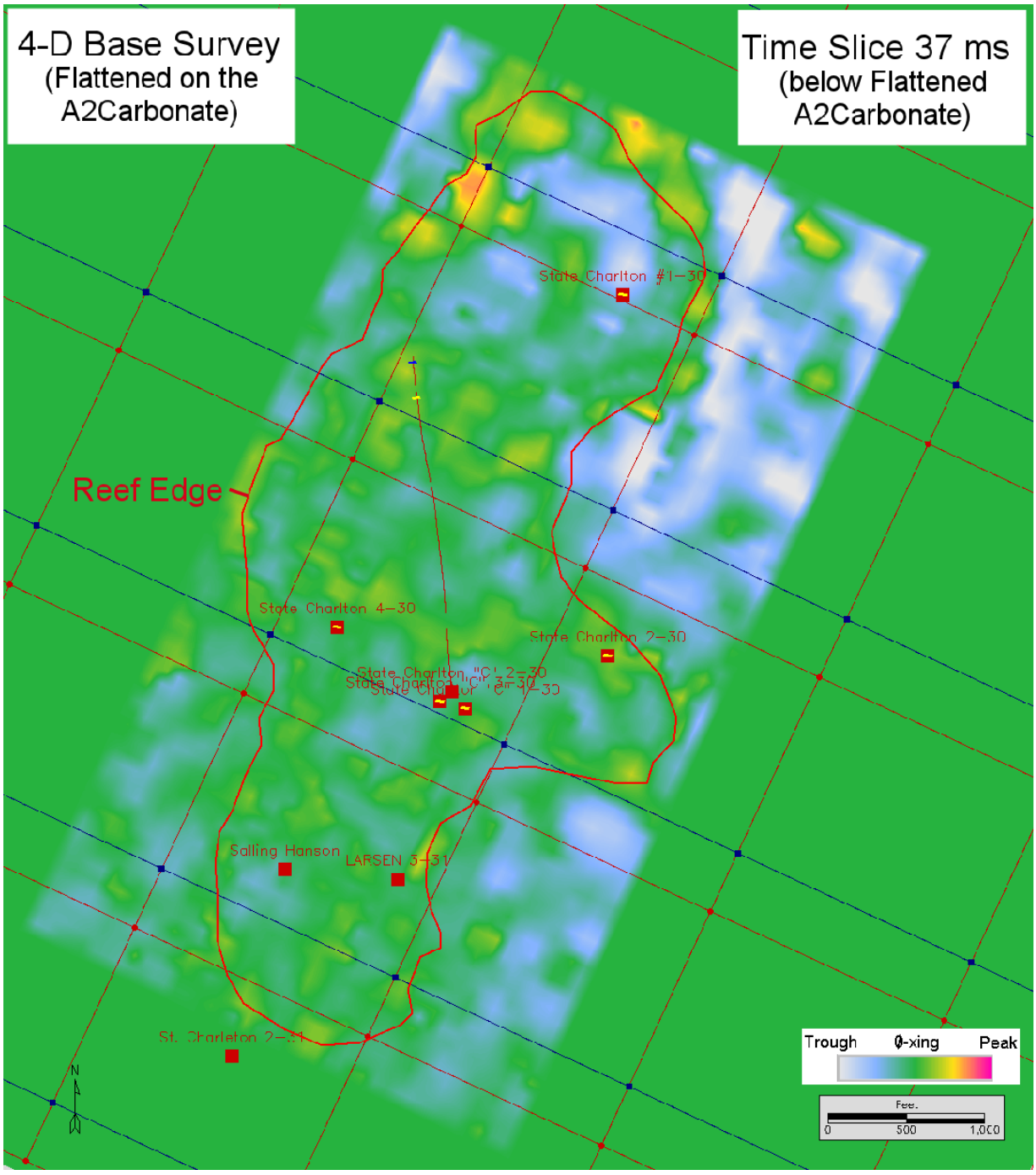
4-D Base Survey
(Flattened on the
A2Carbonate)
Time Slice 37 ms
(below Flattened
A2Carbonate)
State Charlton #1-30
Reef Edge
State Charlton 4-30
State Charlton 2-30
Salling Hanson
LARSEN 3-31
St. Charleton 2-31
Trough
0-xing
Peak
Feet
0
500
1,000
N

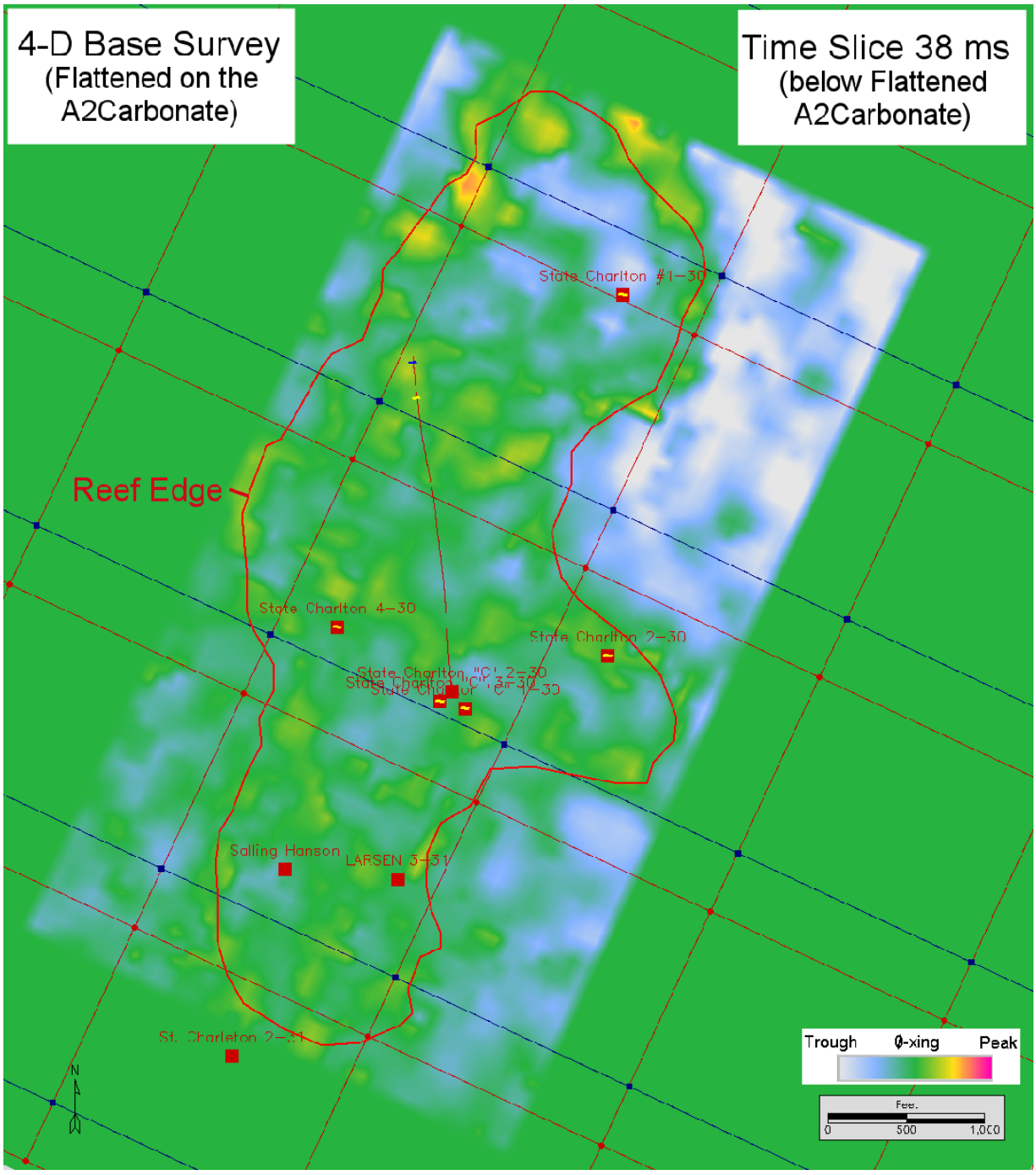
4-D Base Survey
(Flattened on the
A2Carbonate)
Time Slice 38 ms
(below Flattened
A2Carbonate)
State Charlton #1-30
Reef Edge
State Charlton 4-30
State Charlton 2-30
Salling Hanson
LARSEN 3-31
Trough
0-xing
Peak
Feet
0
500
1,000
N

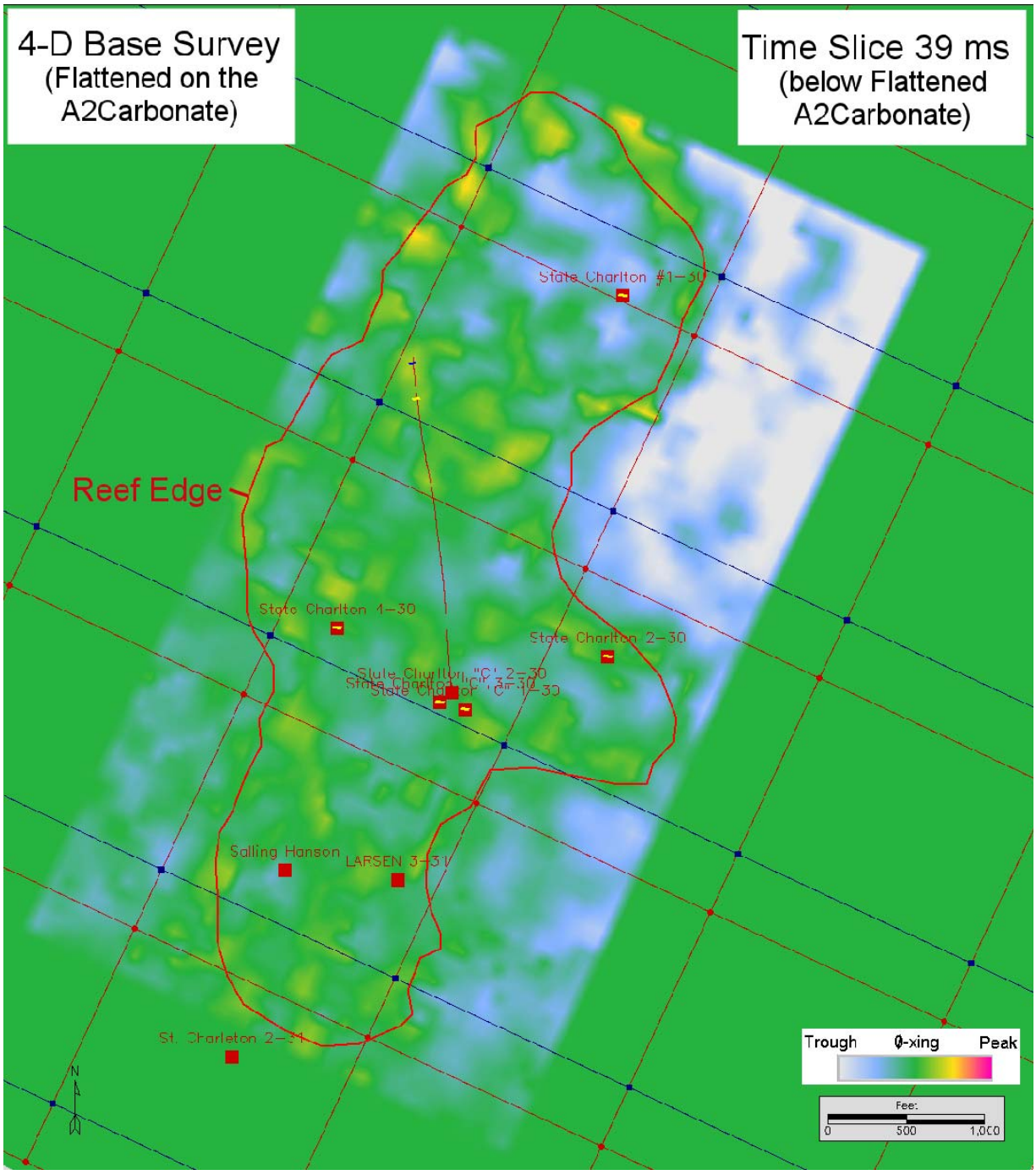
4-D Base Survey
(Flattened on the
A2Carbonate)
Time Slice 39 ms
(below Flattened
A2Carbonate)
State Charlton #1-30
Reef Edge
State Charlton 1-30
State Charlton 2-30
Salling Hanson
LARSEN 3-31
St. Charleton 2-31
Trough
0-xing
Peak
Fee:
0
500
1,000
N

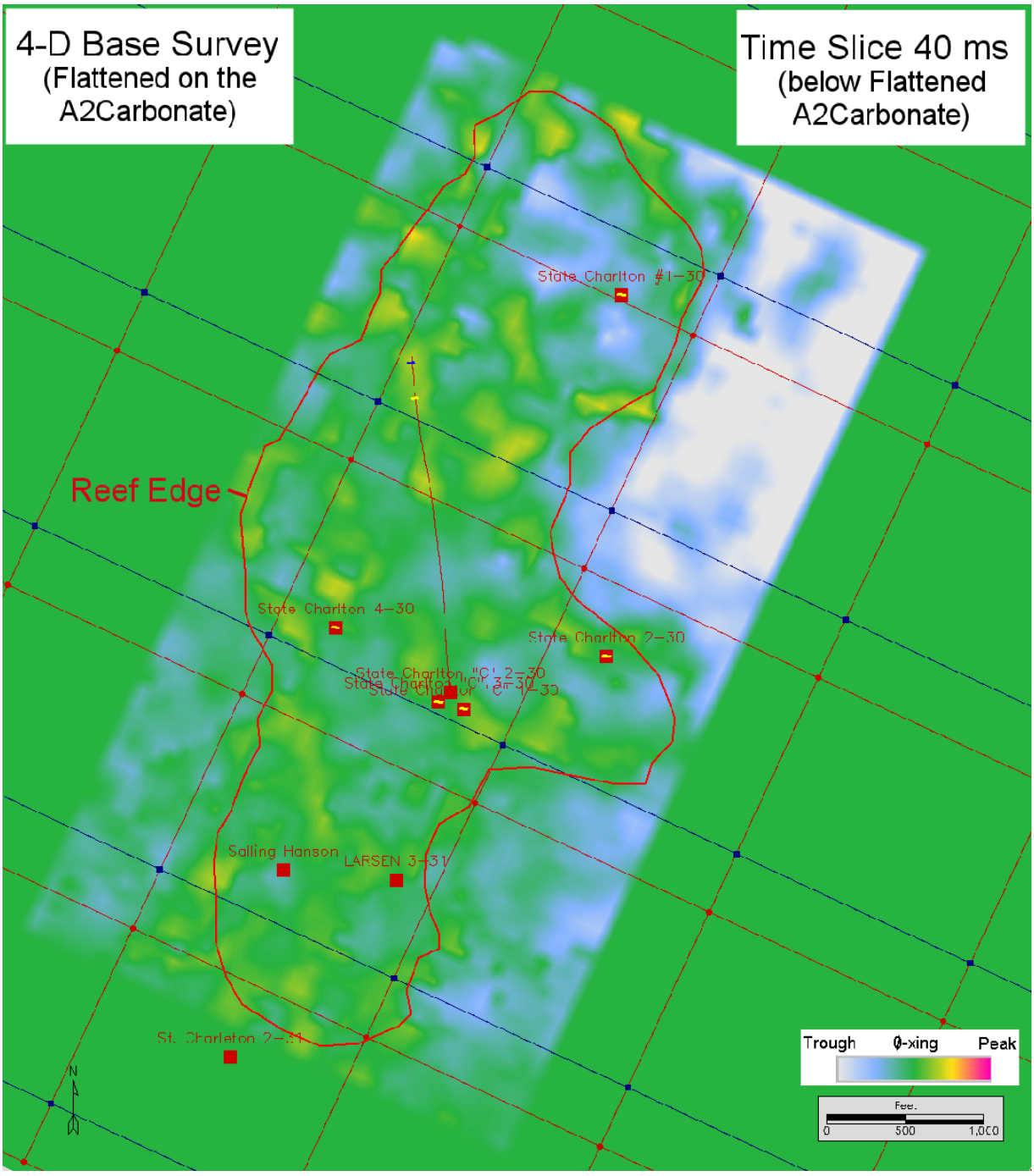
4-D Base Survey
(Flattened on the
A2Carbonate)
Time Slice 40 ms
(below Flattened
A2Carbonate)
State Charlton #1-30
Reef Edge
State Charlton 4-30
State Charlton 2-30
Salling Hanson
LARSEN 3-31
St. Charleton 2-31
N
Trough
0-xing
Peak
Feet
0
500
1,000

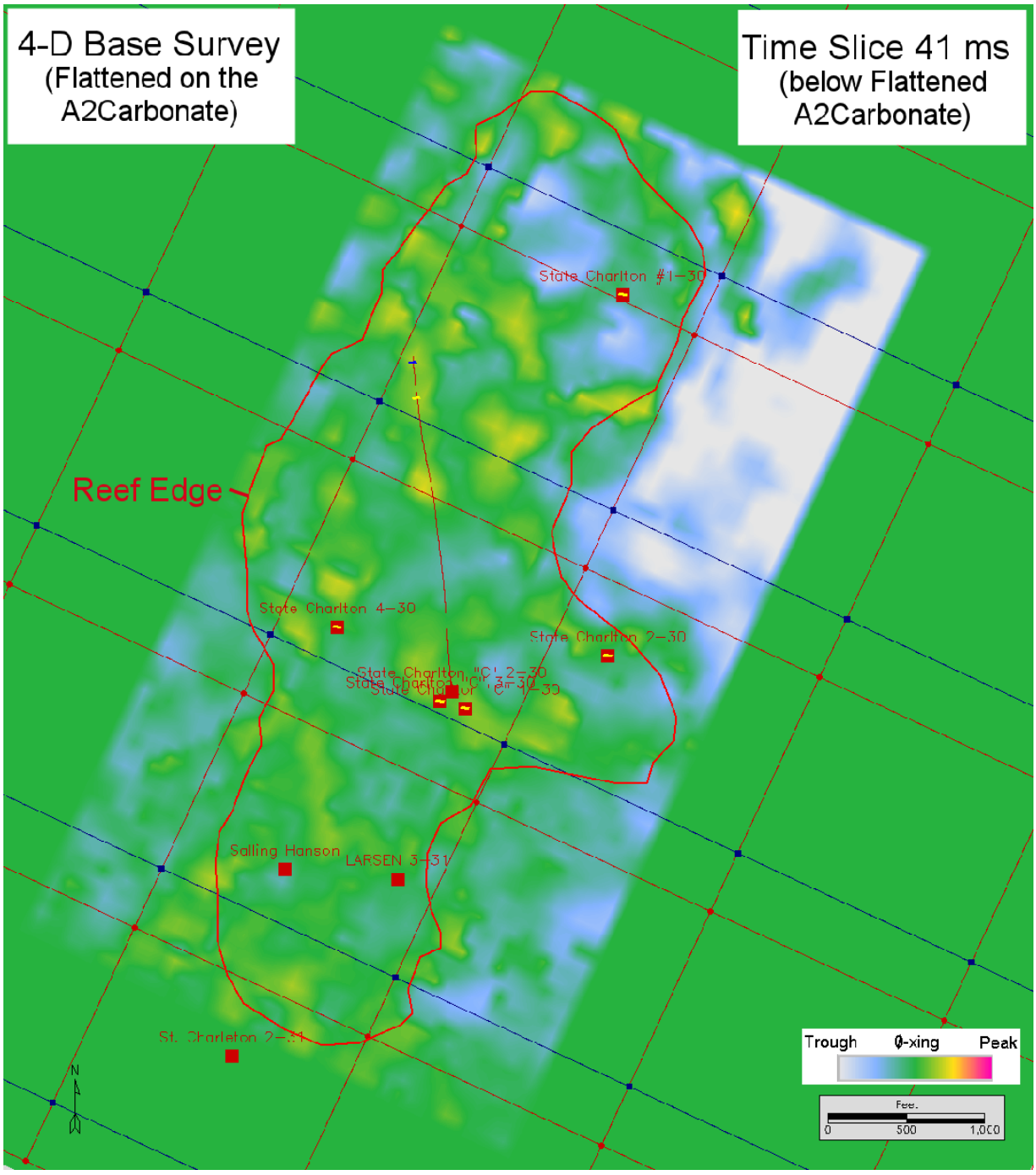
4-D Base Survey
(Flattened on the
A2Carbonate)
Time Slice 41 ms
(below Flattened
A2Carbonate)
State Charlton #1-30
Reef Edge
State Charlton 4-30
State Charlton 2-30
Salling Hanson
LARSEN 3-31
St. Charleton 2-31
N
Trough
0-xing
Peak
Feet
0
500
1,000

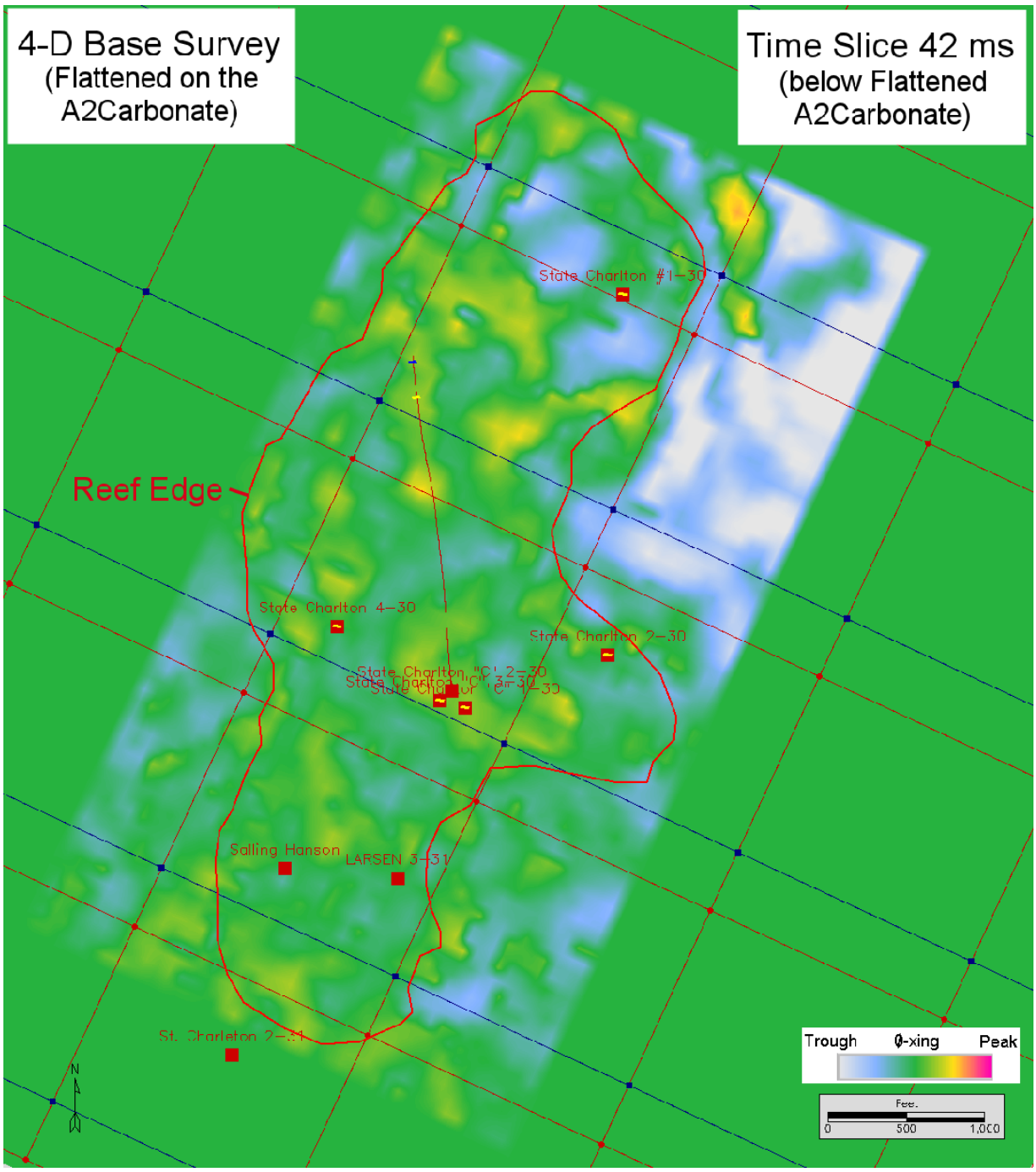
4-D Base Survey
(Flattened on the
A2Carbonate)
Time Slice 42 ms
(below Flattened
A2Carbonate)
State Charlton #1-30
Reef Edge
State Charlton 4-30
State Charlton 2-30
State Charlton "C" 2-30
Salling Hanson
LARSEN 3-31
St. Charleton 2-31
N
Trough
0-xing
Peak
Feet
0
500
1,000

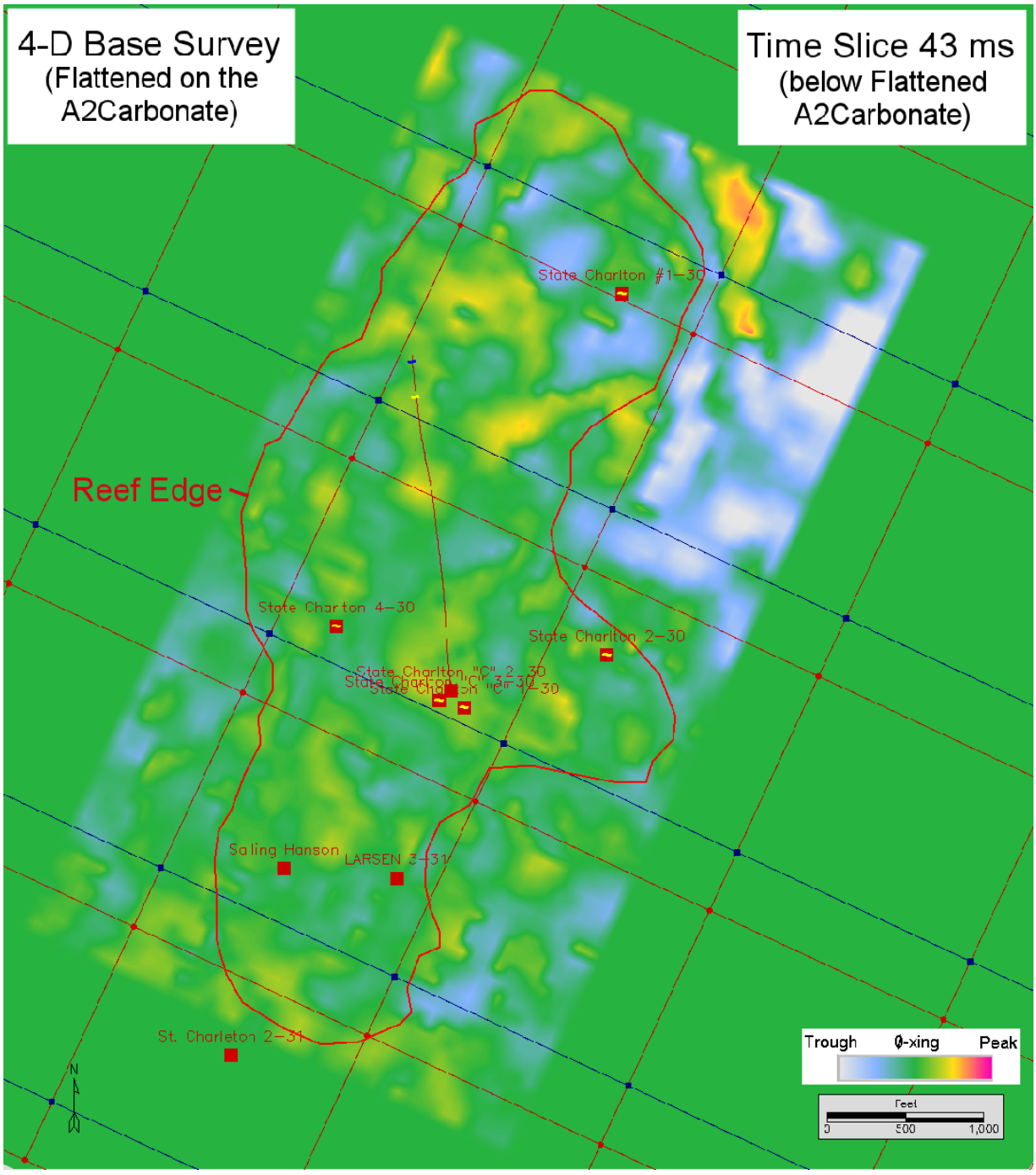
4-D Base Survey
(Flattened on the
A2Carbonate)
Time Slice 43 ms
(below Flattened
A2Carbonate)
State Charlton #1-30
Reef Edge
State Charlton 4-30
State Charlton 2-30
State Charlton "C" 2-30
Saling Hanson
LARSEN 3-31
St. Charleton 2-31
Trough
0-xing
Peak
Feet
0
500
1,000
N

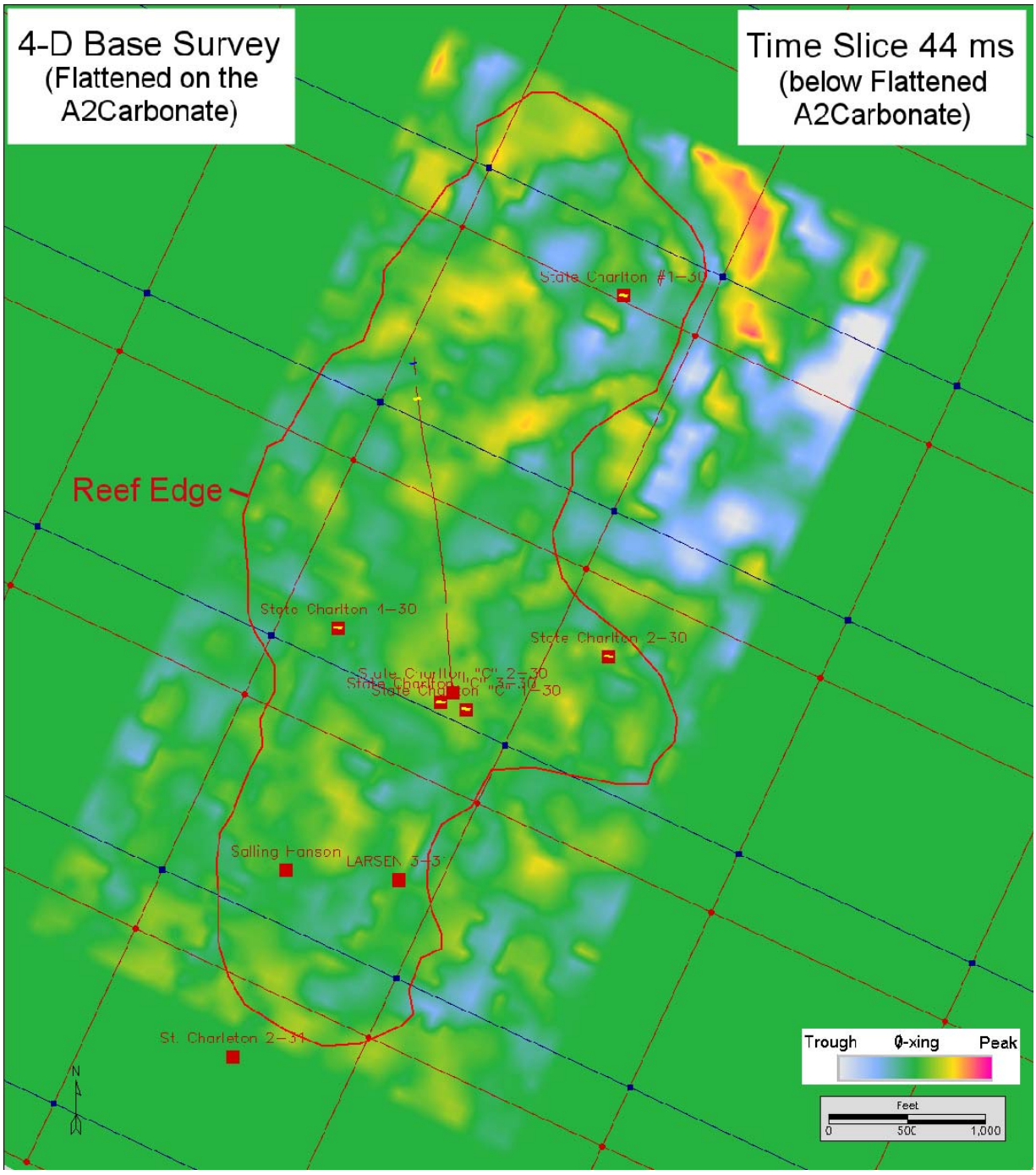
4-D Base Survey
(Flattened on the
A2Carbonate)
Time Slice 44 ms
(below Flattened
A2Carbonate)
Reef Edge
State Charlton #1-30
State Charlton 1-30
State Charlton 2-30
Salling Hanson
LARSEN 3-31
St. Charleton 2-31
Trough
0-xing
Peak
Feet
0
500
1,000
N

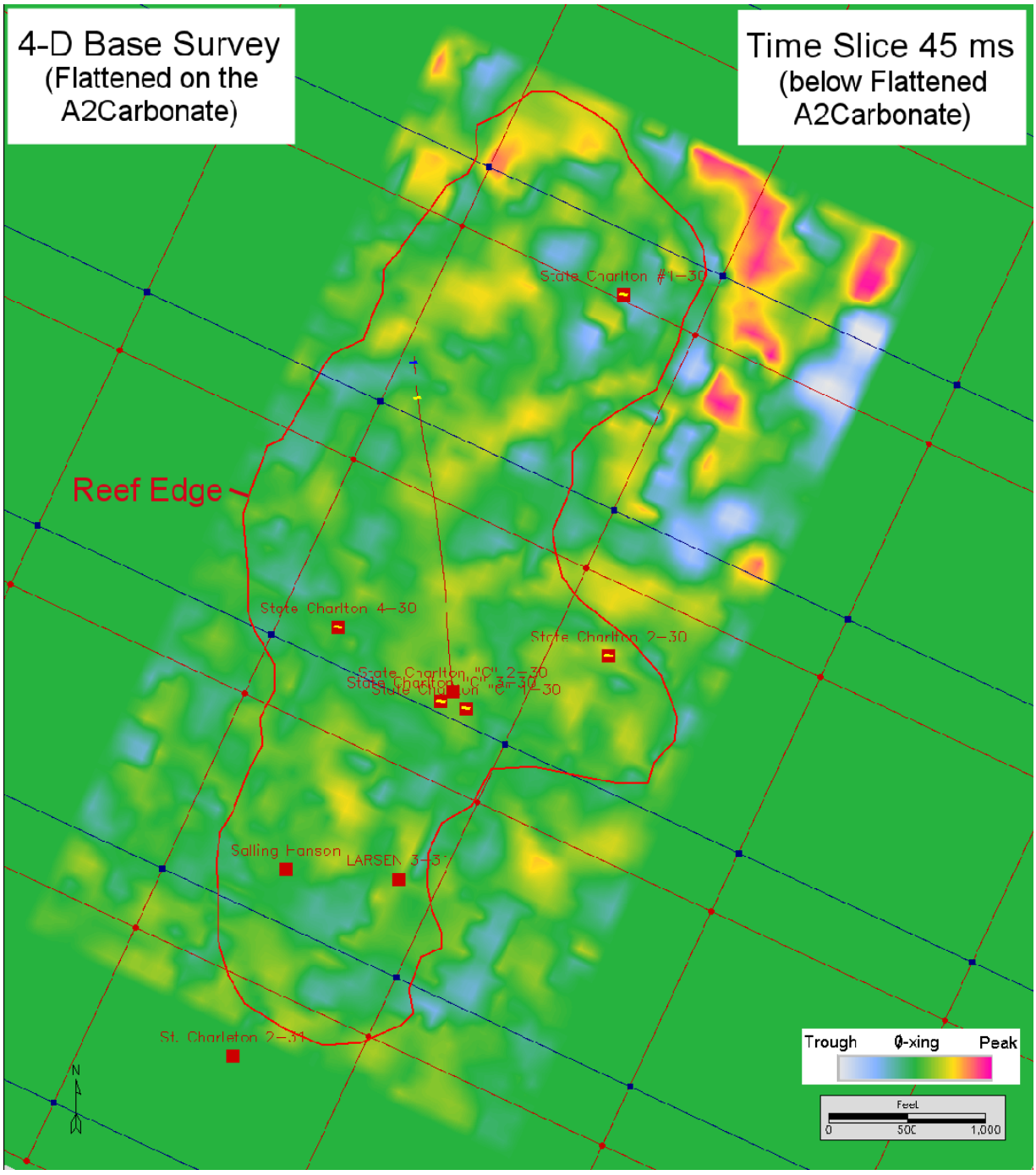
4-D Base Survey
(Flattened on the
A2Carbonate)
Time Slice 45 ms
(below Flattened
A2Carbonate)
State Charlton #1-30
Reef Edge
State Charlton 4-30
State Charlton 2-30
State Charlton "C" 2-30
State Charlton "C" 3-30
State Charlton "C" 4-30
Salling Hanson
LARSEN 3-31
St. Charleton 2-31
N
Trough
0-xing
Peak
Feet
0
500
1,000

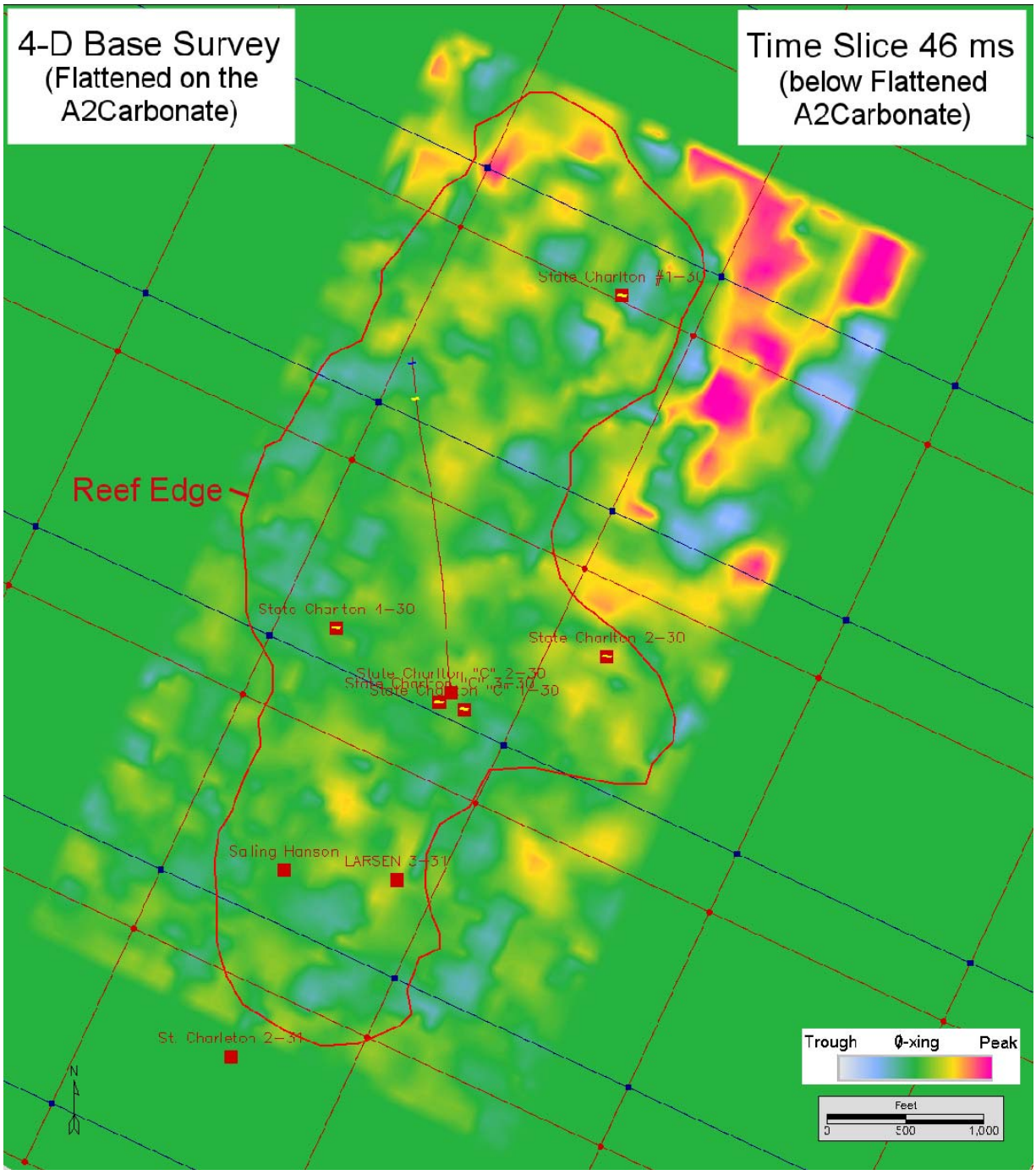
4-D Base Survey
(Flattened on the
A2Carbonate)
Time Slice 46 ms
(below Flattened
A2Carbonate)
State Charlton #1-30
Reef Edge
State Charton 1-30
State Charlton 2-30
Saling Hanson
LARSEN 3-31
St. Charleton 2-31
Trough
0-xing
Peak
Feet
0
500
1,000
N

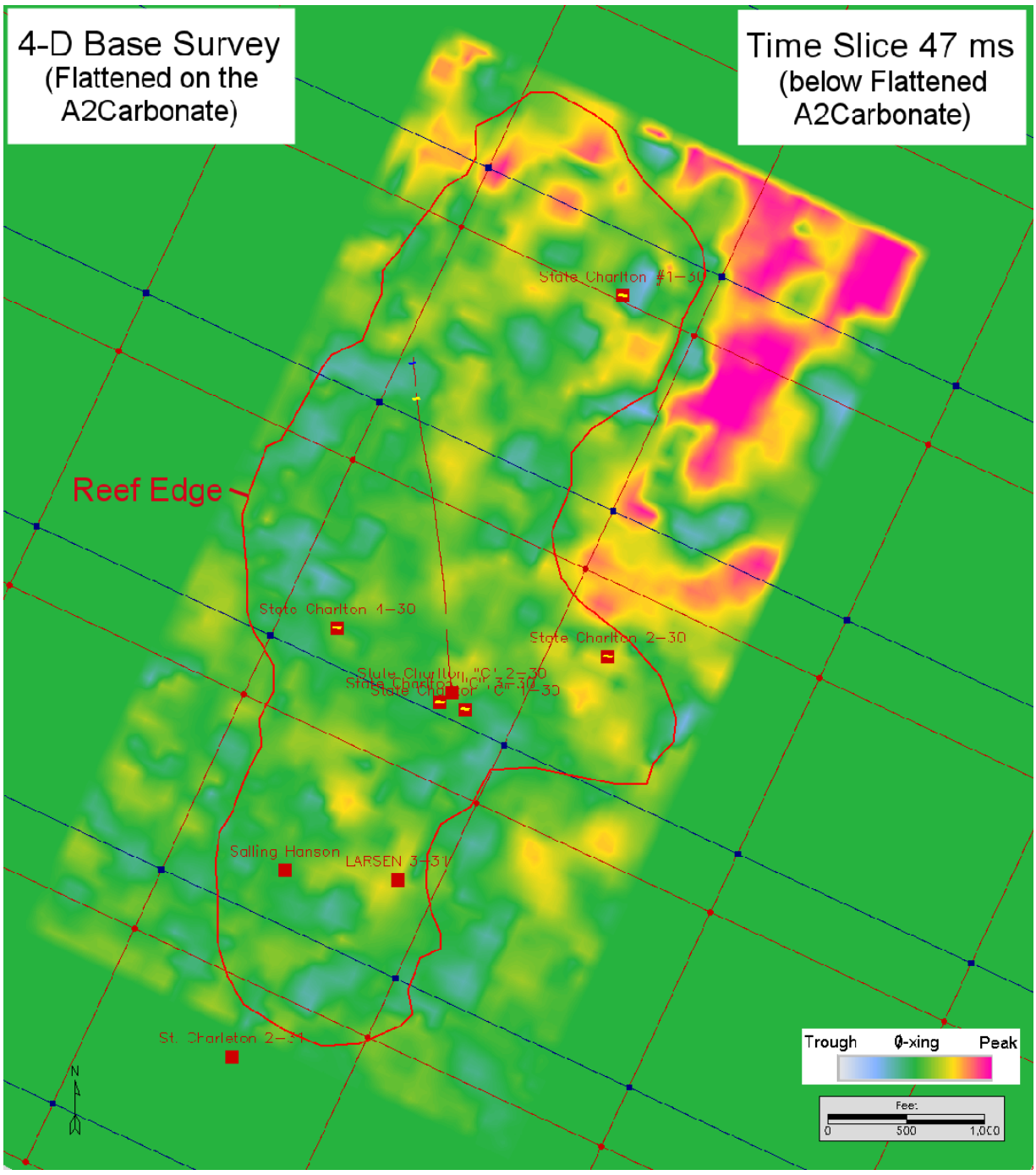
4-D Base Survey
(Flattened on the
A2Carbonate)
Time Slice 47 ms
(below Flattened
A2Carbonate)
State Charlton #1-30
Reef Edge
State Charlton 1-30
State Charlton 2-30
Salling Hanson
LARSEN 3-31
St. Charleton 2-31
N
Trough
0-xing
Peak
Feet
0
500
1,000

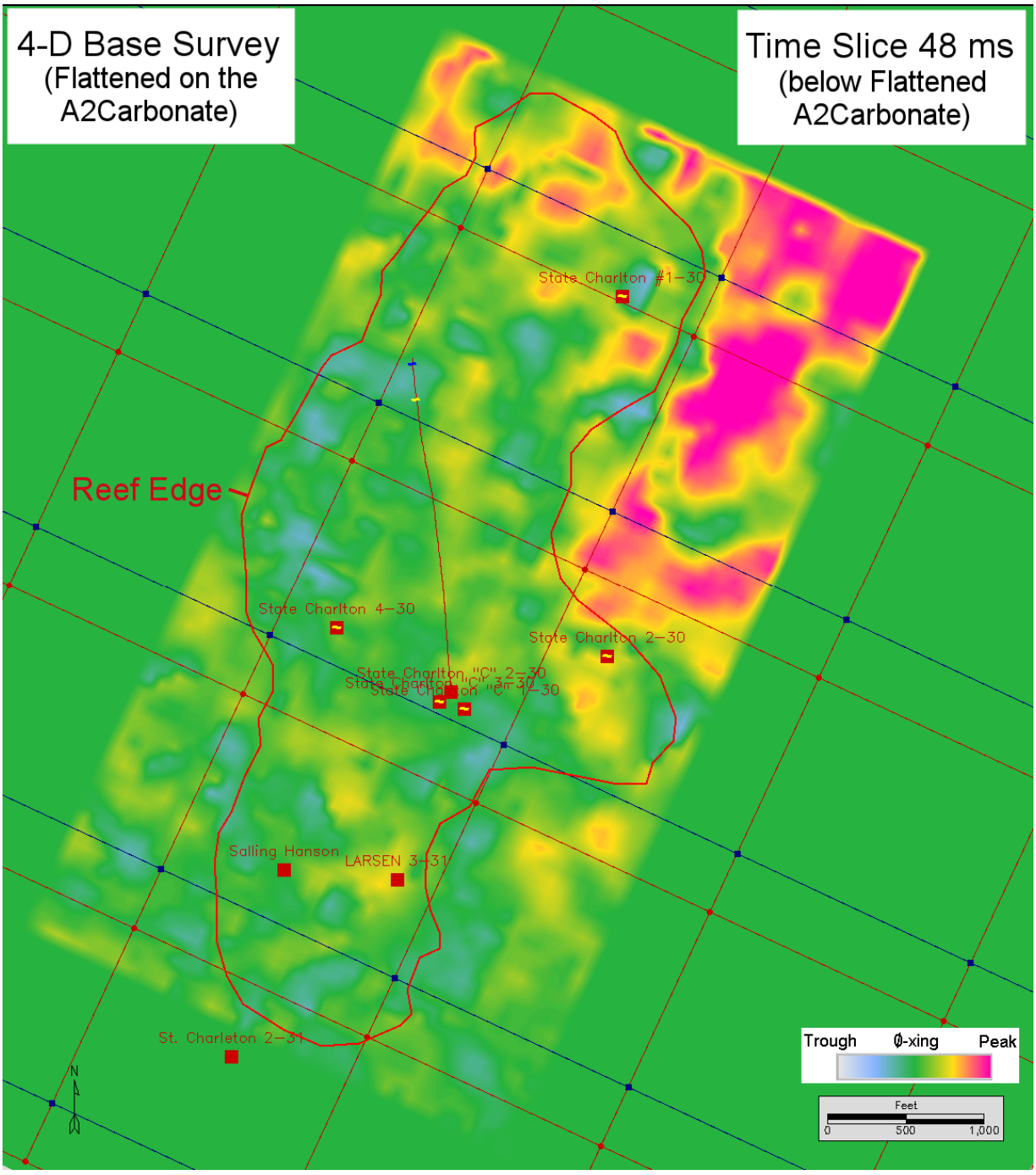
4-D Base Survey
(Flattened on the
A2Carbonate)
Time Slice 48 ms
(below Flattened
A2Carbonate)
State Charlton #1-30
Reef Edge
State Charlton 4-30
State Charlton 2-30
State Charlton "C" 2-30
Salling Hanson
LARSEN 3-31
St. Charleton 2-31
N
Trough
Ø-xing
Peak
Feet
0
500
1,000

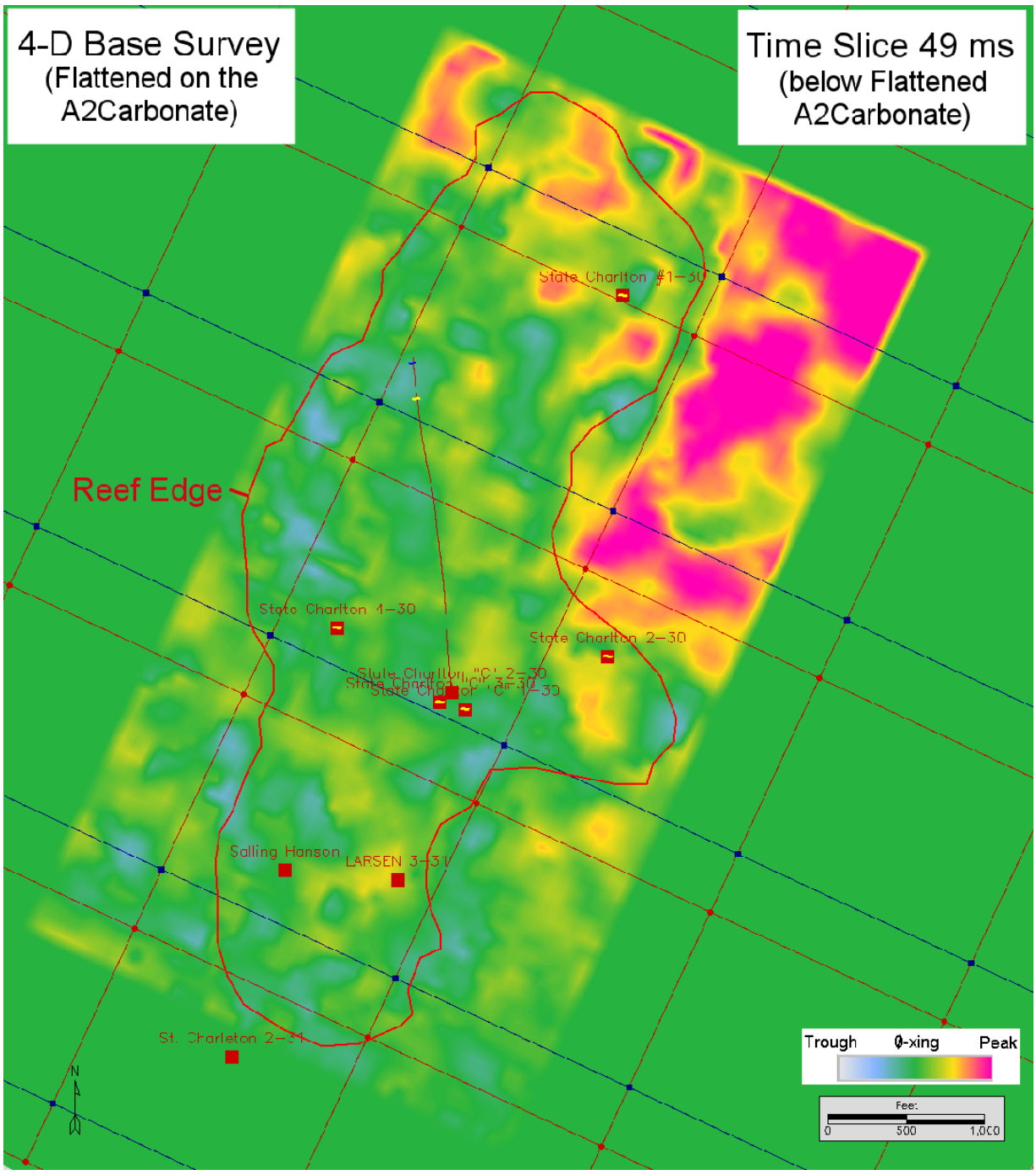
4-D Base Survey
(Flattened on the
A2Carbonate)
Time Slice 49 ms
(below Flattened
A2Carbonate)
State Charlton #1-30
Reef Edge
State Charlton 1-30
State Charlton 2-30
Salling Hanson
LARSEN 3-31
St. Charleton 2-31
N
Trough
0-xing
Peak
Fee:
0
500
1,000

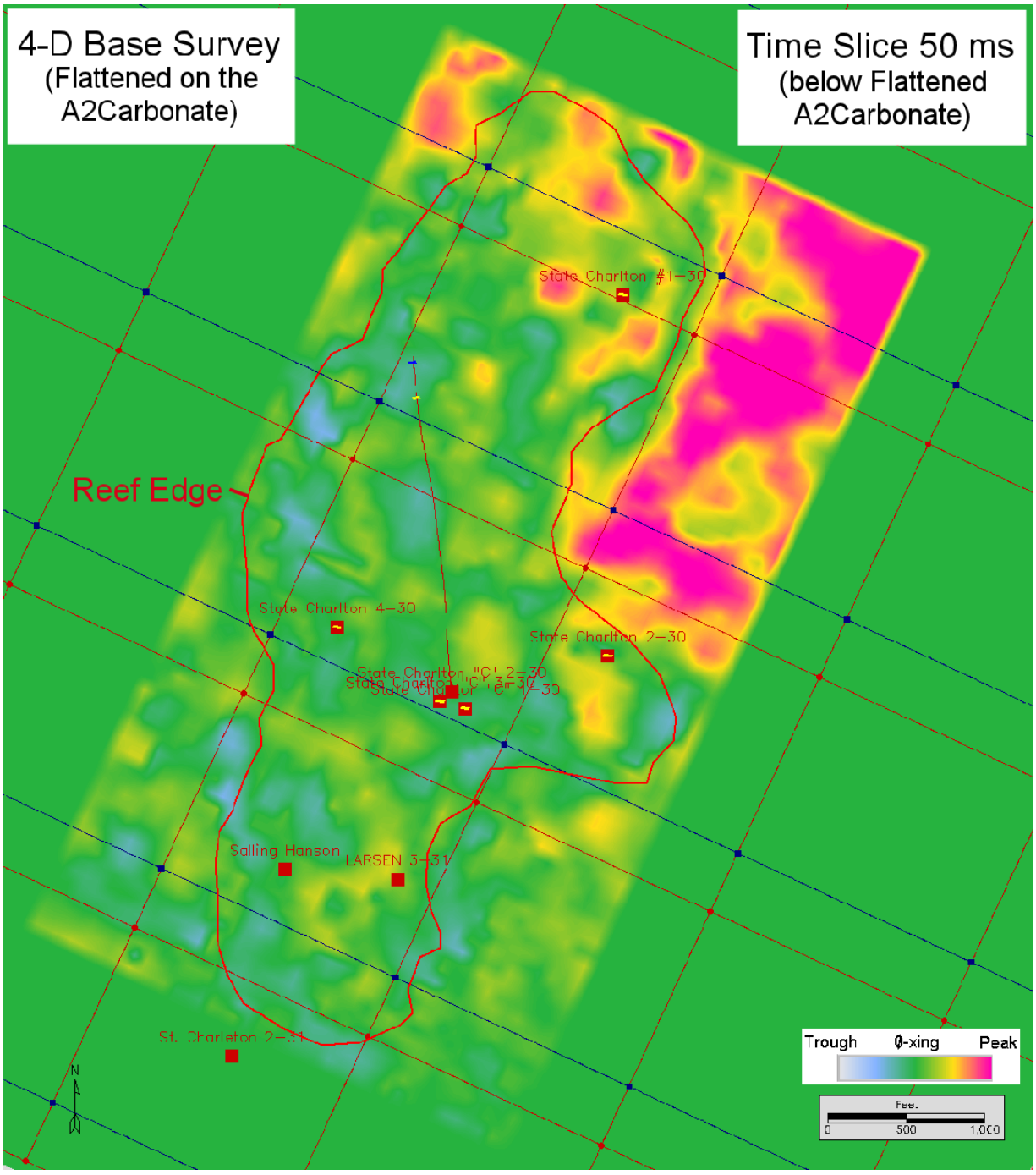
4-D Base Survey
(Flattened on the
A2Carbonate)
Time Slice 50 ms
(below Flattened
A2Carbonate)
State Charlton #1-30
Reef Edge
State Charlton 4-30
State Charlton 2-30
Salling Hanson
LARSEN 3-31
Trough
0-xing
Peak
Feet
0
500
1,000
N

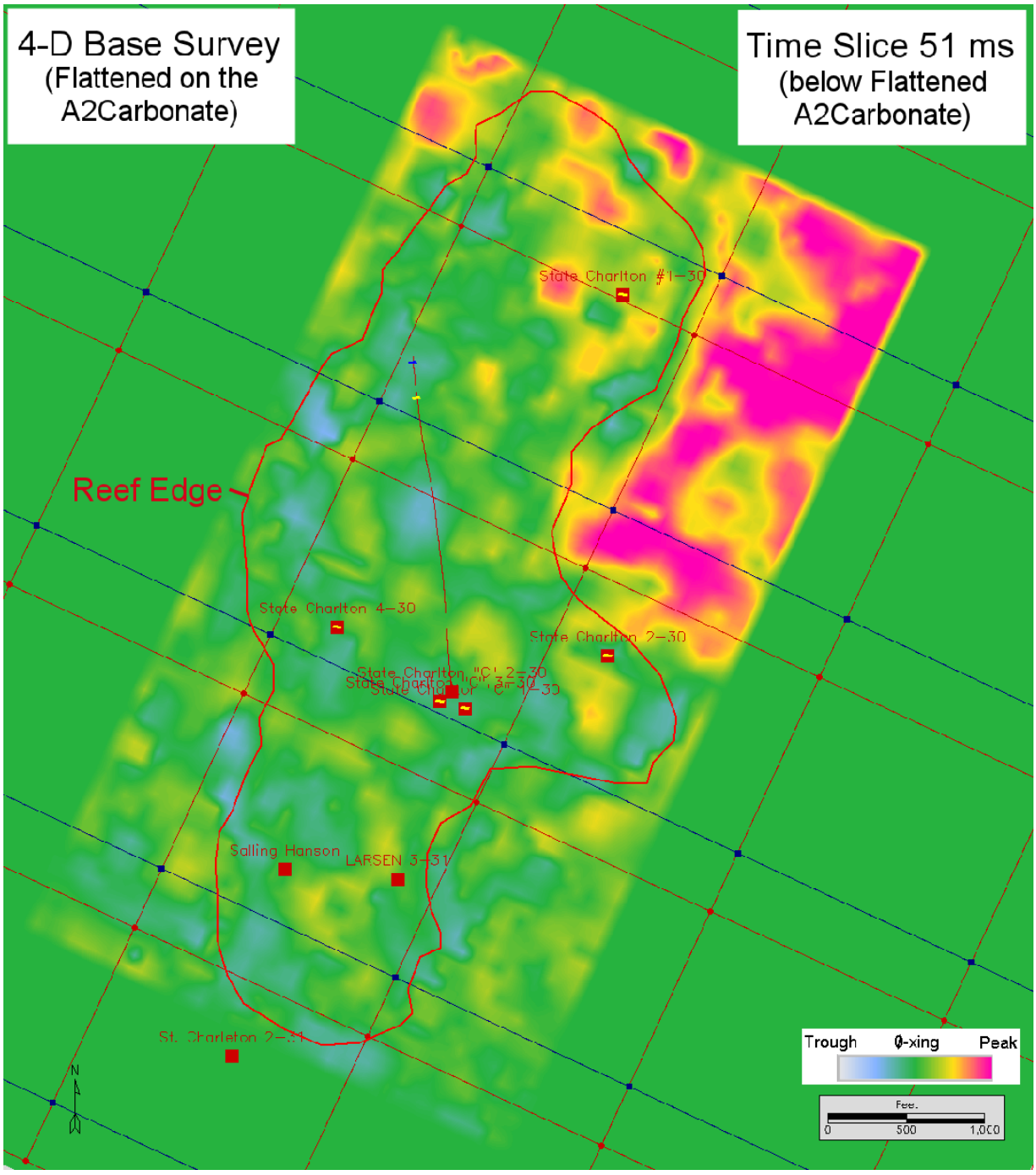
4-D Base Survey
(Flattened on the
A2Carbonate)
Time Slice 51 ms
(below Flattened
A2Carbonate)
State Charlton #1-30
Reef Edge
State Charlton 4-30
State Charlton 2-30
Salling Hanson
LARSEN 3-31
Trough
0-xing
Peak
Feet
0
500
1,000
N

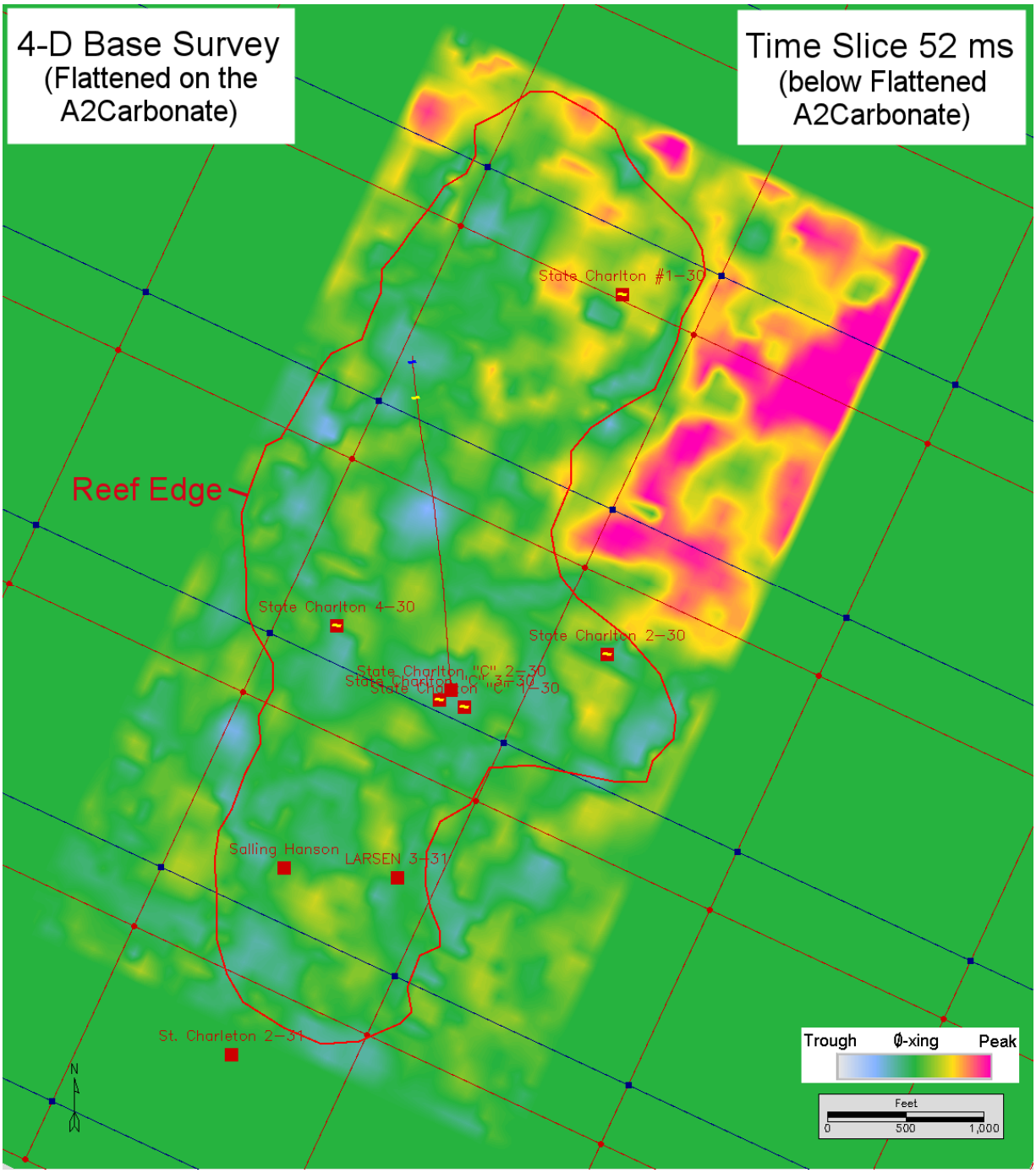
4-D Base Survey
(Flattened on the
A2Carbonate)
Time Slice 52 ms
(below Flattened
A2Carbonate)
State Charlton #1-30
Reef Edge
State Charlton 4-30
State Charlton 2-30
State Charlton "C" 2-30
State Charlton "C" 3-30
State Charlton "C" 1-30
Salling Hanson
LARSEN 3-31
St. Charleton 2-31
N
Trough
Ø-xing
Peak
Feet
0
500
1,000

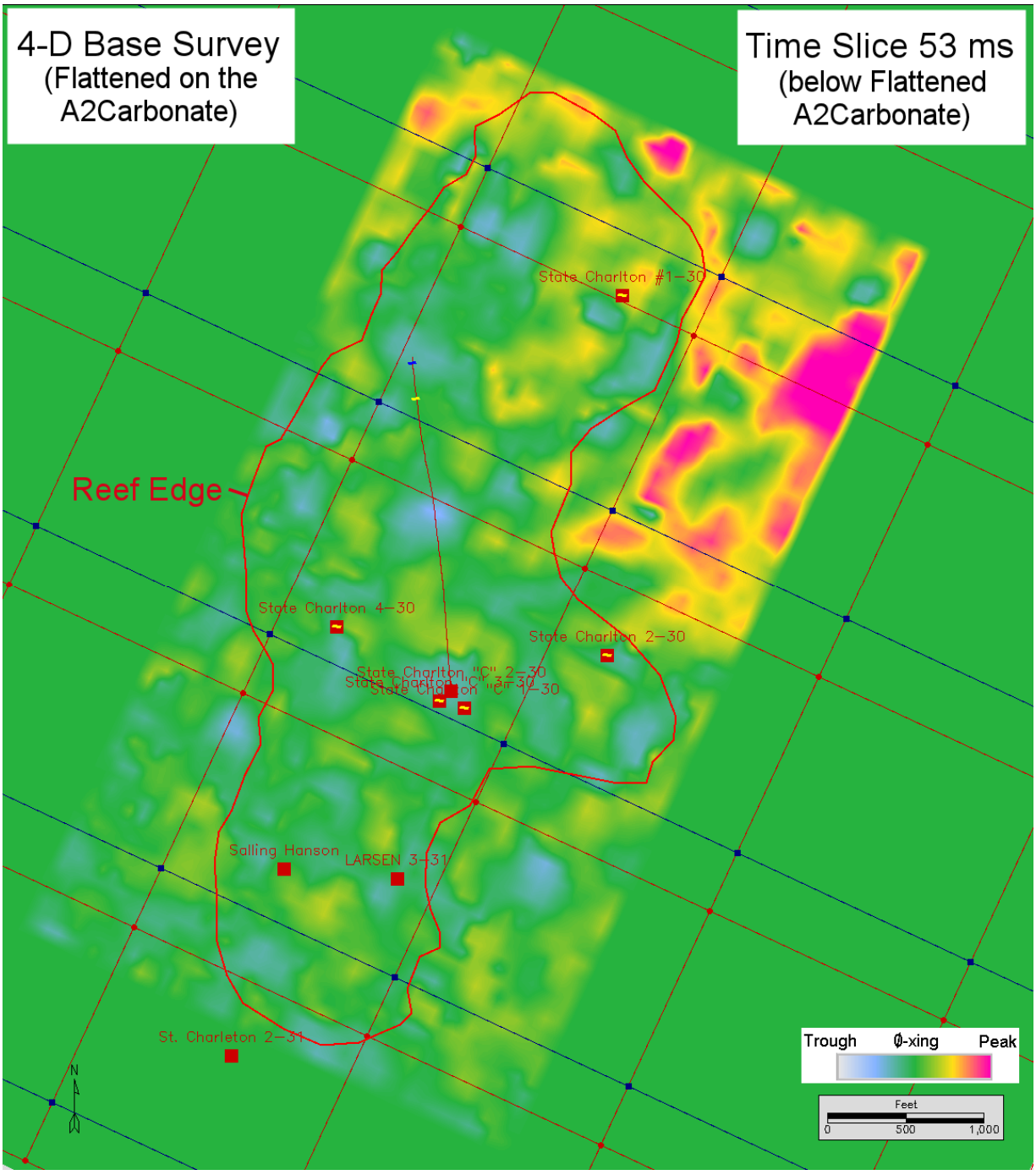
4-D Base Survey
(Flattened on the
A2Carbonate)
Time Slice 53 ms
(below Flattened
A2Carbonate)
State Charlton #1-30
Reef Edge
State Charlton 4-30
State Charlton 2-30
State Charlton "C" 2-30
State Charlton "C" 3-30
State Charlton "C" 1-30
Salling Hanson
LARSEN 3-31
St. Charleton 2-31
N
Trough
Ø-xing
Peak
Feet
0
500
1,000

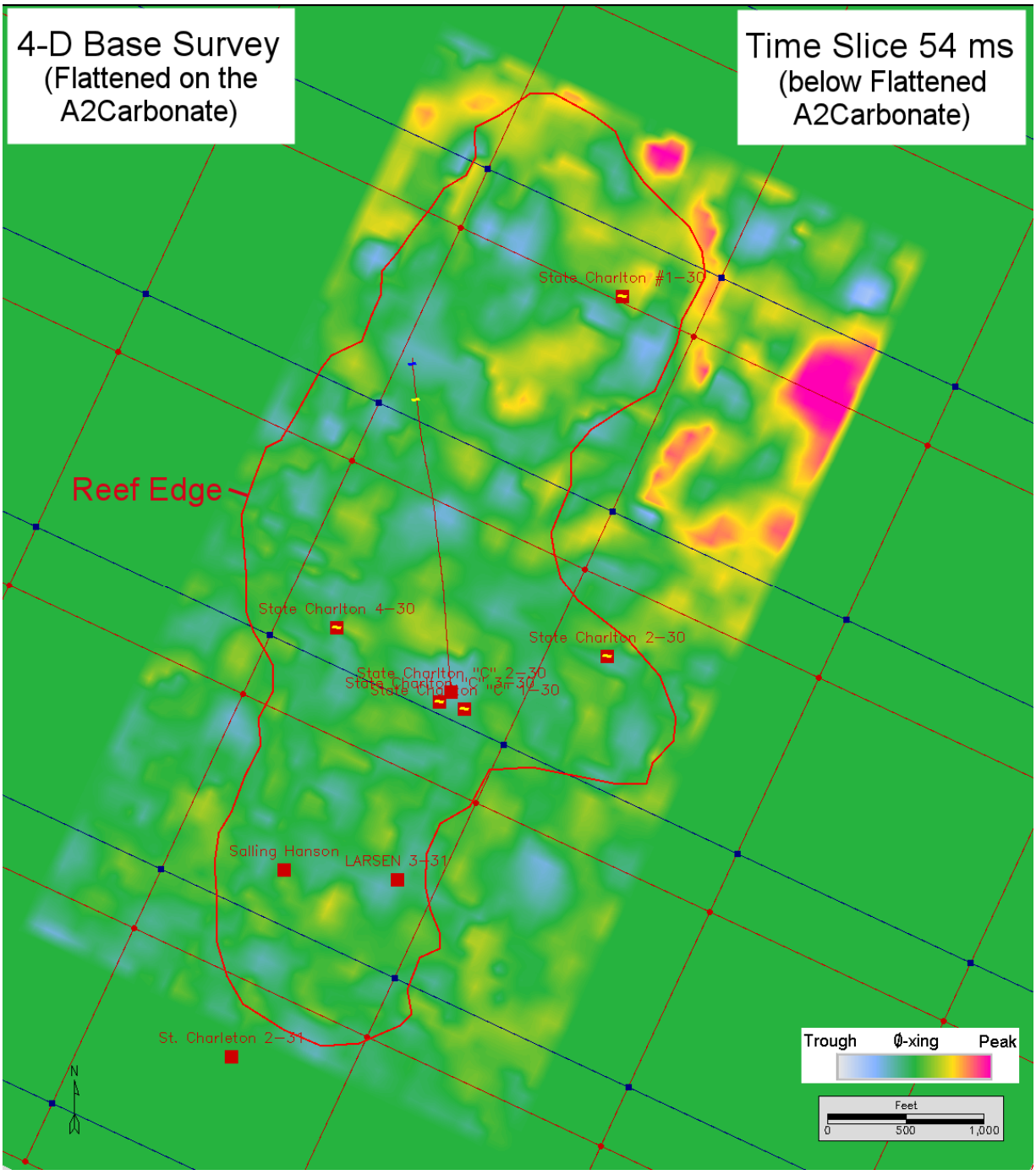
4-D Base Survey
(Flattened on the
A2Carbonate)
Time Slice 54 ms
(below Flattened
A2Carbonate)
State Charlton #1-30
Reef Edge
State Charlton 4-30
State Charlton 2-30
Salling Hanson
LARSEN 3-31
St. Charleton 2-31
Trough
Ø-xing
Peak
Feet
0
500
1,000
N

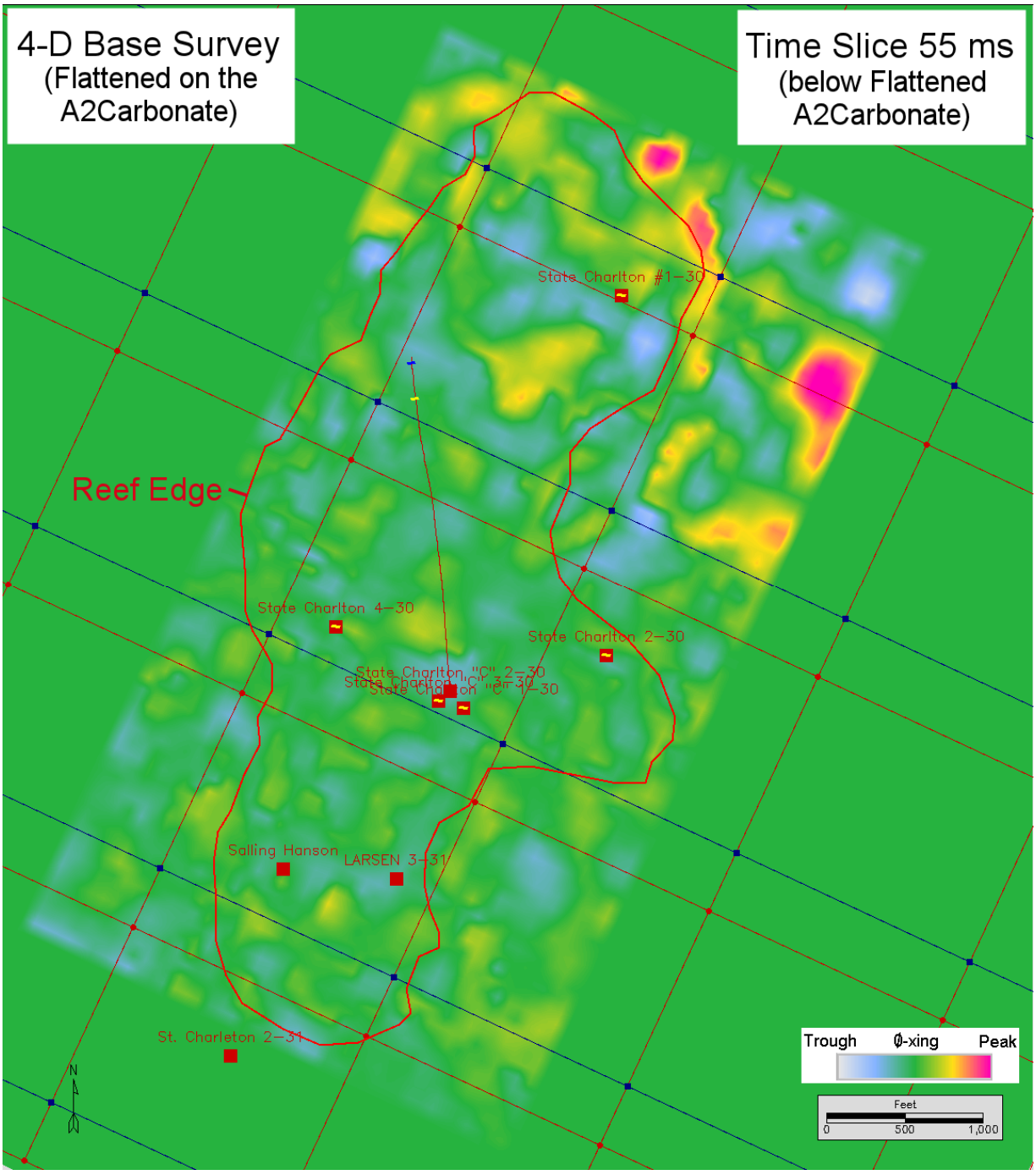
4-D Base Survey
(Flattened on the
A2Carbonate)
Time Slice 55 ms
(below Flattened
A2Carbonate)
State Charlton #1-30
Reef Edge
State Charlton 4-30
State Charlton 2-30
State Charlton "C" 2-30
Salling Hanson
LARSEN 3-31
St. Charleton 2-31
N
Trough
Ø-xing
Peak
Feet
0
500
1,000

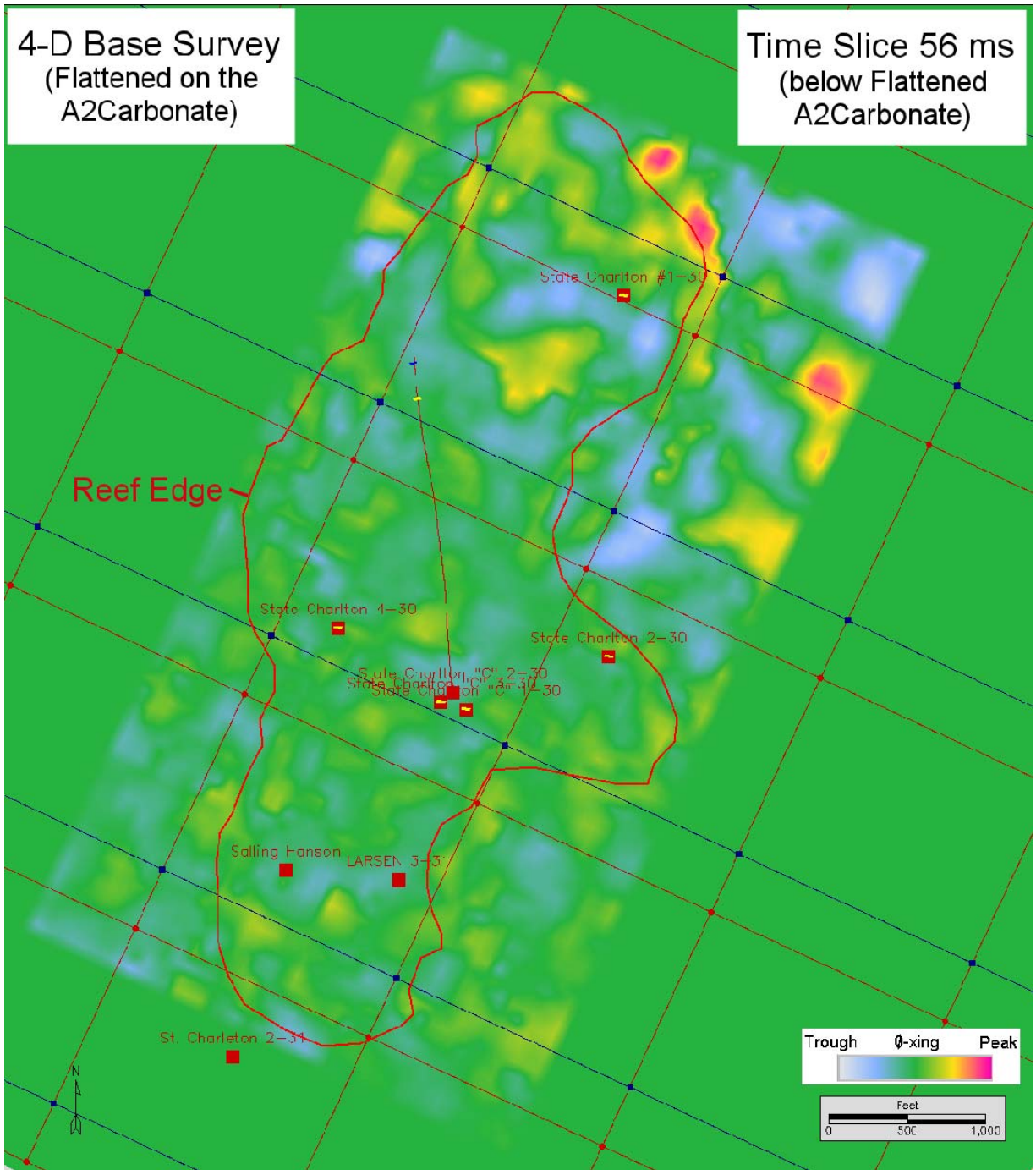
4-D Base Survey
(Flattened on the
A2Carbonate)
Time Slice 56 ms
(below Flattened
A2Carbonate)
State Charlton #1-30
Reef Edge
State Charlton 1-30
State Charlton 2-30
Salling Hanson
LARSEN 3-31
St. Charleton 2-31
N
Trough
0-xing
Peak
Feet
0
500
1,000

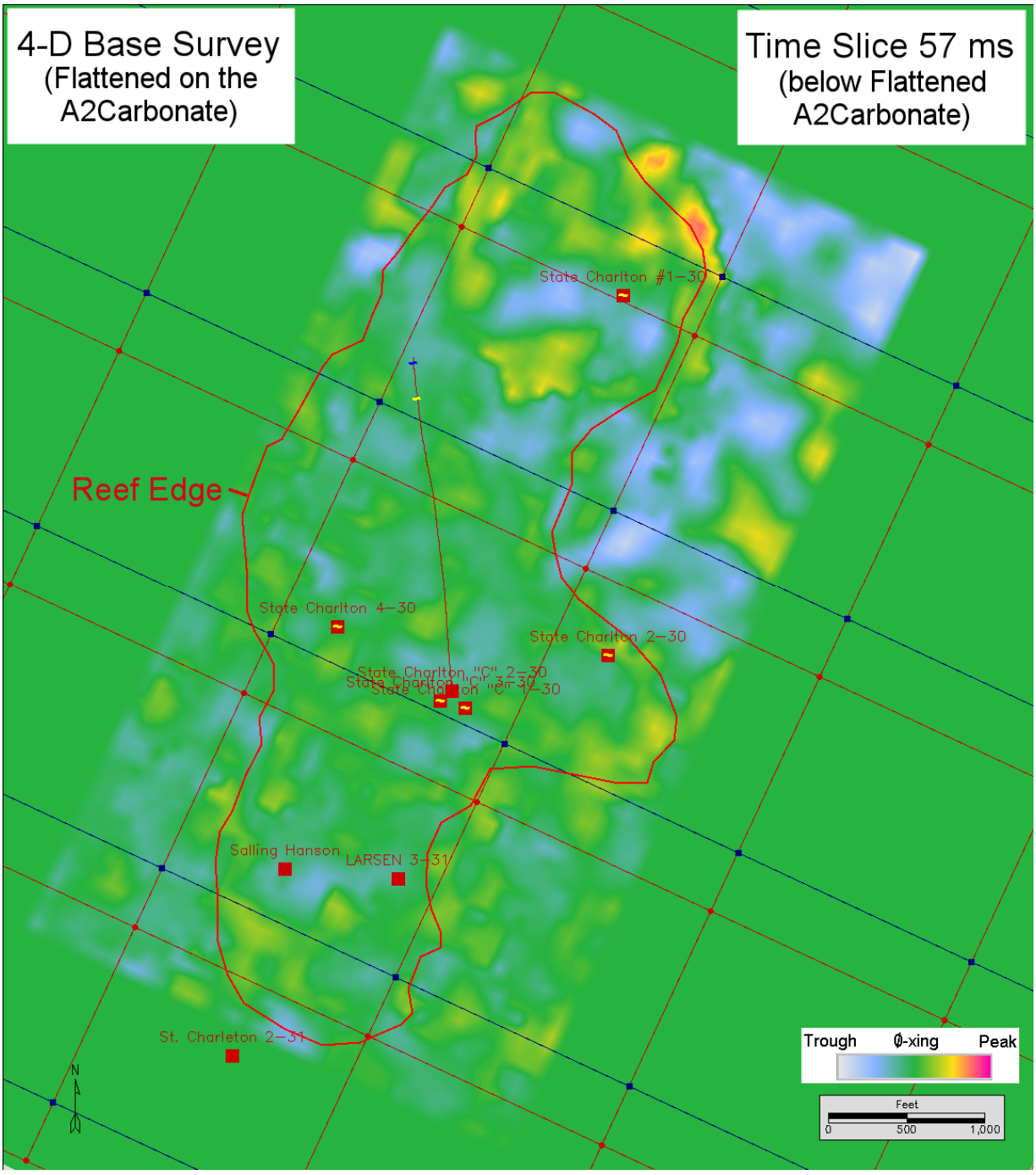
4-D Base Survey
(Flattened on the
A2Carbonate)
Time Slice 57 ms
(below Flattened
A2Carbonate)
State Charlton #1-30
Reef Edge
State Charlton 4-30
State Charlton 2-30
State Charlton "C" 2-30
Salling Hanson
LARSEN 3-31
St. Charleton 2-31
N
Trough
Ø-xing
Peak
Feet
0
500
1,000

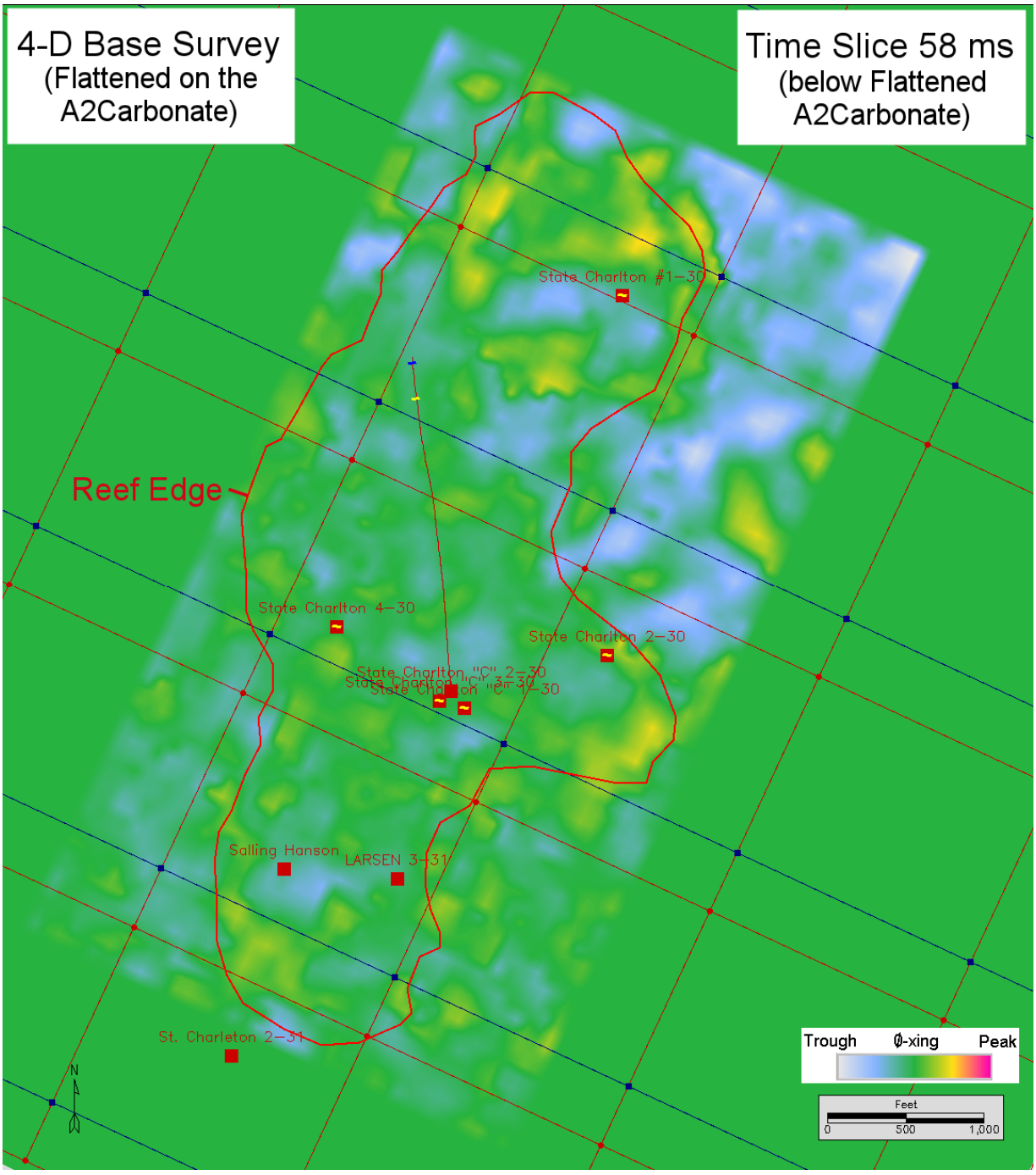
4-D Base Survey
(Flattened on the
A2Carbonate)
Time Slice 58 ms
(below Flattened
A2Carbonate)
State Charlton #1-30
Reef Edge
State Charlton 4-30
State Charlton 2-30
State Charlton "C" 2-30
State Charlton "C" 3-30
State Charlton "C" 1-30
Salling Hanson
LARSEN 3-31
St. Charleton 2-31
N
Trough
Ø-xing
Peak
Feet
0
500
1,000

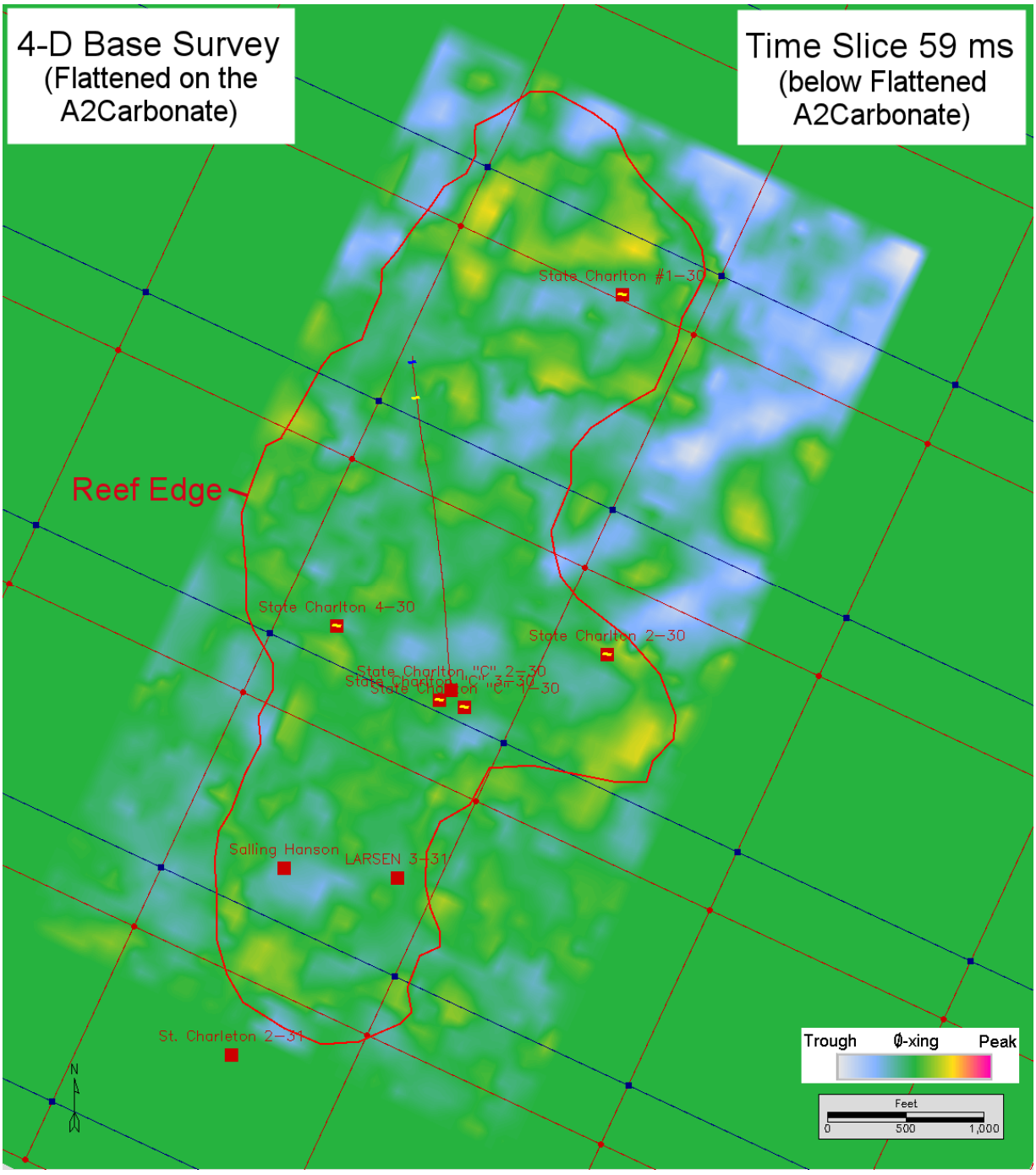
4-D Base Survey
(Flattened on the
A2Carbonate)
Time Slice 59 ms
(below Flattened
A2Carbonate)
State Charlton #1-30
Reef Edge
State Charlton 4-30
State Charlton 2-30
State Charlton "C" 2-30
Salling Hanson
LARSEN 3-31
St. Charleton 2-31
N
Trough
Ø-xing
Peak
Feet
0
500
1,000

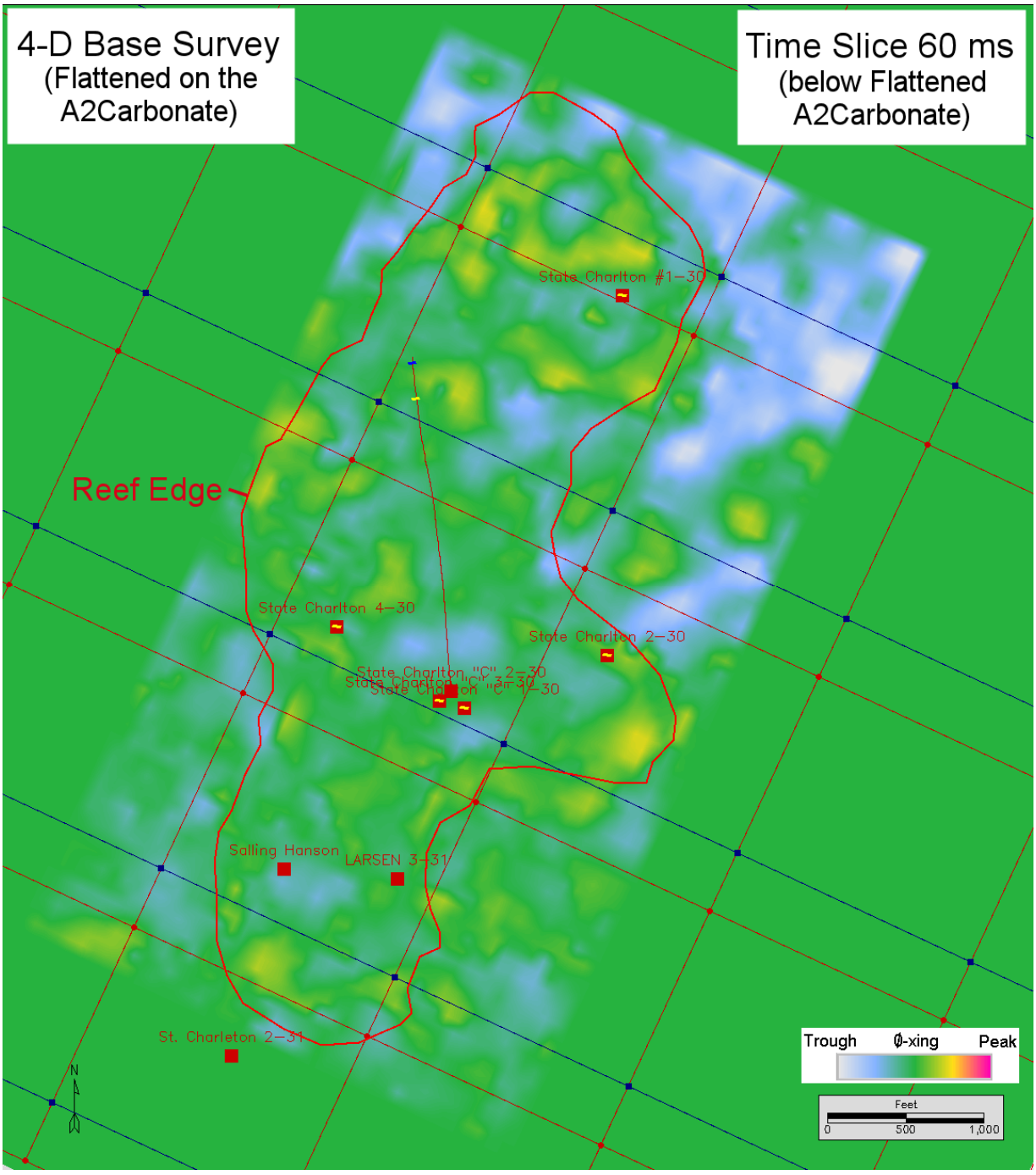
4-D Base Survey
(Flattened on the
A2Carbonate)
Time Slice 60 ms
(below Flattened
A2Carbonate)
State Charlton #1-30
Reef Edge
State Charlton 4-30
State Charlton 2-30
State Charlton "C" 2-30
State Charlton "C" 3-30
State Charlton "C" 1-30
Salling Hanson
LARSEN 3-31
St. Charleton 2-31
N
Trough
Ø-xing
Peak
Feet
0
500
1,000

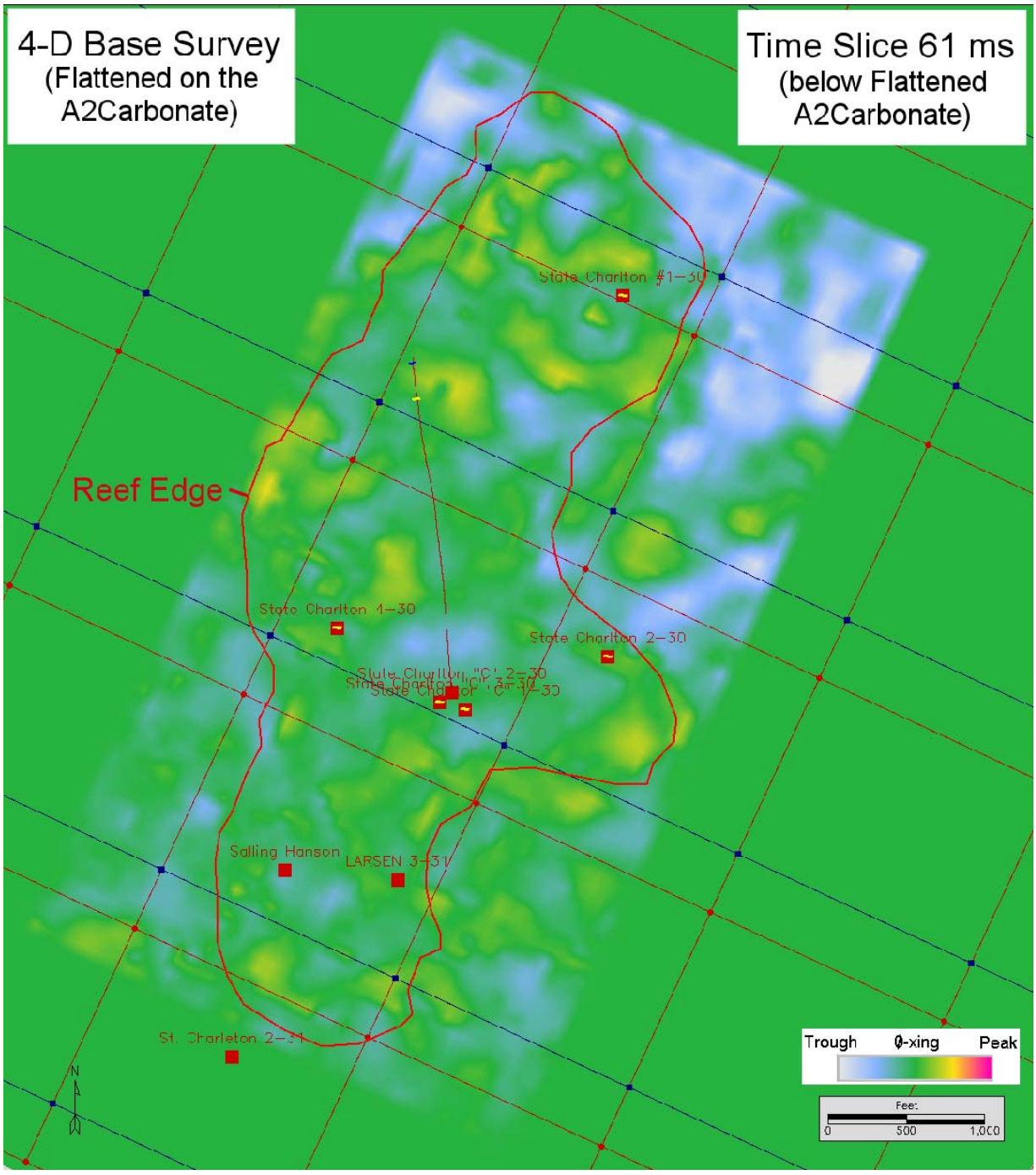
4-D Base Survey
(Flattened on the
A2Carbonate)
Time Slice 61 ms
(below Flattened
A2Carbonate)
State Charlton #1-30
Reef Edge
State Charlton 1-30
State Charlton 2-30
Salling Hanson
LARSEN 3-31
St. Charleton 2-31
Trough
0-xing
Peak
Fee:
0
500
1,000
N

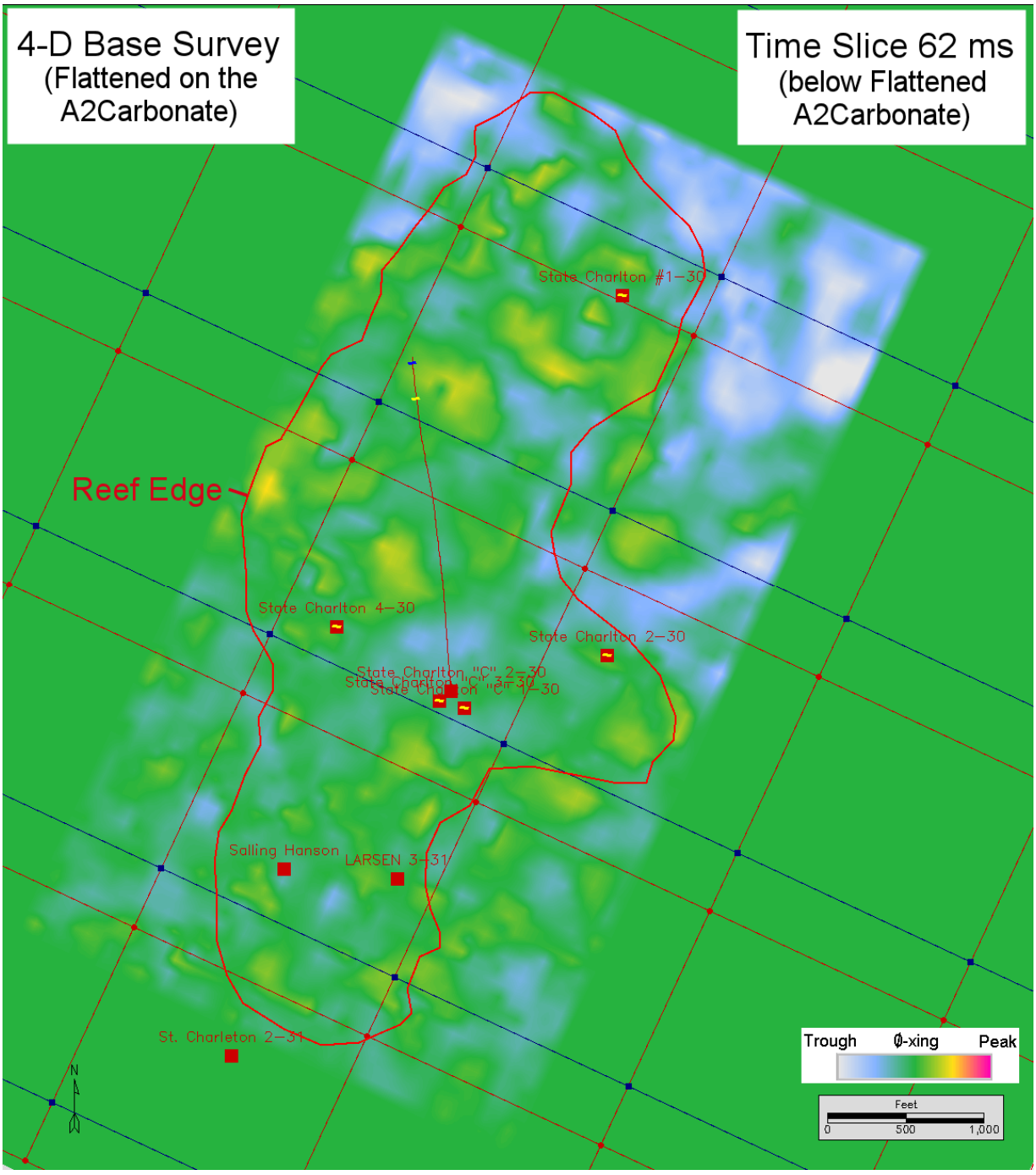
4-D Base Survey
(Flattened on the
A2Carbonate)
Time Slice 62 ms
(below Flattened
A2Carbonate)
State Charlton #1-30
Reef Edge
State Charlton 4-30
State Charlton 2-30
State Charlton "C" 2-30
Salling Hanson
LARSEN 3-31
St. Charleton 2-31
N
Trough
Ø-xing
Peak
Feet
0
500
1,000

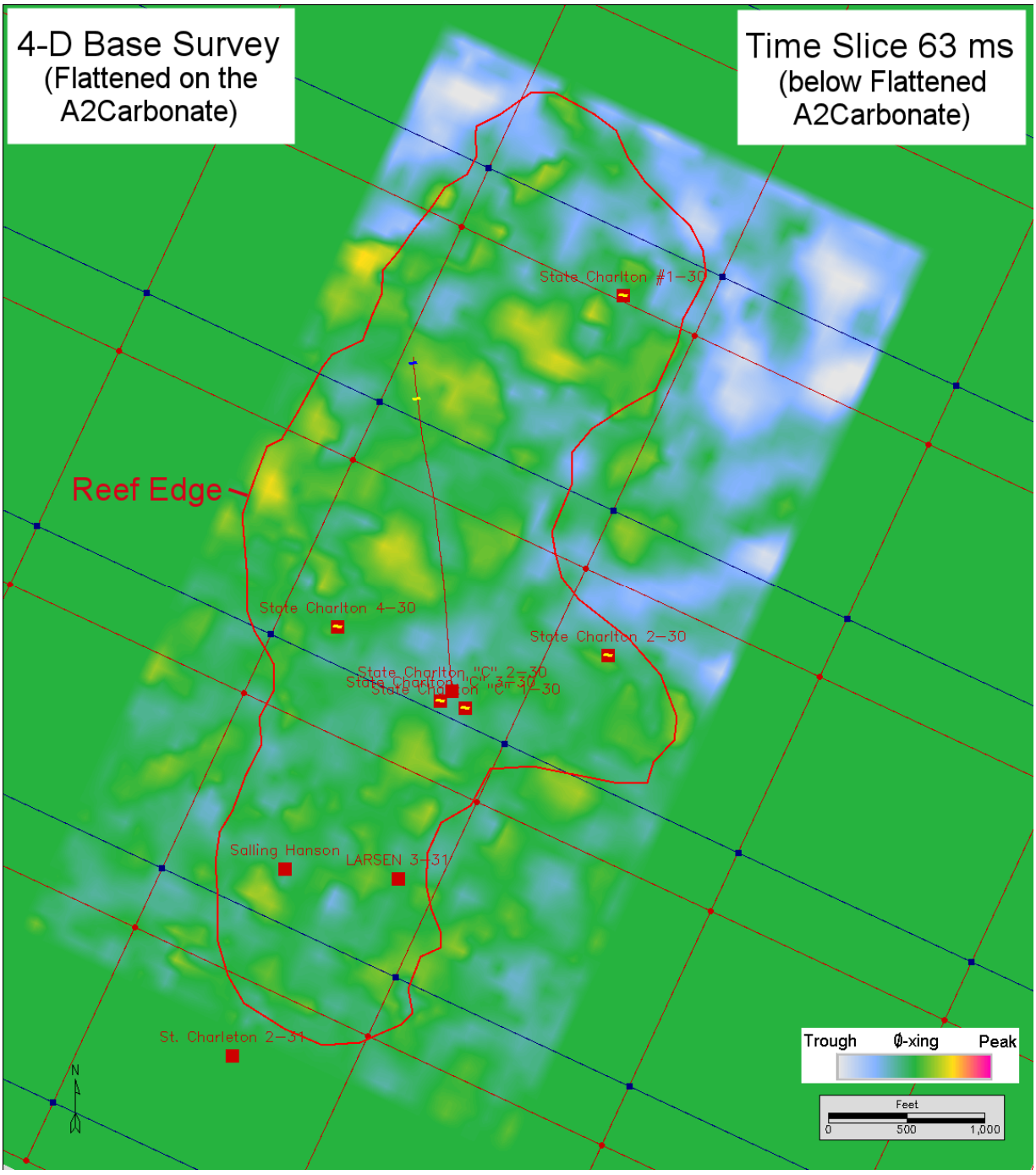
4-D Base Survey
(Flattened on the
A2Carbonate)
Time Slice 63 ms
(below Flattened
A2Carbonate)
State Charlton #1-30
Reef Edge
State Charlton 4-30
State Charlton 2-30
State Charlton "C" 2-30
Salling Hanson
LARSEN 3-31
St. Charleton 2-31
N
Trough
Ø-xing
Peak
Feet
0
500
1,000

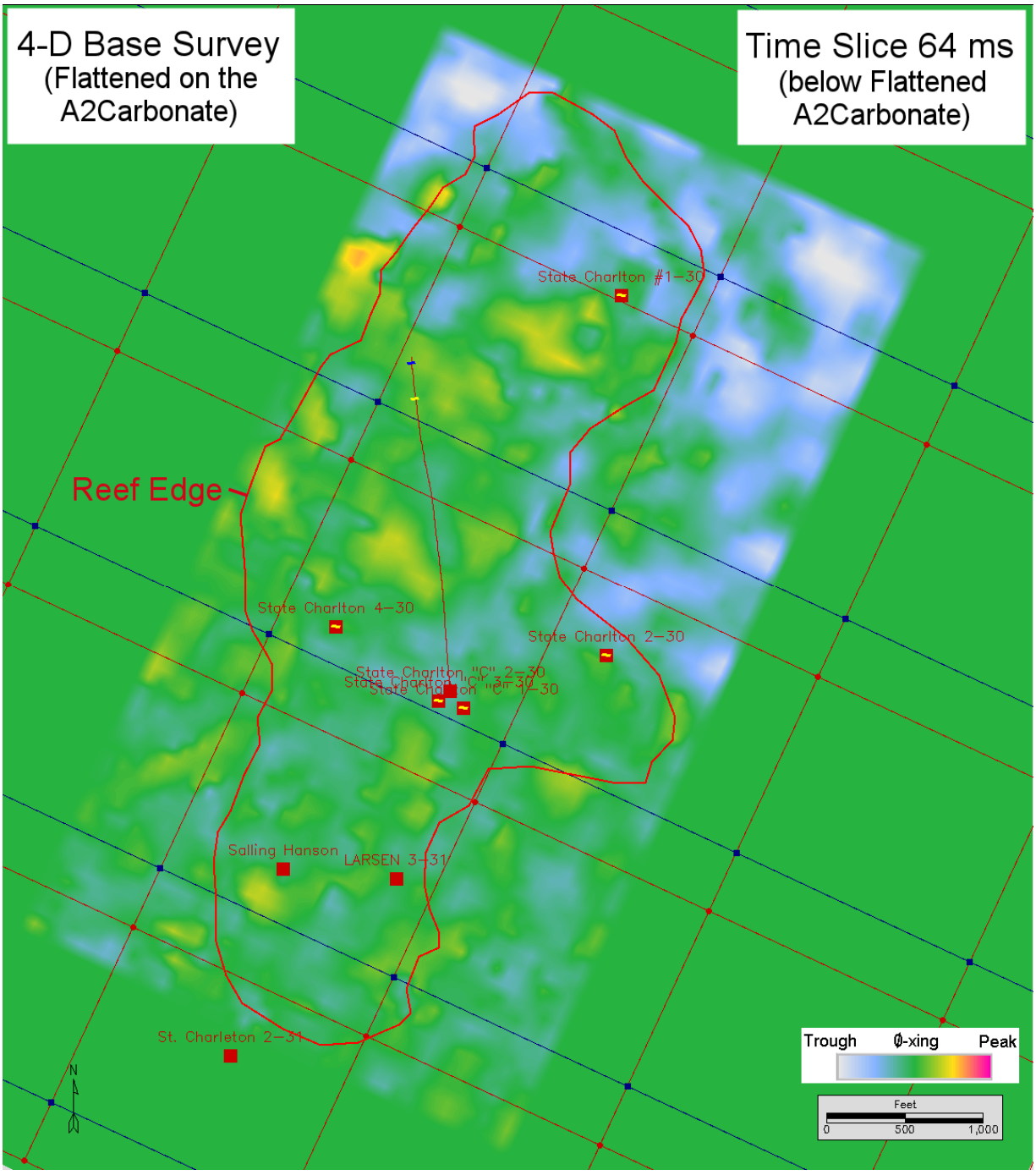
4-D Base Survey
(Flattened on the
A2Carbonate)
Time Slice 64 ms
(below Flattened
A2Carbonate)
State Charlton #1-30
Reef Edge
State Charlton 4-30
State Charlton 2-30
State Charlton "C" 2-30
Salling Hanson
LARSEN 3-31
St. Charleton 2-31
N
Trough
Ø-xing
Peak
Feet
0
500
1,000

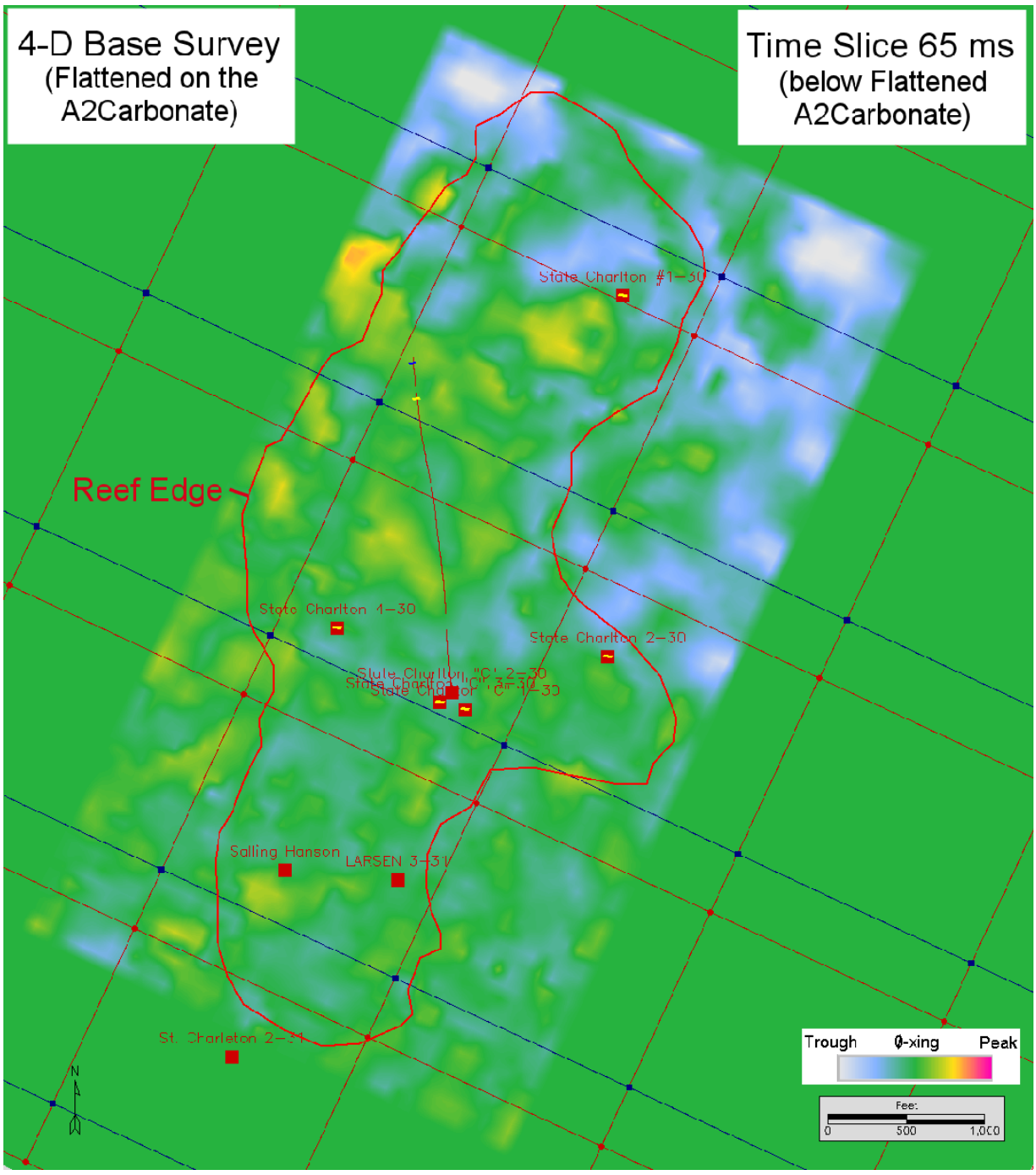
4-D Base Survey
(Flattened on the
A2Carbonate)
Time Slice 65 ms
(below Flattened
A2Carbonate)
State Charlton #1-30
Reef Edge
State Charlton 1-30
State Charlton 2-30
Salling Hanson
LARSEN 3-31
St. Charleton 2-31
Trough
0-xing
Peak
Fee:
0
500
1,000
N

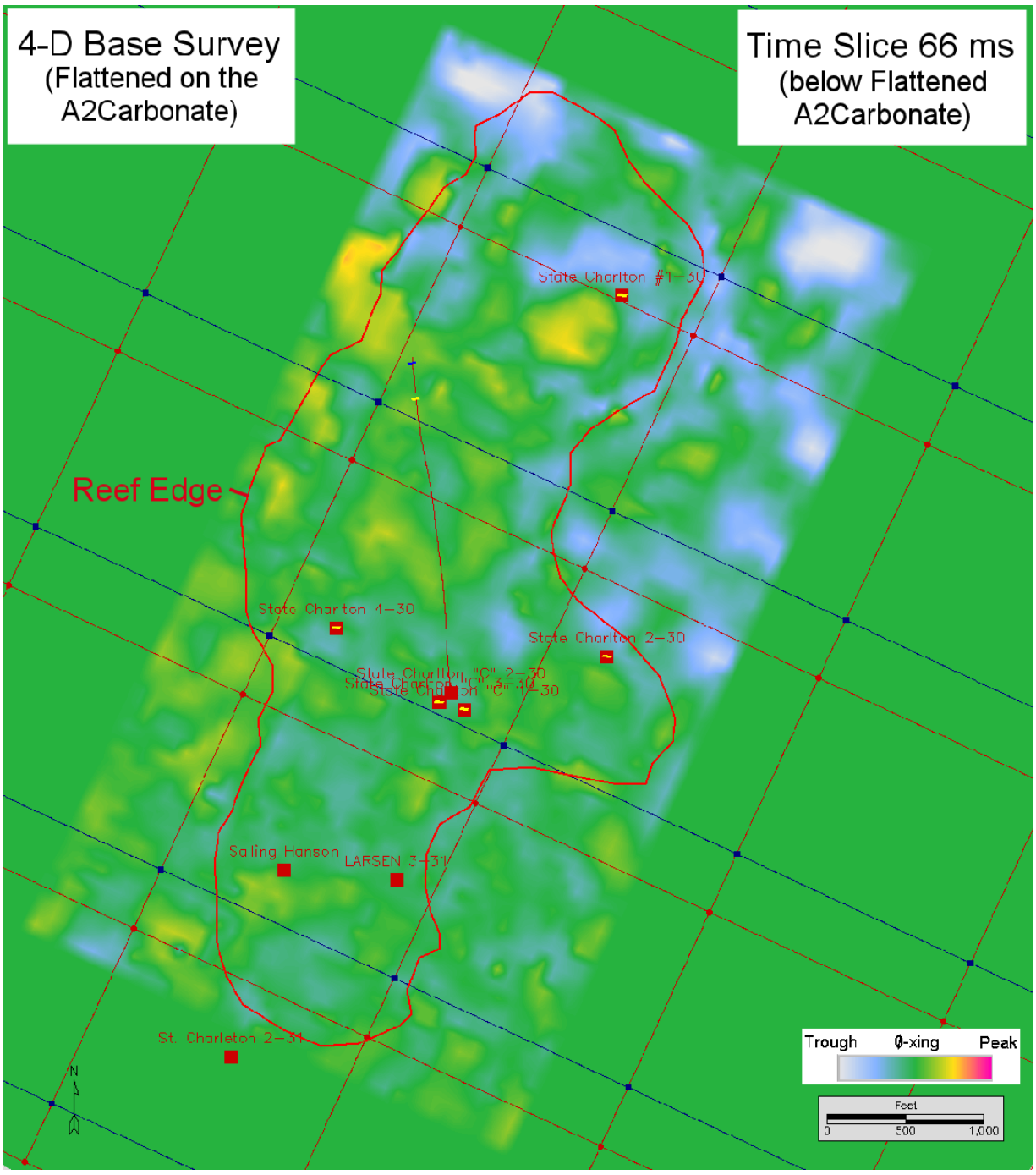
4-D Base Survey
(Flattened on the
A2Carbonate)
Time Slice 66 ms
(below Flattened
A2Carbonate)
State Charlton #1-30
Reef Edge
State Charlton 1-30
State Charlton 2-30
Saling Hanson
LARSEN 3-31
St. Charleton 2-31
N
Trough
0-xing
Peak
Feet
0
500
1,000

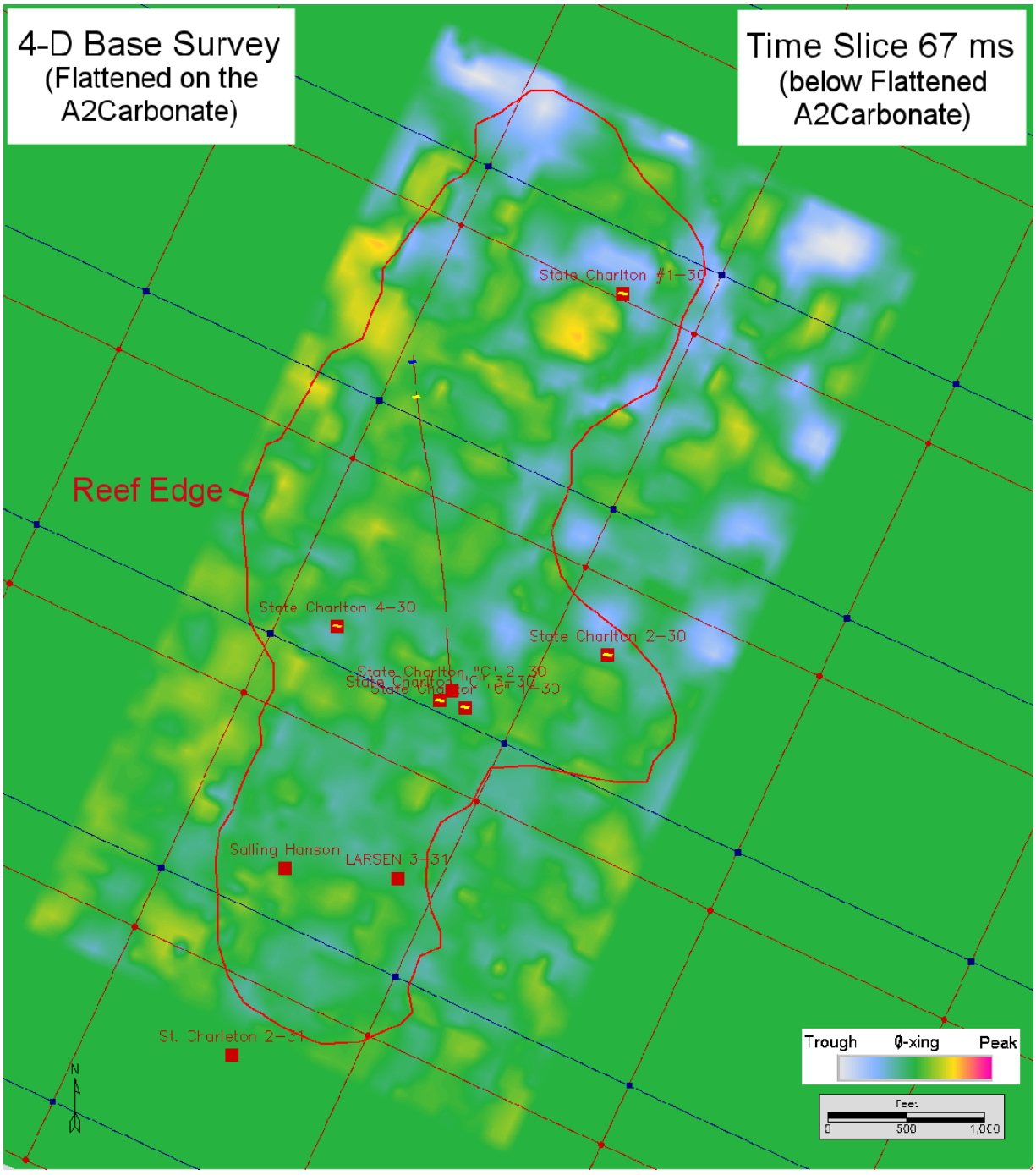
4-D Base Survey
(Flattened on the
A2Carbonate)
Time Slice 67 ms
(below Flattened
A2Carbonate)
State Charlton #1-30
Reef Edge
State Charlton 4-30
State Charlton 2-30
Salling Hanson
LARSEN 3-31
St. Charleton 2-31
Trough
0-xing
Peak
0
500
1,000

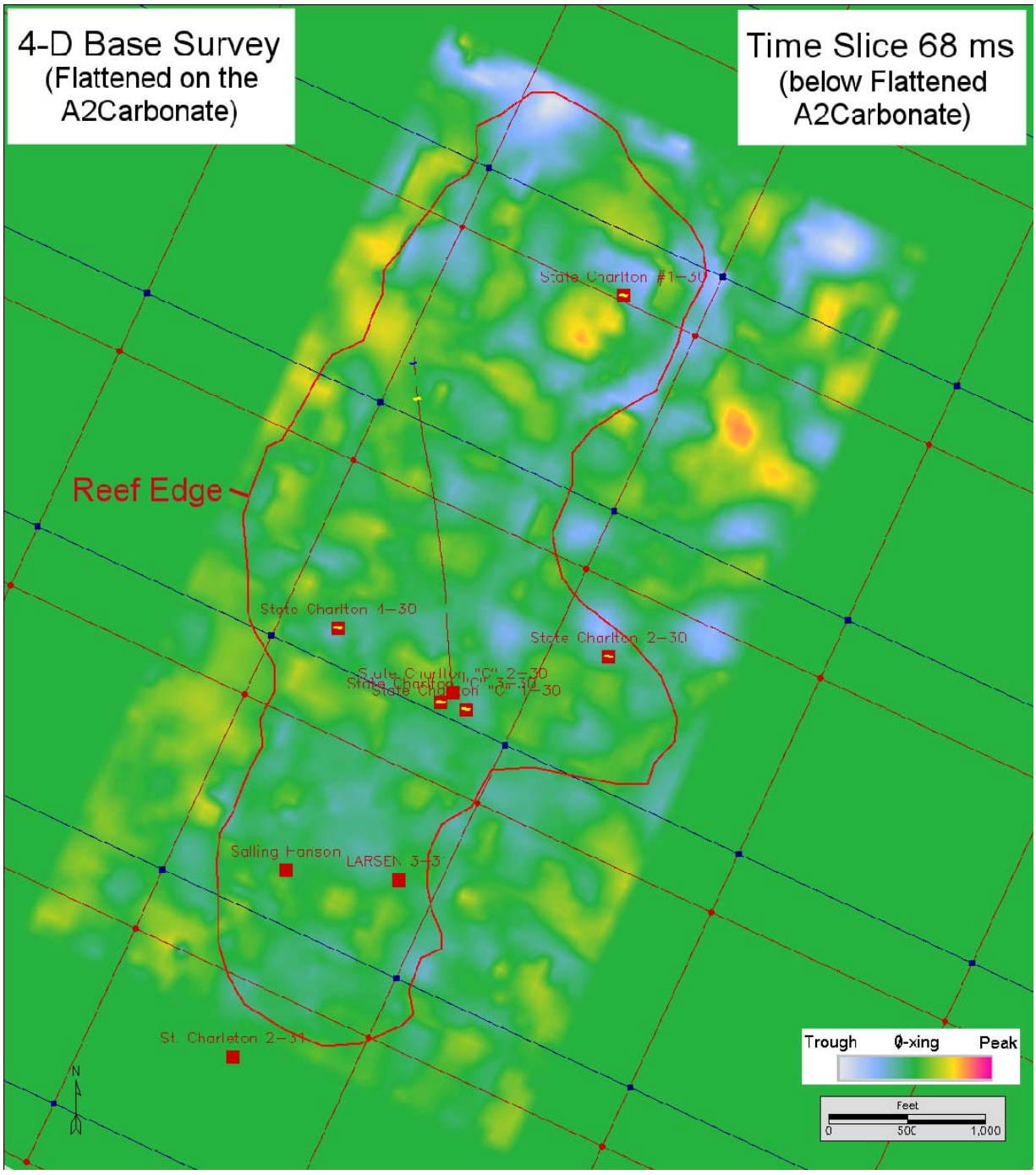
4-D Base Survey
(Flattened on the
A2Carbonate)
Time Slice 68 ms
(below Flattened
A2Carbonate)
State Charlton #1-30
Reef Edge
State Charlton 1-30
State Charlton 2-30
Salling Hanson
LARSEN 3-3
St. Charleton 2-31
N
Trough
0-xing
Peak
Feet
0
500
1,000

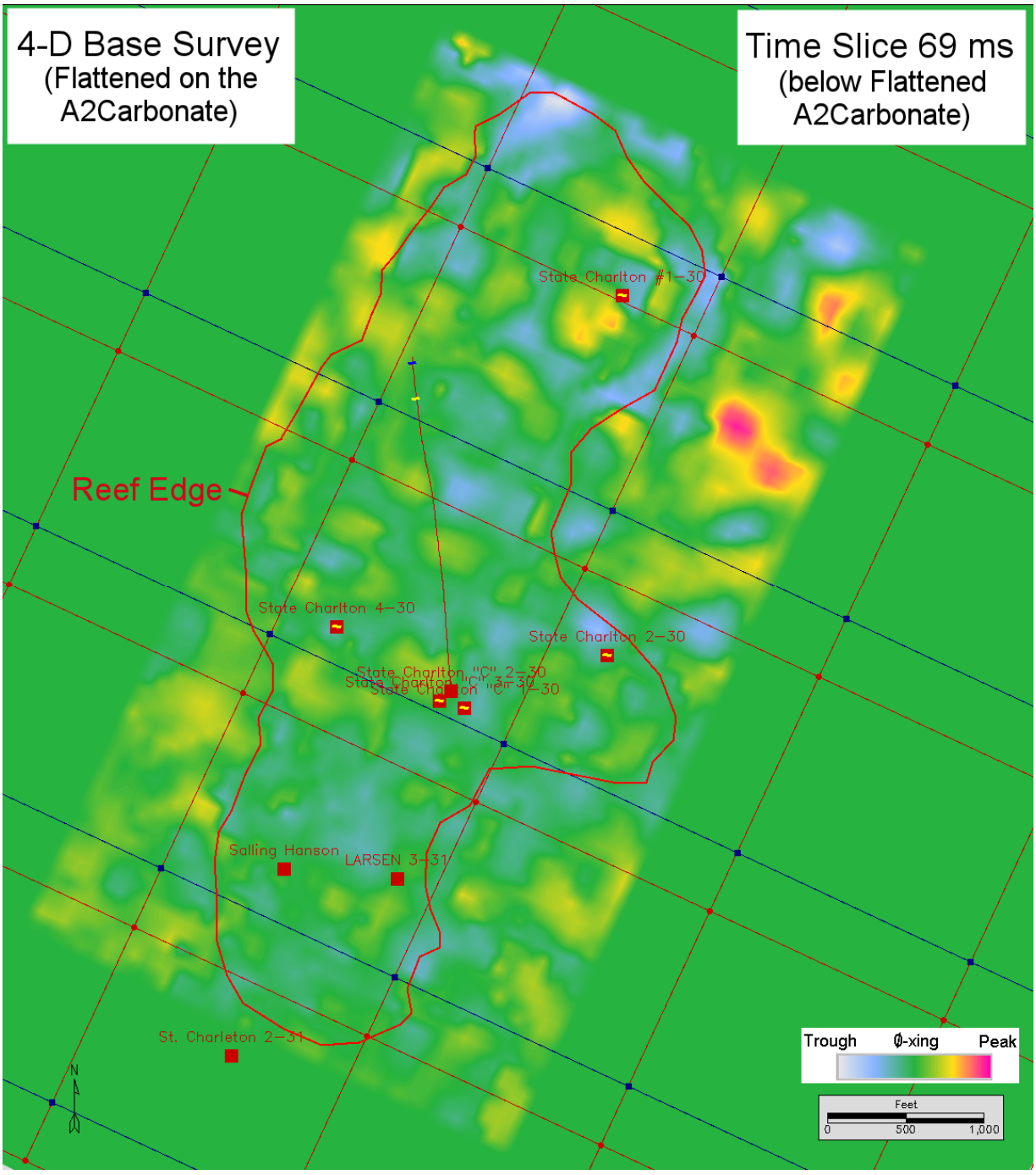
4-D Base Survey
(Flattened on the
A2Carbonate)
Time Slice 69 ms
(below Flattened
A2Carbonate)
State Charlton #1-30
Reef Edge
State Charlton 4-30
State Charlton 2-30
State Charlton "C" 2-30
State Charlton "C" 3-30
State Charlton "C" 1-30
Salling Hanson
LARSEN 3-31
St. Charleton 2-31
N
Trough
Ø-xing
Peak
Feet
0
500
1,000

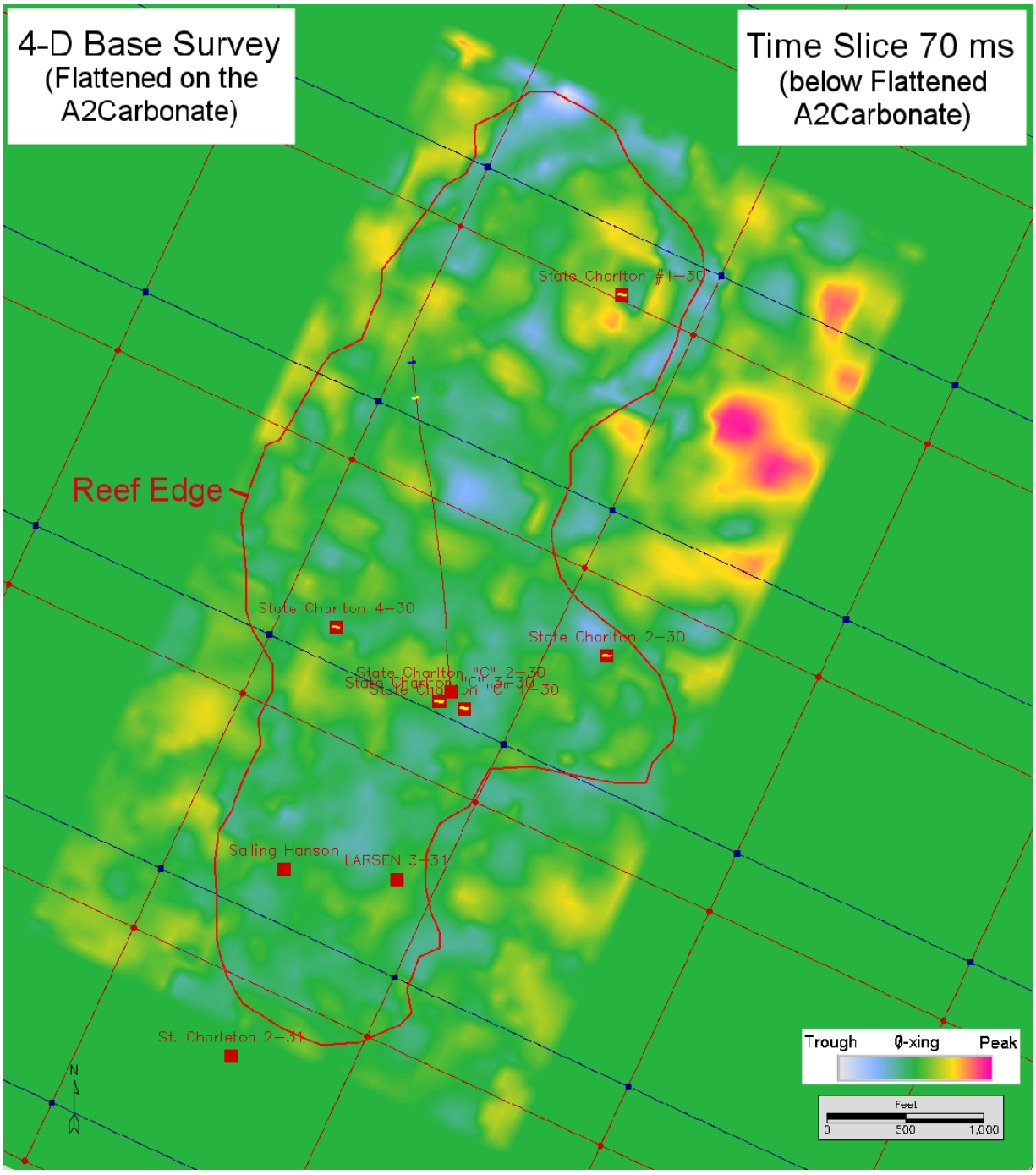
4-D Base Survey
(Flattened on the
A2Carbonate)
Time Slice 70 ms
(below Flattened
A2Carbonate)
State Charlton #1-30
Reef Edge
State Charlton 4-30
State Charlton 2-30
Saling Hanson
LARSEN 3-31
St. Charleton 2-31
Trough
0-xing
Peak
Feet
0
500
1,000
N

10.5 APPENDIX F - 4-D Monitor Seismic Survey (Flattened on A2Carbonate) – Time slices (0-70 ms)

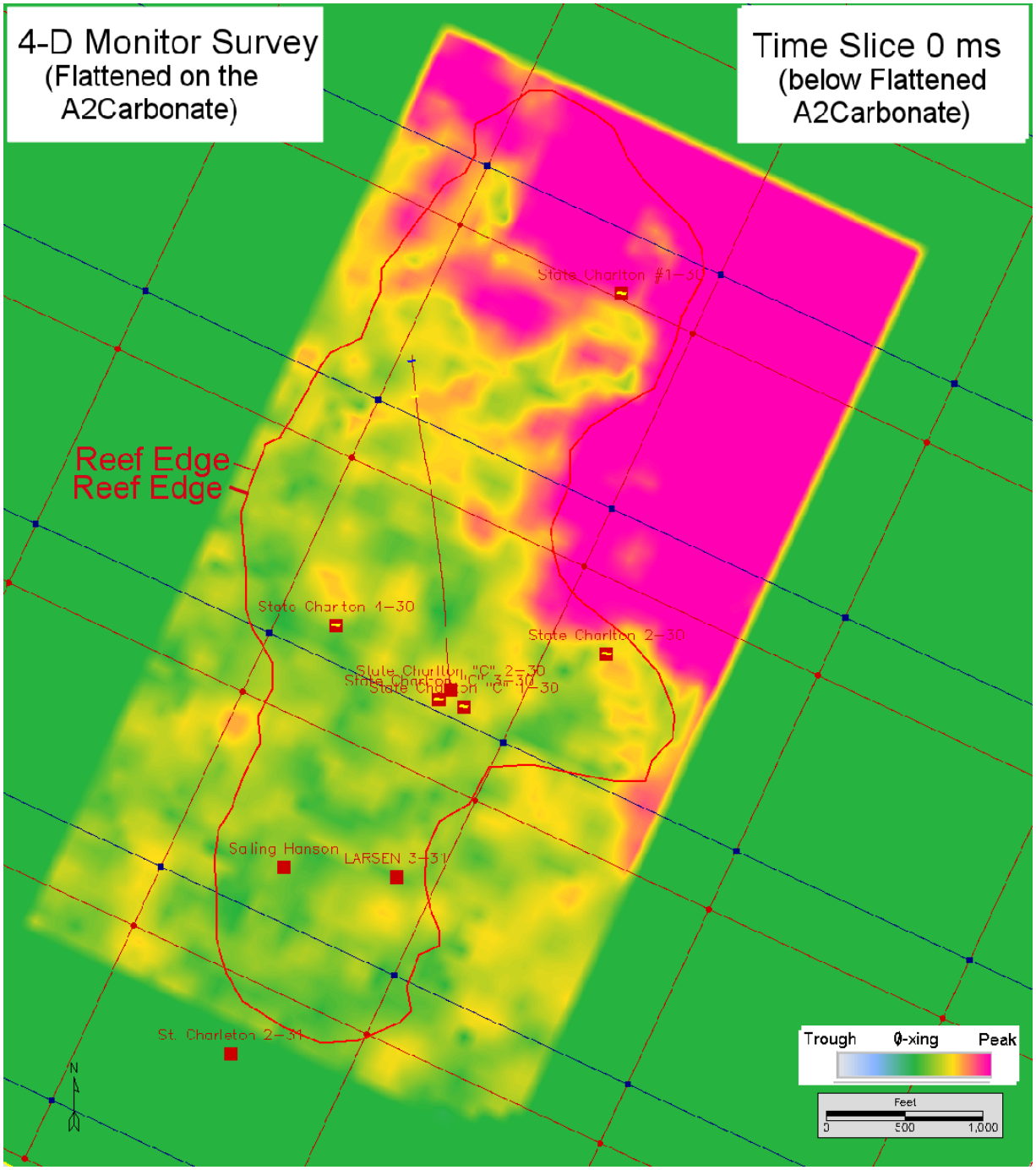

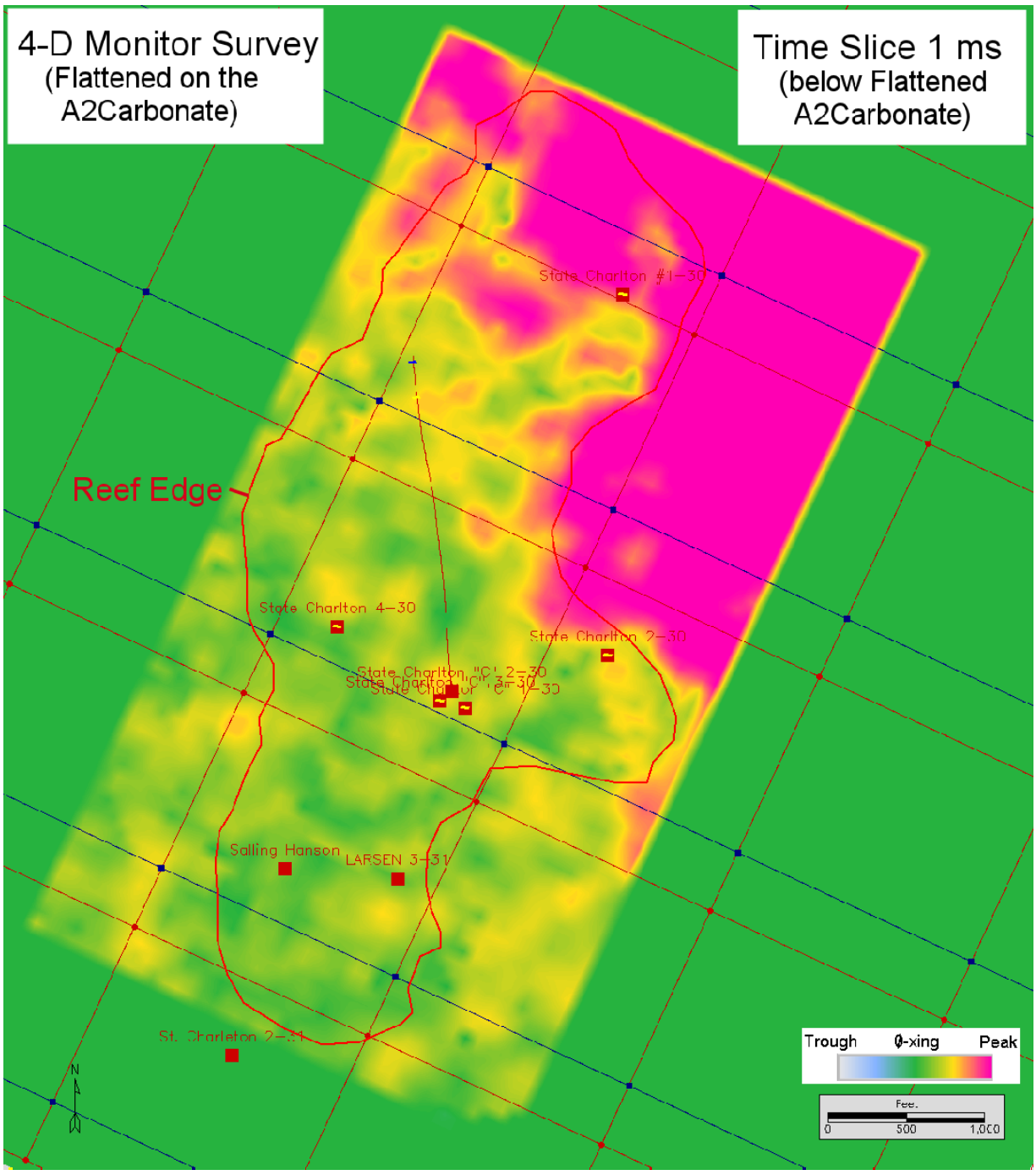
4-D Monitor Survey
(Flattened on the
A2Carbonate)
Time Slice 1 ms
(below Flattened
A2Carbonate)
State Charlton #1-30
Reef Edge
State Charlton 4-30
State Charlton 2-30
Salling Hanson
LARSEN 3-31
Trough
0-xing
Peak
Feet
0
500
1,000

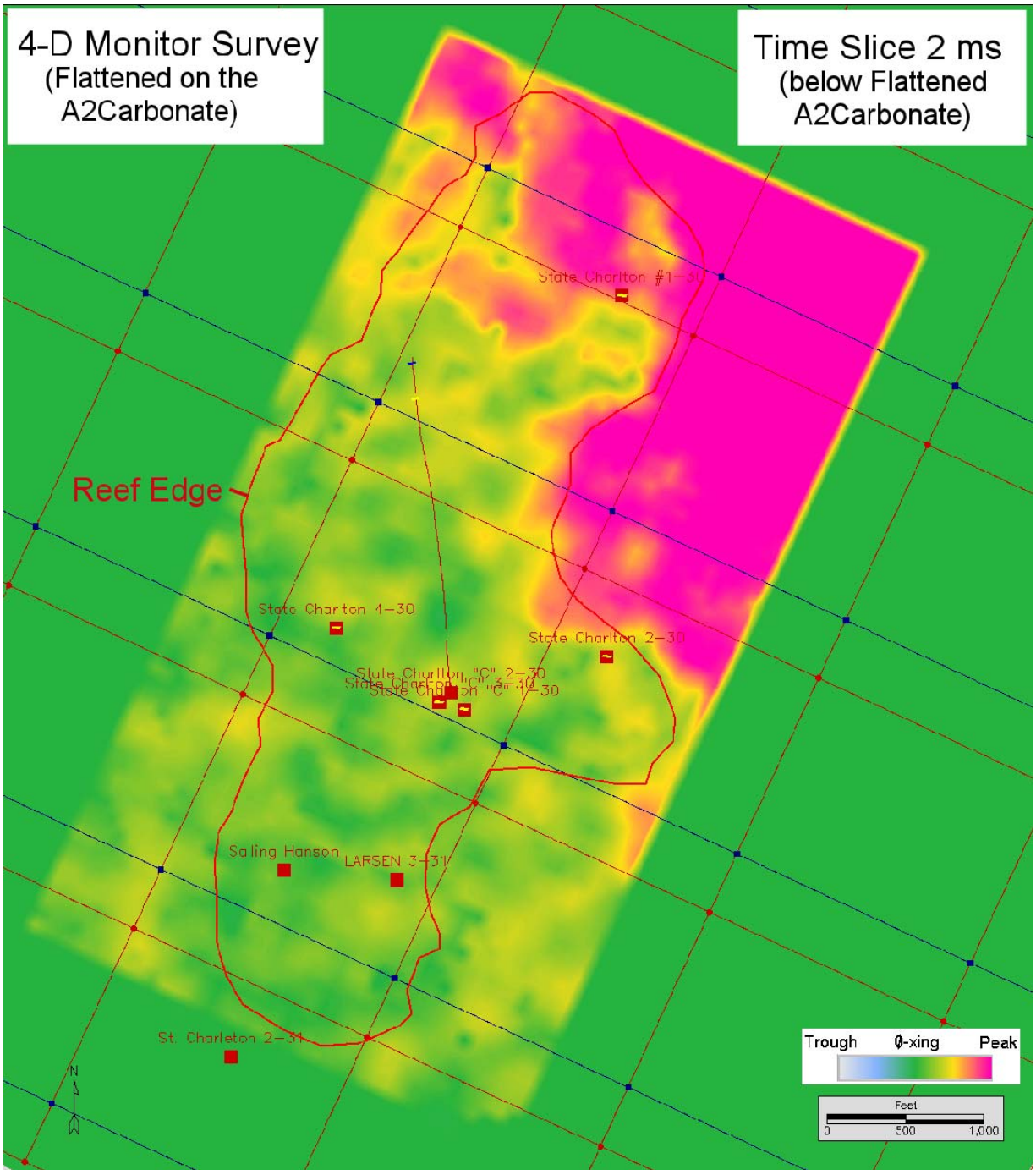
4-D Monitor Survey
(Flattened on the
A2Carbonate)
Time Slice 2 ms
(below Flattened
A2Carbonate)
State Charlton #1-30
Reef Edge
State Charton 1-30
State Charlton 2-30
Slate Charlton "C" 2-30
State Charlton "C" 1-30
Saling Hanson
LARSEN 3-31
St. Charleton 2-31
N
Trough
0-xing
Peak
Feet
0
500
1,000

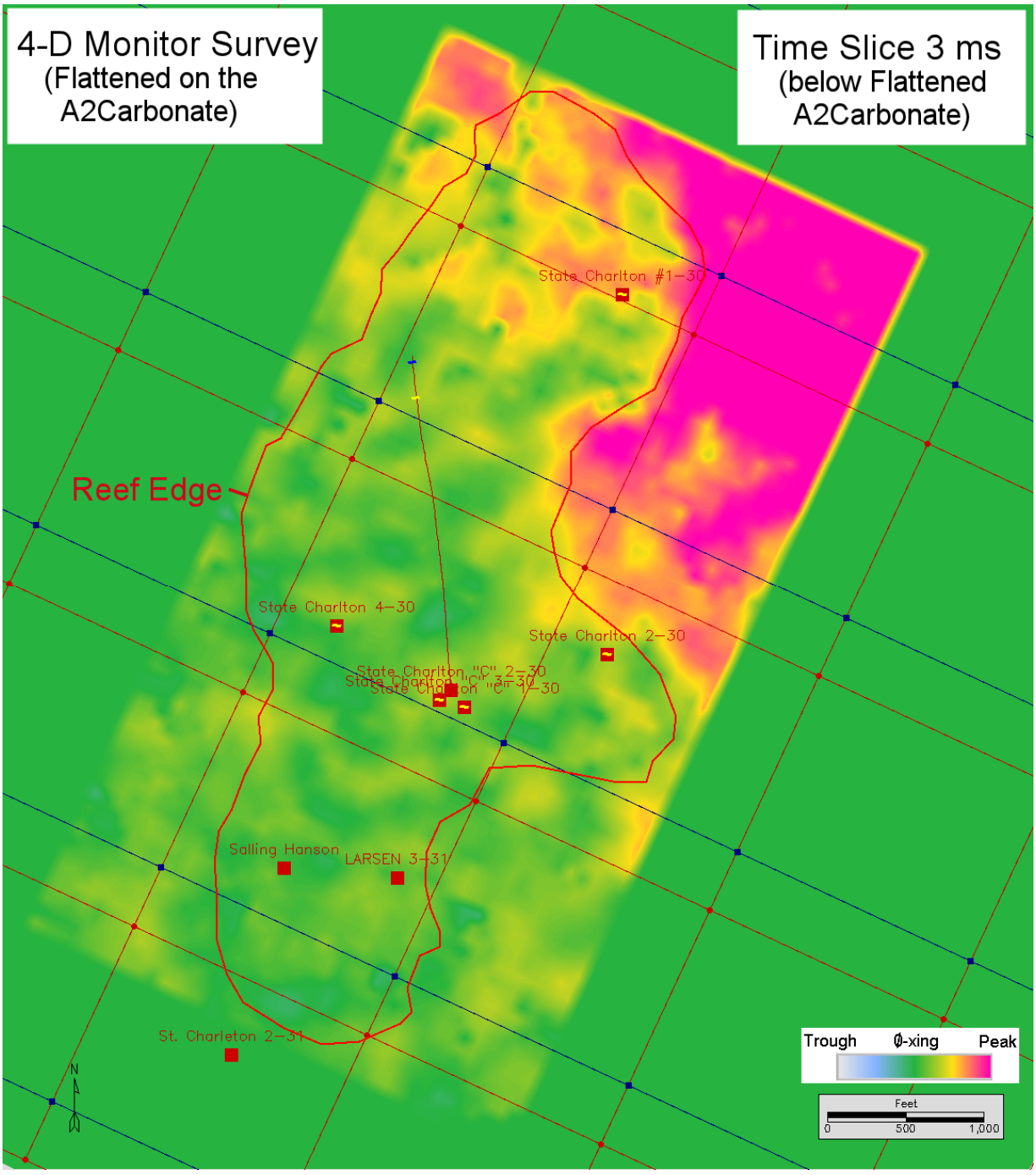
4-D Monitor Survey
(Flattened on the
A2Carbonate)
Time Slice 3 ms
(below Flattened
A2Carbonate)
State Charlton #1-30
Reef Edge
State Charlton 4-30
State Charlton 2-30
State Charlton "C" 2-30
State Charlton "C" 3-30
State Charlton "C" 1-30
Salling Hanson
LARSEN 3-31
St. Charleton 2-31
N
Trough
Ø-xing
Peak
Feet
0
500
1,000

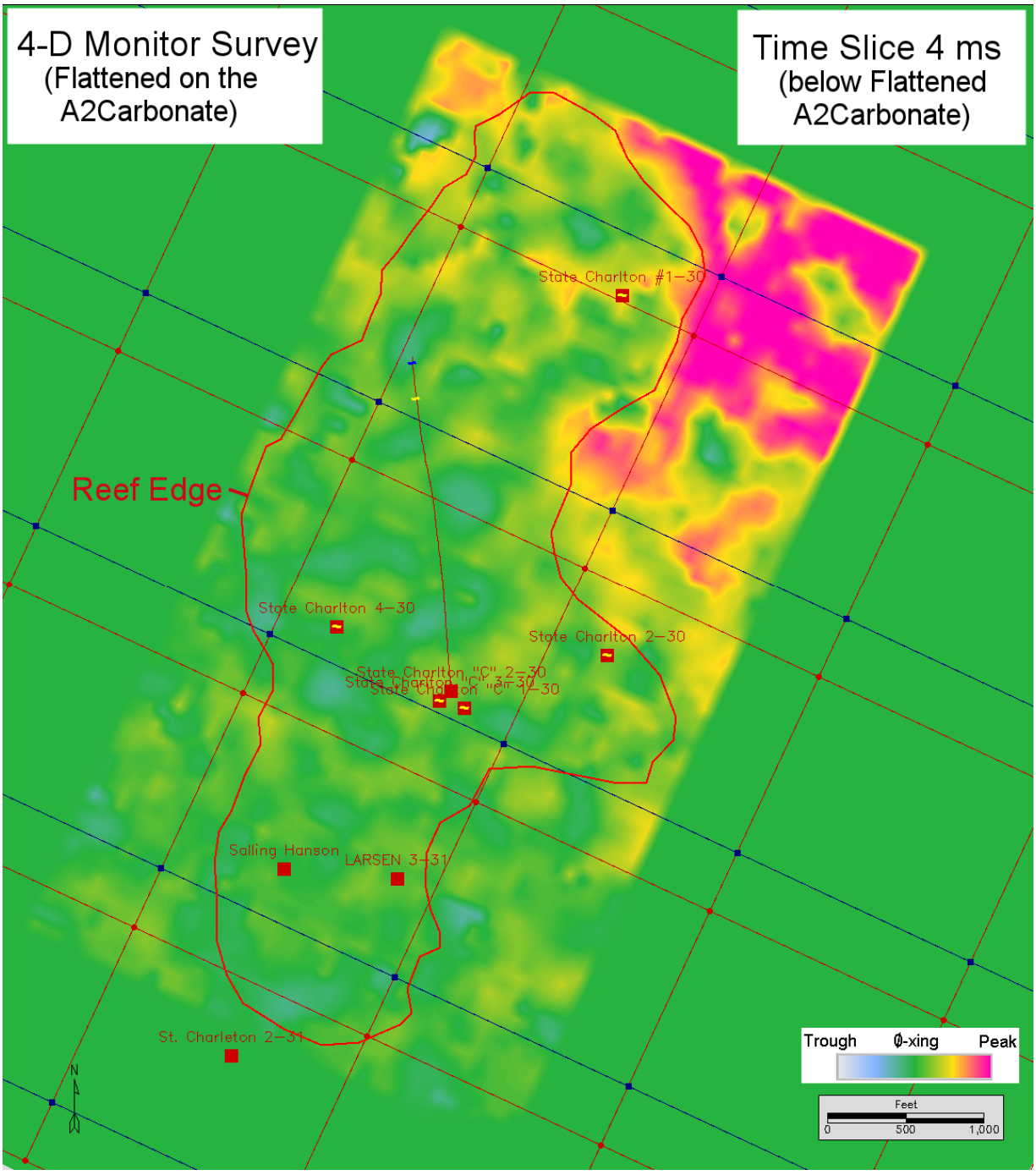
4-D Monitor Survey
(Flattened on the
A2Carbonate)
Time Slice 4 ms
(below Flattened
A2Carbonate)
State Charlton #1-30
Reef Edge
State Charlton 4-30
State Charlton 2-30
State Charlton "C" 2-30
State Charlton "C" 3-30
State Charlton "C" 1-30
Salling Hanson
LARSEN 3-31
St. Charleton 2-31
N
Trough
Ø-xing
Peak
Feet
0
500
1,000

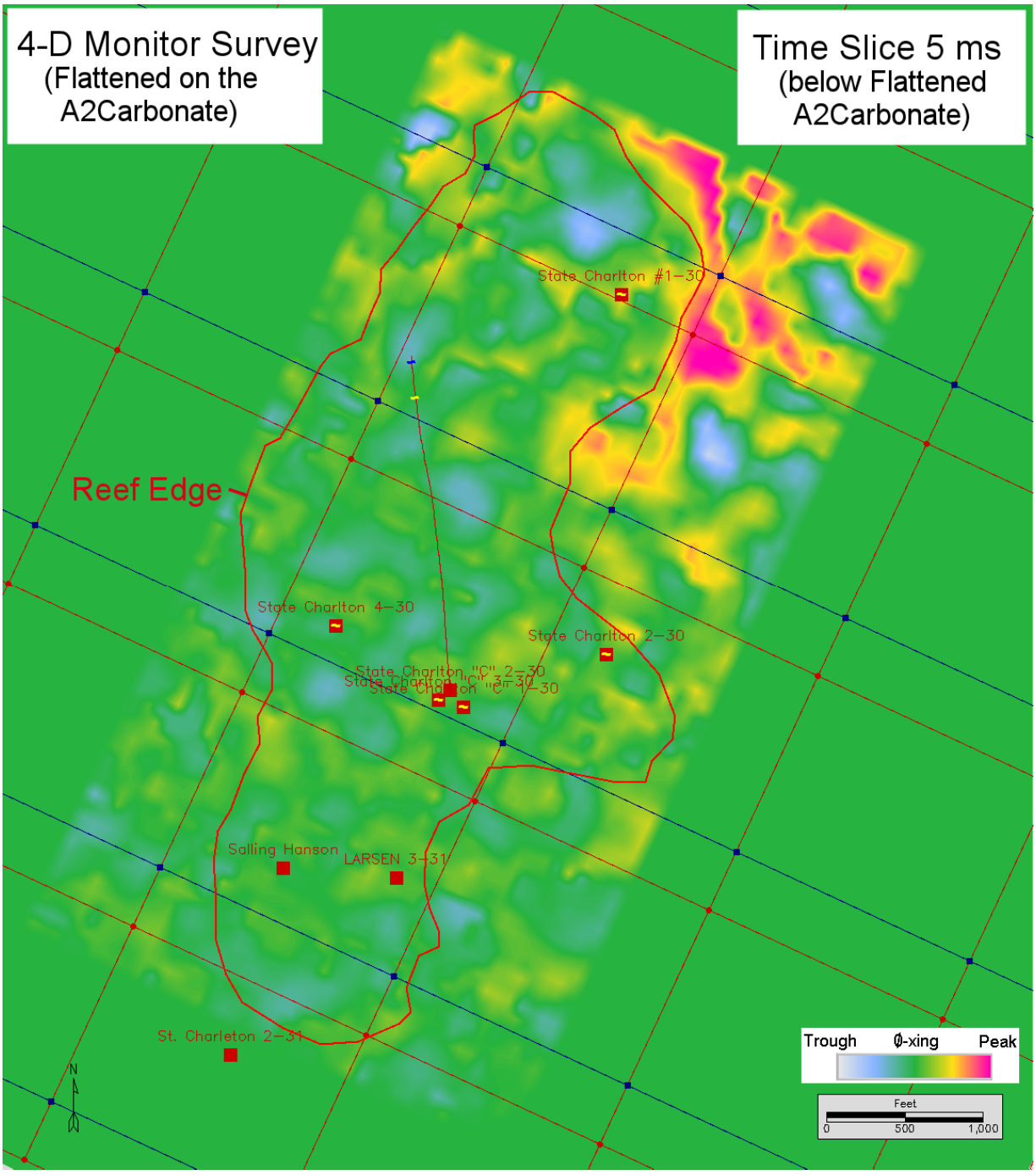
4-D Monitor Survey
(Flattened on the
A2Carbonate)
Time Slice 5 ms
(below Flattened
A2Carbonate)
State Charlton #1-30
Reef Edge
State Charlton 4-30
State Charlton 2-30
State Charlton "C" 2-30
State Charlton "C" 3-30
State Charlton "C" 1-30
Salling Hanson
LARSEN 3-31
St. Charleton 2-31
N
Trough
Ø-xing
Peak
Feet
0
500
1,000

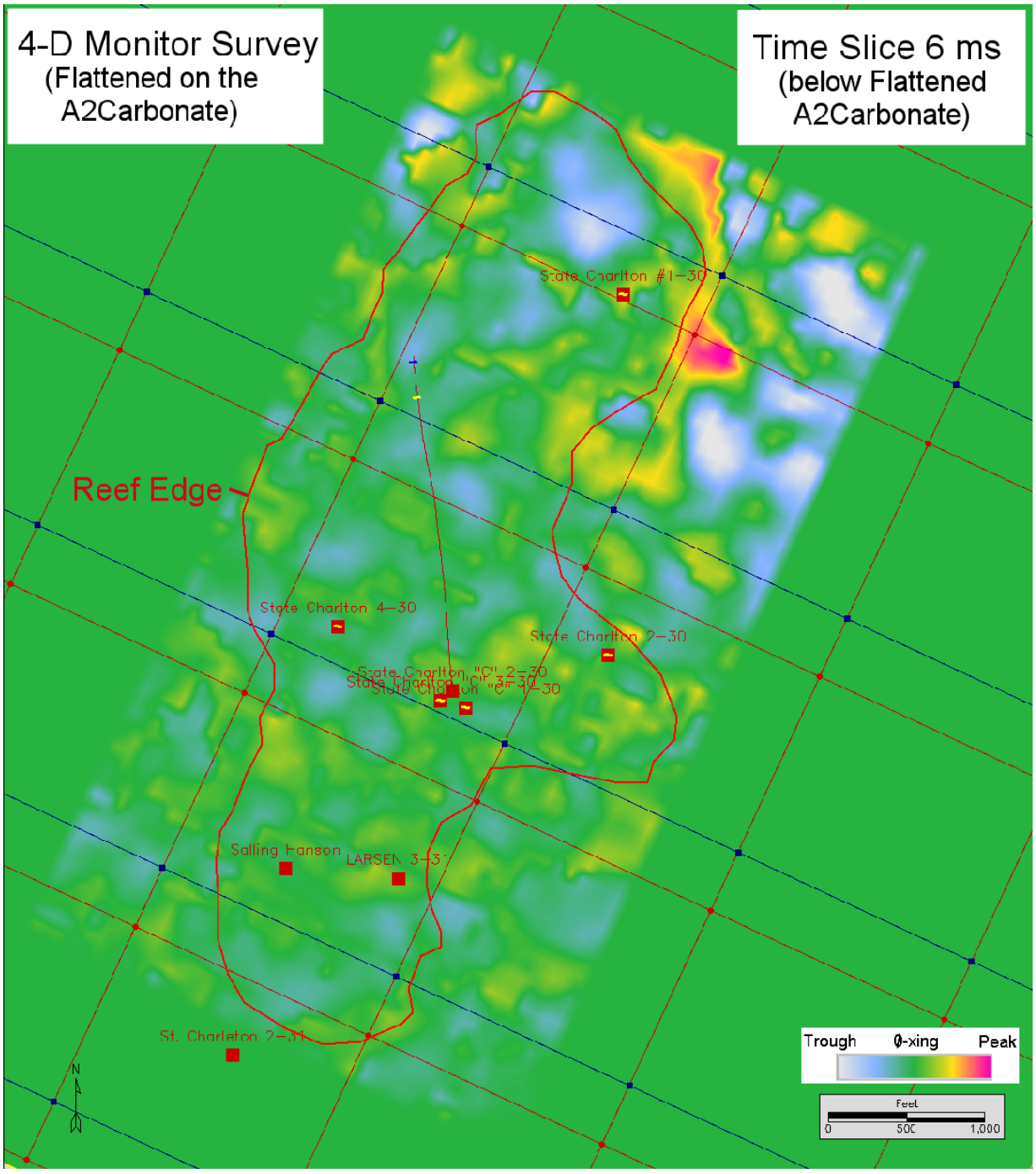
4-D Monitor Survey
(Flattened on the
A2Carbonate)
Time Slice 6 ms
(below Flattened
A2Carbonate)
State Charlton #1-30
Reef Edge
State Charlton 4-30
State Charlton 2-30
Salling Hanson
LARSEN 3-31
St. Charleton 2-31
Trough
0-xing
Peak
Feet
0
500
1,000
N

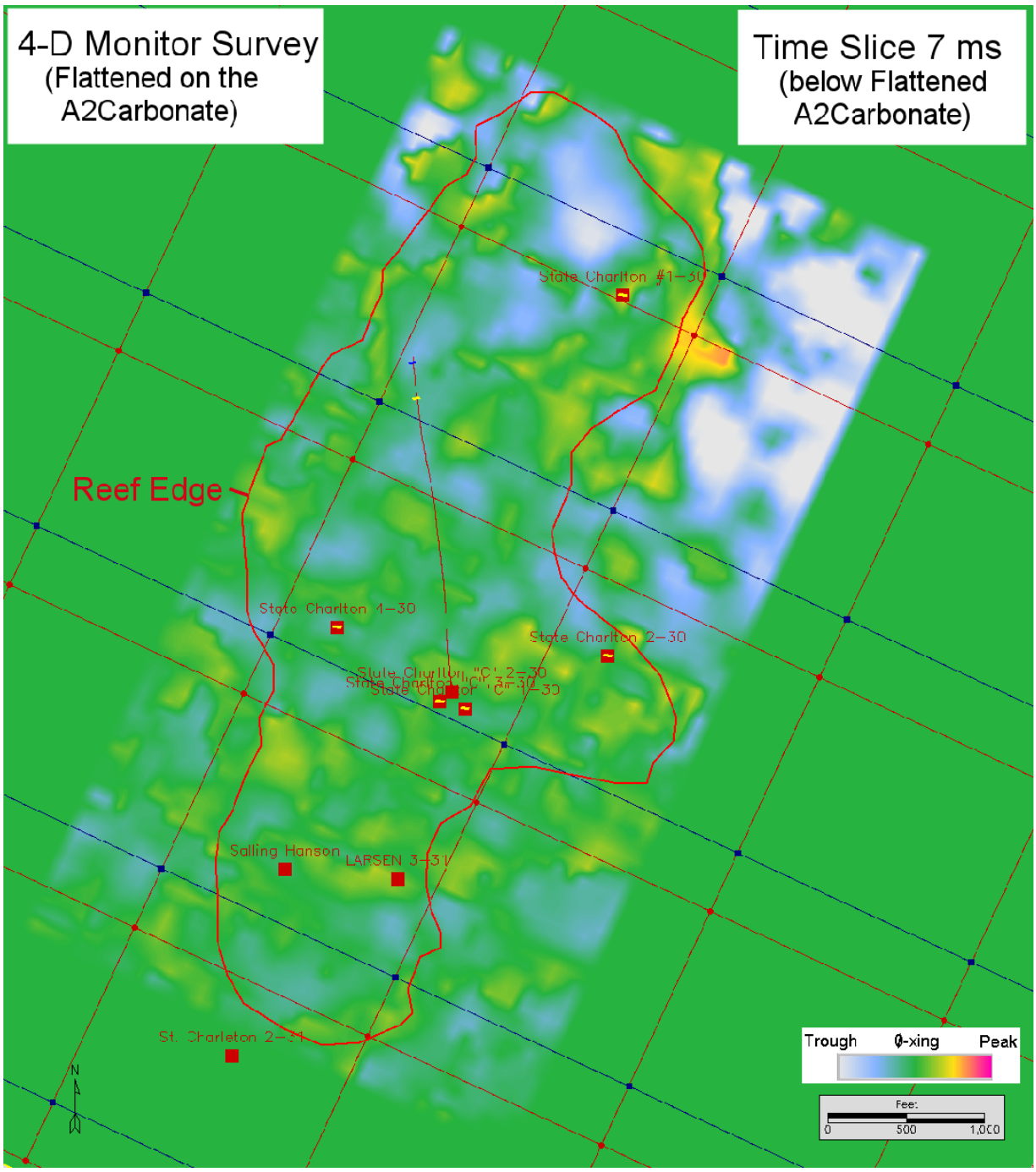
4-D Monitor Survey
(Flattened on the
A2Carbonate)
Time Slice 7 ms
(below Flattened
A2Carbonate)
State Charlton #1-30
Reef Edge
State Charlton 1-30
State Charlton 2-30
Salling Hanson
LARSEN 3-31
St. Charleton 2-31
Trough
0-xing
Peak
Fee:
0
500
1,000
N

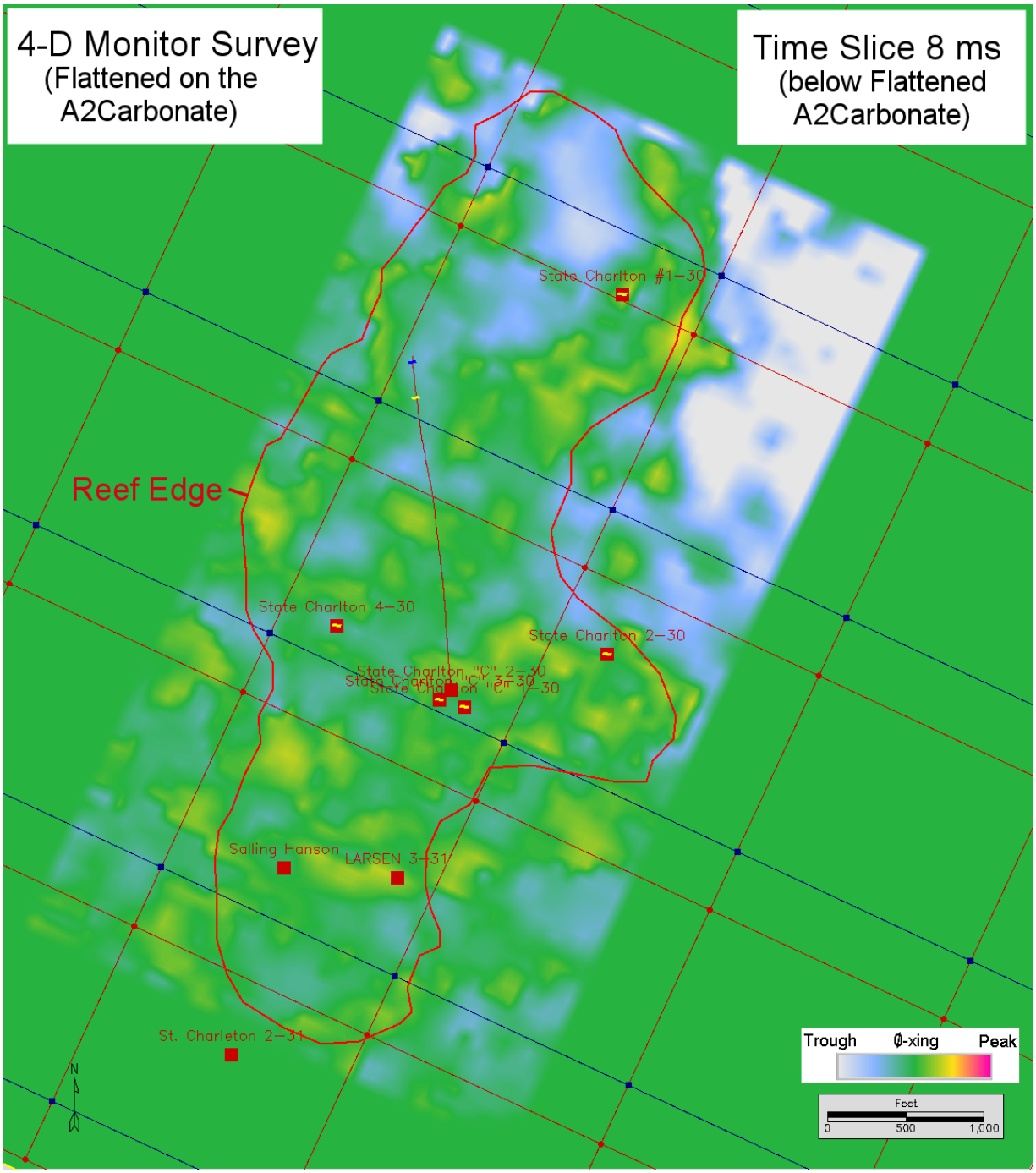
4-D Monitor Survey
(Flattened on the
A2Carbonate)
Time Slice 8 ms
(below Flattened
A2Carbonate)
State Charlton #1-30
Reef Edge
State Charlton 4-30
State Charlton 2-30
State Charlton "C" 2-30
State Charlton "C" 3-30
Salling Hanson
LARSEN 3-31
St. Charleton 2-31
N
Trough
Ø-xing
Peak
Feet
0
500
1,000

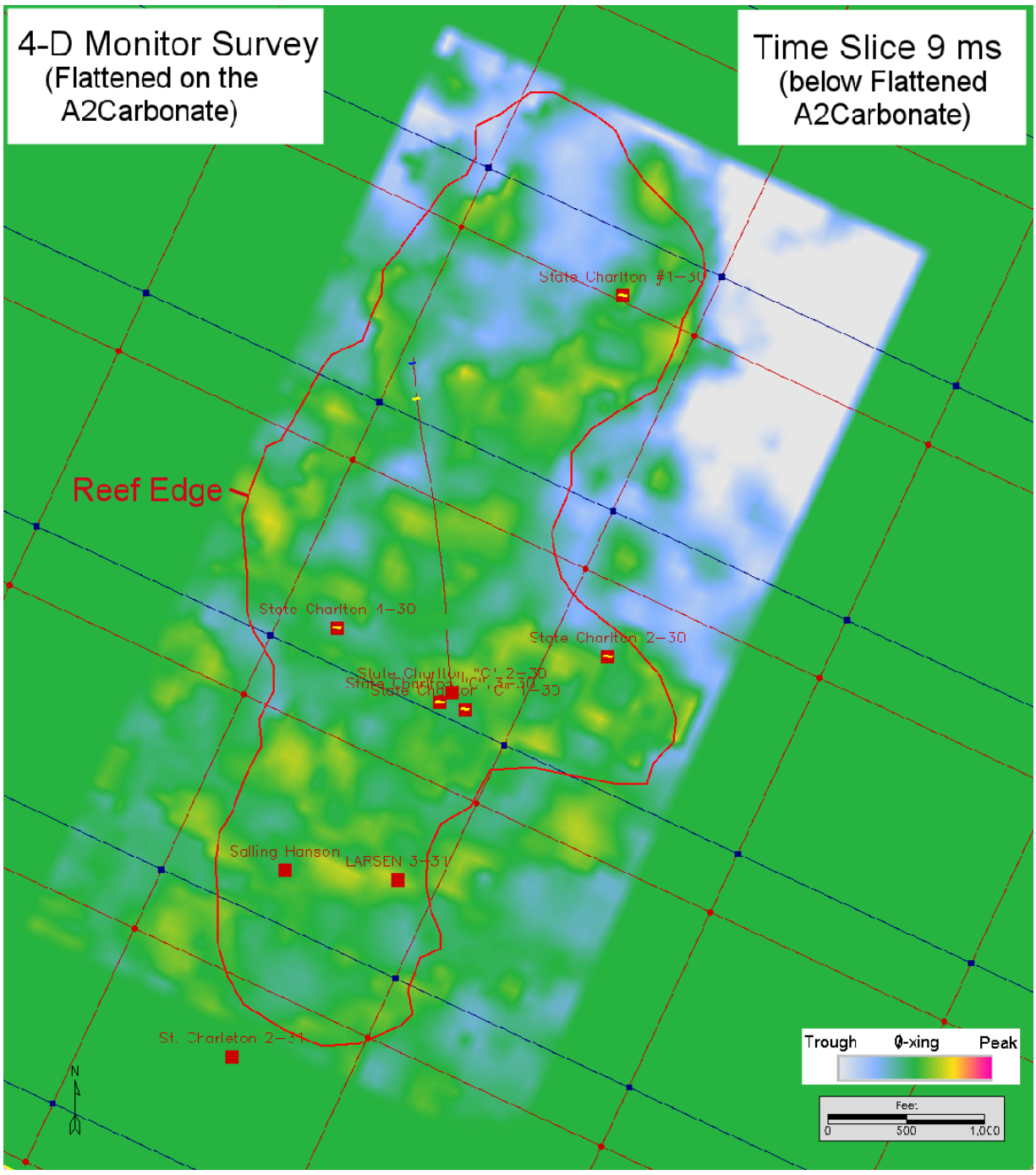
4-D Monitor Survey
(Flattened on the
A2Carbonate)
Time Slice 9 ms
(below Flattened
A2Carbonate)
State Charlton #1-30
Reef Edge
State Charlton 1-30
State Charlton 2-30
Salling Hanson
LARSEN 3-31
St. Charleton 2-31
Trough
0-xing
Peak
Fee:
0
500
1,000
N

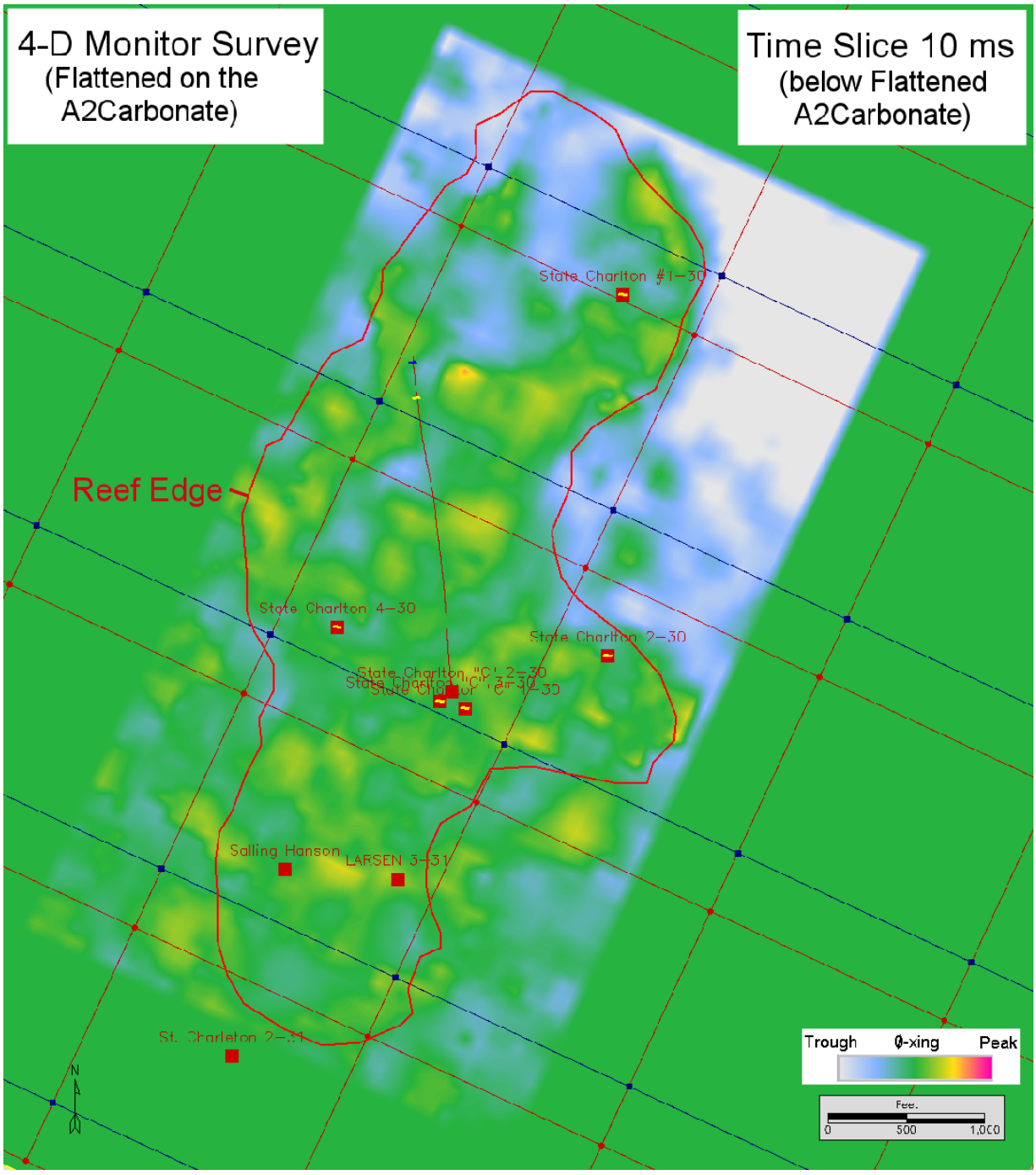
4-D Monitor Survey
(Flattened on the
A2Carbonate)
Time Slice 10 ms
(below Flattened
A2Carbonate)
State Charlton #1-30
Reef Edge
State Charlton 4-30
State Charlton 2-30
Salling Hanson
LARSEN 3-31
Trough
0-xing
Peak
Feet
0
500
1,000
N

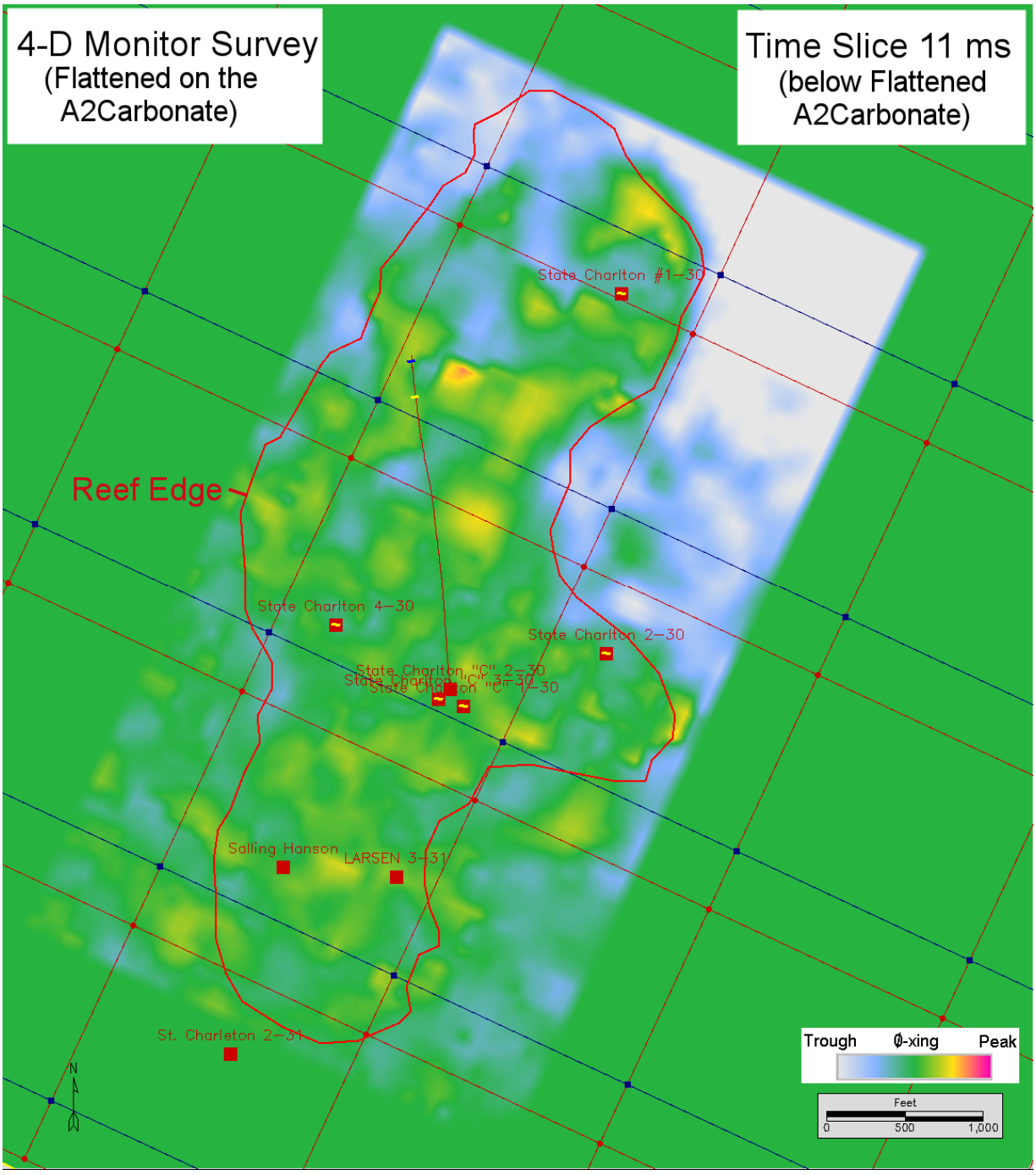
4-D Monitor Survey
(Flattened on the
A2Carbonate)
Time Slice 11 ms
(below Flattened
A2Carbonate)
State Charlton #1-30
Reef Edge
State Charlton 4-30
State Charlton 2-30
State Charlton "C" 2-30
Salling Hanson
LARSEN 3-31
St. Charleton 2-31
Trough
Ø-xing
Peak
Feet
0
500
1,000
N

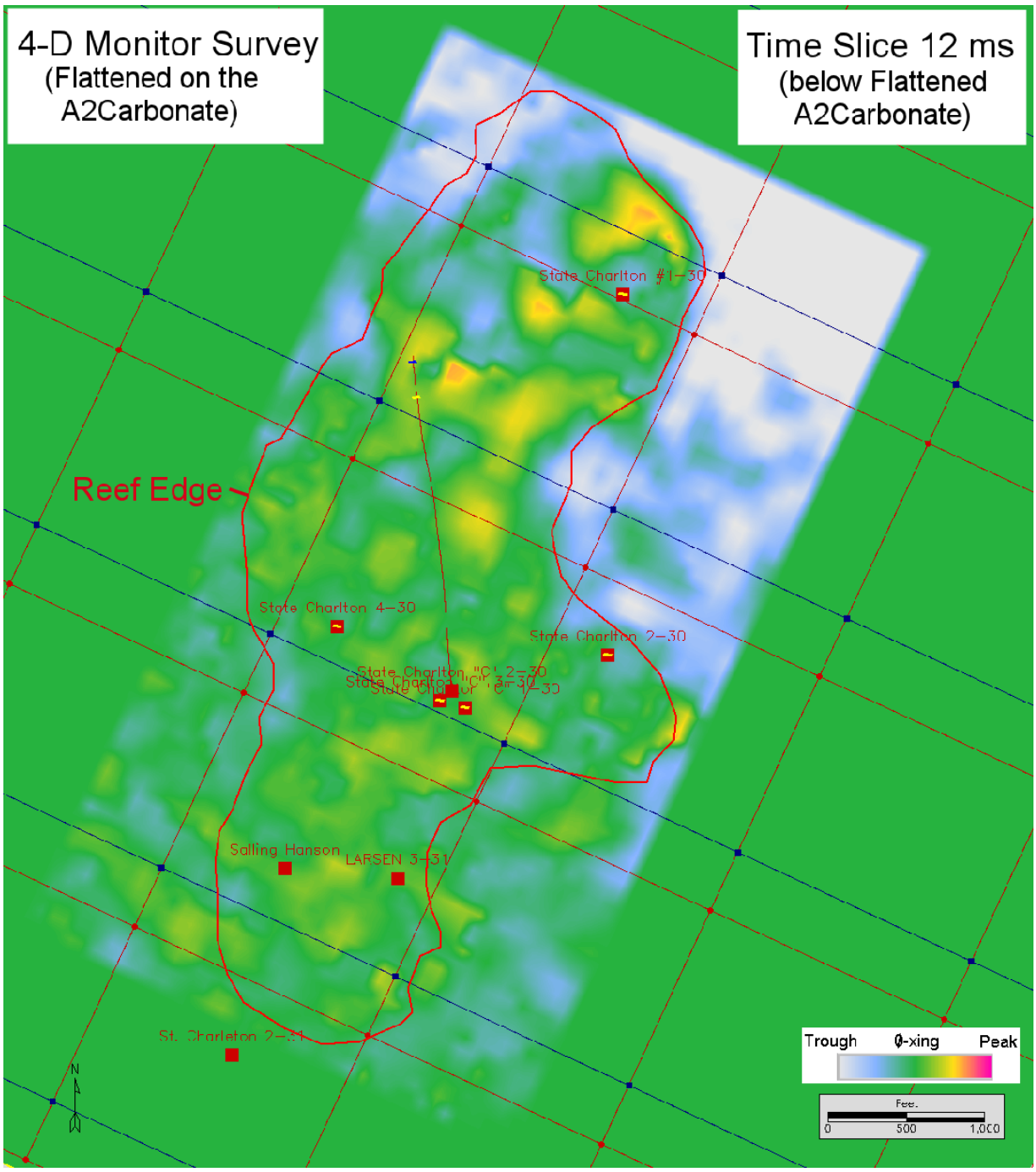
4-D Monitor Survey
(Flattened on the
A2Carbonate)
Time Slice 12 ms
(below Flattened
A2Carbonate)
State Charlton #1-30
Reef Edge
State Charlton 4-30
State Charlton 2-30
Salling Hanson
LARSEN 3-31
St. Charleton 2-31
Trough
0-xing
Peak
Feet
0
500
1,000
N

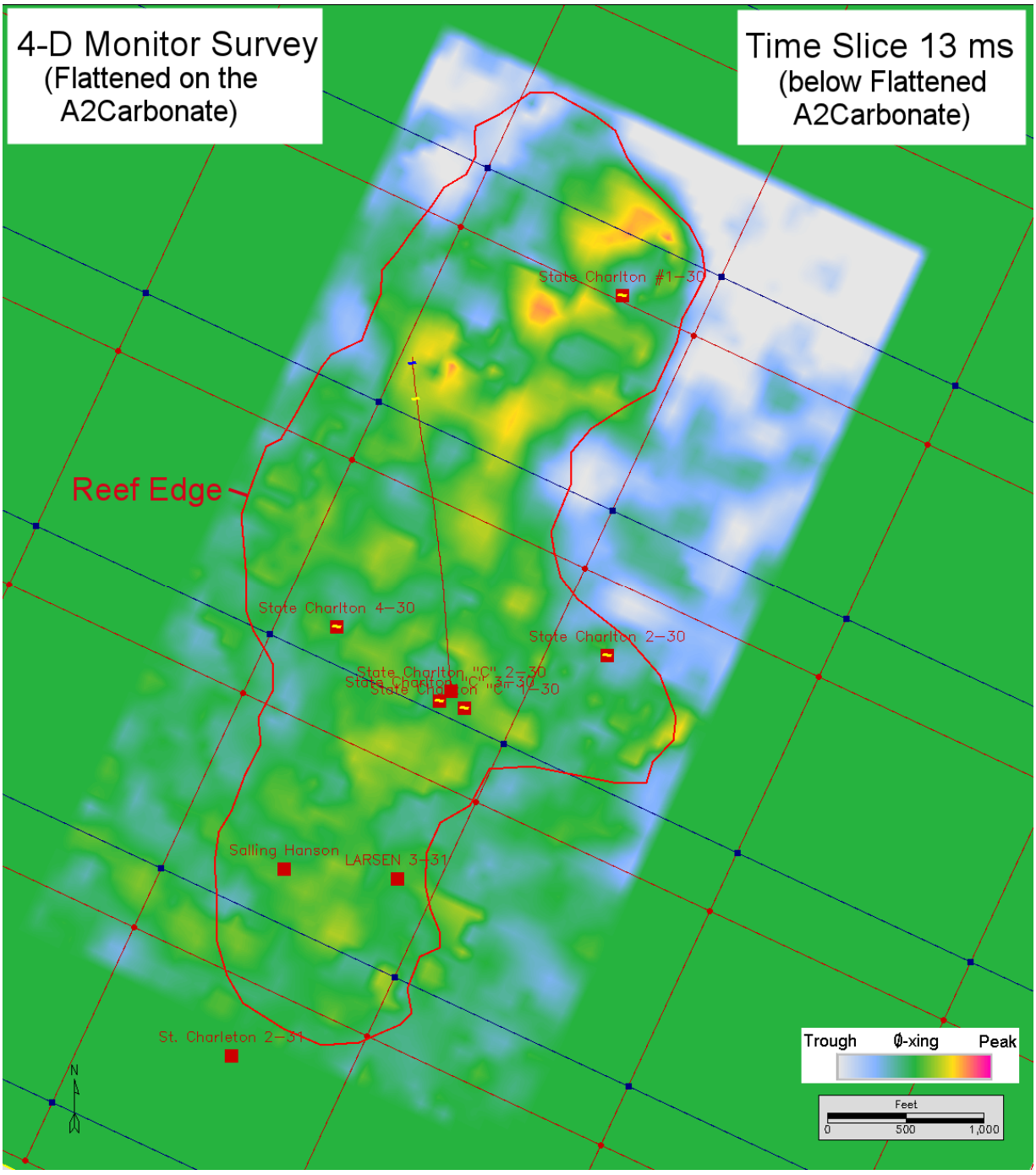
4-D Monitor Survey
(Flattened on the
A2Carbonate)
Time Slice 13 ms
(below Flattened
A2Carbonate)
State Charlton #1-30
Reef Edge
State Charlton 4-30
State Charlton 2-30
State Charlton "C" 2-30
Salling Hanson
LARSEN 3-31
St. Charleton 2-31
N
Trough
Ø-xing
Peak
Feet
0
500
1,000

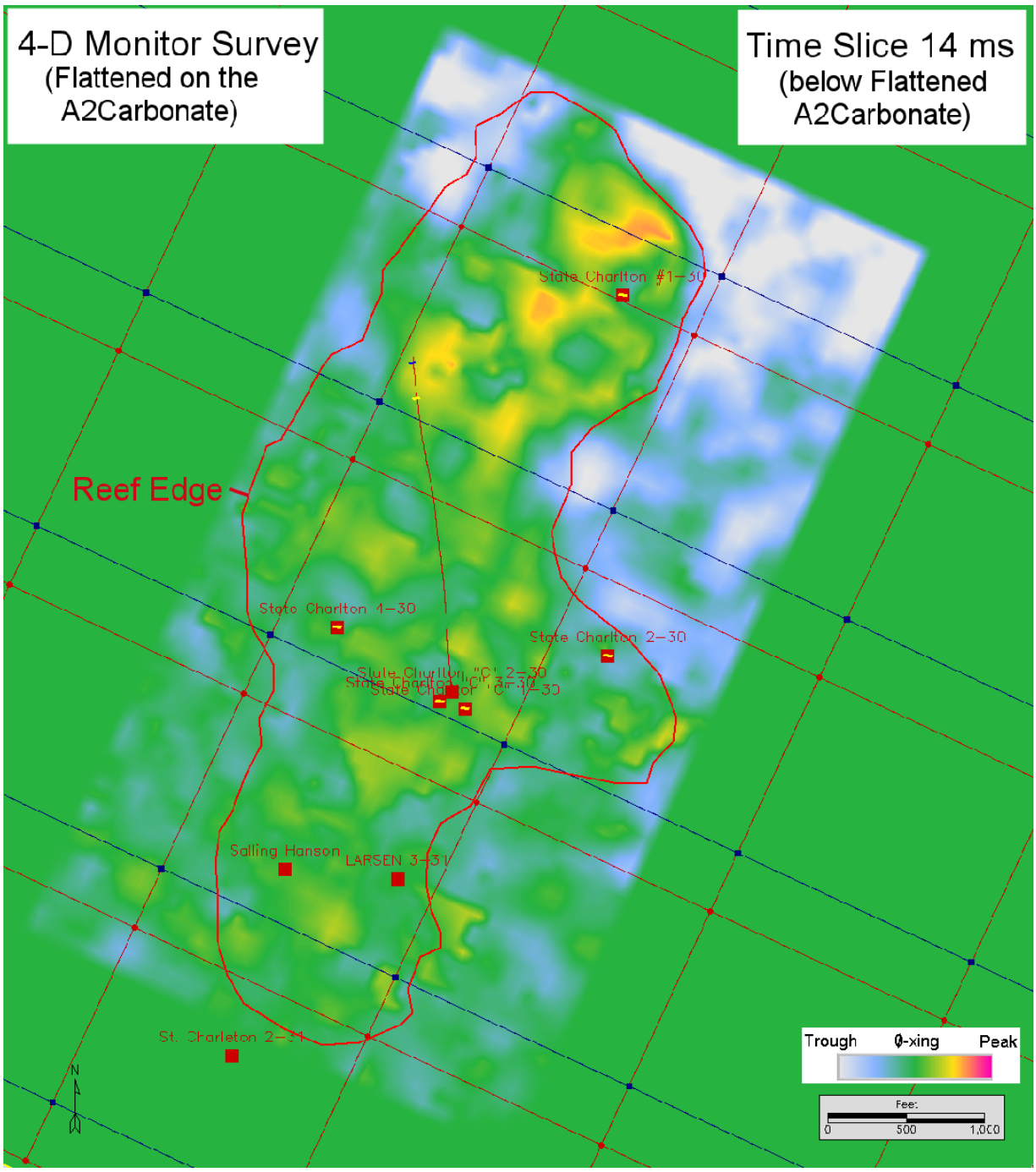
4-D Monitor Survey
(Flattened on the
A2Carbonate)
Time Slice 14 ms
(below Flattened
A2Carbonate)
State Charlton #1-30
Reef Edge
State Charlton 1-30
State Charlton 2-30
Salling Hanson
LARSEN 3-31
St. Charleton 2-31
Trough
0-xing
Peak
Fee:
0
500
1,000
N

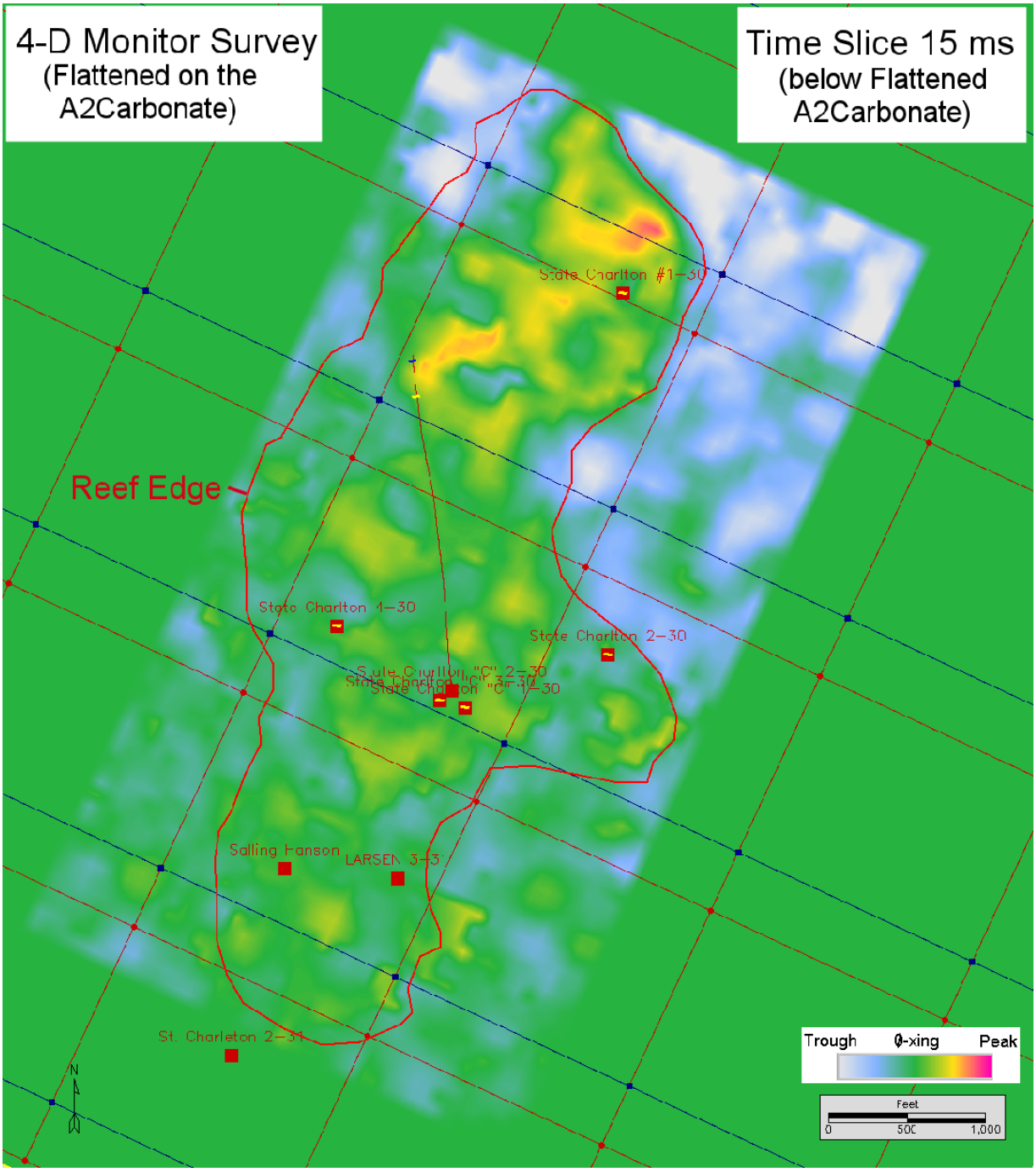
4-D Monitor Survey
(Flattened on the
A2Carbonate)
Time Slice 15 ms
(below Flattened
A2Carbonate)
State Charlton #1-30
Reef Edge
State Charlton 1-30
State Charlton 2-30
Salling Hanson
LARSEN 3-3
St. Charleton 2-31
N
Trough
0-xing
Peak
Feet
0
500
1,000

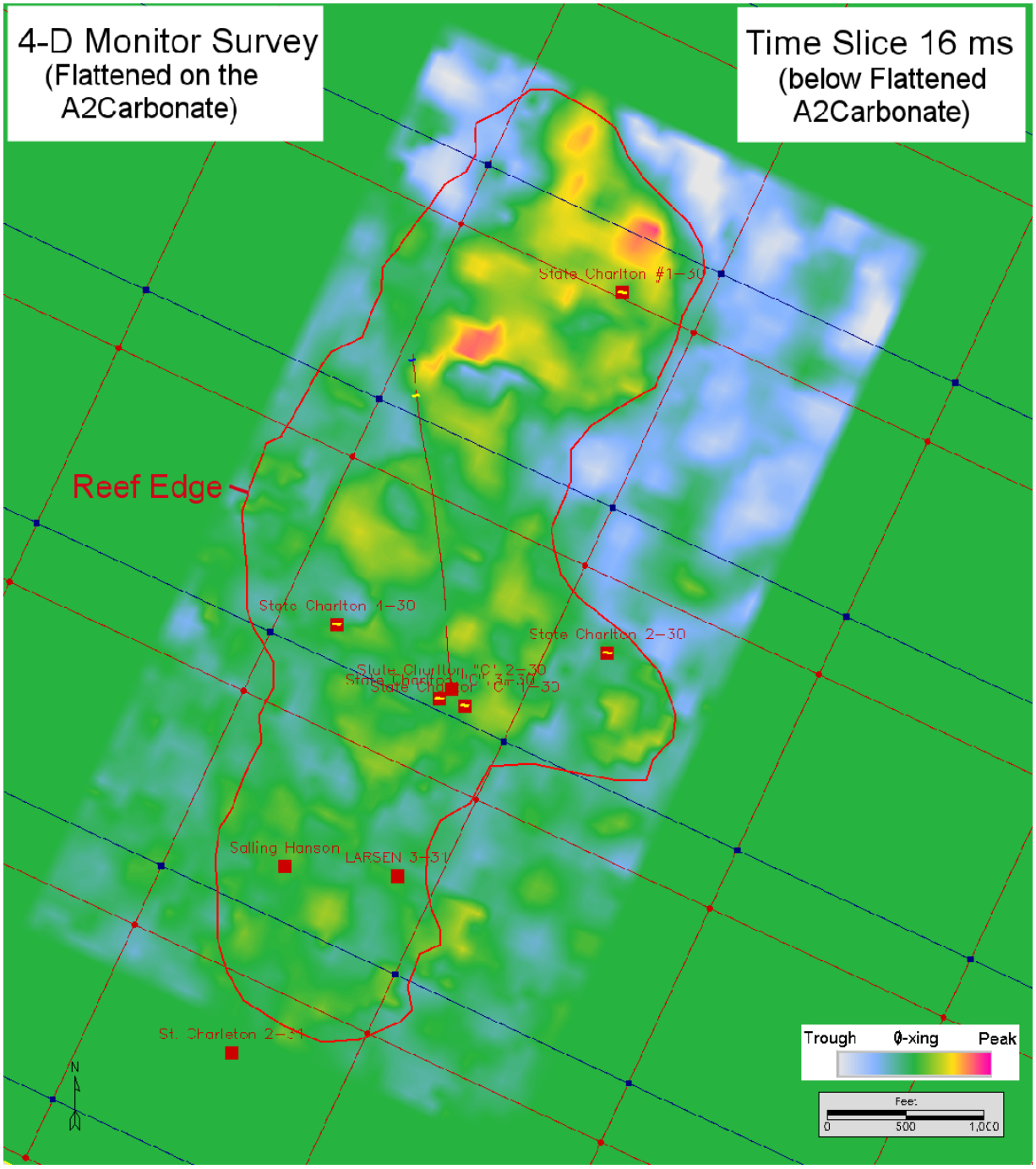
4-D Monitor Survey
(Flattened on the
A2Carbonate)
Time Slice 16 ms
(below Flattened
A2Carbonate)
State Charlton #1-30
Reef Edge
State Charlton 1-30
State Charlton 2-30
Salling Hanson
LARSEN 3-31
St. Charleton 2-31
N
Trough
0-xing
Peak
Fee:
0
500
1,000

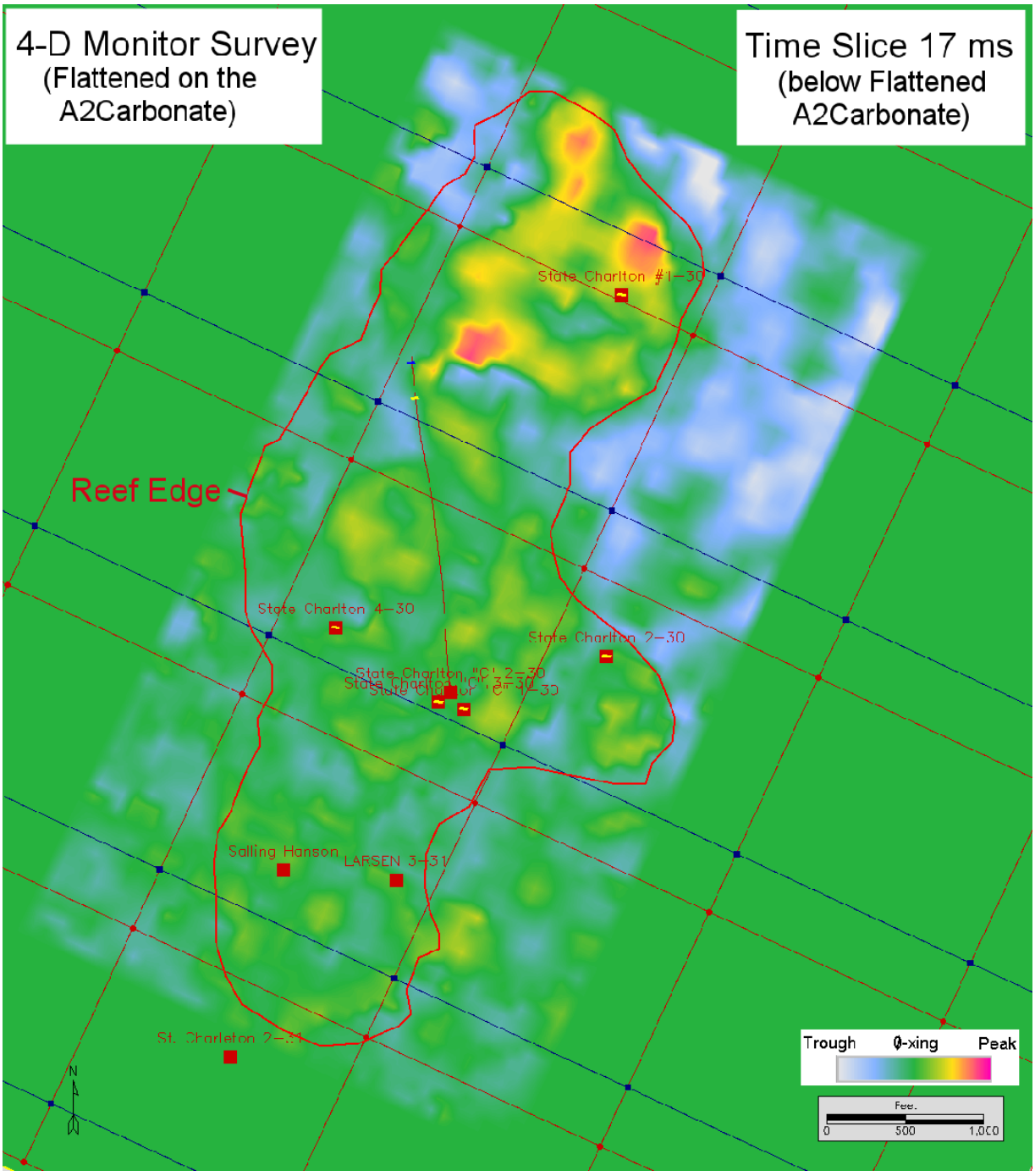
4-D Monitor Survey
(Flattened on the
A2Carbonate)
Time Slice 17 ms
(below Flattened
A2Carbonate)
State Charlton #1-30
Reef Edge
State Charlton 4-30
State Charlton 2-30
Salling Hanson
LARSEN 3-31
Trough
0-xing
Peak
Feet
0
500
1,000
N

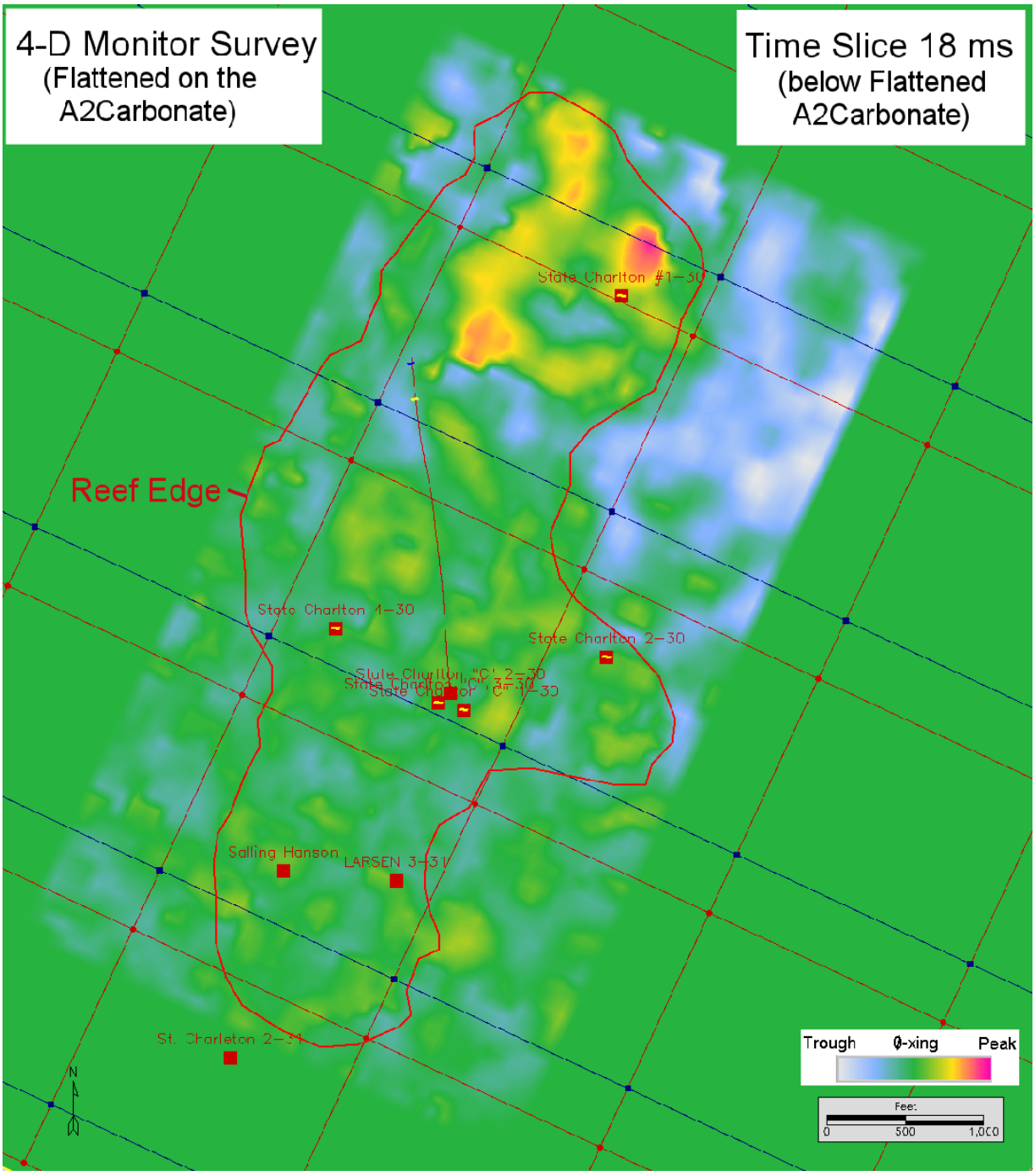
4-D Monitor Survey
(Flattened on the
A2Carbonate)
Time Slice 18 ms
(below Flattened
A2Carbonate)
State Charlton #1-30
Reef Edge
State Charlton 1-30
State Charlton 2-30
Salling Hanson
LARSEN 3-31
St. Charleton 2-31
Trough
0-xing
Peak
Fee:
0
500
1,000
N

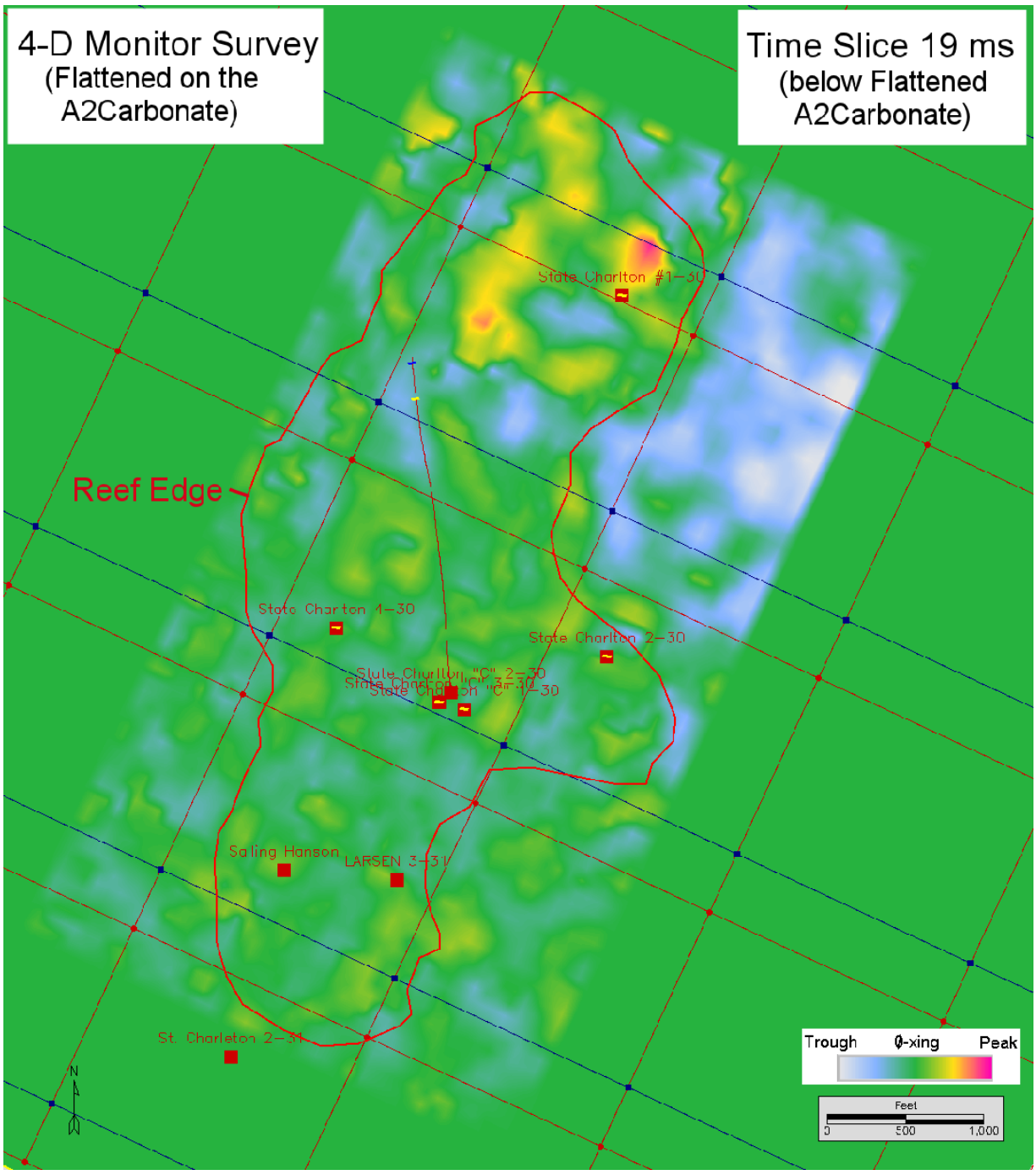
4-D Monitor Survey
(Flattened on the
A2Carbonate)
Time Slice 19 ms
(below Flattened
A2Carbonate)
State Charlton #1-30
Reef Edge
State Charlton 1-30
State Charlton 2-30
Saling Hanson
LARSEN 3-31
St. Charleton 2-31
N
Trough
0-xing
Peak
Feet
0
500
1,000

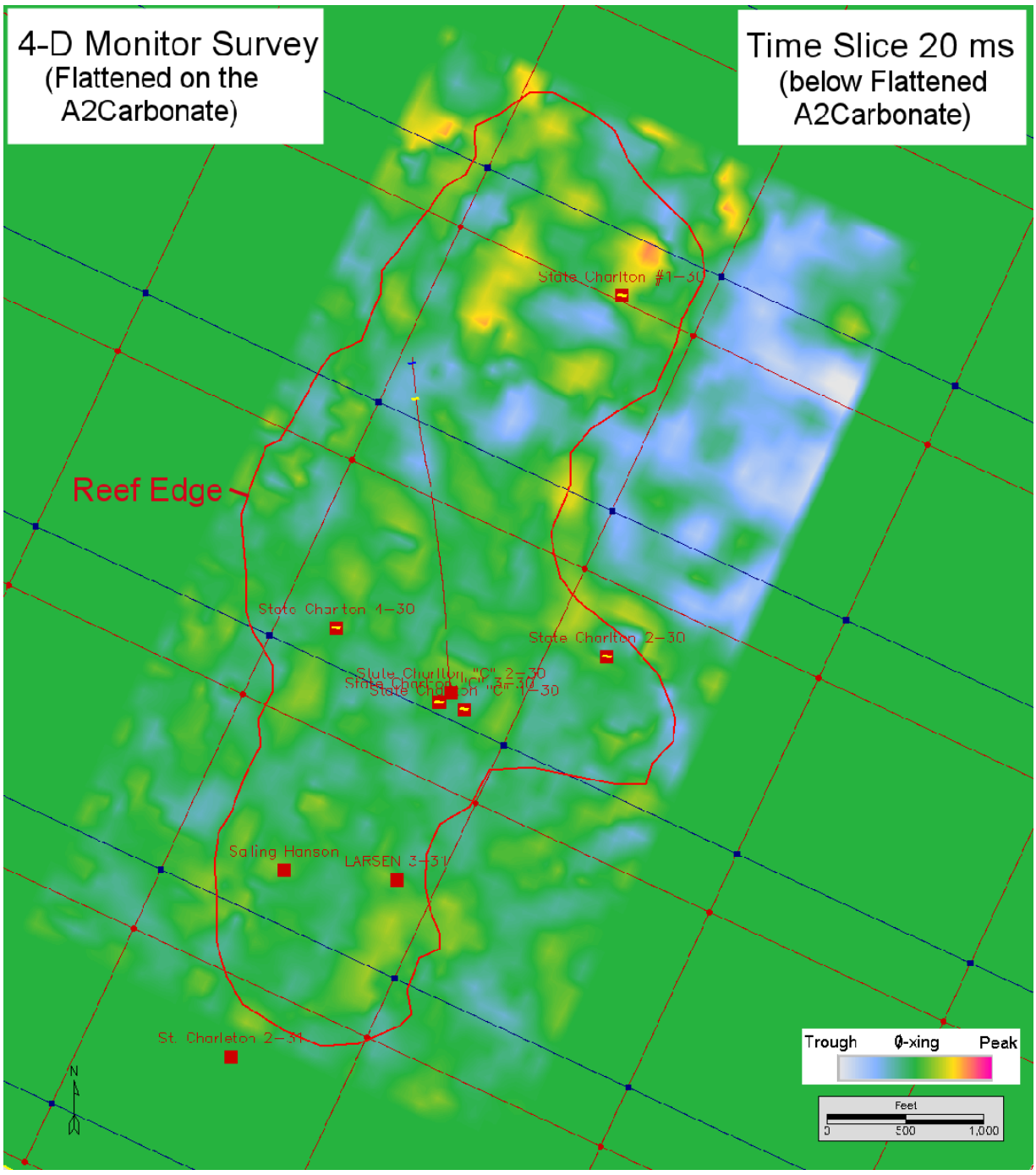
4-D Monitor Survey
(Flattened on the
A2Carbonate)
Time Slice 20 ms
(below Flattened
A2Carbonate)
State Charlton #1-30
Reef Edge
State Charlton 1-30
State Charlton 2-30
Sling Hanson
LARSEN 3-31
St. Charleton 2-31
N
Trough
0-xing
Peak
Feet
0
500
1,000

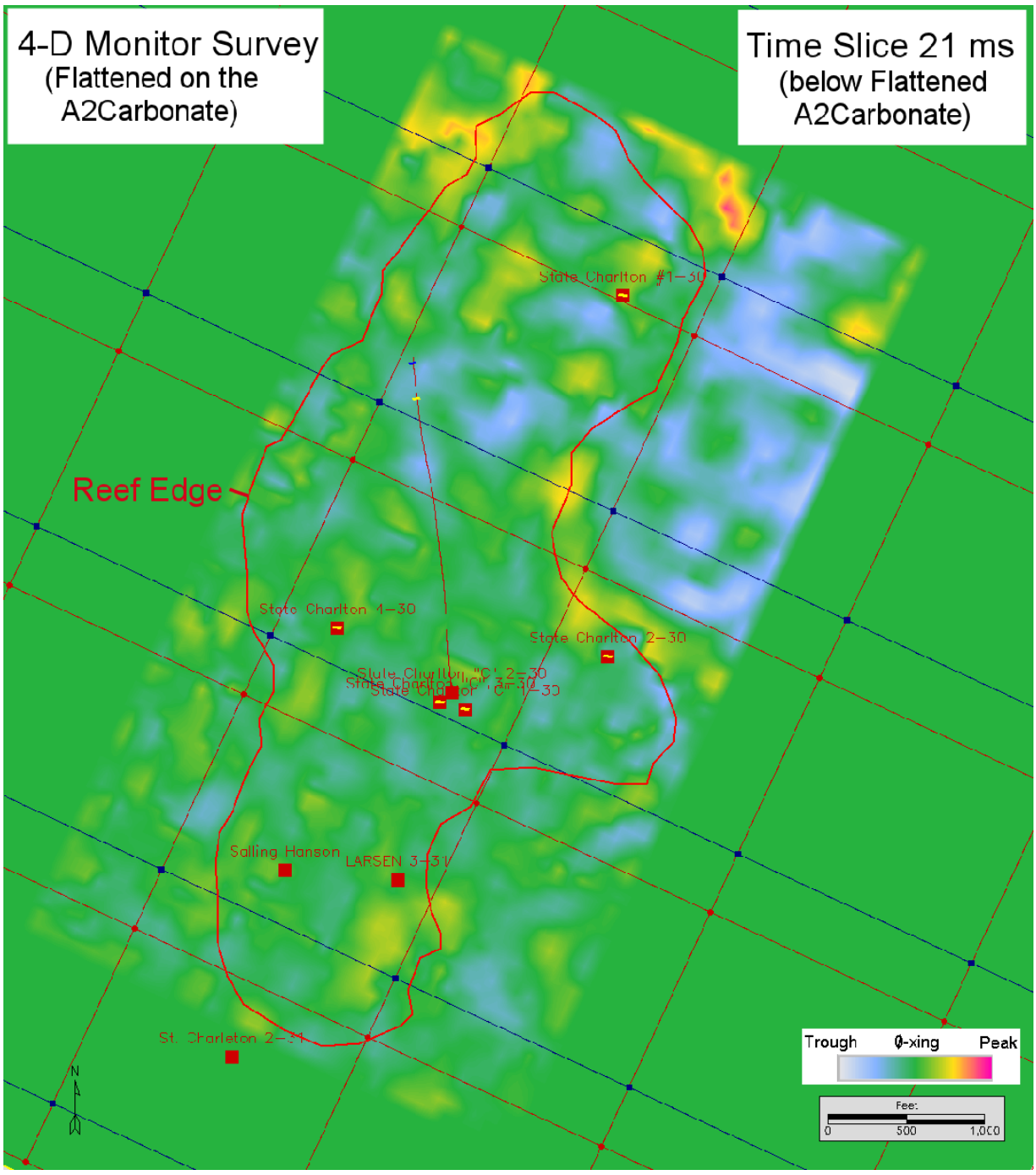
4-D Monitor Survey
(Flattened on the
A2Carbonate)
Time Slice 21 ms
(below Flattened
A2Carbonate)
State Charlton #1-30
Reef Edge
State Charlton 1-30
State Charlton 2-30
Salling Hanson
LARSEN 3-31
St. Charleton 2-31
Trough
0-xing
Peak
Fee:
0
500
1,000
N

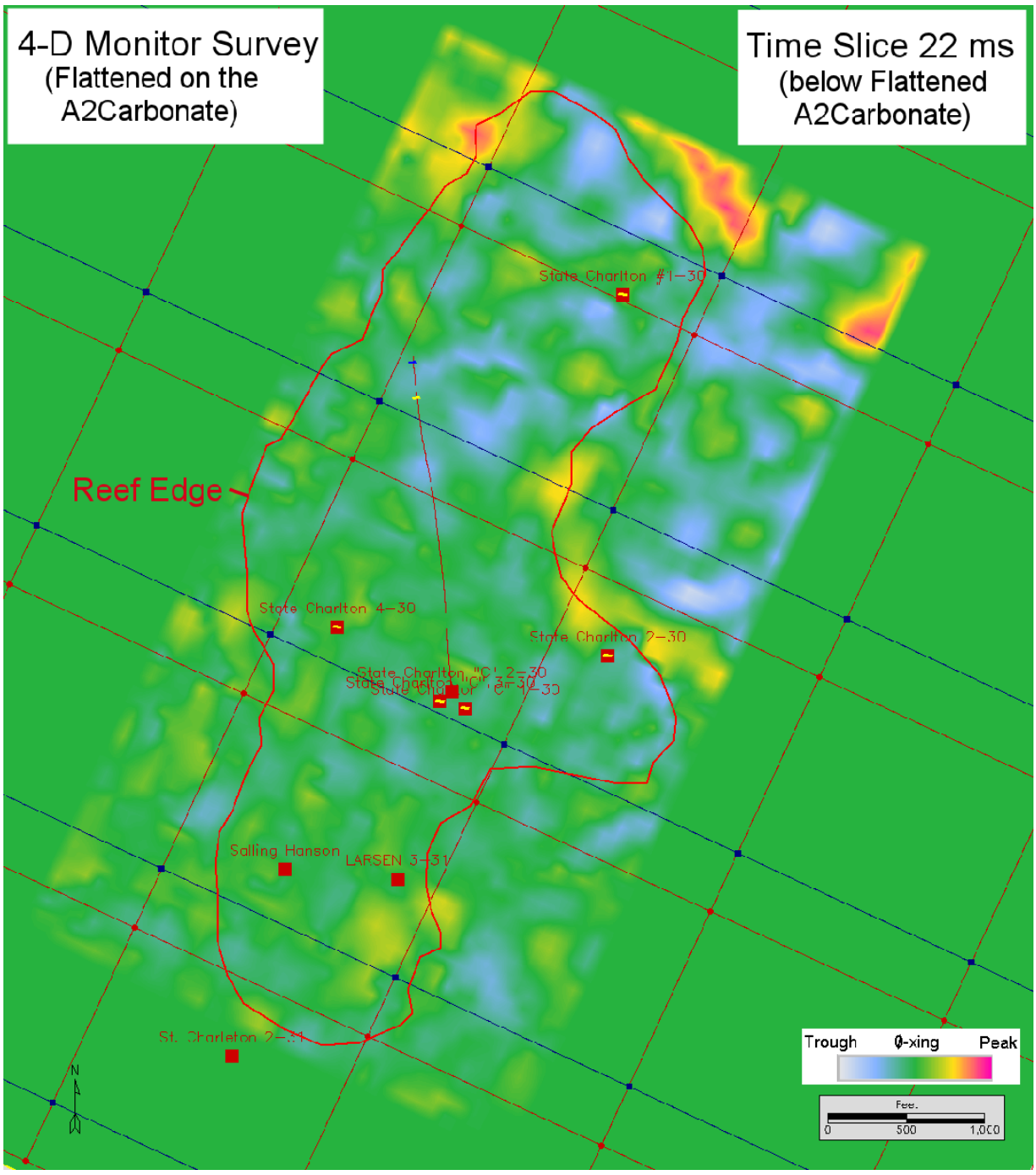
4-D Monitor Survey
(Flattened on the
A2Carbonate)
Time Slice 22 ms
(below Flattened
A2Carbonate)
State Charlton #1-30
Reef Edge
State Charlton 4-30
State Charlton 2-30
Salling Hanson
LARSEN 3-31
Trough
0-xing
Peak
Feet
0
500
1,000
N

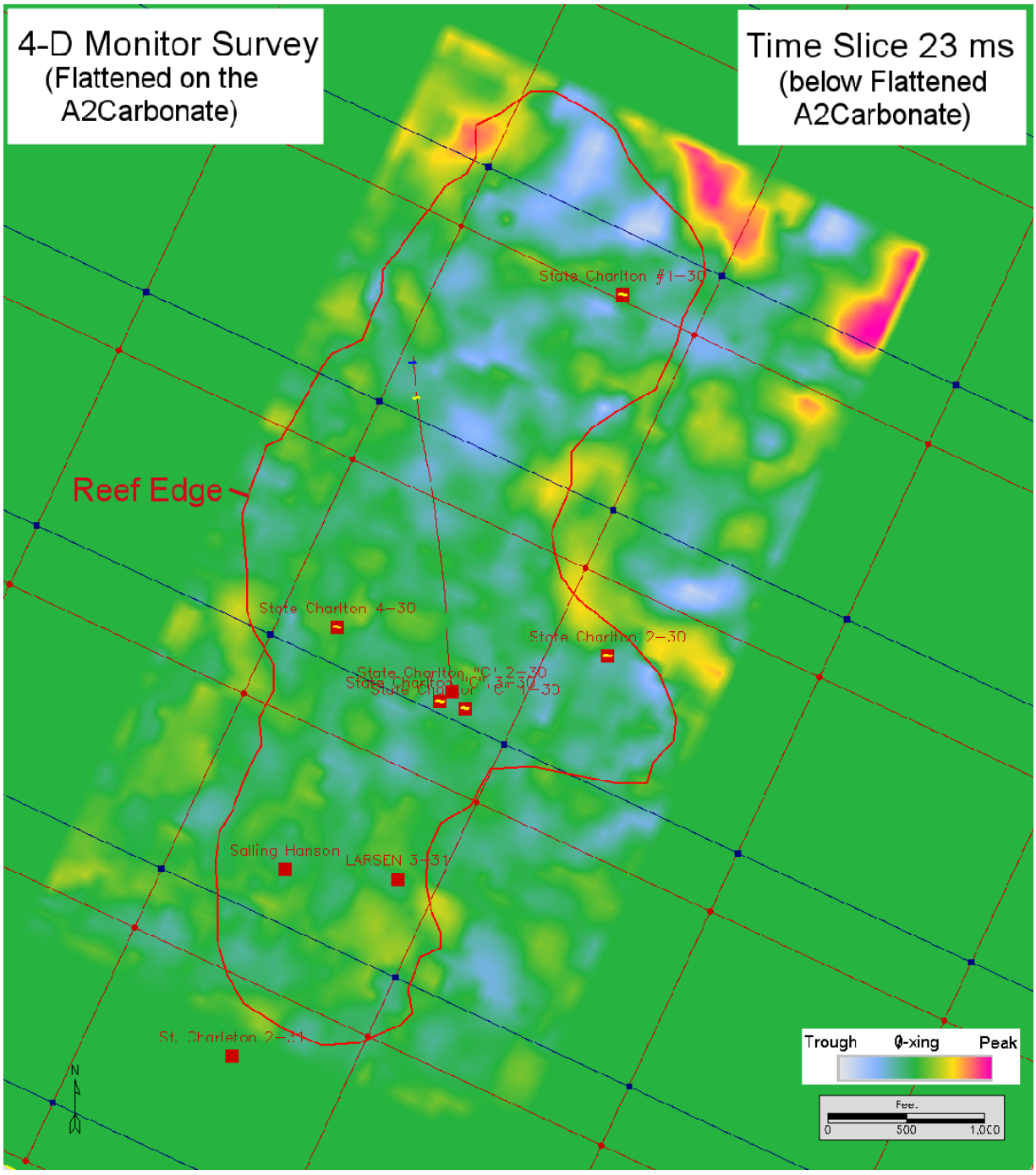
4-D Monitor Survey
(Flattened on the
A2Carbonate)
Time Slice 23 ms
(below Flattened
A2Carbonate)
State Charlton #1-30
Reef Edge
State Charlton 4-30
State Charlton 2-30
Salling Hanson
LARSEN 3-31
Trough
0-xing
Peak
Feet
0
500
1,000
N

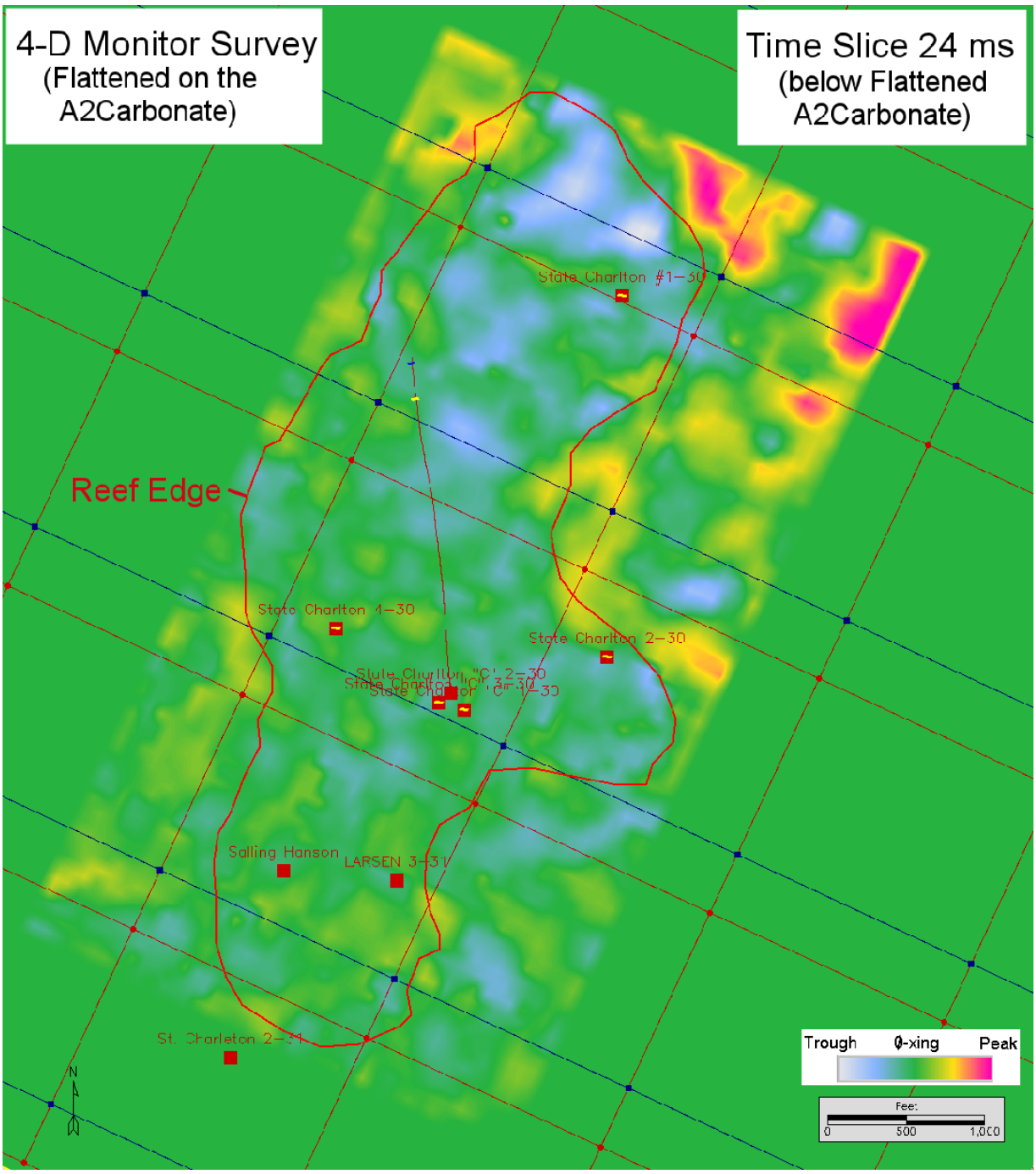
4-D Monitor Survey
(Flattened on the
A2Carbonate)
Time Slice 24 ms
(below Flattened
A2Carbonate)
State Charlton #1-30
Reef Edge
State Charlton 1-30
State Charlton 2-30
Salling Hanson
LARSEN 3-31
St. Charleton 2-31
N
Trough
0-xing
Peak
Fee:
0
500
1,000

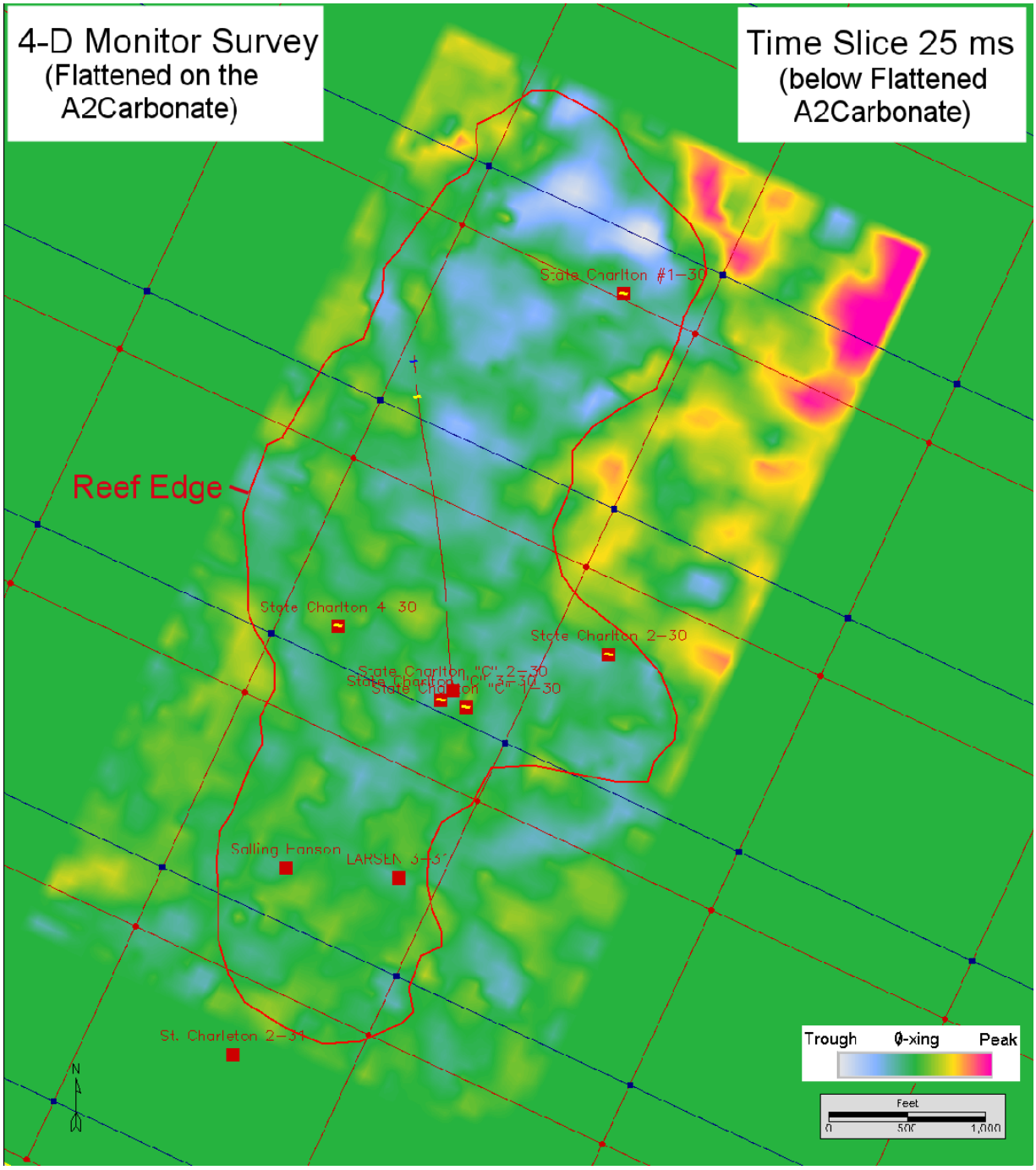
4-D Monitor Survey
(Flattened on the
A2Carbonate)
Time Slice 25 ms
(below Flattened
A2Carbonate)
State Charlton #1-30
Reef Edge
State Charlton 4 30
State Charlton 2-30
Salling Hanson
St. Charleton 2-31
Trough
0-xing
Peak
Feet
0
500
1,000
N

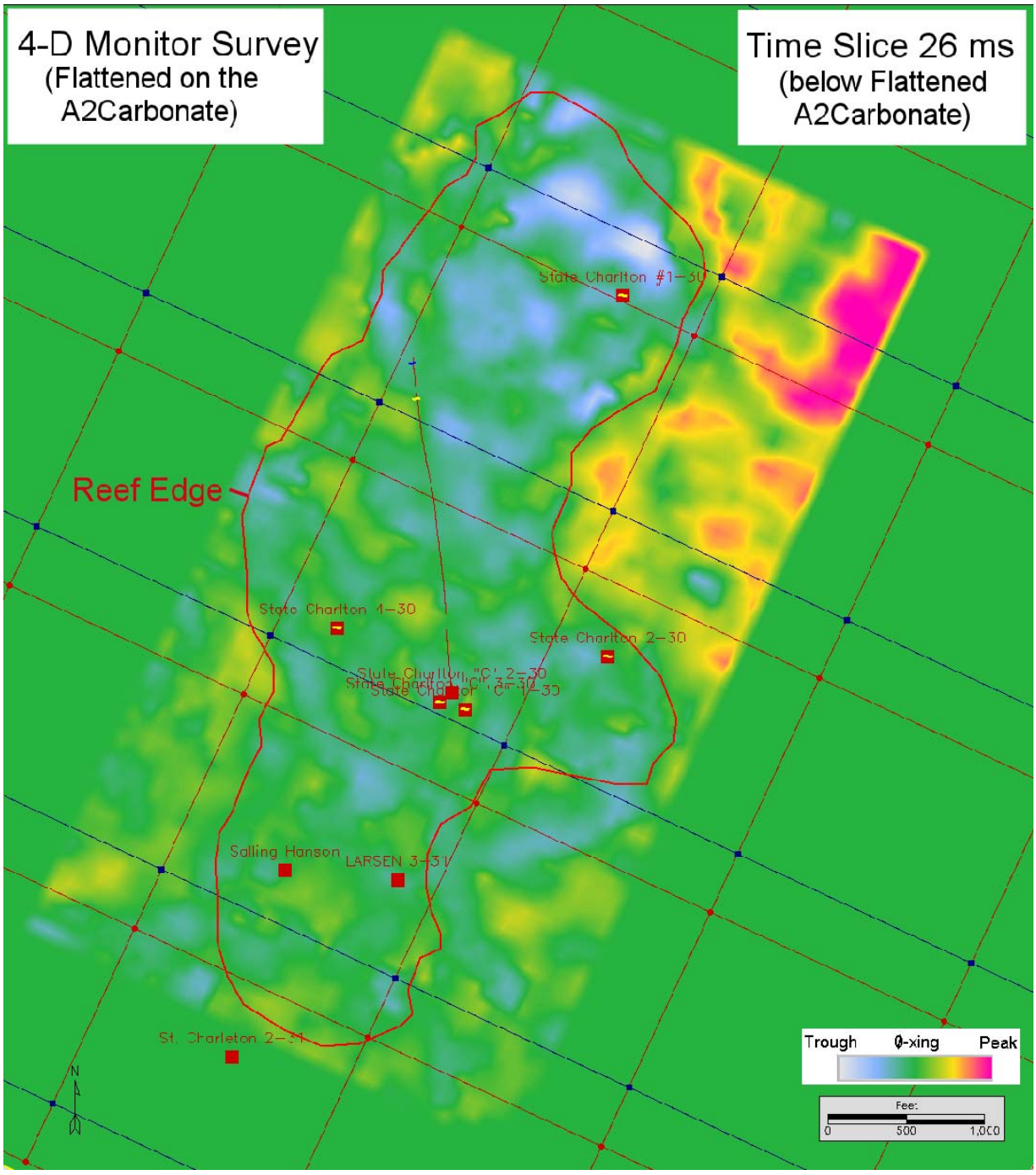
4-D Monitor Survey
(Flattened on the
A2Carbonate)
Time Slice 26 ms
(below Flattened
A2Carbonate)
State Charlton #1-30
Reef Edge
State Charlton 1-30
State Charlton 2-30
Salling Hanson
LARSEN 3-31
St. Charleton 2-31
N
Trough
0-xing
Peak
Fee:
0
500
1,000

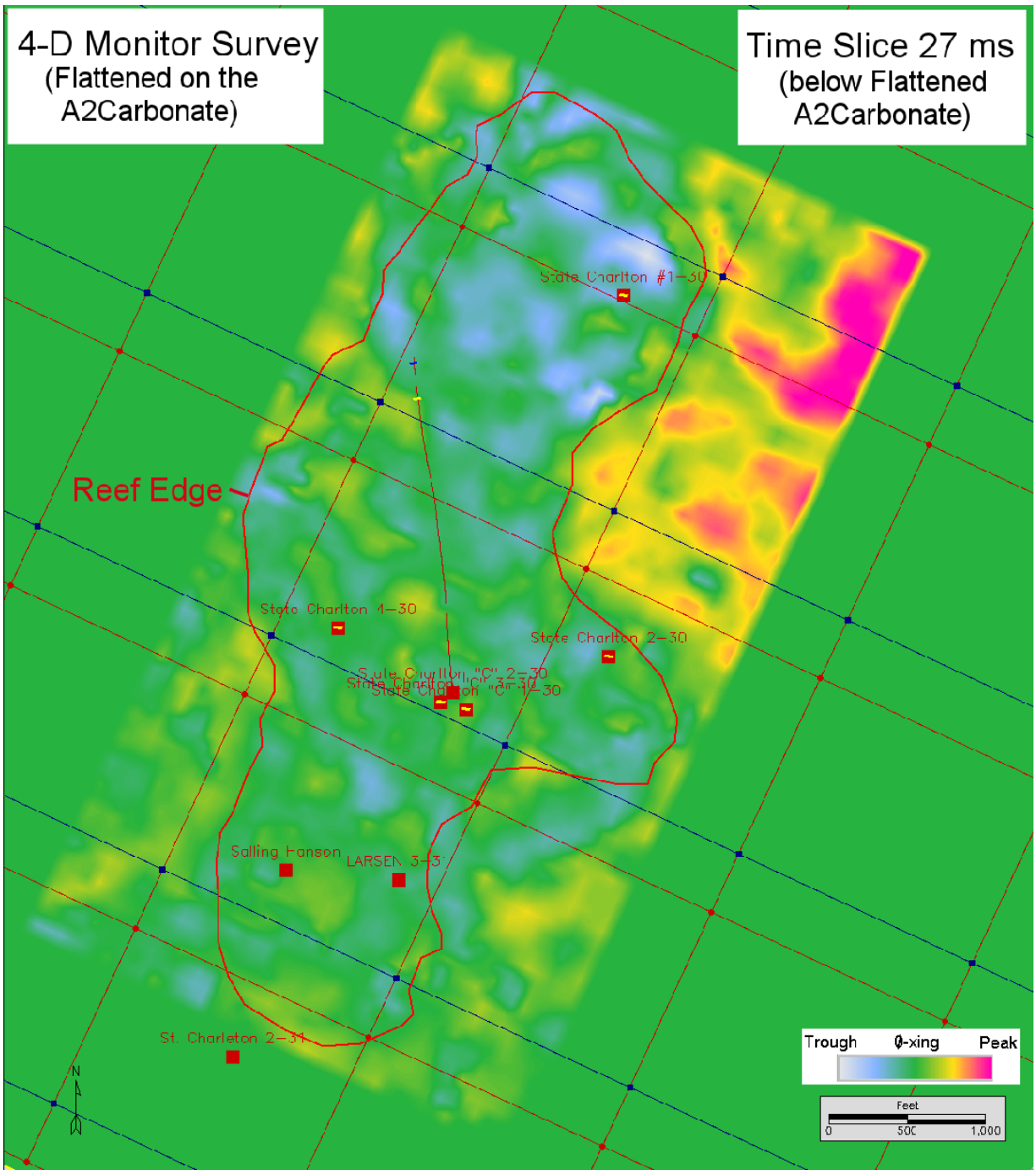
4-D Monitor Survey
(Flattened on the
A2Carbonate)
Time Slice 27 ms
(below Flattened
A2Carbonate)
State Charlton #1-30
Reef Edge
State Charlton 1-30
State Charlton 2-30
Salling Hanson
LARSEN 3-3
St. Charleton 2-31
Trough
0-xing
Peak
Feet
0
500
1,000
N

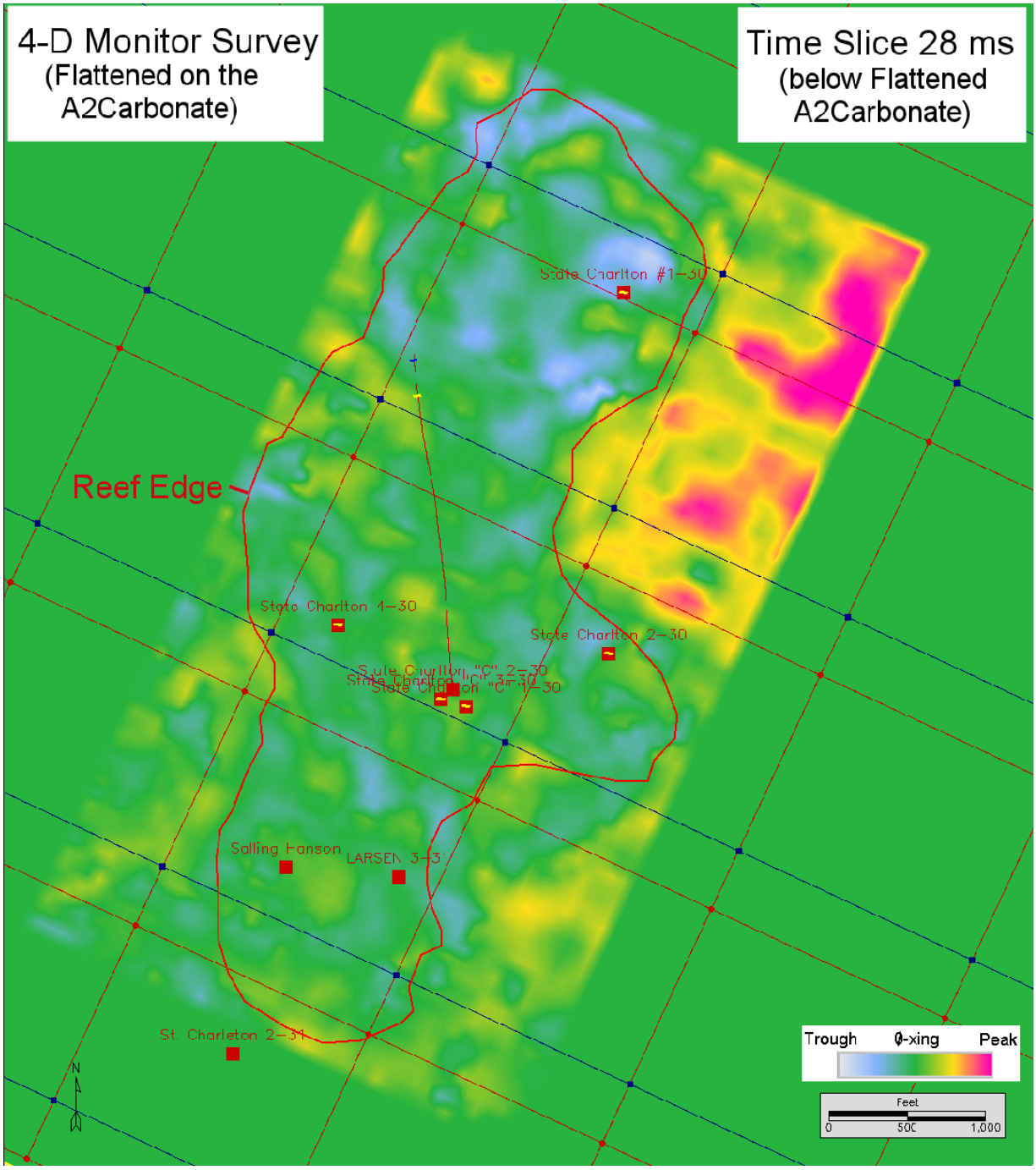
4-D Monitor Survey
(Flattened on the
A2Carbonate)
Time Slice 28 ms
(below Flattened
A2Carbonate)
Reef Edge
State Charlton #1-30
State Charlton 1-30
State Charlton 2-30
Salling Hanson
LARSEN 3-31
St. Charleton 2-31
Trough
0-xing
Peak
Feet
0
500
1,000
N

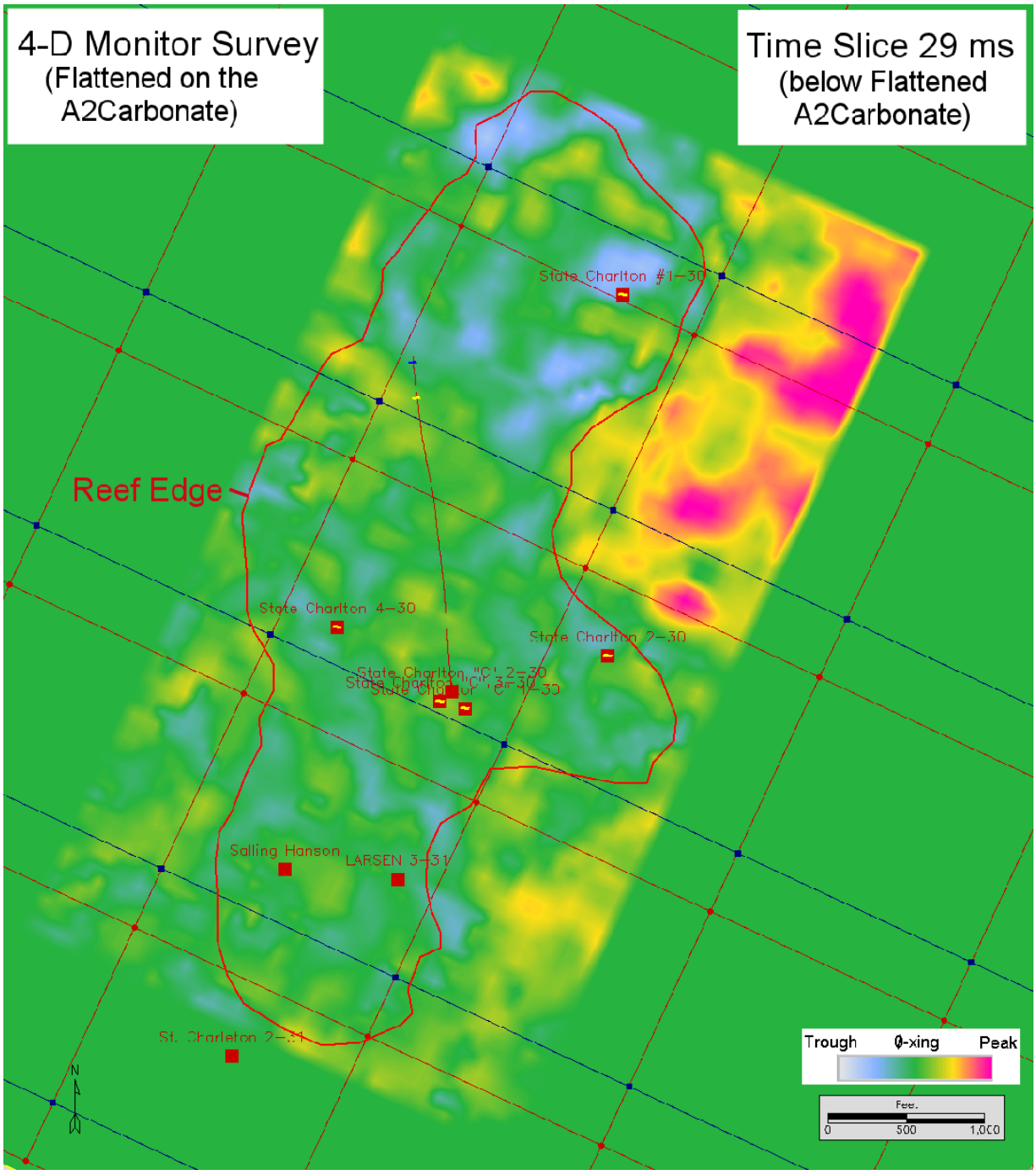
4-D Monitor Survey
(Flattened on the
A2Carbonate)
Time Slice 29 ms
(below Flattened
A2Carbonate)
State Charlton #1-30
Reef Edge
State Charlton 4-30
State Charlton 2-30
Salling Hanson
LARSEN 3-31
Trough
0-xing
Peak
N
0
500
1,000

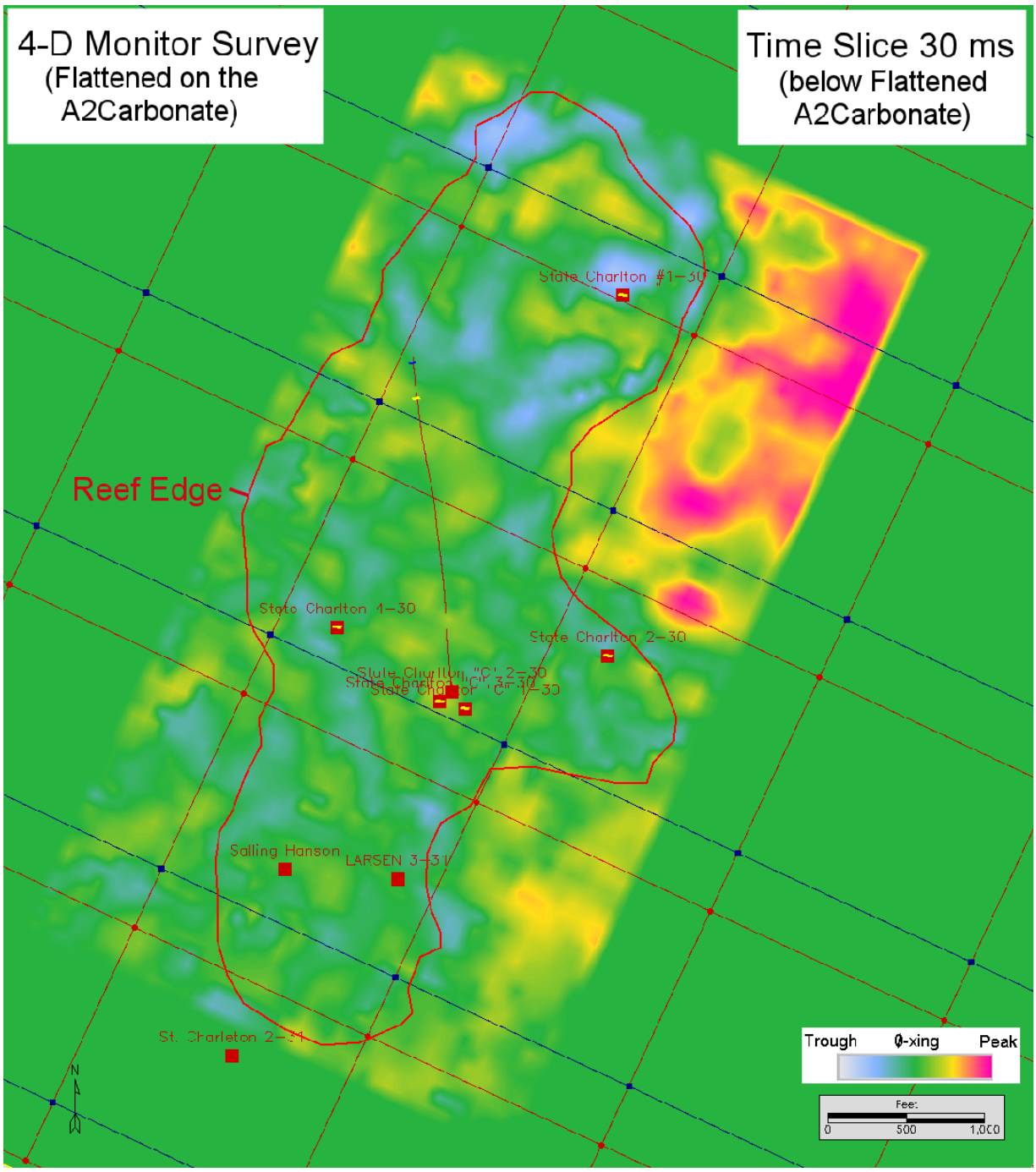
4-D Monitor Survey
(Flattened on the
A2Carbonate)
Time Slice 30 ms
(below Flattened
A2Carbonate)
State Charlton #1-30
Reef Edge
State Charlton 1-30
State Charlton 2-30
Salling Hanson
LARSEN 3-31
St. Charleton 2-31
Trough
0-xing
Peak
Fee:
0
500
1,000
N

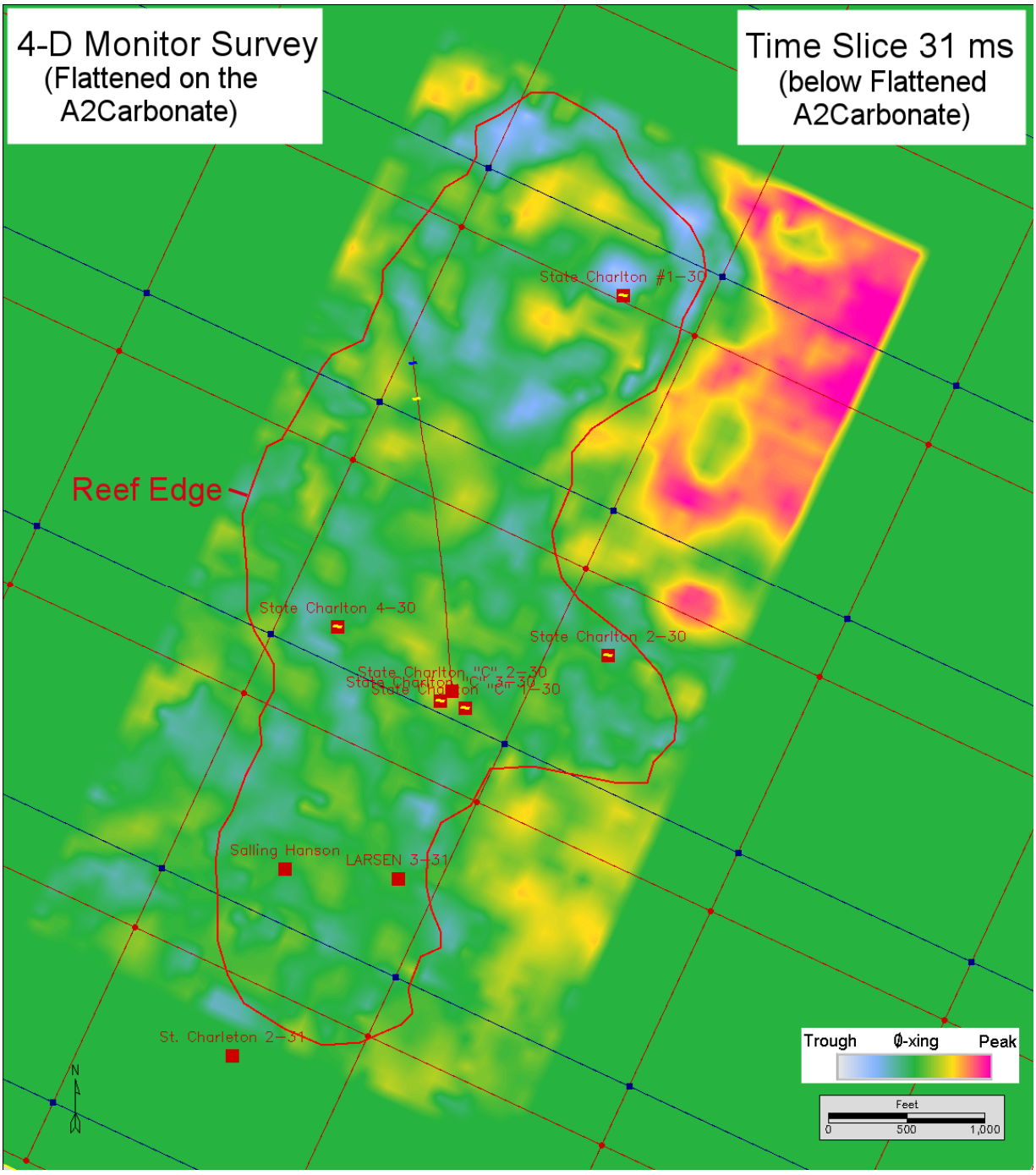
4-D Monitor Survey
(Flattened on the
A2Carbonate)
Time Slice 31 ms
(below Flattened
A2Carbonate)
State Charlton #1-30
Reef Edge
State Charlton 4-30
State Charlton 2-30
State Charlton "C" 2-30
Salling Hanson
LARSEN 3-31
St. Charleton 2-31
N
Trough
Ø-xing
Peak
Feet
0
500
1,000

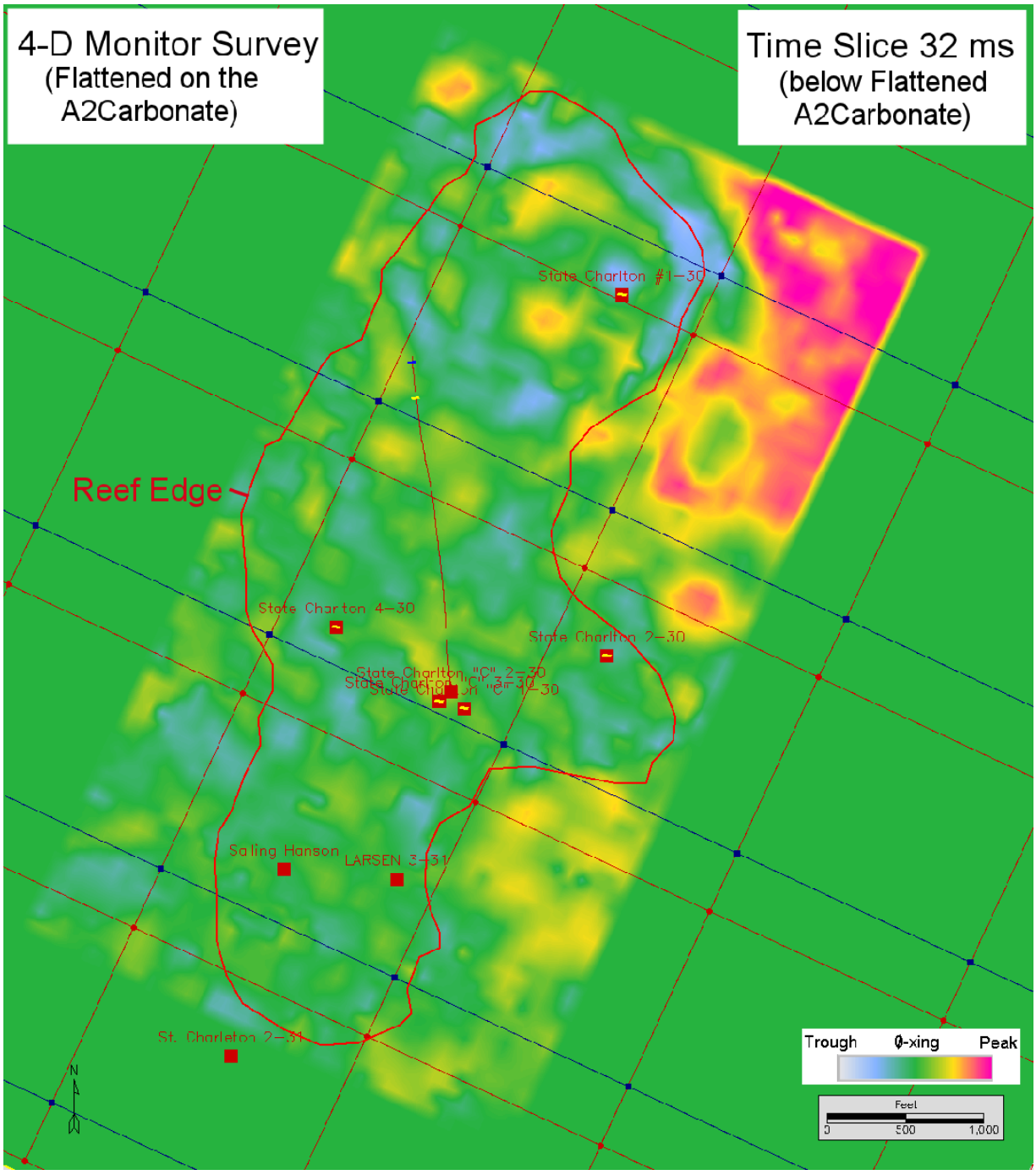
4-D Monitor Survey
(Flattened on the
A2Carbonate)
Time Slice 32 ms
(below Flattened
A2Carbonate)
State Charlton #1-30
Reef Edge
State Charlton 4-30
State Charlton 2-30
State Charlton "C" 2-30
Saling Hanson
LARSEN 3-31
St. Charleton 2-31
N
Trough
0-xing
Peak
Feet
0
500
1,000

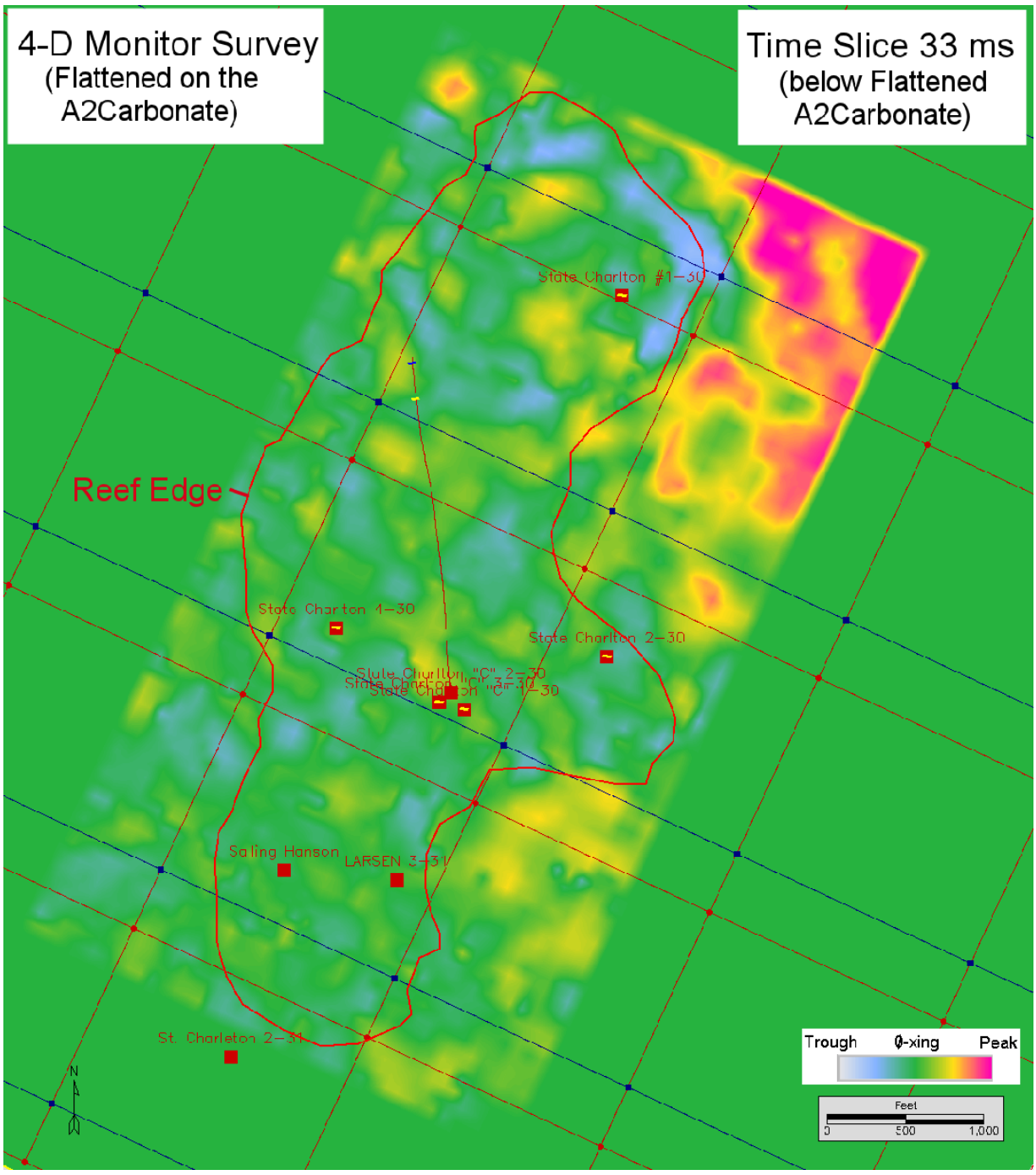
4-D Monitor Survey
(Flattened on the
A2Carbonate)
Time Slice 33 ms
(below Flattened
A2Carbonate)
State Charlton #1-30
Reef Edge
State Charlton 1-30
State Charlton 2-30
Saling Hanson
LARSEN 3-31
St. Charleton 2-31
N
Trough
0-xing
Peak
Feet
0
500
1,000

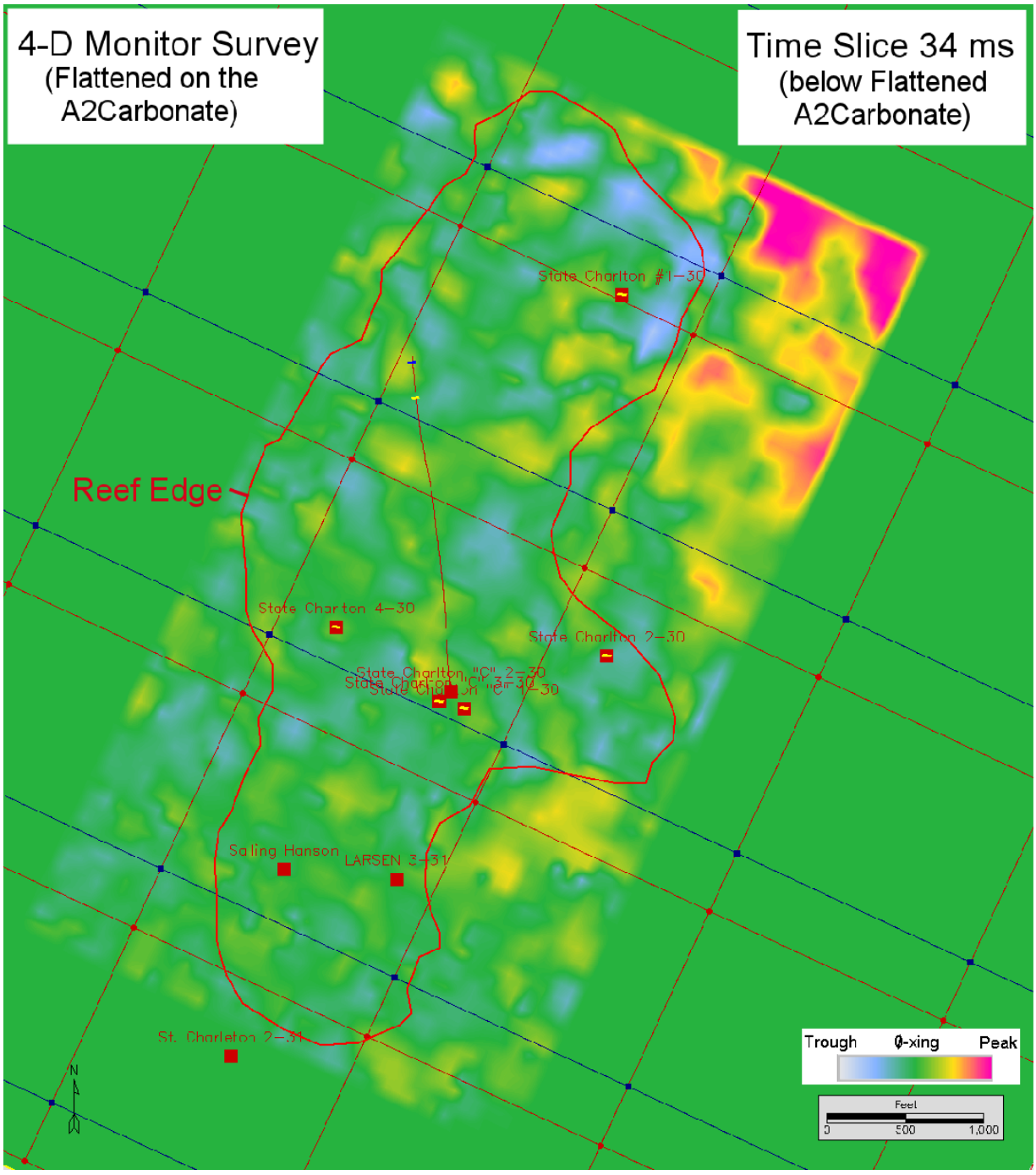
4-D Monitor Survey
(Flattened on the
A2Carbonate)
Time Slice 34 ms
(below Flattened
A2Carbonate)
State Charlton #1-30
Reef Edge
State Charlton 4-30
State Charlton 2-30
Saling Hanson
LARSEN 3-31
St. Charleton 2-31
N
Trough
0-xing
Peak
Feet
0
500
1,000

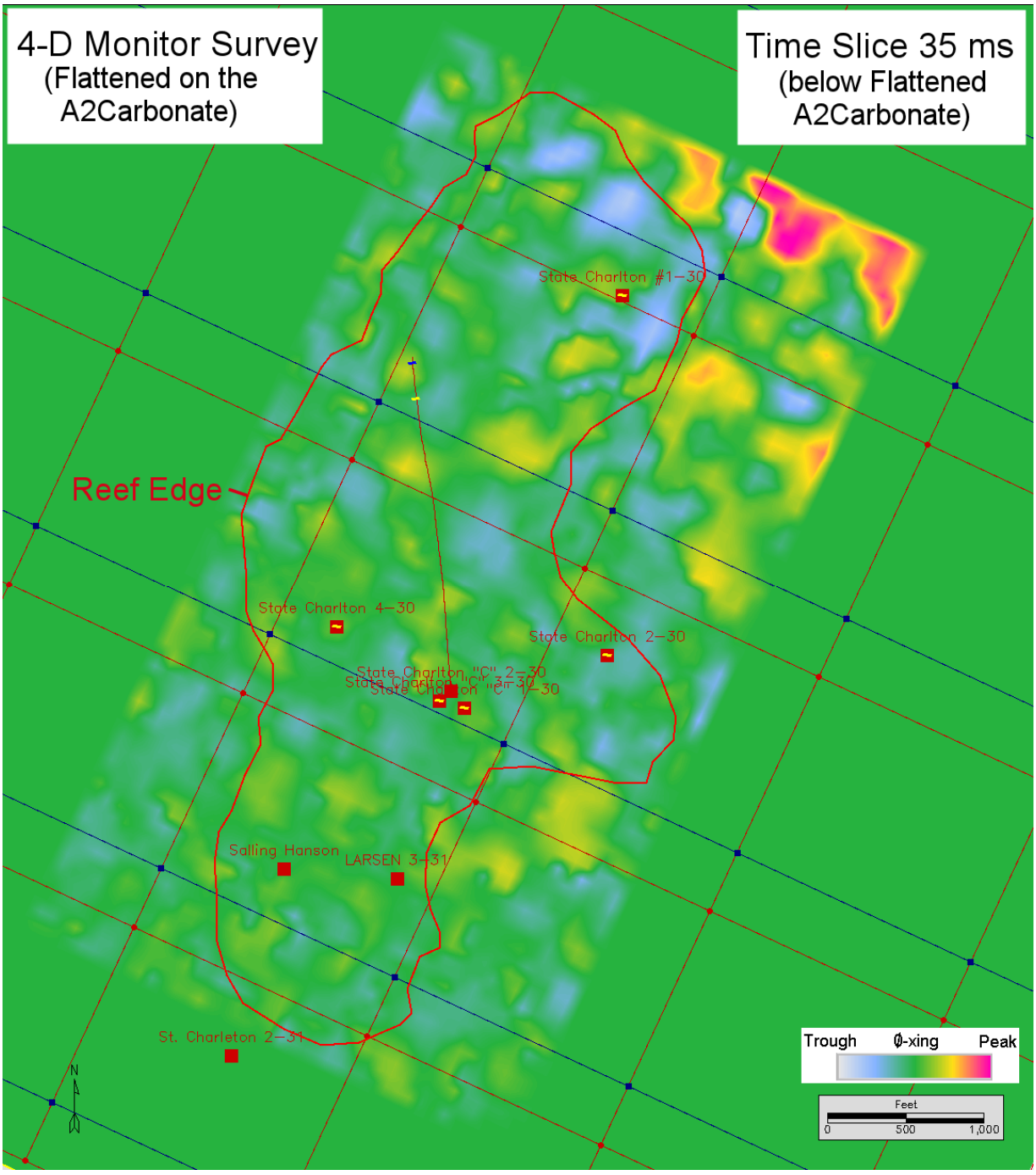
4-D Monitor Survey
(Flattened on the
A2Carbonate)
Time Slice 35 ms
(below Flattened
A2Carbonate)
State Charlton #1-30
Reef Edge
State Charlton 4-30
State Charlton 2-30
State Charlton "C" 2-30
State Charlton "C" 3-30
State Charlton "C" 1-30
Salling Hanson
LARSEN 3-31
St. Charleton 2-31
N
Trough
Ø-xing
Peak
Feet
0
500
1,000

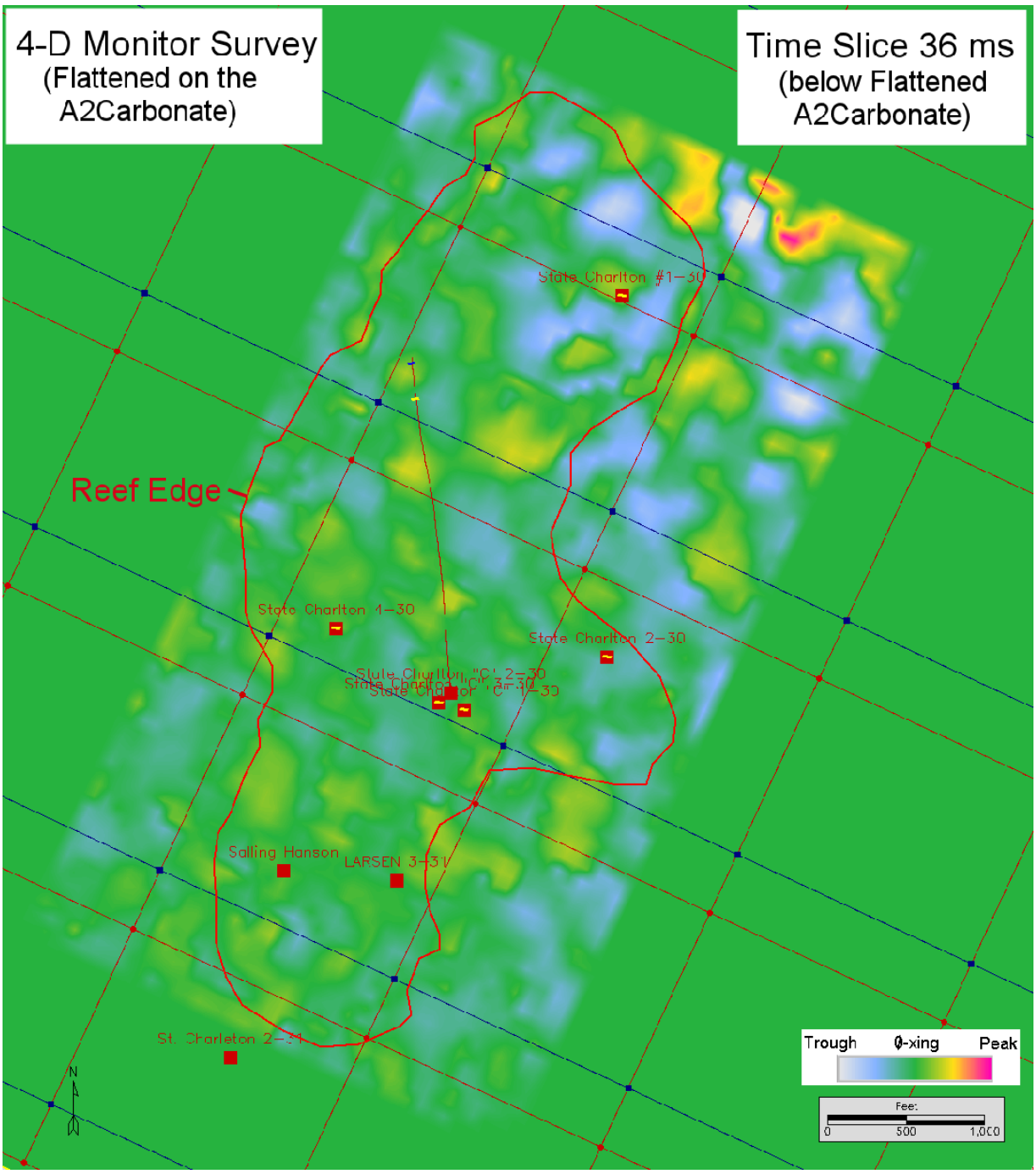
4-D Monitor Survey
(Flattened on the
A2Carbonate)
Time Slice 36 ms
(below Flattened
A2Carbonate)
State Charlton #1-30
Reef Edge
State Charlton 1-30
State Charlton 2-30
Salling Hanson
LARSEN 3-31
St. Charleton 2-31
N
Trough
0-xing
Peak
Fee:
0
500
1,000

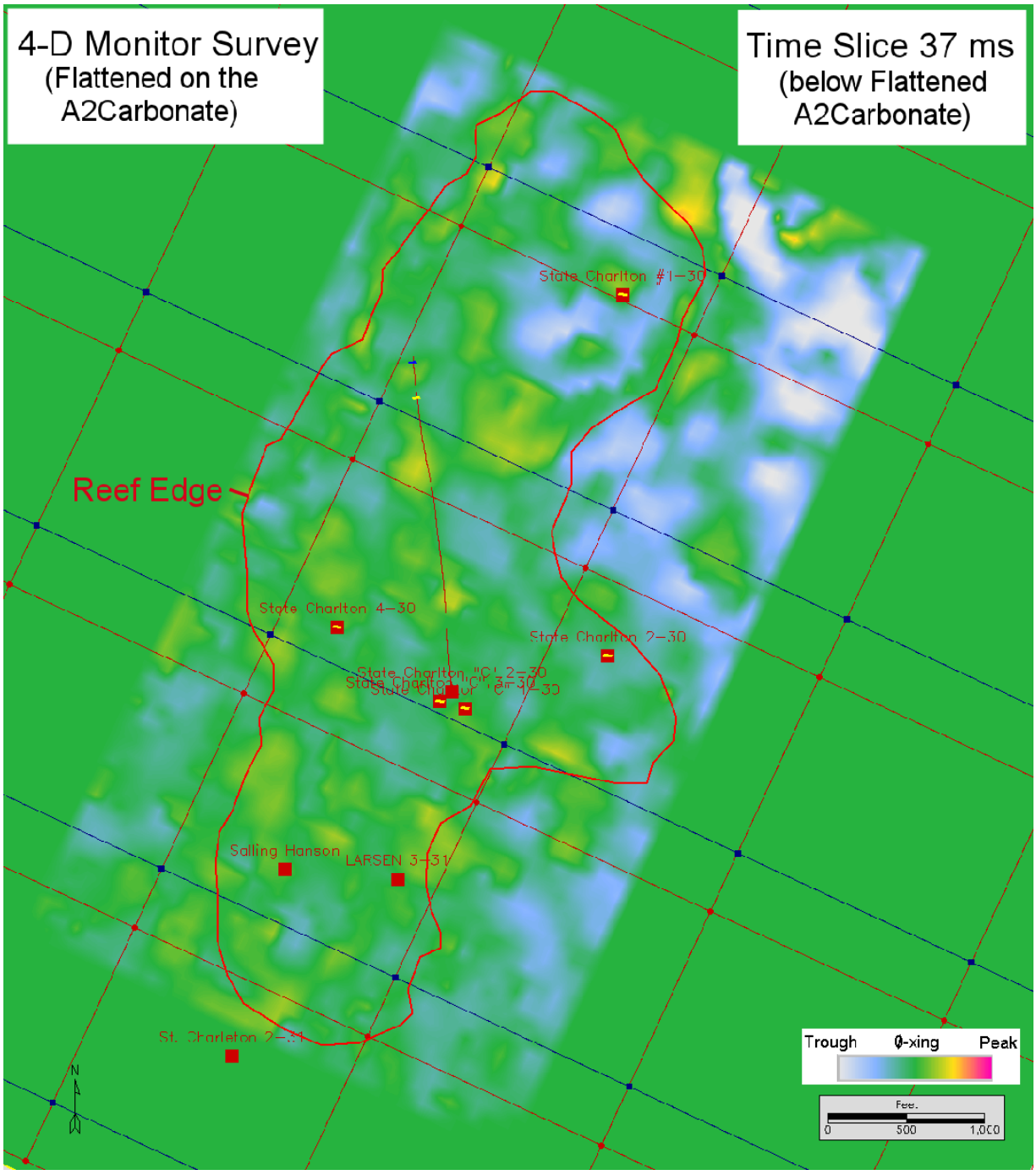
4-D Monitor Survey
(Flattened on the
A2Carbonate)
Time Slice 37 ms
(below Flattened
A2Carbonate)
State Charlton #1-30
Reef Edge
State Charlton 4-30
State Charlton 2-30
Salling Hanson
LARSEN 3-31
Trough
0-xing
Peak
Feet
0
500
1,000
N

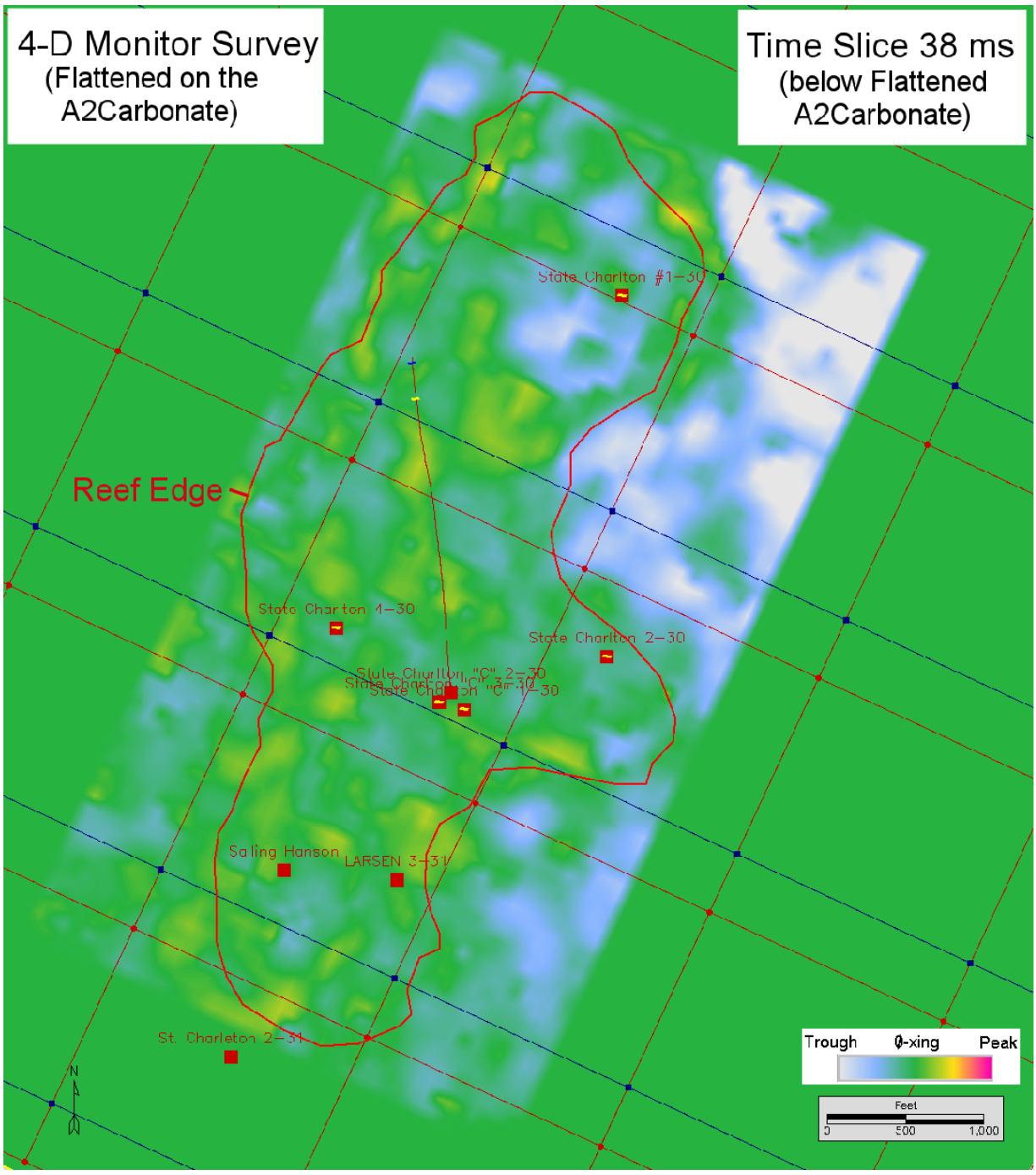
4-D Monitor Survey
(Flattened on the
A2Carbonate)
Time Slice 38 ms
(below Flattened
A2Carbonate)
State Charlton #1-30
Reef Edge
State Charlton 1-30
State Charlton 2-30
Sailing Hanson
LARSEN 3-31
St. Charleton 2-31
Trough
0-xing
Peak
Feet
0
500
1,000
N

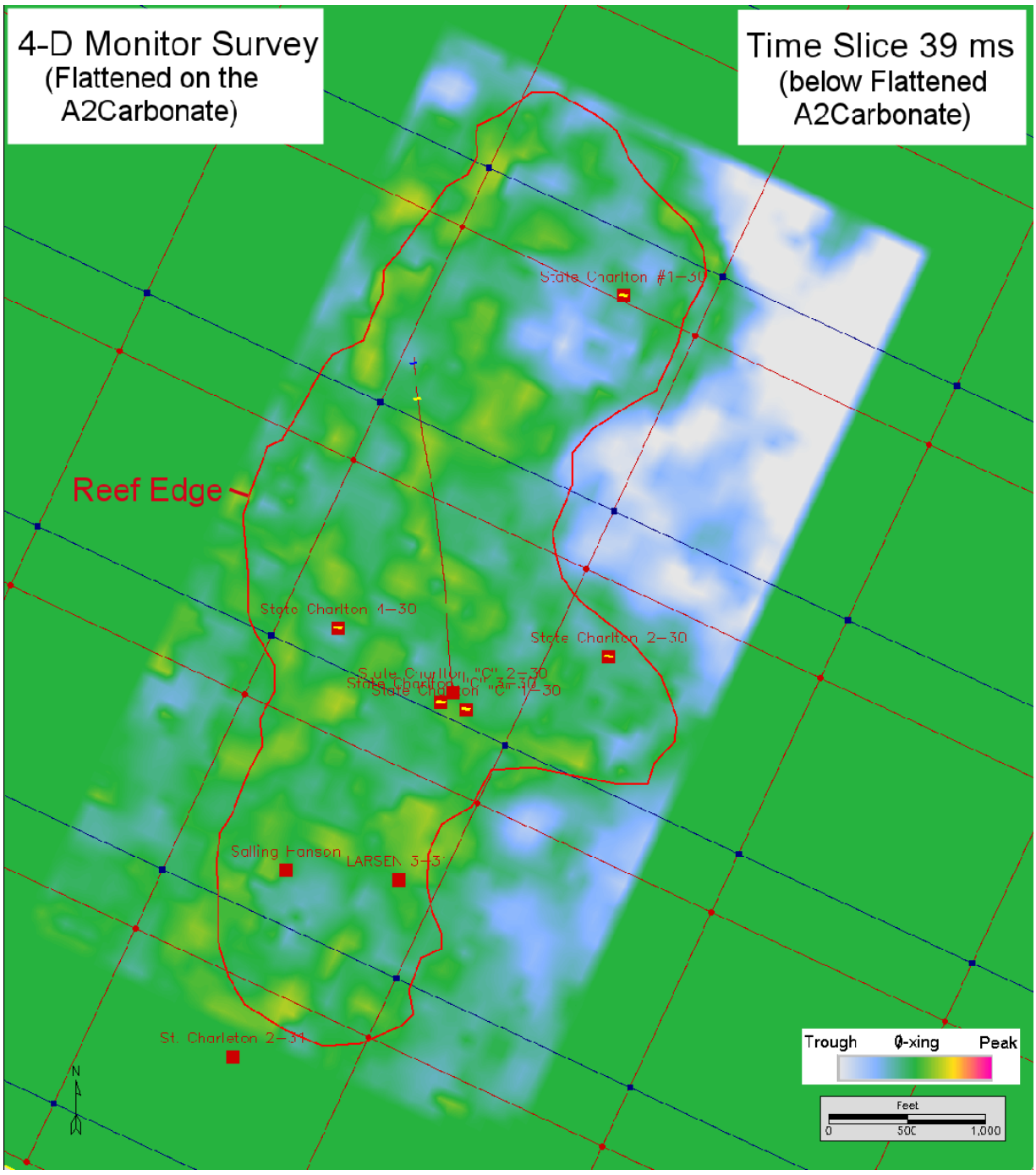
4-D Monitor Survey
(Flattened on the
A2Carbonate)
Time Slice 39 ms
(below Flattened
A2Carbonate)
State Charlton #1-30
Reef Edge
State Charlton 1-30
State Charlton 2-30
Salling Hanson
LARSEN 3-3
St. Charleton 2-31
Trough
0-xing
Peak
Feet
0
500
1,000
N

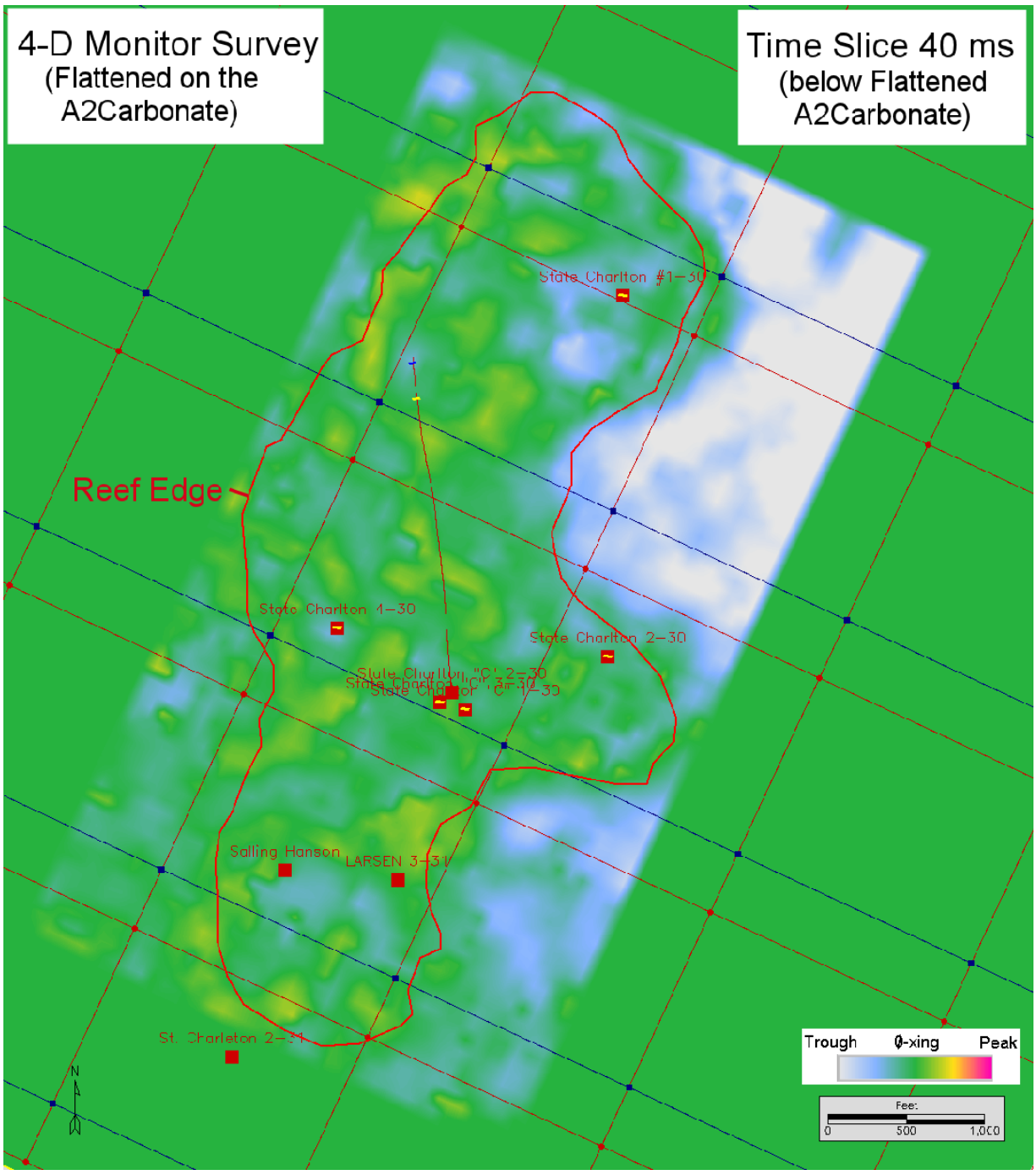
4-D Monitor Survey
(Flattened on the
A2Carbonate)
Time Slice 40 ms
(below Flattened
A2Carbonate)
State Charlton #1-30
Reef Edge
State Charlton 1-30
State Charlton 2-30
Salling Hanson
LARSEN 3-31
St. Charleton 2-31
Trough
0-xing
Peak
Fee:
0
500
1,000
N

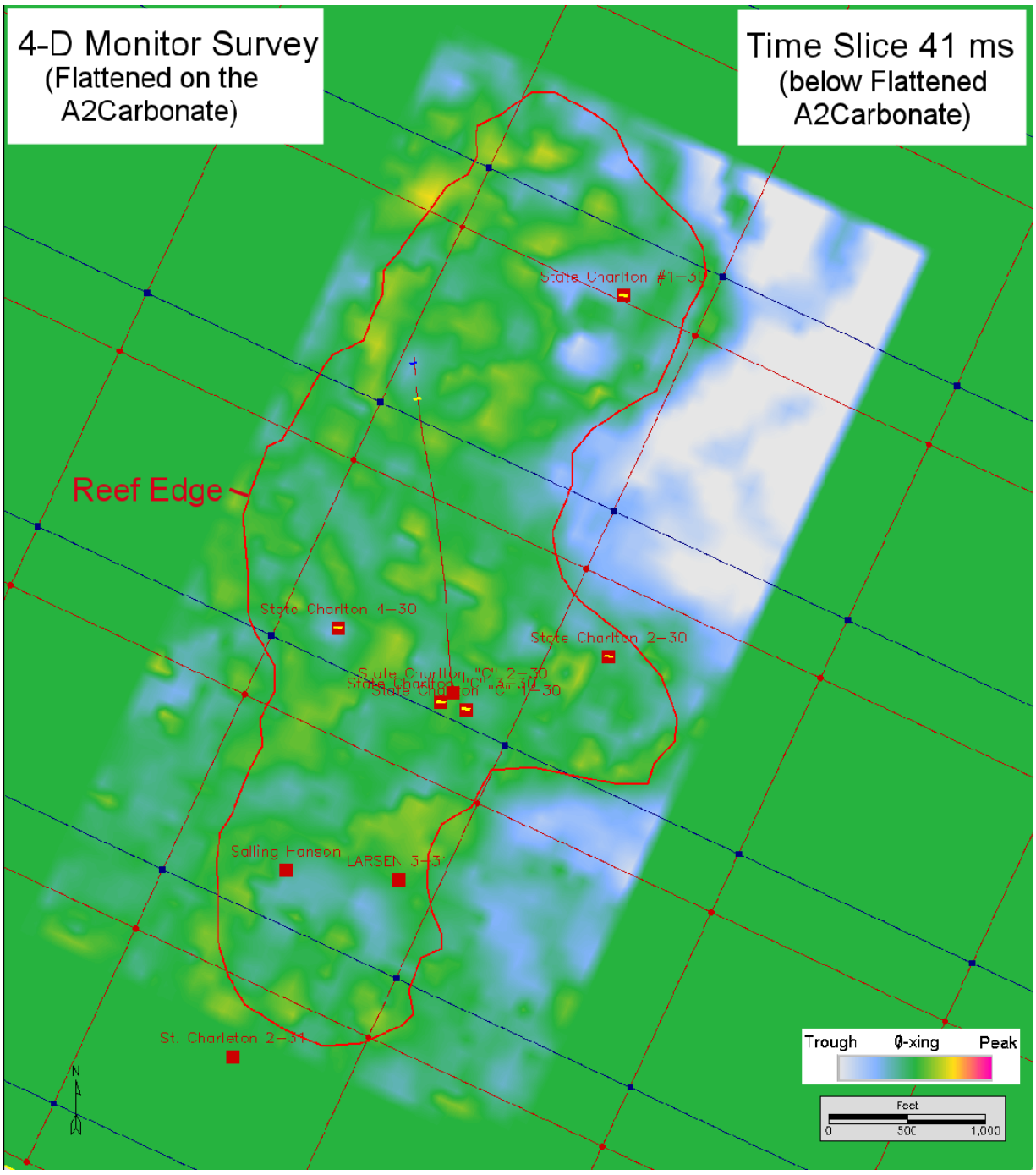
4-D Monitor Survey
(Flattened on the
A2Carbonate)
Time Slice 41 ms
(below Flattened
A2Carbonate)
State Charlton #1-30
Reef Edge
State Charlton 1-30
State Charlton 2-30
Salling Hanson
LARSEN 3-3
St. Charleton 2-31
Trough
0-xing
Peak
Feet
0
500
1,000
N

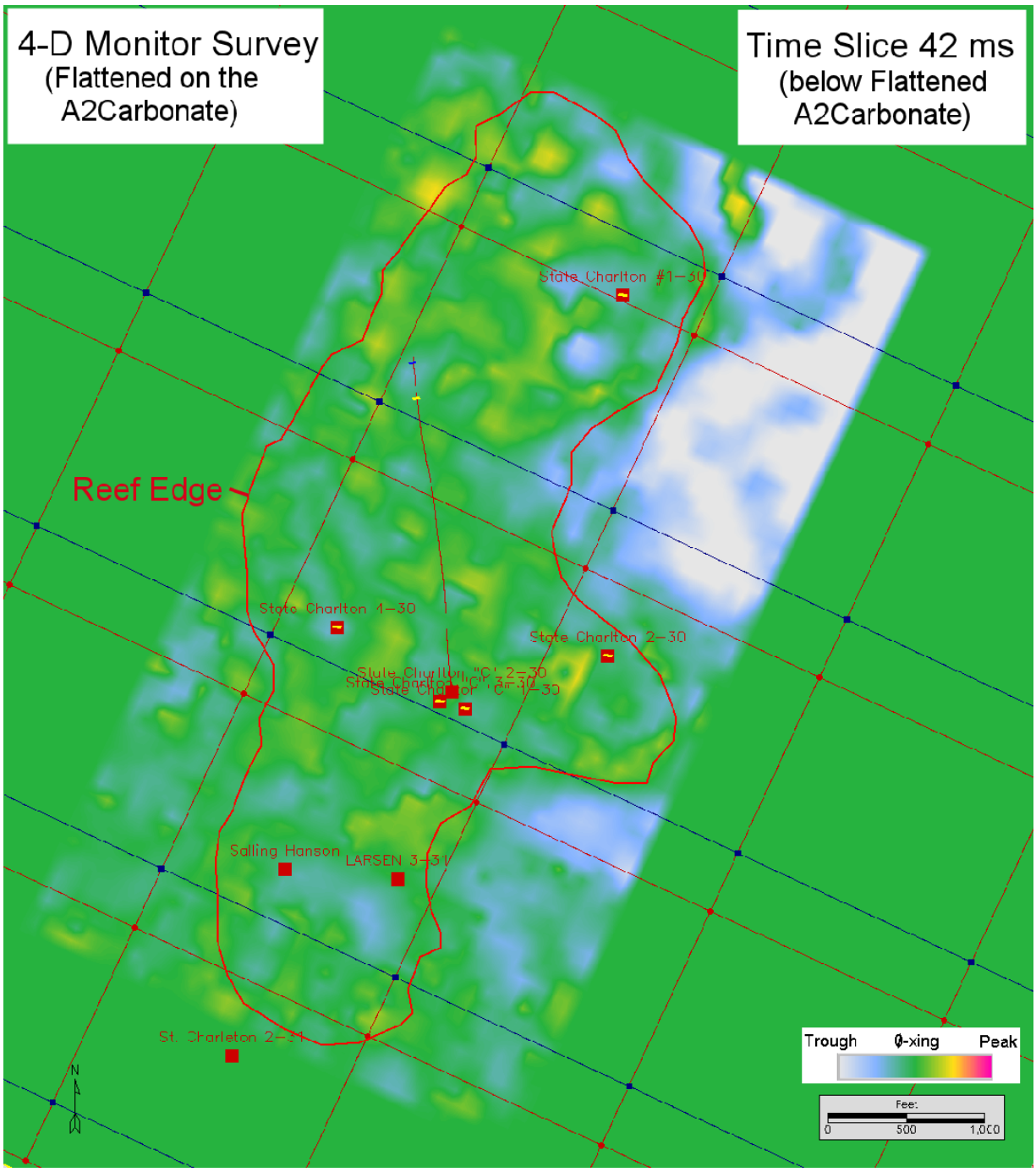
4-D Monitor Survey
(Flattened on the
A2Carbonate)
Time Slice 42 ms
(below Flattened
A2Carbonate)
State Charlton #1-30
Reef Edge
State Charlton 1-30
State Charlton 2-30
Salling Hanson
LARSEN 3-31
St. Charleton 2-31
Trough
0-xing
Peak
Fee:
0
500
1,000
N

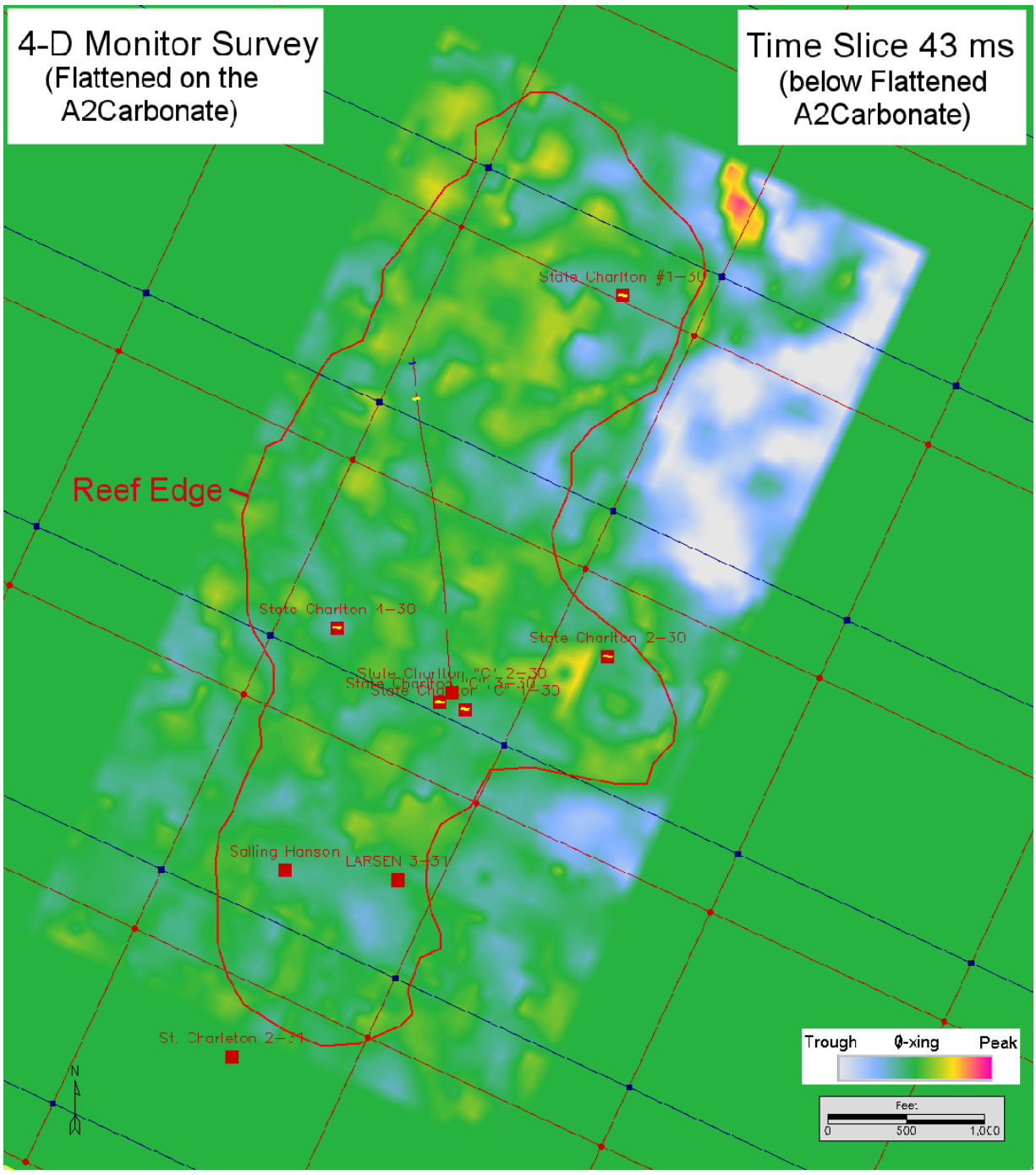
4-D Monitor Survey
(Flattened on the
A2Carbonate)
Time Slice 43 ms
(below Flattened
A2Carbonate)
State Charlton #1-30
Reef Edge
State Charlton 1-30
State Charlton 2-30
Salling Hanson
LARSEN 3-31
St. Charleton 2-31
Trough
0-xing
Peak
Fee:
0
500
1,000
N

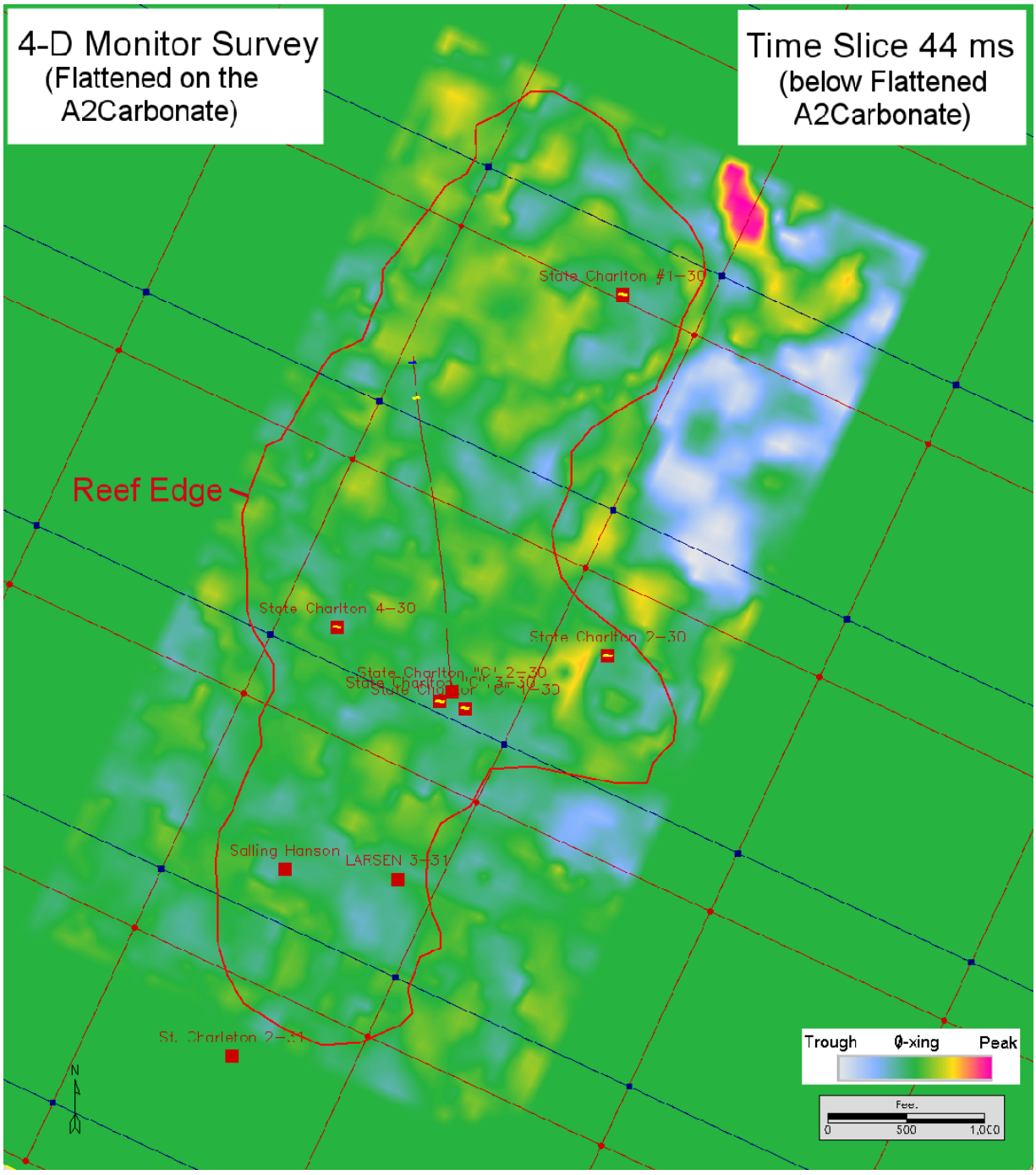
4-D Monitor Survey
(Flattened on the
A2Carbonate)
Time Slice 44 ms
(below Flattened
A2Carbonate)
State Charlton #1-30
Reef Edge
State Charlton 4-30
State Charlton 2-30
Salling Hanson
LARSEN 3-31
Trough
0-xing
Peak
Feet
0
500
1,000
N

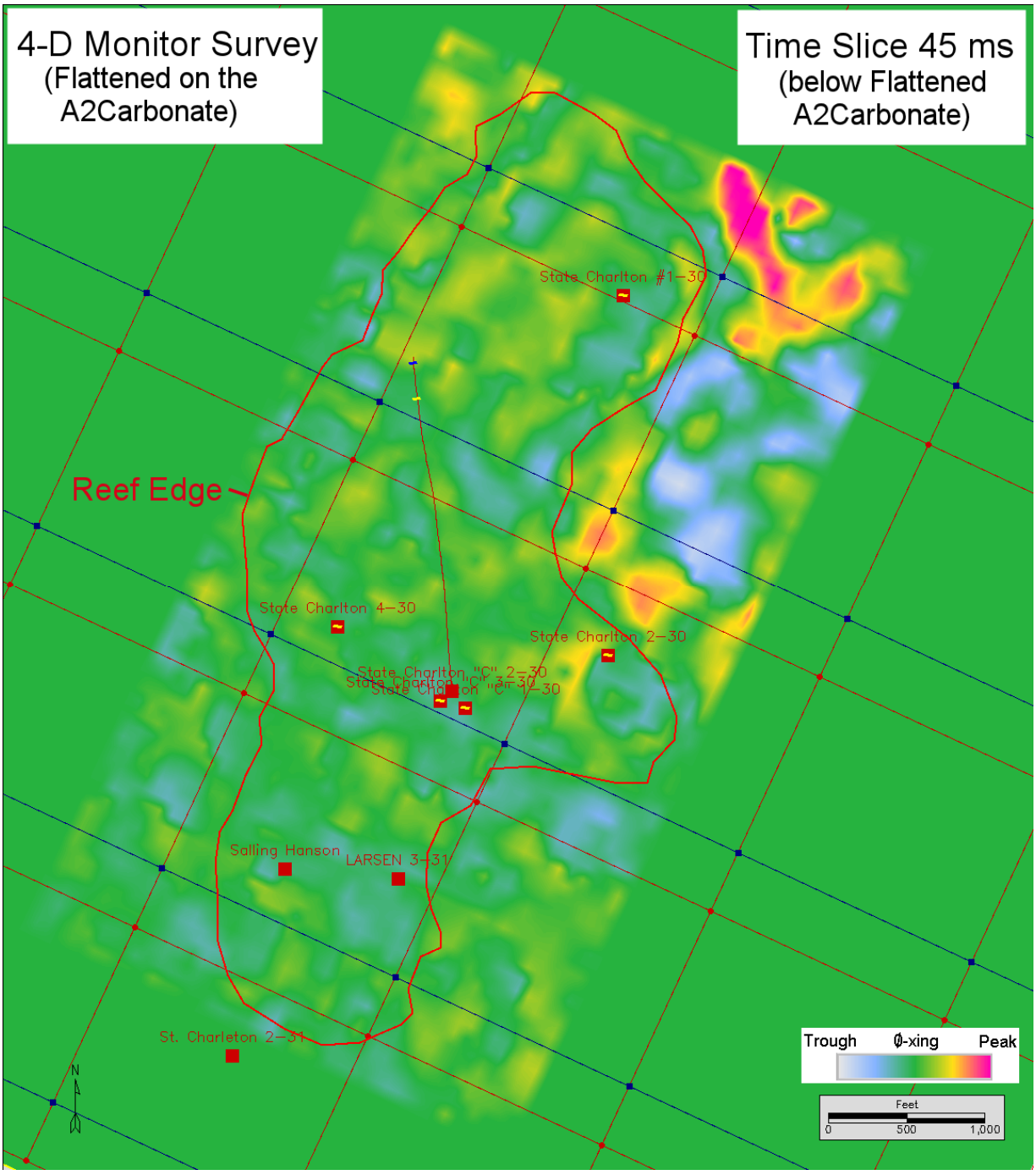
4-D Monitor Survey
(Flattened on the
A2Carbonate)
Time Slice 45 ms
(below Flattened
A2Carbonate)
State Charlton #1-30
Reef Edge
State Charlton 4-30
State Charlton 2-30
State Charlton "C" 2-30
Salling Hanson
LARSEN 3-31
St. Charleton 2-31
N
Trough
Ø-xing
Peak
Feet
0
500
1,000

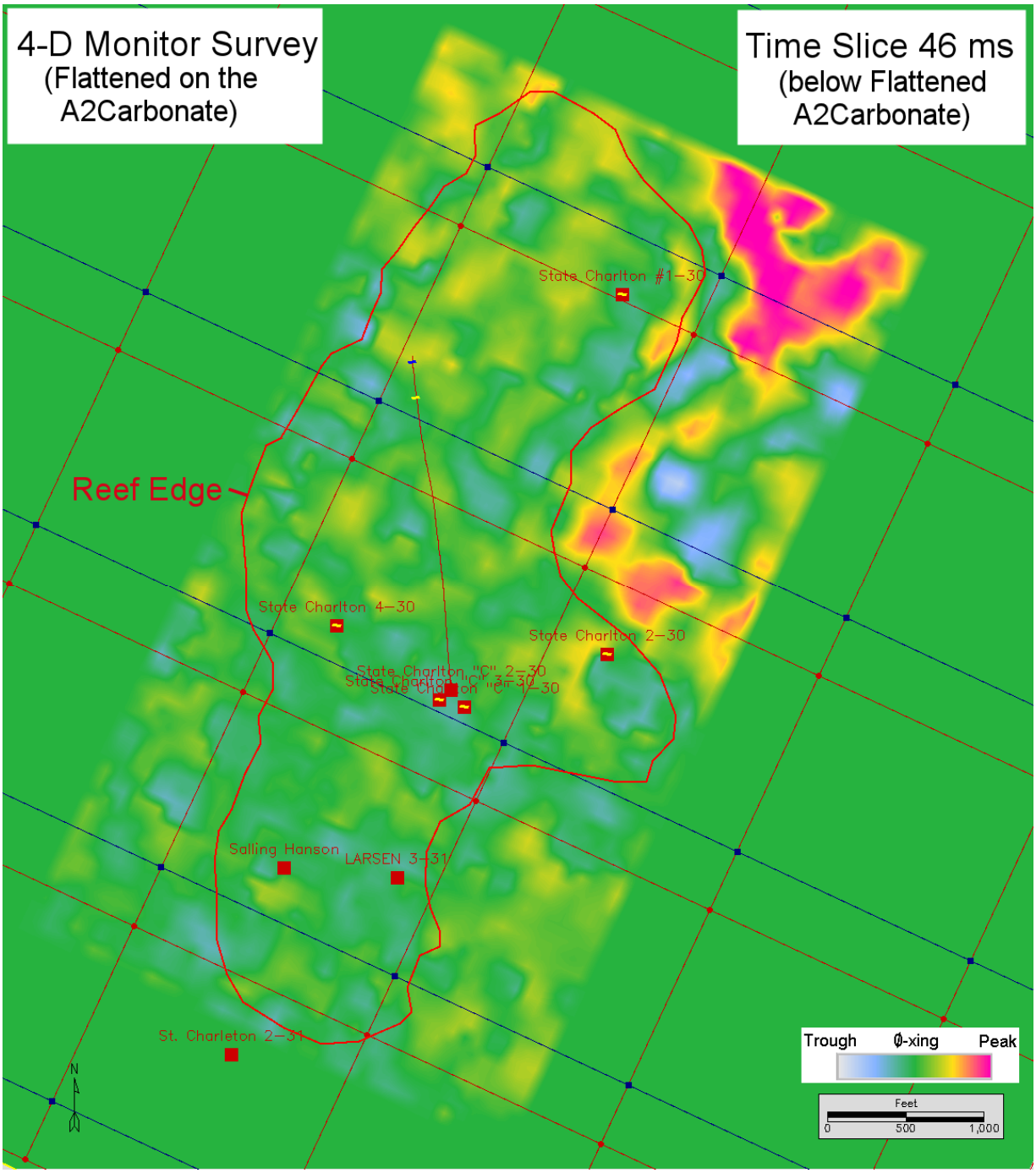
4-D Monitor Survey
(Flattened on the
A2Carbonate)
Time Slice 46 ms
(below Flattened
A2Carbonate)
State Charlton #1–30
Reef Edge
State Charlton 4–30
State Charlton 2–30
State Charlton "C" 2–30
State Charlton "C" 3–30
State Charlton "C" 1–30
Salling Hanson
LARSEN 3–31
St. Charleton 2–31
N
Trough
Ø-xing
Peak
Feet
0
500
1,000

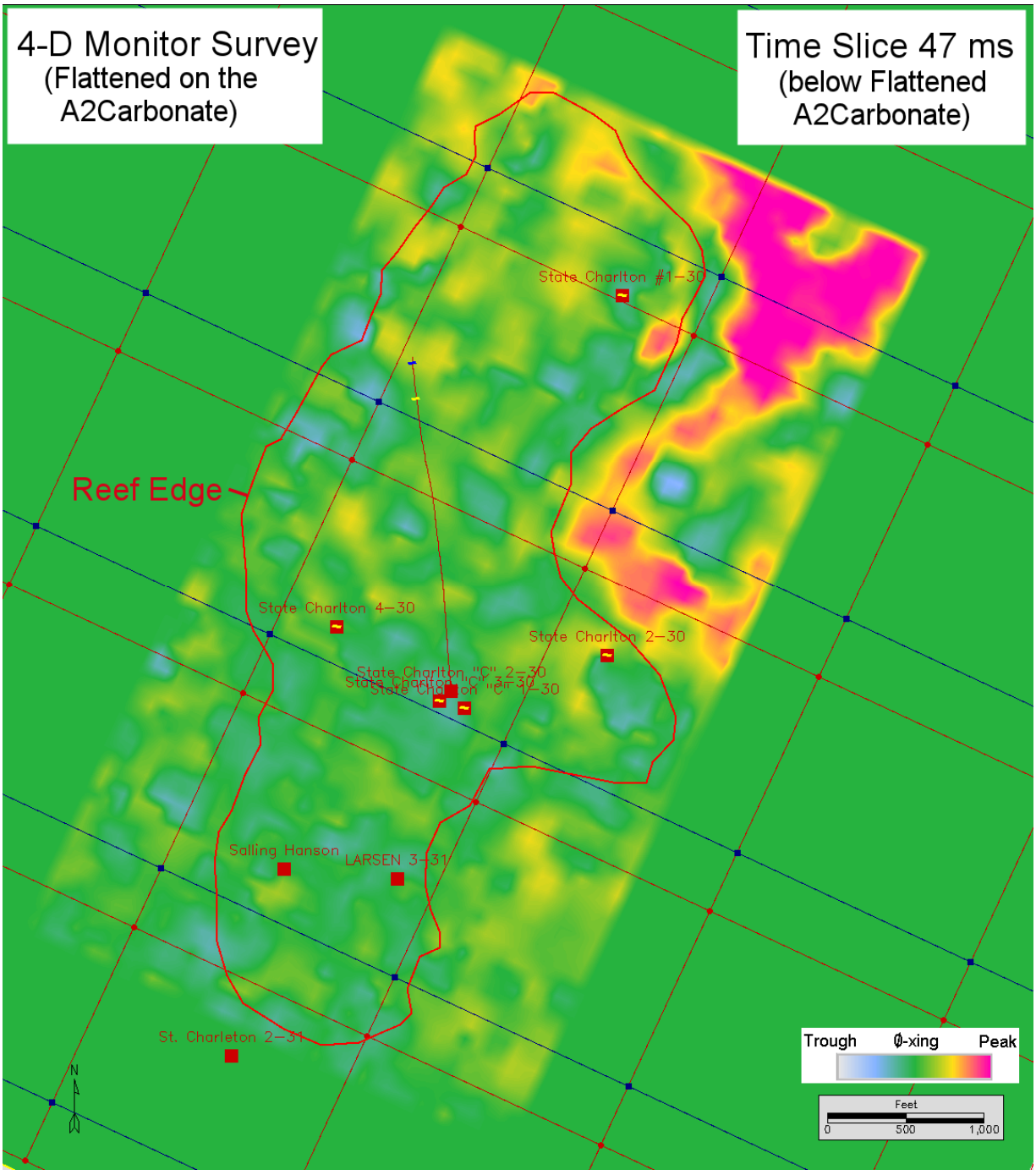
4-D Monitor Survey
(Flattened on the
A2Carbonate)
Time Slice 47 ms
(below Flattened
A2Carbonate)
State Charlton #1-30
Reef Edge
State Charlton 4-30
State Charlton 2-30
State Charlton "C" 2-30
State Charlton "C" 3-30
State Charlton "C" 1-30
Salling Hanson
LARSEN 3-31
St. Charleton 2-31
N
Trough
Ø-xing
Peak
Feet
0
500
1,000

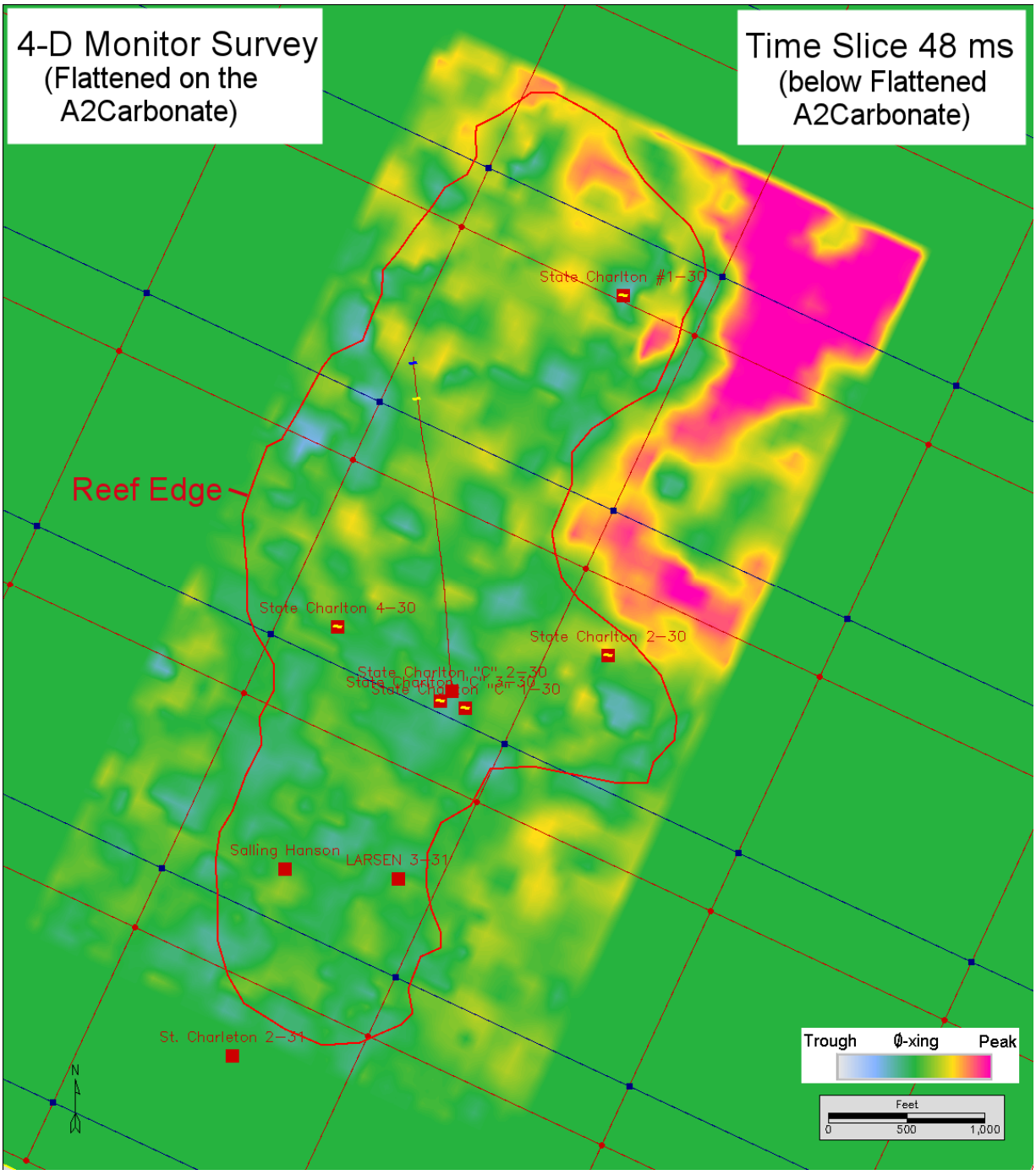
4-D Monitor Survey
(Flattened on the
A2Carbonate)
Time Slice 48 ms
(below Flattened
A2Carbonate)
State Charlton #1-30
Reef Edge
State Charlton 4-30
State Charlton 2-30
State Charlton "C" 2-30
Salling Hanson
LARSEN 3-31
St. Charleton 2-31
N
Trough
Ø-xing
Peak
Feet
0
500
1,000

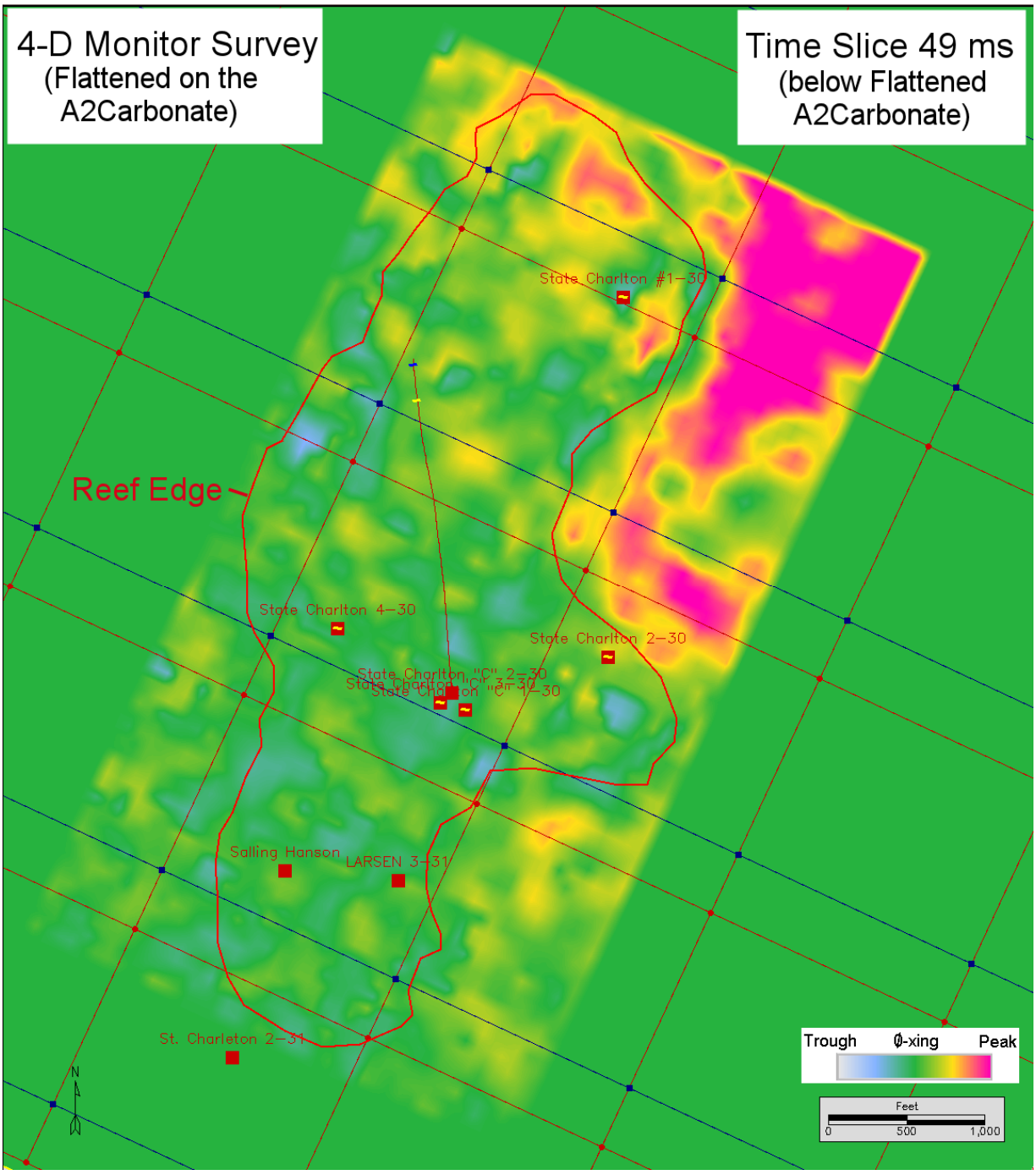
4-D Monitor Survey
(Flattened on the
A2Carbonate)
Time Slice 49 ms
(below Flattened
A2Carbonate)
State Charlton #1-30
Reef Edge
State Charlton 4-30
State Charlton 2-30
State Charlton "C" 2-30
State Charlton "C" 1-30
Salling Hanson
LARSEN 3-31
St. Charleton 2-31
Trough
Ø-xing
Peak
Feet
0
500
1,000
N

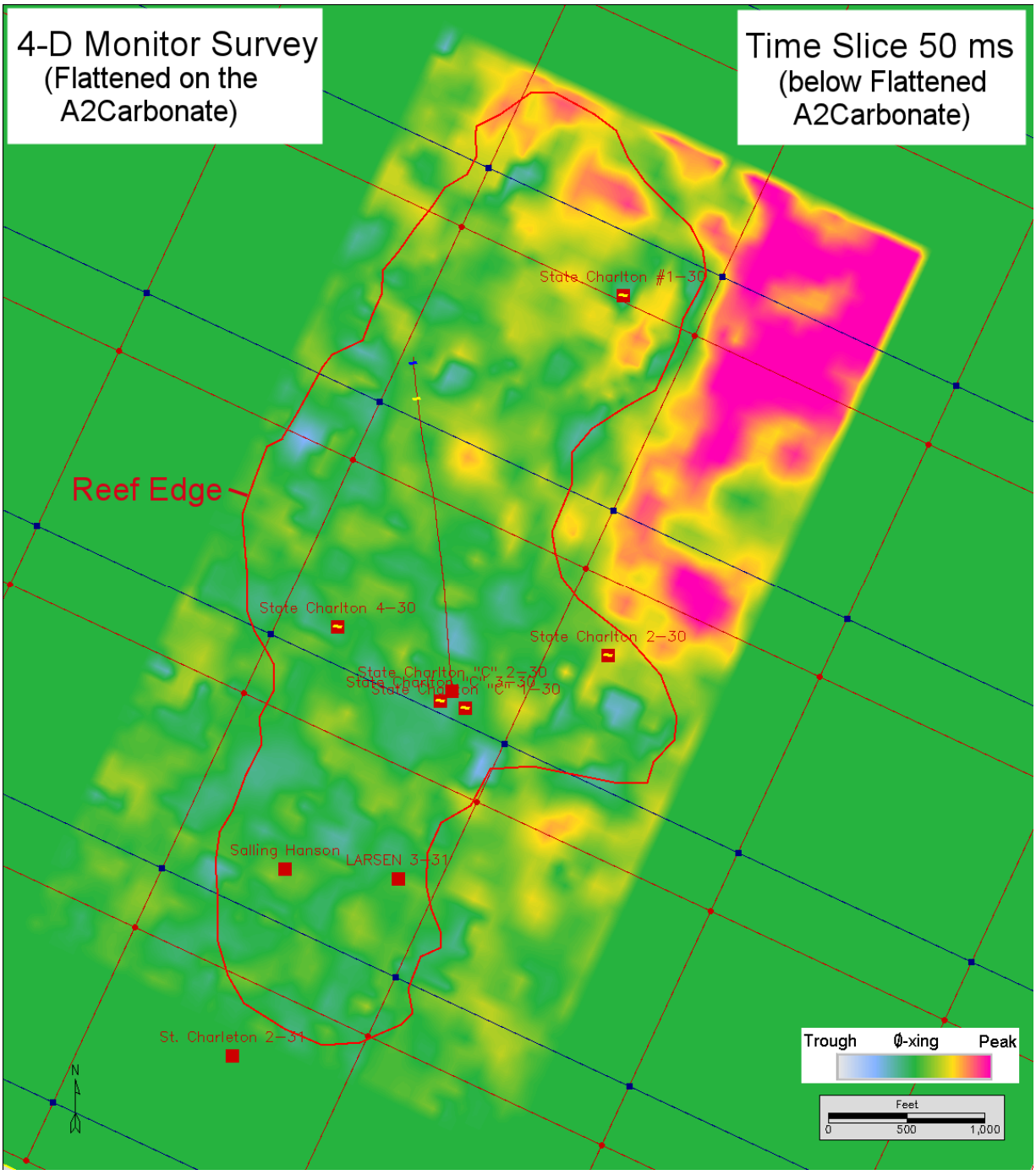
4-D Monitor Survey
(Flattened on the
A2Carbonate)
Time Slice 50 ms
(below Flattened
A2Carbonate)
State Charlton #1-30
Reef Edge
State Charlton 4-30
State Charlton 2-30
State Charlton "C" 2-30
Salling Hanson
LARSEN 3-31
St. Charleton 2-31
N
Trough
Ø-xing
Peak
Feet
0
500
1,000

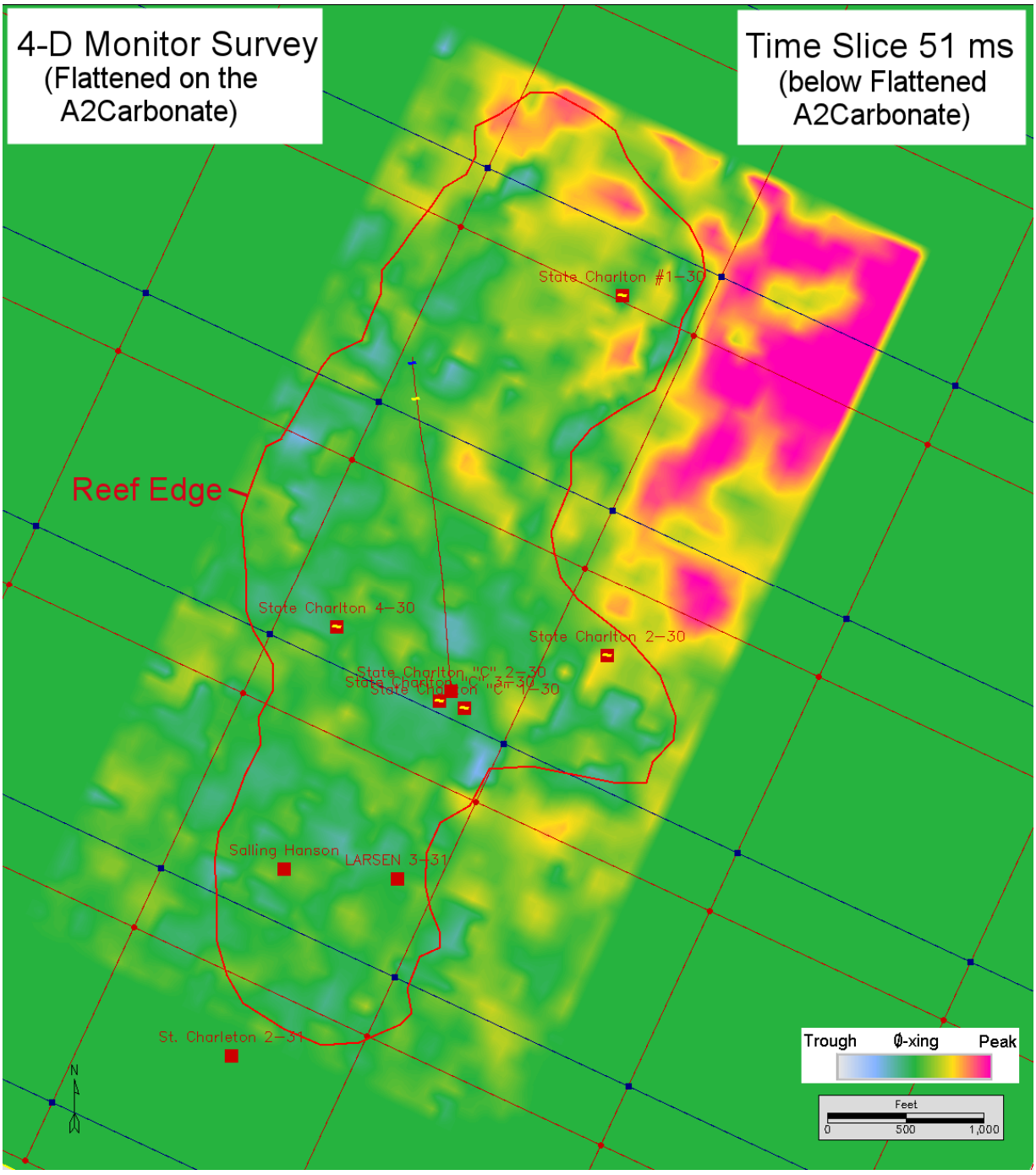
4-D Monitor Survey
(Flattened on the
A2Carbonate)
Time Slice 51 ms
(below Flattened
A2Carbonate)
State Charlton #1-30
Reef Edge
State Charlton 4-30
State Charlton 2-30
State Charlton "C" 2-30
State Charlton "C" 3-30
State Charlton "C" 1-30
Salling Hanson
LARSEN 3-31
St. Charleton 2-31
N
Trough
Ø-xing
Peak
Feet
0
500
1,000

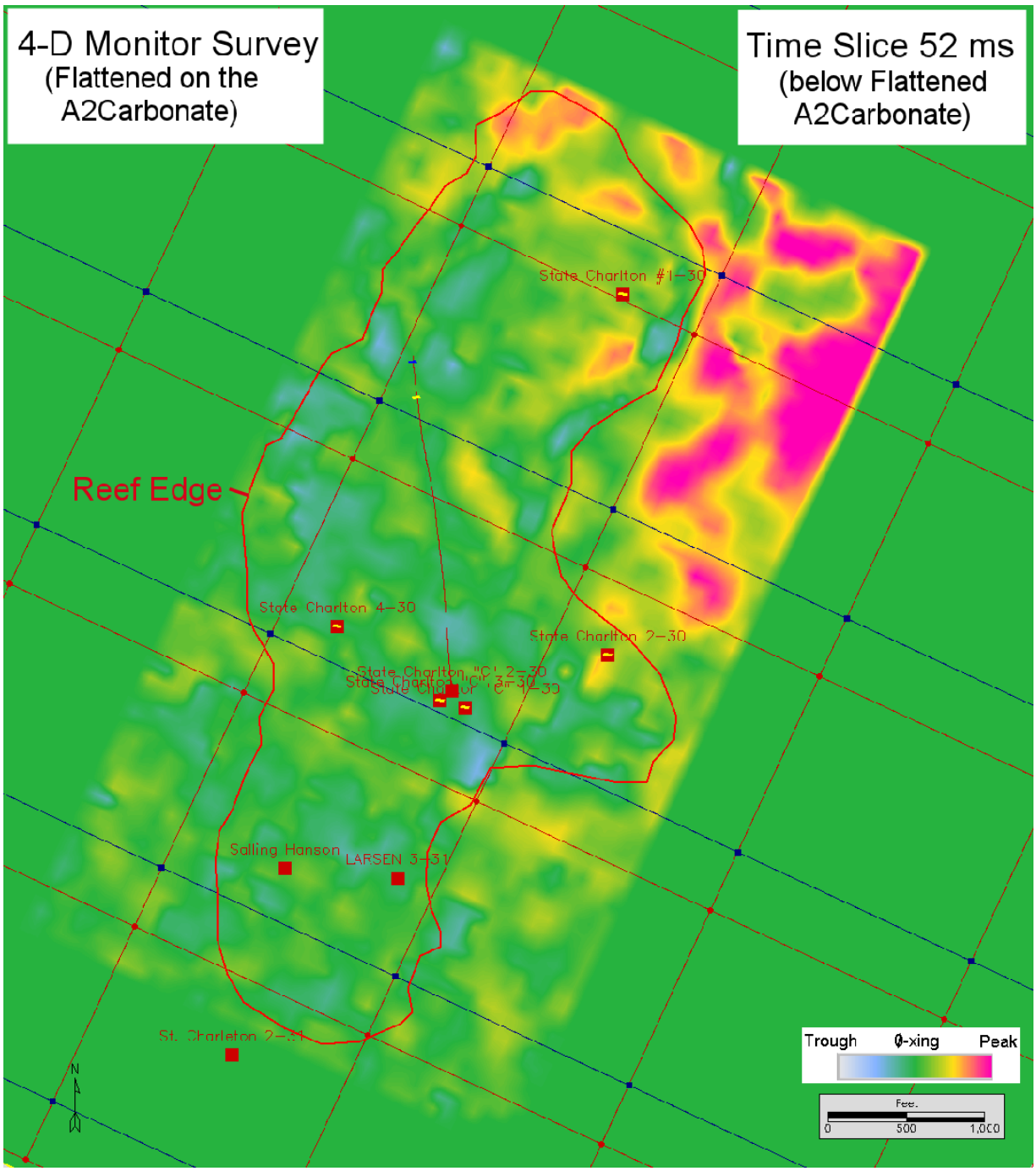
4-D Monitor Survey
(Flattened on the
A2Carbonate)
Time Slice 52 ms
(below Flattened
A2Carbonate)
State Charlton #1-30
Reef Edge
State Charlton 4-30
State Charlton 2-30
Salling Hanson
LARSEN 3-31
St. Charleton 2-31
Trough
0-xing
Peak
Feet
0
500
1,000
N

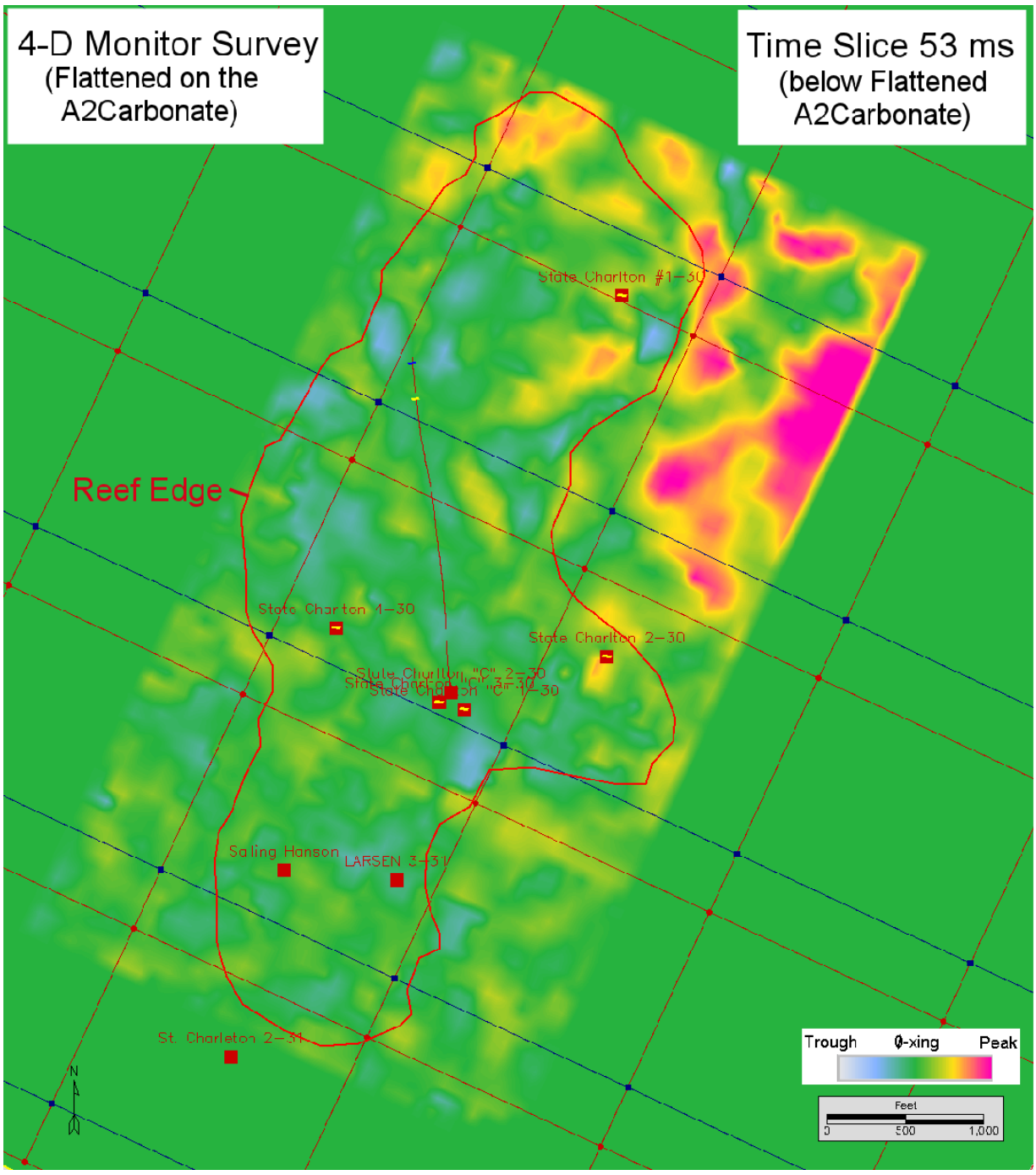
4-D Monitor Survey
(Flattened on the
A2Carbonate)
Time Slice 53 ms
(below Flattened
A2Carbonate)
State Charlton #1-30
Reef Edge
State Charlton 1-30
State Charlton 2-30
Saling Hanson
St. Charleton 2-31
Trough
0-xing
Peak
Feet
0
500
1,000
N

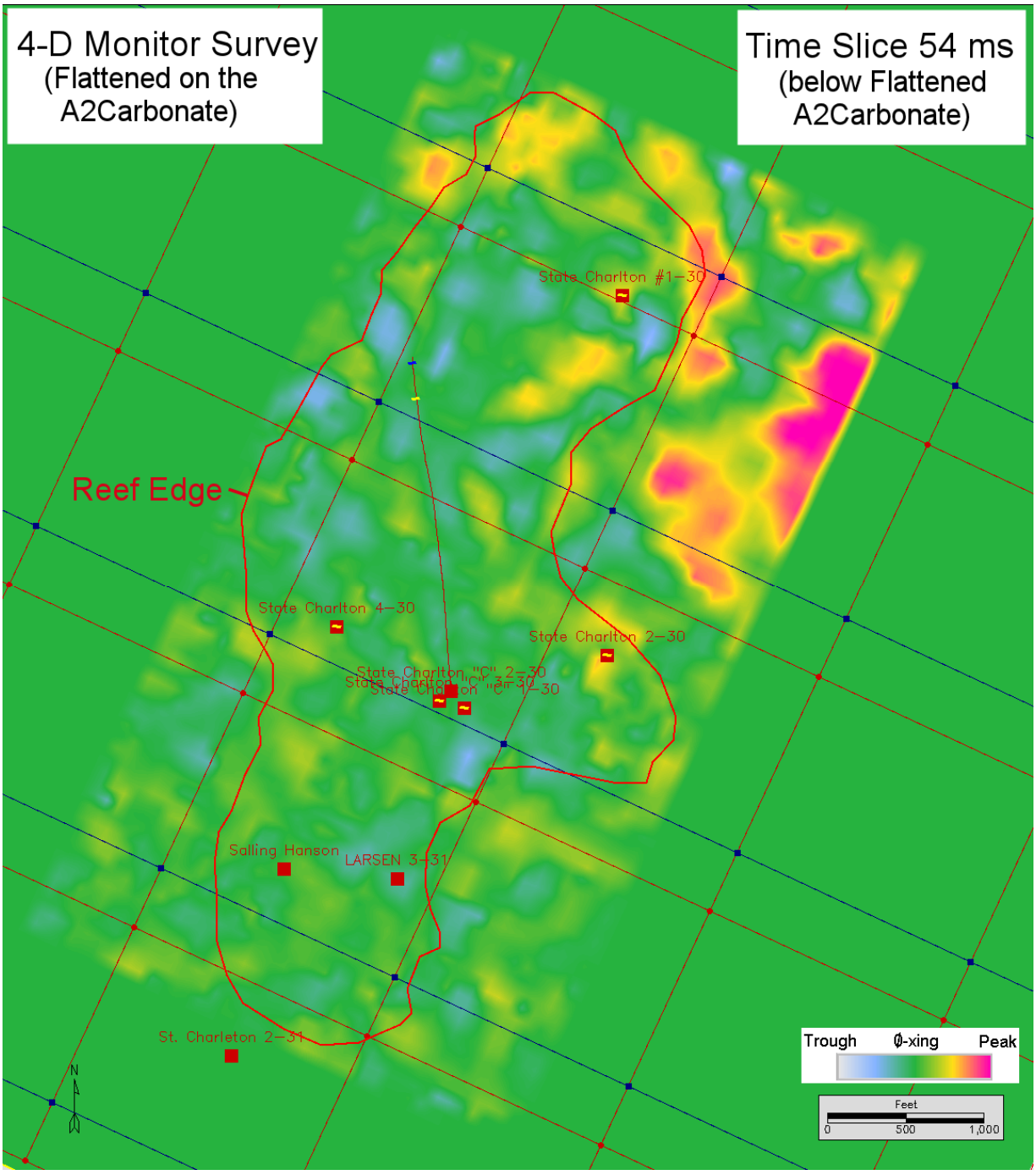
4-D Monitor Survey
(Flattened on the
A2Carbonate)
Time Slice 54 ms
(below Flattened
A2Carbonate)
State Charlton #1-30
Reef Edge
State Charlton 4-30
State Charlton 2-30
State Charlton "C" 2-30
Salling Hanson
LARSEN 3-31
St. Charleton 2-31
N
Trough
Ø-xing
Peak
Feet
0
500
1,000

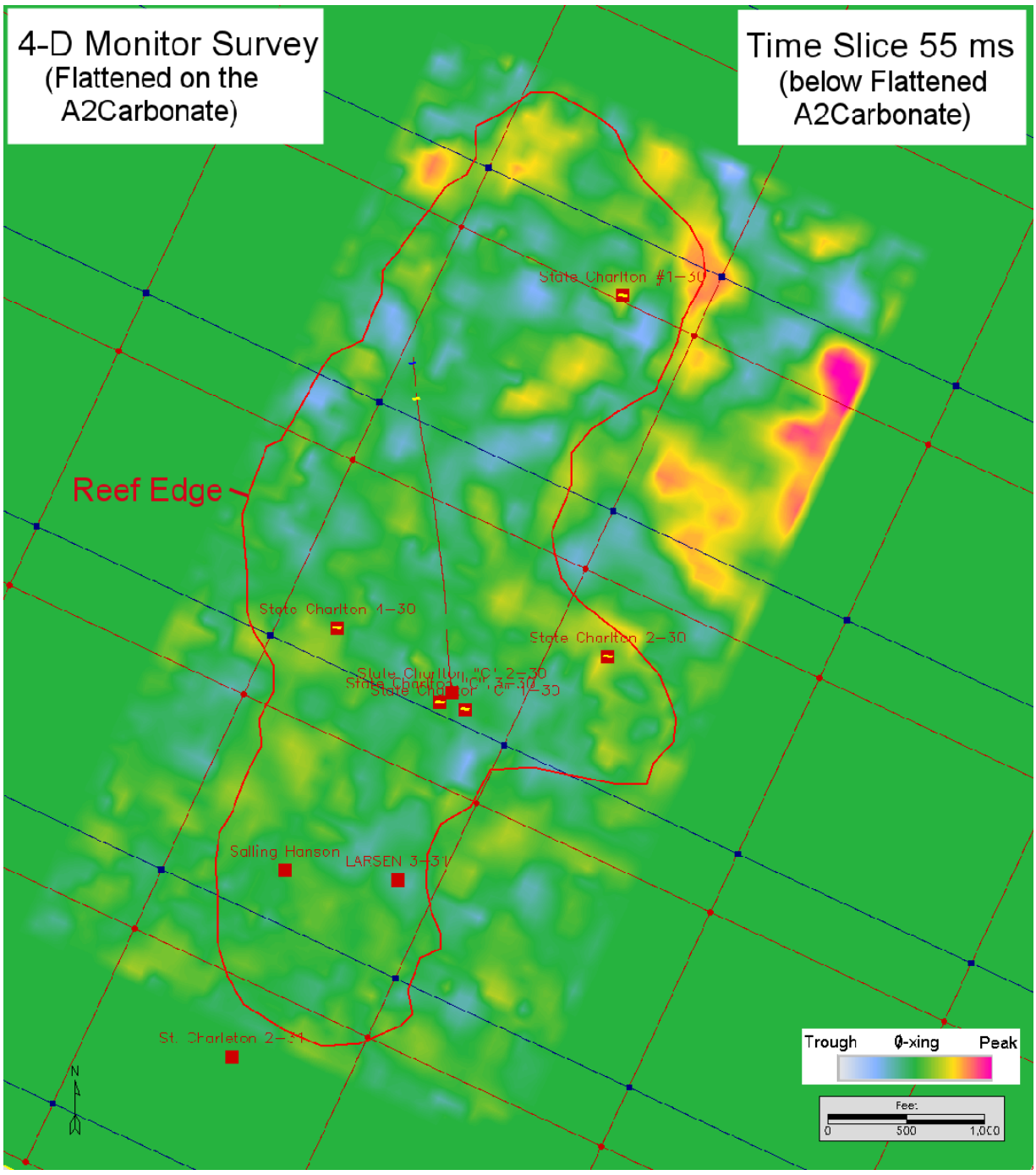
4-D Monitor Survey
(Flattened on the
A2Carbonate)
Time Slice 55 ms
(below Flattened
A2Carbonate)
State Charlton #1-30
Reef Edge
State Charlton 1-30
State Charlton 2-30
Salling Hanson
LARSEN 3-31
St. Charleton 2-31
Trough
0-xing
Peak
Fee:
0
500
1,000
N

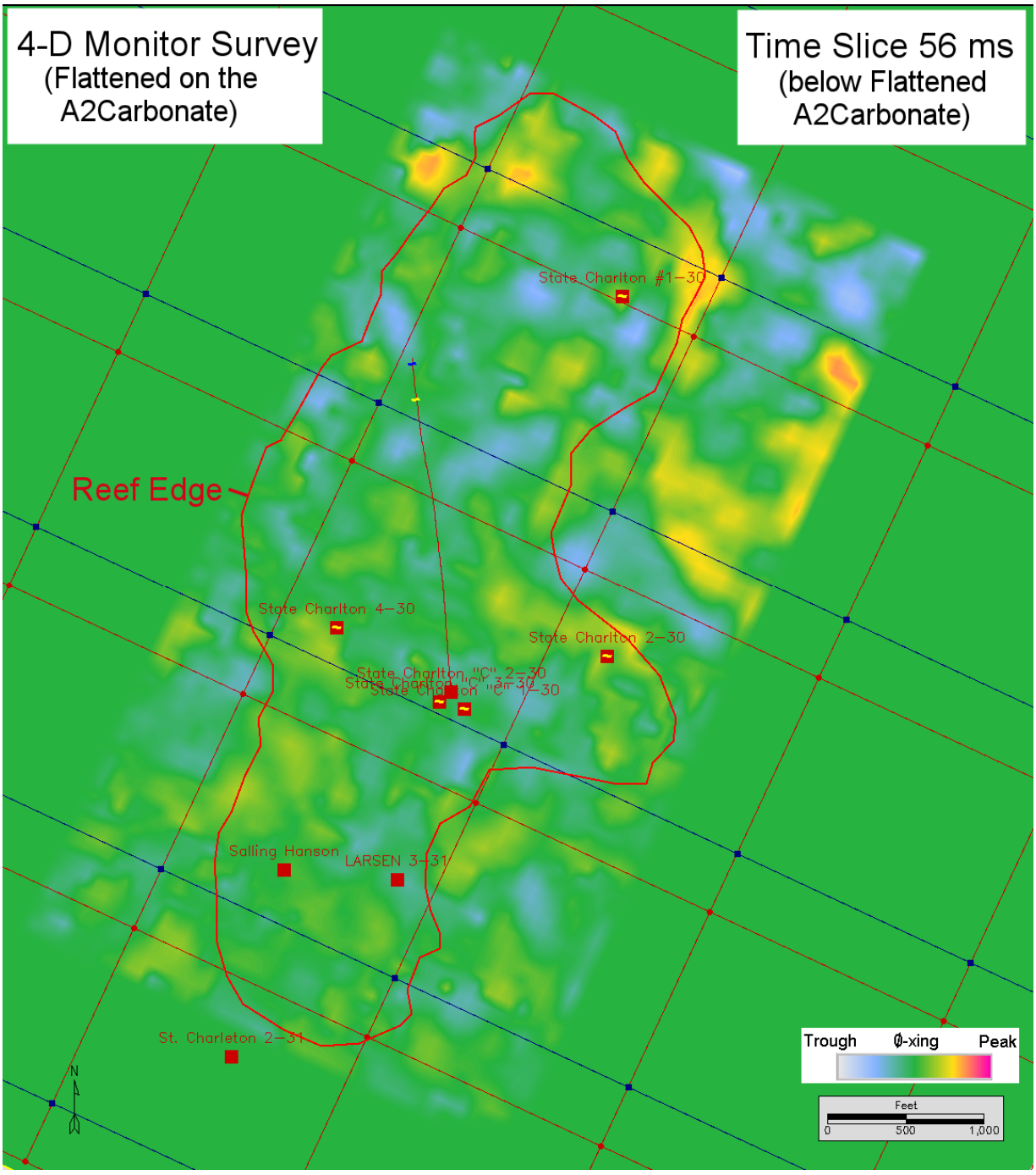
4-D Monitor Survey
(Flattened on the
A2Carbonate)
Time Slice 56 ms
(below Flattened
A2Carbonate)
State Charlton #1-30
Reef Edge
State Charlton 4-30
State Charlton 2-30
Salling Hanson
LARSEN 3-31
St. Charleton 2-31
Trough
Ø-xing
Peak
Feet
0
500
1,000
N

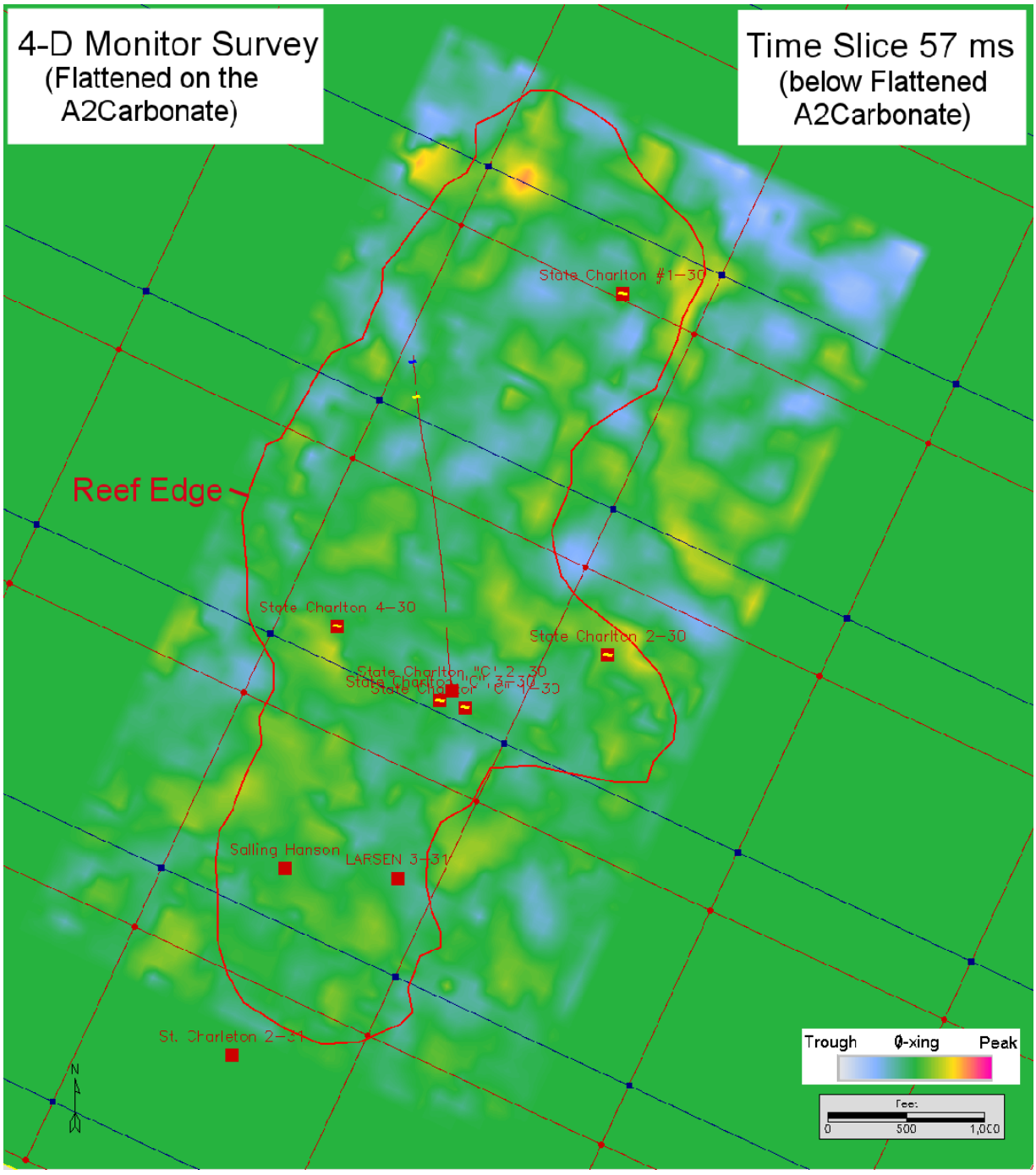
4-D Monitor Survey
(Flattened on the
A2Carbonate)
Time Slice 57 ms
(below Flattened
A2Carbonate)
State Charlton #1-30
Reef Edge
State Charlton 4-30
State Charlton 2-30
Salling Hanson
LARSEN 3-31
St. Charleton 2-31
Trough
0-xing
Peak
0
500
1,000

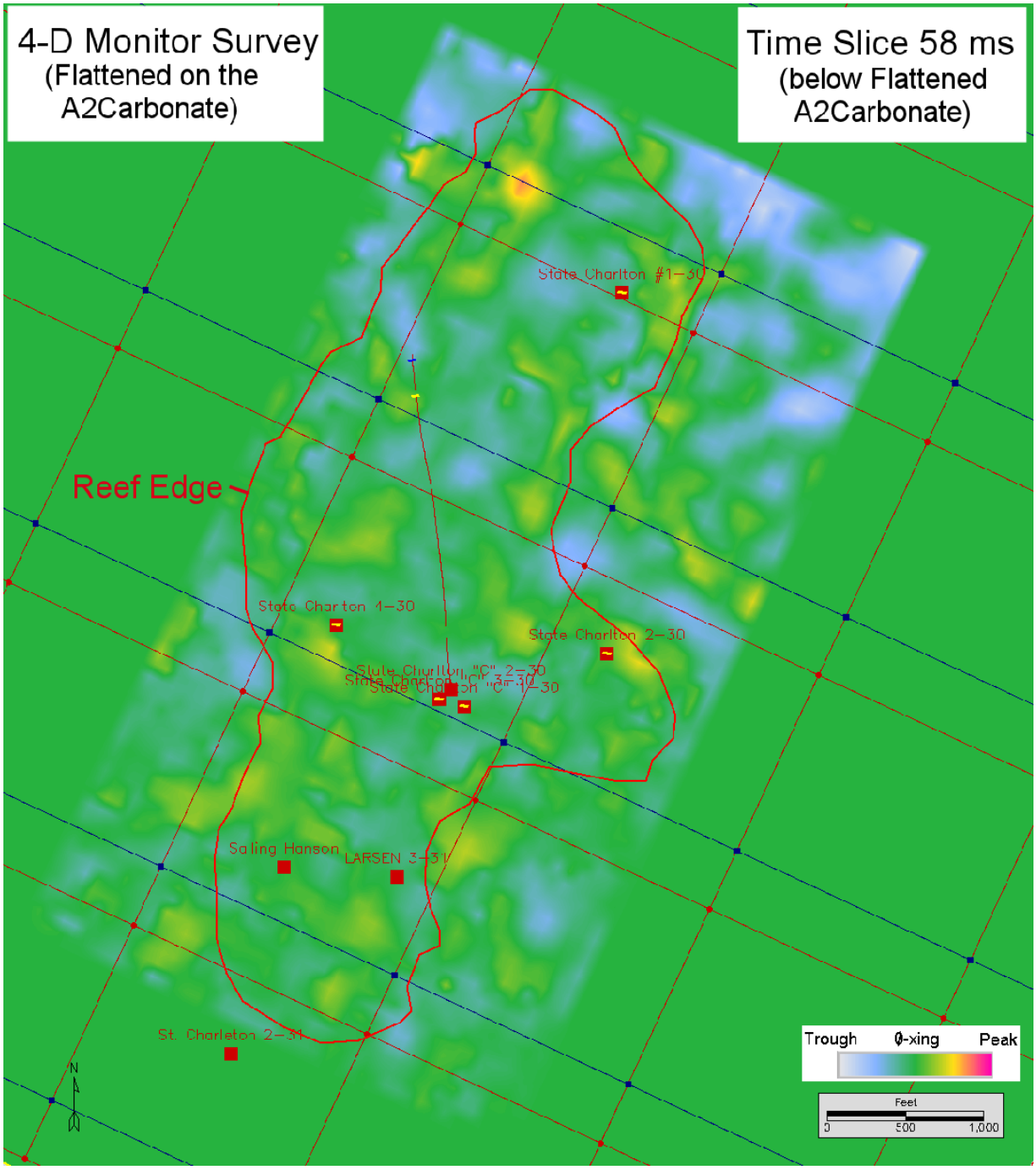
4-D Monitor Survey
(Flattened on the
A2Carbonate)
Time Slice 58 ms
(below Flattened
A2Carbonate)
State Charlton #1-30
Reef Edge
State Charlton 1-30
State Charlton 2-30
Saling Hanson
LARSEN 3-31
St. Charleton 2-31
Trough
0-xing
Peak
Feet
0
500
1,000
N

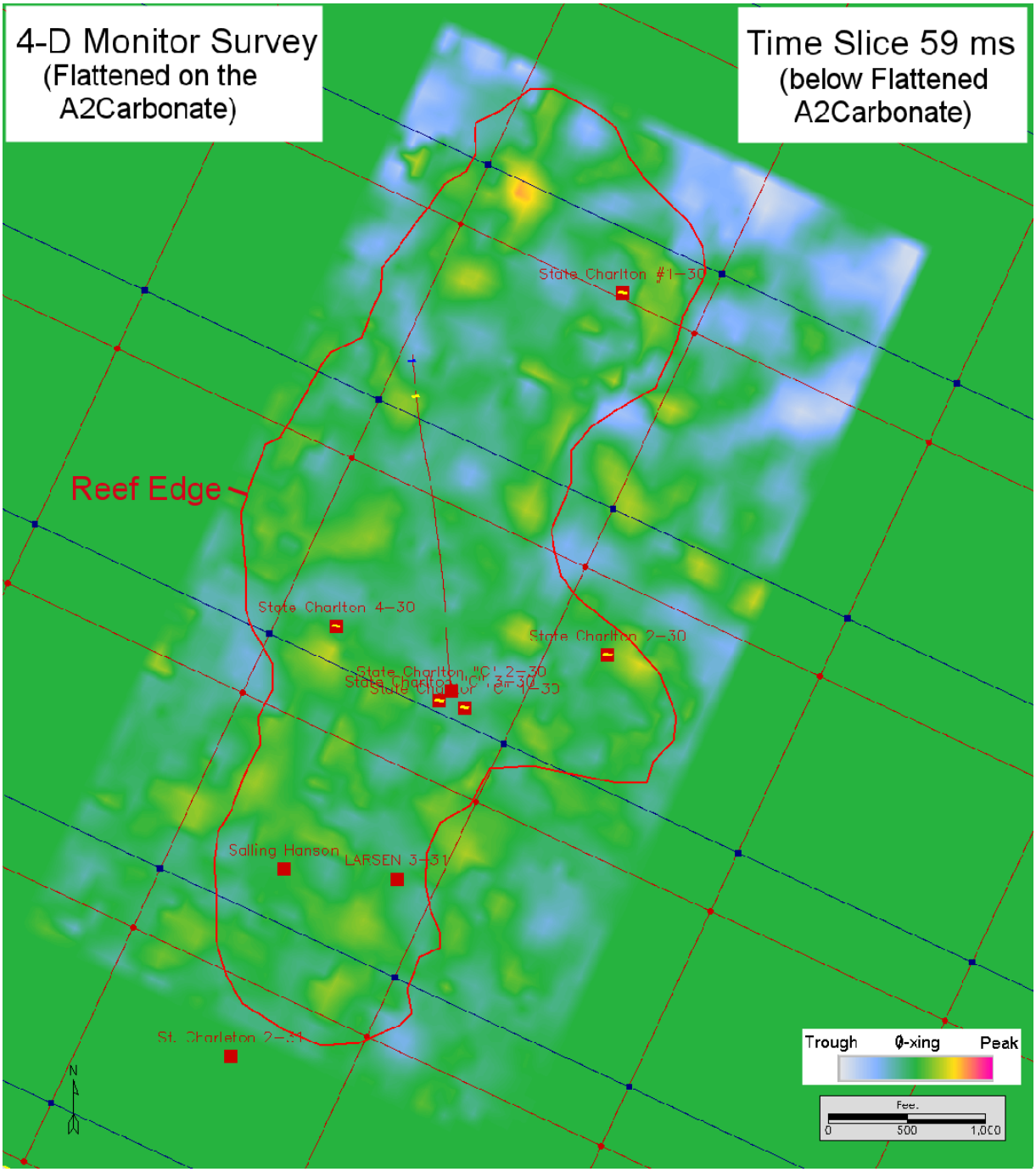
4-D Monitor Survey
(Flattened on the
A2Carbonate)
Time Slice 59 ms
(below Flattened
A2Carbonate)
State Charlton #1-30
Reef Edge
State Charlton 4-30
State Charlton 2-30
Salling Hanson
LARSEN 3-31
St. Charleton 2-31
Trough
0-xing
Peak
Feet
0
500
1,000
N

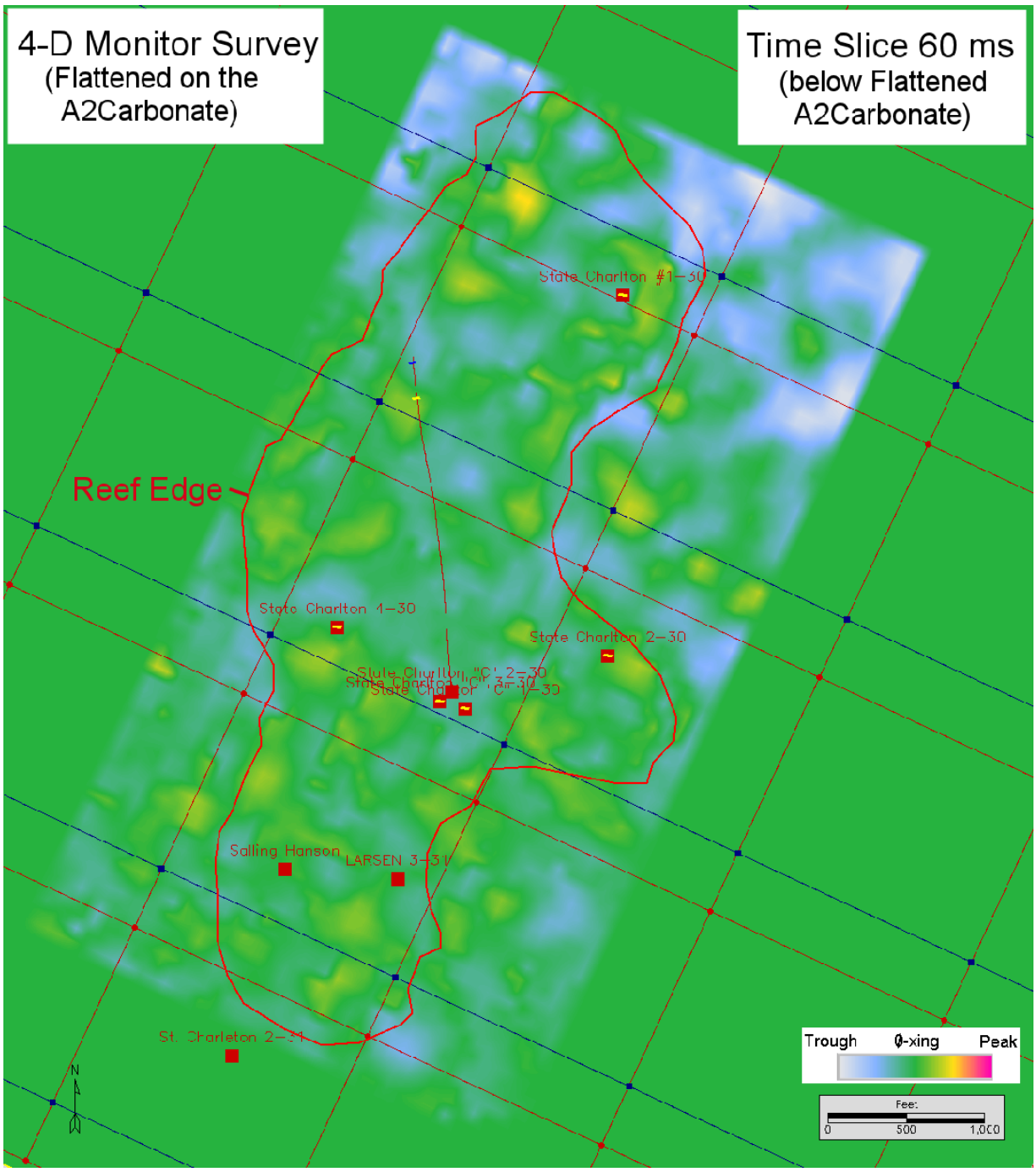
4-D Monitor Survey
(Flattened on the
A2Carbonate)
Time Slice 60 ms
(below Flattened
A2Carbonate)
State Charlton #1-30
Reef Edge
State Charlton 1-30
State Charlton 2-30
Salling Hanson
LARSEN 3-31
St. Charleton 2-31
N
Trough
0-xing
Peak
Fee:
0
500
1,000

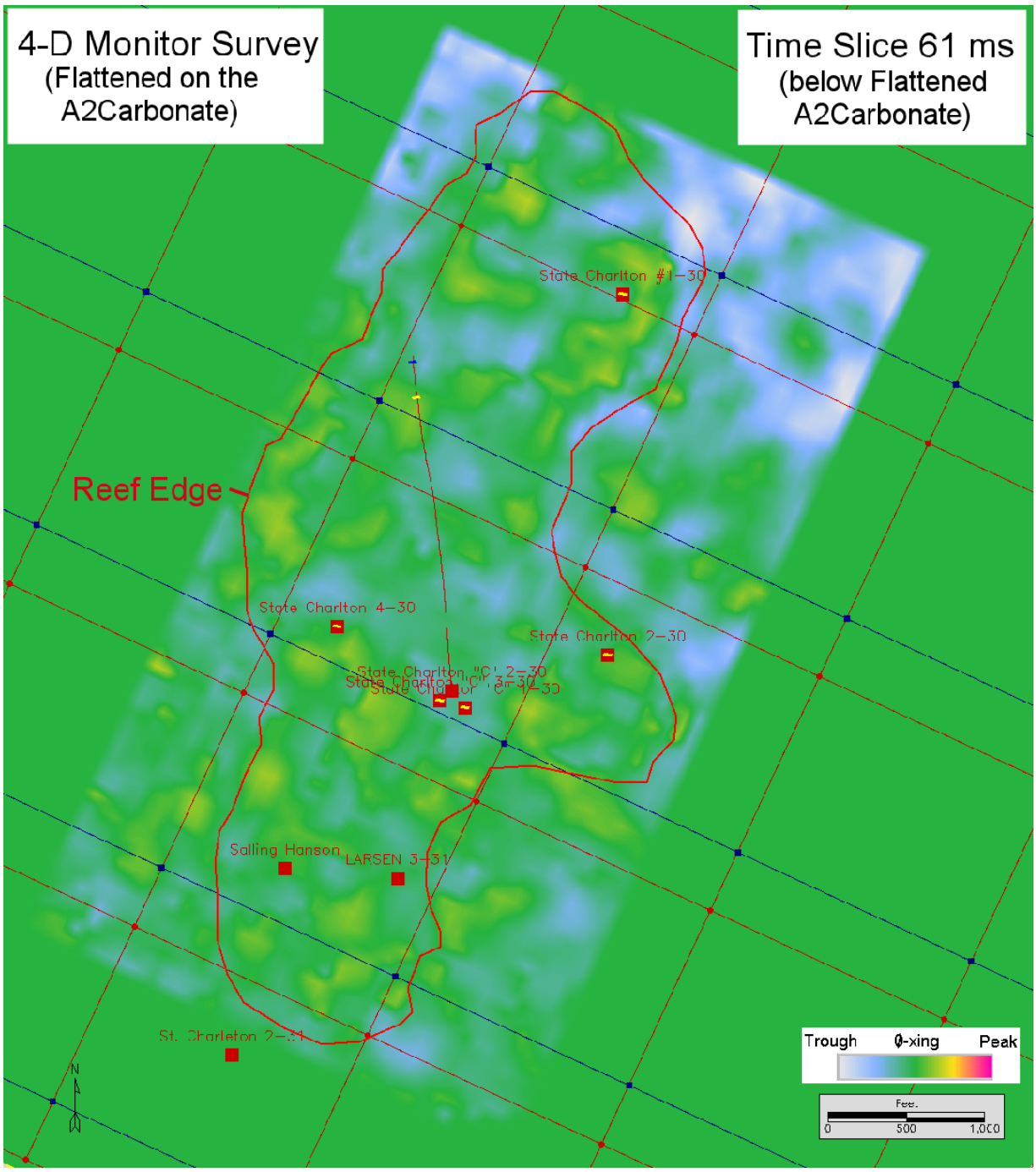
4-D Monitor Survey
(Flattened on the
A2Carbonate)
Time Slice 61 ms
(below Flattened
A2Carbonate)
State Charlton #1-30
Reef Edge
State Charlton 4-30
State Charlton 2-30
Salling Hanson
LARSEN 3-31
St. Charleton 2-31
Trough
0-xing
Peak
Feet
0
500
1,000
N

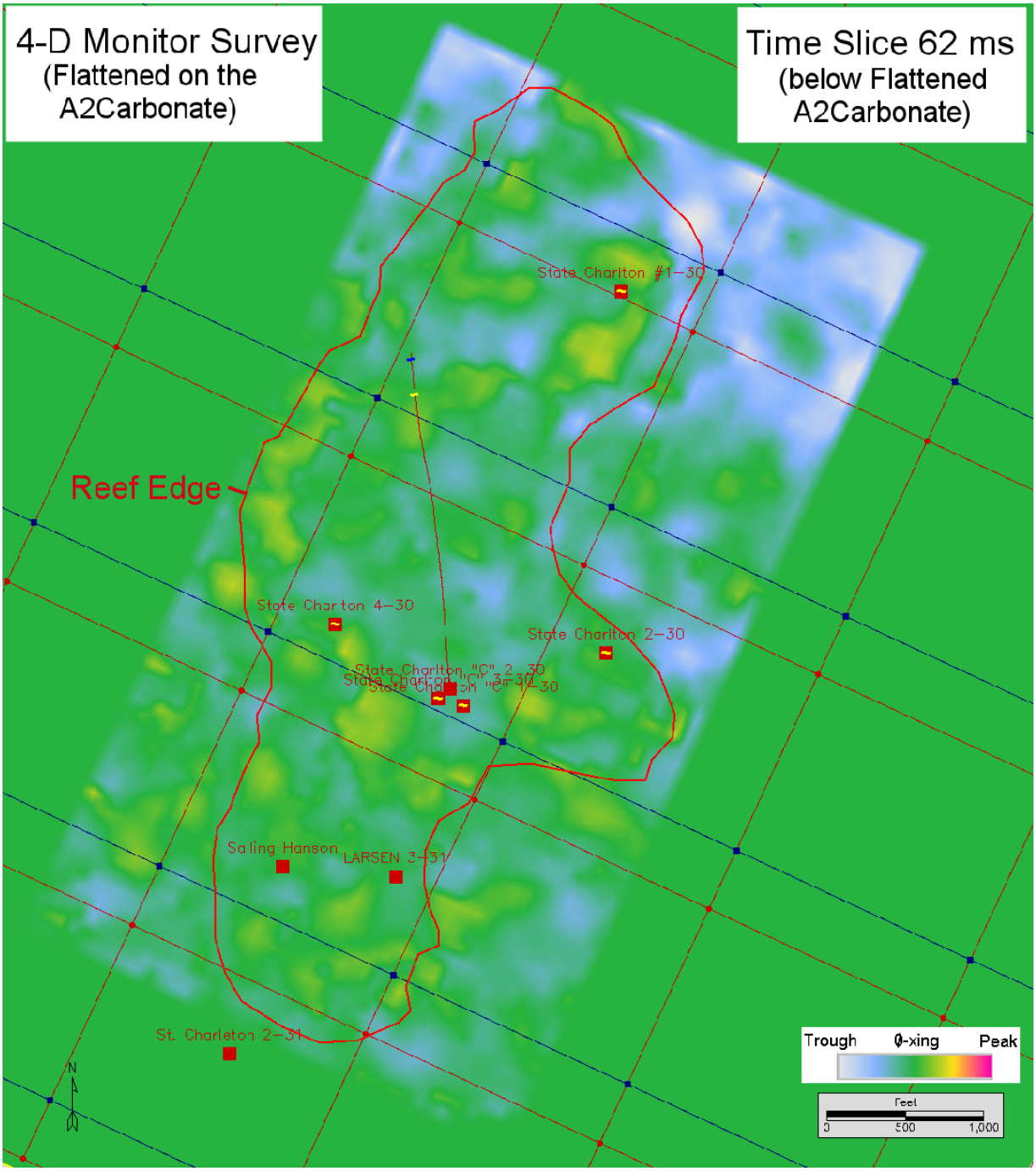
4-D Monitor Survey
(Flattened on the
A2Carbonate)
Time Slice 62 ms
(below Flattened
A2Carbonate)
State Charlton #1-30
Reef Edge
State Charton 4-30
State Charlton 2-30
Saling Hanson
LARSEN 3-31
St. Charleton 2-31
N
Trough
0-xing
Peak
Feet
0
500
1,000

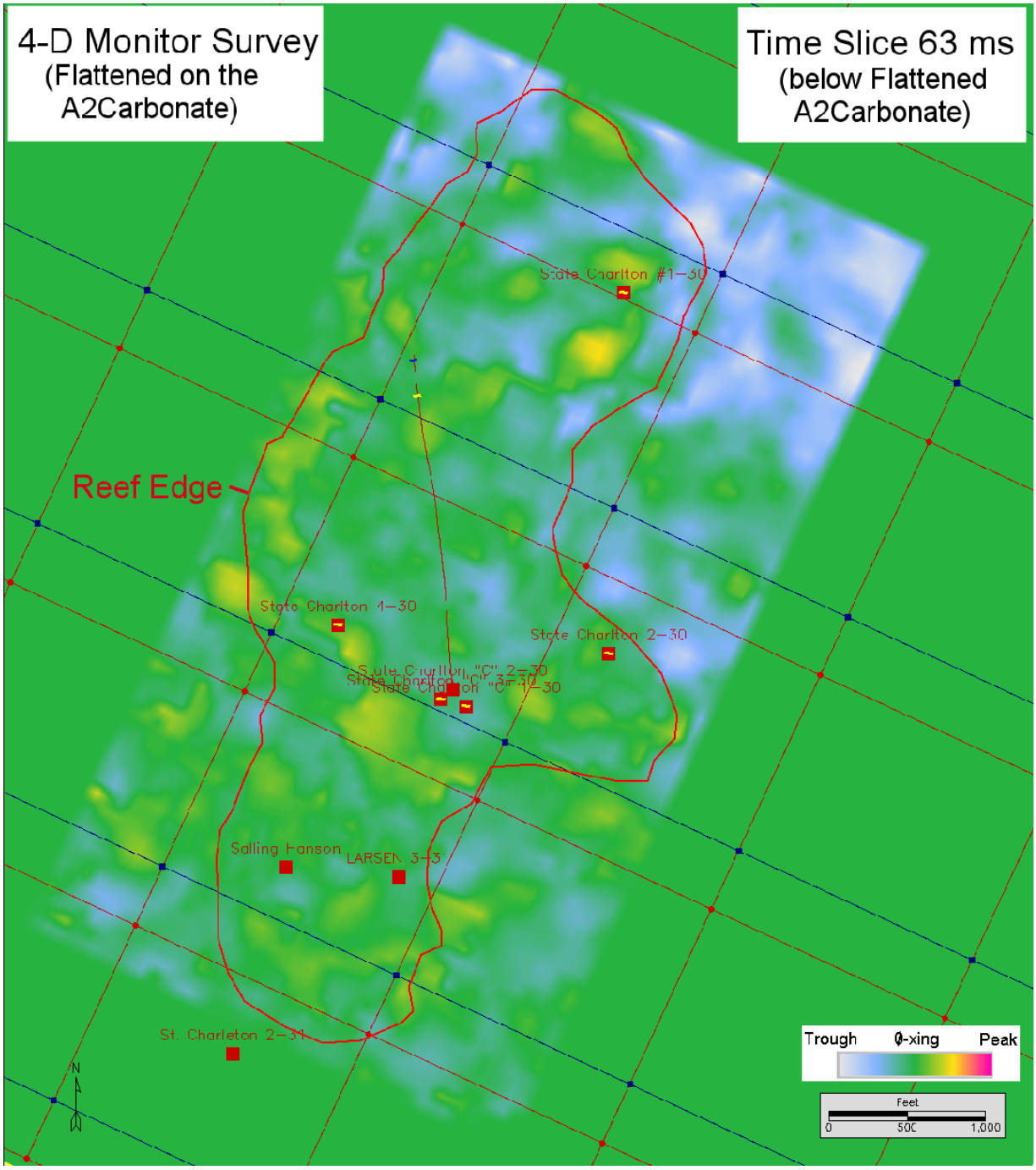
4-D Monitor Survey
(Flattened on the
A2Carbonate)
Time Slice 63 ms
(below Flattened
A2Carbonate)
State Charlton #1-30
Reef Edge
State Charlton 1-30
State Charlton 2-30
Salling Hanson
LARSEN 3-3
St. Charleton 2-31
N
Trough
0-xing
Peak
Feet
0
500
1,000

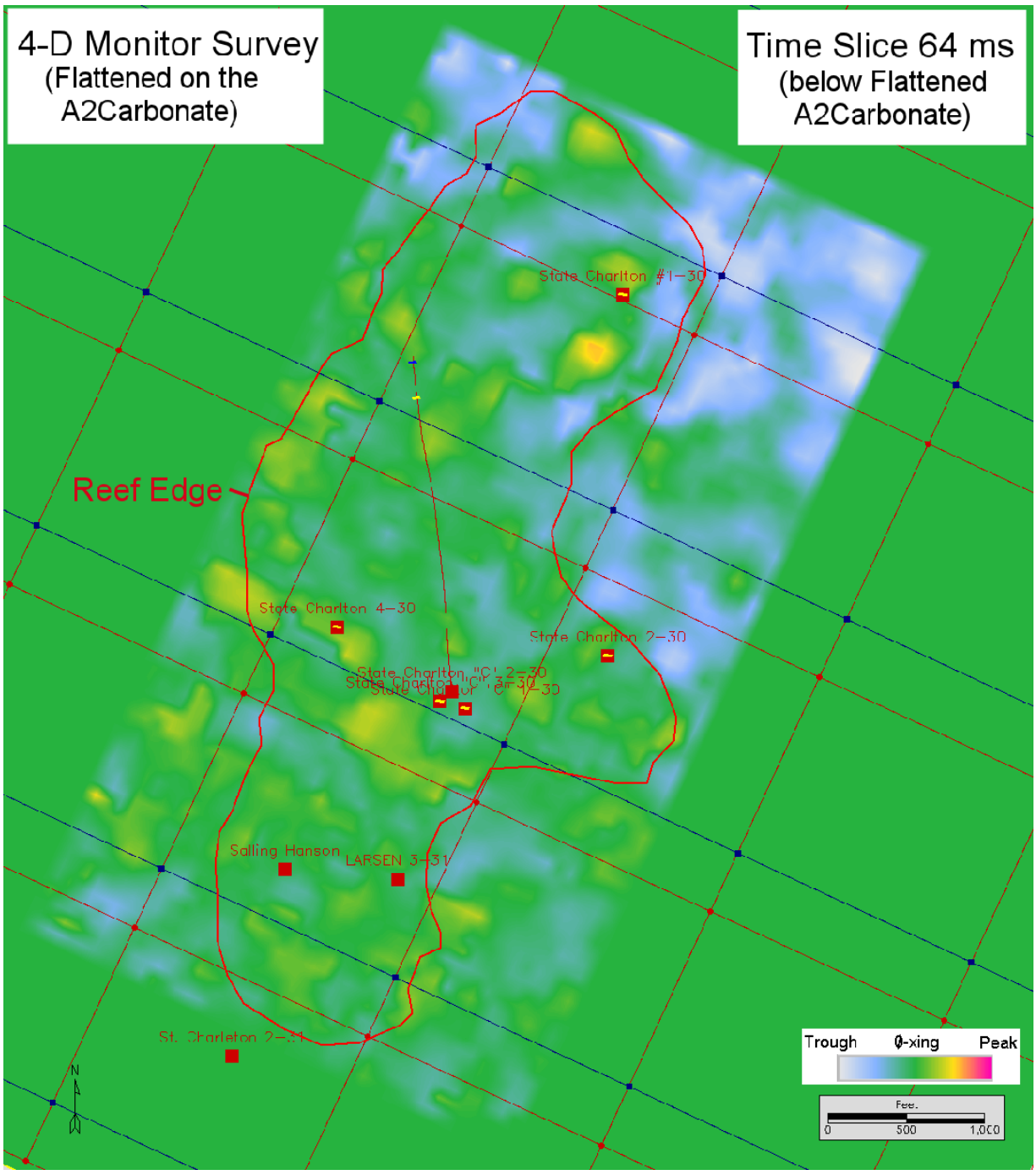
4-D Monitor Survey
(Flattened on the
A2Carbonate)
Time Slice 64 ms
(below Flattened
A2Carbonate)
State Charlton #1-30
Reef Edge
State Charlton 4-30
State Charlton 2-30
Salling Hanson
LARSEN 3-31
Trough
0-xing
Peak
Feet
0
500
1,000
N

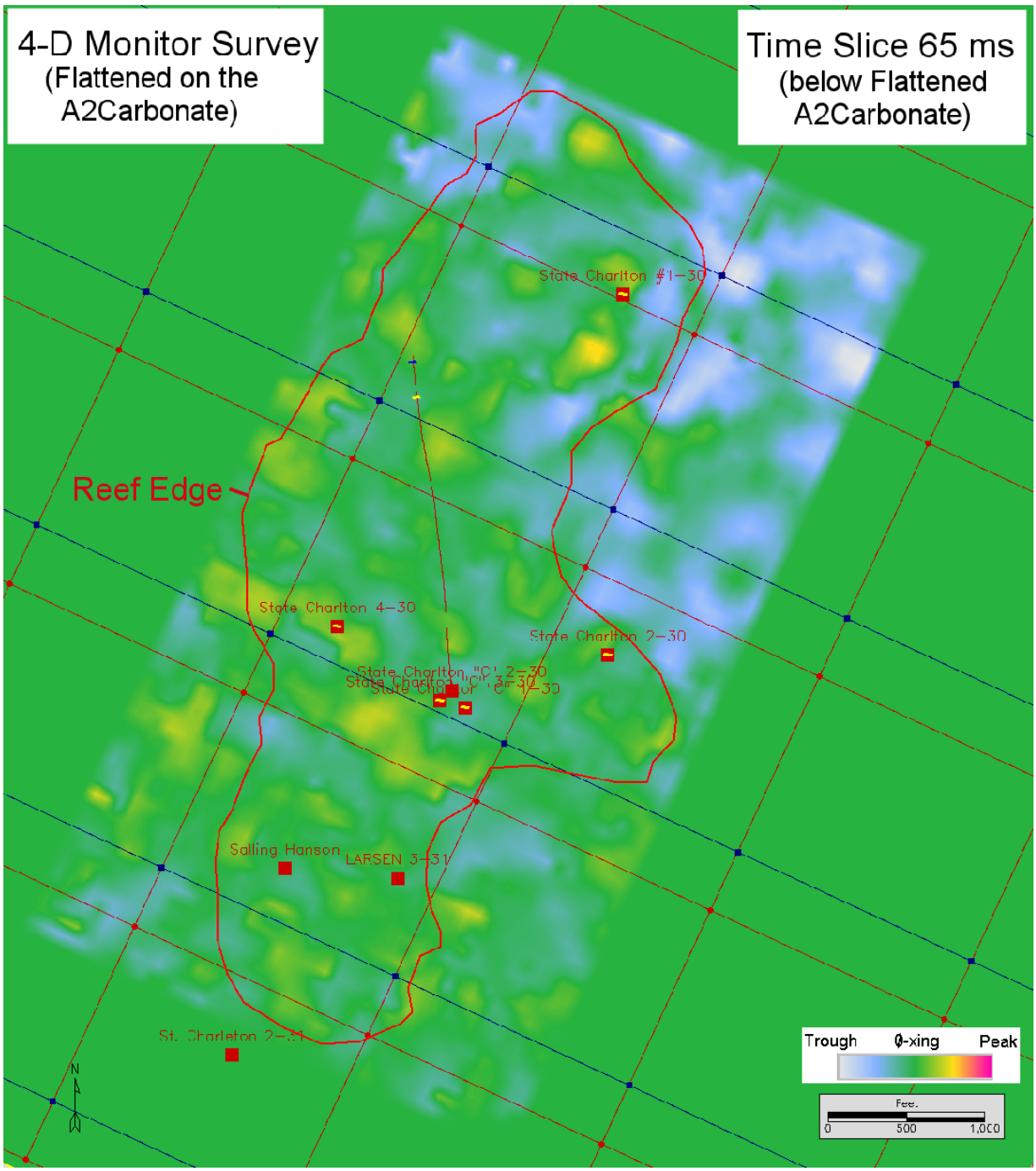
4-D Monitor Survey
(Flattened on the
A2Carbonate)
Time Slice 65 ms
(below Flattened
A2Carbonate)
State Charlton #1-30
Reef Edge
State Charlton 4-30
State Charlton 2-30
Salling Hanson
LARSEN 3-31
Trough
0-xing
Peak
Feet
0
500
1,000
N

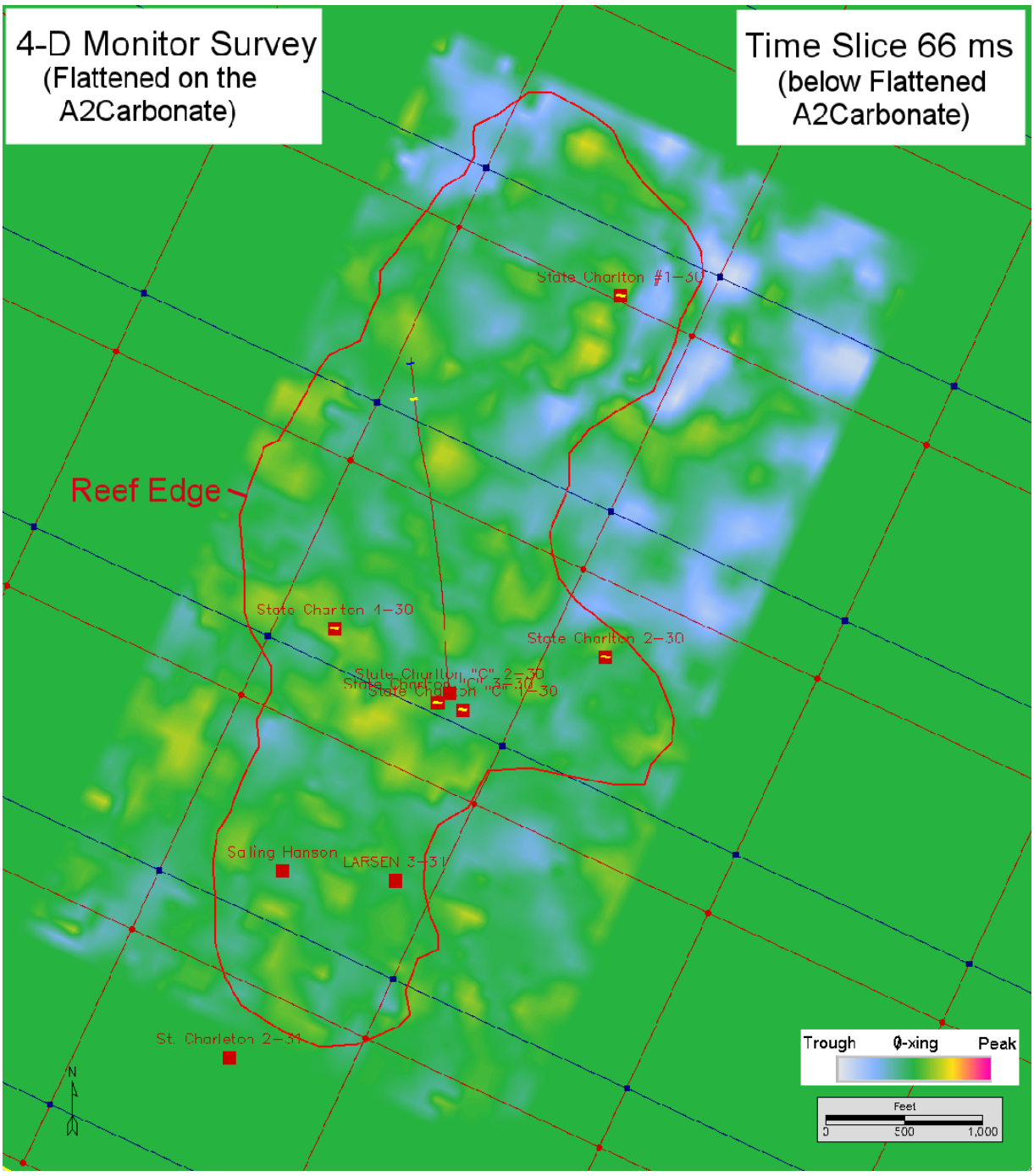
4-D Monitor Survey
(Flattened on the
A2Carbonate)
Time Slice 66 ms
(below Flattened
A2Carbonate)
State Charlton #1-30
Reef Edge
State Charlton 1-30
State Charlton 2-30
Saling Hanson
LARSEN 3-31
St. Charleton 2-31
N
Trough
0-xing
Peak
Feet
0
500
1,000

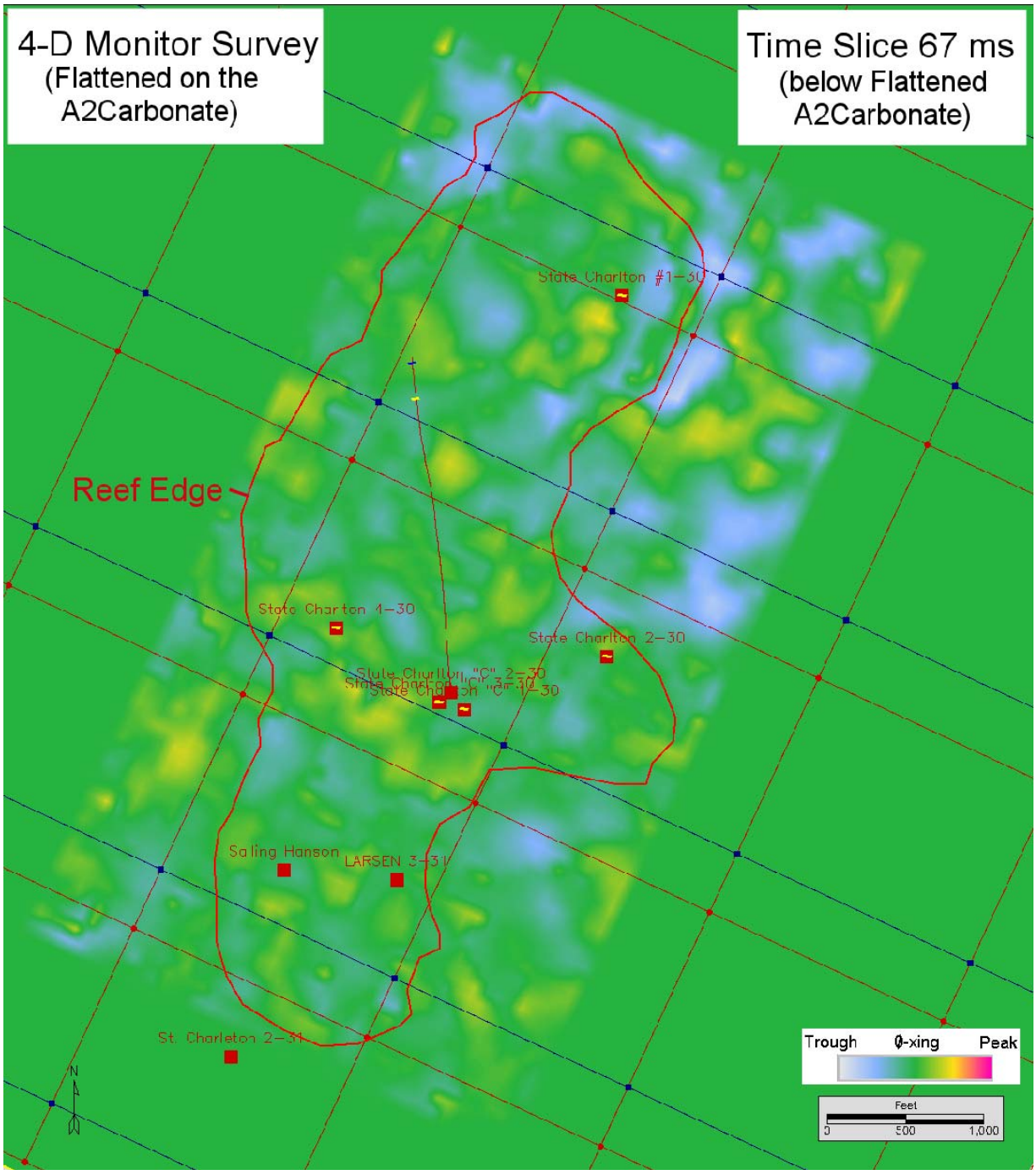
4-D Monitor Survey
(Flattened on the
A2Carbonate)
Time Slice 67 ms
(below Flattened
A2Carbonate)
State Charlton #1-30
Reef Edge
State Charlton 1-30
State Charlton 2-30
Saling Hanson
LARSEN 3-31
St. Charleton 2-31
Trough
0-xing
Peak
Feet
0
500
1,000
N

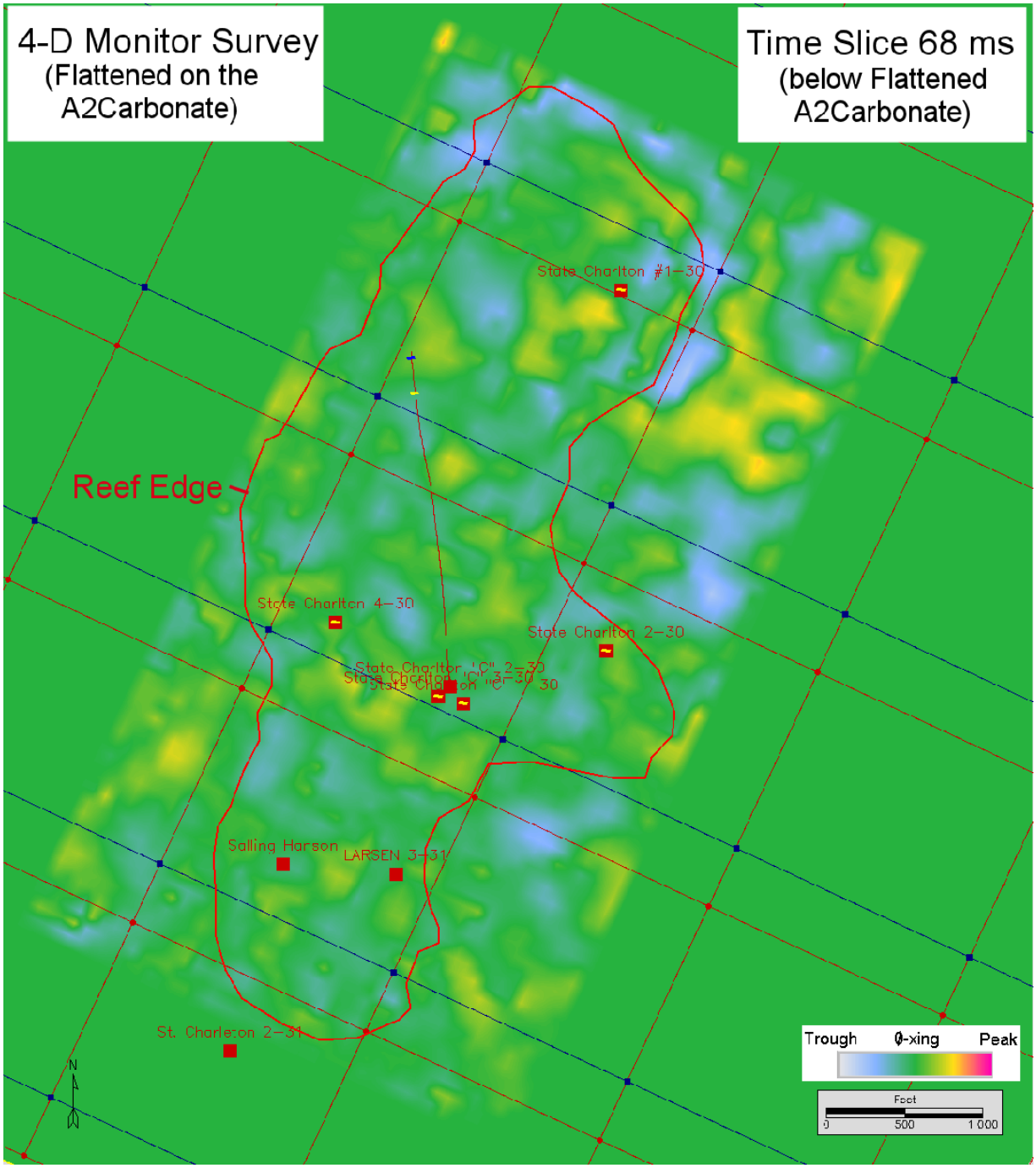
4-D Monitor Survey
(Flattened on the
A2Carbonate)
Time Slice 68 ms
(below Flattened
A2Carbonate)
State Charlton #1-30
Reef Edge
State Charlton 4-30
State Charlton 2-30
Salling Harson
LARSEN 3-31
St. Charleton 2-31
Trough
0-xing
Peak
Feet
0
500
1,000
N

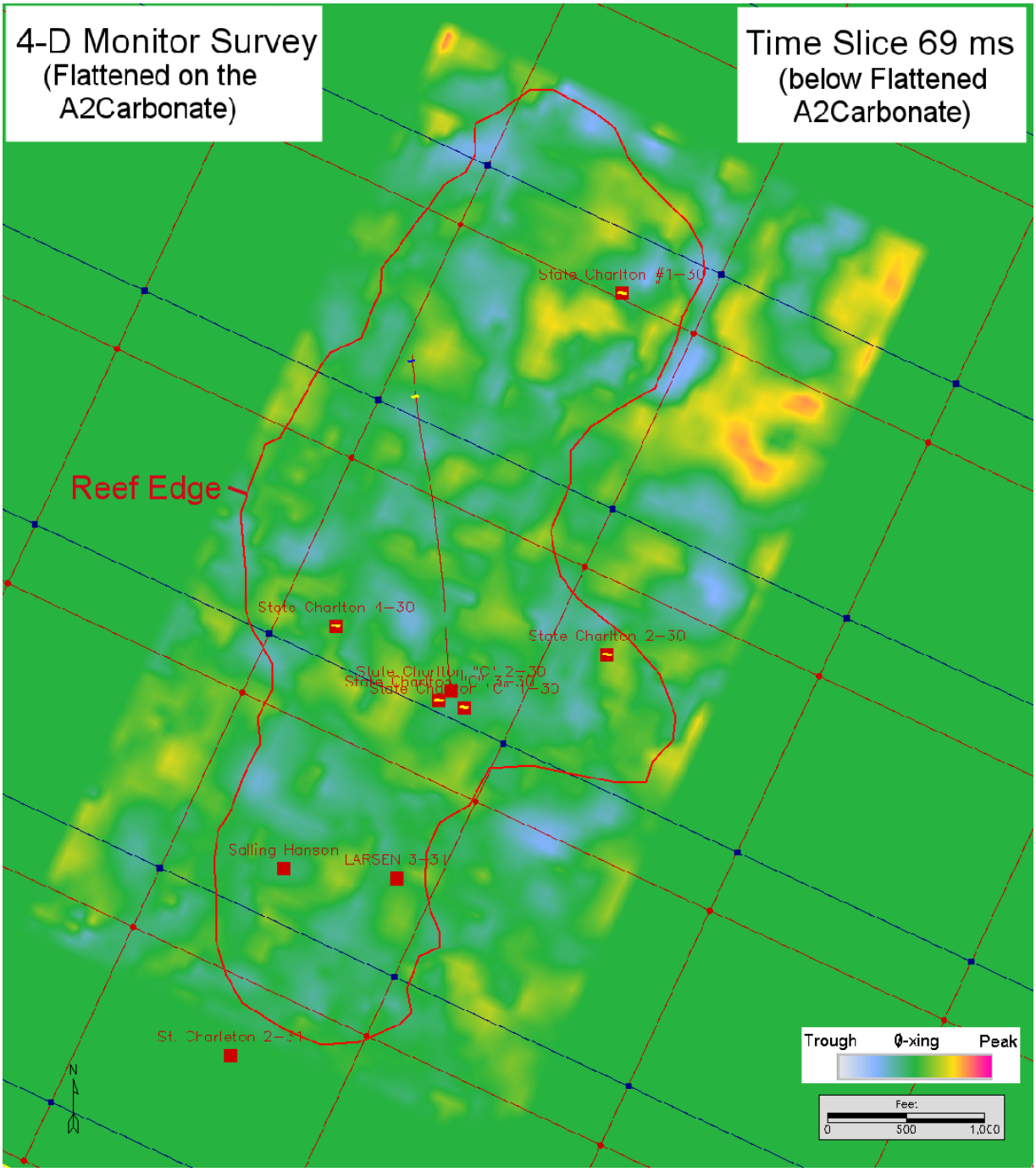
4-D Monitor Survey
(Flattened on the
A2Carbonate)
Time Slice 69 ms
(below Flattened
A2Carbonate)
State Charlton #1-30
Reef Edge
State Charlton 1-30
State Charlton 2-30
Salling Hanson
LARSEN 3-31
St. Charleton 2-31
Trough
0-xing
Peak
Fee:
0
500
1,000
N

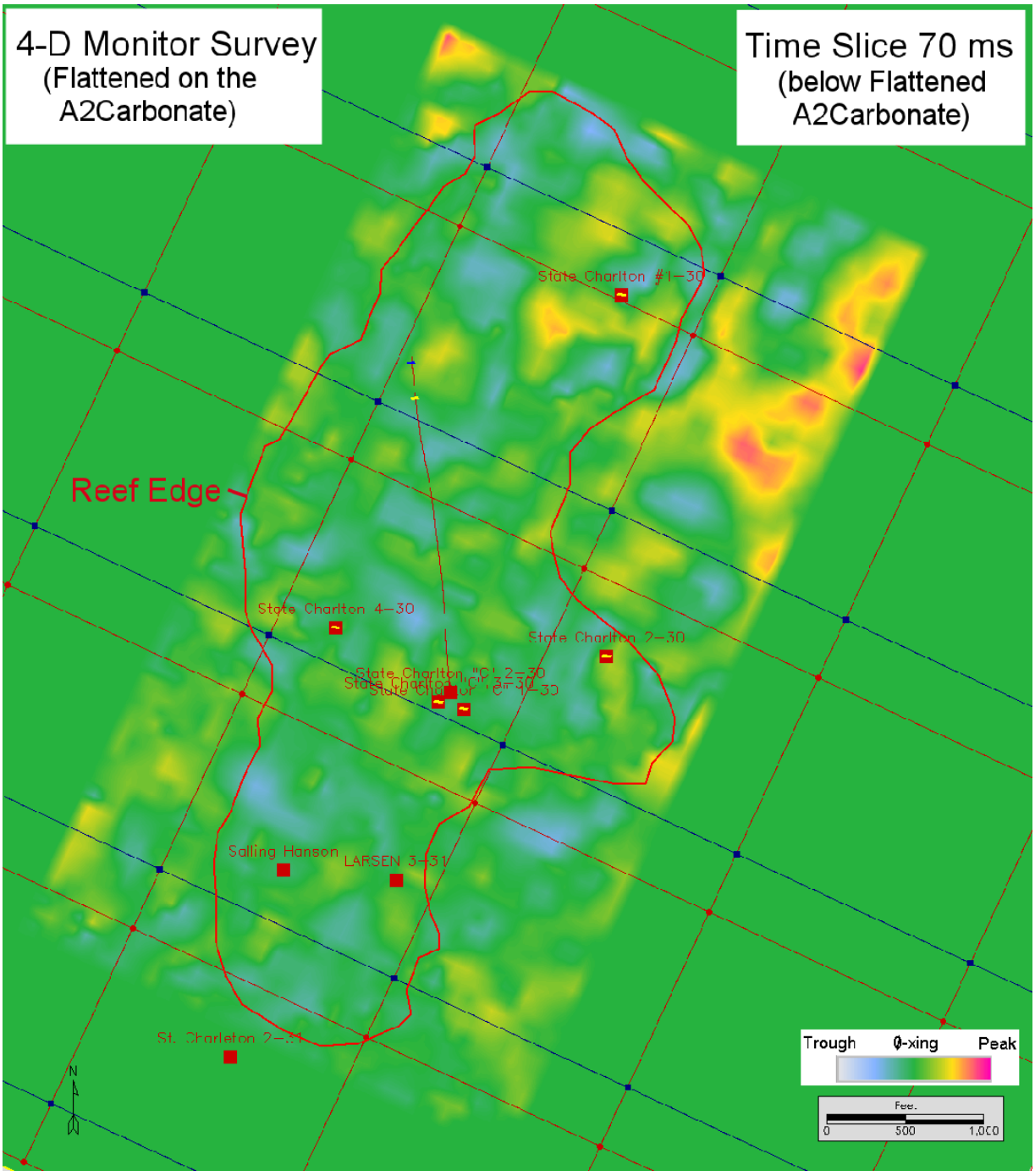
4-D Monitor Survey
(Flattened on the
A2Carbonate)
Time Slice 70 ms
(below Flattened
A2Carbonate)
State Charlton #1-30
Reef Edge
State Charlton 4-30
State Charlton 2-30
Salling Hanson
LARSEN 3-31
Trough
0-xing
Peak
Feet
0
500
1,000
N

10.3 Appendix G - Instantaneous frequency porosity and acoustic amplitude maps generated during the first attempt to characterize the reef's porosity system: 873 – 907 msec

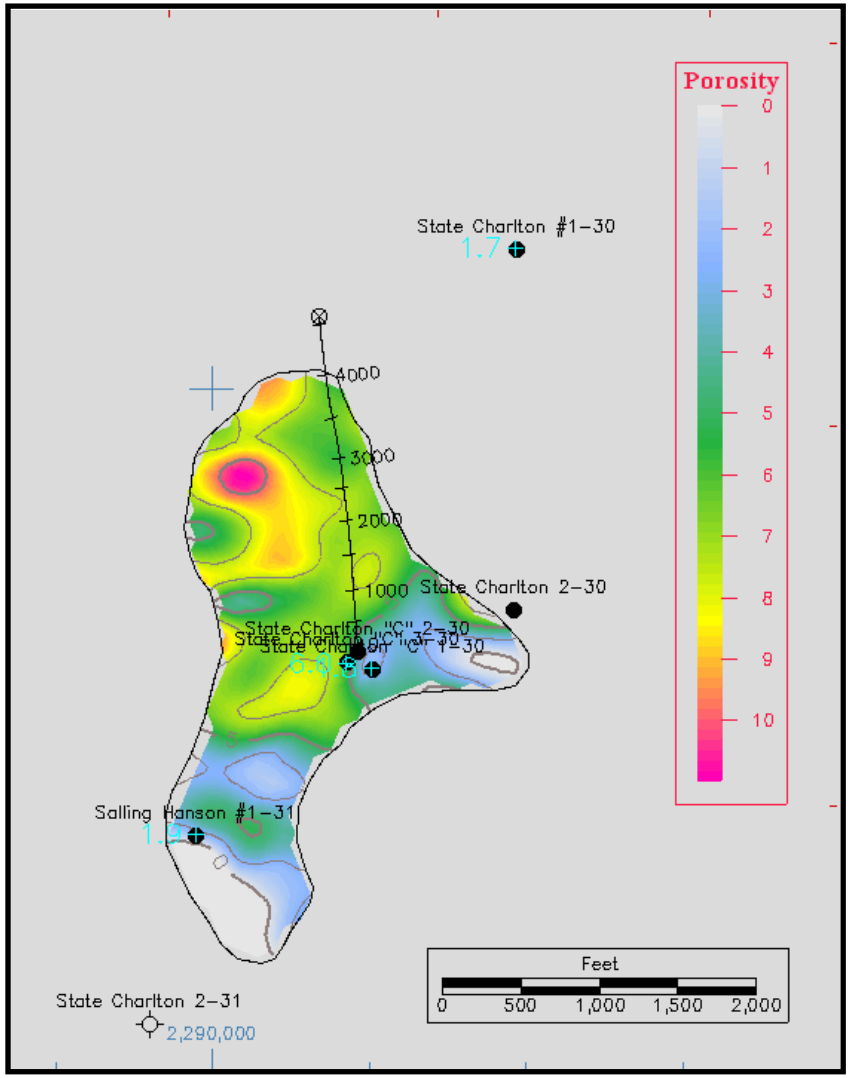

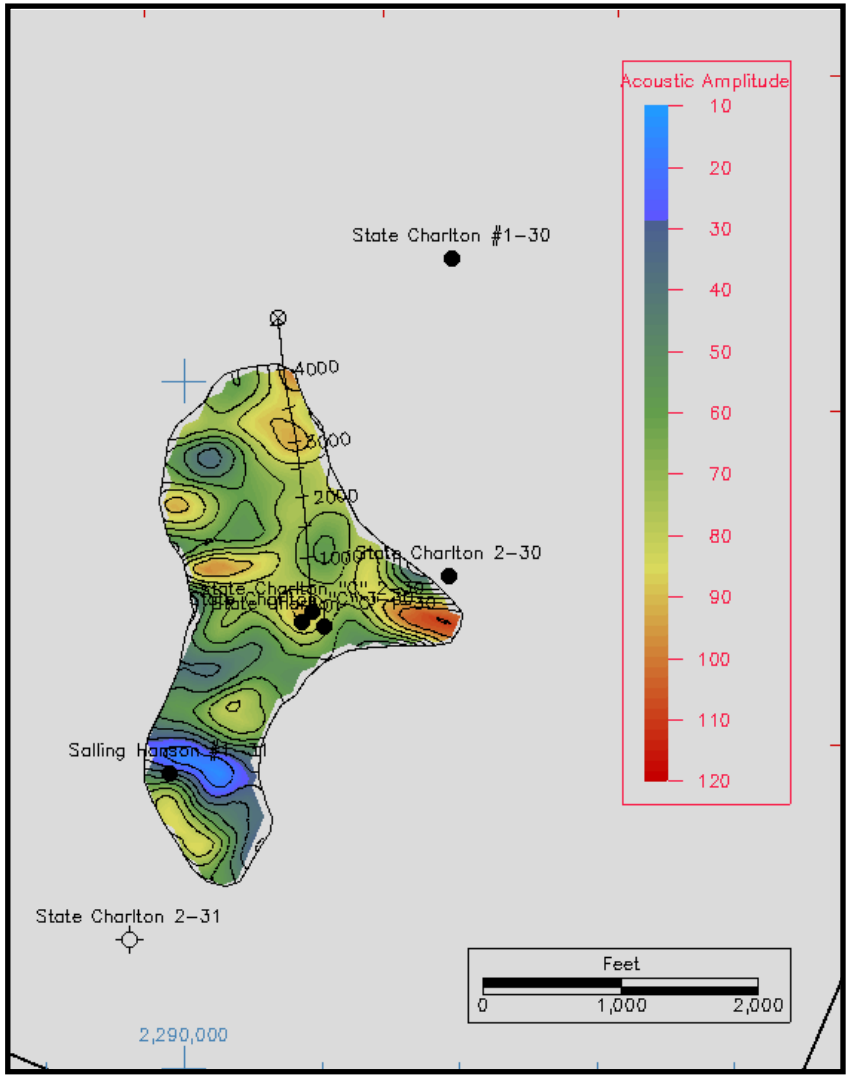

873 msec

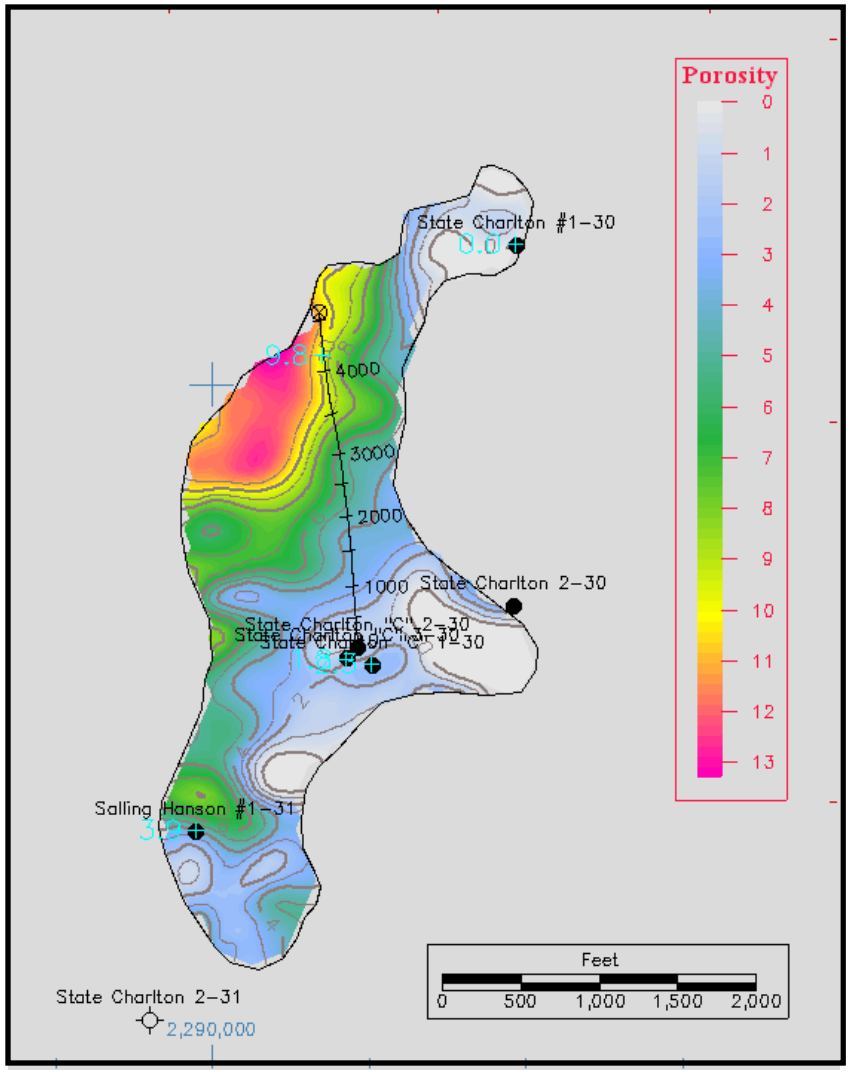
Porosity
0
1
2
3
4
5
6
7
8
9
10
11
12
13
State Charlton #1-30
4000
3000
2000
1000
State Charlton 2-30
Salling Hanson #1-31
State Charlton 2-31
2,290,000
Feet
0
500
1,000
1,500
2,000

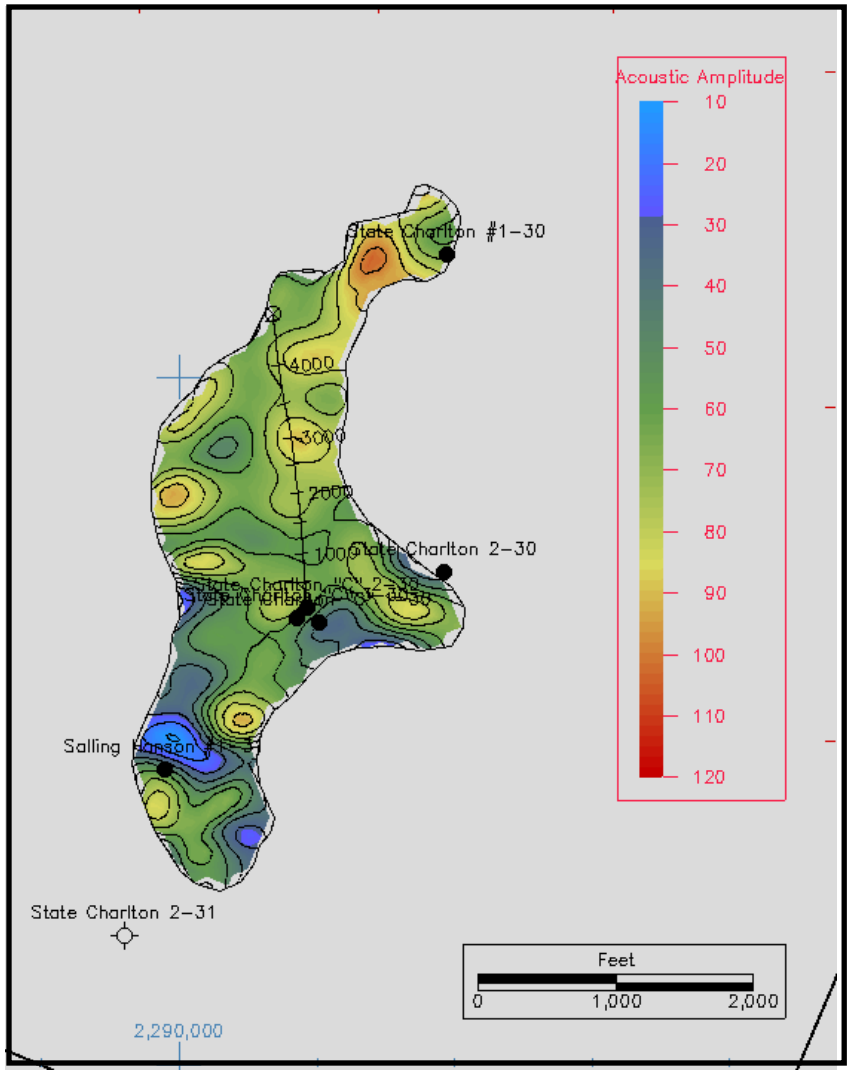
Acoustic Amplitude
10
20
30
40
50
60
70
80
90
100
110
120
State Charlton #1-30
4000
3000
2000
1000
State Charlton 2-30
Salling Hanson
State Charlton 2-31
2,290,000
Feet
0
1,000
2,000

875 msec

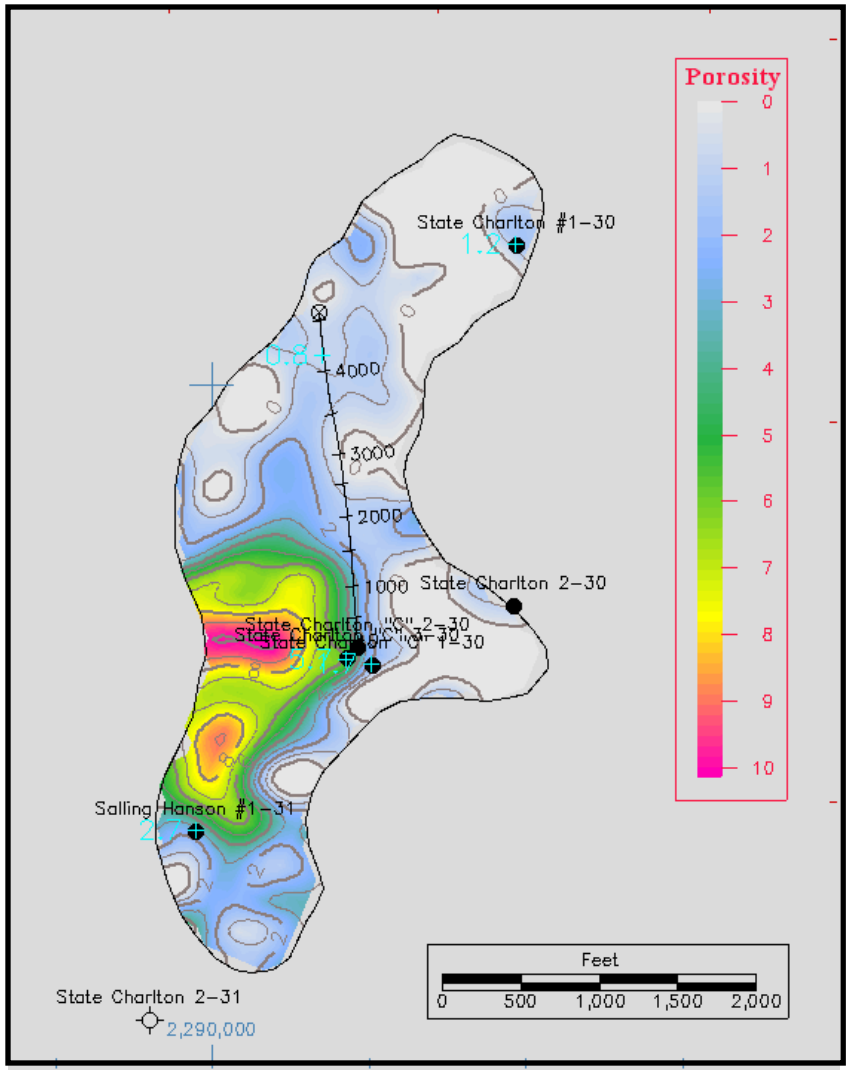
Porosity
0
1
2
3
4
5
6
7
8
9
10
State Charlton #1-30
State Charlton 2-30
Salling Hanson #1-31
State Charlton 2-31
4000
3000
2000
1000
Feet
0
500
1,000
1,500
2,000
2,290,000

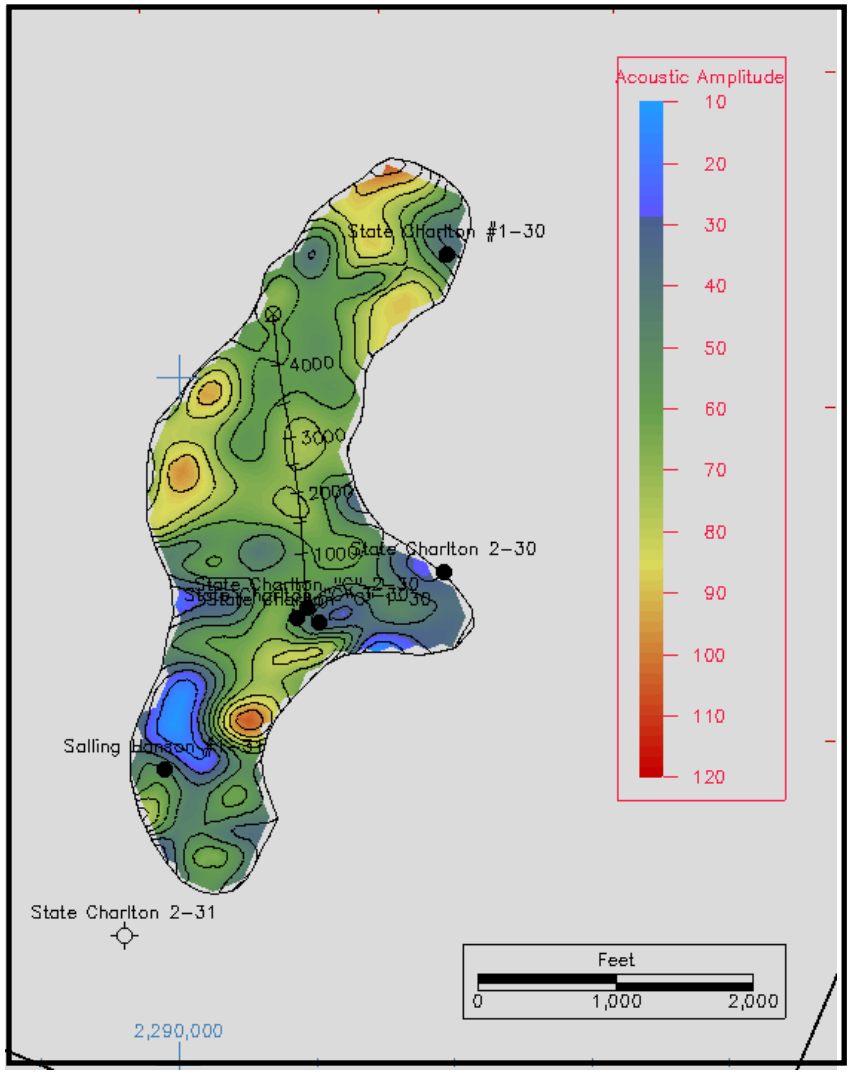
Acoustic Amplitude
10
20
30
40
50
60
70
80
90
100
110
120
State Charlton #1-30
State Charlton 2-30
Salling Hanson #1-31
State Charlton 2-31
4000
3000
2000
1000
Feet
0
1,000
2,000
2,290,000

877 msec

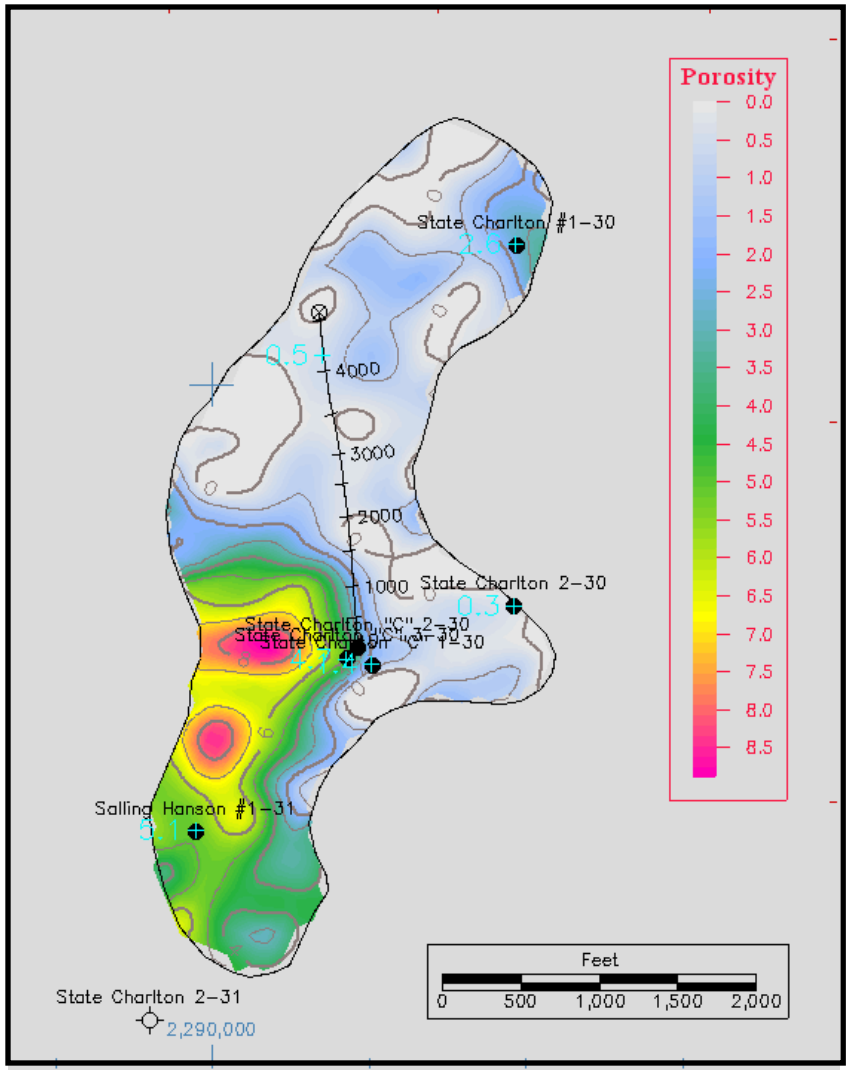
Porosity
0.0
0.5
1.0
1.5
2.0
2.5
3.0
3.5
4.0
4.5
5.0
5.5
6.0
6.5
7.0
7.5
8.0
8.5
State Charlton #1-30
2.6
0.5
4000
3000
2000
1000
State Charlton 2-30
0.3
Salling Hanson #1-31
5.1
State Charlton 2-31
2,290,000
Feet
0
500
1,000
1,500
2,000

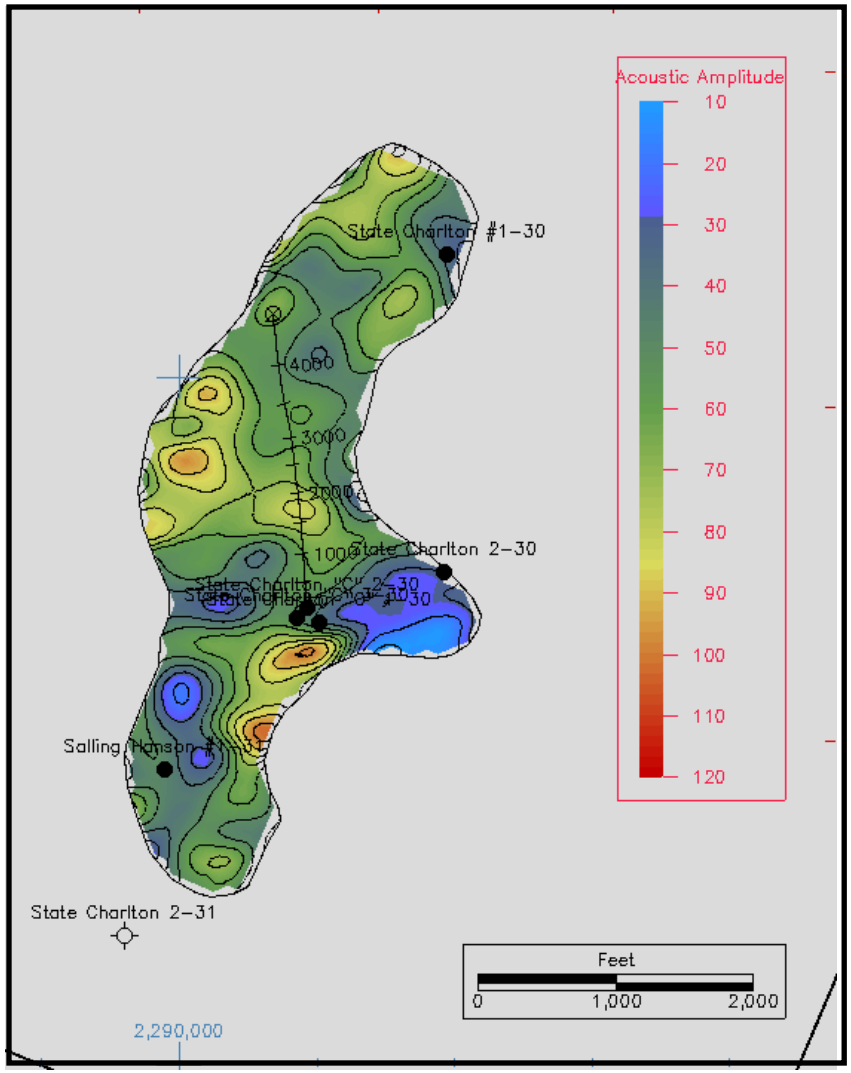
Acoustic Amplitude
10
20
30
40
50
60
70
80
90
100
110
120
State Charlton #1-30
4000
3000
2000
1000
State Charlton 2-30
State Charlton 2-31
2,290,000
Feet
0
1,000
2,000

879 msec

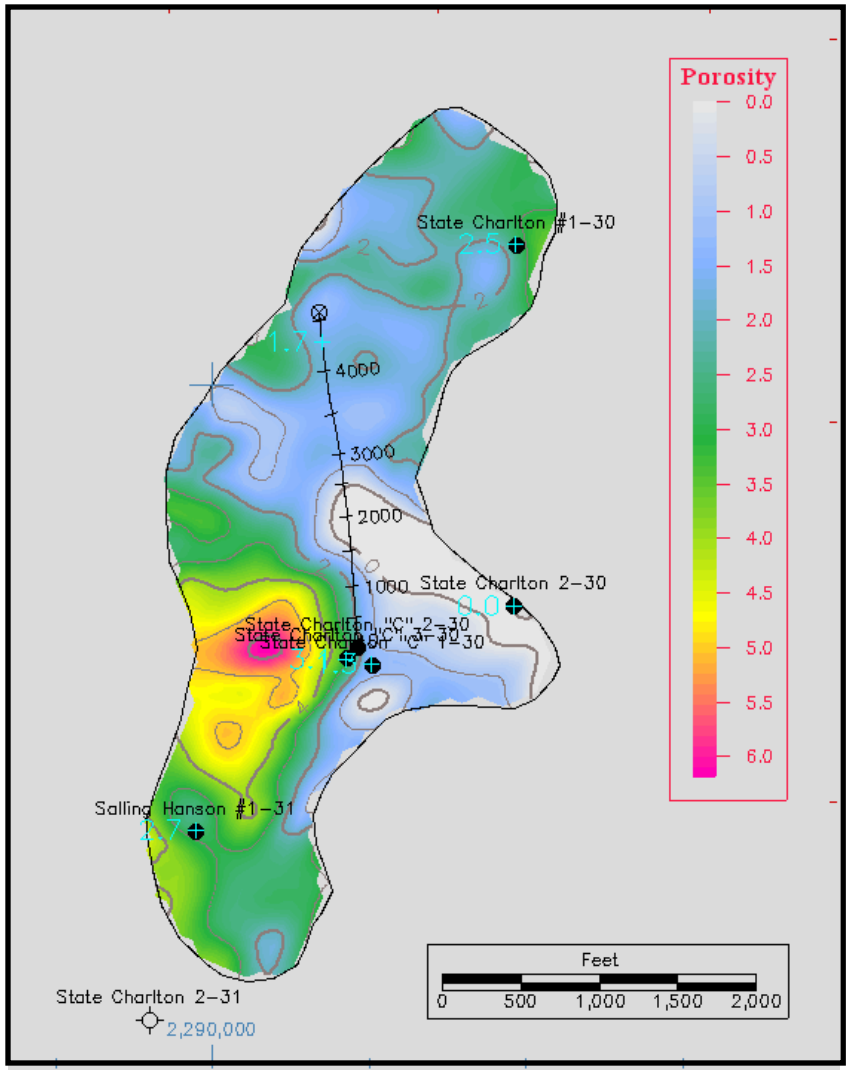
Porosity
0.0
0.5
1.0
1.5
2.0
2.5
3.0
3.5
4.0
4.5
5.0
5.5
6.0
State Charlton #1-30
State Charlton 2-30
Salling Hanson #1-31
State Charlton 2-31
4000
3000
2000
1000
Feet
0
500
1,000
1,500
2,000
2,290,000

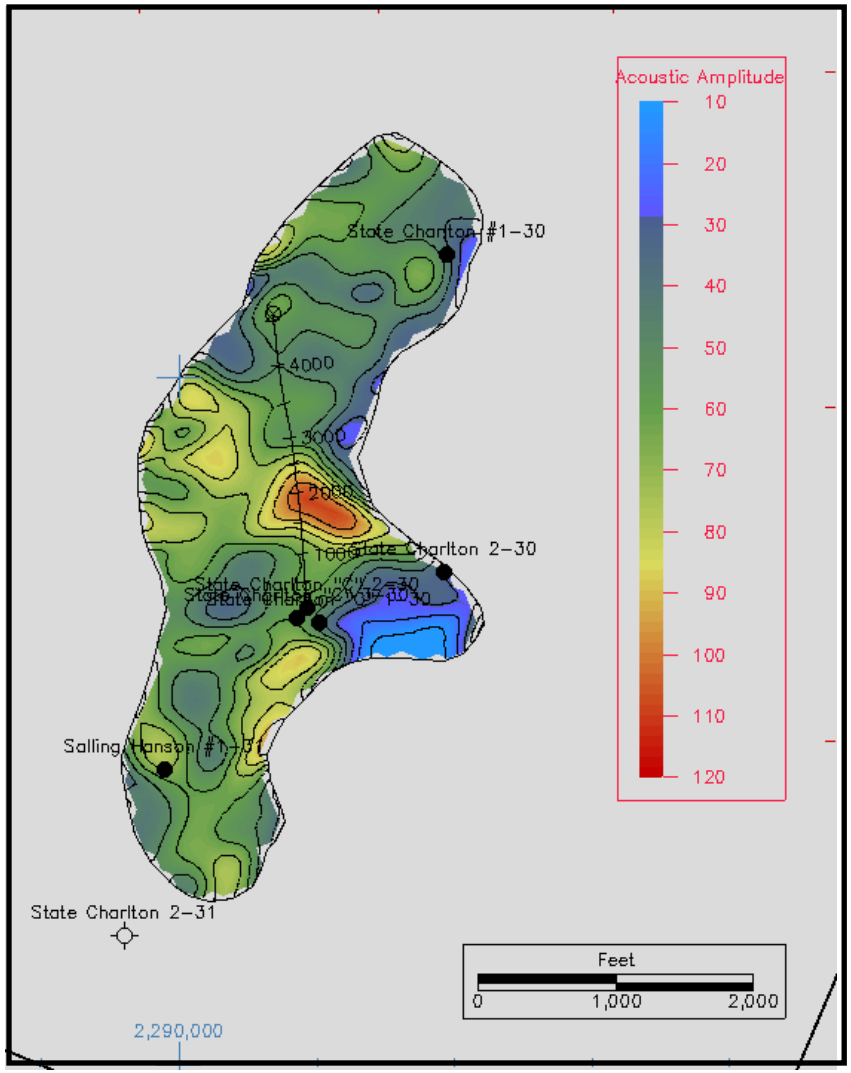
Acoustic Amplitude
10
20
30
40
50
60
70
80
90
100
110
120
State Charlton #1-30
State Charlton 2-30
Salling Hanson #1-31
State Charlton 2-31
4000
3000
2000
1000
Feet
0
1,000
2,000
2,290,000

881 msec

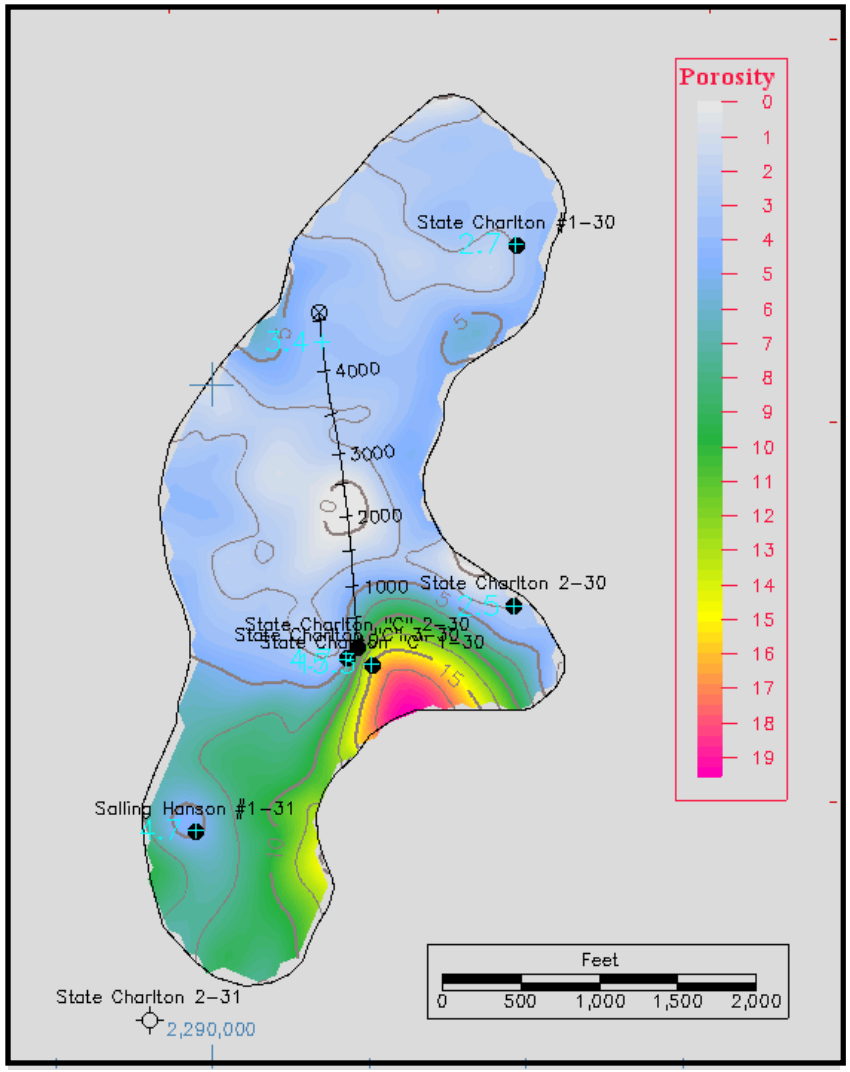
Porosity
0
1
2
3
4
5
6
7
8
9
10
11
12
13
14
15
16
17
18
19
State Charlton #1-30
2.7
4000
3000
2000
1000
State Charlton 2-30
State Charlton "C" 2-30
Salling Hanson #1-31
State Charlton 2-31
2,290,000
Feet
0
500
1,000
1,500
2,000

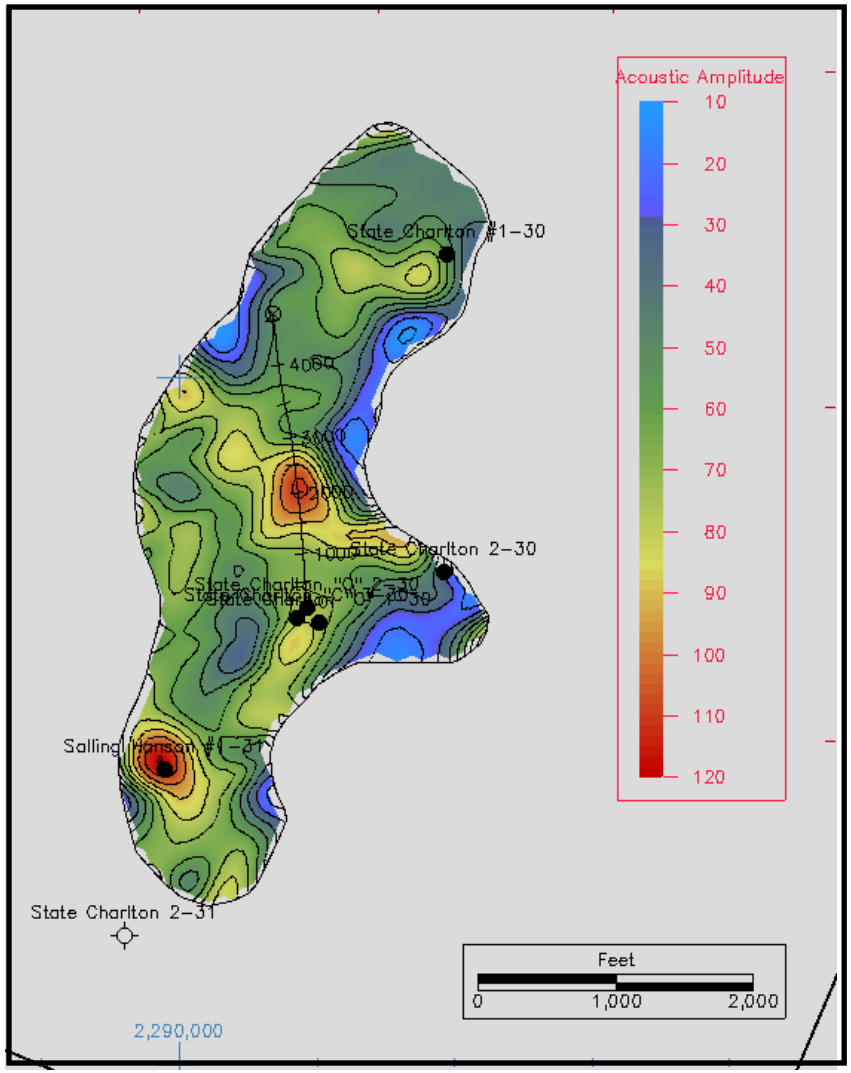
Acoustic Amplitude
10
20
30
40
50
60
70
80
90
100
110
120
State Charlton #1-30
4000
3000
2000
1000
State Charlton 2-30
Salling Hanson #1-31
State Charlton 2-31
2,290,000
Feet
0
1,000
2,000

883 msec

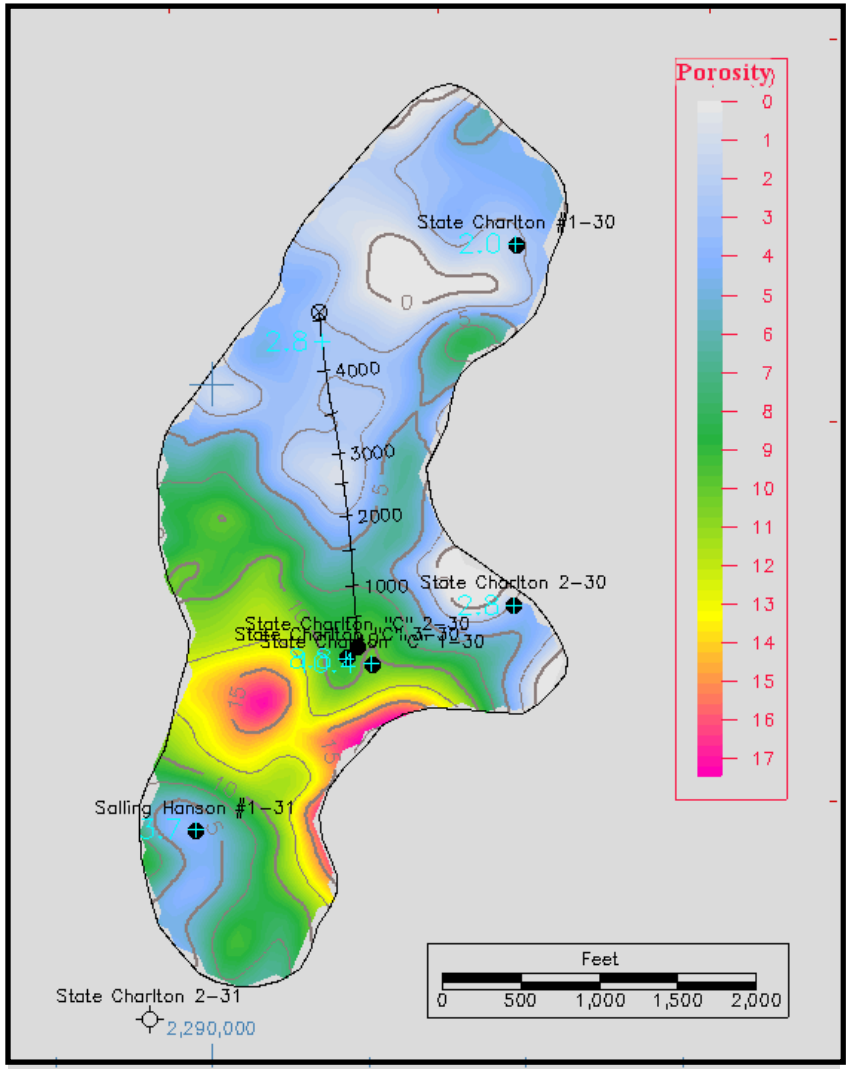
Porosity
0
1
2
3
4
5
6
7
8
9
10
11
12
13
14
15
16
17
State Charlton #1-30
2.0
2.8
4000
3000
2000
1000
State Charlton 2-30
State Charlton "C" 2-30
3.0
Salling Hanson #1-31
State Charlton 2-31
2,290,000
Feet
0
500
1,000
1,500
2,000

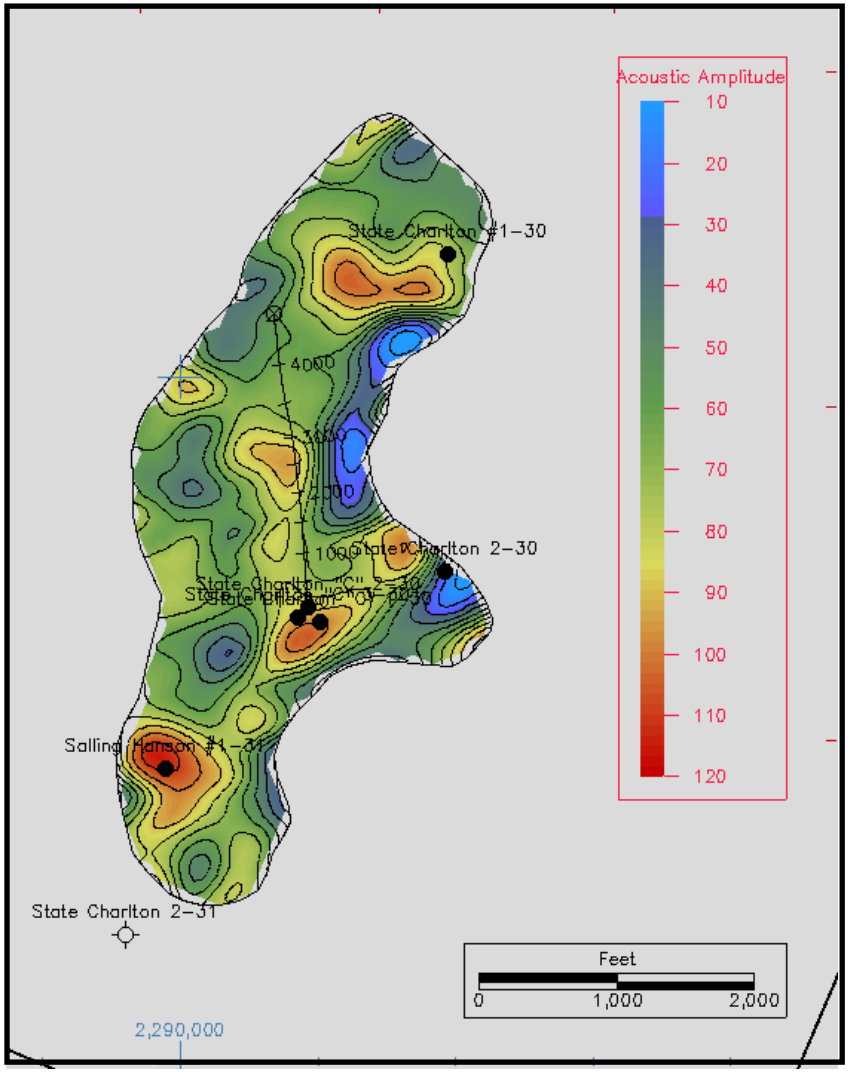
Acoustic Amplitude
10
20
30
40
50
60
70
80
90
100
110
120
State Charlton #1-30
4000
3000
2000
1000
State Charlton 2-30
Salling Hanson #1-31
State Charlton 2-31
2,290,000
Feet
0
1,000
2,000

885 msec

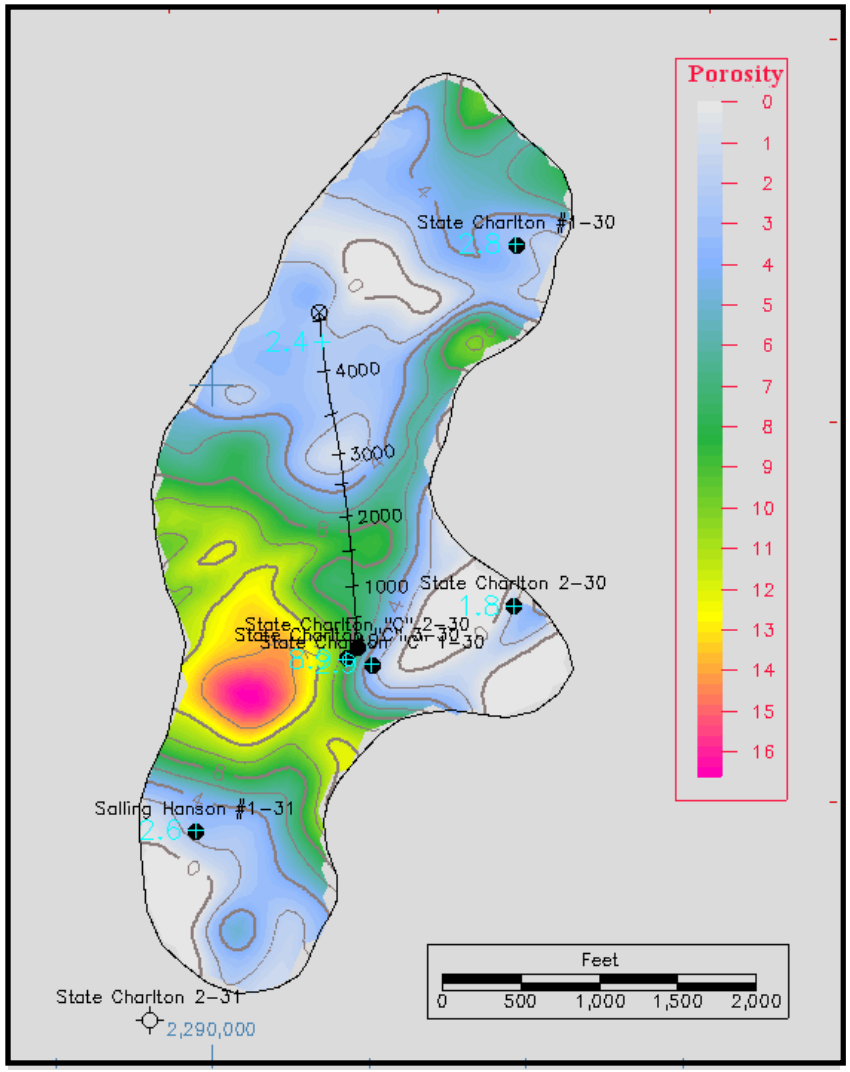
Porosity
0
1
2
3
4
5
6
7
8
9
10
11
12
13
14
15
16
State Charlton #1-30
2.8
2.4
4000
3000
2000
1000
State Charlton 2-30
1.8
5.2
Salling Hanson #1-31
2.6
State Charlton 2-31
2,290,000
Feet
0
500
1,000
1,500
2,000

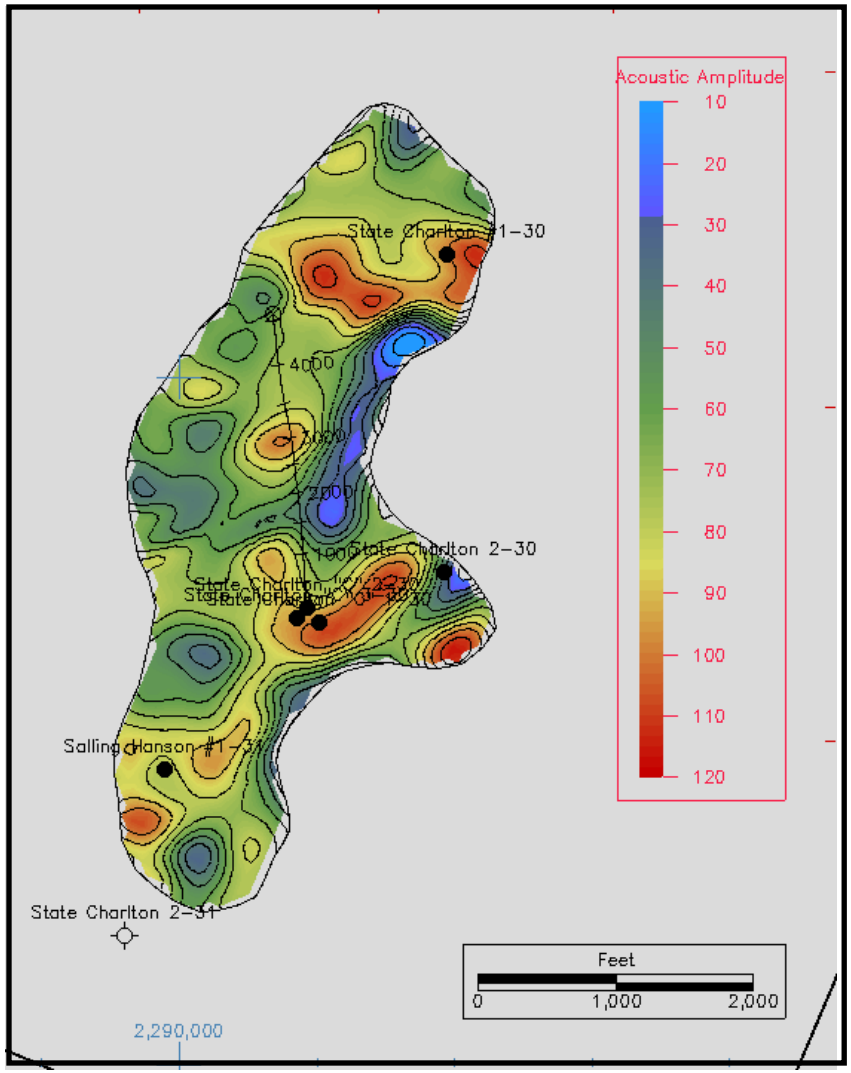
Acoustic Amplitude
10
20
30
40
50
60
70
80
90
100
110
120
State Charlton #1-30
4000
2000
1000
State Charlton 2-30
Salling Hanson #1-31
State Charlton 2-31
2,290,000
Feet
0
1,000
2,000

887 msec

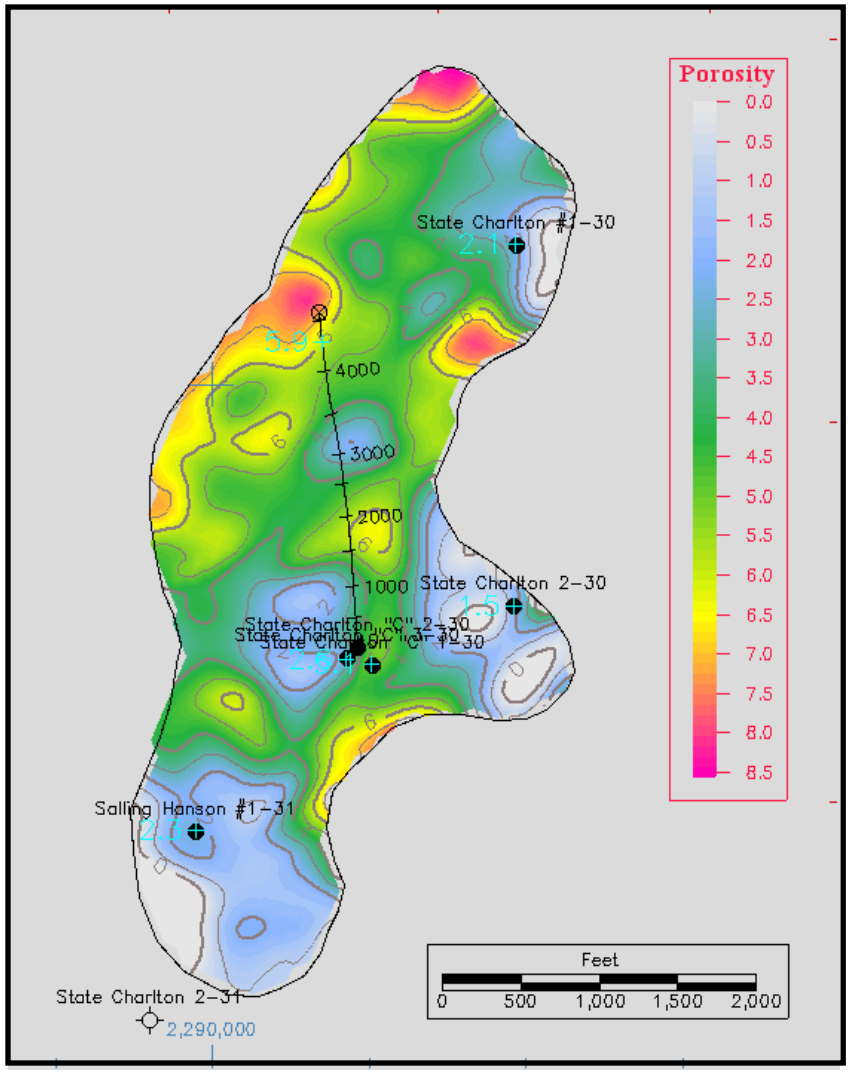
Porosity
0.0
0.5
1.0
1.5
2.0
2.5
3.0
3.5
4.0
4.5
5.0
5.5
6.0
6.5
7.0
7.5
8.0
8.5
State Charlton #1-30
State Charlton 2-30
Salling Hanson #1-31
State Charlton 2-31
4000
3000
2000
1000
Feet
0
500
1,000
1,500
2,000
2,290,000

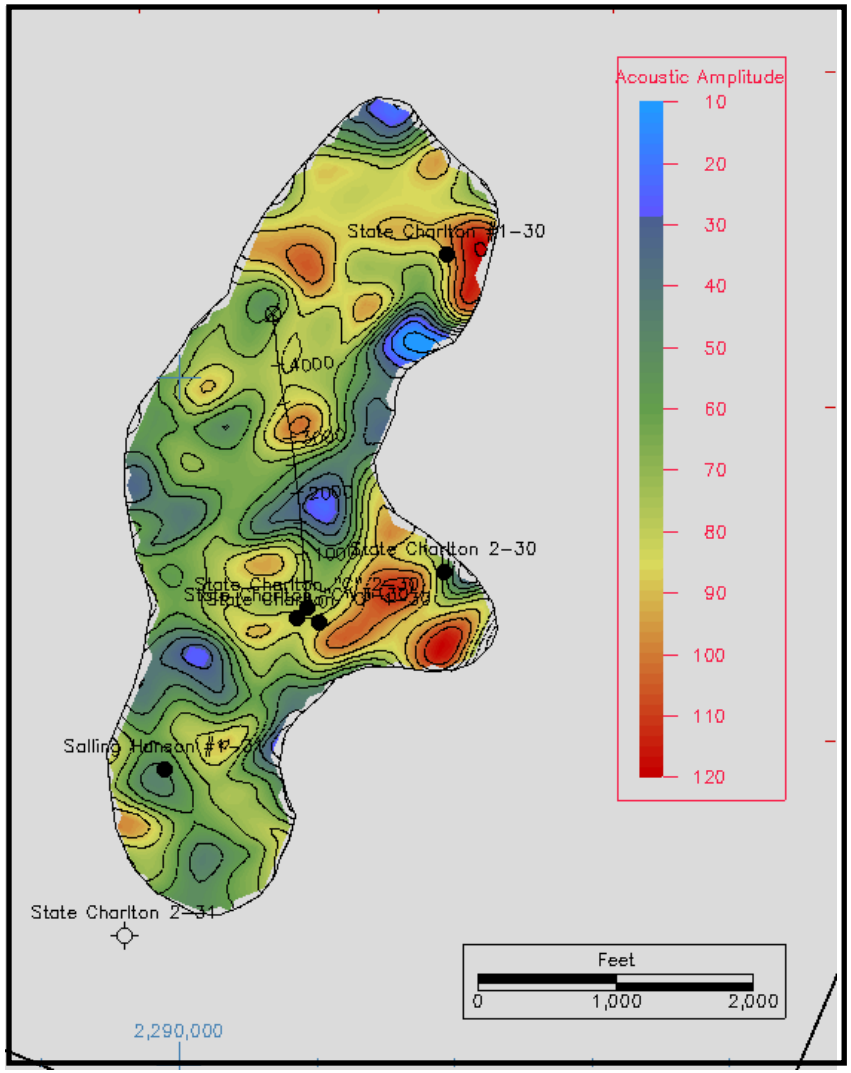
Acoustic Amplitude
10
20
30
40
50
60
70
80
90
100
110
120
State Charlton #1-30
State Charlton 2-30
Salling Hanson #1-31
State Charlton 2-31
4000
2000
1000
Feet
0
1,000
2,000
2,290,000

889 msec

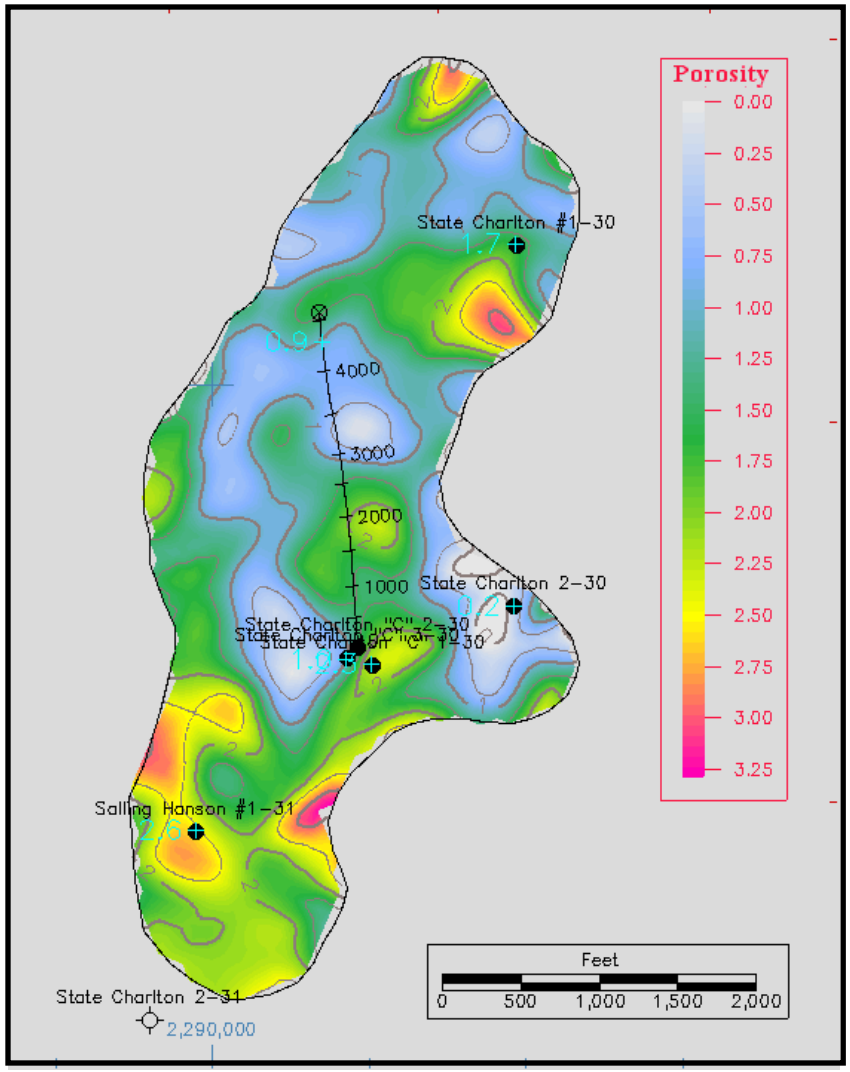
Porosity
0.00
0.25
0.50
0.75
1.00
1.25
1.50
1.75
2.00
2.25
2.50
2.75
3.00
3.25
State Charlton #1-30
State Charlton 2-30
Salling Hanson #1-31
State Charlton 2-31
4000
3000
2000
1000
Feet
0
500
1,000
1,500
2,000
2,290,000

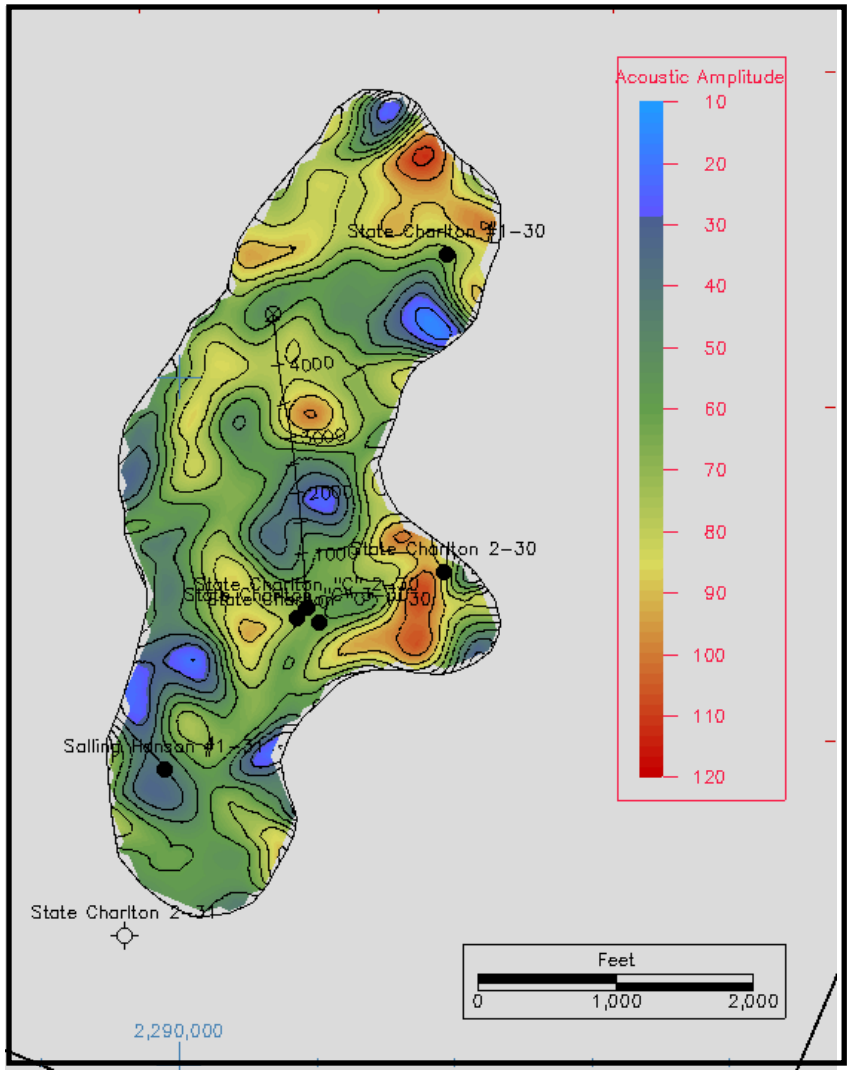
Acoustic Amplitude
10
20
30
40
50
60
70
80
90
100
110
120
State Charlton #1-30
State Charlton 2-30
Salling Hanson #1-31
State Charlton 2-31
4000
2000
1000
Feet
0
1,000
2,000
2,290,000

891 msec

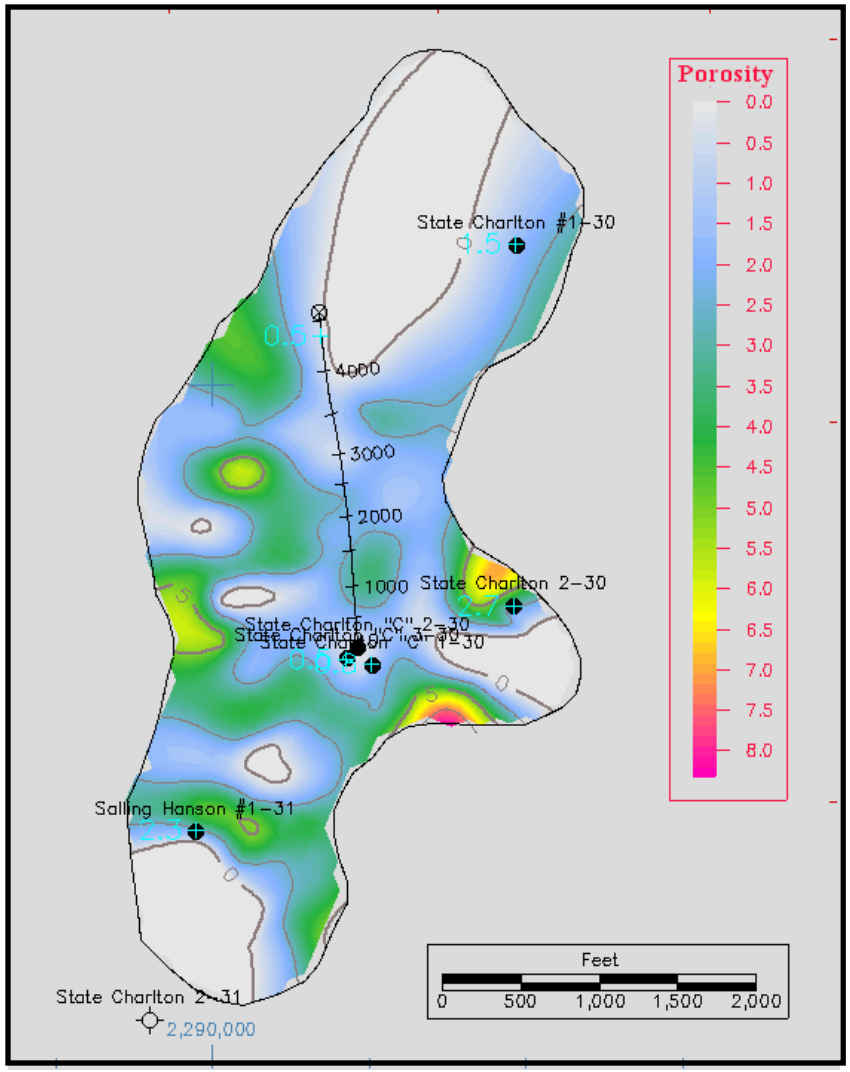
Porosity
0.0
0.5
1.0
1.5
2.0
2.5
3.0
3.5
4.0
4.5
5.0
5.5
6.0
6.5
7.0
7.5
8.0
State Charlton #1-30
0.5
4000
3000
2000
1000
State Charlton 2-30
2.7
State Charlton "C" 2-30
State Charlton "C" 1-30
0.5
Salling Hanson #1-31
2.3
State Charlton 2-31
2,290,000
Feet
0
500
1,000
1,500
2,000

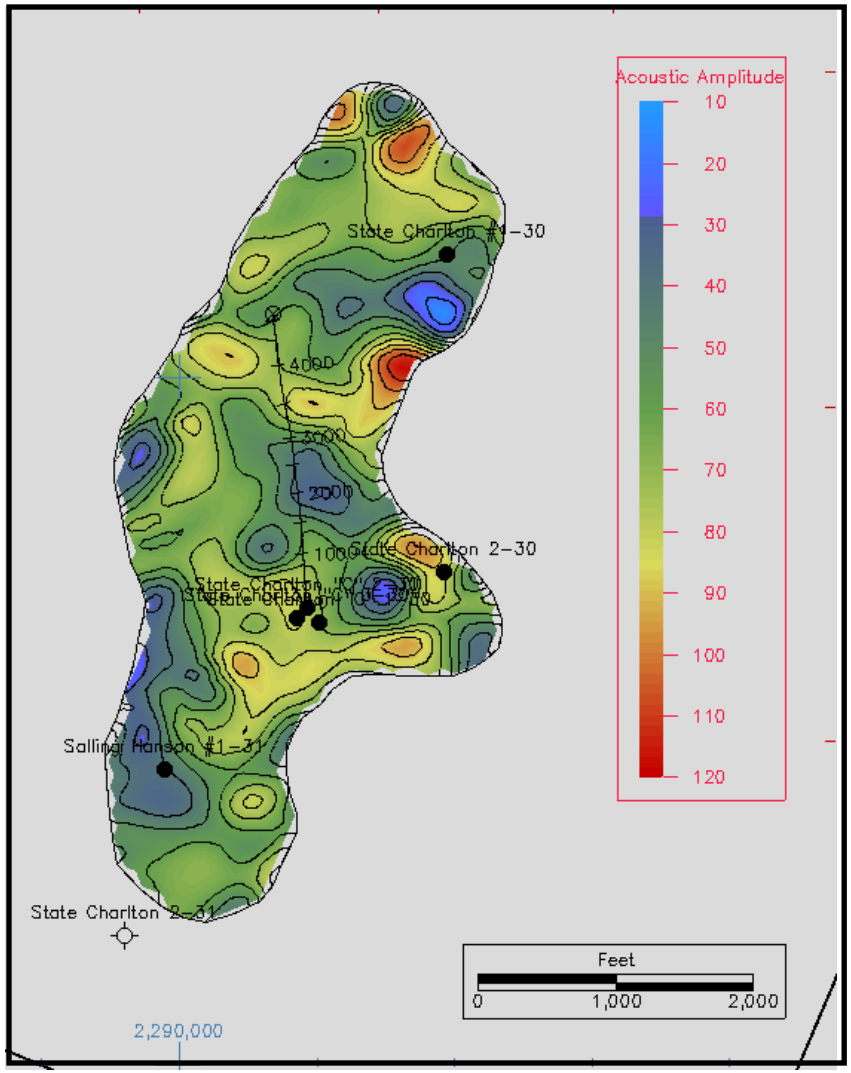
Acoustic Amplitude
10
20
30
40
50
60
70
80
90
100
110
120
State Charlton #1-30
4000
3000
2000
1000
State Charlton 2-30
Salling Hanson #1-31
State Charlton 2-31
2,290,000
Feet
0
1,000
2,000

893 msec

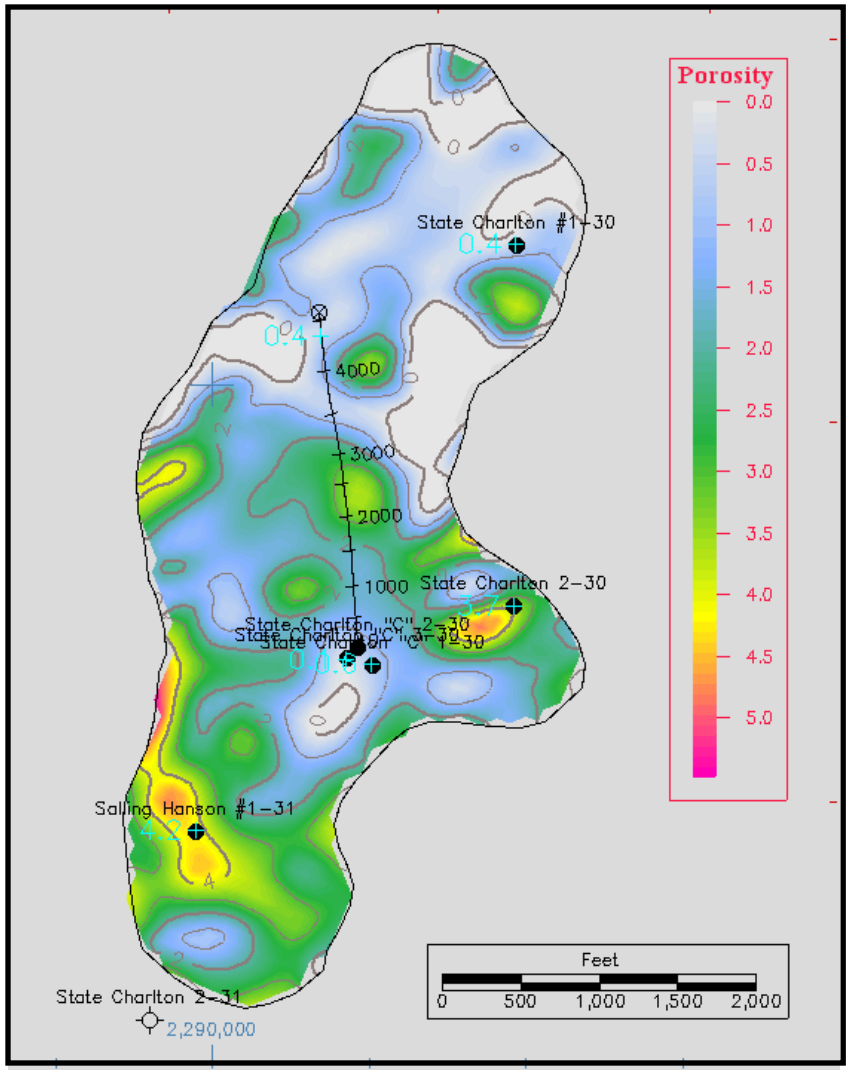
Porosity
0.0
0.5
1.0
1.5
2.0
2.5
3.0
3.5
4.0
4.5
5.0
State Charlton #1-30
0.4
4000
3000
2000
1000
State Charlton 2-30
State Charlton "C" 2-30
Salling Hanson #1-31
4.2
State Charlton 2-31
2,290,000
Feet
0
500
1,000
1,500
2,000

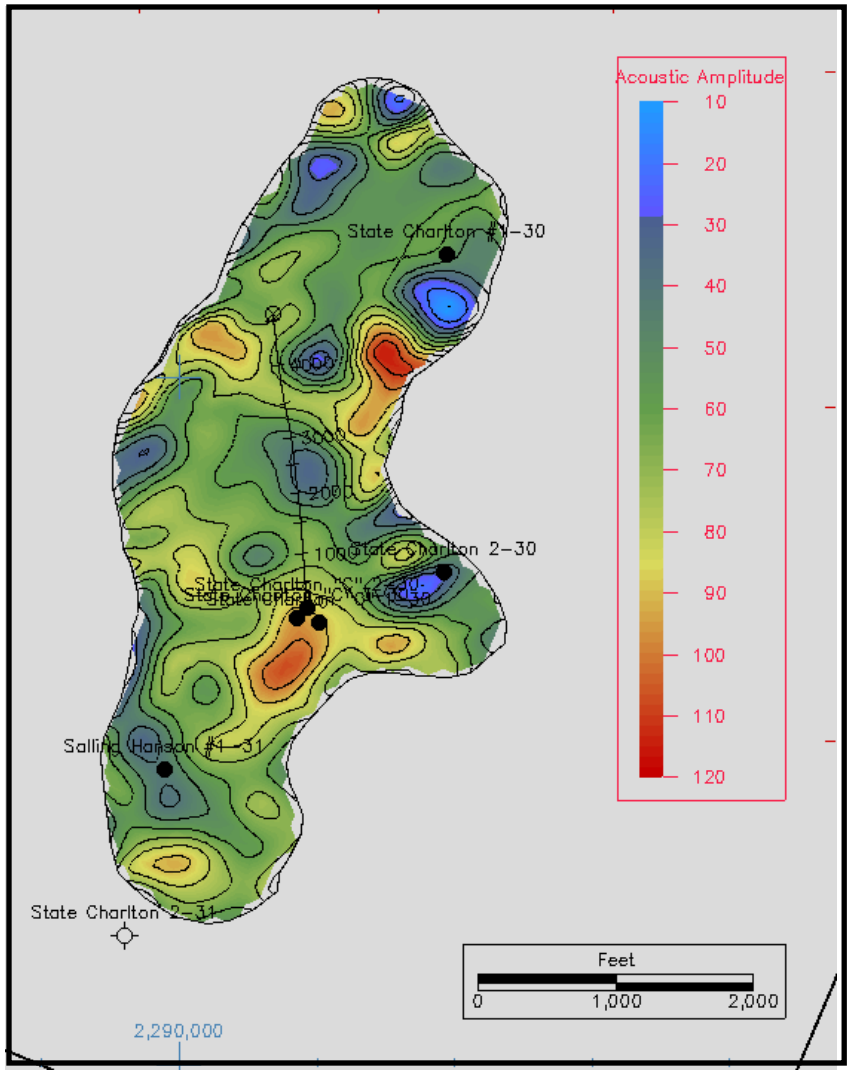
Acoustic Amplitude
10
20
30
40
50
60
70
80
90
100
110
120
State Charlton #1-30
4000
3000
2000
1000
State Charlton 2-30
Salling Hanson #1-31
State Charlton 2-31
2,290,000
Feet
0
1,000
2,000

895 msec

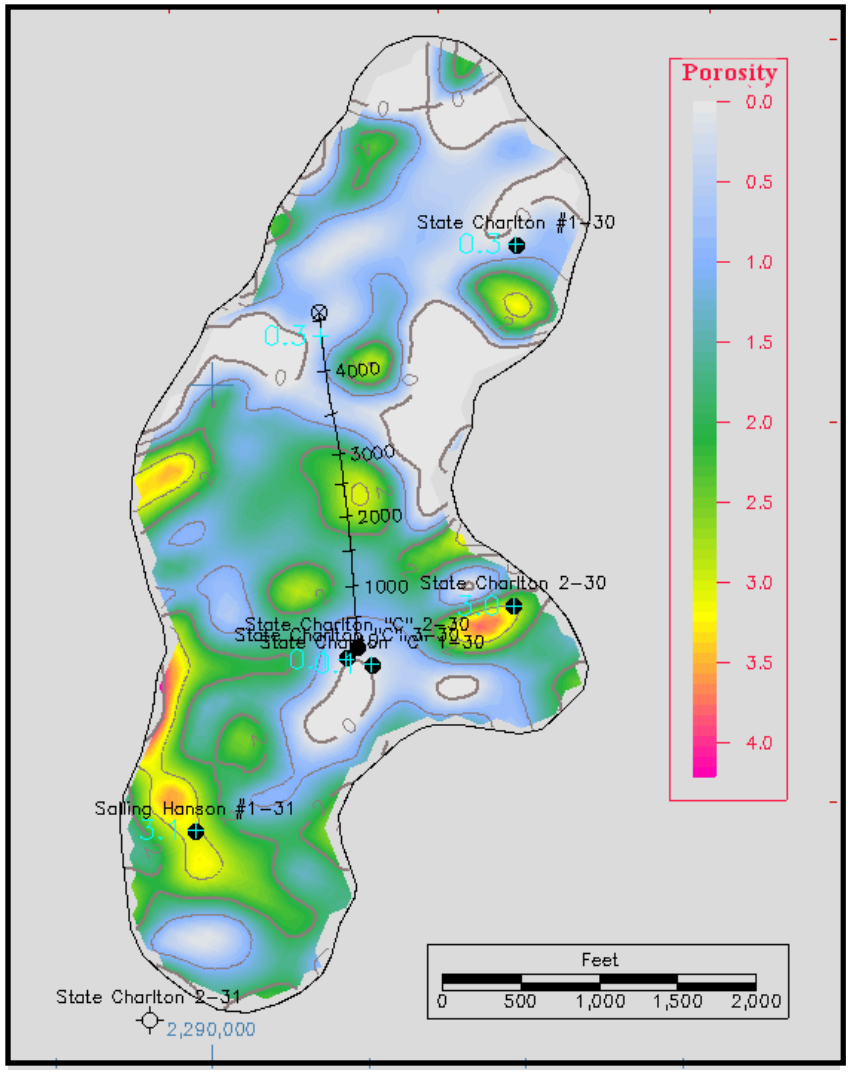
Porosity
0.0
0.5
1.0
1.5
2.0
2.5
3.0
3.5
4.0
State Charlton #1-30
State Charlton 2-30
Salling Hanson #1-31
State Charlton 2-31
4000
3000
2000
1000
Feet
0
500
1,000
1,500
2,000
2,290,000

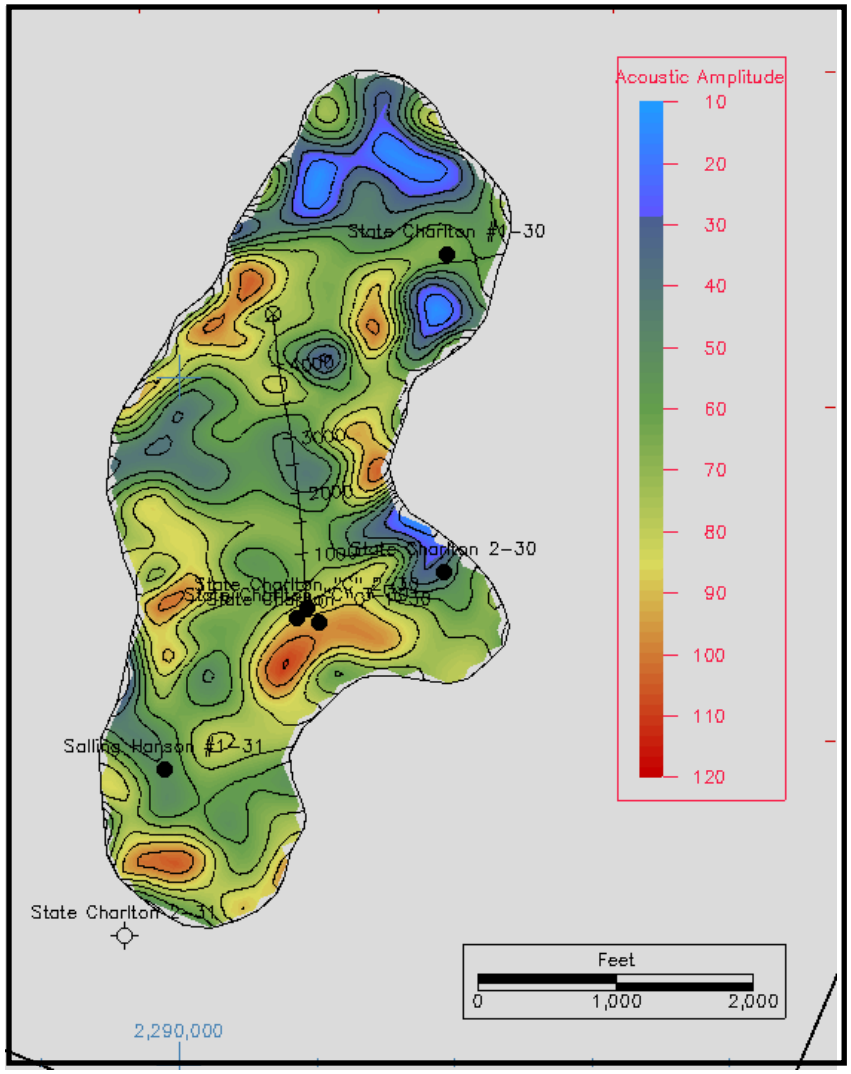
Acoustic Amplitude
10
20
30
40
50
60
70
80
90
100
110
120
State Charlton #1-30
State Charlton 2-30
Salling Hanson #1-31
State Charlton 2-31
Feet
0
1,000
2,000
2,290,000

897 msec

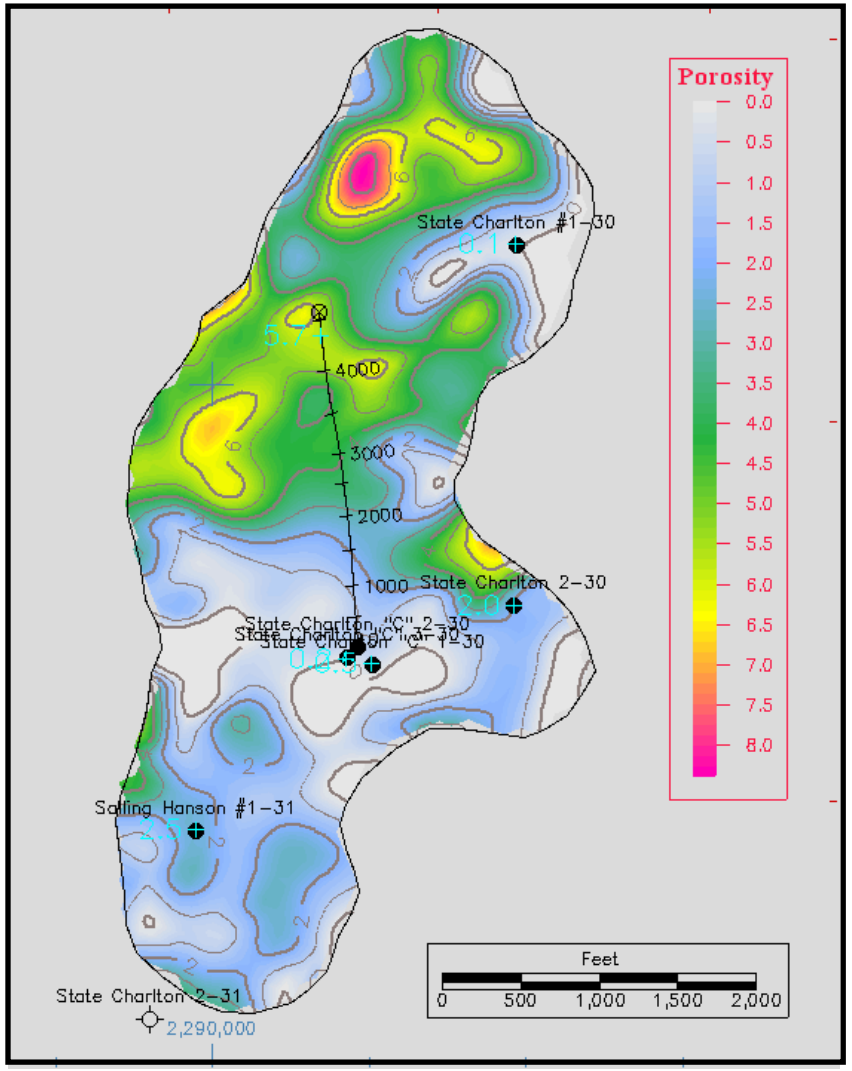
Porosity
0.0
0.5
1.0
1.5
2.0
2.5
3.0
3.5
4.0
4.5
5.0
5.5
6.0
6.5
7.0
7.5
8.0
State Charlton #1-30
4000
3000
2000
1000
State Charlton 2-30
Salling Hanson #1-31
State Charlton 2-31
2,290,000
Feet
0
500
1,000
1,500
2,000

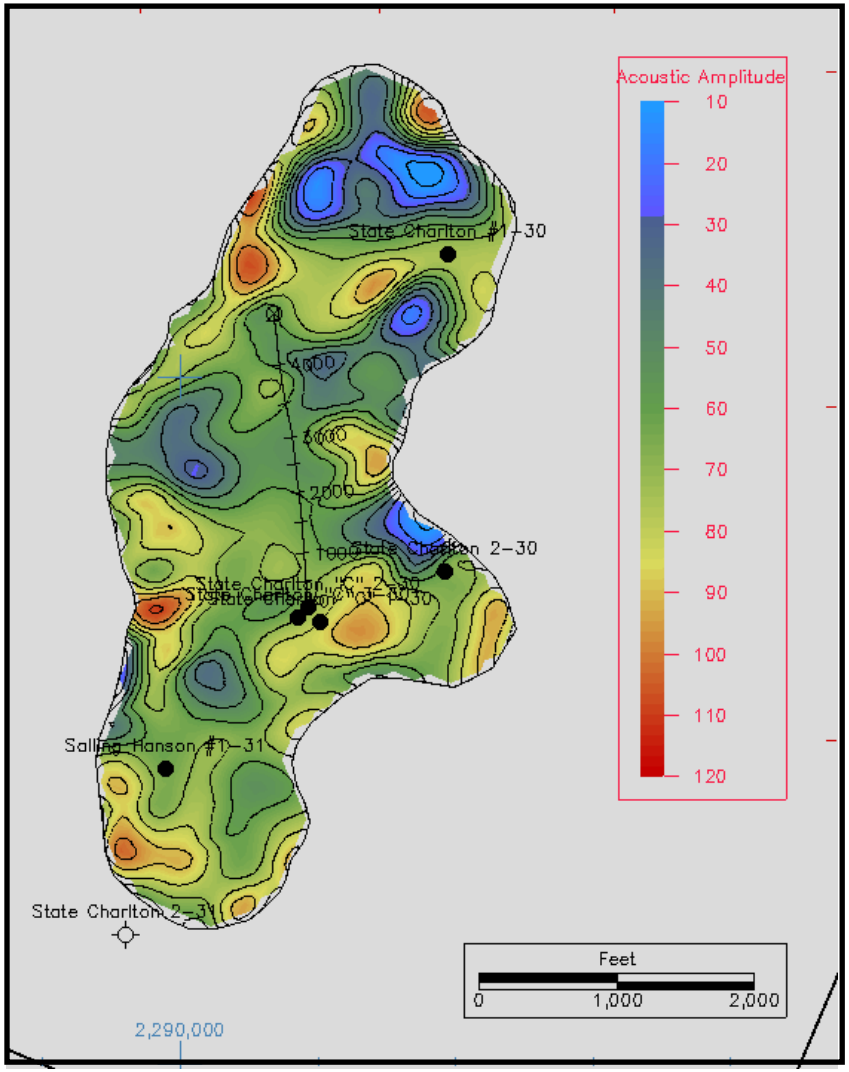
Acoustic Amplitude
10
20
30
40
50
60
70
80
90
100
110
120
State Charlton #1-30
4000
3000
2000
1000
State Charlton 2-30
Salling Hanson #1-31
State Charlton 2-31
2,290,000
Feet
0
1,000
2,000

899 msec

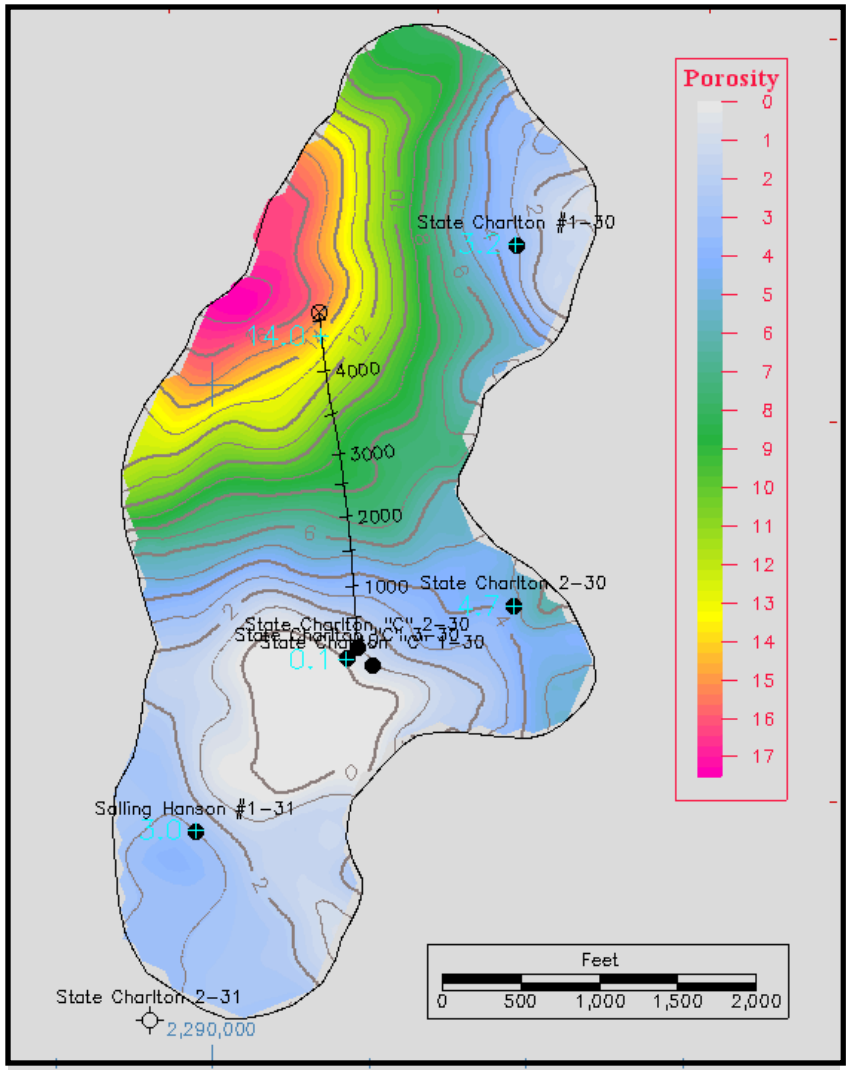
Porosity
0
1
2
3
4
5
6
7
8
9
10
11
12
13
14
15
16
17
State Charlton #1-30
State Charlton 2-30
Salling Hanson #1-31
State Charlton 2-31
14.6
5.2
4.7
6.1
5.0
4000
3000
2000
1000
Feet
0
500
1,000
1,500
2,000
2,290,000

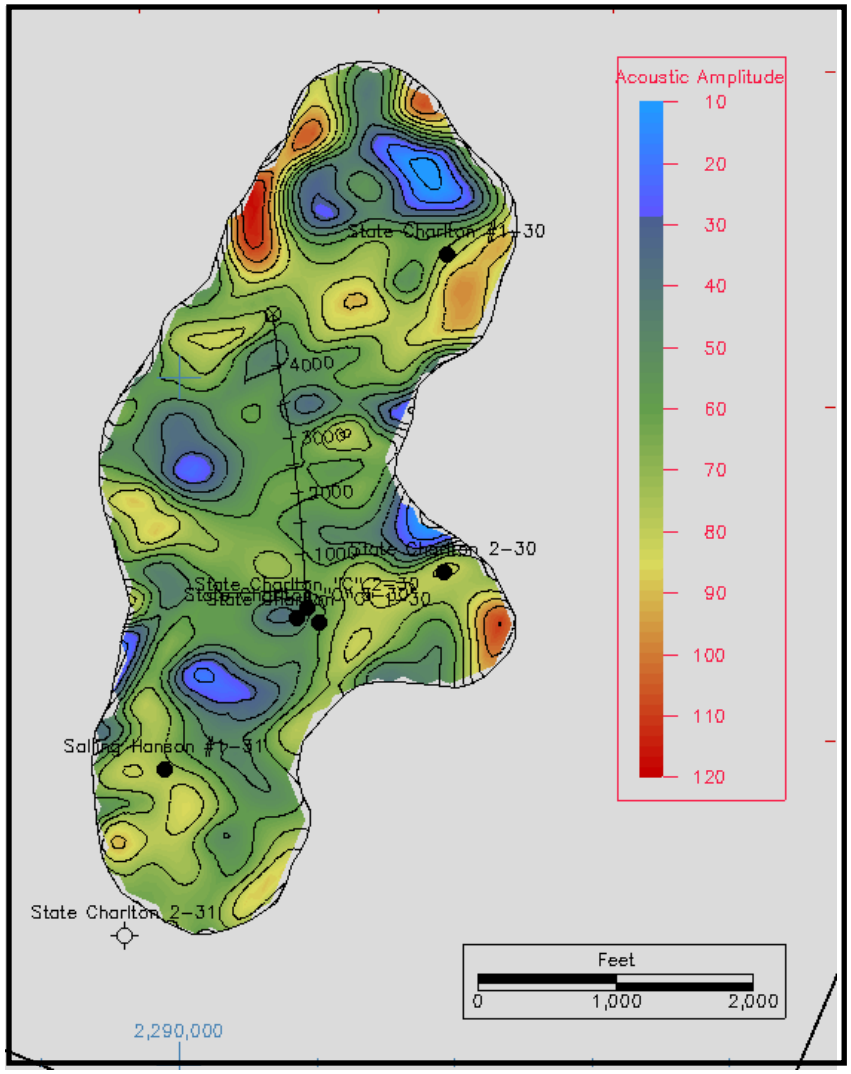
Acoustic Amplitude
10
20
30
40
50
60
70
80
90
100
110
120
State Charlton #1-30
State Charlton 2-30
Salling Hanson #1-31
State Charlton 2-31
4000
3000
2000
1000
Feet
0
1,000
2,000
2,290,000

901 msec

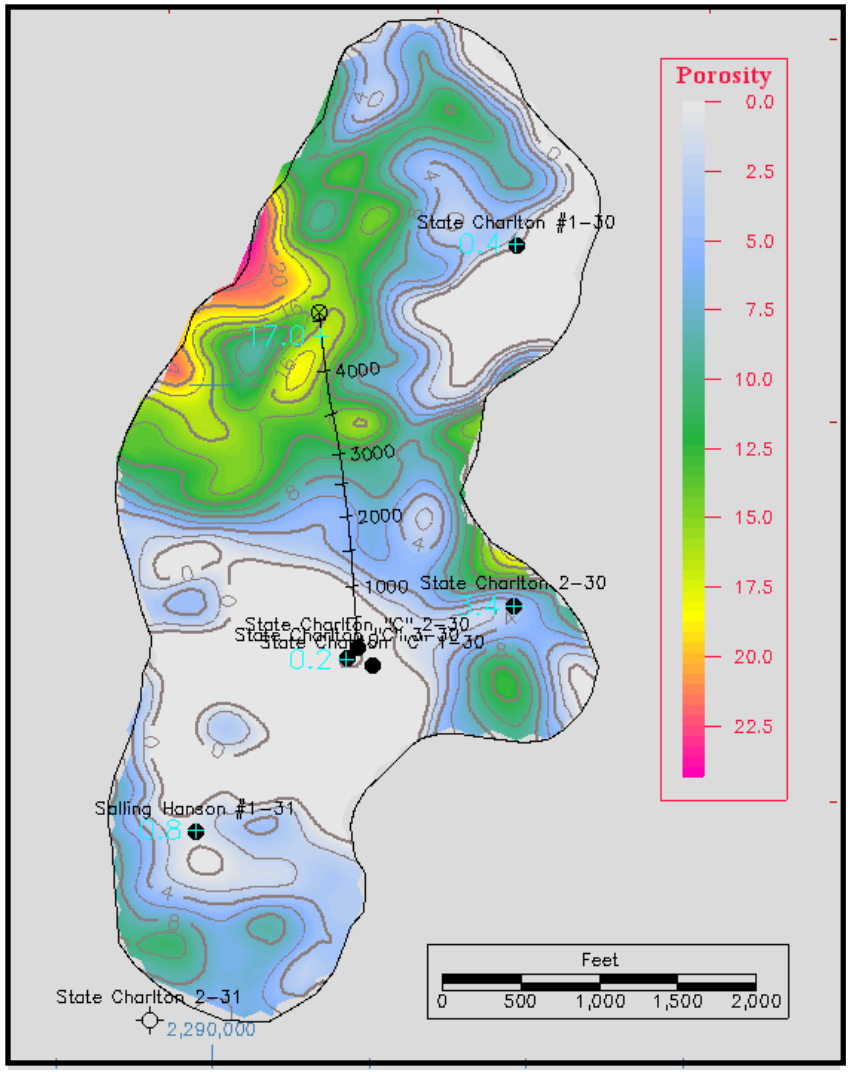
Porosity
0.0
2.5
5.0
7.5
10.0
12.5
15.0
17.5
20.0
22.5
State Charlton #1-30
0.4
17.0
4000
3000
2000
1000
State Charlton 2-30
State Charlton "C" 2-30
State Charlton "C" 1-30
0.2
Salling Hanson #1-31
0.8
State Charlton 2-31
2,290,000
Feet
0
500
1,000
1,500
2,000

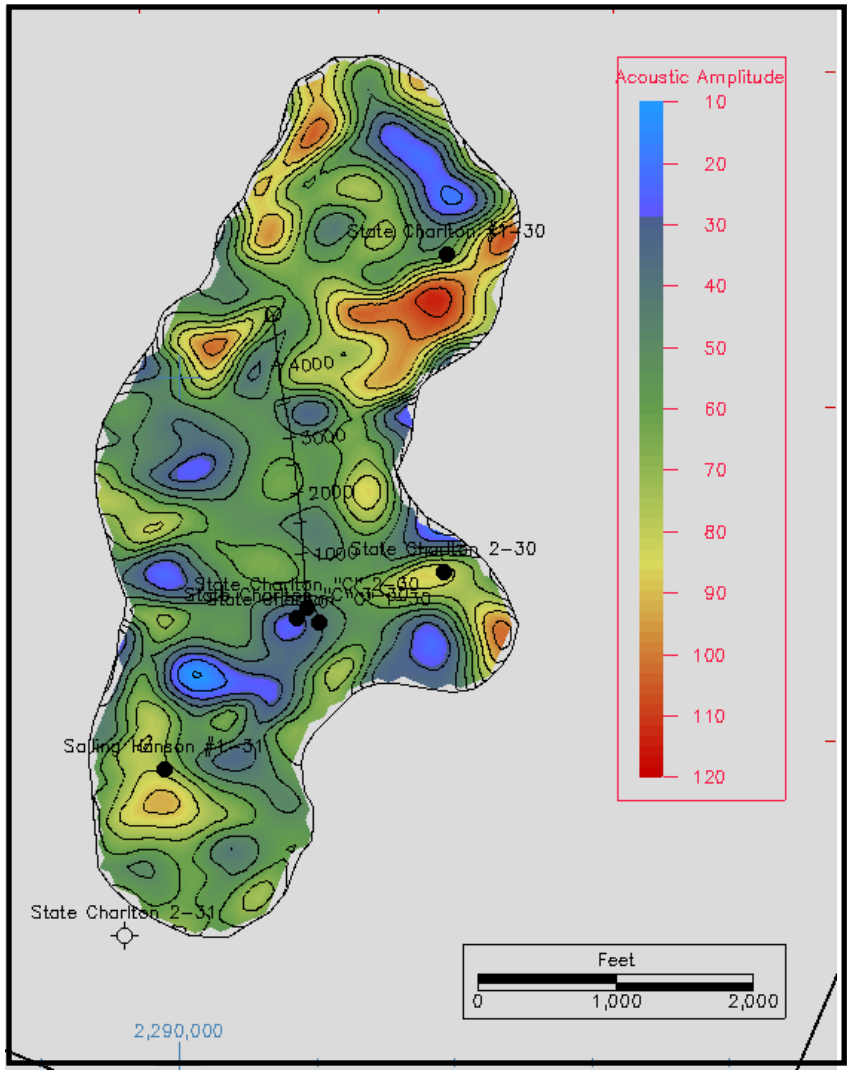
Acoustic Amplitude
10
20
30
40
50
60
70
80
90
100
110
120
State Charlton #1-30
4000
3000
2000
1000
State Charlton 2-30
Salling Hanson #1-31
State Charlton 2-31
2,290,000
Feet
0
1,000
2,000

903 msec

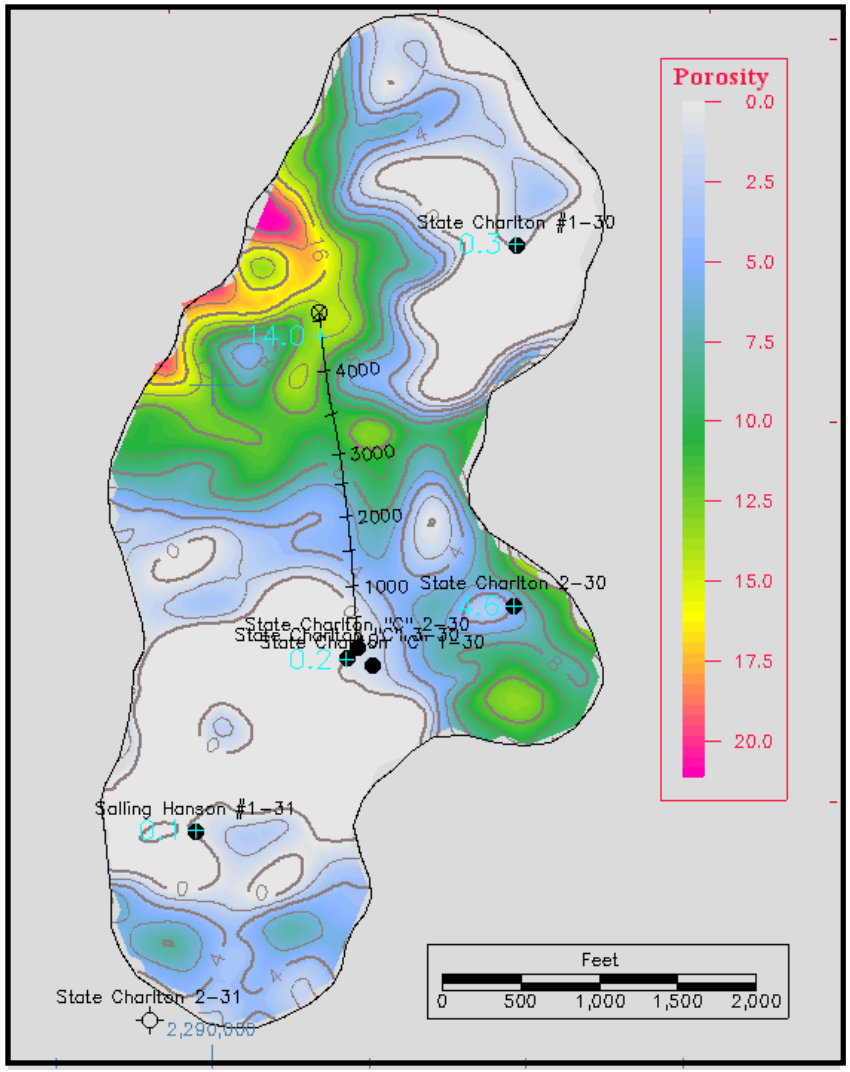
Porosity
0.0
2.5
5.0
7.5
10.0
12.5
15.0
17.5
20.0
State Charlton #1-30
0.3
14.0
4000
3000
2000
1000
State Charlton 2-30
4.6
State Charlton "C" 2-30
State Charlton "C" 1-30
0.2
Salling Hanson #1-31
State Charlton 2-31
2,290,000
Feet
0
500
1,000
1,500
2,000

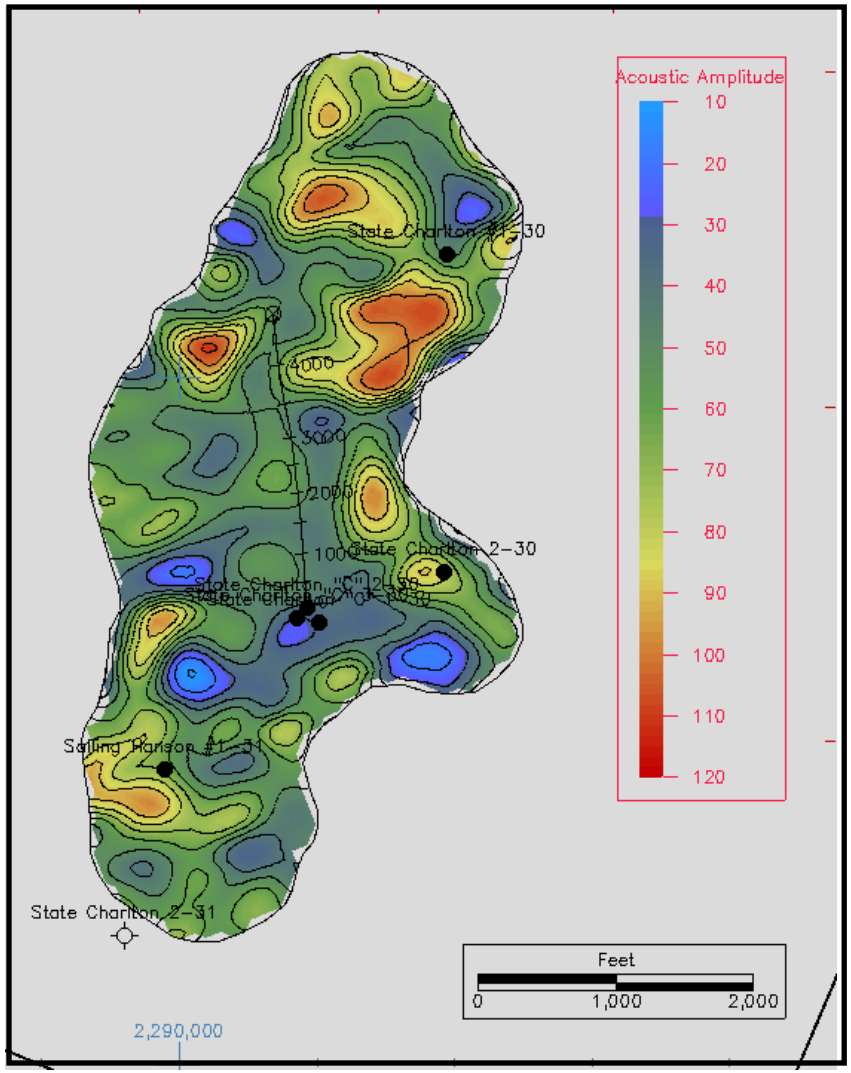
Acoustic Amplitude
10
20
30
40
50
60
70
80
90
100
110
120
State Charlton #1-30
4000
3000
2000
1000
State Charlton 2-30
Salling Hanson #1-31
State Charlton 2-31
2,290,000
Feet
0
1,000
2,000

905 msec

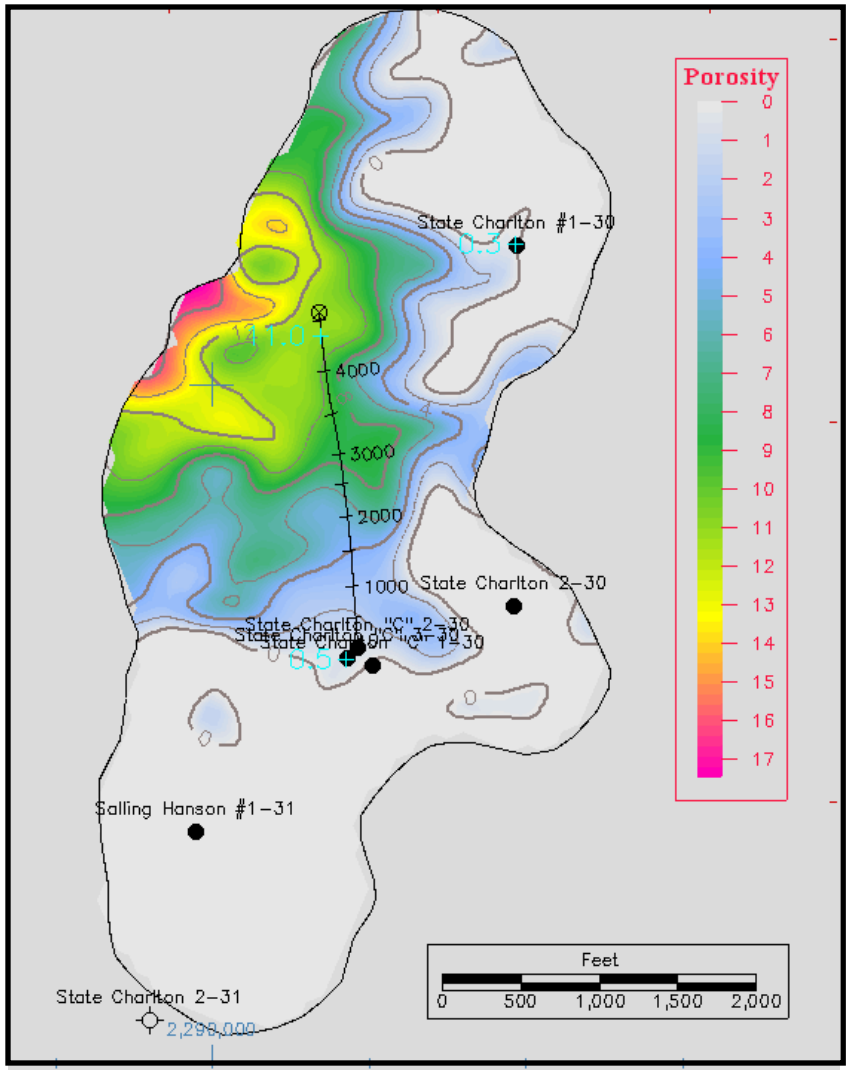
Porosity
0
1
2
3
4
5
6
7
8
9
10
11
12
13
14
15
16
17
State Charlton #1-30
State Charlton 2-30
Salling Hanson #1-31
State Charlton 2-31
4000
3000
2000
1000
Feet
0
500
1,000
1,500
2,000
2,298,000

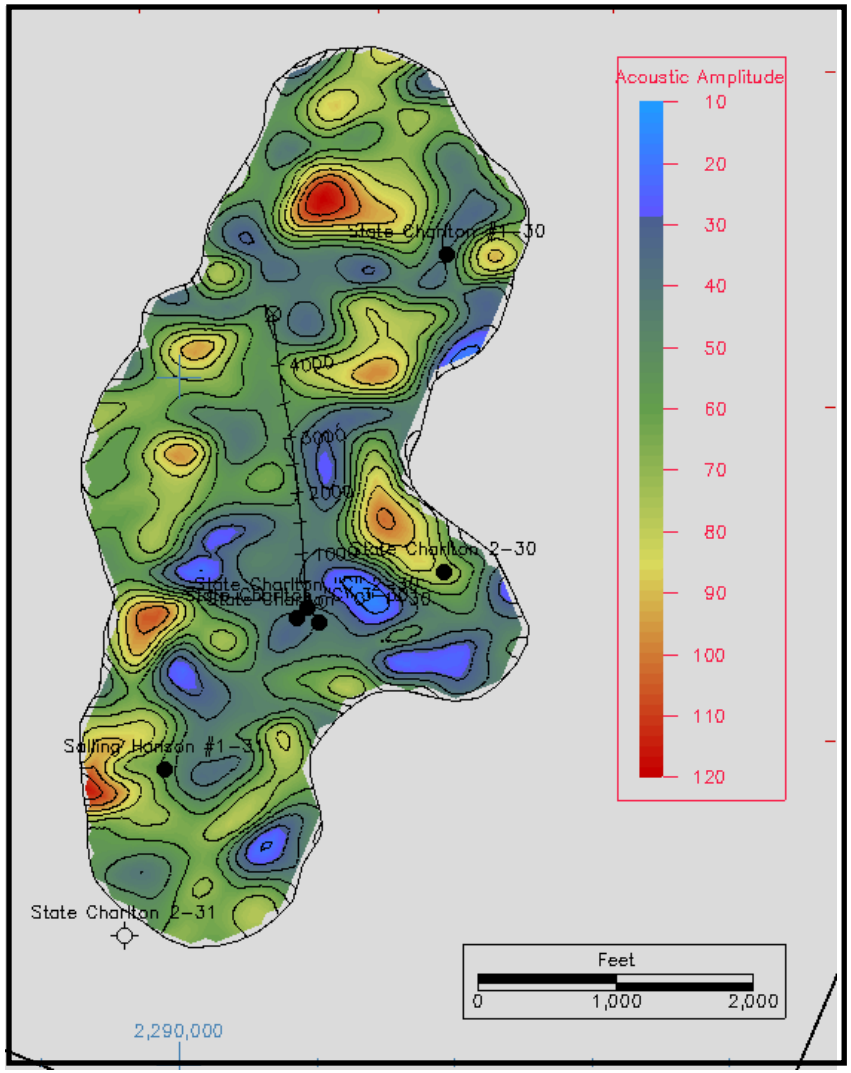
Acoustic Amplitude
10
20
30
40
50
60
70
80
90
100
110
120
State Charlton #1-30
State Charlton 2-30
Salling Hanson #1-31
State Charlton 2-31
4000
3000
2000
1000
Feet
0
1,000
2,000
2,290,000

907 msec

11.8 APPENDIX H – Reservoir Simulation Predictions – Oil Distribution at September, 2007

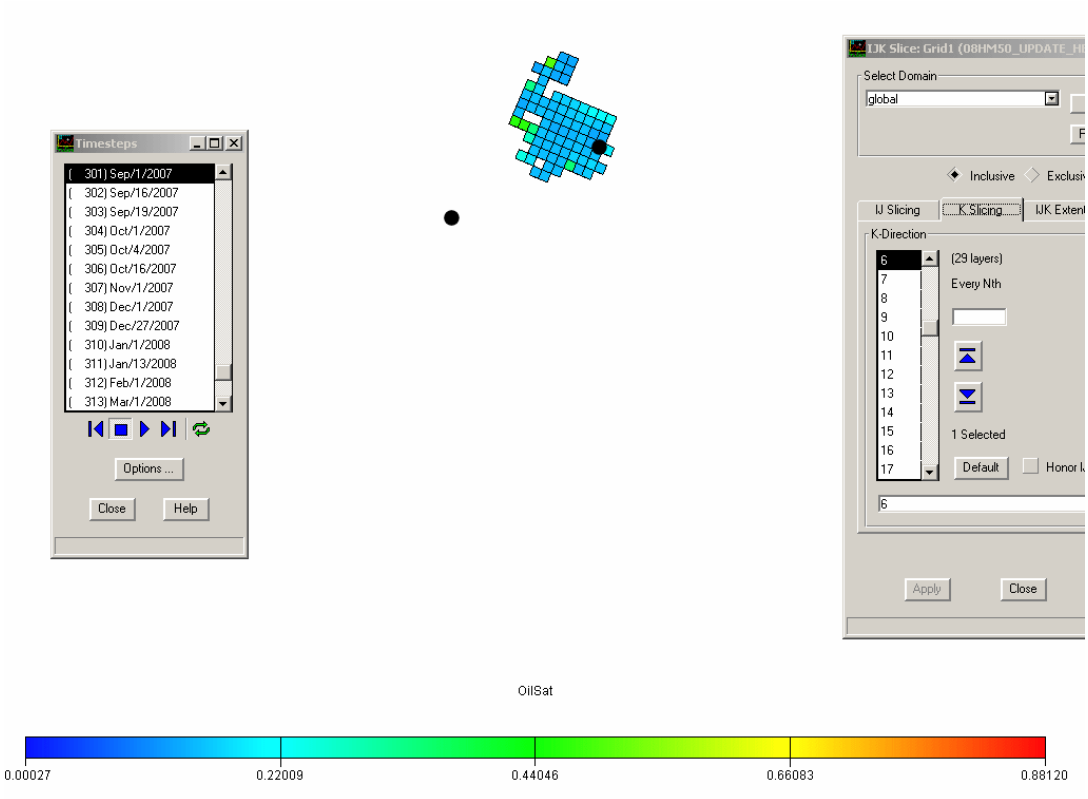

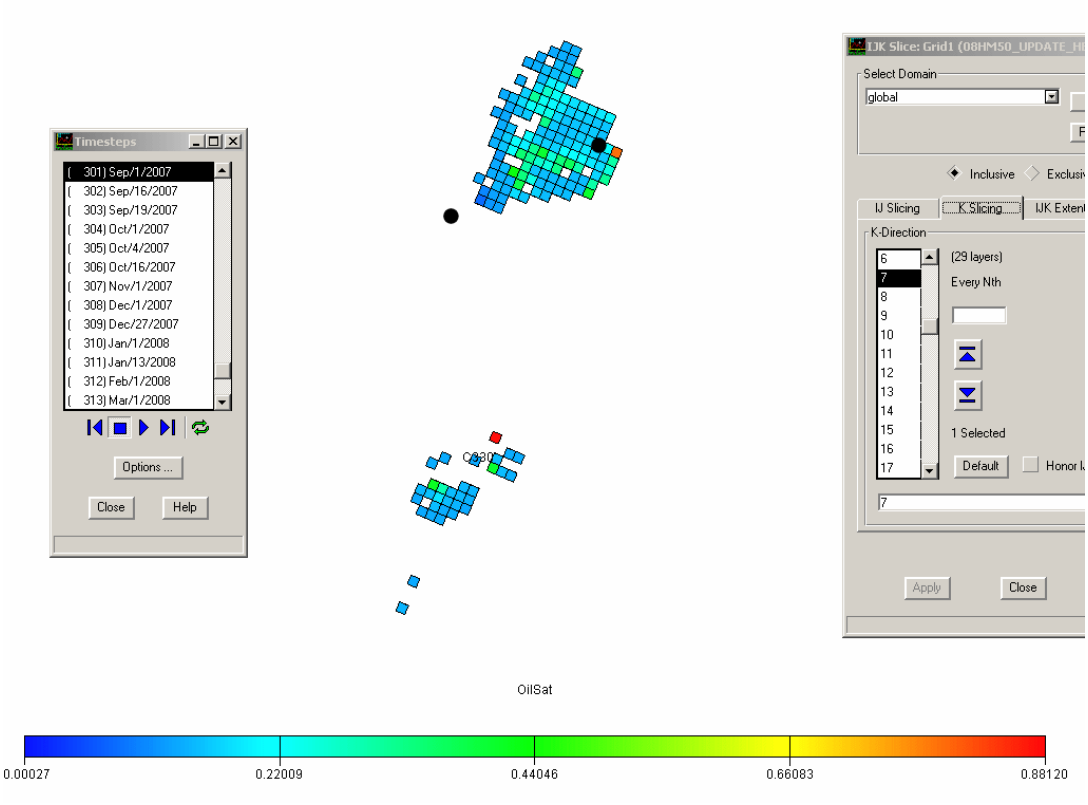
Timesteps
301) Sep/1/2007
302) Sep/16/2007
303) Sep/19/2007
304) Oct/1/2007
305) Oct/4/2007
306) Oct/16/2007
307) Nov/1/2007
308) Dec/1/2007
309) Dec/27/2007
310) Jan/1/2008
311) Jan/13/2008
312) Feb/1/2008
313) Mar/1/2008
Options ...
Close
Help
IJK Slice: Grid1 (08HM50_UPDATE_HI
Select Domain
global
Inclusive
IJ Slicing
K Slicing
K-Direction
(29 layers)
Every Nth
1 Selected
Default
Apply
Close
OilSat
0.00027
0.22009
0.44046
0.66083
0.88120

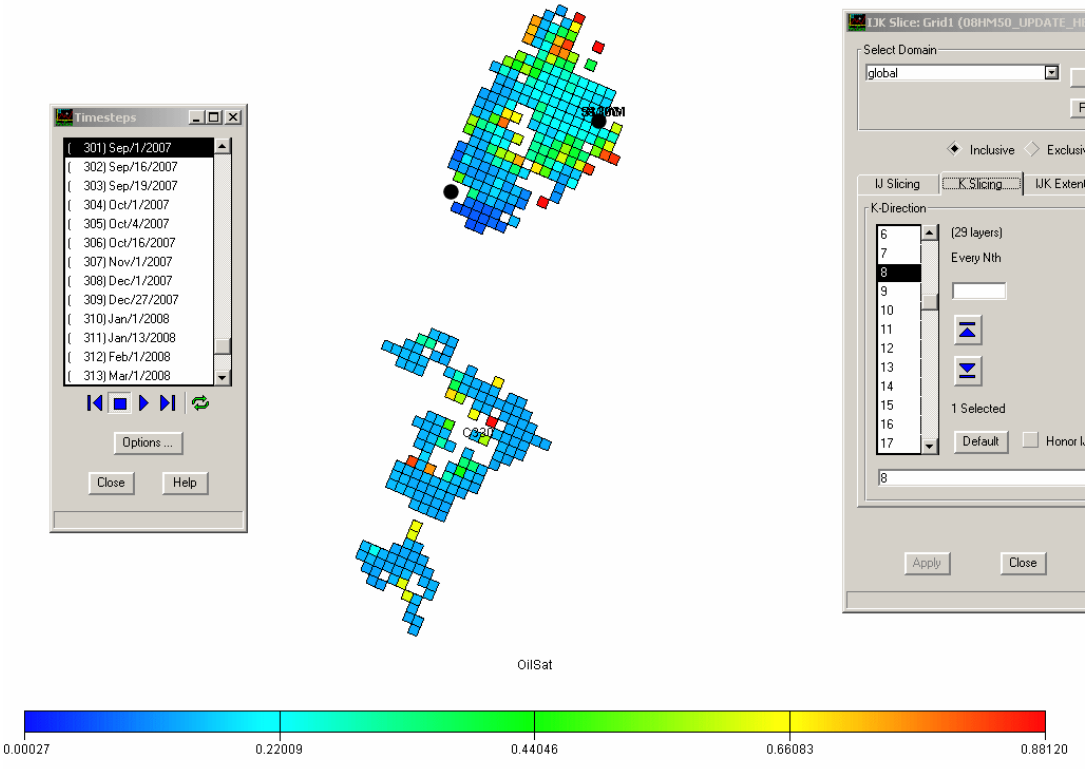
Timesteps
301) Sep/1/2007
302) Sep/16/2007
303) Sep/19/2007
304) Oct/1/2007
305) Oct/4/2007
306) Oct/16/2007
307) Nov/1/2007
308) Dec/1/2007
309) Dec/27/2007
310) Jan/1/2008
311) Jan/13/2008
312) Feb/1/2008
313) Mar/1/2008
Options ...
Close
Help
IJK Slice: Grid1 (08HM50_UPDATE_HI
Select Domain
global
Inclusive
IJ Slicing
K Slicing
K-Direction
(29 layers)
Every Nth
1 Selected
Default
Apply
Close
OilSat
0.00027
0.22009
0.44046
0.66083
0.88120

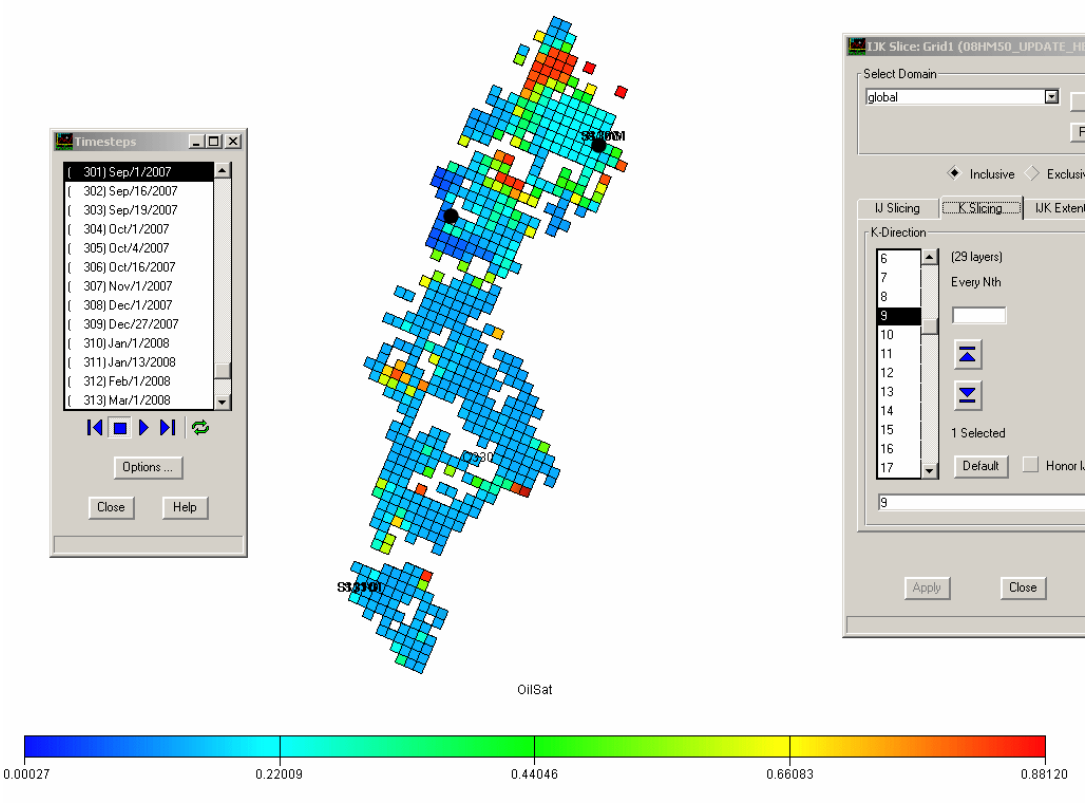
Timesteps
301) Sep/1/2007
302) Sep/16/2007
303) Sep/19/2007
304) Oct/1/2007
305) Oct/4/2007
306) Oct/16/2007
307) Nov/1/2007
308) Dec/1/2007
309) Dec/27/2007
310) Jan/1/2008
311) Jan/13/2008
312) Feb/1/2008
313) Mar/1/2008
Options ...
Close
Help
IJK Slice: Grid1 (08HM50_UPDATE_HI
Select Domain
global
Inclusive
IJ Slicing
K Slicing
K-Direction
(29 layers)
Every Nth
1 Selected
Default
Apply
Close
OilSat
0.00027
0.22009
0.44046
0.66083
0.88120

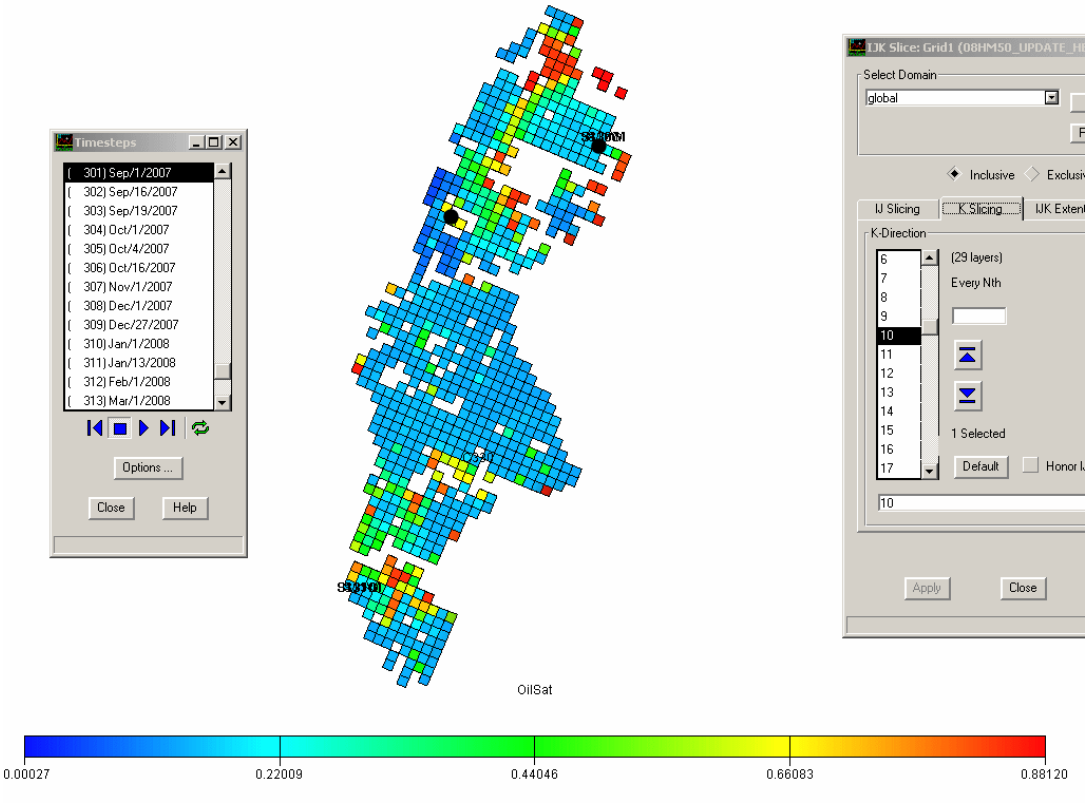
Timesteps
301) Sep/1/2007
302) Sep/16/2007
303) Sep/19/2007
304) Oct/1/2007
305) Oct/4/2007
306) Oct/16/2007
307) Nov/1/2007
308) Dec/1/2007
309) Dec/27/2007
310) Jan/1/2008
311) Jan/13/2008
312) Feb/1/2008
313) Mar/1/2008
Options ...
Close
Help
IJK Slice: Grid1 (08HM50_UPDATE_HI
Select Domain
global
Inclusive
IJ Slicing
K Slicing
K-Direction
(29 layers)
Every Nth
1 Selected
Default
Apply
Close
OilSat
0.00027
0.22009
0.44046
0.66083
0.88120

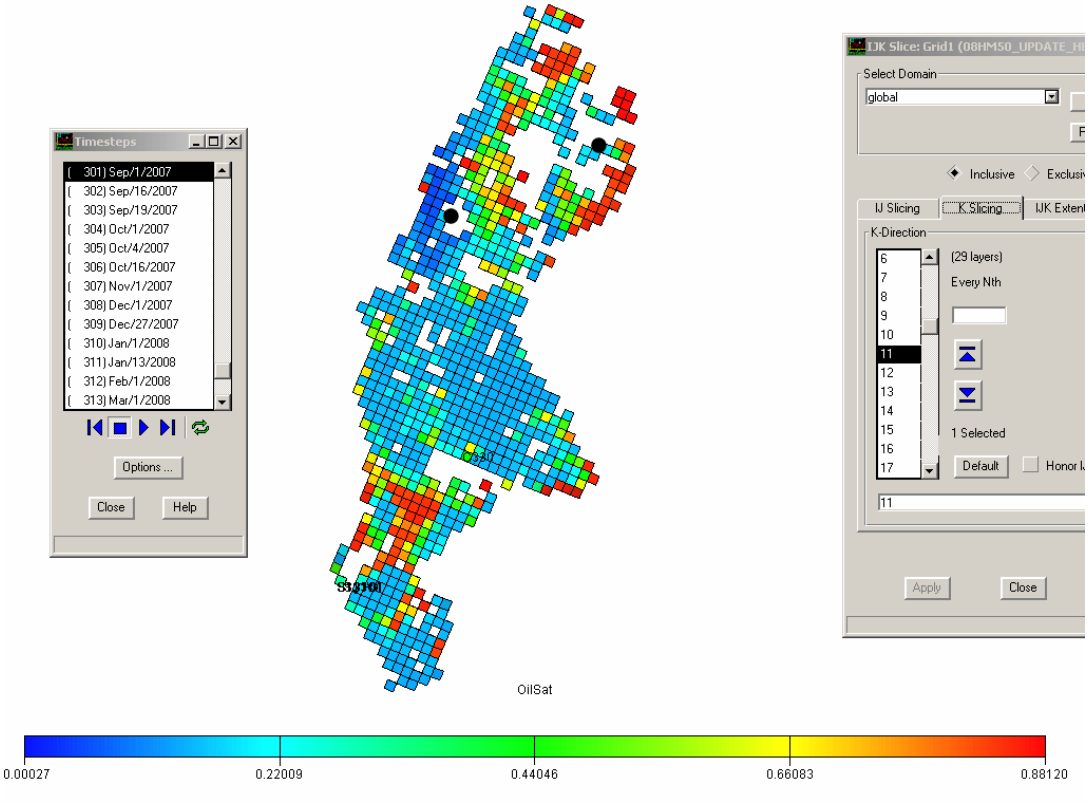
Timesteps
301) Sep/1/2007
302) Sep/16/2007
303) Sep/19/2007
304) Oct/1/2007
305) Oct/4/2007
306) Oct/16/2007
307) Nov/1/2007
308) Dec/1/2007
309) Dec/27/2007
310) Jan/1/2008
311) Jan/13/2008
312) Feb/1/2008
313) Mar/1/2008
Options ...
Close
Help
IJK Slice: Grid1 (08HM50_UPDATE_HI
Select Domain
global
Inclusive
IJ Slicing
K Slicing
K-Direction
(29 layers)
Every Nth
1 Selected
Default
Apply
Close
OilSat
0.00027
0.22009
0.44046
0.66083
0.88120

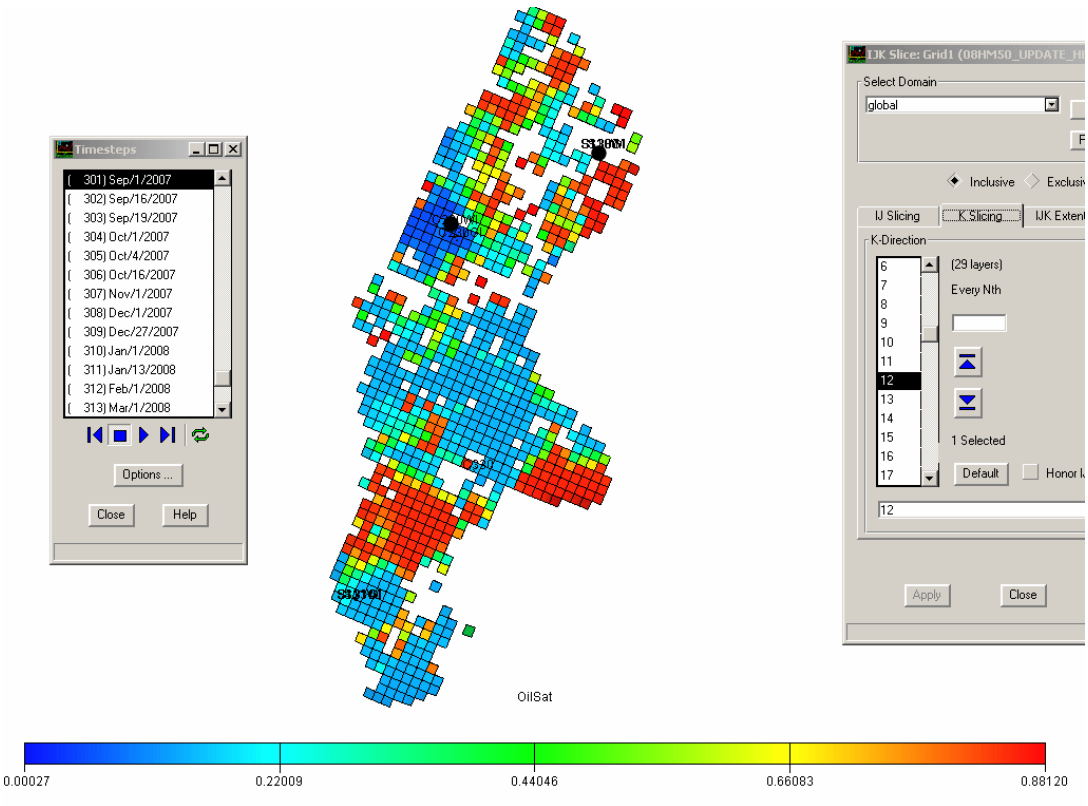
Timesteps
301) Sep/1/2007
302) Sep/16/2007
303) Sep/19/2007
304) Oct/1/2007
305) Oct/4/2007
306) Oct/16/2007
307) Nov/1/2007
308) Dec/1/2007
309) Dec/27/2007
310) Jan/1/2008
311) Jan/13/2008
312) Feb/1/2008
313) Mar/1/2008
Options ...
Close
Help
IJK Slice: Grid1 (08HM50_UPDATE_HI
Select Domain
global
Inclusive
IJ Slicing
K Slicing
K-Direction
(29 layers)
Every Nth
1 Selected
Default
Apply
Close
OilSat
0.00027
0.22009
0.44046
0.66083
0.88120

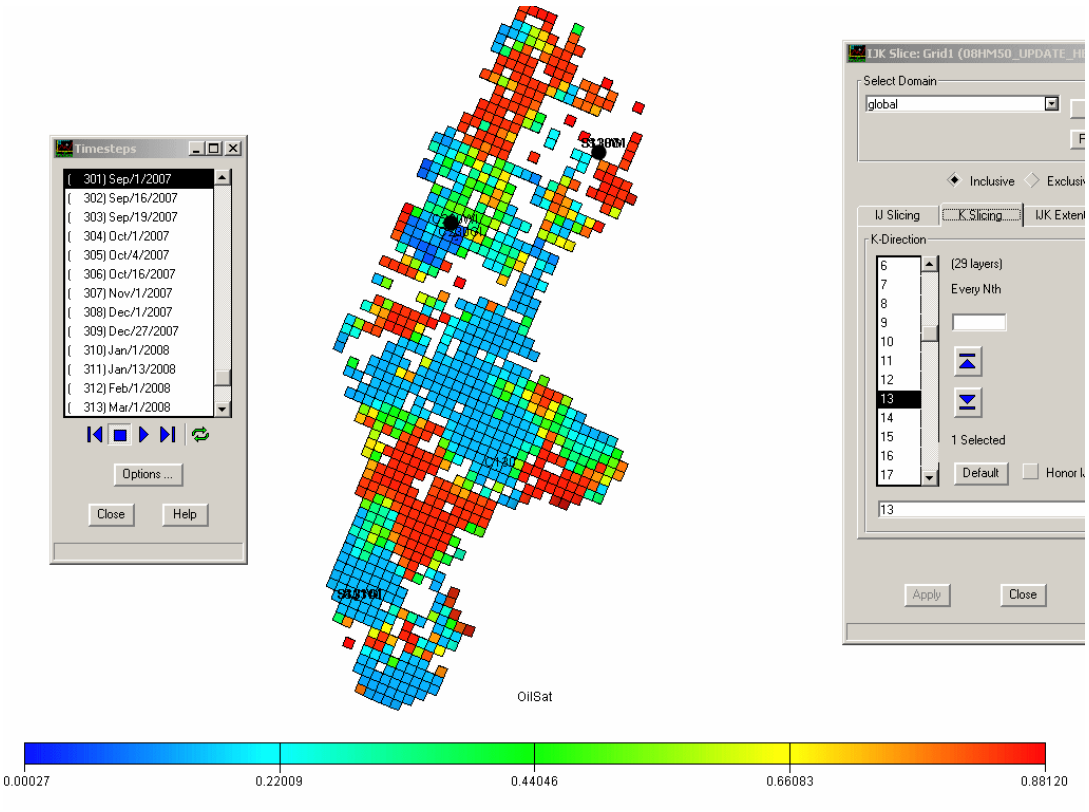
Timesteps
301) Sep/1/2007
302) Sep/16/2007
303) Sep/19/2007
304) Oct/1/2007
305) Oct/4/2007
306) Oct/16/2007
307) Nov/1/2007
308) Dec/1/2007
309) Dec/27/2007
310) Jan/1/2008
311) Jan/13/2008
312) Feb/1/2008
313) Mar/1/2008
Options ...
Close
Help
IJK Slice: Grid1 (08HM50_UPDATE_HI
Select Domain
global
Inclusive
IJ Slicing
K Slicing
IJK Extent
K-Direction
(29 layers)
Every Nth
1 Selected
Default
Apply
Close
OilSat
0.00027
0.22009
0.44046
0.66083
0.88120

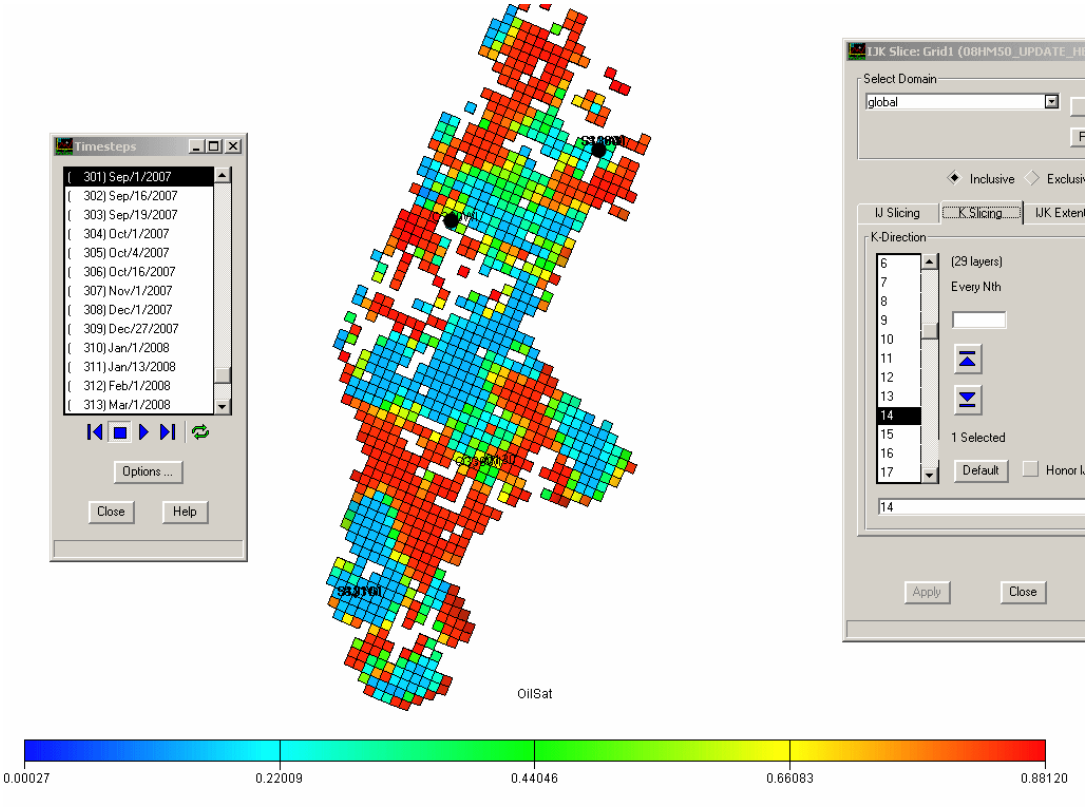
Timesteps
301) Sep/1/2007
302) Sep/16/2007
303) Sep/19/2007
304) Oct/1/2007
305) Oct/4/2007
306) Oct/16/2007
307) Nov/1/2007
308) Dec/1/2007
309) Dec/27/2007
310) Jan/1/2008
311) Jan/13/2008
312) Feb/1/2008
313) Mar/1/2008
Options ...
Close
Help
IJK Slice: Grid1 (08HM50_UPDATE_HI
Select Domain
global
Inclusive
IJ Slicing
K Slicing
IJK Extent
K-Direction
(29 layers)
Every Nth
1 Selected
Default
Apply
Close
OilSat
0.00027
0.22009
0.44046
0.66083
0.88120

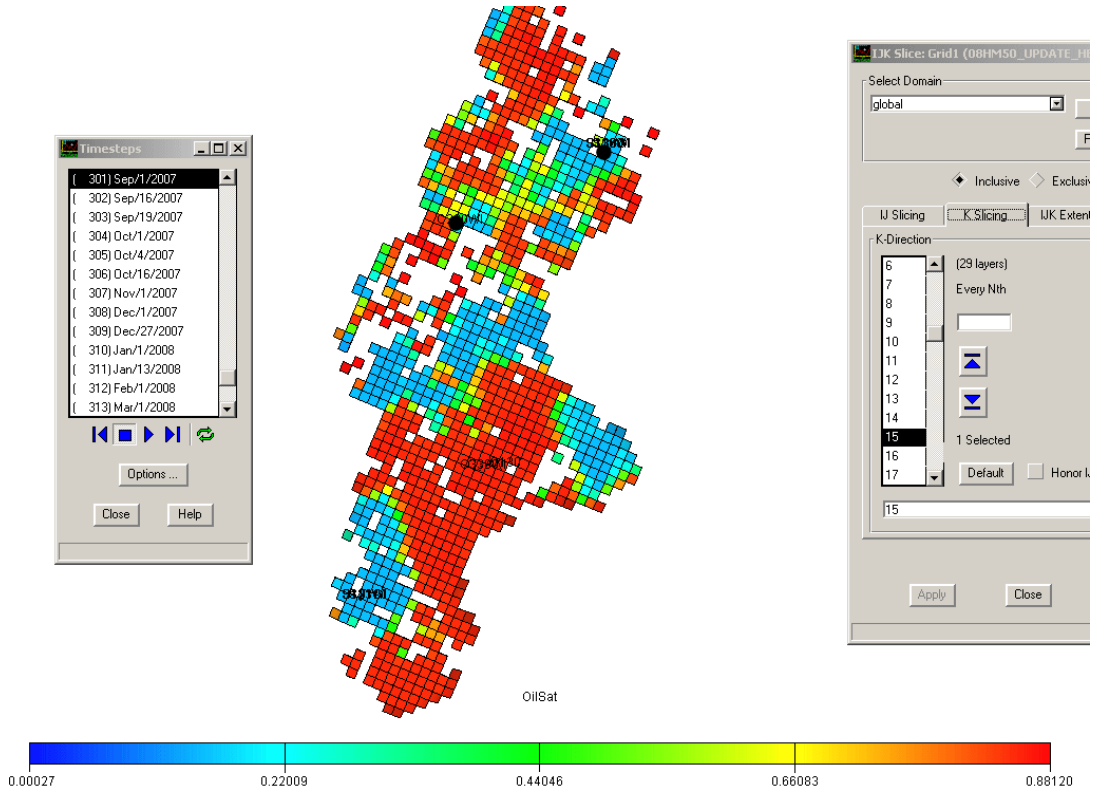
Timesteps
301) Sep/1/2007
302) Sep/16/2007
303) Sep/19/2007
304) Oct/1/2007
305) Oct/4/2007
306) Oct/16/2007
307) Nov/1/2007
308) Dec/1/2007
309) Dec/27/2007
310) Jan/1/2008
311) Jan/13/2008
312) Feb/1/2008
313) Mar/1/2008
Options ...
Close
Help
IJK Slice: Grid1 (08HMS0_UPDATE_HI
Select Domain
global
Inclusive
IJ Slicing
K Slicing
K-Direction
(29 layers)
Every Nth
1 Selected
Default
Apply
Close
OilSat
0.00027
0.22009
0.44046
0.66083
0.88120

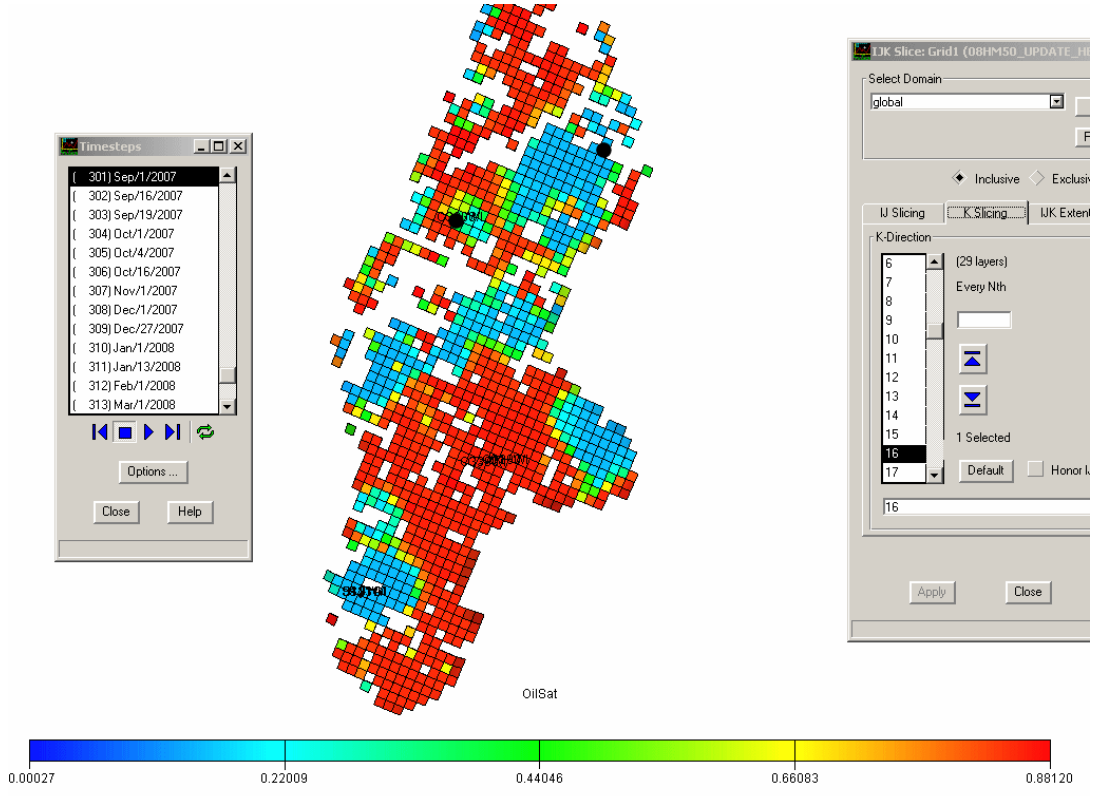
Timesteps
301) Sep/1/2007
302) Sep/16/2007
303) Sep/19/2007
304) Oct/1/2007
305) Oct/4/2007
306) Oct/16/2007
307) Nov/1/2007
308) Dec/1/2007
309) Dec/27/2007
310) Jan/1/2008
311) Jan/13/2008
312) Feb/1/2008
313) Mar/1/2008
Options ...
Close
Help
IJK Slice: Grid1 (08HMS0_UPDATE_HI
Select Domain
global
Inclusive
IJ Slicing
K Slicing
K-Direction
(29 layers)
Every Nth
1 Selected
Default
Apply
Close
OilSat
0.00027
0.22009
0.44046
0.66083
0.88120

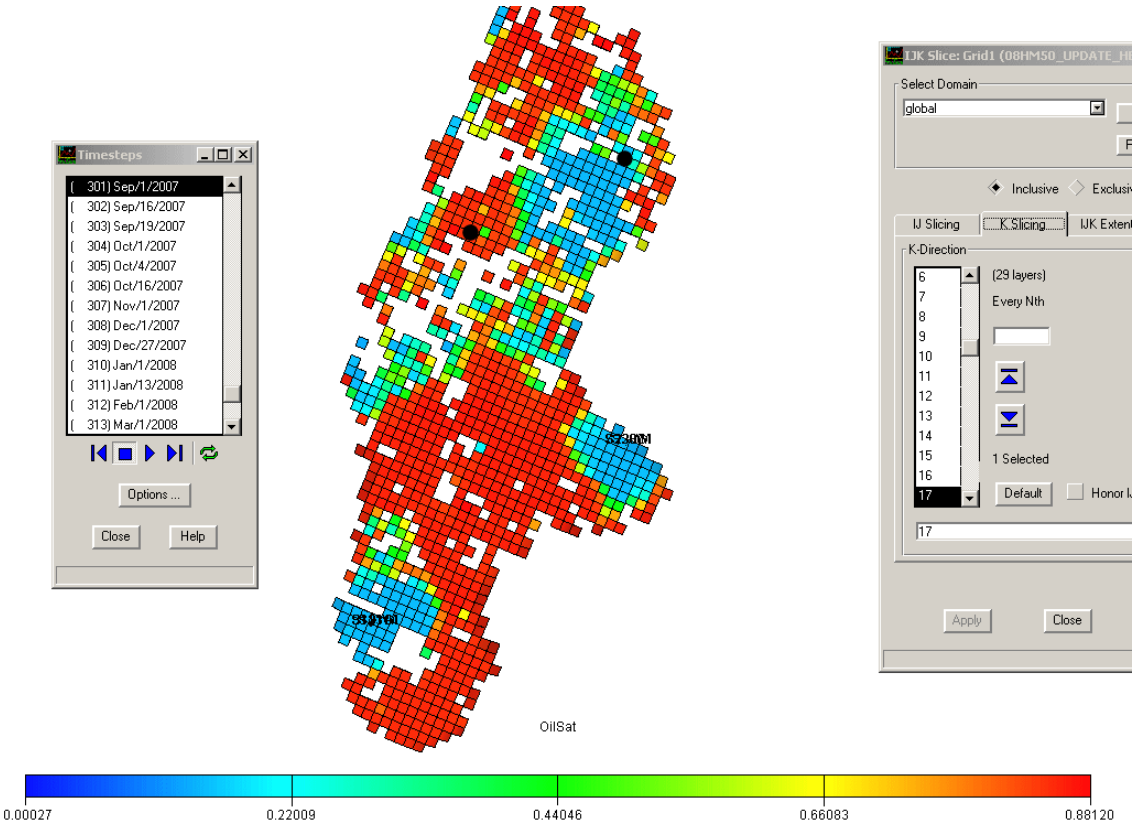
Timesteps
301) Sep/1/2007
302) Sep/16/2007
303) Sep/19/2007
304) Oct/1/2007
305) Oct/4/2007
306) Oct/16/2007
307) Nov/1/2007
308) Dec/1/2007
309) Dec/27/2007
310) Jan/1/2008
311) Jan/13/2008
312) Feb/1/2008
313) Mar/1/2008
Options ...
Close
Help
IJK Slice: Grid1 (08HM50_UPDATE_HI
Select Domain
global
Inclusive
IJ Slicing
K Slicing
IJK Extent
K-Direction
(29 layers)
Every Nth
1 Selected
Default
Apply
Close
OilSat
0.00027
0.22009
0.44046
0.66083
0.88120

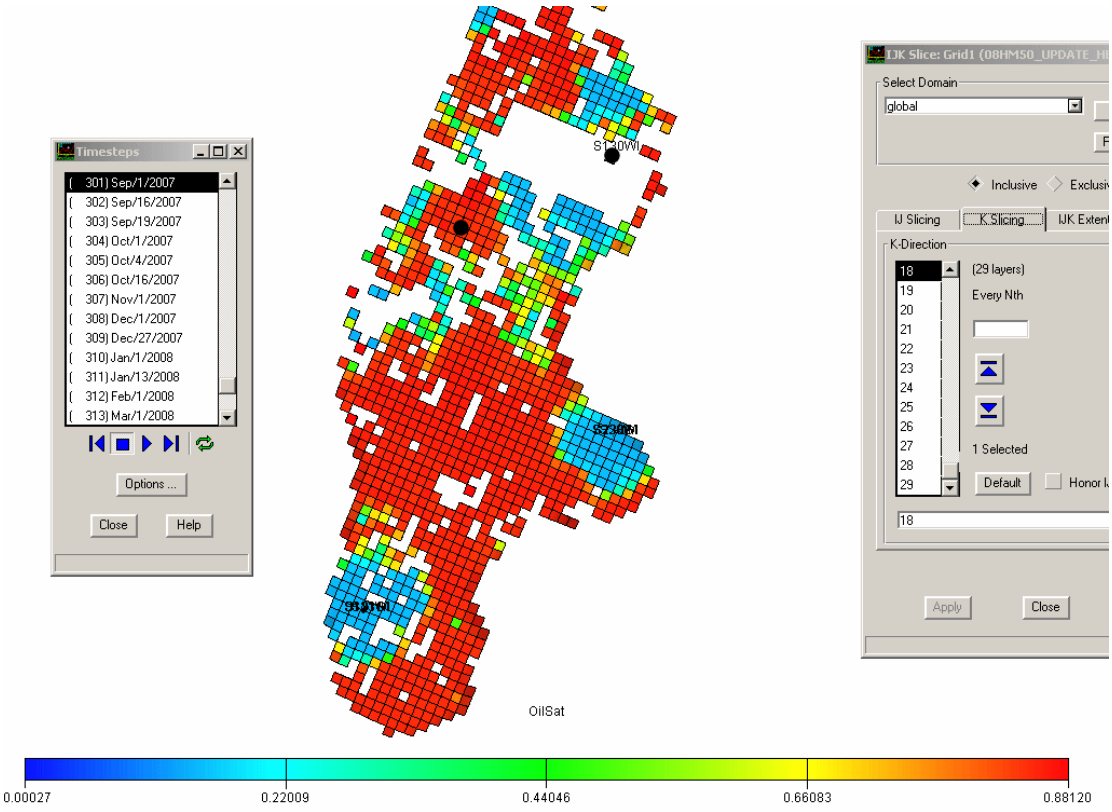
Timesteps
301) Sep/1/2007
302) Sep/16/2007
303) Sep/19/2007
304) Oct/1/2007
305) Oct/4/2007
306) Oct/16/2007
307) Nov/1/2007
308) Dec/1/2007
309) Dec/27/2007
310) Jan/1/2008
311) Jan/13/2008
312) Feb/1/2008
313) Mar/1/2008
Options ...
Close
Help
IJK Slice: Grid1 (08HM50_UPDATE_HI
Select Domain
global
Inclusive
IJ Slicing
K Slicing
IJK Extent
K-Direction
(29 layers)
Every Nth
1 Selected
Default
Apply
Close
OilSat
0.00027
0.22009
0.44046
0.66083
0.88120

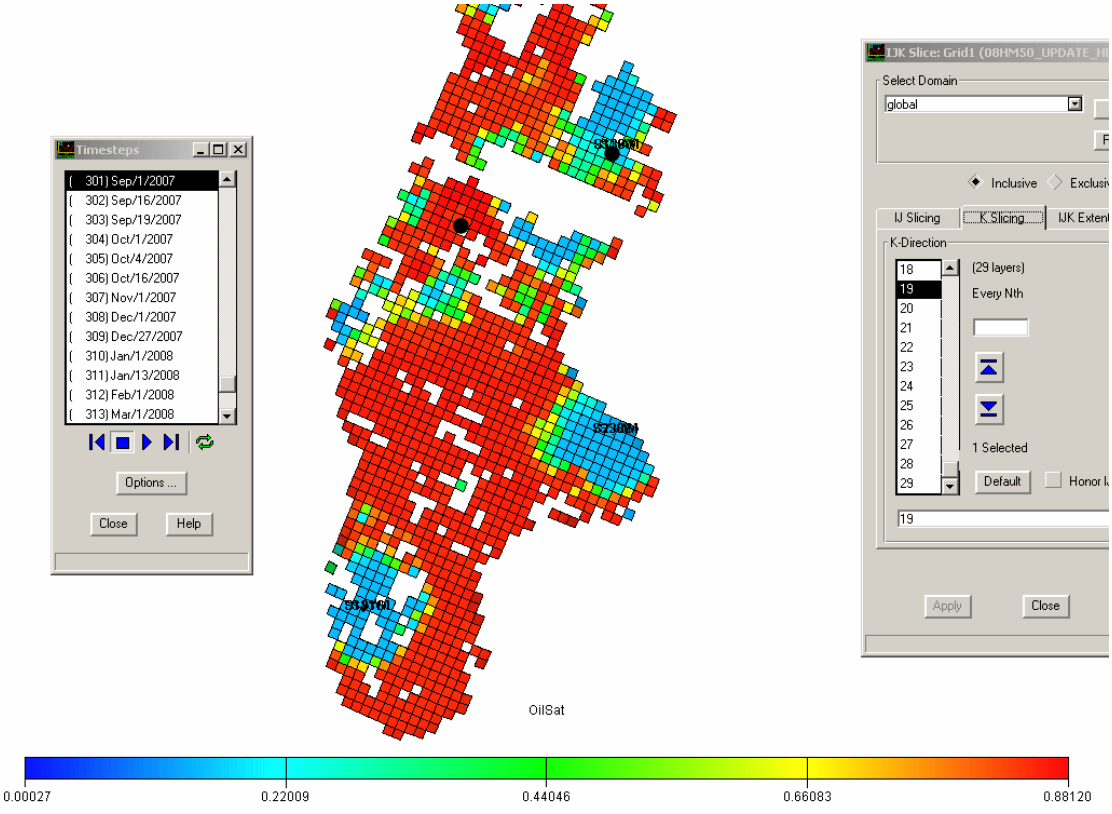
Timesteps
(301) Sep/1/2007
(302) Sep/16/2007
(303) Sep/19/2007
(304) Oct/1/2007
(305) Oct/4/2007
(306) Oct/16/2007
(307) Nov/1/2007
(308) Dec/1/2007
(309) Dec/27/2007
(310) Jan/1/2008
(311) Jan/13/2008
(312) Feb/1/2008
(313) Mar/1/2008
Options ...
Close
Help
IJK Slice: Grid1 (08HM50_UPDATE_HI
Select Domain
global
Inclusive
IJ Slicing
K Slicing
IJK Extent
K-Direction
18
19
20
21
22
23
24
25
26
27
28
29
(29 layers)
Every Nth
1 Selected
Default
19
Apply
Close
OilSat
0.00027
0.22009
0.44046
0.66083
0.88120

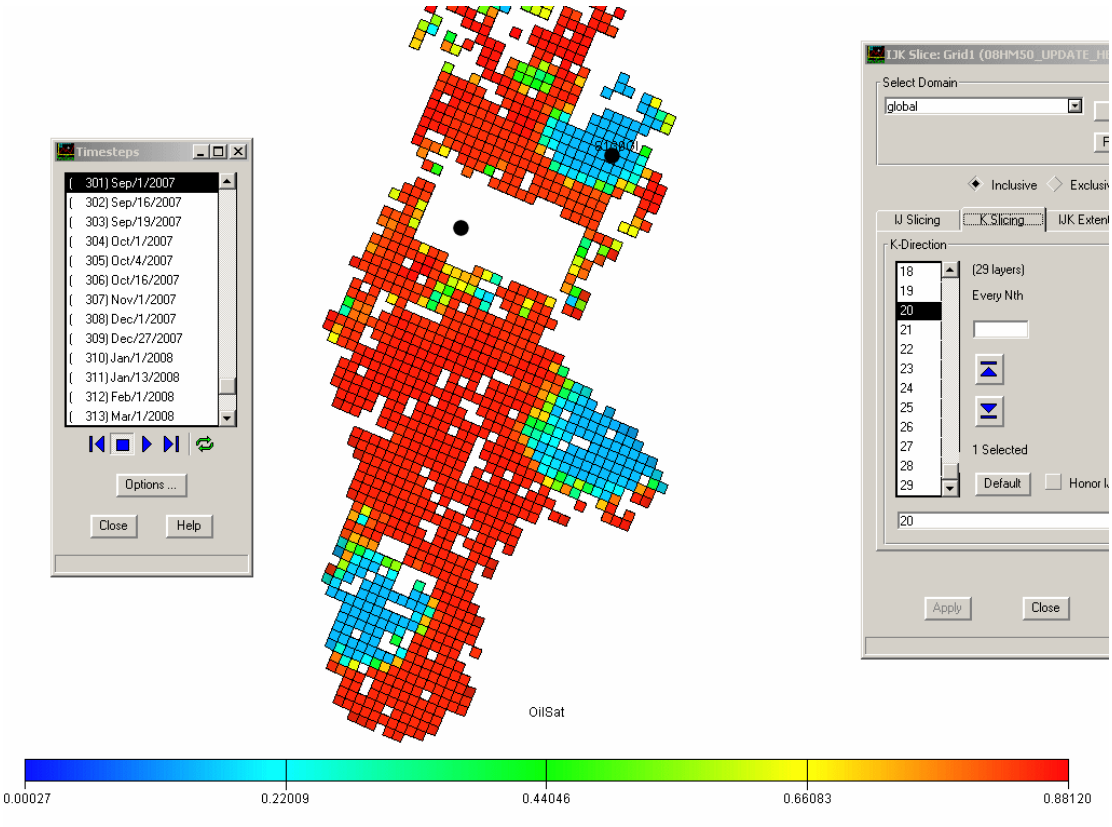
Timesteps
(301) Sep/1/2007
(302) Sep/16/2007
(303) Sep/19/2007
(304) Oct/1/2007
(305) Oct/4/2007
(306) Oct/16/2007
(307) Nov/1/2007
(308) Dec/1/2007
(309) Dec/27/2007
(310) Jan/1/2008
(311) Jan/13/2008
(312) Feb/1/2008
(313) Mar/1/2008
Options ...
Close
Help
IJK Slice: Grid1 (08HM50_UPDATE_HI
Select Domain
global
Inclusive
IJ Slicing
K Slicing
IJK Extent
K-Direction
18
19
20
21
22
23
24
25
26
27
28
29
(29 layers)
Every Nth
1 Selected
Default
20
Apply
Close
OilSat
0.00027
0.22009
0.44046
0.66083
0.88120

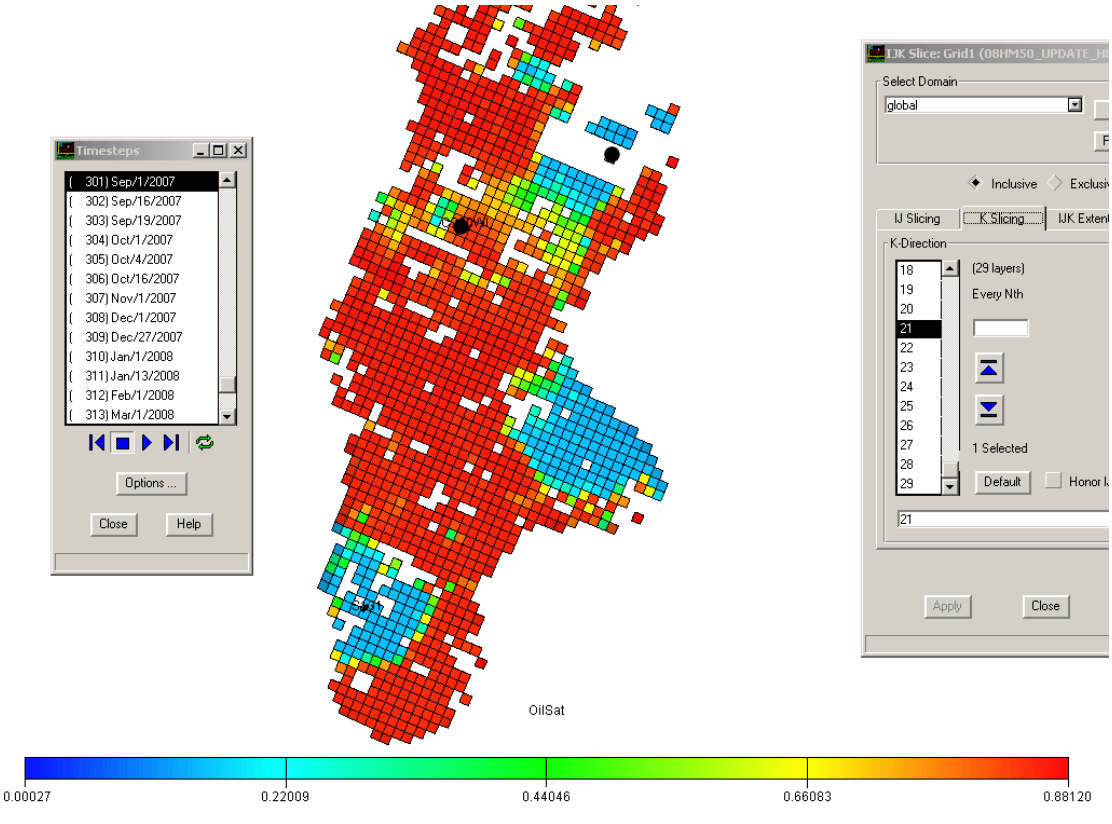
Timesteps
(301) Sep/1/2007
(302) Sep/16/2007
(303) Sep/19/2007
(304) Oct/1/2007
(305) Oct/4/2007
(306) Oct/16/2007
(307) Nov/1/2007
(308) Dec/1/2007
(309) Dec/27/2007
(310) Jan/1/2008
(311) Jan/13/2008
(312) Feb/1/2008
(313) Mar/1/2008
Options ...
Close
Help
IJK Slice: Grid1 (08HM50_UPDATE_HI
Select Domain
global
Inclusive
IJ Slicing
K Slicing
IJK Extent
K-Direction
18
19
20
21
22
23
24
25
26
27
28
29
(29 layers)
Every Nth
1 Selected
Default
21
Apply
Close
OilSat
0.00027
0.22009
0.44046
0.66083
0.88120

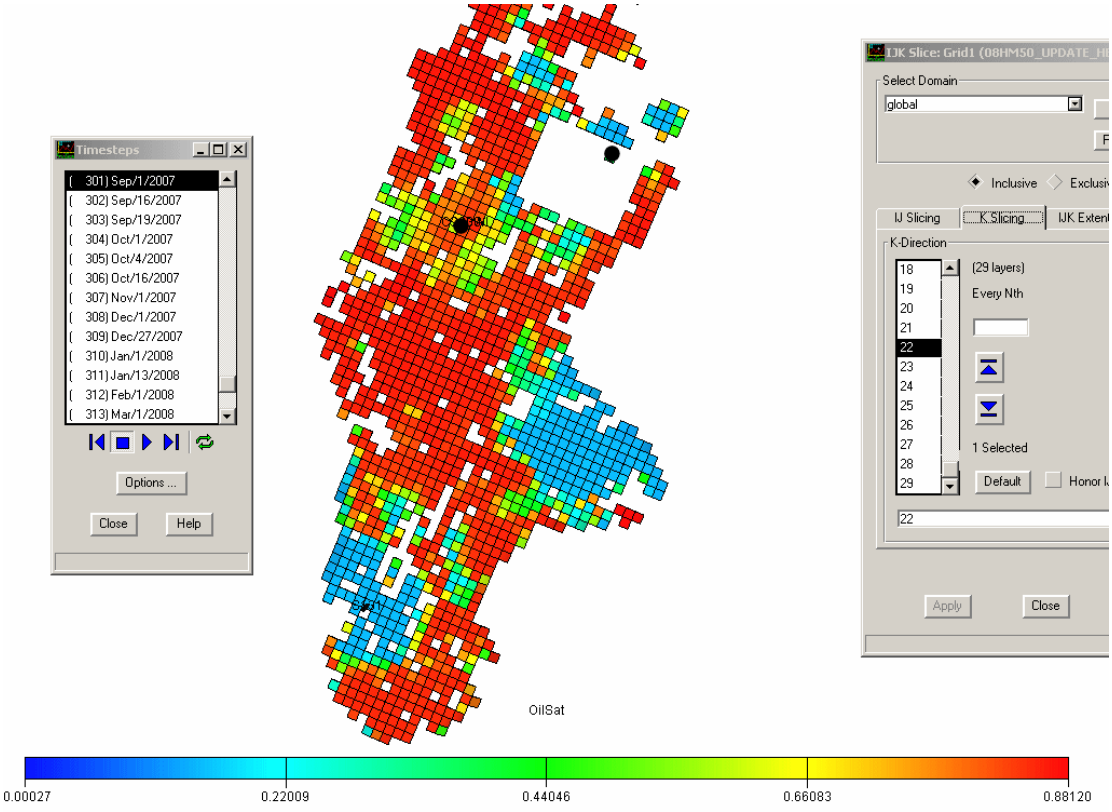
Timesteps
(301) Sep/1/2007
(302) Sep/16/2007
(303) Sep/19/2007
(304) Oct/1/2007
(305) Oct/4/2007
(306) Oct/16/2007
(307) Nov/1/2007
(308) Dec/1/2007
(309) Dec/27/2007
(310) Jan/1/2008
(311) Jan/13/2008
(312) Feb/1/2008
(313) Mar/1/2008
Options ...
Close
Help
OilSat
0.00027
0.22009
0.44046
0.66083
0.88120
IJK Slice: Grid1 (08HM50_UPDATE_HI
Select Domain
global
Inclusive
IJ Slicing
K Slicing
K-Direction
18
19
20
21
22
23
24
25
26
27
28
29
(29 layers)
Every Nth
1 Selected
Default
22
Apply
Close

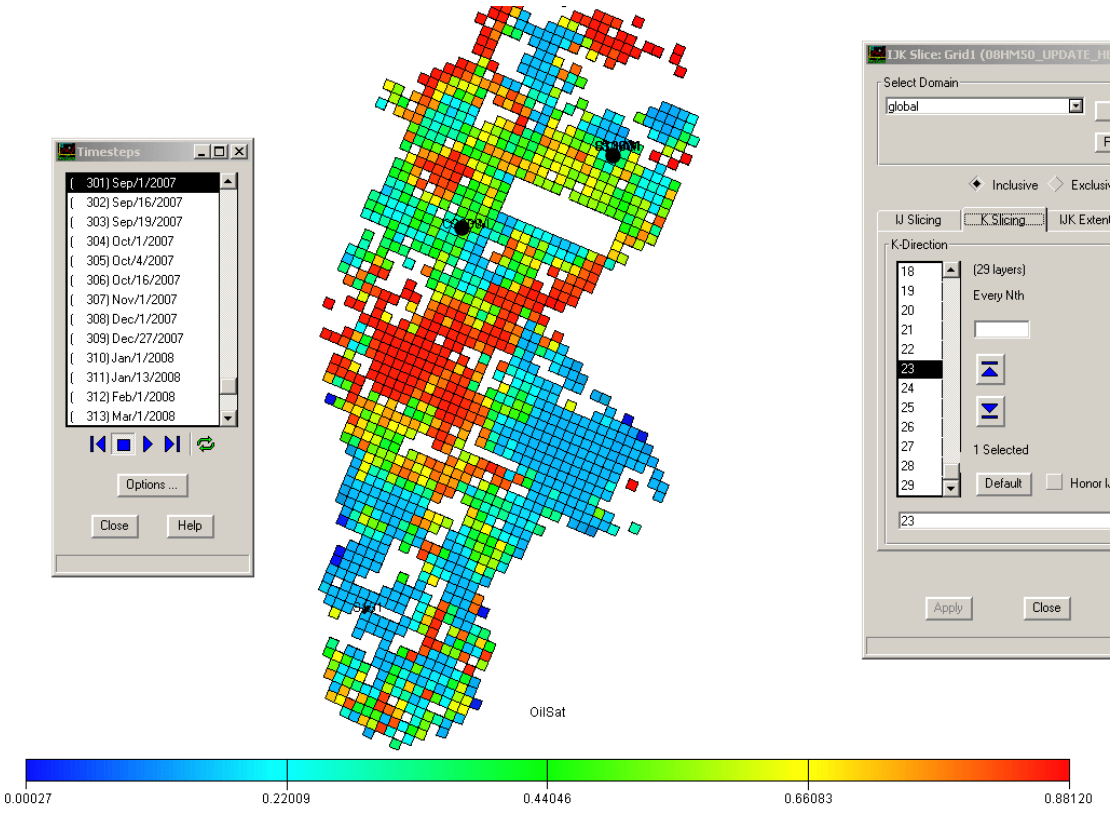
Timesteps
(301) Sep/1/2007
(302) Sep/16/2007
(303) Sep/19/2007
(304) Oct/1/2007
(305) Oct/4/2007
(306) Oct/16/2007
(307) Nov/1/2007
(308) Dec/1/2007
(309) Dec/27/2007
(310) Jan/1/2008
(311) Jan/13/2008
(312) Feb/1/2008
(313) Mar/1/2008
Options ...
Close
Help
IJK Slice: Grid1 (08HM50_UPDATE_HI
Select Domain
global
Inclusive
IJ Slicing
K Slicing
IJK Extent
K-Direction
(29 layers)
Every Nth
1 Selected
Default
Honor
23
Apply
Close
OilSat
0.00027
0.22009
0.44046
0.66083
0.88120

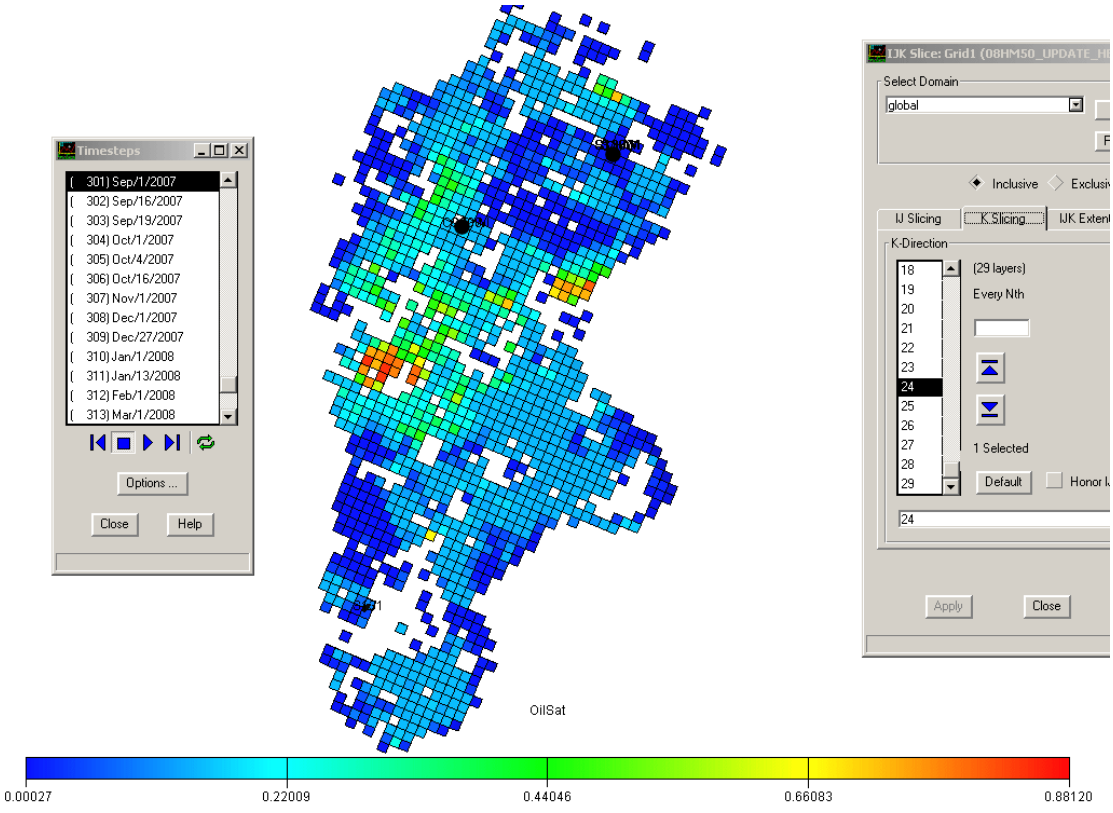
Timesteps
(301) Sep/1/2007
(302) Sep/16/2007
(303) Sep/19/2007
(304) Oct/1/2007
(305) Oct/4/2007
(306) Oct/16/2007
(307) Nov/1/2007
(308) Dec/1/2007
(309) Dec/27/2007
(310) Jan/1/2008
(311) Jan/13/2008
(312) Feb/1/2008
(313) Mar/1/2008
Options ...
Close
Help
IJK Slice: Grid1 (08HM50_UPDATE_HI
Select Domain
global
Inclusive
IJ Slicing
K Slicing
IJK Extent
K-Direction
(29 layers)
Every Nth
1 Selected
Default
Honor
24
Apply
Close
OilSat
0.00027
0.22009
0.44046
0.66083
0.88120

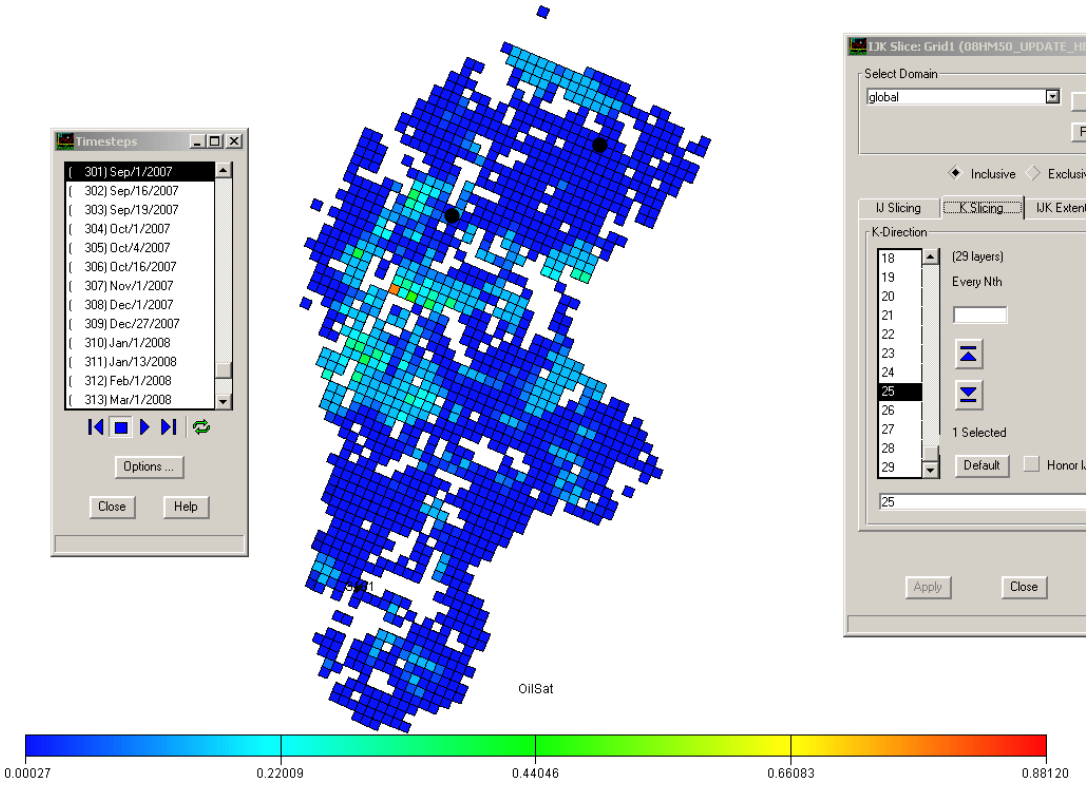
Timesteps
301) Sep/1/2007
302) Sep/16/2007
303) Sep/19/2007
304) Oct/1/2007
305) Oct/4/2007
306) Oct/16/2007
307) Nov/1/2007
308) Dec/1/2007
309) Dec/27/2007
310) Jan/1/2008
311) Jan/13/2008
312) Feb/1/2008
313) Mar/1/2008
Options ...
Close
Help
IJK Slice: Grid1 (08HM50_UPDATE_HI
Select Domain
global
Inclusive
IJ Slicing
K Slicing
K-Direction
(29 layers)
Every Nth
1 Selected
Default
25
Apply
Close
OilSat
0.00027
0.22009
0.44046
0.66083
0.88120

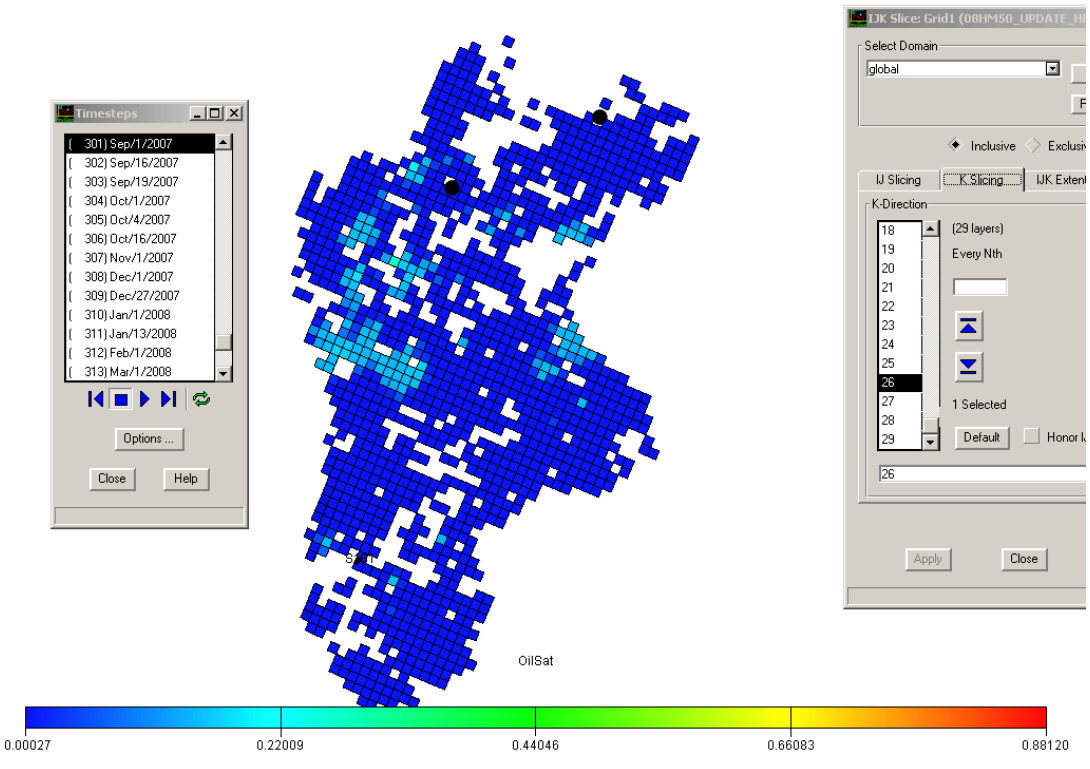
Timesteps
301) Sep/1/2007
302) Sep/16/2007
303) Sep/19/2007
304) Oct/1/2007
305) Oct/4/2007
306) Oct/16/2007
307) Nov/1/2007
308) Dec/1/2007
309) Dec/27/2007
310) Jan/1/2008
311) Jan/13/2008
312) Feb/1/2008
313) Mar/1/2008
Options ...
Close
Help
IJK Slice: Grid1 (08HM50_UPDATE_HI
Select Domain
global
Inclusive
IJ Slicing
K Slicing
K-Direction
(29 layers)
Every Nth
1 Selected
Default
26
Apply
Close
OilSat
0.00027
0.22009
0.44046
0.66083
0.88120

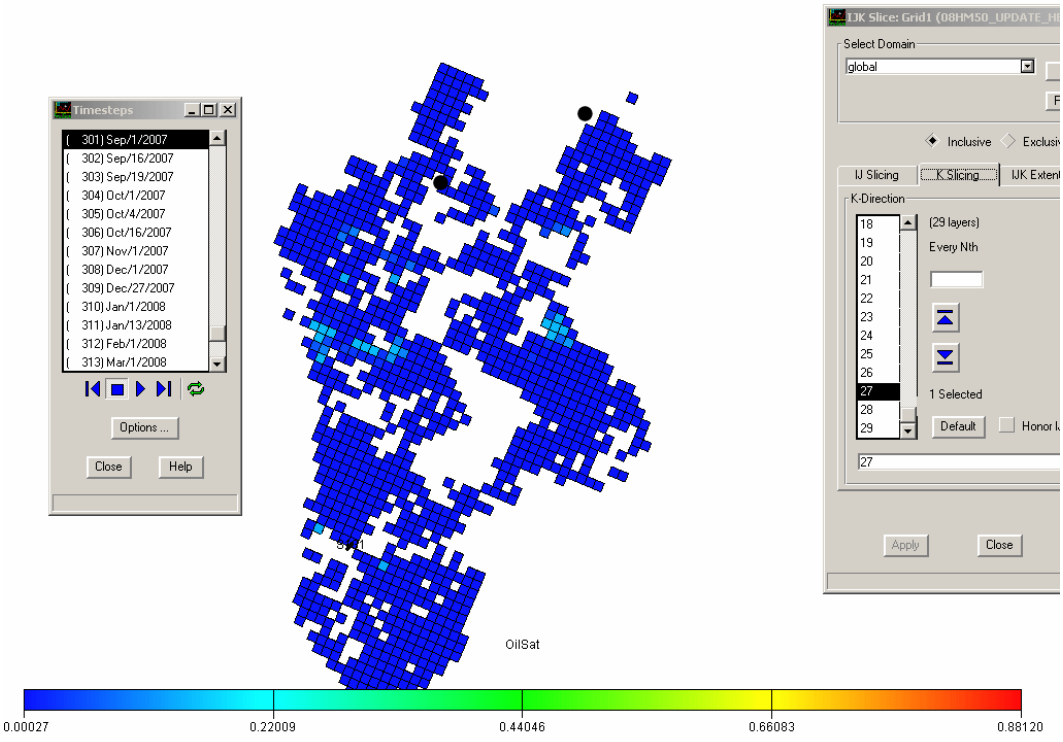
Timesteps
301) Sep/1/2007
302) Sep/16/2007
303) Sep/19/2007
304) Oct/1/2007
305) Oct/4/2007
306) Oct/16/2007
307) Nov/1/2007
308) Dec/1/2007
309) Dec/27/2007
310) Jan/1/2008
311) Jan/13/2008
312) Feb/1/2008
313) Mar/1/2008
Options ...
Close
Help
IJK Slice: Grid1 (08HM50_UPDATE_H
Select Domain
global
Inclusive
IJ Slicing
K Slicing
K-Direction
(29 layers)
Every Nth
1 Selected
Default
27
Apply
Close
OilSat
0.00027
0.22009
0.44046
0.66083
0.88120

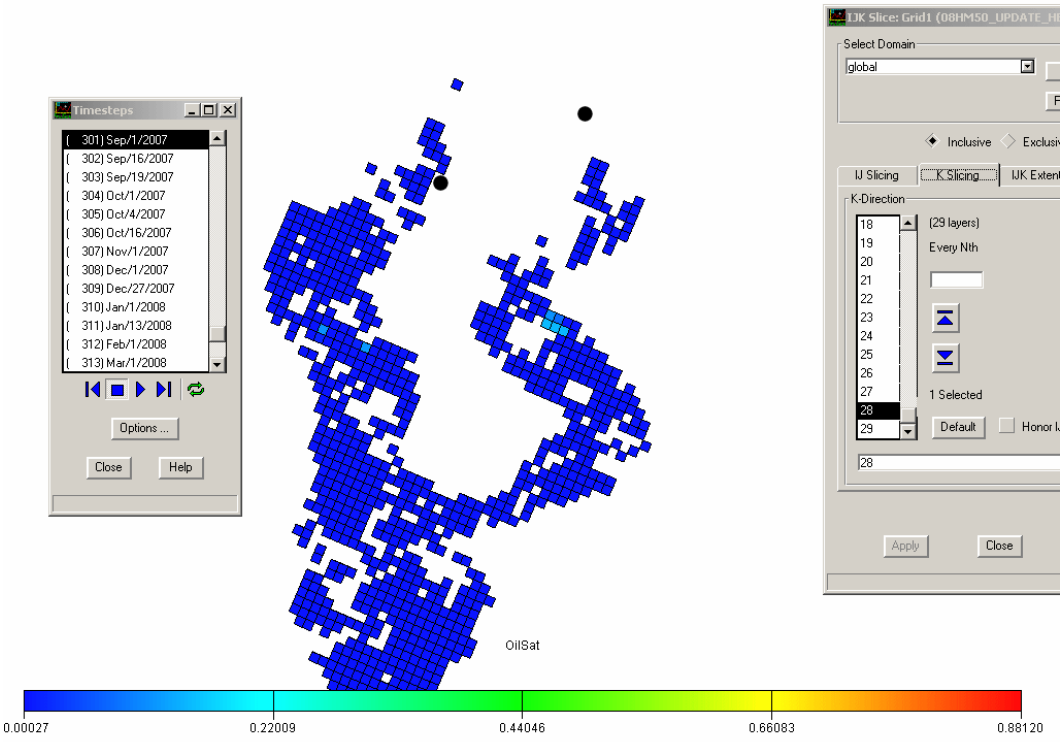
Timesteps
301) Sep/1/2007
302) Sep/16/2007
303) Sep/19/2007
304) Oct/1/2007
305) Oct/4/2007
306) Oct/16/2007
307) Nov/1/2007
308) Dec/1/2007
309) Dec/27/2007
310) Jan/1/2008
311) Jan/13/2008
312) Feb/1/2008
313) Mar/1/2008
Options ...
Close
Help
IJK Slice: Grid1 (08HM50_UPDATE_H
Select Domain
global
Inclusive
IJ Slicing
K Slicing
K-Direction
(29 layers)
Every Nth
1 Selected
Default
28
Apply
Close
OilSat
0.00027
0.22009
0.44046
0.66083
0.88120

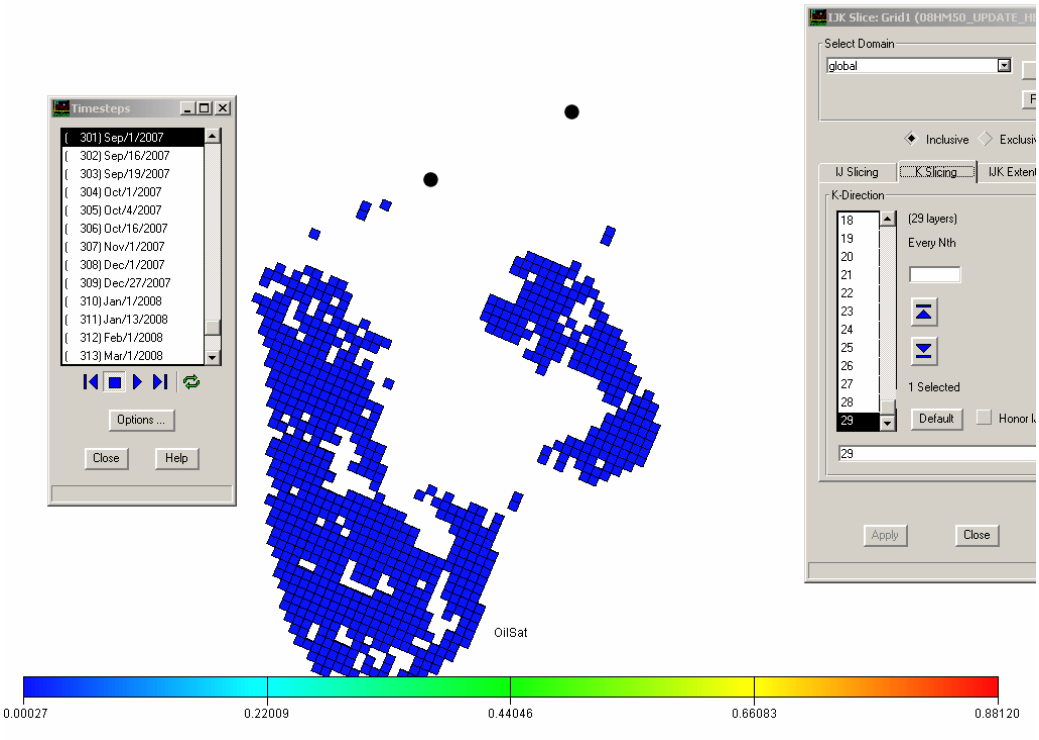
Timesteps
[301] Sep/1/2007
[302] Sep/16/2007
[303] Sep/19/2007
[304] Oct/1/2007
[305] Oct/4/2007
[306] Oct/16/2007
[307] Nov/1/2007
[308] Dec/1/2007
[309] Dec/27/2007
[310] Jan/1/2008
[311] Jan/13/2008
[312] Feb/1/2008
[313] Mar/1/2008
Options ...
Close
Help
IJK Slice: Grid1 (08HM50_UPDATE_HI
Select Domain
global
Inclusive
IJ Slicing
K Slicing
IJK Extent
K-Direction
18
19
20
21
22
23
24
25
26
27
28
29
(29 layers)
Every Nth
1 Selected
Default
29
Apply
Close
OilSat
0.00027
0.22009
0.44046
0.66083
0.88120

National Energy Technology Laboratory

626 Cochrans Mill Road
P.O. Box 10940
Pittsburgh, PA 15236-0940

3610 Collins Ferry Road
P.O. Box 880
Morgantown, WV 26507-0880

One West Third Street, Suite 1400
Tulsa, OK 74103-3519

1450 Queen Avenue SW
Albany, OR 97321-2198

539 Duckering Bldg./UAF Campus
P.O. Box 750172
Fairbanks, AK 99775-0172

Visit the NETL website at:
www.netl.doe.gov

Customer Service:
1-800-553-7681